

**DIRECT AND INDIRECT EFFECTS OF LONG-TERM CLIMATIC CHANGE ON
TERRESTRIAL-AQUATIC ECOSYSTEM INTERACTIONS IN TASMANIA**

KRISTEN K. BECK
ORCID: 0000-0002-8257-9639

Thesis submitted in total fulfilment of
the requirements of the degree of
DOCTOR OF PHILOSOPHY

July 2018

School of Geography
Faculty of Science
The University of Melbourne

“Produced on archival quality paper”

ABSTRACT

Climate influences aquatic ecosystems through two important pathways: (1) directly through temperature or changes in the precipitation/evaporation balance and/or (2) indirectly mediated by changes in the terrestrial environment. However, the indirect impacts of climate on aquatic ecosystems are poorly understood. The aim of this thesis is to better understand how aquatic ecosystems respond to past climate change, using two lakes in western Tasmania as case studies. Palaeoecological research on two multiproxy lake sediment records (Paddy's Lake and Lake Vera) were used to reconstruct chronology (radiometric dating, i.e. ^{14}C); fire regimes (charcoal); vegetation dynamics (pollen); nutrient dynamics (C%, N%, C/N, $\delta^{13}\text{C}$, and $\delta^{15}\text{N}$); catchment geochemistry (μXRF scanning); and aquatic response (diatoms and cladocerans) to determine the impact of climate change on these aquatic ecosystems. Results from Paddy's Lake reveal long-term changes in the cladoceran community are indirectly driven by climate through changing vegetation productivity and available ^{14}N altering the trophic status of the lake. Following the invasion of sclerophyll vegetation caused by increased fire frequency, the indirect climate influences on the aquatic system break down and the cladocerans appear complacent to changing vegetation productivity. At Lake Vera, diatoms respond indirectly to climate through changes in the acidity and dystrophic conditions of the lake with catchment peat formation. An increase in climate variability at ca. 5 ka caused declines in lake level resulting in a shift to a direct response in the diatoms to climate. During a period of increased drying at ca. 2.4 to 0.7 ka, increased fire activity adversely impacts the aquatic system causing a non-linear transition in the diatom community. The findings from this thesis show aquatic ecosystems of Tasmania are predominantly indirectly driven by climate through the formation of thick organic peats. Shifts in vegetation composition alter the surrounding soils and catchment dynamics impacting aquatic ecosystems trophic status and pH. Fire is another important driver of aquatic ecosystem response that causes changes in vegetation composition, altering the nutrient profile of soils and increasing erosion and sediment delivery. Aquatic ecosystems respond with increased pH, disturbance taxa and a shallowing of lake mixing depth in the diatom community. These terrestrial-aquatic ecosystem interactions have the potential to be more widespread across Southern Hemisphere biomes and temperate peatlands worldwide that share similar vegetation-soil dynamics.

DEDICATION

*Dedicated to the Killarney lakes, where my love for palaeo began;
and to Bentley, for being part of my PhD journey from start to end.*

DECLARATION

This is to attest that:

1. This thesis comprises my original work towards Doctor of Philosophy (PhD) degree except where indicated in the Acknowledgment of Collaboration;
2. Due acknowledgement have been made in the text to all other text and/or material used;
3. This thesis is below the 100,000 word limit including all figures, tables, maps, references and appendices.

PUBLICATIONS ARISING FROM THIS THESIS

Chapter 4: Beck, K.K., Fletcher, M.S., Gadd, P.S., Heijnis, H. & Jacobsen, G. (2017) An early onset of ENSO influence in the extra-tropics of the southwest Pacific inferred from a 14,600 year high resolution multi-proxy record from Paddy's Lake, northwest Tasmania. *Quaternary Science Reviews*, 157, 164-175. DOI:10.1016/j.quascirev.2016.12.001

Chapter 5: Beck. K.K., Fletcher, M-S., Kattel, G., Barry, L., Gadd, P.S., Heijnis, H., Jacobsen, G., & Saunders, K.M. (2018) The indirect response of an aquatic ecosystem to long term climate-driven terrestrial vegetation in a subalpine temperate lake. *Journal of Biogeography*, 45, 713-725. DOI:10.1111/jbi.13144

Chapter 6: Beck, K.K., Fletcher, Michael-Shawn, Gadd, P. S., Heijnis, H., Saunders, K. M. & Zawadzki, A. (*in prep*) Direct and indirect aquatic ecosystem response to changes in climate variability: A Holocene diatom record from Tasmania, Australia

Chapter 7: Beck, K. K., Fletcher, M.-S., Gadd, P. S., Heijnis, H., Saunders, K. M., Simpson, G. L., & Zawadzki, A. (2018) Variance and rate-of-change as early warning signals for a critical transition in an aquatic ecosystem state: A test case from Tasmania, Australia. *Journal of Geophysical Research: Biogeosciences*, 123, 495–508. DOI:10.1002/2017JG004135

ACKNOWLEDGEMENT OF COLLABORATION


I hereby acknowledge that some of the work within this thesis was performed in collaboration with other researchers, or carried out in other institutions. Outlined below are the details of collaboration.

Patricia S. Gadd and Henk Heijnis (Australian Nuclear Science and Technology Organisation – ANSTO) performed the μ XRF geochemical analysis for both lake sites (Paddy’s Lake and Lake Vera). Paddy’s Lake Carbon and Nitrogen isotopic and elemental analysis was performed by Linda Barry (ANSTO). For Lake Vera, Mark Rollog (University of Adelaide) performed the Carbon and Nitrogen isotopic and elemental analysis on the long core (TAS1508 N1) and Brent B. Wolfe (Wilfrid Laurier University) on the short core (TAS1108 SC1). Radiocarbon analysis for Paddy’s Lake was performed by Geraldine Jacobsen (ANSTO) and Lead-210 was performed by Atun Zawadzki (ANSTO) for Lake Vera. Remaining radiometric dating was performed by DirectAMS (USA) and The National Ocean Sciences Accelerator Mass Spectrometry (NOSAMS, USA). Giri Kattel (University of Melbourne & Resilience and Transformation Centre in China) provided training and advising for cladoceran analyses. Gavin L. Simpson (University of Regina) was instrumental in the development of the R code for the generalised additive models and early warning signal metrics for Lake Vera. Anthony Romano (University of Melbourne) and Alexa Benson (University of Melbourne) counted macroscopic charcoal for Lake Vera. All the co-authors in the publications arising from this PhD thesis contributed to analysis, interpretation and editing of the manuscripts.

ACKNOWLEDGEMENT OF AUTHORSHIP

I hereby acknowledge that the work included in this thesis contains published papers and scholarly work of which I am a joint author. I have included as part of the thesis a written statement, endorsed by my Primary Supervisor, attesting to my contribution to the joint publications/scholarly work.

I, Kristen Beck, was the primary investigator and lead author of the published articles and in preparation manuscripts included in this Thesis.



Michael-Shawn Fletcher



Kristen Beck

FURTHER ACKNOWLEDGEMENTS

There are many people to thank for their encouragement and support throughout my PhD candidature.

Firstly, my sincerest thanks to my primary supervisor Michael-Shawn Fletcher, for his patience and invaluable guidance. I would not have reached this goal without your intellectual, financial, and emotional support. Thank you as well to my co-supervisors Krystyna Saunders and Russell Drysdale for their guidance. Special thanks to Krystyna for her encouragement and advice; even though we live in different cities you always found time for me.

Thank you to the Australian Research Council (ARC-award: #DI110100019 and IN140100050) and Australian Institute of Nuclear Science and Engineering (AINSE-award: ALNGRA15003 and ALNGRA16023) for funding this project, without which this work would not have been possible. I would also like to thank the University of Melbourne for my endorsement of the MIFRS & MRS scholarships that allowed me to come to Australia to complete my PhD.

Special thanks to Alexa Benson, Agathe Lise-Pronovost, Michela Mariani, Scott Nichols, Angelica Ramierez, William Rapuc, Anthony Romano, Coralie Tate, and Valentina Vanghi for your assistance and persistence on difficult field work. Further gratitude to Michela Mariani for her GIS assistance, intellectual discussion and friendship throughout my PhD. This work was not possible without the hard work of these colleagues.

Thank you to the Department of Primary Industries, Parks, Water and Environment for allowing us to conduct this research (ES 14283 & ES 15221). I would also like to pay my respects to the traditional and original owners of this land and to acknowledge today's Tasmanian Aboriginal community who are the custodians of this land.

Thanks to colleagues and friends in the School of Geography for your guidance and friendship. To friends and family far and wide who have supported me throughout my PhD.

I would like to thank my dad, Chris, for his encouragement. My mum, Karen, and sister, Megan, for their unwavering support and always reassuring me. Ryan, my partner, for his fortitude and understanding through this crazy journey and Allyson Griffith who had the patience to read and edit the final draft of this thesis.

Finally, I would like to thank my examiners for taking the time to review my thesis and for their helpful suggestions.

TABLE OF CONTENTS

Abstract	iii
Dedication	v
Declaration.....	vi
Publications arising from this Thesis.....	vii
Acknowledgement of Collaboration.....	viii
Acknowledgement of Authorship.....	ix
Further Acknowledgements.....	xi
List of Figures.....	xxiii
List of Tables	xxxiv
CHAPTER 1: INTRODUCTION.....	1
1.1 Thesis Aim:.....	1
1.2 The Critical Knowledge Gap	1
1.3 Study Area: Tasmania.....	5
1.4 Research Questions.....	6
1.5 Palaeoecology and Research Design	7
1.6 Thesis Layout.....	9
1.7 Chapter Closing	11
CHAPTER 2: BACKGROUND.....	13
2.1 Chapter Aim.....	13

2.2 Modern Tasmanian Climate.....	13
2.2.1 Southern Westerly Winds (SWW).....	15
2.2.2 El Niño Southern Oscillation (ENSO).....	16
2.3 Modern Tasmanian Vegetation.....	16
2.4 Legacy of Fire in Tasmania	19
2.5 Holocene Climate and Vegetation History	20
2.5.1 Holocene Climate	21
2.5.2 Vegetation History of Tasmania	22
2.6 Tasmanian Geology	23
2.7 Tasmanian Soils.....	24
2.8 Limnology of Tasmania.....	25
2.8.1 Limnological Characteristics	26
2.8.2 Tyler’s Line	27
2.8.3 Aquatic Ecology	28
2.9 Terrestrial-Aquatic Ecosystem Interactions.....	30
2.9.1 Direct Drivers of Catchment Dynamics and Vegetation Change	30
2.9.2 Direct Drivers of Aquatic Ecosystem Change	32
2.9.3 Indirect Drivers of Aquatic Ecosystem Change.....	34
2.10 Non-Linear Ecosystem System Response to Environmental Change	37
2.11 Chapter Closing	38
CHAPTER 3: METHODS	39

3.1 Chapter Aim.....	39
3.2 Palaeoecological Approach.....	39
3.3 Site Selection	40
3.3.1 Paddy's Lake	41
3.3.2 Lake Vera.....	43
3.4 Sediment Coring	45
3.4.1 Coring Equipment.....	45
3.4.2 Coring Methods	46
3.5 Radiometric Dating.....	53
3.5.1 Radiocarbon Dating	54
3.5.2 Lead-210 Dating	58
3.6 Age-depth Modelling	60
3.6.1 Standard Methods	61
3.6.2 Advantages to Age-depth Modelling.....	63
3.6.3 Limitation to Age-Depth Modelling	64
3.7 Micro-X-ray Fluorescence (XRF) Scanning.....	64
3.7.1 Standard Method of μ XRF Scanning.....	65
3.7.2 Advantages to μ XRF Scanning.....	66
3.7.3 Limitation to μ XRF Scanning.....	67
3.8 Elemental and Isotopic Carbon and Nitrogen Analysis.....	67
3.8.1 Carbon.....	68

3.8.2 Nitrogen	71
3.8.3 Standard Method.....	72
3.8.4 Advantages to Carbon and Nitrogen Organic Proxies	73
3.8.5 Limitations to Carbon and Nitrogen Organic Proxies	74
3.9 Palynology	75
3.9.1 Standard Method.....	76
3.9.2 Advantages to Palynology	78
3.9.3 Limitation of Palynology	79
3.10 Diatoms.....	79
3.10.1 Standard Method.....	81
3.10.2 Advantages to Diatom Analysis	82
3.10.3 Limitations to Diatom Analysis	82
3.11 Cladocerans.....	83
3.11.1 Standard Method.....	84
3.11.2 Advantages of Cladoceran Analysis	85
3.11.3 Limitations to Cladoceran Analysis.....	85
3.12 Charcoal	86
3.12.1 Standard Method.....	87
3.12.2 Advantages to Charcoal Analysis	88
3.12.3 Limitations of Charcoal Analysis	88
3.13 Statistical Methods and Data Analysis	89

3.13.1 Cluster Analysis (CONISS).....	90
3.13.2 Ordination Analysis.....	91
3.13.3 Lead and Lag Analyses.....	94
3.13.4 Sequential t-test analysis of regime shifts.....	97
3.13.5 Rate-of-change.....	99
3.13.6 Generalised Additive Modelling (GAMs).....	101
3.14 Chapter Closing.....	102
PART ONE: PADDY'S LAKE.....	103
CHAPTER 4: DISCUSSION.....	105
4.1 Chapter Aim.....	105
4.2 Abstract.....	105
4.3 Introduction.....	106
4.4 Western Tasmania.....	109
4.4.1 Regional Geography.....	109
4.5 Methods.....	112
4.5.1 Sediment Recovery.....	112
4.5.2 Chronology.....	112
4.5.3 Charcoal Analysis.....	113
4.5.4 Palynology.....	114
4.5.5 Geochemistry.....	114
4.6 Results.....	115

4.6.1 Sediment Recovery	115
4.6.2 Chronology	115
4.6.3 Charcoal	118
4.6.4 Palynology	119
4.6.5 Geochemistry	122
4.7 Discussion.....	124
4.7.1 Palaeoenvironmental History.....	124
4.7.2 Long-term Climate Change [SWW to ENSO].....	129
4.7.3 Sclerophyll Invasion	133
4.8 Conclusions.....	133
4.9 Acknowledgements.....	134
CHAPTER 5: DISCUSSION	135
5.1 Chapter Aim.....	135
5.2 Abstract.....	135
5.3 Introduction.....	136
5.4 Geographical Setting of Tasmania.....	138
5.4.1 Cladocerans of Subalpine Temperate Australasia	139
5.4.2 Site Description	139
5.5 Materials and Methods.....	140
5.5.1 Core Collection and Chronology	140
5.5.2 Cladoceran Analysis	141

5.5.3 Geochemistry	141
5.5.4 Pollen and Charcoal Analysis	142
5.5.5 Numerical Analyses	142
5.6 Results.....	143
5.6.1 Chronology	143
5.6.2 Cladoceran Analysis	144
5.6.3 Geochemistry	147
5.6.4 Pollen and Charcoal Analysis	147
5.6.5 Numerical Analyses.....	149
5.7 Discussion.....	150
5.7.1 Vegetation Change and Lake nutrient Dynamics	150
5.7.2 Vegetation Change and Aquatic ecosystem Dynamics.....	154
5.8 Conclusion	157
5.9 Acknowledgements.....	158
PART TWO: LAKE VERA	159
CHAPTER 6: DISCUSSION	161
6.1 Chapter Aim.....	161
6.2 Abstract.....	161
6.3 Introduction.....	162
6.4 Regional Geography and Site Description.....	163
6.5 Methods	165

6.5.1 Coring and Chronology	165
6.5.2 μ XRF Geochemistry.....	166
6.5.3 Carbon Nitrogen	166
6.5.4 Charcoal.....	167
6.5.5 Diatoms.....	167
6.5.6 Canonical Correspondence Analysis	168
6.6 Results.....	168
6.6.1 Coring and Chronology	168
6.6.2 μ XRF Geochemistry.....	170
6.6.3 Carbon and Nitrogen.....	171
6.6.4 Charcoal.....	173
6.6.5 Diatoms.....	173
6.6.6 Canonical Correspondence Analysis	175
6.7 Discussion.....	176
6.7.1 Ecological Interpretation of Diatoms.....	176
6.7.2 Indirect Climate Impacts on Aquatic Ecosystems	177
6.7.3 Direct Climate Impacts on Aquatic Ecosystems.....	180
6.7.4 Multi-millennial to Millennial Climate Shifts	184
6.8 Conclusion	184
CHAPTER 7: DISCUSSION	187
7.1 Chapter Aim.....	187

7.2 Abstract.....	187
7.3 Introduction.....	188
7.3.1 Biogeography of Tasmania.....	190
7.3.2 Study Site.....	191
7.4 Materials and Methods.....	192
7.4.1 Coring and Chronology	192
7.4.2 Geochemical Analysis	193
7.4.3 Diatom Analysis	194
7.4.4 Palynology and Charcoal Analysis	194
7.4.5 Numerical Analyses.....	195
7.5 Results.....	196
7.5.1 Coring and Chronology	196
7.5.2 Geochemical Analysis	198
7.5.3 Diatom Analysis	199
7.5.4 Palynology and Charcoal Analysis.....	202
7.5.5 Numerical Analyses.....	204
7.6 Discussion.....	207
7.6.1 Fire-driven Changes in Aquatic Ecosystem Dynamics	207
7.6.2 Critical Transitions and Early Warning Signals	211
7.7 Conclusion	213
7.8 Acknowledgments	214

Chapter 8: Synthesis	215
8.1 Chapter Aims	215
8.2 Chapter Introduction	215
8.3 Aquatic Ecosystem Response to Climate	216
8.4 Aquatic Ecosystems, Climate and Catchment Relationships.....	222
8.5 Aquatic Ecosystems and Fire Disturbance	226
8.6 Critique and Unresolved Gaps	228
8.7 Chapter Closing	231
Chapter 9: Conclusion and Future work.....	233
9.1 Thesis Conclusion.....	233
9.2 Future work.....	234
REFERENCES	235
Appendix I.....	297
Appendix II.....	300
Appendix III	303
Appendix IV	318
Appendix V	338
Appendix VI.....	341

LIST OF FIGURES

Figure 1.1: Schematic of potential climate pathways (direct and indirect) that influence aquatic ecosystem response.....	3
Figure 1.2: Flow chart of thesis layout.....	10
Figure 2.1: Average monthly Tasmanian precipitation (blue bars), maximum monthly temperature (line with cross symbols), and minimum monthly temperature (line with circle symbols). Data was retrieved from Bureau of Meteorology (http://www.bom.gov.au/) for every Tasmanian weather station and all recorded years (as early as 1890 CE).....	14
Figure 2.2: Precipitation correlation maps for a) Southern Annular Mode and b) Southern Oscillation Index in Tasmania (Mariani et al., 2016a).....	14
Figure 2.3: Schematic of atmospheric circulation cells and surface winds (Figure 1.2; Holden, 2011).	15
Figure 2.4: Vegetation groups of western Tasmanian provided by TASVEG3.0 (Department of Primary Industries, 2017).	17
Figure 2.5: Factors influencing fire across space and time. Loops on the triangles indicate potential feedbacks (Figure 1, Parisien et al., 2009). The shaded box indicates the scales relevant to this study.	20
Figure 2.6 Map of Tasmanian geological groups.	24
Figure 2.7: Map of surface hydrology in Tasmania.	26
Figure 2.8: Map of Tyler’s Line (map revised from Tyler, 1992; Rees et al., 2010b).	28
Figure 2.9: A conceptual model for critical transitions where low resilience (a and b), longer recovery rates (c to e) increase the temporal autocorrelation and variance (g and h) indicate the early warning signals of a critical transitions (Figure 2; Scheffer et al., 2015).	38
Figure 3.1: Map of Tasmania, Tyler’s Line (red solid, dashed and dotted lines) (Tyler, 1992) and satellite images of study site locations: (1) Paddy’s Lake and (2) Lake Vera.	40
Figure 3.2: Photo of Paddy’s Lake (by: Kristen Beck, 2016).....	42

Figure 3.3: Vegetation groups defined by TASVEG 3.0 (Department of Primary Industries, 2017) surrounding Paddy’s Lake and Lake Vera.....	43
Figure 3.4: Photo of Lake Vera (by: Kristen Beck, 2015).....	45
Figure 3.5: University of Melbourne Palaeoecology Laboratory coring platform equipped with two pontoons, a wood deck and the Nesje tripod (by: Kristen Beck, 2015).....	47
Figure 3.6: a) Schematic of the Universal percussion corer (Aquatic Research Instruments, 2016). b) Photograph of the Universal Corer and extruding stand (by: Jonathon Garber, 2017).....	48
Figure 3.7: Attaching the aluminium chamber to the Nesje coring head at Paddy’s Lake (by: Alexa Benson, 2014).....	49
Figure 3.8: Hammering the Nesje at Lake Vera (by: Michela Mariani, 2015).....	50
Figure 3.9: Winching the Nesje back to the platform after core collection (by: William Rapuc, 2014).....	50
Figure 3.10: Sediment core inside aluminium chamber on the platform at Paddy’s Lake (by: Alexa Benson, 2014).	51
Figure 3.11: Core splitter at University of Melbourne. Splitting a Universal Core from Rebecca’s Lagoon, northwest Tasmania (by: Bianca Dickson, 2016).....	52
Figure 3.12: Examples of split Lake Vera cores a) TAS1508 N1, b) TAS1508 N1 archive half, and c) TAS1508 N2 (by: Kristen Beck, 2015).	52
Figure 3.13: Core slicing apparatus with a sediment sample on the metal cradle (by: Kristen Beck, 2016).	53
Figure 3.14: Example calibration of radiocarbon date 1,295 ¹⁴ C yrs ± 33 (1σ) from a Northern Territory, Australia sediment sample (NT1501). Dark grey shading demonstrates the 95% cal yr BP probability.	57
Figure 3.15: Uranium decay series including principal radionuclides and their associated half-lives (Figure 1, Appleby, 2001).....	59
Figure 3.16: Classical age-depth model examples of a) linear interpolation; b) linear regression; c) cubic spline; and d) smooth spline functions of an example dataset in clam (Blaauw, 2010).....	62
Figure 3.17: Example of Bayesian age-depth modelling in Bacon (Blaauw et al., 2013) using the in program example “RLGH3”.	63

Figure 3.18: ITRAX core scanner (Figure 1; Croudace et al., 2006).	66
Figure 3.19: Schematic of the Nitrogen cycle (O.M.= organic matter and DIN= dissolved inorganic Nitrogen) (Figure 1; Talbot, 2001).	71
Figure 3.20: Schematic of C and N elemental and isotopic analysis apparatus and method (Figure 2; Talbot, 2001).	73
Figure 3.21: Photograph of pollen grains, <i>Amperea xiphoclada</i> and Ericaceae (TAS1401 N1), under a light microscope at 400x magnification (by: Kristen Beck, 2015).	75
Figure 3.22: Flowchart of pollen processing, specific to the University of Melbourne Protocol (Berglund, 1986b; Faegri et al., 1989).	77
Figure 3.23: Photograph of <i>Eunophora tasmanica</i> under a light microscope at 1000x magnification (TAS1508 N1E) (by: Kristen Beck, 2016).	80
Figure 3.24: Photograph of preserved cladoceran <i>Bosmina meridionalis</i> on the left from Paddy's Lake under light microscope at 630x magnification (TAS1401 N1) (by: Kristen Beck, 2015). On the right a sketch of important cladoceran body parts that preserve in sediment (Figure 2; Korhola et al., 2001).	83
Figure 3.25: Photography of microscopic charcoal fragment under a light microscope at 20x magnification (TAS1508 N1C) (by: Kristen Beck, 2016).	86
Figure 4.1: Maps of Tasmanian precipitation correlated to a) Southern Annular Mode and b) Southern Oscillation Index (modified from Mariani and Fletcher, 2016). Black dots indicate site locations: 1) Paddy's Lake, Black Bluff; 2) Wombat Pool, Cradle Mountain; 3) Lake Gwendolyn and Lake Nancy, Frenchman's Cap; 4) Lake Dobson, Mount Field National Park; and 5) Lake Osborne, Hartz Ranges. c) A satellite image of Paddy's Lake.	111
Figure 4.2: Age-depth model developed in clam v2.2 (Blaauw, 2010) using SHCal13 (Hogg et al., 2013) and employing a smooth spline (factor=0.50; goodness-of-fit of 83.38). Outliers are marked in red.	117
Figure 4.3: Paddy's Lake charcoal data: a) Fire return interval (FRI) (years per/fire); b) Signal-to-noise (SNI) index. SNI above the grey dashed line indicates fire events above the noise threshold (>3); c) background charcoal (particles/cm ² yr ⁻¹); d) Microscopic charcoal (particles/cm ² yr ⁻¹ x 10 ³); e) Macroscopic charcoal (particles/cm ² yr ⁻¹)	

¹); and f) Peak Magnitude (particles/cm² yr⁻¹). Red plus symbols indicate significant charcoal peaks (peaksFinal).

.....118

Figure 4.4: Pollen stratigraphy of Paddy's Lake important pollen types. Pollen data is presented as percentages and grouped by rainforest taxa (green), sclerophyll taxa (maroon), trees and shrubs (teal), graminoids (yellow) and aquatic taxa (grey). Group percentage totals are stacked by their associated colour. Microscopic charcoal is presented as particles cm⁻² yr⁻¹ x 10³. The DCA axis 1 scores estimate trends in the terrestrial pollen percentage data (variance=52.0%). CONISS cluster analysis represents the significant cluster groups and subzones of the terrestrial pollen types. The grey dashed line represents the break in Zones 1, 2, and 3 while the red dashed lines separate the subzones of Zone 3.....121

Figure 4.5: ITRAX stratigraphy for Paddy's Lake composite core of important μ XRF geochemicals, normalised by $kcps_n$, with a 1.5 smooth spline.123

Figure 4.6: Summary plot of Paddy's Lake data including: a) terrestrial pollen DCA axis score 1; b) grass and herbs pollen percentages; c) geochemical PCA axis 1 scores with weighted average (window width=51); d) *Phyllocladus aspleniifolius* pollen percentages; e) sclerophyll taxa pollen percentages with weighted average in red (window width=7); f) macroscopic charcoal (particles/cm² yr⁻¹) on log scale with weighted average in red (window width=11); and g) bromine ($kcps_n \times 10^{-3}$) in grey with weighted average (black, window width=51). With Antarctic climate data from: h) $\delta^{18}O$ record from Taylor Dome Antarctic (Grootes et al., 2001) raw data in grey with weighted average in dark grey (window width=11); and i) Antarctic ice core $\delta^{18}O$ composite curve (Pedro et al., 2016). Blue box indicates the ACR and Zone 1 while the grey dashed line separates Zones 2 and 3.127

Figure 4.7: Summary plot of Holocene palaeoecological data: a) Lake Nancy and Lake Gwendolyn combined charcoal z-score regression (red) interpolated to 80-year time- steps and z-scores calculated from an average of pre-European (12-0.2 ka) charcoal values and smoothed weighted averaging regression (window width = 9) (Fletcher et al., 2015); b) Paddy's Lake bromine data ($kcps_n \times 10^{-3}$) in grey with weighted grey dashed lines show shifts average (black, window width=51); Paddy's Lake pollen percent data (grey line - scatter) with a weighted average (black line, window width= 7) for: c) *Phyllocladus aspleniifolius*; d) *Nothofagus cunninghamii*; e) sclerophyll taxa; f) Poaceae; g) Paddy's Lake macroscopic charcoal (particles/cm² yr⁻¹); and h) the number of El

Niño events in 100-year overlapping windows from inorganic sediment deposits in Laguna Pallcacocha, Ecuador (Moy et al., 2002) with red shading indicates significant El Niño events. Red dashed lines indicate significant fire events and vegetation response and blue triangles indicate locations of ^{14}C dates. Grey dashed lines show shifts in *P. aspleniifolius* (signalling regional hydroclimate) that occur during periods of increased El Niño frequency...132

Figure 5.1: Digital elevation map of Tasmania and location of Paddy's Lake (yellow dot), on the left, featuring Tyler's Line (Tyler, 1992) determined by precipitation (solid blue line), rainforest boundary (dotted blue line) and the dolerite edge (blue dashed line). On the right, a photograph of Paddy's Lake (by: Kristen Beck, 2016).....140

Figure 5.2: Age-depth model of Paddy's Lake, Tasmania with a smooth spline model (factor=0.50; goodness-of-fit of 83.38) calibrated using SHCal13 (Hogg et al., 2013). Outlier dates are marked in red (Chapter 4).....143

Figure 5.3: Stratigraphy of Paddy's Lake cladoceran taxa. Cladoceran species are presented as percentage composition and grouped by Pelagic (blue), Littoral (green) and Eurytopic (yellow) taxa. The DCA axis 1 (variance= 25.1%) and 2 (variance= 14.3%) scores estimate trends in the cladoceran percentage data. Red dashed lines indicate breaks in the seven significant CONISS zones.146

Figure 5.4: Summary figure of Paddy's Lake vegetation types and nutrient indicators. a) $\delta^{15}\text{N}$ (‰); b) $\delta^{13}\text{C}$ (‰); c) C/N ratio; d) sediment Nitrogen percentage; e) sediment Carbon percentage; f) percent woody plant pollen (grey) with a weighted average (black, window width=5); g) percent grass and herb pollen (grey) with a weighted average (black, window width=5); and h) bromine ($\text{kcps}_n \times 10^3$)(grey) and weighted average (dark green, window width=61) (Chapter 4).148

Figure 5.5: Summary figure of aquatic and terrestrial ecosystem changes at Paddy's Lake. a) bromine ($\text{kcps}_n \times 10^3$)(grey) with a weighted average (dark green, window width=61) (Chapter 4); b) percent sclerophyll pollen (grey) with a weighted average (black, window width=3) (Chapter 4); c) *Botryococcus* spp. AR (grains/cm² yr⁻¹ x 10⁻³)(light green) with a weighted average (black, window width=3); d) Pollen DCA axis 2 (grey) with a weighted average (black, window width=5); e) Cladoceran DCA axis 1 (blue); f) $\delta^{15}\text{N}$ (‰) (orange); g) oligotrophic:eutrophic cladoceran taxa ratio (green); h) pollen AR (grains/cm² yr⁻¹ x 10⁻⁵)(grey) with a weighted average (black, window width=5); and i) background charcoal particles/cm² yr⁻¹ (red) (Chapter 4). Shaded background colours indicate generic climate transitions.....153

Figure 5.6: Cross-correlation analysis of Paddy's Lake data with four lags of 400 year bins for: a) $\delta^{15}\text{N}$ vs. pollen AR; b) pollen DCA axis 2 vs. cladoceran DCA axis 1; and c) $\delta^{15}\text{N}$ vs. oligotrophic:eutrophic cladoceran ratio. The grey dashed lines indicate the upper and lower confidence intervals of the Cross-correlation analysis. The grey shaded areas are the significant relationships between the two time series. The red dashed line indicates the start lag time which the two time series have a significant relationship.156

Figure 6.1: A map of Tasmania's Tyler's Line (Tyler, 1992) is on the left determined by precipitation (black solid line), rainforest boundary (black dashed line) and the dolerite edge (black dotted line) with a precipitation correlation heat map of the Southern Oscillation Index and location of Lake Vera (pink dot). On the right a satellite image of Lake Vera with the coring location (pink dot) overlaid with bathymetry determined by Peterson (1966), isobath intervals equal 10 feet (3.05 m).....165

Figure 6.2: Age model for Lake Vera, Tasmania. a) ^{210}Pb CIC age-depth model with error bars. b) Activity of total and supported ^{210}Pb with errors by depth (cm). c) Bacon age-depth (red dotted line) model with probability distribution of the radiocarbon ages (blue) and age probability of ^{210}Pb dates (green). Yellow symbols represent the radiocarbon dates with an applied age offset. The 1000 iterations of potential depth ages (Bayesian statistic, black dotted lines) are shown with the 95% confidence interval (grey dotted lines).170

Figure 6.3: A summary of Paddy's Lake geochemistry results. a) $\delta^{15}\text{N}$ (‰) (grey) and weighted average (lime green, window width= 3); b) Carbon/Nitrogen ratio (grey) and weighted average (dark green, window width=3); c) percent carbon (grey) and weighted average (light brown, window width=3) and d) percent nitrogen (grey) and weighted average (olive, window width=3); e) Ca (grey) and weighted average (black, window width =101); f) Ti (grey) and weighted average (brown, window width=101); g) Fe/Mn (grey) and weighted average (dark green, window width=101); h) Fe (grey) and weighted average (green, window width=101); i) Br (grey) and weighted average (light green, window width=101); and j) charcoal accumulation rate (light red) and weight average (dark red, window width=5).....172

Figure 6.4: Stratigraphy of Lake Vera diatoms. Most abundant diatom species presented as relative abundance. The PCA axis 1, 2, and 3 estimate trends in the diatom percentage data (explained variance of PCA 1 =29.6 %, PCA 2=13.7 % and PCA 3= 4.6 %). Significant zones are separated by red dashed lines, significant zones from

Chapter 7 are separated by grey dashed lines. Planktonic:benthic ratio estimate trends in the sum of planktonic taxa to benthic taxa.....	173
Figure 6.5: Summary plot of multi-proxy dataset from Lake Vera. a) western Tasmania palaeofire (Mariani et al., 2017b); b) <i>Phyllocladus aspleniifolius</i> pollen percent (grey) weighted average (dark green, window width=5); c) <i>Isoetes</i> pollen percent (grey) weighted average (teal, window width=5); d) <i>Lagarostrobos franklinii</i> pollen percent (grey) weighted average (light green, window width=5); e) diatom PCA axis 1 scores (grey) weighted average (dark blue, window width=3); f) <i>Discostella stelligera</i> percentage (grey) weighted average (light blue, window width=3); g) charcoal accumulation rate (light red) weighted average (dark red, window width=5).....	179
Figure 6.6: Schematic representative of Lake Vera bathymetry and planktonic versus littoral habitat extent at differing lake levels.	181
Figure 6.7: CCA biplot of important diatom taxa (red) and significant environmental geochemicals (a) and vegetation (b) (blue arrows) overlaying depth samples (grey circles). Zone 1 is indicated by black dots, Zone 2 is indicated by white dots and Zone 3 by grey dots.	183
Figure 7.1: Map of Australia, inset map of Tasmania with site location (blue dot) and a photo of Lake Vera, Tasmania (by: Kristen Beck, 2015).....	192
Figure 7.2: Age-depth model for Lake Vera, Tasmania. a) Total and supported ^{210}Pb activity concentrations with uncertainties, b) ^{210}Pb chronology based on the CIC model, c) Age-depth model developed in Bacon, the blue symbols indicate probability distribution of the ^{14}C ages and the green symbols age probability of ^{210}Pb dates. The black dotted lines demonstrate the 1,000 iterations of Bayesian statistic and potential depth ages in a 95% confidence interval. The red line demonstrates the weighted mean ages.....	197
Figure 7.3: A summary of Lake Vera geochemical results of a) Carbon/Nitrogen ratio; b) Carbon percent; c) Nitrogen percent; d) Fe/Mn fit with a weighted average (window width= 51); e) Fe fit with a weighted average (window width= 51); and f) Ti ratios fit with a weighted average (window width= 51). Grey dashed line indicates the non-linear shift in the diatom community.	199

- Figure 7.4: Stratigraphy of the important Lake Vera diatom species presented as percentage composition. The PrC estimate trends in the diatom percentage data (PrC explained variance=60.0%). Red dashed lines show breaks in CONISS cluster analysis for the diatoms (four significant zones). X-axis scale varies by taxa.201
- Figure 7.5: Summary stratigraphy of percent terrestrial pollen, ferns and aquatic taxa (x-axis varies) with four significant CONISS.....203
- Figure 7.6: A summary plot of Lake Vera data. a) percent disturbance pollen taxa (*Urticaceae* and *Bauera rubioides*) (brown); b) total percent fern pollen taxa (orange); c) total diatom valves (valves/mL $\times 10^8$) (light green) fitted with a fitted GAM (black); d) *Pediastrum* spp. influx ($\times 10^3$)(green); e) *Discostella stelligera* percentages (blue) with a fitted GAM (black); f) Fe/Mn ratios (grey $\times 10^3$) fitted with a weighted average in black (window width= 33); g) Carbon/Nitrogen ratio (brown); h) diatom variance (blue) and confidence interval (grey dashed) of GAM residuals; i) diatom PrC (green) with fitted GAM (black) and confidence intervals (grey dashed); j) diatom ROC (orange); and k) charcoal sum z-scores (red) with a fitted GAM (black). Grey dotted line indicates the timing of the non-linear shift.206
- Figure 7.7: Early warning signals statistical summary of the Lake Vera diatoms (left) and pollen (right) including: a and e) ROC (orange); b and f) GAM fitted variance (blue) and confidence intervals (grey dashed line); c and g) PrC (green) fitted GAM (black) and confidence intervals (grey dashed); d and h) charcoal (CHAR in red) sum z-scores and fitted GAM (black). Vertical grey dashed lines indicate the timing of the diatom non-linear shift.210
- Figure 8.1: Paddy's Lake a) interpolated cladoceran DCA axis 1 scores (blue) with RSI curve (red, window width of 6); b) significant RSI shifts (p-value <0.05). SEA analysis on interpolated Paddy's Lake data for c) pollen DCA axis 2 scores and d) pollen accumulation rate (AR). Dark grey bars represent the significant SEA p<0.05, black bars p<0.01.219
- Figure 8.2: Lake Vera a) interpolated diatom PCA axis 1 scores (black) with RSI curve (red, window width of 20) and significant RSI shifts (blue, p-value <0.05). Grey bar is the response event excluded from the analysis. b-g) SEA analysis on interpolated Lake Vera data split into response events pre 5 ka (right) and post 5 ka (left) for: b & e) $\delta^{15}\text{N}$; c & f) pollen PCA axis 1; and d & g) Fe. Dark grey bars represent the significant SEA p<.05, black bars p<0.01220

Figure 8.3: Summary figure of Paddy’s Lake cladoceran diversity including a) cladoceran species richness with RSI index (red, window width=15); b) cladoceran Shannon diversity with RSI index (red, window width=15); c) cladoceran Pielou’s evenness with RSI index (red, window width=15); and d) percent sclerophyll pollen with weighted average (orange, window width=15). Diversity indices were calculated using the package <i>vegan v.2.4-4</i> (Oksanen et al., 2016) in R.....	224
Figure 8.4: Revised Figure 1.1 schematic of the climate influences on aquatic ecosystem to highlight the important pathways determined by this thesis.....	225
Figure 8.5: Revised Figure 1.1 schematic highlighting fire influences on an aquatic ecosystem.	228
Figure I.1: Optical image of Paddy’s Lake recovered cores: TAS1401 SC1 (93 cm) and TAS1401 N1 (227 cm). TAS1401 N1 was cut in two [TAS1401 N1A (113 cm) and TAS1401 N1B (114 cm)] for analysis.	297
Figure I.2: PCA biplot for geochemical (ITRAX) of important geochemical elements (Al, Si, P, S, Cl, K, Ca, Sc, Ti, Mn, Fe, Ni, Cu, Zn, Br, Rb, Sr, Zr, and Pb) and Mo incoherence/coherence ratio axis 1 and 2. Data converted to z-scores and PCA analysis conducted in PC-Ord v4.27 (McCune et al., 2011), variance of axis 1= 42.391 and axis 2= 7.114.	298
Figure I.3: DCA biplot for terrestrial pollen data axis 1 and 2. DCA was performed in <i>R v3.1.1</i> (R Development Core Team, 2014) using the <i>rioja</i> package (Juggins, 2016) on square root transformed data with rare taxa down weighted. Percent variance described by axis 1 is 26.06% and 4.16% for axis 2.....	299
Figure III.1: Scatter plot of $\delta^{13}\text{C}$ and C/N results from Lake Vera.....	304
Figure III.2: PCA biplot of TAS1108SC1 +TAS1508 N1 Hellinger transformed fossil diatom data with important taxa presented here in red. Grey circles indicate sample depths. Explained variance of axis 1 is 29.6% and axis 2 is 13.7%.....	305
Figure III.3: Stratigraphy of Lake Vera diatoms. Most abundant diatom species presented as percentage composition. The PCA axis 1 estimate trends in the diatom percentage data (explained variance of PCA 1 29.6%). Significant zones determined by CONISS are separated by red dashed lines and significant zones from Chapter 7 are separated by grey dashed lines. Planktonic:benthic ratio estimate trends in the sum of planktonic taxa to benthic taxa.....	306

Figure III.4: Absolute abundance of a) tychoplanktonic taxa; b) <i>Eunotia</i> spp.; c) <i>Achnantheaceae</i> spp.; d) <i>Discostella stelligera</i> ; and e) Total diatom valves for Lake Vera.....	307
Figure III.5: PCA biplot of TAS1108SC1 +TAS1508 N1 Hellinger transformed terrestrial pollen percentages with important taxa presented here in red. Grey circles indicate sample depths. Explained variance of axis 1 is 37.2% and axis 2 is 15.3%.....	308
Figure III.6: Stratigraphy of Lake Vera pollen. Important pollen taxa are presented as percentage composition. <i>Botryococcus</i> and <i>Pediastrum</i> are presented as influx and microscopic charcoal as an accumulation rate. Zones determined by CONISS are separated by red dashed lines.....	309
Figure III.7: μ XRF stratigraphy for Lake Vera composite core of important XRF geochemicals, normalised by Mo incoherence/coherence, with a smooth spline of 1.5.....	310
Figure III.8: Cluster analysis and broken stick model for Lake Vera μ XRF data. The broken stick shows up to 10 significant cluster. The age and depth of the first six significant breaks in the dendrogram are highlighted in red.....	311
Figure IV.1: Extended diatom summary stratigraphy of percent diatoms (x-axis varies), cyst:diatoms, total valves ($\text{mLx}10^9$) and PrC with four significant CONISS zones.....	320
Figure IV.2: Geochemical μ XRF summary stratigraphy of important geochemical elements. Ti, Zn, Ca, K, include the detrital elements, Si/Ti is a bio indicator for diatom productivity, and S and Fe/Mn indicate terrestrial inputs and redox conditions, Br and Mo Inc/Coh are indicators of terrestrial organic matter inputs. All summarised elements are normalised values by Mo Inc/Coh with the exception of *.....	321
Figure IV.3: Diatom principal curve biplot with an explained variance of 60.0%. The fitted curve uses 133.978 degrees of freedom and correspondence analysis method with a penalty =1.4.....	322
Figure IV.4: Species response plots of diatoms taxa included in the principal curve (PrC) performed using analogue (Simpson et al., 2016). Higher abundances indicate the PrC score the species is most associated with.	327
Figure IV.5: Pollen principal curve biplot with an explained variance 60.7 %. The fitted curve uses 75.2732 degrees of freedom and correspondence analysis method with penalty =1.4.	328

Figure IV.6: Species response plots of the terrestrial pollen for all taxa included in the PrC performed using analogue (Simpson et al., 2016). Higher abundances indicate the PrC score the species is most associated with.	331
Figure IV.7: Lake Vera diatom PrC curve (green) fit with the mean RSI curve (red, window width of 5) and significant RSI shifts (blue bar, p-value <0.01). Outputs with larger window widths (i.e. 20 and 30) showed the same result.	331
Figure V.1: Extended SEA analysis results for interpolated Paddy's Lake data (100 yrs) for Chapter 8. Dark grey bars represent the significant SEA p<0.05, black bars p<0.01.	338
Figure V.2: Extended SEA analysis results for interpolated Lake Vera data (50 yrs) for Chapter 8. Dark grey bars represent the significant SEA p<0.05, black bars p<0.01.	339

LIST OF TABLES

Table 3.1: List of C/N ratios and $\delta^{13}\text{C}$ values associated with different terrestrial and aquatic sources (Table 1; Meyers et al., 2001).....	70
Table 3.2: CharAnalysis outputs and definitions (Whitlock et al., 2001; Higuera, 2009).	88
Table 4.1: Radiocarbon laboratory results for Paddy's Lake. Dates are organised in chronological sequence and the core code is identified at the top of the depths. Samples measured at AMSDirect are labelled with lab code D-AMS and samples analysed at ANSTO are labelled with the lab code OZS. The two <i>bold italicised</i> dates were removed as outliers from the age model and * indicate the paired macrofossil-bulk sediment samples. Square brackets designate depths within the continuous sedimentary sequence.....	116
Table 5.1: Summary of significant CONISS cladoceran zones (N=7) from Paddy's Lake, displayed by age (ca. ka) and sample depths (cm). Key taxa are reported with their approximate mean, maximum and minimum percent abundance.....	144
Table 5.2: Cross Correlation analysis results including standard deviation, standard error, upper and lower confidence intervals (CI).....	150
Table 6.1: Radiocarbon results table for Lake Vera (TAS1108 SC1 & TAS1508 N1), including the laboratory identification number, sample depth (cm), sample type, the F modern (pMC) and error (1σ), the radiocarbon age (BP) and error, and $\delta^{13}\text{C}$ (per mil).....	169
Table 7.1: Radiocarbon results for Lake Vera, including NOSAMS laboratory identification number, sample depth (cm), sample type, the F modern and error, the radiocarbon age (BP) and error (1σ), and $\delta^{13}\text{C}$ (per mil)....	197
Table II.1: Radiocarbon laboratory results for Paddy's Lake. Dates are organised in chronological sequence, core code identified at the top of depths. The two <i>bold italicised</i> dates were removed as outliers from the age model and * indicate the paired macrofossil-bulk sediment samples. Square brackets designate depths within the continuous sedimentary sequence (Chapter 4).	300
Table III.1: Age offset for bulk sediment dates. Calculated by differencing macrofossil and bulk sediment radiocarbon dates from the same depth sample.....	303

Table III.2: Diatom authorities Lake Vera TAS1108SC1+TAS1508 N1 composite core (Chapter 6). Diatom taxonomic nomenclature was verified using Algaebase (<http://www.algaebase.org/>).....311

Table IV.1: Lead-210 extended results table, analysis conducted at Australian Nuclear Science and Technology Organisation.319

Table IV.2: Diatom authorities for Lake Vera TAS1108SC1 (Chapter 7). Diatom taxonomic nomenclature was verified using Algaebase (<http://www.algaebase.org/>).....331

CHAPTER 1: INTRODUCTION

1.1 THESIS AIM:

The aim of this thesis is to understand the relative roles of changes in climate and terrestrial environments on long-term aquatic ecosystem dynamics in Tasmania. I aim to use palaeoecological data derived from lake sediments to reconstruct past environmental changes over the Holocene. The Holocene is the targeted time frame because it represents a period broadly analogous to today's climate, yet with sufficient variability to test for relationships between climate and aquatic ecosystem response. I will employ geochronology to determine age of the lake sediments; the analysis of charcoal to inform fire history and past climate; pollen as an indicator of surrounding vegetation change and climate history; elemental geochemistry and organic matter isotopes will allow understanding of catchment dynamics such as soil development, nutrient cycling, and lake chemistry; and diatom and cladoceran remains will inform on aquatic ecosystem change. To assess the terrestrial and aquatic ecosystem reconstructions I perform a variety of statistical methods to determine timing of changes recorded in the palaeoecological data and to test the direct and indirect linkages between climate and aquatic ecosystem change.

1.2 THE CRITICAL KNOWLEDGE GAP

Freshwater is essential to life on earth, it is crucial for many ecosystem services and hosts a significant component of global biodiversity (Costanza et al., 1997; Postel et al., 1997; Carpenter et al., 2009; Grizzetti et al., 2016). These freshwater systems are primarily driven by climate, influencing aquatic ecosystem structure, function, and mechanisms (Petchey et al., 1999; Ball et al., 2010; Fritz et al., 2013). Understanding how aquatic systems respond to climatic changes over multiple scales of space and time is imperative for sustainable management of our environment. Aquatic ecosystems respond 'directly' to climatic change through abiotic factors such as temperature, lake level change, and altered thermoclines (Schindler et al., 1996; Schindler, 1997; Smol et al., 2000; Gell et al., 2005; Prebble et al., 2005; Saunders, 2011; Gell et al., 2012; Saunders et al., 2012). Climate-

driven impacts on aquatic ecosystems can also be mediated through the surrounding terrestrial environment via vegetation altering soil dynamics and nutrient input to water bodies ('indirect' responses) (Figure 1.1) (Huvane et al., 1996; Korsman et al., 1998; Lancashire et al., 2002; Tibby et al., 2007b; Augustinus et al., 2008; Moos et al., 2009; Fritz et al., 2013; Timbal et al., 2013)[†]. Despite acknowledgement of the influences of these two climate pathways over aquatic systems, research on aquatic ecosystem response to climate is imbalanced with ample evidence that aquatic ecosystems respond directly to climate (Laird et al., 1996; Gasse et al., 1997; Fritz et al., 1999; Korhola et al., 2000; Smol et al., 2000; Gell et al., 2005; Prebble et al., 2005; Gell et al., 2012). The paucity of research into indirect pathways exposes a critical knowledge gap in our understanding of aquatic ecosystem response to climate.

[†] In this thesis, I have identified two pathways that climate influences aquatic ecosystems: direct and indirect. I use 'direct' to express an environmental phenomenon that alters a system without acting through other processes (e.g. the effect of temperature change on the thermal state of a water body and its impact on aquatic ecosystems); and 'indirect' to indicate an environmental phenomenon acting through other processes to create change in a system (e.g. the effect of temperature on the vegetation composition and the subsequent impact that change has on soil nutrients and trophic status of aquatic ecosystems).

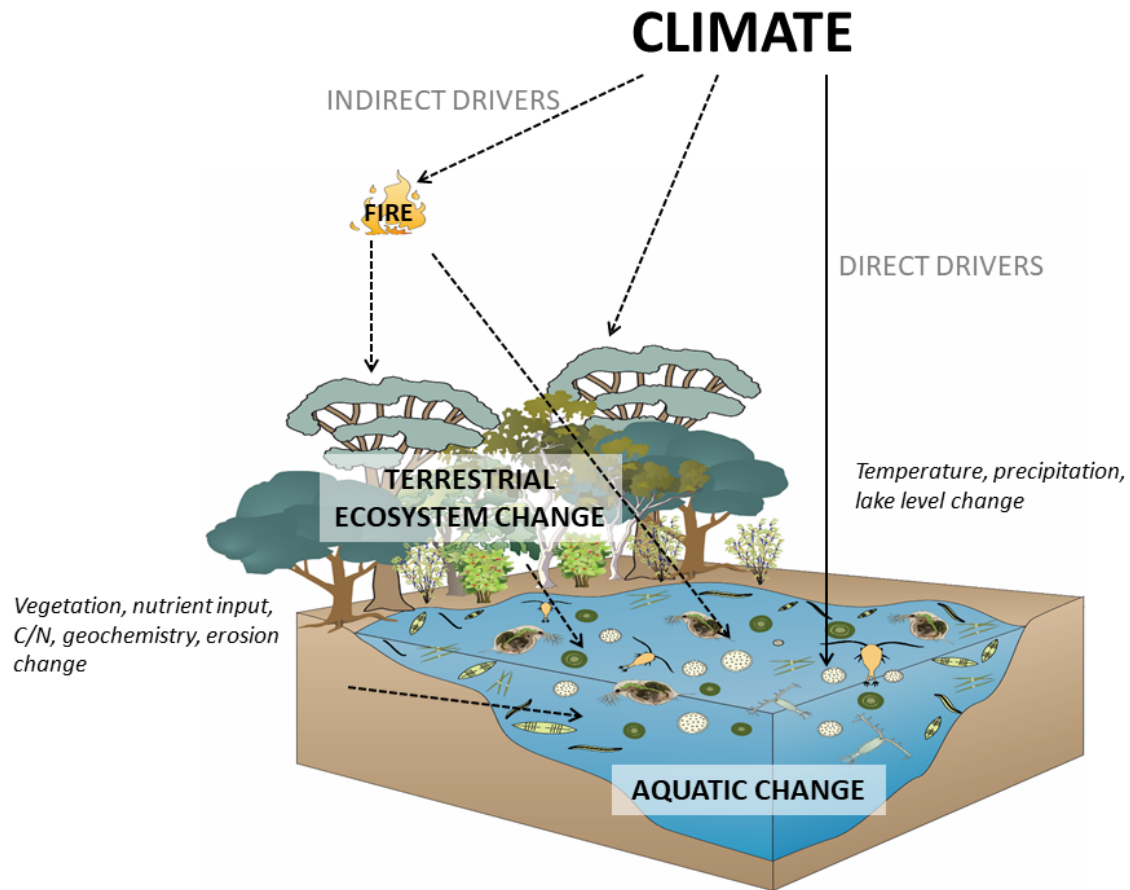


Figure 1.1: Schematic of potential climate pathways (direct and indirect) that influence aquatic ecosystem response.

Terrestrial environments are predominantly driven by climate, and these in turn indirectly influence aquatic ecosystems. There is evidence worldwide that climate drives soil development and vegetation change over multiple spatial and temporal scales (Crocker et al., 1955; Iverson, 1964; Pastor et al., 1986; Engstrom et al., 2000; Moreno et al., 2003; Pearson et al., 2003; Fritz et al., 2013). For example, long-term fluxes in CO₂ and temperature result in changes in vegetation structure and spatial patterns, in turn, these shifts in vegetation dynamics also alter soils (e.g. nutrient cycling and carbon storage) (Kershaw, 1995; Cowling, 1999; Cramer et al., 2001; Prentice et al., 2009). Climate-driven changes in the terrestrial environment such as vegetation change, nutrient cycling, and soil development can alter aquatic ecosystem nutrient status, pH, water chemistry, and

species composition (Crocker et al., 1955; Sreenivasa et al., 1973; Whitehead et al., 1989; Huvane et al., 1996; Engstrom et al., 2000; Fritz et al., 2013; Law et al., 2015).

Studies that investigate both terrestrial and aquatic ecosystems environmental change at a single site reveal a remarkably tight coupling in response to a range of environmental drivers including climate, non-climate-related nutrient dynamics, lake ontogeny, bedrock weathering, erosion, and human impact (Bradbury, 1986; Huvane et al., 1996; Engstrom et al., 2000; Moos et al., 2009; Barr et al., 2013; Fritz et al., 2013; Law et al., 2015; Perren et al., 2017). Yet, most of this research has been conducted in the Northern Hemisphere with relatively few studies from the Southern Hemisphere.

Australia is a continent sensitive to climate change yet our understanding of the aquatic ecosystem response to climate in this region is lacking. The Australian government recognises the importance of future climate change and the potential impacts on ecosystems (CSIRO and Bureau of Meteorology, 2015; DPIPW, 2016). The 2016 management plan for the Tasmanian World Heritage Area presents a detailed synopsis of the potential impacts of climate change on the terrestrial environment (e.g. increased wild fires and the loss of endemic plant systems). Critically, this region hosts the highest density of freshwater systems in Australia; however, in the 2016 management plan the potential impacts to aquatic systems barely receives mention with no detail of any future threats or management responses presented. Thus, there is a crucial knowledge gap in how climatic change influences aquatic ecosystems in this region and more broadly across Australia presenting a major barrier to sustainably manage these systems.

. Fire occurrence, frequency and intensity has also shaped the Australian terrestrial environment by altering the vegetation composition, species propagation, soil structure and vegetation-soil feedbacks (Jackson, 1968; Gill, 1975; Bowman et al., 2009b; Wood et al., 2012; Murphy et al., 2013; Enright et al., 2015; Holz et al., 2015). Past occurrence of fire in Australia is tightly linked to climate (Turney et al., 2004; Bradstock, 2010; Mariani et al., 2016a; Mariani et al., 2016b) and the magnitude and intensity of wild fires is predicted to increase with future

rises in temperature increasing drought stress brought on by climate change (Pitman et al., 2007; Flannigan et al., 2009; Bradstock, 2010; Fox-Hughes et al., 2014); yet there is little to no understanding of the effects of these environmental drivers on aquatic ecosystems in Australia.

1.3 STUDY AREA: TASMANIA

In this thesis, I use western Tasmania as a case study for understanding how aquatic ecosystems are influenced by climatic change (directly and indirectly). Western Tasmania is an ideal region to better understand the influences of climate on aquatic ecosystem response because: (1) freshwater is abundant (Buckney et al., 1973; Tyler, 1992); (2) aquatic ecosystems are oligotrophic, dystrophic, and acidic (Tyler, 1974, 1992) – the inert geology leads to a predominance of organic soils that potentially contribute substantially to the nutrient budget of associated aquatic ecosystems (Buckney et al., 1973; Tyler, 1992); (3) changes in vegetation structure and composition are tightly coupled with changes in climate and fire activity (Jackson, 1968; Macphail, 1979; Colhoun et al., 1999; Hopf et al., 2000; Fletcher et al., 2007a); and (4) long-term fire activity is modulated by climate (rainfall) (Nicholls et al., 2007; Styger et al., 2015; Mariani et al., 2016a).

In the terrestrial environment of Tasmania, fire frequency and vegetation flammability are the overriding factors governing vegetation and soil type (Jackson, 1968; Bowman et al., 1981; Bowman et al., 1986b; Bowman et al., 2009b; Wood et al., 2012). A positive feedback model proposed by Jackson (1968) (the ecological drift model) depicts a spectrum from rainforest to treeless vegetation (moorland) in which fire frequency and soil development interact to create discrete states. In rainforested states, a positive feedback between low fuel flammability and low fire frequency allows the prolonged accumulation of organic matter (deep soil profiles) that facilitates the further establishment of rainforest trees. Respectively, high fire frequency results in the dominance of flammable and low-nutrient tolerant sclerophyll vegetation that produce nutrient-poor soils resulting in a positive feedback between high fire frequency, sclerophyll vegetation, and low soil nutrient status (Jackson, 1968). These vegetation

feedbacks are corroborated by vegetation stable state research in Tasmania (Wood et al., 2012; Fletcher et al., 2014b; Holz et al., 2015).

Based on our understanding of Jackson's ecological drift model (fire-vegetation soil relationships) and the current understanding of Tasmanian limnology (oligotrophic dystrophic systems atop inert bedrock), I hypothesise vegetation and soil dynamics will be important for aquatic ecosystems. The dystrophic nature of these lakes and the unyielding geology where these lakes are located suggests the terrestrial environment provides organic matter and essential nutrients to aquatic systems. These essential nutrients are provided by the surrounding peats derived from decomposing local vegetation. Therefore, under climatic conditions that favour rainforest vegetation; nutrient rich organic peat soils will dominate the catchment, and thus, deliver essential nutrients into the aquatic system indirectly influencing response. Under this scenario I expect direct climate influences will be less important than indirect influences. However, under moisture-deficient conditions fire frequency will increase and strip soils favouring sclerophyll vegetation, a vegetation group adapted to nutrient poor environments. Under this scenario, I expect indirect climate influences to be less important because aquatic systems will rely more on internal nutrient cycling. Additionally, I anticipate the effects of increased fire frequency will also impact aquatic ecosystems. These hypotheses lead to the following research questions.

1.4 RESEARCH QUESTIONS

- 1. How does long-term climatic change influence aquatic ecosystems in Tasmania: directly, indirectly or both?*
- 2. If a direct pathway is evident, what is the principal mechanism influencing the aquatic ecosystem?*
- 3. If an indirect pathway is evident, what is the principal mechanism through which terrestrial environmental change influences the aquatic environment?*
- 4. How do aquatic ecosystems respond to fire disturbance in western Tasmania?*

If climate is impacting both terrestrial and aquatic environments the timing of environmental change will be important to determine the pathways of influence. The longer life span of terrestrial vegetation compared to aquatic organisms suggests aquatic ecosystems would respond before the terrestrial environment if climate is directly impacting both systems. However, if aquatic ecosystem response to climate is mediated by the terrestrial environment, an aquatic ecosystem response will occur after a change in the terrestrial environment.

Additionally, to understand the climatic influences on aquatic ecosystem response, data with sufficient natural variability is needed to determine ecological response to climate at different magnitudes and scales. Long-term time series datasets provide necessary climate variability to test ecological response. For fast responding systems, monitoring can be done to test responses to environmental change; however, monitoring is frequently inadequate in length to assess important climate transitions (Scheffer et al., 2012; Dakos et al., 2015). With a lack of time series data (i.e. monitoring data) to encompass enough climate variability, palaeoecological methods can be used to retrieve past information. To test my hypotheses, I will use palaeoecological methods and an array of statistical applications to (1) model important changes in the terrestrial and aquatic ecosystems and (2) test the timing of important transitions related to climate using time series analysis. For full details of statistical applications see Section 3.13.

1.5 PALAEOECOLOGY AND RESEARCH DESIGN

Palaeoecology is the study of past ecosystem change using proxy data principally drawn from natural archives that record long-term ecosystem dynamics on a variety of spatial and temporal scales. Proxy data portrays information for environmental variables that accumulate in natural archives (Last et al., 2001). For example, pollen is a proxy for vegetation and charcoal is a proxy for fire. Lake sediments trap a range of proxies that can be used as powerful datasets of long-term environmental change, such as terrestrial and aquatic ecosystem dynamics,

well suited to address the questions of this thesis (Smol, 1992; Reid et al., 1995; Smol et al., 2000; Cohen, 2003; Anderson et al., 2006; Birks et al., 2006; Smol, 2010; Kattiel, 2012; Fritz et al., 2013).

A number of palaeoecological studies display the efficacy of pollen analysis as a tool for testing the response of vegetation systems to climate changes in the Australasian region (Kershaw, 1976; Macphail, 1979; Macphail, 1986; Colhoun et al., 1991b; Shulmeister et al., 1995; Haberle, 2005; Donders et al., 2007; Fletcher et al., 2007b; Vandergoes et al., 2013). Some also include charcoal analysis to understand climate-fire-vegetation dynamics (Kershaw, 1986; Haberle et al., 2006; Denham et al., 2009; Fletcher et al., 2010b; Fletcher et al., 2014a; Stahle et al., 2016). Aquatic ecosystem proxies, such as diatom valves and cladoceran remains, have also been used in the Australasian region to reconstruct aquatic ecosystem responses to climate (Tibby et al., 2007b; Kattiel et al., 2010; Gell et al., 2012), human impact (Taffs et al., 2007; Kattiel et al., 2015), and lake development (Bradbury, 1986; Hodgson et al., 1996; Gell et al., 2005). Though some aquatic records do exist in Tasmania (Bradbury, 1986; Cameron et al., 1993; Hodgson et al., 1996; Hodgson et al., 2000; Saunders et al., 2013a), they are relatively few.

To address my research aims, I present two Holocene multi-proxy lake sediment records from western Tasmania. My study design uses palaeoecological methods to constrain the influences of climate on terrestrial and aquatic ecosystems and the relationship between them through time. High-resolution sampling of sediment sequences enabled me to capture multi-decadal to multi-centennial scale dynamics. Radiometric dating was used to determine the geochronology; charcoal to infer changes in fire history; pollen to determine past climate and vegetation change; organic and inorganic geochemistry to provide understanding of catchment dynamics and nutrient cycling in the terrestrial and aquatic environment; and diatoms and cladoceran remains to understand aquatic ecosystem response.

1.6 THESIS LAYOUT

This thesis contains nine chapters (Figure 1.2). *Chapter 1: Introduction* presents the knowledge gap, hypotheses and research questions, as well as, the research design of this thesis. *Chapter 2: Background* reviews the current literature and understanding of the study region, and potential relationships of the aquatic ecosystem to climate (direct and indirect). *Chapter 3: Methods* outlines the methods used for this research and the justifications for each proposed method. The discussion chapters are broken into two parts for each study site, **Part 1: Paddy's Lake** (*Chapters 4 & 5*) and **Part 2: Lake Vera** (*Chapters 6 & 7*). In **Part 1**, *Chapter 4* presents the modified published work on the Paddy's Lake terrestrial environmental response to climate from the Late-Pleistocene to Holocene. *Chapter 5* is a modified published cladoceran record from Paddy's Lake outlining aquatic ecosystem response to the terrestrial environment and climate. In **Part 2**, *Chapter 6* is a prepared manuscript of a Holocene diatom record from Lake Vera that observes the aquatic ecosystem response and terrestrial environmental changes and climate. *Chapter 7* is a modified published article that reveals a critical transition in a diatom record from Lake Vera caused by fire disturbance. The information presented in each discussion chapter is synthesised to address the specific research questions and caveats of this thesis in *Chapter 8*. A brief summary in *Chapter 9* summarises the main findings of this thesis. Supporting material for publications, unpublished results and additional material is presented in the appendices.

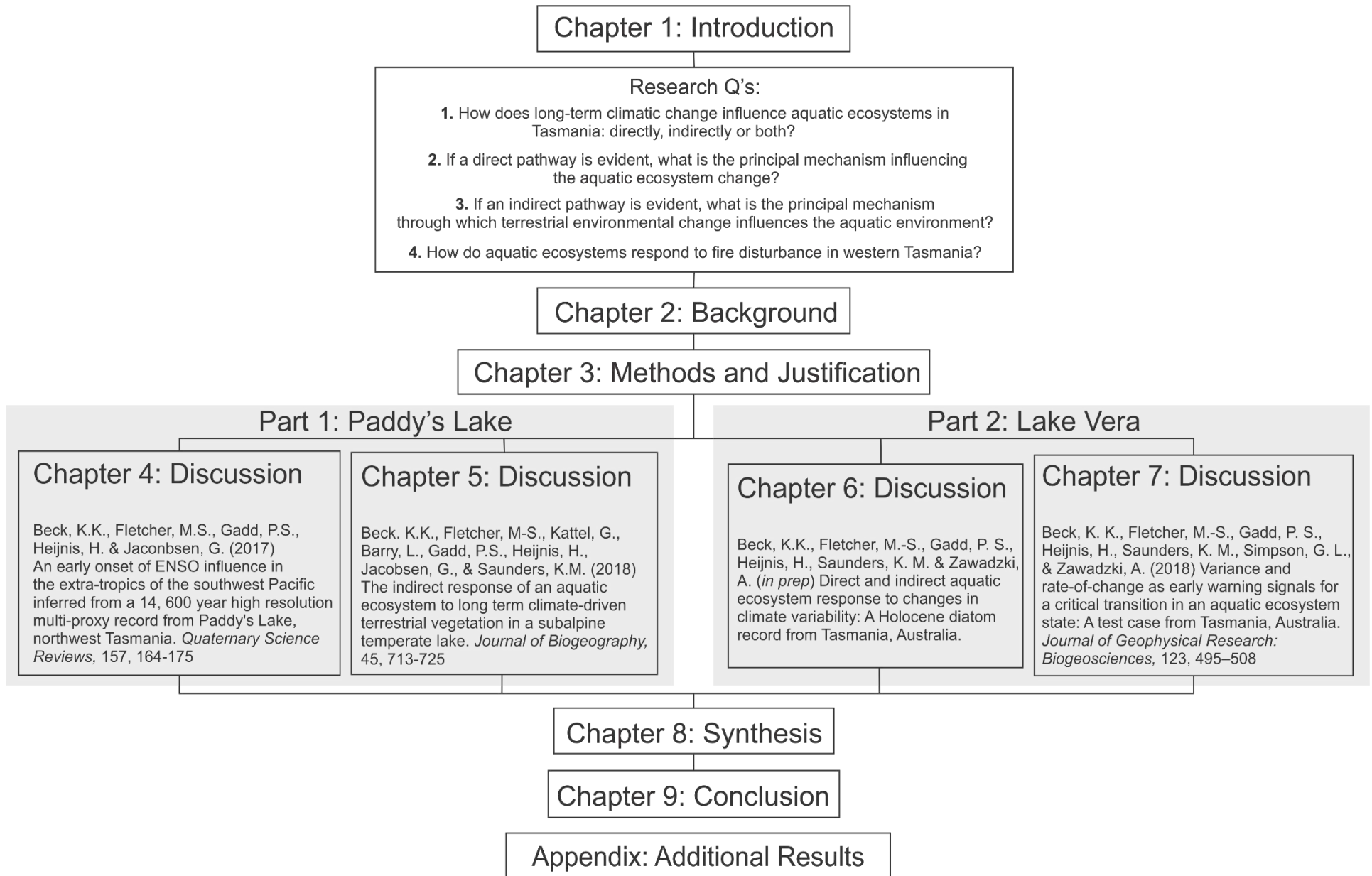


Figure 1.2: Flow chart of thesis layout.

1.7 CHAPTER CLOSING

Aquatic ecosystems are under threat of climate change, yet their long-term response to climate is still poorly understood. Using Tasmania as a case study, this thesis aims to disentangle how aquatic ecosystems respond to climate change, particularly over long timescales (Holocene). I use a multi-proxy environmental reconstruction based on lake sediment archives (palaeoecology) to provide insight into the relationship between terrestrial (pollen and organic and XRF geochemistry), and aquatic ecosystem response (diatoms and cladocerans) e to changes in climate and disturbance (charcoal).

CHAPTER 2: BACKGROUND

2.1 CHAPTER AIM

The aim of this chapter is to provide the context for this project. An overview of the Tasmanian environment will be presented here including climate, vegetation, geology, and limnological characteristics. Additionally, this chapter will provide current understanding of aquatic ecosystems, and their connection to climate through direct and indirect interactions.

2.2 MODERN TASMANIAN CLIMATE

Tasmanian climate is temperate maritime, driven by the absorption and storage of heat from the surrounding ocean causing mild winters and cool summers (Williams, 1974; Jackson, 1999a; Kitchener et al., 2013). It sits between 40-44°S and 144-148°E with an average annual maximum temperature of 15.7°C and minimum temperature of 4.7°C (Figure 2.1) (Bureau of Meteorology, 2017). Tasmanian precipitation is driven by storm tracks embedded in the southern westerly winds (SWW) that dominate the mid- to high latitudes of the Southern Hemisphere. Because Tasmania is bisected by northwest to south running mountain ranges, a rain shadow results in high rainfall in the west and comparatively dry conditions in the east (Macphail, 1979; Tyler, 1992). Western Tasmania receives precipitation >1200 mm annually with some alpine regions receiving >3200 mm. The drier eastern regions receive <750 mm annually, with as little as 400 mm falling in the driest parts (Macphail, 1979; Jackson, 1999a; Kitchener et al., 2013). Snowfall does occur in Tasmania and is widespread across the alpine regions; however, it is never permanent (Jackson, 1999a; Kitchener et al., 2013). Supra-annual trends in rainfall are influenced mainly by two key components of the Southern Hemisphere climate system: the El Niño Southern Oscillation (ENSO) in the north (McBride et al., 1983; Hill et al., 2009) and the Southern Annular Mode (SAM) in the west (Figure 2.2).

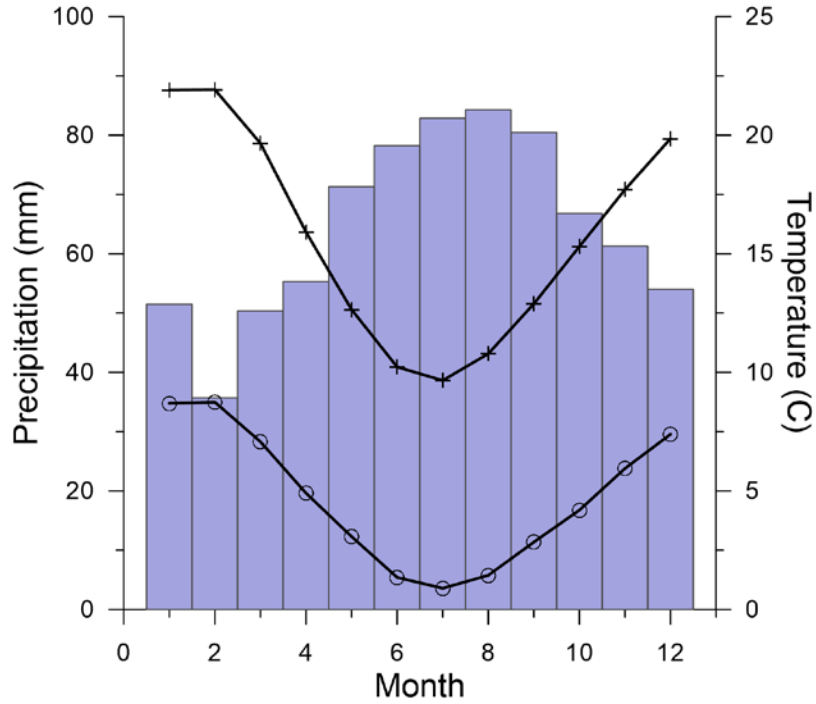


Figure 2.1: Average monthly Tasmanian precipitation (blue bars), maximum monthly temperature (line with cross symbols), and minimum monthly temperature (line with circle symbols). Data was retrieved from Bureau of Meteorology (<http://www.bom.gov.au/>) for every Tasmanian weather station and all recorded years (as early as 1890 CE).

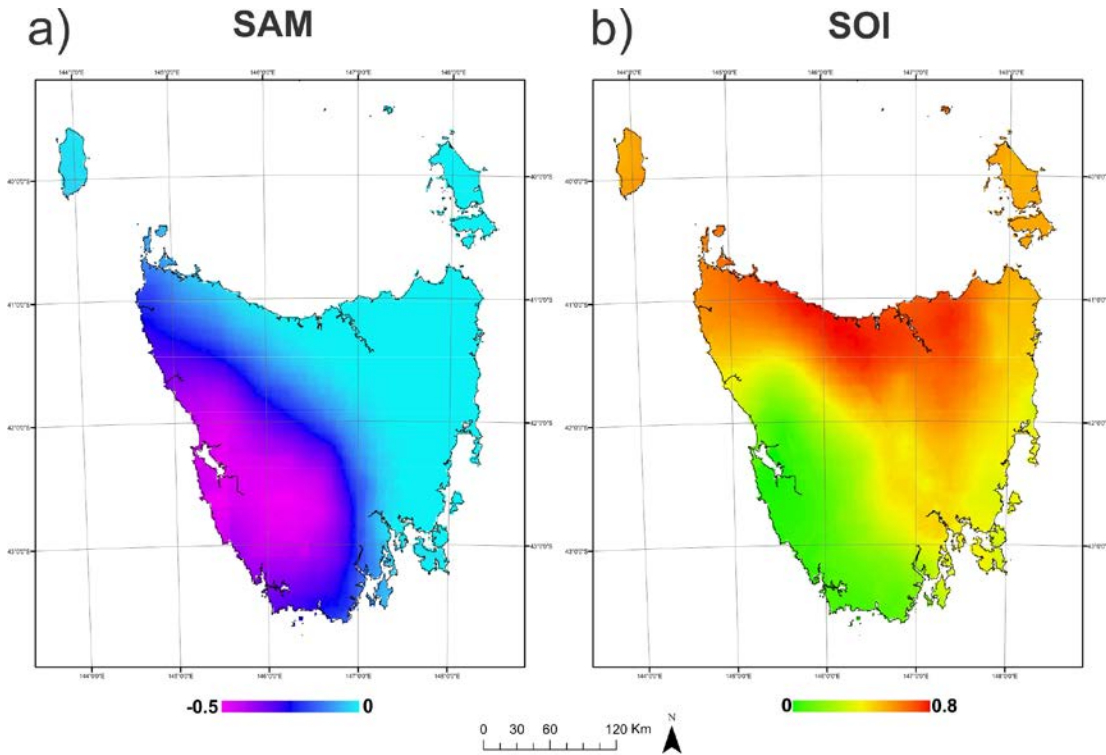


Figure 2.2: Precipitation correlation maps for a) Southern Annular Mode and b) Southern Oscillation Index in Tasmania (Mariani et al., 2016a).

2.2.1 SOUTHERN WESTERLY WINDS (SWW)

SWW are the mid- to high latitude (30-60°) prevailing winds of the Southern Hemisphere. They sit in the Ferrel cell, between the rising air of the Polar cell and the descending air of the Hadley cell (Figure 2.3) (Holden, 2011; Bryant, 2013). Latitudinal shifts (north-south) in the position and intensity of the SWW occur at a range of temporal scales (Lamy et al., 2010; Fletcher et al., 2011; Varma et al., 2011; Fletcher et al., 2012; Voigt et al., 2015) occur at interannual to multi-decadal time-scales are linked to the Southern Annular Mode (SAM) (Abram et al., 2014; Mariani et al., 2016a). Positive atmospheric pressure in the mid-latitudes accompanied by negative atmospheric pressures at high latitudes is defined as a positive SAM phase, and the opposite pressure anomalies are representative of a negative SAM phase (Gillett et al., 2006; Stammerjohn et al., 2008). During a positive SAM phase mid-latitude regions such as Tasmania, southern Australia, New Zealand, Chile, and Argentina experience southward movement of the SWW and decreased air advection over the ocean causing warming and decreased precipitation at latitudes lying above the core of the SWW (between 40-60°S) (Figure 2.2a) (Gillett et al., 2006; Hill et al., 2009).

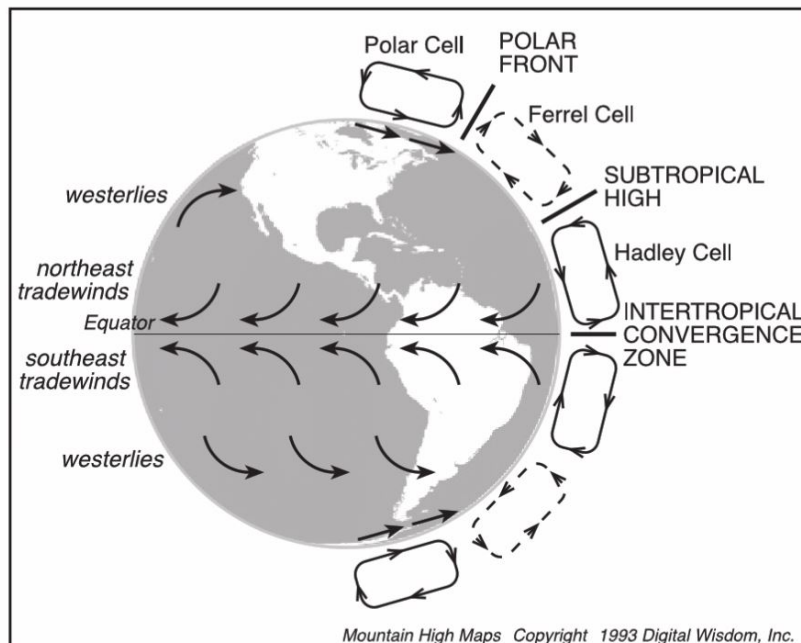


Figure 2.3: Schematic of atmospheric circulation cells and surface winds (Figure 1.2; Holden, 2011).

2.2.2 EL NIÑO SOUTHERN OSCILLATION (ENSO)

ENSO is the interaction between large scale oceanic and atmospheric pressure systems (the Walker Circulation) in the tropical Pacific Ocean that acts on a supra-annual timescale (interannual to decadal) (Philander, 1983; Shulmeister et al., 1995; Chiew et al., 1998; Tudhope et al., 2001; Moy et al., 2002; Turney et al., 2004; Yan et al., 2011). The connection between ENSO and rainfall is determined by the strength of air convection in the trans-Pacific Ocean Walker Cell. During the warm (El Niño) phase of ENSO, southeast Australia experiences decreased rainfall that can result in drought conditions caused by weakened atmospheric convection over Indonesia and Australia due to dissipating trade wind strength toward the west Pacific. The weakened trade winds produce an upwelling of warm waters and increased atmospheric convection in the eastern Pacific Ocean off the coast of South America, and thus increased rainfall in the eastern Pacific (Philander, 1983; Shulmeister et al., 1995; Chiew et al., 1998; Shulmeister, 1999; Conroy et al., 2009; Hill et al., 2009; Yan et al., 2011; Timbal et al., 2013). Hill *et al.* (2009) revealed that years characterised by high frequency of El Niño events are strongly correlated to a significant decrease in rainfall in northern Tasmania and the Southern Oscillation Index (SOI), an ENSO index (Figure 2.2b). With the onset of recent climate change and increasing global temperatures, El Niño events have begun to increase in frequency and strength (Lenton et al., 2008; Power et al., 2013; Cai et al., 2014).

2.3 MODERN TASMANIAN VEGETATION

Variability in climate, altitude, fire, and soil type in Tasmania causes a diversity of vegetation. Climate is the strongest determinant of vegetation type with fire acting as a secondary influence (Kitchener et al., 2013). There are six main vegetation types in Tasmania: rainforest, wet sclerophyll, alpine-subalpine, dry sclerophyll, coastal, and moorland-sedgeland-scrubland, with temperate rainforest and moorland dominating the west (Figure 2.4) (Jackson, 1999b). Below are the six vegetation types described by Jackson.

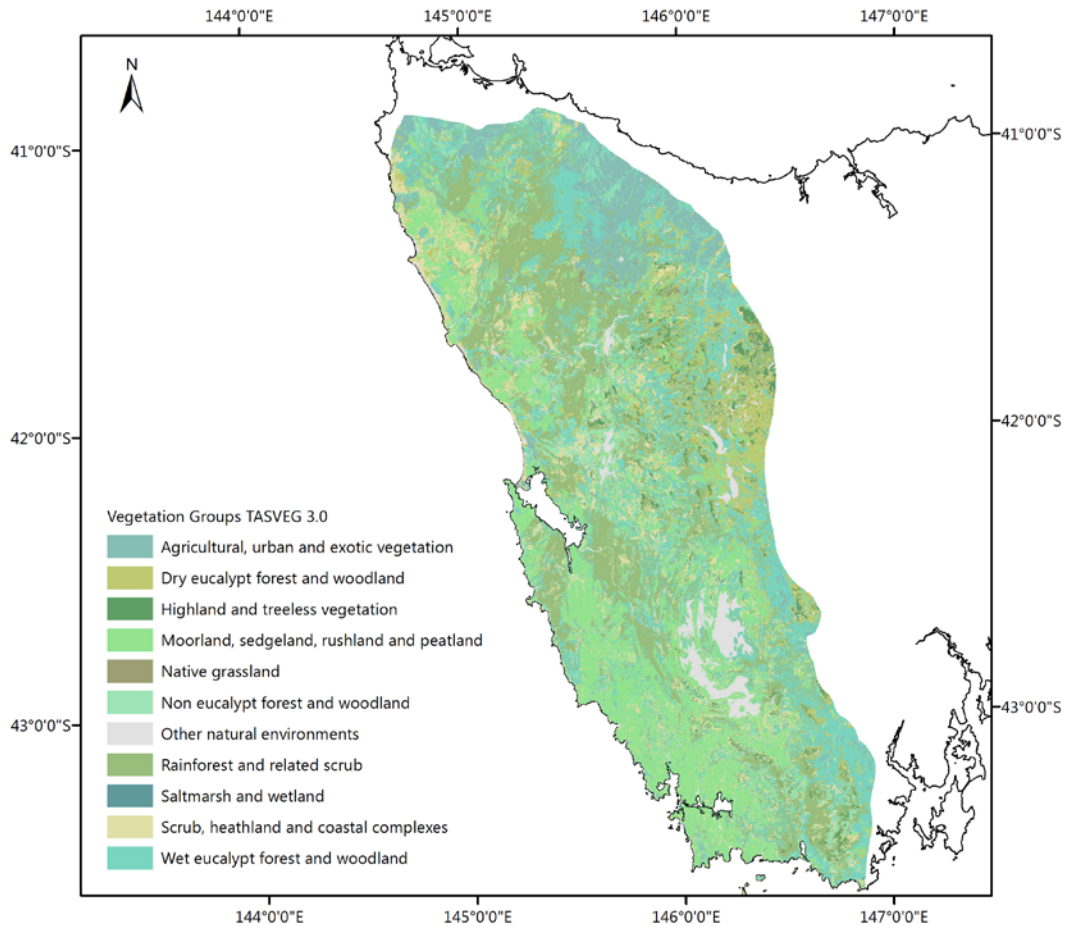


Figure 2.4: Vegetation groups of western Tasmanian provided by TASVEG3.0 (Department of Primary Industries, 2017).

2.3.1 Rainforest

Rainforests occur in the wettest western regions of Tasmania where rain exceeds 1000 mm per year and fire frequency is low (Jackson, 1968; Macphail, 1979; Busby, 1986; Hill et al., 1988). Rainforests can be divided into two subgroups: montane and lowland. Montane rainforests are dominated by *Nothofagus gunnii* and *Athrotaxis cupressoides*, while lowland rainforests consist of *Nothofagus cunninghamii*, *Atherosperma moschatum*, *Eucryphia lucida*, *Phyllocladus aspleniifolius*, *Lagarostrobos franklinii*, and *Anodopetalum biglandulosum*. These lowland forests have acid- and nutrient-poor soils (Read et al., 1985; Kitchener et al., 2013).

2.3.2 Wet sclerophyll

This biome receives 500-700 mm of rainfall per year and slight fire disturbance (Jackson, 1999b). These forest types consist of *Eucalyptus delegatensis*, *E. nitida*, *E. obliqua* and tall shrubs: *Acacia* spp., *Olearia* spp., *Bedfordia salicina*, *Pomaderris apetala*, *Phebalium daviesii*, and mesophyll shrubs (Kitchener et al., 2013).

2.3.3 Alpine-subalpine

Alpine environments occur above 700 m elevation in the southwest and 1,400 m in the central northeast (Kirkpatrick, 1983). Vegetation consists of conifers (*A. cupressoides*), woody plants (*Eucalyptus* spp. and *Nothofagus* spp.), microshrubs (*Diselma archeri* and *Microstrobos niphphilus*), and bolster plants (Epacridaceae, *Donatia novae-zelandiae* and *D. tasmanica*) (Kirkpatrick et al., 1984; Kitchener et al., 2013). Alpine vegetation is tolerant of both wet and dry environments, with precipitation between 790 to 3,600 mm; yet intolerant of fire (Kirkpatrick, 1983). The open landscape and poor coverage from the wind causes devastating fire effects in these regions (Kirkpatrick et al., 1984).

2.3.4 Dry sclerophyll

Dry sclerophyll vegetation occupies 26 percent of Tasmanian central and eastern regions (Jackson, 1999b; Kitchener et al., 2013). This biome contains *Eucalyptus* spp., low trees (*Exocarpus cupressiformis*, *Allocasuarina littoralis*, *Banksia marginata*, and *Bursaria spinosa*), and low shrubs (Asteraceae, Fabaceae, Epacridaceae and Myrtaceae). Transitional taxa from wet to dry sclerophyll consist of *Bedfordia salicina*, *Acacia dealbata*, and *Ziera arborescens* (Williams et al., 1996; Kitchener et al., 2013). These forests can survive high frequency low intensity fires (Jackson, 1968; Brown et al., 1982b).

2.3.5 Coastal

Coastal vegetation is tolerant of wind and salt spray (Kitchener et al., 2013). Spray zone coastal complexes, mainly restricted to King Island, support low-growing halophytic species such as *Disphyma crassifolium*, *Carpobrotus rossii* and *Sarcocornia quinqueflora*, *Leucophyta brownii* and *Alyxia buxifolia*.

Rocky southwest coasts consist of shrubs (*Cyathodes* spp., *Correa*, *Stipa*, and *Plantago*), and diverse heathlands (Epacridaceae, Proteaceae, Fabaceae, Myrtaceae, Orchidaceae, Cyperaceae, Restionaceae, Asteraceae and *Leptospermum* spp.), while the vegetation of the southwest coast is highly disturbed by wind. Coastal scrubs, common in the north, are dominated by *Acacia logifolia* subsp. *sophorae* and *Leptospermum laevigatum* and shrubland taxa (*Allocasuarina verticillata*, *Banksia marginata*, *Beyeria lechenaultii*, *Myoporum insulare*, *Lepidosperma concavum*, and *Leucopogon parviflorus*) (Jackson, 1999b; Kitchener et al., 2013).

2.3.6 Moorland-sedgeland-scrubland

Moorlands are the most dominant vegetation type in cool western Tasmania, below the alpine zone. They occupy a large area of Tasmania which is suitable for rainforest but their overall coverage has been increased due to Aboriginal burning (Fletcher et al., 2010a; Fletcher et al., 2010b; Kitchener et al., 2013). The characteristic species of moorland vegetation is *Gymnoschoenus sphaerocephalus* associated with taxa such as Ericaceae, Restionaceae, Proteaceae and Myrtaceae spp. (Kantvilas et al., 1988; Fletcher et al., 2010a; Kitchener et al., 2013).

2.4 LEGACY OF FIRE IN TASMANIA

After climate, fire is arguably the most important non-climatic factor governing the global distribution of vegetation and occurs at a variety of spatial and temporal scales depending on the environment (Bond et al., 2005; Scott et al., 2014). The important factors that influence fire on multi-decadal scales are ignition source, fuel type, and climate conditions (Figure 2.5). High biomass and ample ignition, caused by the presence of humans for the past 40,000 years, suggests climate is the primary driver of fire occurrence in Tasmania. Fire is also dependent on vegetation type, topography, and soil type (Jackson, 1968; Wood et al., 2011b). North-facing slopes with high exposure to sun and wind are prone to sclerophyll vegetation, low fertility of soils, and increased probability of fire (Wood et al., 2011b).

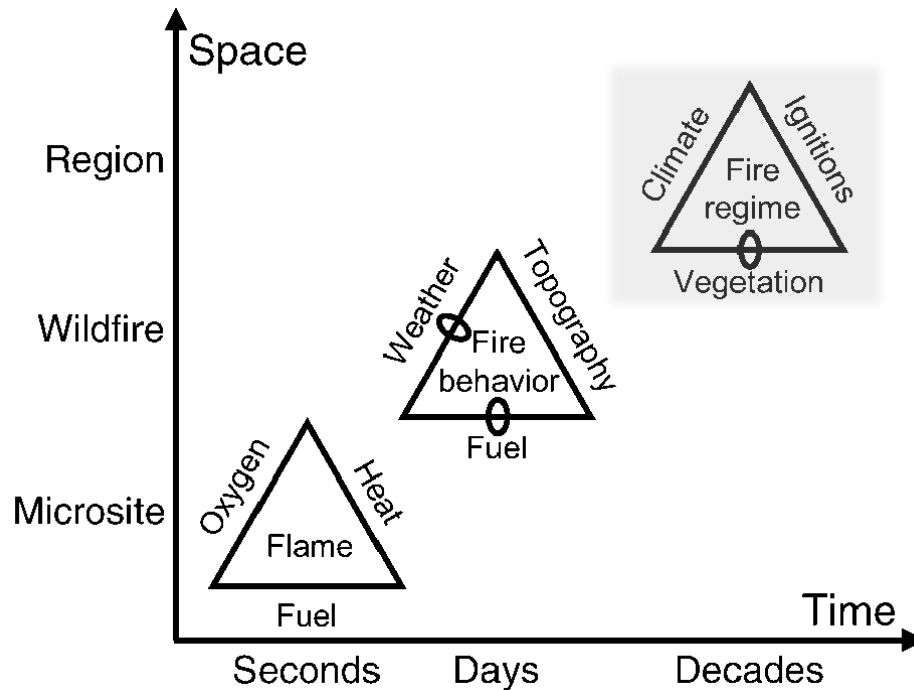


Figure 2.5: Factors influencing fire across space and time. Loops on the triangles indicate potential feedbacks (Figure 1, Parisien et al., 2009). The shaded box indicates the scales relevant to this study.

In Australia, fire occurrence has a strong spatial relationship with influences of ENSO and SAM (Hill et al., 2009; Mariani et al., 2016a; Mariani et al., 2016b). A synthesis of historic fire records and 14 charcoal records from southwest Tasmania reveals that fire activity is tightly coupled to SAM over a historical period of the past 1 kyr (thousands of years) (Mariani et al., 2016a). Across southeast Australia and eastern Tasmania, ENSO shows a correlation with fire occurrence and area burnt in the past <100 years (Mariani et al., 2016b). Aside from climate, an increase in subsequent fires in the European period have decimated rainforest stands across the entire western high rainfall zone of Tasmania (Bowman, 1998) resulting in a decline in vegetation coverage and change in the structure of endemic vegetation; as well as, habitat loss and animal extinctions (Bowman, 1998).

2.5 HOLOCENE CLIMATE AND VEGETATION HISTORY

In western Tasmania, Holocene climate change is often described as a shift from dominant multi-millennial climate variability driven by the SWW (from early to mid-Holocene) followed by an amplification of multi-

decadal ENSO (mid- to late Holocene) climate variability (Fletcher et al., 2015; Rees et al., 2015). Though other climate influences are present during the Holocene in Tasmania, this climatic framework will support the findings in this thesis.

2.5.1 HOLOCENE CLIMATE

The onset of the Holocene marks a rapid increase in temperature and greenhouse gases, with upwards of a 7°C increase in temperature at the termination of the Late Glacial (Dansgaard et al., 1989; Chappellaz et al., 1993; Pedro et al., 2016). In western Tasmania, Antarctic warming and peak SST occurred during the early Holocene (ca. 12 to 9 ka) contributing to a southward shift in the core belt of the SWW delivering less moisture to the 41-42°S latitudes (Reeves et al., 2013; Fletcher et al., 2015; Rees et al., 2015). From ca. 9 to 5 ka, the SWW moved north with strong flow at 41-42°S latitudes resulting in increased precipitation (Moreno et al., 2003; Moreno, 2004; Fletcher et al., 2012; Fletcher et al., 2015). A speleothem record from Lynd's Cave in northern Tasmania suggests the mid-Holocene period (ca. 9 to 5 ka) had a variable climate of wet and dry conditions (Xia et al., 2001), a transitional period between SWW and ENSO dominant climate systems (Rees et al., 2015). Other evidence suggests the opposite position and strength of the SWW during the early and mid-Holocene, but agrees that the SWW strength was weakened into the late Holocene with the onset of ENSO (Moros et al., 2009).

After ca. 6 ka, El Niño events increased in strength and frequency causing drying in south east Australia (Markgraf et al., 2000; Moy et al., 2002; Moros et al., 2009). Changes in the frequency and amplitude of the ENSO system is believed to be the result of orbital forcing, leading to a change in the tropical Pacific SST gradient. This gradient is weaker during periods when El Niño events are more frequent (Shulmeister et al., 1995; Tudhope et al., 2001; Conroy et al., 2008; Yan et al., 2011). In the most recent ca. 3 ka, climate variability has become more extreme due to increase frequency and amplitude of El Niño and positive SAM causing extremely dry phases state wide with increased fire frequency and the invasion of sclerophyll vegetation (Abram et al., 2014;

Mariani et al., 2016a; Fletcher et al., 2018a). In the 20th and 21st century, anthropogenic climate change has led to rapid warming in Tasmania (Cook et al., 1991; Johnson et al., 2011).

2.5.2 VEGETATION HISTORY OF TASMANIA

The onset of the Holocene in Tasmania was marked by a warming and wet climate resulting in the development of moorland and cool temperate rainforest (van de Geer et al., 1989; van de Geer et al., 1994; Colhoun et al., 1999; Fletcher et al., 2010b; Rees et al., 2010a). Post-glacial vegetation change was influenced by human use of fire which has remained fairly stable throughout the Holocene until the arrival of Europeans (Fletcher et al., 2010a; Fletcher et al., 2010b, c; Wood et al., 2012; Stahle et al., 2016; Stahle et al., 2017). The rainforest vegetation expanded into areas where it was protected from fire (low-lying topography and south-facing slopes) (Wood et al., 2011b), extending across western Tasmania including large areas around Frenchman's Cap (Macphail, 1979). Here, I have grouped the main trends in vegetation in response to the climatic paradigm used in this thesis (SWW to ENSO dominant system).

2.5.2.1 Early Holocene - 11.7 to 9 ka

The transition to Holocene vegetation in Tasmania following the glacial maximum was preceded by an expansion in *Phyllocladus aspleniifolius*, which is indicated by increases in the relative abundance of *P. aspleniifolius* pollen in sediment records across the island (Macphail, 1979; Van de Geer et al., 1991; Stahle et al., 2016). With warming and dry conditions, communities of moorland and heath were favoured (Hopf et al., 2000; Stahle et al., 2016; Mariani et al., 2017a; Stahle et al., 2017); however, rainforest still continued to expand throughout the early Holocene (Hopf et al., 2000; Stahle et al., 2016; Mariani et al., 2017a; Stahle et al., 2017).

2.5.2.2 Mid-Holocene - 9 to 6 ka

Increased strength of SWW during the mid-Holocene caused warm and wet conditions resulting in the highest abundance of temperate rainforest taxa (i.e. *Nothofagus cunninghamii*) (Macphail, 1979; Harle et al., 1999; Hopf et al., 2000; Stahle et al., 2017). In coastal regions, increased moisture and a higher sea level led to inundated coastal wetlands and increased abundance of water-logged taxa (Cyperaceae and Restionaceae) (Fletcher et al., 2010a).

2.5.2.3 Mid to Late Holocene - 6 ka to present

Increased frequency of El Niño events caused increased dry conditions and fire frequency (Moy et al., 2002; Turney et al., 2004), resulting in the increased abundance of sclerophyll vegetation and the loss of rainforest (Macphail, 1979; Harle et al., 1999; Hopf et al., 2000; Fletcher et al., 2014a; Stahle et al., 2016; Stahle et al., 2017). With European arrival (ca. 1850's CE) vegetation structure was altered with the introduction of exotic vegetation (i.e. *Pinus*) and increased fire activity (Bowman, 1998; Romanin et al., 2016; Mariani et al., 2017b).

It is important to note that these vegetation mainly patterns reflect changes in climate drivers. The distribution and extent of the moorland vegetation community over this period reflects human management (Fletcher et al., 2010b), and the extent of this vegetation community is underestimated due to the poor dispersal of the key pollen taxa *Gymnoschoenus sphaerocephalus* (Mariani et al., 2017a).

2.6 TASMANIAN GEOLOGY

Tasmania's folded and faulted landscape, underlying bedrock, topography, and soil types are all important to vegetation composition and aquatic ecosystem characteristics. The geological basement of metamorphic rock is siliceous in nature and thus very resistant to weathering (Buckney et al., 1973; Jackson, 1999b). Bedrock in the west is comprised of Precambrian metamorphic Cambrian sediments with volcanic and Quaternary sediments, and Jurassic dolerite and Carboniferous-Triassic sediments in the east (Figure 2.6) (di Folco, 2007). Soil

formation across Tasmania is slow and, nutrient leeching from bedrock is poor (Jackson, 1968; Buckney et al., 1973; Kitchener et al., 2013).

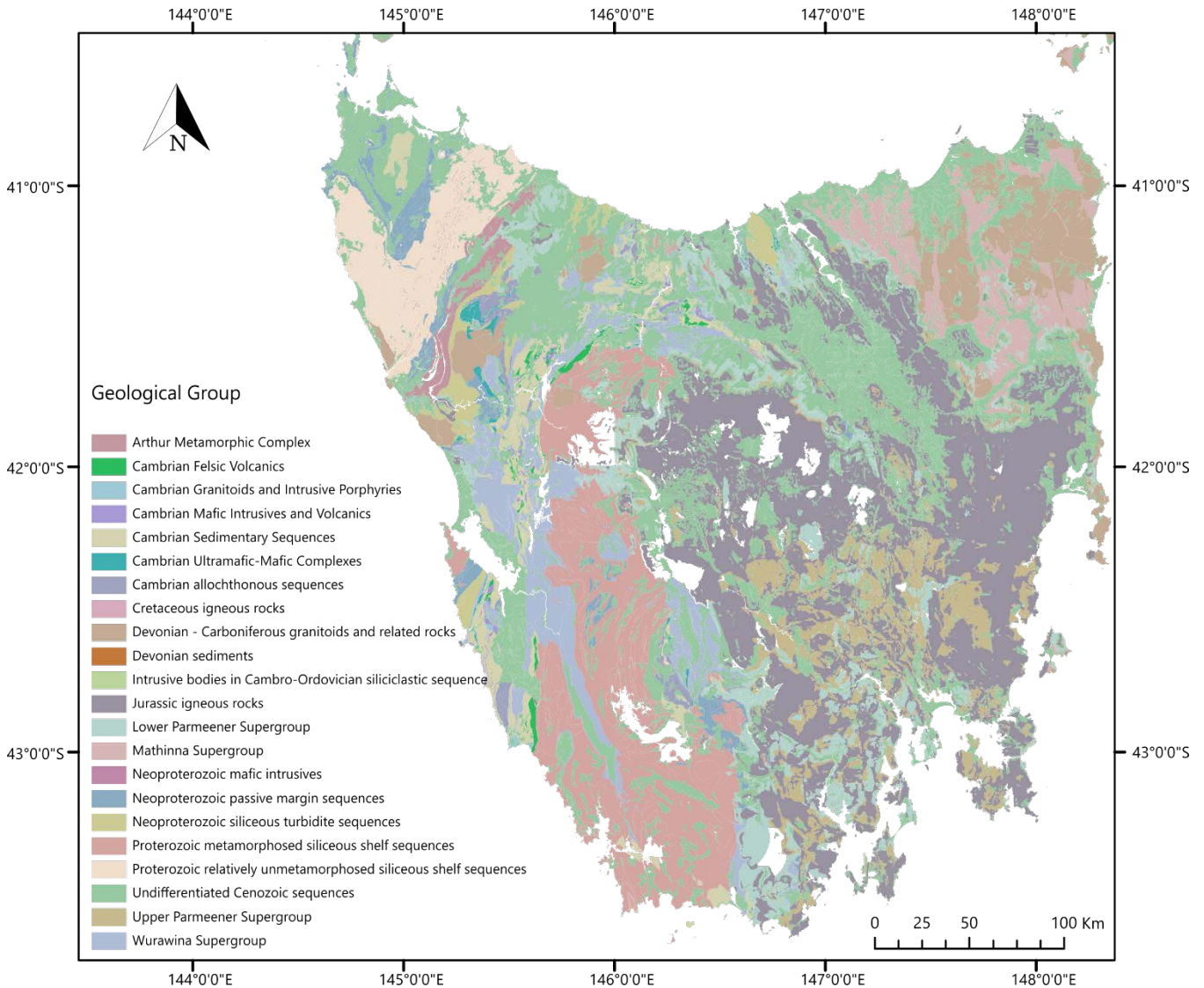


Figure 2.6 Map of Tasmanian geological groups.

2.7 TASMANIAN SOILS

Western Tasmanian soils are predominantly organic peats (organosols), defined by their organic carbon and nitrogen content, depth and degree of humification (Isbell, 2002; di Folco, 2007). These organic soils form from

plant and animal decomposition (Lal, 1993), while soil structure and accumulation rate is determined by climate, topography, biota, geology, topography, fire, and time (di Folco, 2007).

In western Tasmania, organic peat soils are associated with humid, high rainfall and low evaporative environments (Stace, 1968; Pemberton, 1989). Organosols occur on the nutrient-poor inert quartzite substrate in the west. Mineral rich peats occur on the softer substrates, such as the limestones and sandstones, toward central and eastern Tasmania (Pemberton, 1989; Kirkpatrick et al., 1998; di Folco, 2007). Soil development is directly related to time. When undisturbed by fire or erosion, Tasmanian organic soils will date back to the last glaciation (Pemberton, 1988; Macphail et al., 1999). Accumulation of soils is directly related to temperature and plant production, for instance, as altitude increases soil accumulation decreases (Bridle et al., 1997). Additionally, humidity is a determiner of soil accumulation, where low-lying topography with poor drainage and shallow slopes have high soil accumulation rate (di Folco, 2007).

Vegetation is also an important determinant for organic soil development in Tasmania (di Folco, 2007) with humified organosols present under herbaceous vegetation in alpine regions and neutral to alkaline fibrous peats are formed under *Eucalyptus* forests (Stace, 1968). Forested regions accumulate more organic nutrient-rich soils compared to non-forested regions where burning results in nutrient-poor soils (Jackson, 1968; Wood et al., 2012). Burning destroys peats and alters organic matter accumulation and nutrient stocks (Bowman et al., 1981; Bridle et al., 2003; González-Pérez et al., 2004; di Folco, 2007; Orians et al., 2007). Charcoal in soils also reduces water tables and soil permeability affecting organic matter decomposition (di Folco, 2007).

2.8 LIMNOLOGY OF TASMANIA

Tasmania has over 4,000 inland lakes (Figure 2.7), many formed by part glaciation (Tyler, 1974, 1992). These lakes are largely unexplored and thus the majority of lake physiology is assumed (Tyler, 1974).

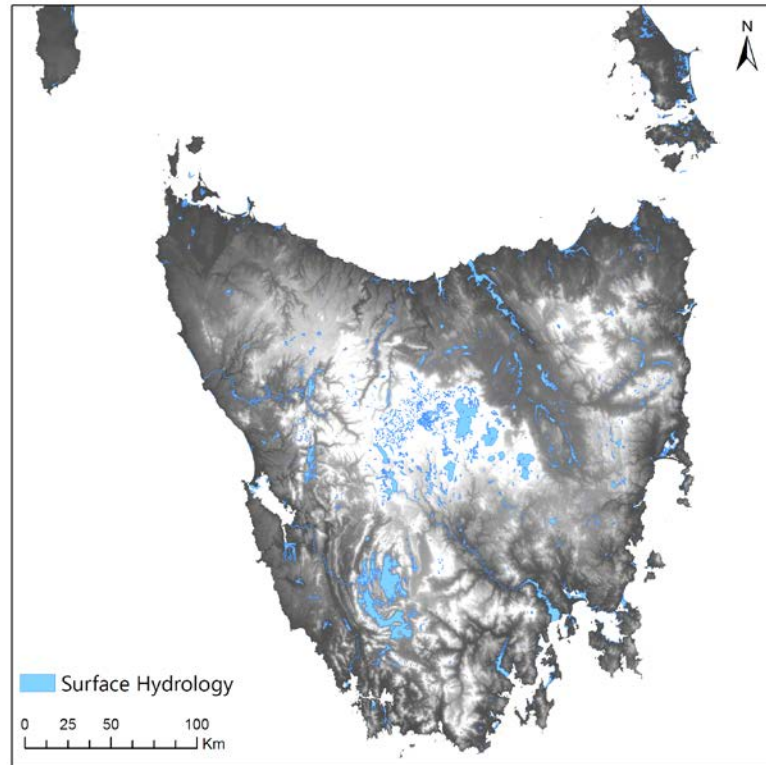


Figure 2.7: Map of surface hydrology in Tasmania.

2.8.1 LIMNOLOGICAL CHARACTERISTICS

Tasmanian lakes range in size from 150 km² to greater than a hectare with the majority located within 650-1,100 masl on the Central Plateau. Water temperature of Tasmanian lakes varies by altitude, lake morphology and stratification. Lake temperatures range from ~0-25°C and frozen lakes are uncommon (Tyler, 1974). Most of the lakes are unstratified and homothermic. Exploration of Lake Picton and Lake Riveaux in southwest Tasmania shows evidence of stratification, thus it is likely that some mountainous lakes stratify in summer months (Tyler, 1974). A range of mixing regimes exist in Tasmania from monomictic, polymictic, meromictic, and dimictic (for lakes that freeze) (Tyler, 1992). Many Tasmanian lakes are fishless (Tyler, 1974).

Lakes range from freshwater to hypersaline with geology and climate as predominant factors that influence lake chemistry. Bedrock has a minor influence on water chemistry, where chemical makeup is mostly derived from

external inputs such as sea spray and precipitation (Tyler, 1972; Buckney et al., 1973). In the southwest, most minerals and nutrients are delivered by precipitation via the humic acids from surrounding peat. On the Central Plateau, Tasmanian waters are the clearest with 70% of dissolved material derived from terrestrial inputs. Saline lakes (>300 ppm) of Tasmania are all located in the east where conditions are dry and evaporation is higher than precipitation (Tyler, 1974, 1992). The trophic status of these lakes ranges from ultra-oligotrophic to eutrophic. Eastern lakes are shallow and turbulent due to the frequency of winds and lie outside of the glacial margins (Tyler, 1992), while western lakes are not well described. The clear division in the ecology of these lakes from east to west is a product of Tyler's Line, discussed in the next section.

2.8.2 TYLER'S LINE

Peter Tyler (1992) recognised an ecological bisection of Tasmania running from northwest to southeast along the central ranges. This is now termed 'Tyler's Line' (Figure 2.8). It marks a clear division in the Tasmanian landscape in climate, geology, vegetation, and soils. Tyler (1992) describes the west as wet, heavily rainforested, and dominated by poor mineral organic peats atop Precambrian siliceous bedrock. The east of Tasmania is flat with open *Eucalyptus* forests and enriched mineral soils (Tyler, 1992). Lake salinity transitions from very pure in the montane regions to hypersaline (7x sea water) in the midlands of Tasmania (Tyler, 1992). The eastern lakes have a higher euphotic (light penetration) zone of 10 m and are more alkaline with light absorption in blue-green wavelengths. Western lakes have a euphotic zone of 2 m and are acidic with light absorption in red coloured wavelengths due to humic matter (Tyler, 1992). Though bisection is apparent, the transition is not sharp and has an intermediate limnology zone or 'corridor' (Tyler, 1992). This limnological division of east-west regions and the transitional corridor dictate aquatic species composition (Tyler, 1972; Croome et al., 1973; Tyler, 1974; Croome, 1986; Shiel et al., 1989; Tyler, 1992; Vyverman et al., 1995; Vyverman et al., 1996; Walsh et al., 2001; Walsh et al., 2004; Rees et al., 2010b).

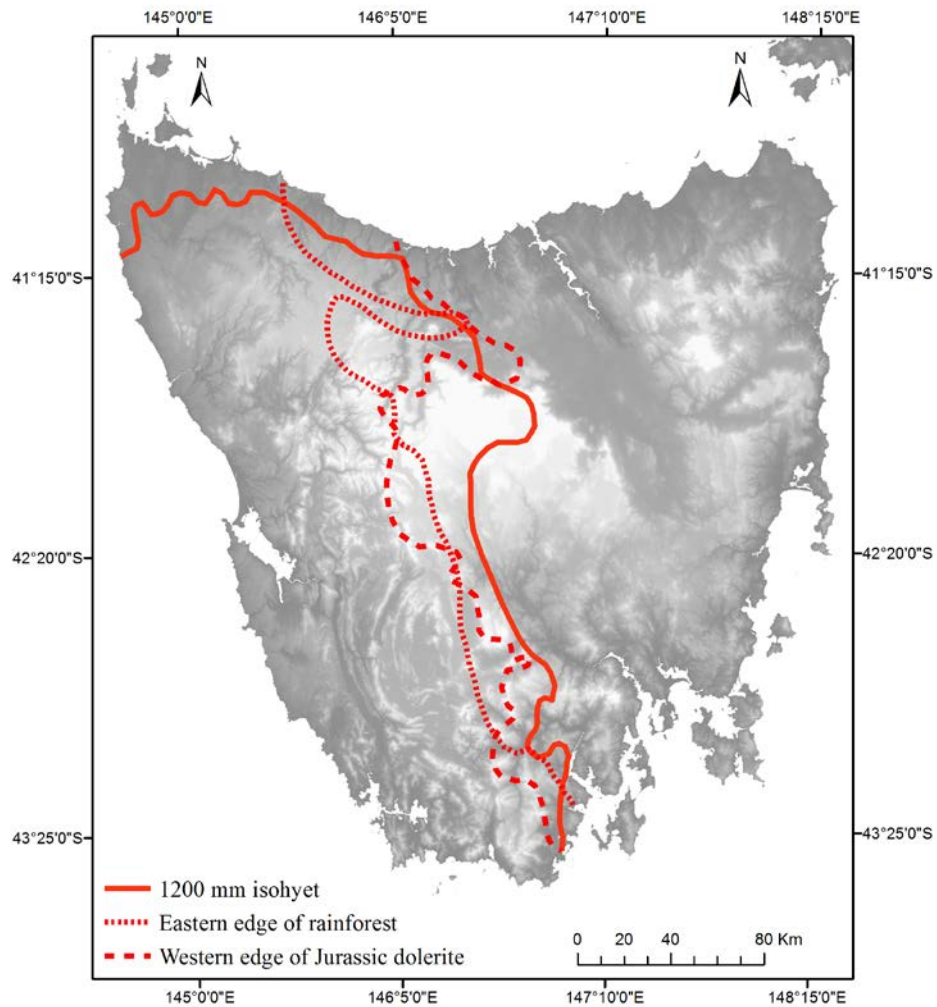


Figure 2.8: Map of Tyler's Line (map revised from Tyler, 1992; Rees et al., 2010b).

2.8.3 AQUATIC ECOLOGY

There are many organisms found in lake ecosystems (e.g. algae, fish, zooplankton, aquatic plants, biting midges) and many of these (or parts of these) organisms are preserved in lake sediments. For this project, I will be investigating diatoms and cladocerans. This section will focus on these organisms.

2.8.3.1 Tasmanian Aquatic Biota

The freshwater biota of Tasmania is widely unknown. Species distribution is dictated by chemical and physical properties characterised by Tyler's Line and is more similar to New Zealand than mainland Australia (Tyler, 1974, 1992). Most of the ecological work on zooplankton of Tasmania focuses on cataloguing taxonomy, yet it is still incomplete (Green, 1976; Smirnov et al., 1983; Koste et al., 1986; Shiel et al., 1986; Koste et al., 1987a; Koste et al., 1987b; Geddes, 1988; Koste et al., 1989a, b; Shiel et al., 1989; Frey, 1991a; Green et al., 1992; Shiel et al., 1995; Shiel, 1995; Walsh et al., 2001; Walsh et al., 2004). Similarly, diatom taxonomy is also lacking (Vyverman et al., 1995; Sabbe et al., 2001; Kilroy et al., 2003; Kociolek et al., 2004; Vanhoutte et al., 2004). Diatom species assemblages in Tasmania are strongly influenced by Tyler's Line and respond firstly to pH, as well as, calcium and sodium with strong correlations to changes in alkalinity, gilvin (an indicator of stain or colour), and chloride (Vyverman et al., 1995; Vyverman et al., 1996).

2.8.3.2 Hemisphere Ubiquity

It is understood that the biogeography of the earth produces regions of species endemism, particularly when comparing Northern and Southern Hemispheres. Australia has a high degree of species endemism (Chapman, 2009); however, algal communities are surprisingly cosmopolitan and comparable to the Northern Hemisphere (Tyler, 1996). Concerns have risen that Southern Hemisphere aquatic taxonomy has been forced to follow European taxonomy due to a lack of identification material (Shiel et al., 1995; Tyler, 1996). It is difficult to prove a species' endemism, and it becomes increasingly challenging with increased habitat fragmentation, removal, and a lack of historical data (Shiel et al., 1995; Walsh et al., 2001). However, more recent work determines local environmental factors alone are not predictors for biogeographical patterns and community diversity in aquatic ecosystems. More likely diversity is dependent on large scale processes, such as evolution, dispersal, and community heterogeneity (Vyverman et al., 2007; Verleyen et al., 2009). Ubiquity of aquatic biota is difficult to

quantify and still debated subject matter. However, there appears to be a degree of cosmopolitan and endemic species in Australia (Walsh et al., 2001).

2.9 TERRESTRIAL-AQUATIC ECOSYSTEM INTERACTIONS

Direct and indirect influences of climate can impact aquatic ecosystems through multiple pathways. For example, climate can directly influence thermal stratification of a lake, as well as, indirectly via vegetation and catchment processes that alter lake chemistry and trophic status (Wang et al., 2016). This section will review how terrestrial and aquatic ecosystems are directly and indirectly impacted by climate using examples from the literature with a focus on the Australian region.

2.9.1 DIRECT DRIVERS OF CATCHMENT DYNAMICS AND VEGETATION CHANGE

For the purposes of this thesis I will focus on climate and fire-related drivers of vegetation and catchment dynamics.

2.9.1.1 Climate

Climate and catchment dynamics (e.g. the effects of temperature on soils) are complicated and poorly understood (Woods, 2003; Orians et al., 2007; Köhler et al., 2009). A rise in soil temperature can increase soil decomposition resulting in exchange of atmospheric carbon. Carbon cycling is complex and different substrates, such as peatland, permafrost, or upland mineral soils, have different responses to climate and impacts on the carbon budget (Davidson et al., 2006). Change in soil temperature can cause root resistance, altered decomposition, changes in microbial respiration, nitrogen mineralisation and atmospheric CO₂ release, which can all impact vegetation composition and ecosystem function (Bunnell et al., 1977; Running et al., 1980; Kirschbaum, 1995; Zak et al., 1999; Ball et al., 2010).

Climate can alter moisture availability and temperature regimes influencing vegetation extent and composition (Liu, 1990; McAndrews et al., 1993; Shulmeister et al., 1995; St. Jacques et al., 2000; Moreno, 2004; Hill et al., 2009; Moos et al., 2011; Fletcher et al., 2014a). In the Southern Hemisphere, climatic influences of ENSO alter moisture variability and fire regimes resulting in dry tolerant vegetation taxa with amplification of El Niño activity (Moreno, 2004; Moy et al., 2009; Fletcher et al., 2014a; Fletcher et al., 2015; Rees et al., 2015).

2.9.1.2 Fire Dynamics

Fire impacts vegetation and catchment dynamics by destruction of biomass, change in vegetation composition, and altered soil structure, nutrient status and hydrological pathways (Raison, 1979; Kirkpatrick et al., 1984; Kutiel et al., 1993; Benda et al., 1998; González-Pérez et al., 2004; Fletcher et al., 2014a). Living root systems are important for binding soils and the death of plants can leave soils vulnerable to increased erosion and mass wasting (Kutiel et al., 1993; Benda et al., 1998). Further, heavy rains following fire events can strip soil profiles (Bowman et al., 1981; Pemberton, 1988, 1989; di Folco et al., 2011). Fires can also directly alter soil chemistry by decreasing the organic content (lowering humic acids content), and thickness of the humus layer, thus, increasing exchangeable cations and soil pH (Raison, 1979; Korhola et al., 1996; González-Pérez et al., 2004; Certini, 2005; Leys et al., 2016). Importantly, fire can result in the removal and addition of organic matter through the deposition of ash (Raison, 1979; Certini, 2005) and change the available nutrients within soils for export (Kirkpatrick et al., 1984; González-Pérez et al., 2004; Orians et al., 2007; Leys et al., 2016). Local high severity fires have shown a pulse of nutrients, such as N and P, into the sediment record (Morris et al., 2015). However, long term trends show declines in C, P, and N concentrations and increases in stable N isotopes, Ti, Ca, K, and Al caused by the removal of terrestrial biomass and erosion (Durán et al., 2008; Dunnette et al., 2014; Leys et al., 2016). Low post-fire recovery of C and N suggests low terrestrial N availability (Dunnette et al., 2014). Thus, soil nutrient dynamics and vegetation change following burning are complex and not well

understood (Raison, 1979; Kirkpatrick et al., 1984; Kutiel et al., 1993; González-Pérez et al., 2004; Lane et al., 2008).

Vegetation type and fire frequency can also dictate the nutrient availability within a soil profile. This is the particular case in Tasmania. The Jackson (1968) “ecological drift” model suggests low fire frequency perpetuates more productive vegetation types, such as rainforest. These vegetation groups maintaining wet environments and produce more organic and fertile peat soils due to their fuel type (Beadle, 1966; Beadle, 1968). Increased frequency of fires results in sclerophyll dominant vegetation types. These vegetation types are adapted to low nutrient environments and produce lower nutrient litter (Beadle, 1966; Beadle, 1968; Bowman et al., 1986b; Oriens et al., 2007; Wood et al., 2012). This is confirmed by a gradient from high to low P, Fe, and C found within the soil profiles from rainforest, *Eucalyptus* forests, and moorland vegetation types (Bowman et al., 1986b; Wood et al., 2011a). If fire frequency remains unchanged, these relationships produce a positive feedback perpetuating the same vegetation and soil type (Jackson, 1968; Wood et al., 2012). Drainage and topography can also have an effect on nutrient availability and soil profiles (di Folco, 2007; Wood et al., 2011a).

2.9.2 DIRECT DRIVERS OF AQUATIC ECOSYSTEM CHANGE

Some examples of abiotic climate factors that directly influence aquatic ecosystems are temperature (Battarbee, 2000; Brooks et al., 2000; Smol et al., 2000; Schindler, 2001), salinity (De Deckker, 1982; Fritz et al., 1993; Gasse et al., 1997; Saunders et al., 2007; Tibby et al., 2007a; Gell et al., 2012), lake level (Alhonen, 1970; Hofmann, 1998; Korhola et al., 2000), and thermal stratification (Fee et al., 1996; Schindler et al., 1996; Sommaruga-Wögrath et al., 1997).

2.9.2.1 Evidence from Past Climate Change

The direct relationship between climate and aquatic ecosystems can manifest through changes in temperature and the precipitation/evaporation balance altering the aquatic biota and ecosystem (Lotter et al., 1997; Schindler, 1997; Brooks et al., 2000; Smol et al., 2000). For example, diatom assemblages from coastal lagoons of Tasmania (Saunders, 2011) and north-west Victorian wetlands (Tibby et al., 2007a) show the direct influences of climate through altered lake salinity and lake volume. In many circumstances smaller lakes experience direct drivers of climate, due to greater impacts on water balance with low lake volume (De Deckker, 1982; Michelutti et al., 2003; Smol et al., 2007; Dangles et al., 2017); although, large lakes also experience the direct effects of climate (Gasse, 2000; Michelutti et al., 2015; Reavie et al., 2017; Giles et al., 2018).

Typically, the ratio between planktonic (pelagic) and benthic (or littoral) aquatic taxa are used as indicators of lake level changes, where high ratios indicate more available planktonic to benthic habitat of fuller lakes (Alhonen, 1970; Hofmann, 1998; Fritz et al., 1999; Jeppesen et al., 2001). For example, a diatom reconstruction from Walala Lake on Vanderlin Island in the Gulf of Carpentaria in the Northern Territory shows shifts in the dominance between planktonic and benthic diatoms. These shifts are interpreted as indicating changes in lake depth arising from changes in effective precipitation (Prebble et al., 2005). In the wet tropics of northern Queensland, a Holocene diatom record from Lake Euramoo strongly tracks climate through changes in effective precipitation and the effects on lake level (Tibby et al., 2007b).

The direct effects of climate are also shown in Lake Purrumbete in Koallah, Victoria (Tibby et al., 2012).

Turbulent tolerant diatom taxa dominate during periods of high regional effective moisture and strong wind-driven mixing (Jones et al., 1998; Tibby et al., 2012). Similarly, temperate regions of New Zealand show the direct effects of climate on cladocerans and diatoms communities. Low lake levels were interpreted during the Last Glacial Cold Period with high abundance of littoral cladocerans and diatoms, followed by a shift to higher

moisture conditions and a warming climate. This was inferred as higher lake levels from abundant planktonic cladoceran and diatom taxa (Kattel et al., 2010; Augustinus et al., 2012).

2.9.3 INDIRECT DRIVERS OF AQUATIC ECOSYSTEM CHANGE

Climate can indirectly drive aquatic ecosystem change through changes in vegetation and catchment dynamics (Ball et al., 2010). Shifts in vegetation can alter hydrology (Huxman et al., 2005), organic matter inputs (St. Jacques et al., 2000; Whitcraft et al., 2008), and nutrient dynamics (Bernhardt et al., 2005; Cairns et al., 2005; Perren et al., 2017). For example, increased woody material and decreased ground water delivery can decrease carbon inputs; as well as, increase nitrogen into aquatic ecosystems with more nutrient litter from surrounding vegetation (Ball et al., 2010; Morris et al., 2015). This section will outline the potential indirect climate impacts on aquatic ecosystems through vegetation, catchment, and fire dynamics.

2.9.3.1 Evidence from Past Climate-driven Vegetation Change and Catchment Dynamics

Aquatic ecosystems may respond to catchment dynamics (i.e. bedrock weathering, nutrient leaching/delivery, sediment loading and soil development) often driven by climate mediated by vegetation change. These processes can elicit a change in soil acidity, organic soil content, and soil nutrient structure- termed lake ontogeny (Crocker et al., 1955; Jacobson et al., 1980; Whiteside, 1983; Whitehead et al., 1989; Engstrom et al., 2000; Fritz et al., 2013). Lake ontogeny is the succession or historical development of the lake environment. The development of soil biochemistry induced by vegetation change can cause a progression of leached base cations from local soils resulting in natural lake acidification, as well as, an increase in nutrient inputs that lead to natural eutrophication of a lake (Whiteside, 1983; Whitehead et al., 1989; Engstrom et al., 2000; Fritz et al., 2013). More specifically, vegetation succession can increase organic carbon within catchment soils (Crocker et al., 1955; Korsman et al., 1998; St. Jacques et al., 2000; Ball et al., 2010; Fritz et al., 2013), which can lower soil base saturation (Tamm,

1991), resulting in poorly buffered water runoff, intensifying the trend toward acidification and eutrophication of aquatic ecosystems (Liu, 1990; Korsman et al., 1998; Engstrom et al., 2000; St. Jacques et al., 2000).

A record from Lake Makkassjon, Sweden shows an example of lake ontogeny with demonstrates the natural acidification caused by soil formation and vegetation change. The acidification period is driven by organic soil development causing increased leaching of humic acids by a subsequent shift from deciduous to coniferous dominant forest, lowering the base saturation of the soils (Tamm, 1991). This transition results in poorly buffered catchment runoff and, thus a decrease in diatom inferred pH. In another example, shifts in the position of the Arctic front have driven oscillations between tundra and forest vegetation in North America that alter the pH of runoff into lake systems, driving clear diatom compositional change (MacDonald et al., 1993).

Lake ontogeny can also be expressed in the palaeoecological records as change in nutrient status induced by vegetation change. Engstrom et al. (2000) highlight the processes and mechanisms involved in lake ontogeny by using chronosequences of lakes in the Glacial Bay region of Alaska. The Glacial Bay lakes limnic development is connected to biochemical changes with vegetation succession following deglaciation. These lakes experience soil changes such as carbonate leaching, increased dissolved organic carbon (DOC), base cations and nitrogen inputs associated with vegetation succession (Engstrom et al., 2000). Climate-driven shifts in the boreal zone of Canada from low- to high- vegetation productivity increase the nutrient content of runoff caused by increased leaf litter decomposition driving substantial changes in lake trophic status and transitions between oligotrophy and mesotrophy (Crocker et al., 1955; Jacobson et al., 1980; St. Jacques et al., 2000; Moos et al., 2009; Moos et al., 2011). This phenomenon is also observed in southern Ontario, Canada, where climate-driven shifts from coniferous *Pinus*-dominated forest to mixed forest results in an increase in soil nutrient content with more nutrient rich leaf litter and more nutrient tolerant aquatic taxa (St. Jacques et al., 2000; Beck et al., 2016).

Across Australia aquatic ecosystem respond indirectly to climate through changes in nutrient inputs as the result of vegetation change (Bradbury, 1986; Barr et al., 2013). In south-east Queensland, Blue Lake experiences a shift

in pH and nutrient concentrations inferred from changes in diatom species assemblages (Barr et al., 2013) caused by a decline in Casuarinaceae pollen and an increase in drought-tolerant taxa consistent with the impacts of increased El Niño events (Shulmeister et al., 1995; Moy et al., 2002). In Tasmania, two Pleistocene/Holocene diatom records from Tasmania (Lake Vera and Eagle Tarn) reveal the indirect influences of climate following deglaciation through lake ontological processes (Bradbury, 1986). In the late Pleistocene, these lakes were deeper, oligotrophic and more alkaline with dominance of planktonic taxa. They progressed to shallower, dystrophic and more acidic lakes, a symptom of the organic acidic soils developing under Tasmanian rainforest vegetation. Bradbury (1986) concludes that these aquatic shifts are the response to climate mediated through local vegetation.

2.9.3.2 Impact of Fire Dynamics on Aquatic Ecosystems

Fire can impact aquatic ecosystems through nutrient inputs, pollutant transport, and sediment delivery resulting in changes in trophic status, water clarity, and lake mixing (Ball et al., 2010; Brown, 2016). Fire increases the erosion of terrestrial material and heavy metals creating turbid waters and/or altering lake chemistry (Korhola et al., 1996; Birks, 1997; Dunnette et al., 2014; Leys et al., 2016). In the Beartooth Mountains of Wyoming, USA severe fires caused declining water clarity resulting in decreased planktonic:benthic diatom ratios and productivity caused by less light penetration post fire altering lake stratification and mixing depth (Brown, 2016). Fire can also alter the nutrient status of lakes where increased inputs of organic nutrients (e.g. DOC, P and N) can alter the trophic status of aquatic ecosystems (Renberg et al., 1993; Birks, 1997; White et al., 2006; Smith et al., 2011; Leys et al., 2016). Conversely, a lack of fire can decrease N export and nutrient delivery into aquatic ecosystems (Ball et al., 2010). However, the removal of biomass caused by fire can decrease nutrient delivery over the long-term (Durán et al., 2008; Dunnette et al., 2014; Morris et al., 2015; Leys et al., 2016).

Frequent burning can increase lake pH through the destruction of the acid humus soil layer and release base cations from ash deposition (Korhola et al., 1996; Birks, 1997). Fire events induced by local agricultural activity

at Lake Makkassjon, Sweden corresponded to a period of increased alkalisation and shift in aquatic composition, but no significant impact on forest type (Korsman et al., 1998). Similarly, these relationships were found in North Pond, Massachusetts, USA where a decline in *Tsuga* following a fire event transformed soils causing an increase in nutrients and lake pH (Huvane et al., 1996). The impact of fire on aquatic chemistry is dependent on the vegetation type on the landscape, soil and geology, and the frequency of fire (Renberg et al., 1993; Birks, 1997; Dunnette et al., 2014).

2.10 NON-LINEAR ECOSYSTEM SYSTEM RESPONSE TO ENVIRONMENTAL CHANGE

Ecosystems exposed to prolonged stressors such as nutrient influx, climate and land-use change are at risk of crossing a tipping point or critical transition into a new stable state (Carpenter et al., 2006; Bunting et al., 2016). These non-linear responses to external drivers are becoming more important in understanding ecosystem states, dynamics and regime shifts (Scheffer et al., 2009; Seddon et al., 2014).

Critical transitions occur when a system is exposed to added environmental pressure or perturbations (Scheffer et al., 2009; Wang et al., 2012). When a system approaches a critical transition, also known as a bifurcation, recovery from small perturbations slows and a threshold is exceeded, driving the system to a new state (Figure 2.9) (Scheffer et al., 2009). The lack of understanding of the mechanisms of critical transitions and how to predict them has brought attention to this ecological phenomenon. Early warning signals have been identified to better understand and predict this process (Carpenter et al., 2006; Scheffer et al., 2009; Scheffer et al., 2012; Wang et al., 2012; Dakos et al., 2015; Bunting et al., 2016). Some examples of early warning signals include increases in autocorrelation, variance, skewness, and flickering prior to a critical transition (Scheffer et al., 2009; Wang et al., 2012; Dakos et al., 2015). Critical transitions are rarely observed in nature, though there are examples of critical transitions in aquatic ecosystems (Carpenter et al., 2011; Wang et al., 2012; Gell et al., 2014; Capon et al., 2015; Bunting et al., 2016). However, there has been criticism that many reported non-linear transitions in aquatic ecosystems have misleading language and do not provide enough statistical evidence to be suggest a critical

transition or new stable state (Capon et al., 2015). Therefore, these caveats must be carefully considered when interpreting non-linear shifts.

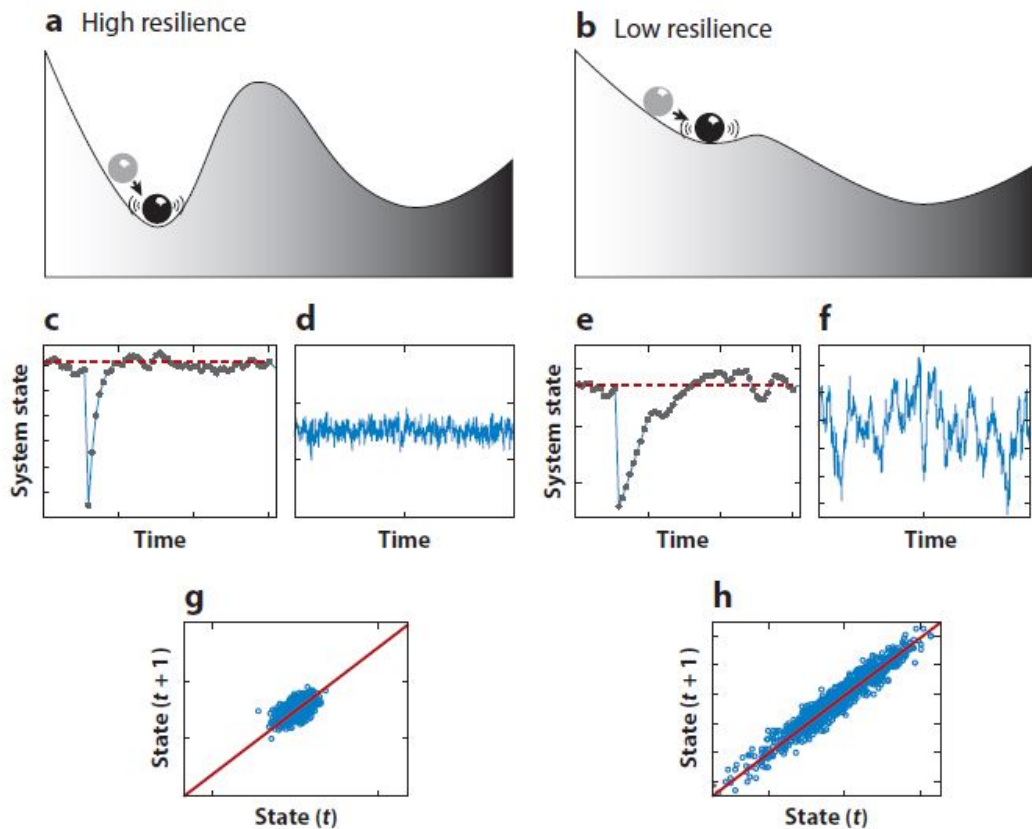


Figure 2.9: A conceptual model for critical transitions where low resilience (a and b), longer recovery rates (c to e) increase the temporal autocorrelation and variance (g and h) indicate the early warning signals of a critical transitions (Figure 2; Scheffer et al., 2015).

2.11 CHAPTER CLOSING

This chapter has framed the environmental setting of Tasmania, as well as, provided an understanding of the interactions between terrestrial and aquatic ecosystems. The current understanding of direct and indirect influences of climate on aquatic ecosystems were explored using examples from Australia and other regions of the world. Lastly, critical transitions and non-linear responses were introduced.

CHAPTER 3: METHODS

3.1 CHAPTER AIM

Outlined in this chapter are palaeoecological approaches, site selection, chronology, geochemical and biological proxy methods, and statistical approaches.

3.2 PALAEOECOLOGICAL APPROACH

Palaeoecological research can be used to capture ecosystem and/or environmental changes over long periods of time using proxy data preserved in natural archives. Natural archives exist in many forms such as ice cores, loess deposits, lake and ocean sediments, and accumulations of peat (Anderson et al., 2007; Raper et al., 2009).

Palaeoecological research has three key assumptions:

1. The law of superposition - material laid at the bottom of the deposit is older than the material laid on top;
2. Diagenesis, equifinality, provenance, and taphonomy - the physical, chemical and biological processes that occurred when and where the deposit was laid;
3. Uniformitarianism and neocatastrophism - the present ecological or geological processes are the same as the past (Anderson et al., 2007).

Here I employ lake sediment archives as they contain information on both terrestrial and aquatic ecosystem change that, under selected environmental conditions, are well preserved and continuous. The vast majority of lakes in western Tasmania began accumulating sediment following the retreat of ice formed during the Last Glacial Maximum (Macphail, 1979; Colhoun et al., 1991a; Colhoun, 1996; Colhoun et al., 1999; Fletcher et al., 2007a; Fletcher et al., 2015; Rees et al., 2015; Stahle et al., 2016; Mariani et al., 2017a). For this research, glacially formed lakes are targeted to retrieve a sediment record spanning the Holocene. The Holocene includes substantial climate variability which can be used to test terrestrial and aquatic ecosystem response to long-term

climatic change. (Prentice, 1978; Prentice, 1985; Berglund, 1986a; Faegri et al., 1989; Sugita, 1993; Punning et al., 1997; Cáceres et al., 2002; Bunting et al., 2004; Warfe et al., 2013) Small lakes with low hydrological connectivity were selected to focus on local terrestrial and aquatic signals.

3.3 SITE SELECTION

Lake archives from Paddy's Lake and Lake Vera (Figure 3.1) were selected to reveal the influences of climate and fire on vegetation change, catchment dynamics, and aquatic systems. A multiple proxy approach will be employed on each lake to understand influences of climate (charcoal), and the terrestrial environment (pollen, XRF and CN) on aquatic (CN, diatoms and cladocerans) ecosystem response.

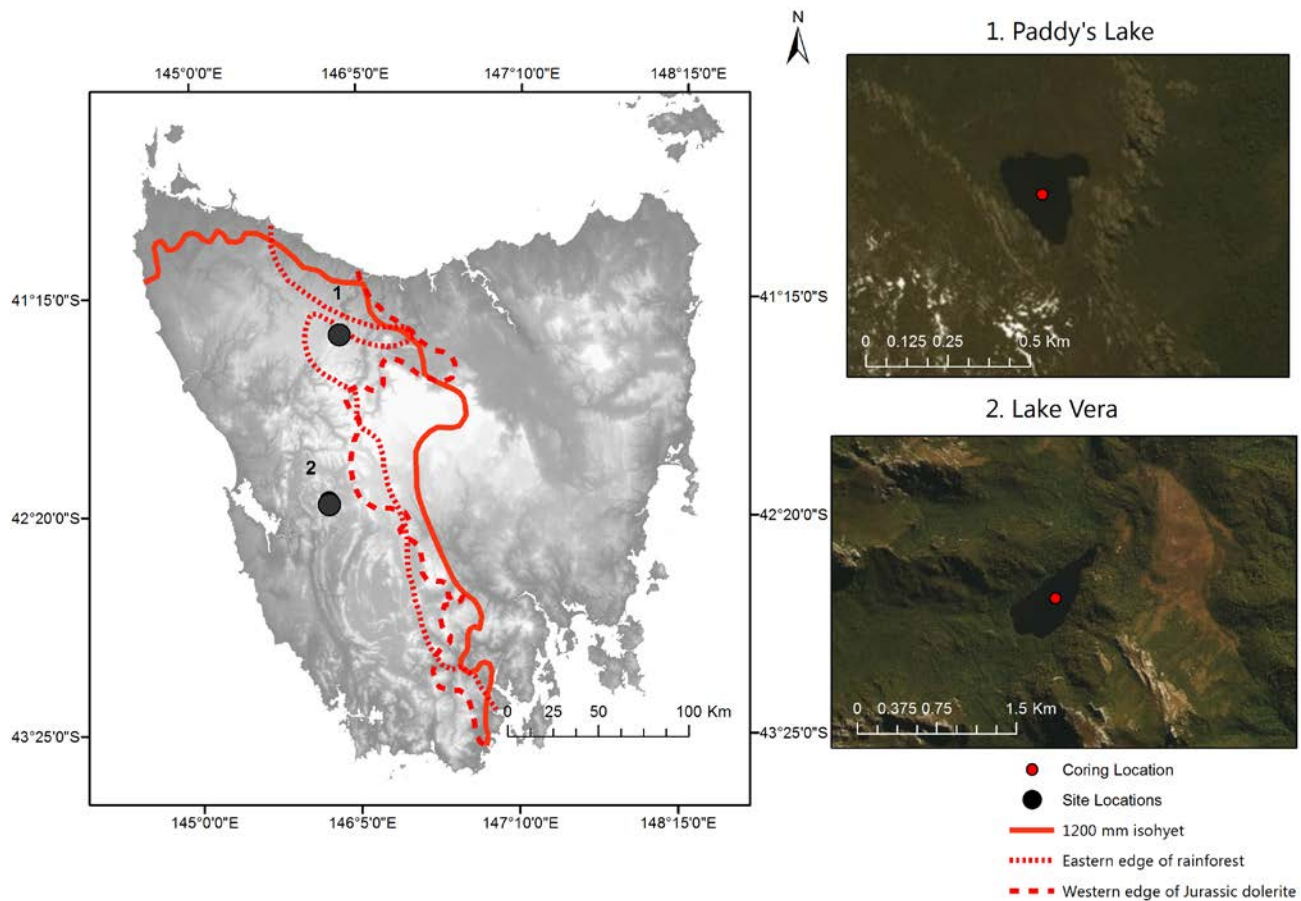


Figure 3.1: Map of Tasmania, Tyler's Line (red solid, dashed and dotted lines) (Tyler, 1992) and satellite images of study site locations: (1) Paddy's Lake and (2) Lake Vera.

3.3.1 PADDY'S LAKE

Paddy's Lake (41°27' S, 145°57' E) is a glacially formed cirque lake, located in northern Tasmania, at 1065 masl on Black Bluff (Figure 3.2). Paddy's Lake has a maximum depth of ~21.5 m and an area of 26 km². Its total catchment area is 174.258 km². The mean annual precipitation interpreted from the closest weather stations [Loongana 4.4 km (468 masl) and Waratah 36 km (609 masl)] is ~1,740 mm. The suggested minimum and maximum temperature at Paddy's Lake by application of the adiabatic lapse rate is ~4.6°C and ~14°C (Bureau of Meteorology, 2016b). Local geology consists of Quaternary deposits of quartzite; conglomerate talus and moraine deposits with traces of Cambrian volcanic clastic conglomerate breccia, sandstone, pink sandstone and siltstone; and pebble-cobble conglomerate (Seymour et al., 1995; Pemberton et al., 2004). Surrounding vegetation consists of eastern alpine heathland and lichen lithosphere (Figure 3.3) (Harris et al., 2005; Kitchener et al., 2013; Department of Primary Industries, 2017) with dominant taxa: *Athrotaxis selaginoides*, *Baeckea gunniana*, *Eucalyptus* spp., *Nothofagus cunninghamii*, *Orites* spp., and *Richea* spp. (Parks & Wildlife Service, 2008).



Figure 3.2: Photo of Paddy's Lake (by: Kristen Beck, 2016).

Paddy's Lake is an ideal site for this project due to the (1) small size of the lake with one outflow; (2) location within the zone of strongest correlation between ENSO and precipitation in Tasmania; (3) the glacially formed lake, abandoned by ice before the Holocene (ca. 11.7 ka) (Barrows et al., 2002); and (4) oligotrophic dystrophic waters.

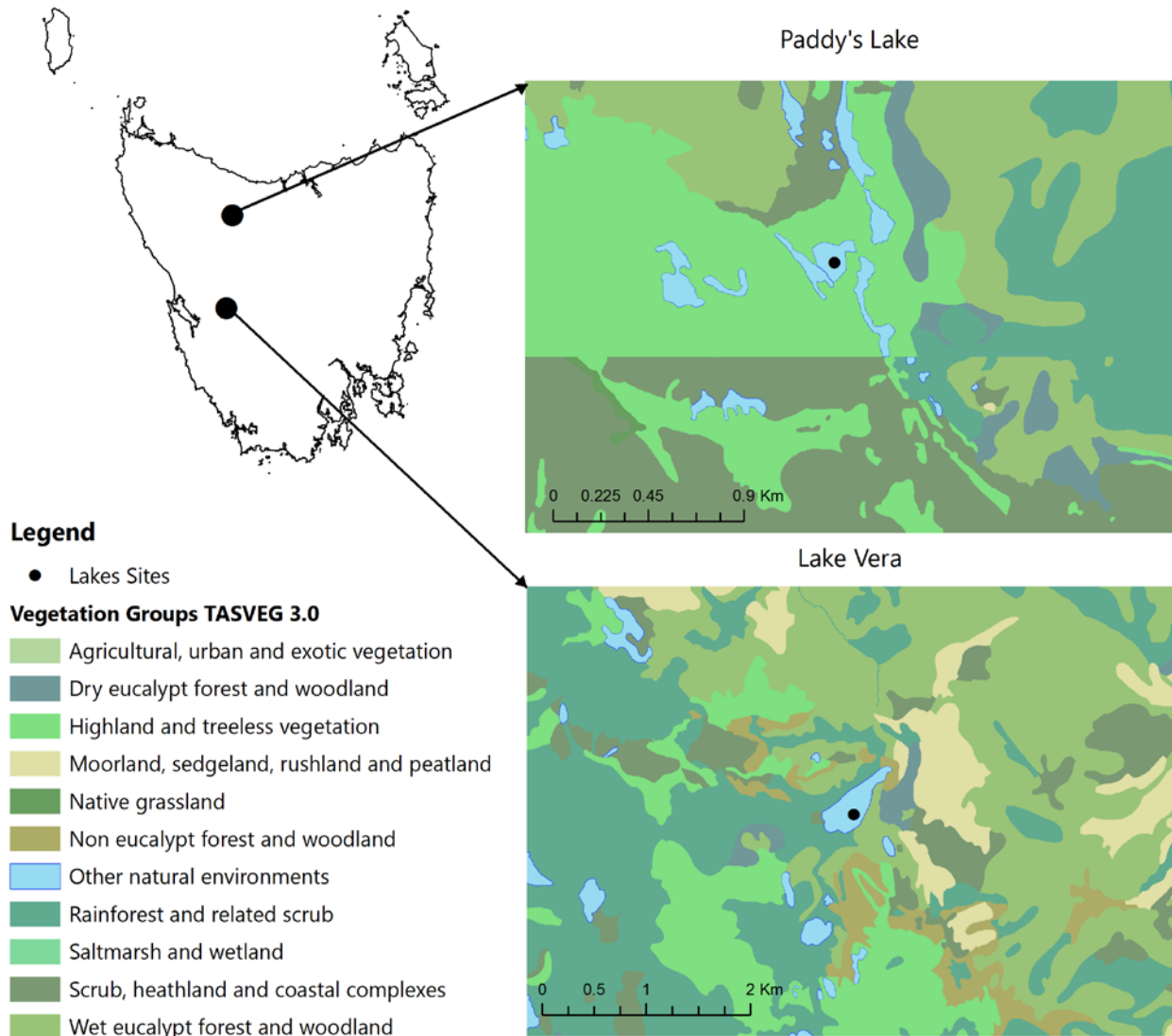


Figure 3.3: Vegetation groups defined by TASVEG 3.0 (Department of Primary Industries, 2017) surrounding Paddy's Lake and Lake Vera.

3.3.2 LAKE VERA

Lake Vera (42°16' S, 145°52' E) is a small moraine-bound lake formed in a glacial valley located on Frenchman's Cap, western Tasmania at 550 masl (Figure 3.4). The maximum water depth at Lake Vera is ~50 m, with a total surface area of 158.486 km² and a catchment area of 5,204.385 km². Lake Vera's annual mean precipitation is ~2,800 mm with a mean annual temperature of ~8.7°C (Macphail, 1979; Bradbury, 1986; Markgraf et al., 1986). Vegetation surrounding Lake Vera is diverse with four vegetation types surrounding the lake: (1) rainforest and

related scrubland; (2) scrub, heathland and coastal complexes; (3) wet eucalypt forest and woodland; and (4) non-eucalypt forest and woodland (Figure 3.3). The dominant taxa include: *Anodopetalum biglandulosum*, *Atherosperma moschatum*, *Athrotaxis selaginoides*, *Eucryphia lucida*, *Eucalyptus delegatensis*, *Lagarostrobos franklinii*, *Leptospermum nitidum*, *Phyllocladus aspleniifolius* and *Nothofagus cunninghamii* (Harris et al., 2005; Kitchener et al., 2013; Department of Primary Industries, 2017). Geology contains mainly quartzite Precambrian metamorphic bedrock (Peterson, 1966; Macphail, 1979; Bradbury, 1986).

Lake Vera is located in the zone of strongest correlation between SAM and rainfall in Tasmania (Hill et al., 2009). Critically, the site records more than 10,000 years (10 kyrs), from 12.5 ka to 2.5 ka, of substantial climate-driven vegetation change that occurred in the absence of fire (Fletcher et al., in review). Vegetation transitions track shifts in the position of the SWW, with relatively dry conditions from ca. 12 to 7 ka dominated by dry tolerant rainforest taxa to peak moisture delivery from ca. 7 to 5 ka with dominant wet rainforest species. Drought tolerant vegetation types increase in abundance with the onset of ENSO at ca. 5 ka. Increased fire disturbance at ca. 2.3 ka increased the abundance of disturbance taxa (Fletcher et al. in review). Thus, Lake Vera is an appropriate site to evaluate climatically driven aquatic ecosystem changes in the absence of fire. It is also an ideal site for this project because it has (1) a sediment record of ca. 19 ka (Macphail, 1979; Fletcher et al., in review); (2) vegetation change driven by climate throughout the Holocene (Fletcher et al., in review); and (3) oligotrophic dystrophic waters with preserved diatoms (Bradbury, 1986).



Figure 3.4: Photo of Lake Vera (by: Kristen Beck, 2015)

3.4 SEDIMENT CORING

The collection of an undisturbed continuous sediment sequence is a critical part of palaeoecological research. The deepest point of the lake typically allows for the most complete record, highest sedimentation and least disturbed sediments (Birks et al., 1980).

3.4.1 CORING EQUIPMENT

To retrieve an entire Holocene sediment sequence, a water-sediment interface (“surface”) core and “long” cores are needed. Surface corers are designed to retrieve an intact water-sediment interface. Upper layers of sediment typically have high water content and surface corers are designed to capture this sediment-water interface

undisturbed and with minimum compaction. Long sediment corers are designed to capture the consolidated sediment, further down the sediment stratigraphy. For this research, the Universal Corer (Aquatic Research Instruments, 2016) was used to collect a surface core and a Nesje corer (Nesje, 1992) to collect a continuous long core.

The Universal corer uses gravity, as well as a percussion hammer to collect sediment. Percussion corers can collect more sediment than traditional gravity corers; however, compaction of the sediment while hammering can occur (Glew et al., 2001). Long cores are frequently retrieved using piston corers, such as the Livingston (Livingstone, 1955) or Nesje (Nesje, 1992). The selected lakes in this study are >20 m deep, therefore the Nesje Corer piston coring system is used because it is not limited by lake depth. The Nesje corer uses a suspension cable, a hammer and a winch rather than drive rods to collect a continuous long sediment record (Nesje, 1992). The Nesje operates similar to the Livingston with a piston creating a vacuum in a core chamber. Core collection starts slightly in the sediment (~20 to 50 cm), then the piston is fixed in place. Once the piston is fixed at the desired depth the core chamber is hammered around the piston to collect a continuous record up to 6 to 9 m in a single drive. The Nesje does have some drawbacks as this system is very heavy (~400 kg) and less portable than other systems. Due to hammering, the Nesje does not collect pristine surface sediments, this is why the Universal was used in conjunction with the Nesje.

3.4.2 CORING METHODS

Sediment sequences are collected from the deepest basin of a lake off a floating platform. The University of Melbourne Palaeoecology Laboratory platform is designed to be assembled onshore for Nesje, piston, and gravity coring. The platform has two pontoons with a wooden deck fixed to a specialised frame for the Nesje tripod (Figure 3.5). The platform is then paddled to the deepest basin and anchored in place to keep the platform from moving. Accurate depth and GPS coordinates are recorded before coring begins.



Figure 3.5: University of Melbourne Palaeoecology Laboratory coring platform equipped with two pontoons, a wood deck and the Nesje tripod (by: Kristen Beck, 2015).

3.4.2.1 Universal Coring

The Universal Corer is used from the side of the floating platform to collect an undisturbed surface core (Figure 3.6). The Universal is suspended by two cables in the water; one attached to the corer and one to the hammer. The cable attached to the corer is kept taut in one hand and lowered through the water using gravity to penetrate the sediment. The PVC tube that collects the core sample penetrates the surface sediment. The corer cable is held taut, then using the hammer cable from the other hand the hammer is lifted and lowered in a controlled motion to collect more sediment. Caution must be taken not to over penetrate the corer into the sediment. Some water should remain in the top of the PVC tube (1.5 m in length) to maintain a good surface sediment interface.

Once hammering is completed the corer in entirety is pulled to the surface, with the sediment remaining inside the PVC tube. The Universal has a mechanism that closes the top of the corer when pulled up through the water (it

remains open when falling through the water). This mechanism plugs the top of the corer, creating a vacuum that retains the sediment inside the tube (Figure 3.6). Once the Universal is pulled to the surface it remains slightly in the water, to maintain a vacuum, before the PVC tube is plugged at the bottom to retain the sediment.

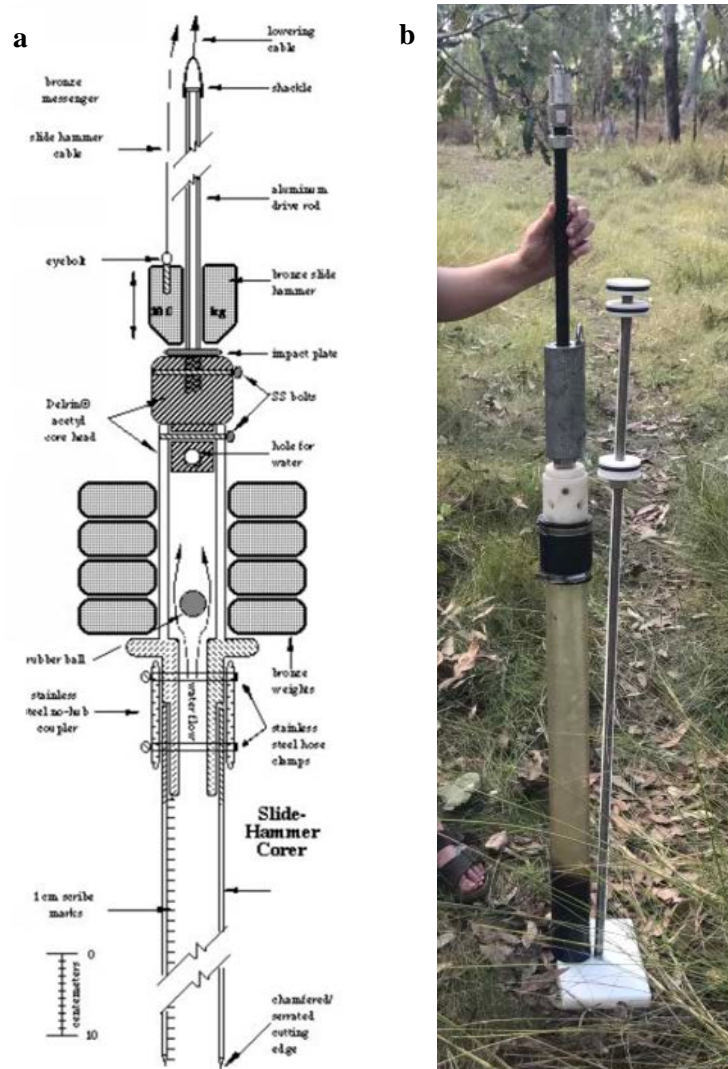


Figure 3.6: a) Schematic of the Universal percussion corer (Aquatic Research Instruments, 2016). b) Photograph of the Universal Corer and extruding stand (by: Jonathon Garber, 2017).

3.4.2.2 Nesje Coring

Nesje coring is completed from the centre of the floating platform. First the piston is adjusted to fit the core chamber by two rubber bungs to create a good seal. Then the aluminium chamber is attached to the head of the

Nesje corer and lowered to the desired depth using the winch (Figure 3.7). A tape measure is fastened to the top of the Nesje to keep track of the distance travelled.



Figure 3.7: Attaching the aluminium chamber to the Nesje coring head at Paddy's Lake (by: Alexa Benson, 2014).

The Nesje is lowered ~20 to 50 cm into the sediment, then the piston is fixed in place to the platform using vice grips. The hammer is then raised and lowered collecting sediment inside the core chamber by the vacuum created by the fixed piston (Figure 3.8). The attached tape measure continues to track the progress of sediment collection. The Nesje aluminium chamber is typically 6 m in length, therefore hammering cannot exceed this distance or will stop when the bedrock is reached. Once hammering stops, the Nesje and the piston cable are winched to the platform with the sediment inside the aluminium chamber (Figure 3.9). When the Nesje reaches the platform the core chamber is detached from the head of the Nesje and hoisted onto the platform to be measured and capped for transport (Figure 3.10).



Figure 3.8: Hammering the Nesje at Lake Vera (by: Michela Mariani, 2015).

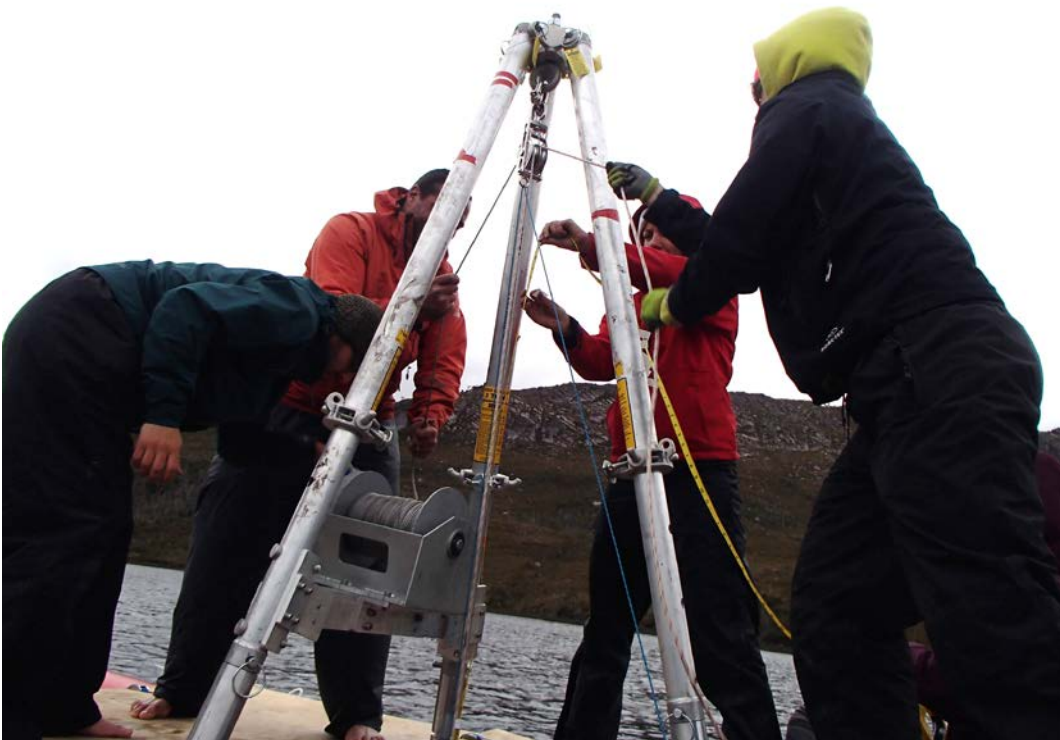


Figure 3.9: Winching the Nesje back to the platform after core collection (by: William Rapuc, 2014).

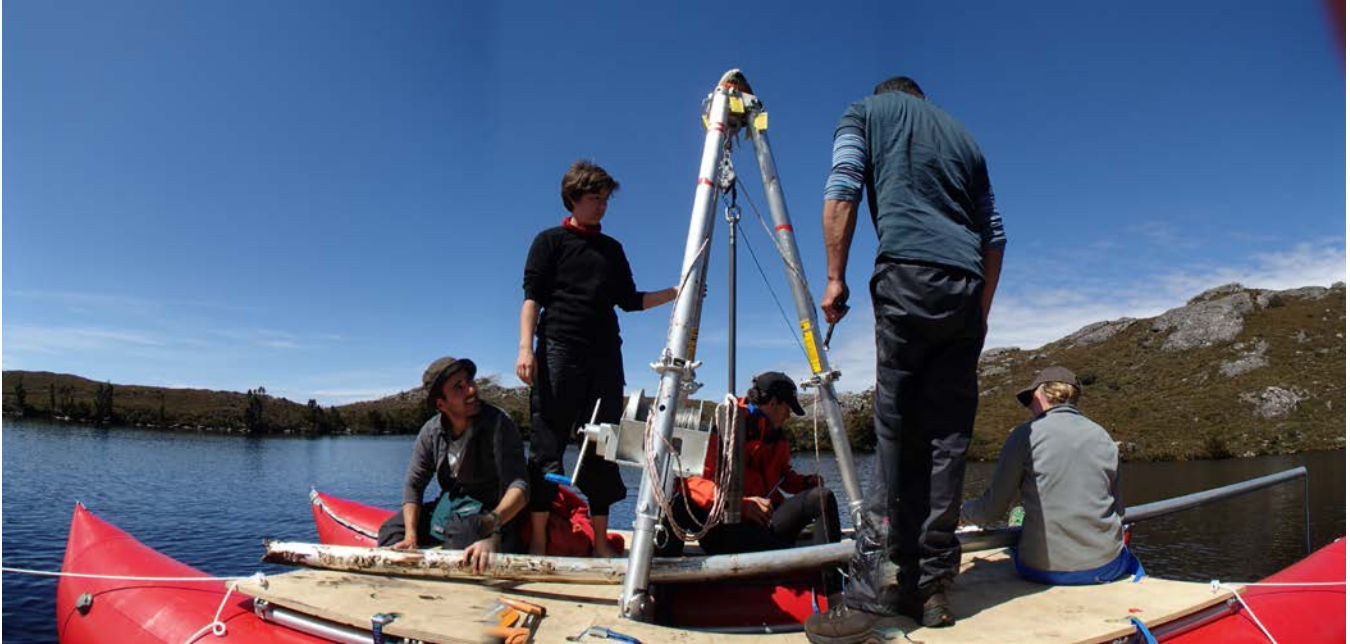


Figure 3.10: Sediment core inside aluminium chamber on the platform at Paddy's Lake (by: Alexa Benson, 2014).

3.4.2.3 Extruding Cores in the Laboratory

A custom core splitter at the University of Melbourne is used to split the cores in half longitudinally. The core splitter has an adjustable cradle for the cores to sit horizontally and a moving handsaw that cuts the core tube (Figure 3.11). The core splitter is designed to cut different coring tube material, i.e. aluminium or PVC. The core is halved using a wire or fishing line run through the longitudinal cuts creating two equal halves (Figure 3.12). Cores longer than 1.3 m must be cut into smaller sections to be split by this apparatus.



Figure 3.11: Core splitter at University of Melbourne. Splitting a Universal Core from Rebecca's Lagoon, northwest Tasmania (by: Bianca Dickson, 2016).

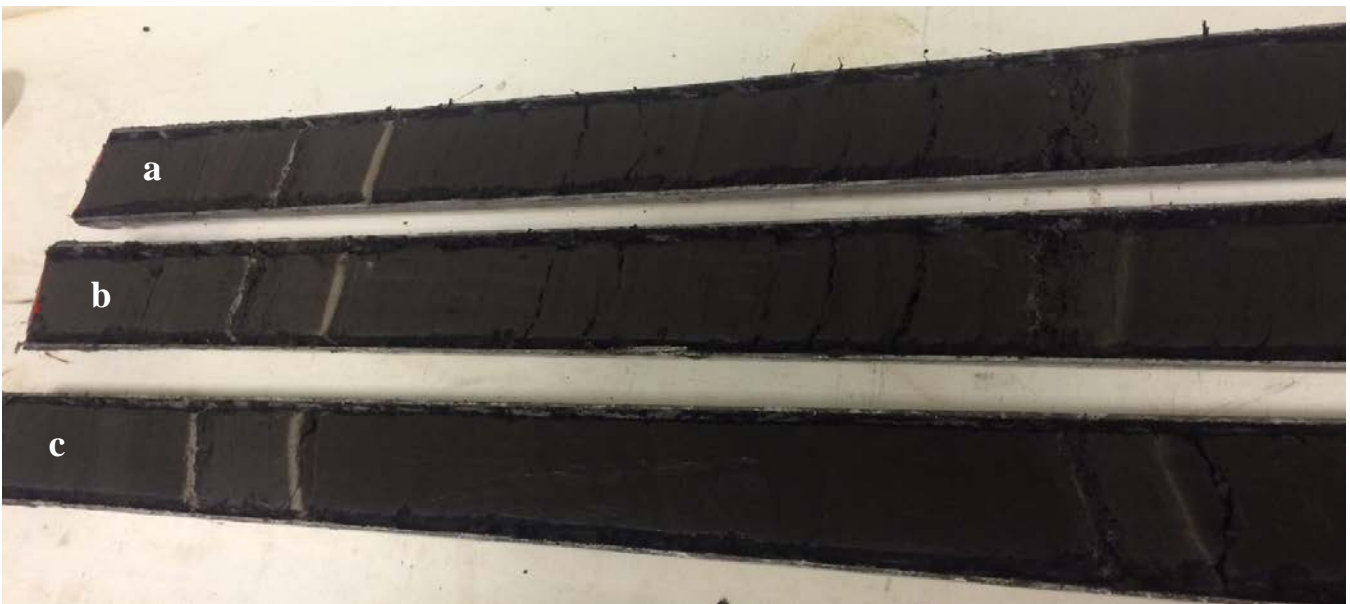


Figure 3.12: Examples of split Lake Vera cores a) TAS1508 N1, b) TAS1508 N1 archive half, and c) TAS1508 N2 (by: Kristen Beck, 2015).

To maintain accurate resolution and depth samples, the sediment cores are sliced into 0.5 cm intervals from one half of the split core. The other half of the core is archived and stored in a refrigerator for further analysis if

needed. The core slicing apparatus has a metal cradle for cores to sit; a ruler to measure sample intervals, and a moving semicircular blade to cut each sample interval (Figure 3.13). Sediment intervals are bagged in sterile Whirl-Bags for future subsampling.

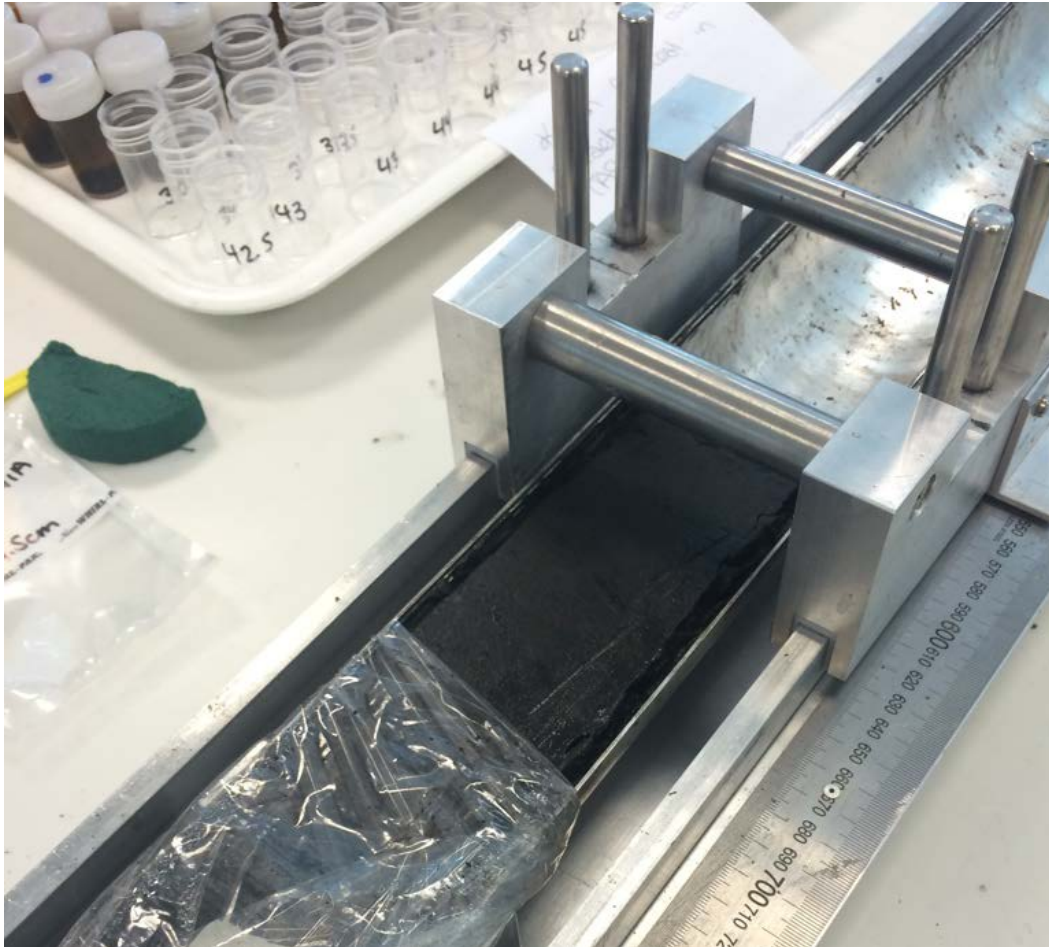


Figure 3.13: Core slicing apparatus with a sediment sample on the metal cradle (by: Kristen Beck, 2016).

3.5 RADIOMETRIC DATING

An accurate chronology is pivotal to the success of this project. There are several techniques for dating palaeoecological archives: radiocarbon dating (^{14}C), lead-210 dating (^{210}Pb), atmospheric nuclear fallout (^{137}Cs), luminescence dating, varve chronology, uranium series, palaeomagnetism, electron spin resonance dating, and tephrochronology (Chappell, 1978; Håkanson et al., 1983; Olsson, 1986; Last et al., 2001). Radiocarbon dating is

the most widely used technique in palaeoecology for dating lake sediments (Chappell, 1978; Håkanson et al., 1983; Blaauw et al., 2012), and will be used to date the lake sediment in this project. Radiocarbon dating uses carbonate (organic) material and radiometric dating methods to date material up to 60,000 years in age; however is unreliable for the past few hundred years due to the atmospheric weapons testing and the burning of fossil fuels (Hedges, 1981; Björck et al., 2001). Therefore short-lived isotopes such as ^{210}Pb is commonly used to measure the ages of younger lake sediments (the past 150 years) (Hedges, 1981; Björck et al., 2001). Thus, combining ^{14}C and ^{210}Pb dating techniques can adequately date lacustrine sediment cores spanning the Holocene and will be the dating techniques used in this thesis.

3.5.1 RADIOCARBON DATING

Radiocarbon is extensively used for dating sediments <60,000 years old due to the short-lived age of the radioactive carbon isotope used in the technique (^{14}C). Carbon-14 is a radioactive isotope and exists for an average of 8,270 years before it decays back to the stable element ^{14}N (Björck et al., 2001). Heavy ^{14}C atoms react with oxygen and are incorporated into the biosphere as $^{14}\text{CO}_2$. This $^{14}\text{CO}_2$ is freely incorporated into living organisms with the consumption of CO_2 . When the organism dies, the uptake of CO_2 stops and the heavy ^{14}C begins to decay. To determine the age of fossil material, the amount of ^{14}C is compared to the known ^{12}C ($^{14}\text{C}/^{12}\text{C}$) to measure how much decay has occurred (Olsson, 1986; Björck et al., 2001) using the known ^{14}C half-life of 5,568 years (Mook, 1986; Mook et al., 1986).

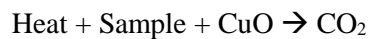
There are two methods for ^{14}C dating: conventional radiocarbon dating, and Accelerator Mass Spectrometry (AMS) dating. The conventional ^{14}C dating technique counts decaying C atoms and requires pure carbon to determine the age; this is problematic in sediments with low organic matter. However, the technique is often more precise than AMS when enough organic material is available. Conventional ^{14}C dating is less commonly used since the development of AMS radiocarbon dating. The AMS method can use very small amounts of C with

improved time resolution and age uncertainty (Björck et al., 2001) and will be the method used for radiocarbon dating in this thesis.

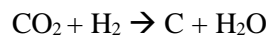
3.5.1.1 Standard Method of AMS Radiocarbon dating

In the laboratory, subsamples are selected for ^{14}C dating. Macrofossils provide more accurate dates but bulk sediment can be used when macrofossils are not available. Samples (macrofossils and bulk sediments) are dried at 60°C for ~24 hours to remove any water content. Contaminating rootlets are removed then samples are pre-treated with a series of chemical digestions. First, the addition of HCl followed by NaOH, then acidification to pH of ~3 is performed to remove any contaminant C. Once pre-treated, the samples go through a process of combustion and graphitisation where they are heated with CuO to produce CO_2 , then H_2 is added to produce solid C (Björck et al., 2001).

Combustion:



Graphitisation:



This solid C is put into the accelerator mass spectrometer where energy and different isotopes of C are injected to move the C sample along the spectrometer. The AMS technique counts the number of ^{12}C , ^{13}C and ^{14}C atoms in the high-voltage spectrometer (Blaauw et al., 2012). This produces an array of ^{14}C particles that can be measured and compared to the standard levels of ^{14}C to determine the radiocarbon age (Olsson, 1986; Björck et al., 2001).

3.5.1.2 Calibration

Radiocarbon age is not a true calendar age due to changes in the atmospheric production rate of $^{14}\text{C}/^{12}\text{C}$ (Olsson, 1986; Björck et al., 2001). To correct ^{14}C age to calendar age, radiocarbon dates are calibrated to an international calibration curve developed using dendrochronology (Olsson, 1986; Björck et al., 2001). There are three calibration curves used to correct radiocarbon dates: INTCal13 for Northern Hemisphere environments (Reimer et al., 2013); Marine13 for oceanic environments (Niu et al., 2013); and SHCal13 for the Southern Hemisphere (Hogg et al., 2013). Calibration accuracy is dependent on: (1) error in analysed radiocarbon date and (2) range of probabilities in the associated portion of the calibration curve (Björck et al., 2001). Depending where the radiocarbon date intersects the calibration curve, multiple calendar dates are possible. Therefore ^{14}C age is given a calendar year probability (Figure 3.14) (Blaauw et al., 2012). These results are not always normal distributions and can be multimodal depending on the intersecting region of the calibration curve. Therefore, calibration distributions are reduced to 68% or 95% calibration ranges regardless of age distributions (asymmetric to multi-peak) (Blaauw, 2010; Blaauw et al., 2012).

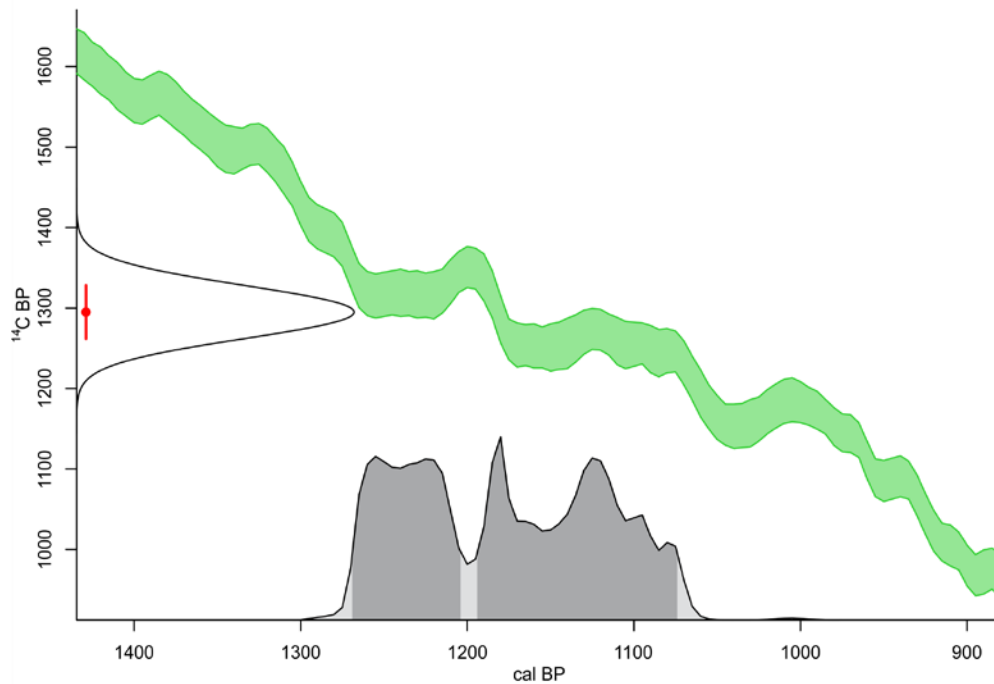


Figure 3.14: Example calibration of radiocarbon date 1,295 ^{14}C yrs \pm 33 (1σ) from a Northern Territory, Australia sediment sample (NT1501). Dark grey shading demonstrates the 95% cal yr BP probability.

The calendar age 1950 AD has been standardised to 0 calibrated years (cal yr) BP. Calibrating ^{14}C dates is now performed within age-modelling programs by selecting the relevant calibration curves that are appropriate for the data. For the age modelling purposes of this project SHCal13 has been used to calibrate the ^{14}C dates and the median or maximum density age (intercept) is used within the age-depth models (Blaauw, 2010 Version 2.2).

3.5.1.3 Advantages to Radiocarbon dating

Radiocarbon dating is widely used in the Quaternary research community and advantageous for several reasons:

1. It is ideal for Holocene sequences dating between 500 to 50,000 cal yr BP (Chappell, 1978);
2. It has simple sample preparation (DirectAMS, 2017);
3. Analysis can be run on small amounts of material, bulk sediment, or macrofossil as low as 0.1 g dry weight (Björck et al., 2001; DirectAMS, 2017);

4. Methods and accuracy are constantly improving (Björck et al., 2001).

3.5.1.4 Limitations to Radiocarbon dating

Radiocarbon dating does have caveats.

1. Contamination – exposure to old or young C can contaminate samples such as sediment reworking, exposure to modern C during processing or the penetration of rootlets (Olsson, 1986; Björck et al., 2001).
2. Reservoir effects – if the $^{14}\text{C}/^{12}\text{C}$ ratio in the lake is lower than the atmospheric ratio all of the radiocarbon dates may have an offset (Olsson, 1986; Björck et al., 2001).
3. Radiocarbon error – the standard deviations associated with the radiocarbon age obtained may vary between laboratories; some use a mean of multiple sample runs, others use Poisson distribution to approximate error and can be overly optimistic (Olsson, 1986; Björck et al., 2001).
4. Due to fossil fuel burning the atmospheric $^{14}\text{C}/^{12}\text{C}$ ratio has been altered over the past 200 years, thus radiocarbon should not be used to date younger sediments (Björck et al., 2001).
5. Radiocarbon dating has high uncertainties compared to other methods such as luminescence (Lian et al., 2001), and Uranium series (Chappell, 1978).

3.5.2 LEAD-210 DATING

Lead-210 dating is a method used on younger sediments. Lead-210 is a natural occurring radioisotope part of the uranium decay series with a half-life of 22.3 years (Figure 3.15). It is deposited into archives from the atmosphere (unsupported ^{210}Pb) and from soils and substrate (supported ^{210}Pb) (Håkanson et al., 1983; Appleby, 2001).

Deposited ^{210}Pb will decay at a constant rate from which sediment accumulation rates can be determined (Olsson, 1986). Lead-210 activity is determined via two methods: alpha radiation or gamma ray emission, and the choice

of method is governed by ^{210}Pb activity (Håkanson et al., 1983). Alpha spectrometry is most common and is used on small and low activity samples, and thus will be the method used in this thesis (Appleby, 2001). The ratio of supported and unsupported forms of ^{210}Pb provides an age for the sediments determined by two possible age models constant rate of supply (CRS) or constant initial concentration (CIC).

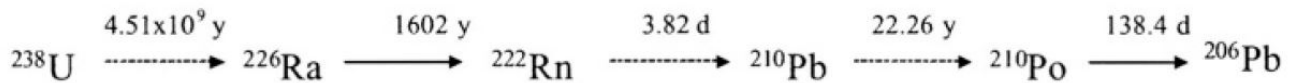


Figure 3.15: Uranium decay series including principal radionuclides and their associated half-lives (Figure 1, Appleby, 2001).

3.5.2.1 Standard Method Alpha Spectrometry and Age determination

The alpha radiation method measures the emitted ^{210}Po extracted by chemical digestion in a low-background alpha spectrometer (Appleby, 2001). The emitted ^{210}Po is used to measure ^{210}Pb activity when the two radionuclides are in equilibrium (Appleby, 2001). Once ^{210}Pb activity is determined a model (CRS or CIC) must be applied to determine age of the sediments.

The CRS model is widely used with homogeneous sediments with constant unsupported ^{210}Pb deposition from the atmosphere to freshwater (Olsson, 1986; Appleby, 2001). The CIC model assumes constant initial concentration of ^{210}Pb regardless of sediment accumulation rate, and therefore the ^{210}Pb varies in proportion to the sedimentation rate (Appleby, 2001). Model choice is site dependent. Typically, sites with no changes to sediment forcing or known hiatuses will be suitable for the CRS model. If surface ^{210}Pb concentration is inversely related to sedimentation rate, CRS will likely be the appropriate model. Additionally, model choice is commonly validated by a ^{137}Cs spike used to verify the model methods. Global fallout of ^{137}Cs began in 1954 CE following testing of nuclear weapons and measured ^{137}Cs can verify the 1954 CE horizon (Appleby, 2001). However, the ^{137}Cs signal is not always detected in Southern Hemisphere records. Details of the selected ^{210}Pb models are found in individual chapters (Chapter 6 & 7).

3.5.2.2 Advantages of Lead-210 dating

The advantages to using ^{210}Pb dating are:

1. ^{210}Pb can accurately date recent sediments where radiocarbon cannot (Olsson, 1986);
2. ^{210}Pb can be performed on small samples with low activity (Appleby, 2001);
3. ^{210}Pb dating methods and models can be validated by ^{137}Cs in many environments (Appleby, 2001).

3.5.2.3 Disadvantages of Lead-210 Dating

Lead-210 does have its limitations.

1. Complex catchments can have transport scenarios in which the CRS and CIC models are not well suited for the ^{210}Pb activity (Appleby, 2001).
2. Vertical mixing, particularly in the upper unconsolidated layer of sediment, will alter ^{210}Pb profiles and produce inaccurate age outputs (Olsson, 1986; Appleby, 2001)
3. Lead-210 can only be used to date the past 150 years (Appleby, 2001).

3.6 AGE-DEPTH MODELLING

Dating cannot be done on every sample depth used for proxy analysis because it is expensive, uses valuable resources, and is time-consuming. Therefore, to assign sample depths ages, mathematical models have been developed to produce age-depth models for archive sequences. Age-depth models are produced using statistical methods to predict the best age per sample depth with the smallest possible error. Software programs that develop age-depth models allows for selection of model type, calibration curves, and outliers. Popular software packages include: Bacon (Blaauw et al., 2013), clam (Blaauw, 2010), and OxCal (Ramsey, 2005).

3.6.1 STANDARD METHODS

There are two types of age models: classical (basic and mixed-effect) and Bayesian (Blaauw et al., 2012). The basic age model assumes errors only associated with the dates provided, while a mixed-effect models account for various forms of error such as: sample error, radiocarbon error (Section 3.5.1.4), and calibration error (Section 3.5.1.2) (Blaauw, 2010; Blaauw et al., 2012). Classical age-depth models can be performed using clam whereby model function (linear interpolation, polynomials, splines and power functions; Figure 3.16), calibration curve (INTCal13, Marine13, and SHCal13), calibration age estimate (midpoints, weighted means, medians and maximum densities), and outlier can be selected (Blaauw, 2010; Blaauw et al., 2012).

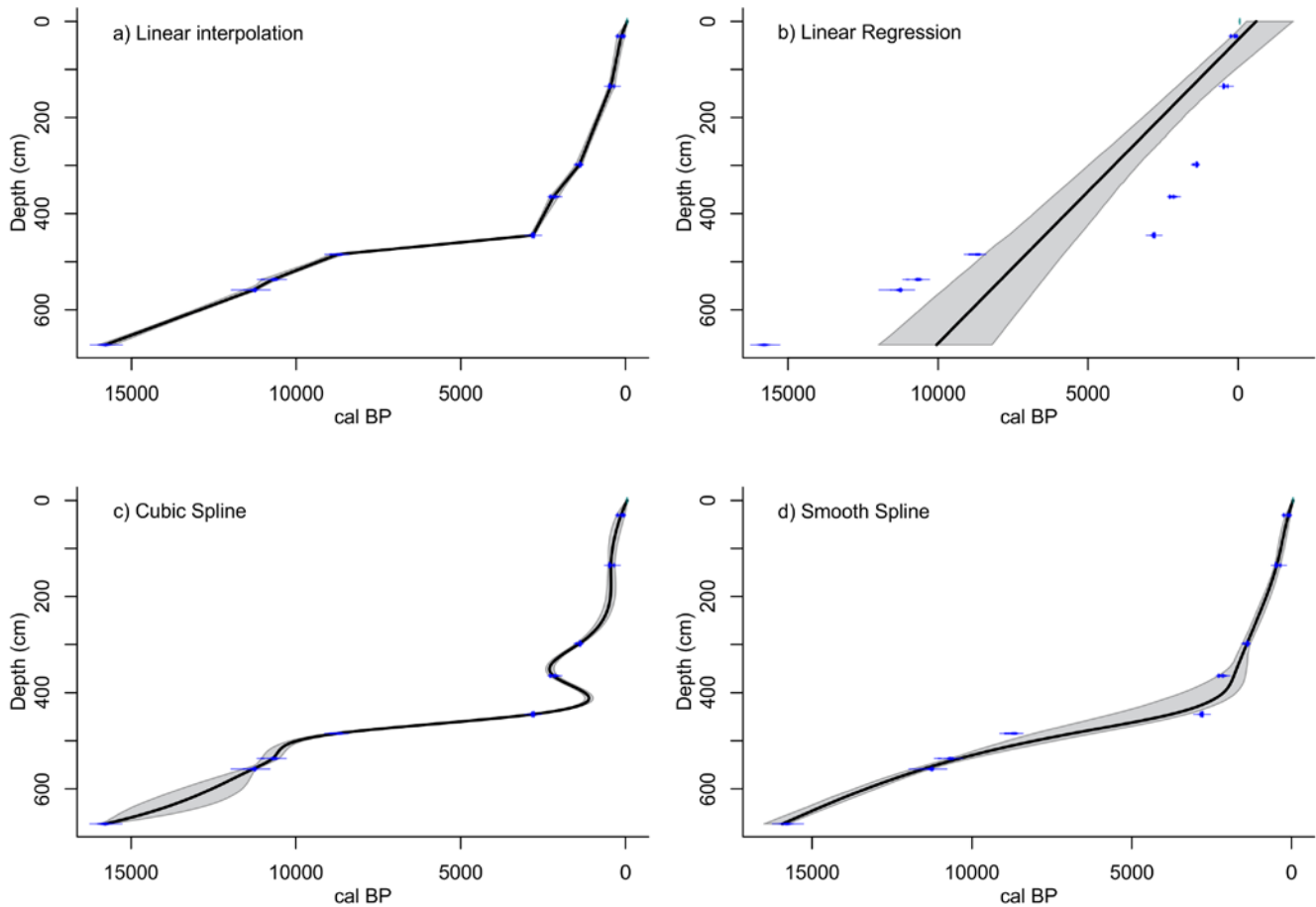


Figure 3.16: Classical age-depth model examples of a) linear interpolation; b) linear regression; c) cubic spline; and d) smooth spline functions of an example dataset in clam (Blaauw, 2010).

Bayesian models use Bayesian statistics and prior information, such as accumulation rates and variability over time, from the dating sequence to inform error in Bacon and OxCal software (Blaauw et al., 2012; Blaauw et al., 2013). Bayesian statistics provide the opportunity to produce the most “logical” age-depth model with constraint on positive accumulation rates, where classical statistics used for age-depth model selection can be subjective (Blaauw et al., 2012). The software package Bacon performs Bayesian age-depth modelling and separates the sediment core into many thin vertical sections and estimates the accumulation rate through thousands of probability sampling iterations (Markov Chain Monte Carlo) in years/cm. The model determines outliers using student-t distribution test (Blaauw et al., 2013). These parameters are then combined to create date estimates for each depth interval and the age-depth model (Figure 3.17) (Blaauw et al., 2013).

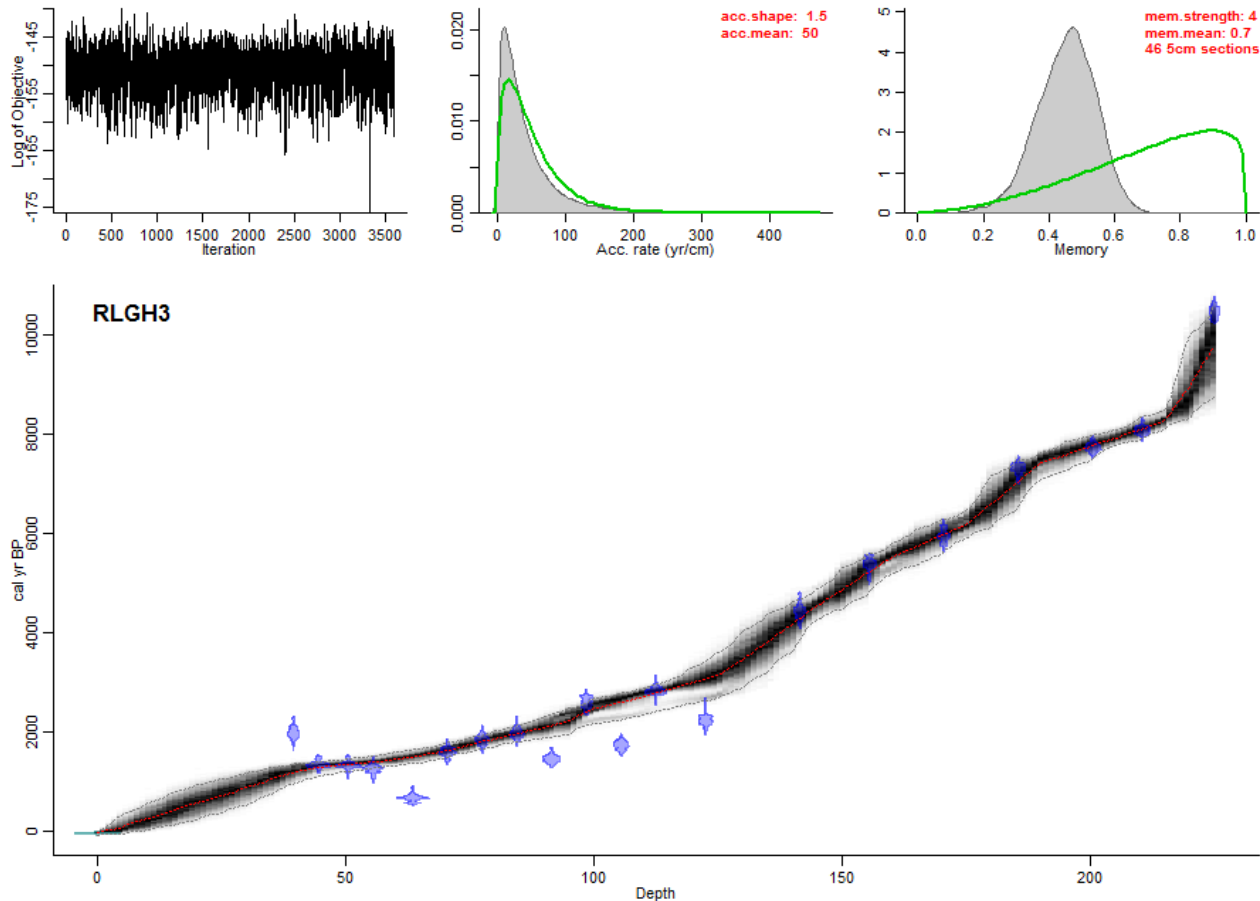


Figure 3.17: Example of Bayesian age-depth modelling in Bacon (Blaauw et al., 2013) using the in program example “RLGH3”.

3.6.2 ADVANTAGES TO AGE-DEPTH MODELLING

Age-depth modelling is advantageous to palaeoecological research because:

1. It provides robust chronologies for interpreting patterns and trends in time series data (Blaauw et al., 2012);
2. It produces probable age for sample depths without dating the entire sediment sequence (Blaauw et al., 2012);
3. It is a widely used technique (Blaauw et al., 2012);

4. All model outputs produce an age-depth model and its 95% confidence interval (Blaauw, 2010).

3.6.3 LIMITATION TO AGE-DEPTH MODELLING

Age-depth modelling can also be problematic.

1. Some age-depth models are prone to underestimating confidence intervals by not accounting for errors of radiocarbon dating and calibrated ages (Blaauw et al., 2012).
2. Models that fit data points too closely are likely “over fitting” and underestimating uncertainties (Blaauw et al., 2012).
3. Calibration errors or sediment sequences with multiple reversals will decrease the accuracy of the date and thus the age-depth model (Björck et al., 2001).
4. Different models used (i.e. linear regression, splines or linear interpolation) produce different age-depth model results (Telford et al., 2004).

Therefore caution must be employed when dating sediment, as well as, understanding the limitations of dating and age-depth models when interpreting palaeoecological results. Here I employ both classical and Bayesian age-depth modelling techniques using clam (Blaauw, 2010 Version 2.2) and Bacon (Blaauw et al., 2011). The technique selected will be dependent on site characteristics and radiocarbon dating results. Detailed methods and results of age models can be found in discussion chapters 4, 5, 6, and 7.

3.7 MICRO-X-RAY FLUORESCENCE (XRF) SCANNING

Micro-X-ray fluorescence (μ XRF) is a non-destructive analysis that applies X-ray fluorescence spectrometry to detect elemental variability (Croudace et al., 2006). Data retrieved are sedimentary indicators for organic C content, biological activity, detritus deposition, grain size, seawater inputs, erosion, contaminants, volcanic ash,

climate deterioration, rock type, mineralisation, and productivity (Croudace et al., 2006; Rothwell et al., 2006; Zuo, 2013; Croudace et al., 2015). The μ XRF scanner also provides a high-quality optical image useful for examining physical properties of sediment cores.

Some examples of μ XRF indices in palaeoecological research include: Sr/Ca ratio as an indicator of water freshening (Mischke et al., 2010); Ca/Fe ratios to indicate changes in carbonate deposition in response to climatic change (Balsam et al., 1987); Incoherence/Coherence, Br/Cl and S/Cl ratios as indicators of changes in organic productivity (Croudace et al., 2006); Fe/Mn ratios inform redox conditions such as lake anoxia (Koinig et al., 2003; Kylander et al., 2011; Augustinus et al., 2012); and Ti indicates erosion and sediment deposition (Croudace et al., 2006; Rothwell et al., 2006). Therefore, μ XRF scanning will provide geochemical information for this project to reveal changes in sediment properties and delivery, organic inputs, and chemical weathering from the surrounding catchment.

3.7.1 STANDARD METHOD OF μ XRF SCANNING

An ITRAX core scanner gathers micro-X-ray fluorescence mass spectrometry of element profiles and optical and radiographic core images (Croudace et al., 2006). The core is loaded into a cradle for scanning after core parameters (core length, core tube type etc.) are input into the initiating software. First, a surface scan is performed to create an optical and radiograph image of the core, then calibration is performed. Core details are entered into the software (core name, file storage location, scan limits and scanning resolution) before the ITRAX core scanner analyses the core for elemental data (Figure 3.18) (Croudace et al., 2006). Raw data retrieved from ITRAX core scanning requires some transformation before interpretation or statistical analysis. There are numerous ways to transform or normalise μ XRF data by: Al or Ti (Croudace et al., 2015); Incoherence/Coherence ratio (Inc/Coh) to account for water content; core tube type; central logged ratio; or total counts (kcps) (Croudace

et al., 2015). For this research, I will use the common normalisation methods of total counts (kcps) and Inc/Coh (Chapters 4, 5, 6 & 7).



Figure 3.18: ITRAX core scanner (Figure 1; Croudace et al., 2006).

3.7.2 ADVANTAGES TO μ XRF SCANNING

μ XRF is a useful tool in palaeoecological research because:

1. It produces high resolution data as fine as 200 μm (Croudace et al., 2015);
2. It collects multiple elemental signatures at once (Croudace et al., 2006);
3. It gathers imagery helpful for lithological analysis (Croudace et al., 2006);
4. The analysis is non-destructive to sediment (Croudace et al., 2006; Rothwell et al., 2006; Zuo, 2013).

3.7.3 LIMITATION TO μ XRF SCANNING

μ XRF scanning also has limitations.

1. The elemental data retrieved from μ XRF scanning are relative trends, not extract elemental quantities (Croudace et al., 2015).
2. Lighter elements down core are susceptible to water content variability causing unrelated geochemical change (Davies et al., 2015).
3. Normalisation techniques are not standardised and many scientists use different methods (Croudace et al., 2015).

For the purposes of this study elemental quantities are not necessary; elemental trends are sufficient to understand the sediment sequence. The μ XRF geochemical data in this project is used to produce a high resolution geochemical signature of past environmental change. Specific μ XRF methods and results can be found in discussion chapters 4, 5, 6, and 7.

3.8 ELEMENTAL AND ISOTOPIC CARBON AND NITROGEN ANALYSIS

Organic matter can be a large portion of lake sediments. Elements found in organic matter (carbon, nitrogen, sulphur, hydrogen, oxygen) have biosphere cycles and produce multiple isotopes that can be analysed to better understand natural environments (Peterson et al., 1987). Bioindicators Carbon (C) and Nitrogen (N) are useful indicators of production in terrestrial and aquatic environments, changes in vegetation types, soil dynamics and nutrient cycling (Birks et al., 1980; Håkanson et al., 1983; Bengtsson et al., 1986; Siegenthaler et al., 1986; Meyers et al., 2001). In palaeoecological research, measures of C and N are represented as total percent content, ratios, or isotopic signature (%C, %N, C/N, $\delta^{13}\text{C}$ and $\delta^{15}\text{N}$) and used to understand their role in the terrestrial and aquatic environment.

3.8.1 CARBON

Carbon is found in all organic matter and provides important energy sources for heterotrophic organisms (Håkanson et al., 1983). Thus organic C preserved in sediments indicate biomass, organic matter origins, and delivery routes (Meyers et al., 2001). Organic C has two sources: allochthonous (from the surrounding environment), or autochthonous (from the lake environment). In highly dystrophic environments nearly all the organic C is allochthonous (Håkanson et al., 1983; Meyers et al., 2001). Organic C is only a fraction of organic matter that escapes remineralisation during sedimentation preserved in sediment (Meyers et al., 2001). Further, organic C content can be diluted from bicarbonate and clastic sediments (Håkanson et al., 1983; Meyers et al., 2001). In Tasmanian lake sediments bicarbonate is low (Buckney et al., 1973), therefore C content will be a good indicator for organic matter. There are multiple sedimentary measures of organic matter content including: Loss-on-ignition (LOI), Total organic Carbon (TOC or %C) and μ XRF geochemical scanning. In this project, %C and μ XRF geochemistry (See Section 3.7) will be used as indicators of organic content.

Carbon has two stable isotopes, ^{12}C and ^{13}C , and their ratio ($^{13}\text{C}/^{12}\text{C}$) characterises lake processes (Siegenthaler et al., 1986). Typically, values are attributed to changes in hydrological C, C exchange between the atmosphere and lake, biological productivity, residence time of lake water, and terrestrial vegetation composition (Birks et al., 1980; Siegenthaler et al., 1986; Meyers, 1994; Meyers et al., 2001; Wolfe et al., 2001; Lamb et al., 2004). For example, increased river water lowers the $\delta^{13}\text{C}$ between -10 and -15, values will increase toward +2 if the lake and atmosphere are at equilibrium, and high biological activity will enrich ^{13}C because aquatic plants prefer the lighter C (Siegenthaler et al., 1986; Meyers et al., 2001). $\delta^{13}\text{C}$ is also a good indicator for shifts in C_3 and C_4 plants (Birks et al., 1980). Tasmania does not have many C_4 plant types (Kitchener et al., 2013), therefore trends in $\delta^{13}\text{C}$ will not track vegetation compositional changes well. Additionally, due to the dystrophic environment of many Tasmanian lakes, including the ones selected for this thesis, C is likely allochthonous making interpreting the $\delta^{13}\text{C}$ isotopic signature difficult. Pairing isotopic C signatures with C/N ratios will allow a better understanding of the dynamics of terrestrial and aquatic environments in Tasmania.

The C/N can reveal information about the terrestrial and aquatic environment of a lake (Meyers et al., 2001). The values of C/N are dependent on the organic soil composition; however, understanding the physiology of the site is important. For example, low C or N environments produce high ratios; although, lakes with high organic content dominated by humic soils will also have a high C/N ratio (Håkanson et al., 1983). In some systems C/N ratios can provide a signature of vegetation type due to different levels of cellulose in vegetation. When, compared with $\delta^{13}\text{C}$ values, the source of plant material can be determined (Meyers, 1994). Examples of C/N and $\delta^{13}\text{C}$ isotope values helpful for interpreting organic matter trends can be found in Table 3.1.

Table 3.1: List of C/N ratios and $\delta^{13}\text{C}$ values associated with different terrestrial and aquatic sources (Table 1; Meyers et al., 2001).

Organic Matter Source	Location	C/N (atomic)	$\delta^{13}\text{C}$ (‰)	Reference
C₃ Vascular Plants				
willow leaves	Walker Lake, Nevada	38	-26.7	Meyers (1990)
poplar leaves	Walker Lake, Nevada	62	-27.9	Meyers (1990)
cottonwood leaves	Grosse Ile, Michigan	31	-30.5	Meyers & Lallier-Verges (1999)
yellow poplar leaves	Ann Arbor, Michigan	33	-29.1	Meyers & Lallier-Verges (1999)
white oak leaves	Ann Arbor, Michigan	22	-29.0	Meyers & Lallier-Verges (1999)
red oak leaves	Ann Arbor, Michigan	29	-29.8	Meyers & Lallier-Verges (1999)
American beech leaves	Grosse Ile, Michigan	17	-28.3	Meyers & Lallier-Verges (1999)
European beech leaves	Ann Arbor, Michigan	17	-30.2	Meyers & Lallier-Verges (1999)
pinyon pine needles	Walker Lake, Nevada	42	-24.8	Meyers (1990)
white spruce needles	Ann Arbor, Michigan	42	-25.1	Meyers et al. (1995)
white spruce bark	Ann Arbor, Michigan	57	-23.5	Meyers et al. (1995)
white spruce wood	Ann Arbor, Michigan	163	-23.1	Meyers et al. (1995)
white pine needles	Ann Arbor, Michigan	42	-25.2	Meyers & Lallier-Verges (1999)
red pine needles	Ann Arbor, Michigan	39	-27.1	Meyers & Lallier-Verges (1999)
palm fronds	Lake Bosumtwi, Ghana	91	-25.5	Talbot & Johannessen (1992)
<i>Sphagnum</i>	Newfoundland Canada	9	-27.5	Macko et al. (1991)
C₄ Vascular Plants				
salt grass	Walker Lake, Nevada	160	-14.1	Meyers (1990)
tumbleweed	Walker Lake, Nevada	68	-12.5	Meyers (1990)
blood grass	Lake Bosumtwi, Ghana	42	-11.1	Talbot & Johannessen (1992)
wild millet	Lake Bosumtwi, Ghana	156	-10.8	Talbot & Johannessen (1992)
Soil Organic Matter				
Lake Baikal watershed	Siberia, Russia	20	-23.4	Prokopenko et al. (1993)
Willamette valley	Oregon, USA	13	-26.2	Prahl et al. (1994)
peat bog	Washington, USA	17	-28.7	Ertel and Hedges (1984)
Lake Algae				
mixed plankton	Lake Baikal, Russia	9	-30.9	Prokopenko et al. (1993)
mixed plankton	Walker Lake, Nevada	8	-28.8	Meyers (1990)
mixed plankton	Pyramid Lake, Nevada	6	-28.3	Meyers (1994)
mixed plankton	Lake Michigan	7	-26.8	Meyers (1994)
mixed plankton	Lake Biwa, Japan	7	-27.5	Nakai & Koyama (1987)
Lake Surface Sediments				
Lake Biwa	Honshu, Japan	6	-25.3	Meyers & Horie (1993)
Lake Ontario	North America	8	-26.2	Hodell & Schelske (1998)
Lake Michigan	North America	8	-26.3	Rea et al. (1980)
Walker Lake	Nevada, USA	8	-24.2	Meyers (1990)
Baldeggersee	Switzerland	8	-33.1	Teranes & Bernasconi (unpub.)
Lake Baikal	Russia, Siberia	11	-29.9	Qiu et al. (1993)
Lake Bosumtwi	Ghana, Africa	14	-26.4	Talbot & Johannessen (1992)

3.8.2 NITROGEN

Nitrogen is essential to life and is often a limiting nutrient (Talbot, 2001). Inorganic and organic N occurs in a variety of forms and are cycled through the environment by a series of oxidation stages. Therefore the N biogeochemical cycle is incredibly complex (Figure 3.19) and interpreting the trends in N indicators in palaeoecology can be challenging (Meyers et al., 2001; Talbot, 2001). In palaeoecology, N content is either expressed by total percent N, or C/N, typically referring to the source of organic N. Whereas isotopic N ($\delta^{15}\text{N}$) values are used to infer biological processes and production (Talbot, 2001). Total percent N contains both organic and inorganic forms of N, and the components that make up the organic content (such as aquatic plants and algae vs. terrestrial vegetation and soils) will have differing amounts of N. For example, phytoplankton are rich in N while terrestrial vegetation have relatively low N. N-fixing microorganisms in soils can increase nutrient enrichment (Talbot, 2001).

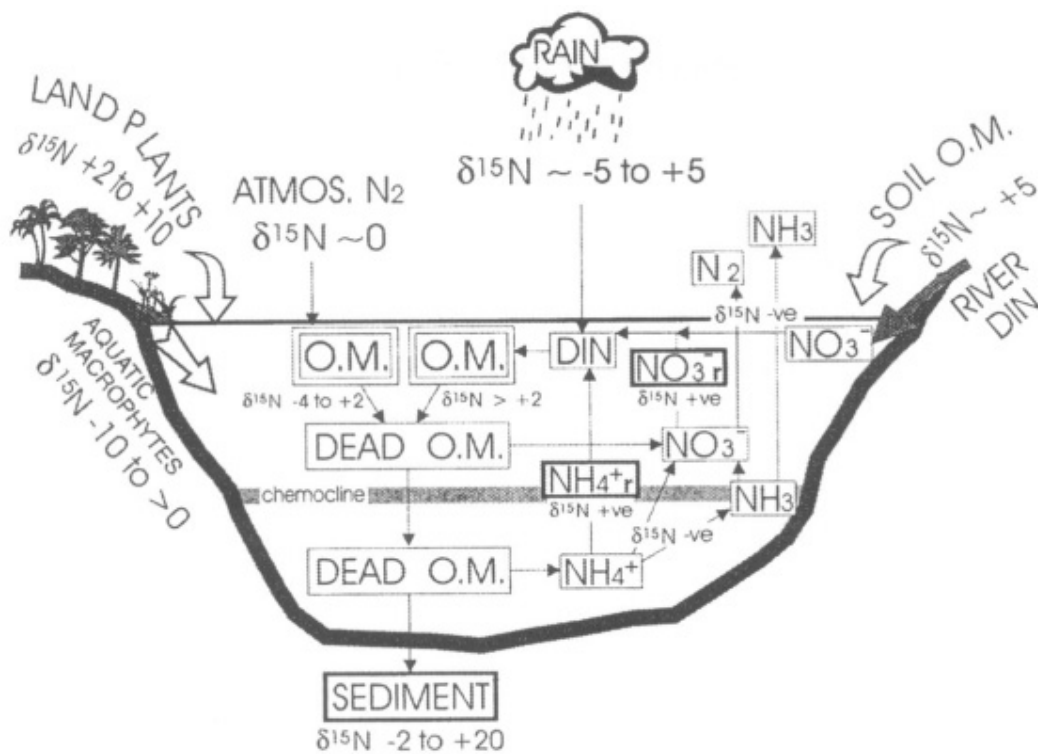


Figure 3.19: Schematic of the Nitrogen cycle (O.M.= organic matter and DIN= dissolved inorganic Nitrogen) (Figure1; Talbot, 2001).

Isotopic N is particularly useful for understanding changes in available N for aquatic organisms. $\delta^{15}\text{N}$ values identify organic sources of N through trends in the $^{15}\text{N}/^{14}\text{N}$ (Meyers et al., 2001). $\delta^{15}\text{N}$ values represent the dissolved NO_3^- (used by aquatic plants and algae) and atmospheric N_2 (used by terrestrial vegetation). The difference between these two sources make up the preserved N in the $\delta^{15}\text{N}$ values (Meyers et al., 2001; Juggins et al., 2012). Algae prefer to consume the lighter isotope (^{14}N) of inorganic N and when available ^{15}N becomes enriched and the $\delta^{15}\text{N}$ values will increase. This phenomenon is known as the Rayleigh distillation (Meyers et al., 2001; Talbot, 2001). Trends in $\delta^{15}\text{N}$ values can indicate algal productivity (Talbot et al., 2000), terrestrial N inputs (Talbot, 2001), and precipitation (Hobbie et al., 2012). However, trends in can be misinterpreted on account of the activity of N-fixation, terrestrial plants, or trophic level (Howarth et al., 1988; Meyers et al., 2001; Talbot, 2001; Vander Zanden et al., 2001).

3.8.3 STANDARD METHOD

A coupled Elemental Analyser and Isotope Ratio Mass Spectrometer is used to determine the elemental and isotopic C and N (Figure 3.20). Carbonates are a problem when determining $\delta^{13}\text{C}$ and C/N ratios in sediments, therefore samples high in carbonates are not recommended for this type of analysis. Small amounts of carbonates can be removed by reacting sediments with HCl. After pre-treatment of HCl, samples are dried (by either a convection oven or freeze-drying) and ground into a homogenous powder. The dried samples are weighed into aluminium cups and sealed to be analysed.

The elemental analyser uses flash combustion at 1,700-1,800°C in an oxidising atmosphere to determine C and N content of the organic matter. After combustion, a vacuum transfer system isolates CO_2 and N_2 gas for isotopic analysis in the mass spectrometer. A molecular sieve is very important to isotopic N analysis, assisting with gas release into the mass spectrometer. Without this sieve isotopic fractionation transpires too early and results in

potential errors (Meyers et al., 2001; Talbot, 2001). Figure 3.20 demonstrates the element analyser and mass spectrometer apparatus.

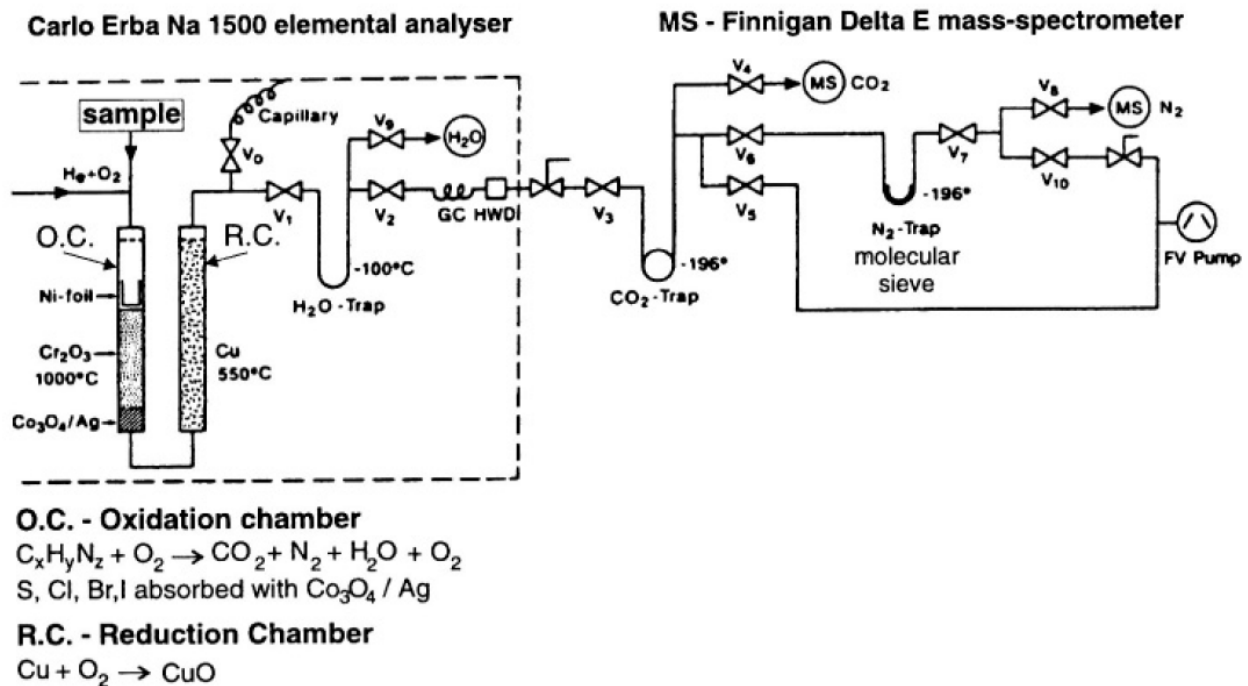


Figure 3.20: Schematic of C and N elemental and isotopic analysis apparatus and method (Figure 2; Talbot, 2001).

Data collected from C and N analysis requires normalisation before interpretation. Organic C and N content are normalised to a commercial certified reference standard and isotopic results are normalised to International Atomic Energy Agency (IAEA) reference material (Böhlke et al., 1995; Gonfiantini et al., 1995; Le Clercq et al., 1998).

3.8.4 ADVANTAGES TO CARBON AND NITROGEN ORGANIC PROXIES

There are a number of advantages to using C and N elemental and isotopic signatures in palaeoecological data.

1. They provide signatures for both terrestrial and aquatic environments (Siegenthaler et al., 1986; Meyers et al., 2001).

2. They indicate organic matter content, as well as, the source of material (Siegenthaler et al., 1986; Meyers et al., 2001; Talbot, 2001).
3. Despite repositioning of organic C and N, their isotopes maintain their signature with minimal error (Meyers et al., 1993; Meyers, 1994).

3.8.5 LIMITATIONS TO CARBON AND NITROGEN ORGANIC PROXIES

Some limitations of C and N elemental and isotopic analysis include:

1. Sites with low algal productivity compared to organic C inputs can be problematic for $\delta^{13}\text{C}$ interpretation because the sediment loses C in post-deposition (Meyers et al., 2001);
2. C/N values are guidelines not discrete boundaries. Within lake processes, limited N and aquatic composition, can alter these values (Meyers et al., 2001);
3. Diagenetic processes can alter isotopic signatures, particularly $\delta^{15}\text{N}$ ratios, because N rich compounds decompose rapidly after death (Talbot, 2001);
4. Inorganic N from non-organic sources can contaminate bulk N samples (Talbot, 2001);
5. N released by diatoms during diagenesis can alter isotopic N composition (Talbot, 2001; Wolfe et al., 2001).

In the selected sites for this project elemental and isotopic C and N are used to decipher important the landscape and within lake nutrient processes. Detailed methods and results of C and N analysis can be found in discussion chapters 5, 6, and 7.

3.9 PALYNOLOGY

Palynology (pollen and spore analysis) is a widely used palaeoecological technique for determining chronology, vegetation dynamics and climate change (Birks et al., 1980; Berglund, 1986b; Bennett et al., 2001). Pollen and spores are the sexual part of plants produced by angiosperms, gymnosperms and ferns. Pollen and spores possess a highly resistant layer called the exine, made of cellulose and sporopollenin that is highly resistant to chemical and physical degradation under certain sedimentary conditions, allowing indefinite preservation. Pollen and spores vary in shape, size (from 10-200 μm), and texture that allows identification to family, genus or species level under a light microscope (Figure 3.21) (Faegri et al., 1989; Bennett et al., 2001). Palynology provides valuable information of past vegetation dynamics and climate change.



Figure 3.21: Photograph of pollen grains, *Amperea xiphoclada* and Ericaceae (TAS1401 N1), under a light microscope at 400x magnification (by: Kristen Beck, 2015).

3.9.1 STANDARD METHOD

Pollen processing follows standard methods by Faegri and Iversen (1989). Approximately 0.5 mL of sediment is treated with several chemical digestions to prepare microscope slides for pollen identification (Figure 3.22). First the samples are treated with hot 10% KOH to remove humic acid and deflocculate the sediment. Next the sample is sieved (180 μm) to remove any coarse material. A small sieve is not used for Tasmanian sediments because small pollen grains such as *Eucryphia* spp. (<10 μm) may be lost. A known number of exotic pollen grains (*Lycopodium* spp.) is added, in the form of a tablet, to the sample with 10% HCl and heated to assist in dissolving the exotic pollen tablet, as well as, remove any calcium carbonate material. Next, 48% HF is added and heated to remove any inorganic material, mainly silica. Following this step, glacial acetic acid is used to rinse the sample before acetolysis because this solution reacts violently with water. Acetolysis solution (1-part sulphuric acid and 9-parts acetic anhydride) is then added and heated for a short period to remove any unwanted organic material and polysaccharides present on the outside of the pollen grains. A repeat of the glacial acetic acid rinse is followed by tert-butyl alcohol (TBA). TBA is used to wash the sample into an archive vial and will evaporate out of the mounting medium. The mounting medium used in this research is glycerol. Once added to the sample and stirred, a pollen slide can be prepared (Berglund, 1986b; Faegri et al., 1989; Bennett et al., 2001).

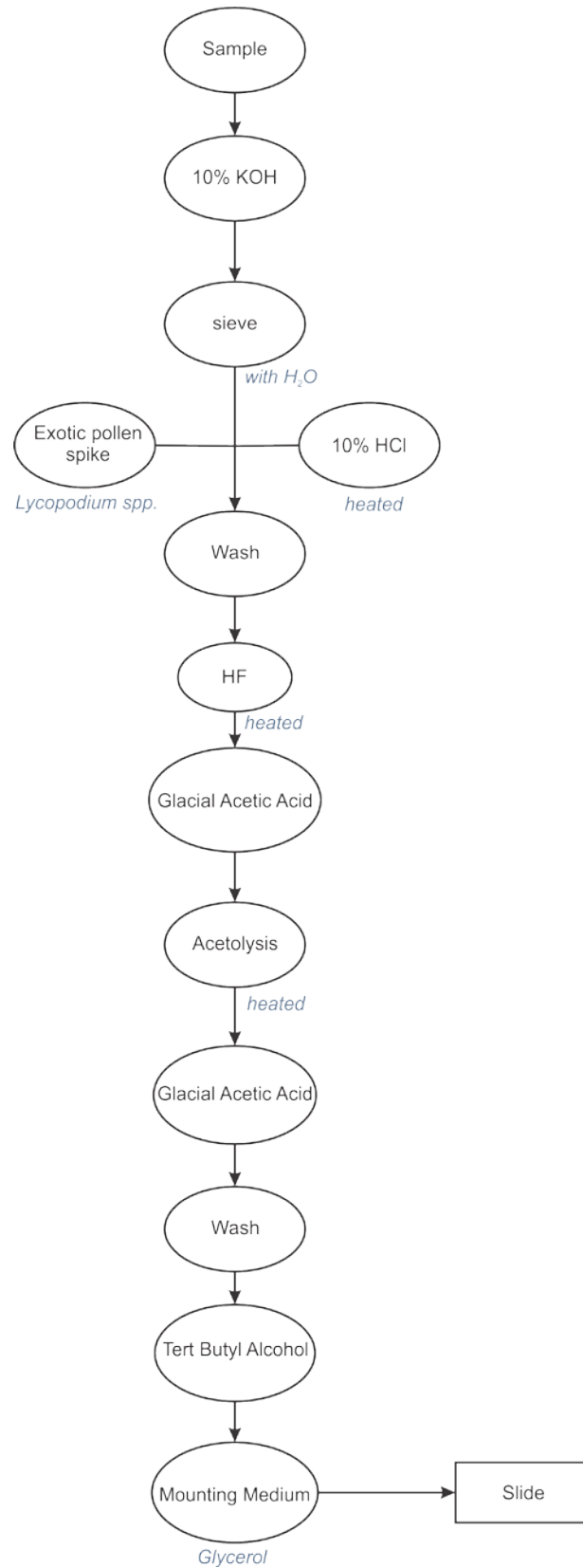


Figure 3.22: Flowchart of pollen processing, specific to the University of Melbourne Protocol (Berglund, 1986b; Faegri et al., 1989).

Pollen is identified at 400x magnification using a bright field objective on a light microscope. In palaeoecological research, typically 300 terrestrial pollen grains are identified. Taxonomy for this research will be determined using reference collections from: the University of Melbourne, the University of Tasmania, Macphail's personal collection, and the Newcastle Pollen collection (Hopf et al., 2002). Pollen data is presented as a percentage of the terrestrial pollen sum, while percentage aquatic and spore pollen are based on the supersum inclusive of all pollen and spores. The *Lycopodium* spp. spike is used to determine the accumulation rates using concentration values divided by depositional time. Detailed methods and results of pollen processing and analysis can be found in discussion chapters 4 and 7.

3.9.2 ADVANTAGES TO PALYNOLOGY

Pollen has a number of characteristics that are well suited to palaeoecological research.

1. Pollen is highly abundant and well preserved in anaerobic environments (Birks et al., 1980; Bennett et al., 2001).
2. It mixes in the atmosphere to produce a uniform pollen rain (Bennett et al., 2001).
3. They are identifiable by microscopy with reasonably well defined taxonomy at an international standard (Berglund, 1986a).
4. Pollen is correlated to surrounding vegetation when extracted at a known space and time (Birks et al., 1985; Bennett et al., 2001).

3.9.3 LIMITATION OF PALYNOLOGY

Palynology also has several limitations.

1. Taxonomic uncertainty – some pollen grains can only be identified to genus or family and trends may be lost from species level (Bennett et al., 2001). For example, *Eucalyptus* spp. pollen can only be identified to genus level even though there are hundreds of different species of *Eucalyptus* in Australia (Atlas of Living Australia, 2016).
2. Difficult to control source of signal – pollen can travel large distances, thus, the origin of the pollen rain can be difficult to constrain. However, good site selection can assist in controlling the local or regional signals (Prentice, 1985; Berglund, 1986a; Sugita, 1993; Bunting et al., 2004).
3. Pollen analysis assumes quantity and dispersal of grains is uniform but this is not true of pollen dispersal (Birks et al., 1980; Birks et al., 1985; Faegri et al., 1989; Bennett et al., 2001).

There are a number of pollen records from Australia that highlight the responsiveness of vegetation systems in this region to environmental change over a range of timescales (Shulmeister et al., 1995; Harle et al., 1999; Haberle, 2005; Williams et al., 2009; Fletcher et al., 2014a). Importantly, Australian palynology research has revealed that vegetation is highly sensitive to the influences of fire and changing climate (Shulmeister et al., 1995; Fletcher et al., 2007a; Williams et al., 2009; Fletcher et al., 2012), justifying the use of this proxy to address indirect climate response research questions of this project.

3.10 DIATOMS

Diatoms are an important indicator of aquatic ecosystem change. They are sensitive to a number of chemical and physiological lake characteristics, and species assemblages can provide both qualitative and quantitative measures of changes in past lake conditions (Battarbee, 1986; Battarbee et al., 2001). Diatoms are unicellular yellow brown

algae under the division Bacillariophyta. They have a siliceous cell wall (frustule) made up of two identical halves (valves) that preserves in lake sediments (Birks et al., 1980; Battarbee et al., 2001). These valves have intricate patterns, unique to each species (Figure 3.23). Diatoms can be solitary or exist in colonies (*Aulacoseira* spp., *Fragilaria* spp. and *Tabellaria* spp.) and generally have two potential habitats: planktonic or benthic (Battarbee et al., 2001).



Figure 3.23: Photograph of *Eunophora tasmanica* under a light microscope at 1000x magnification (TAS1508 N1E) (by: Kristen Beck, 2016).

Diatoms are short-lived organisms that rapidly respond to number of within-lake environmental conditions such as: trophic status, productivity, pH, water quality, and salinity (Birks et al., 1980; Battarbee, 1986; Dixit et al., 1992; Battarbee et al., 2001). Therefore, their autoecologies can be linked to external drivers and often used to reconstruct past lake environments. For example, shifts in planktonic to benthic habitat or salinity can reveal changes in lake level (Fritz et al., 1993; Gasse et al., 1997; Battarbee, 2000; Tibby et al., 2007a; Saunders, 2011). Changes in acidity can track the succession of vegetation on the landscape (Engstrom et al., 2000; Fritz et al., 2013; Law et al., 2015). As well, trophic status can determine changes in nutrient inputs (Engstrom et al., 2006; Moos et al., 2009; Bennion et al., 2015).

3.10.1 STANDARD METHOD

Diatom processing follows standard methods by Battarbee (1986) to digest sediments for microscope slide preparation. Samples of 0.5 mL react with 30% hydrogen peroxide to remove organic matter from the sediment. If the reaction is not too vigorous the samples can be heated in a hot bath to speed up the process. If samples contain carbonates they first need to be treated with hot 10% HCl; however, carbonates are not typically present in Tasmanian sediments. Hydrogen peroxide can be continually added in small amounts (~5 mL) until there is no more reaction. Once all the organic matter is removed, the samples are washed a few times before a stock dilution is made with a known concentration of sample to water. A known dilution of sample is then evaporated onto a cover slip and mounted with Naphrax® to prepare a slide. Slides are examined using a DIC oil immersion objective and identified at 1000x on a light microscope. At least 300 diatom valves are identified per slide following standard methods. Taxonomy of diatoms from Tasmanian lakes will be determined using the following literature: Foged (1978); Krammer et al. (1986, 1988, 1991b, 1991a); Haworth et al. (1993); and Vyverman et al. (1995); Sabbe et al. (2001); Kilroy et al. (2003); Kociolek et al. (2004); Vanhoutte et al. (2004). Full cover slip transects need to be identified for diatoms to calculate a known volume of counted material to determine diatom concentration (equation below).

$$\text{Total valves} = \# \text{ of diatoms counts} \times \frac{\text{coverslip area}}{\text{area counted}} \times \frac{\text{sample volume}}{\text{subsample volume}}$$

Diatom species data can be presented as percentages of the total diatom species assemblage, sample concentration, or fluxes. More detailed methods and results of diatom processing and analysis can be found in discussion chapters 6 and 7.

3.10.2 ADVANTAGES TO DIATOM ANALYSIS

A number of characteristics predispose diatoms to be an effective proxy of aquatic ecosystem change.

1. High abundance and good preservation in most aquatic environments (Hall et al., 1992; Reid et al., 1995; Stoermer et al., 1999; Smol et al., 2000).
2. Well-developed diatom ecology and taxonomy (Hustedt, 1930-1966; Foged, 1978; John, 1983; Krammer et al., 1986, 1988, 1991a, b; Round, 1993).
3. High sensitivity and rapid responders to changes in environmental conditions (Dixit et al., 1992; Hall et al., 1992; Fritz et al., 1993; Reid et al., 1995; Stoermer et al., 1999; Smol et al., 2000).

3.10.3 LIMITATIONS TO DIATOM ANALYSIS

Diatoms are not without limitations.

1. Diatoms can be subject to dissolution. Generally diatoms preserve well in cold soft water in the mid- to high latitudes, and have poorer preservation in warm, alkaline, or saline waters or from low latitude lakes (Battarbee et al., 2001; Ryves et al., 2009).
2. Excessive species diversity. Environments easily contain over 100 diatom taxa, additionally some diatom species ecology remains poorly understood (Battarbee, 1986; Vanormelingen et al., 2008).
3. Taxonomy is incomplete, particularly in Australia (Vyverman et al., 2007; Vanormelingen et al., 2008).
4. Problems with taphonomy. Unknown movement of a fossil from the time the organisms dies to when the fossil is discovered, as well as, differential preservation (Battarbee et al., 2001).

Even though, taxonomy and ecology of Tasmanian diatoms is limited, diatoms have proven to be useful indicators for aquatic ecosystem response to environmental changes (Hodgson et al., 1996; Hodgson et al., 2000; Vyverman et al., 2007; Saunders et al., 2012) and the research questions of this project. Using diatoms in this research will also advance the application of diatoms in Australian palaeoecological research.

3.11 CLADOCERANS

Cladocerans are another useful indicator of aquatic ecosystem change in palaeoecological research because they preserve in lacustrine sediment and are sensitive to climate, food web dynamics, trophic status, disturbance, water chemistry, and watershed processes (Frey, 1986; Korhola et al., 2001). Cladocerans are zooplankton under the class and order *Branchiopoda Cladocera*. They are small (<1 mm) grazing aquatic crustaceans and can be herbivorous or carnivorous. They are diverse and occupy niche aquatic habitats (littoral or planktonic) with preferred substrate such as vegetation, rock, mud sand or open water (Korhola et al., 2001). Cladocerans reproduce asexually and sexually. Under stress they reproduce sexually by laying resting eggs called ephippia. Ephippia are highly resistant and preserve in sediments along with the body parts of the cladocerans (Frey, 1986; Korhola et al., 2001). After the zooplankton die they moult their exoskeleton made up of carapaces, post-abdomens, claws, mandibles, antennae and head shields (Figure 3.24). These parts contain chitin which is very resistant to decay and degradation, allowing cladoceran body parts to fossilise in the sediment (Frey, 1986; Korhola et al., 2001).

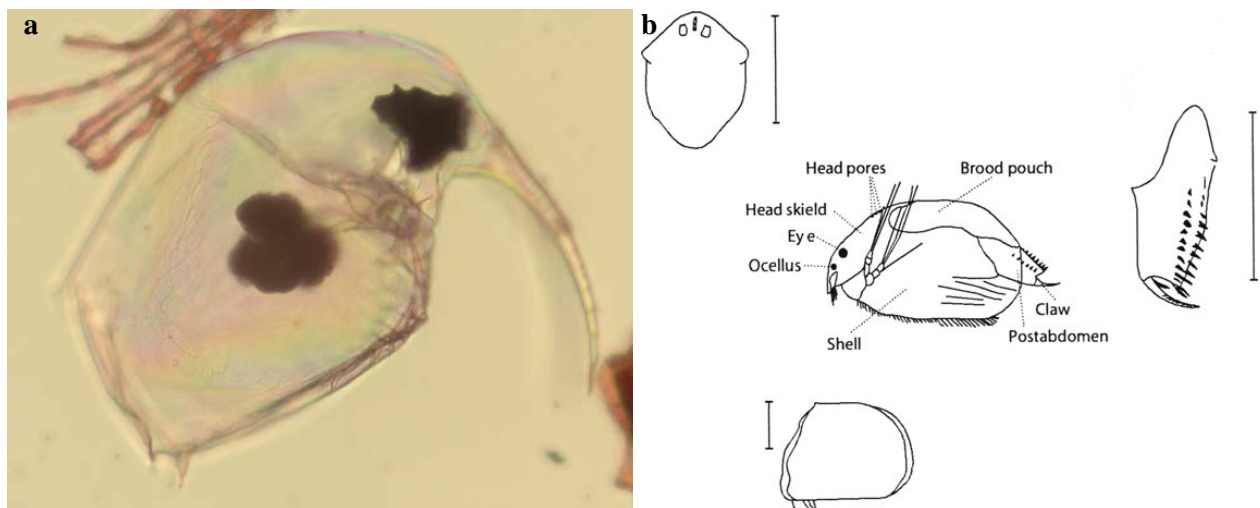


Figure 3.24: Photograph of preserved cladoceran *Bosmina meridionalis* on the left from Paddy's Lake under light microscope at 630x magnification (TAS1401 N1) (by: Kristen Beck, 2015). On the right a sketch of important cladoceran body parts that preserve in sediment (Figure 2; Korhola et al., 2001).

Similar to diatoms, cladoceran species are sensitive to a variety of environmental factors and can be used in palaeoecological research. Their assemblages have been used to reconstruct changes in temperature (Lotter et al., 1997), lake level (Hofmann, 1998), changes in food web dynamics (Battarbee, 2000) and lake nutrient status (Kamenik et al., 2007). Though using cladocerans remains in palaeoecological research is fairly new to the Australasian region, work from Victoria, Australia (Ogden, 1997, 2000; Kattel et al., 2015) and New Zealand (Kattel et al., 2010) demonstrate the potential of these aquatic indicators for reconstructing past environmental change.

3.11.1 STANDARD METHOD

Cladocerans processing follows standard methods by Frey (1986) for slide preparation. A 1.25 mL sample is digested in 100 mL of 10% KOH and heated for 45 minutes to remove humic material. The sample is then sieved with a 38 μm mesh to remove any fine material. Instead of determining concentration by dry sediment mass (Frey, 1986), an exotic pollen spike, similar to pollen analysis (Faegri et al., 1989), is used to determine concentration. Following the pollen spike, the sample is stained with safranin and evaporated on a cover slip. The dried sample is mounted with glycerol jelly for slide preparation. Cladoceran remains are examined using a light microscope bright field objective at 100x magnification. Typically a total of 200 cladoceran individuals are identified per sample; however, 100 individuals are sufficient with low diversity. The literature used to identify cladoceran species in this research includes: Alonso, 1996; Brehm, 1953; Shiel and Dickson, 1995; Shiel, 1995; and Szeroczyńska and Sarmaja-Korjonen, 2007. More detailed methods for cladoceran analysis can be found in discussion Chapter 5.

3.11.2 ADVANTAGES OF CLADOCERAN ANALYSIS

Cladocerans are an excellent proxy for palaeoecological research because:

1. They have good preservation. All cladoceran species leave some sort of remains that can preserve (Frey, 1986);
2. Distinct microhabitats and ecological niches allow inference of changing environments (Kattel, 2012);
3. Rapid ecological responses due to short life span (Frey, 1986; Korhola et al., 2001; Kattel, 2012);
4. Presence in many aquatic environments (Korhola et al., 2001).

3.11.3 LIMITATIONS TO CLADOCERAN ANALYSIS

There are limitations to the use of cladocerans as a proxy for palaeoecological research.

1. Not all cladocerans preserve equally in sediments; some species have better preservation of more body parts than others (Korhola et al., 2001).
2. There can be issues with distribution and abundance of remains due to bioturbation, lake morphology, water depth and movement (Whiteside et al., 1988; Korhola et al., 2001).
3. Taxonomic diversity can be lost in identifying cladoceran remains (Whiteside et al., 1988) and is incomplete, particularly in Australia.

Limited cladoceran research in Australia has been performed; however the use of cladocerans as a palaeoecological indicator was successful in Australia and New Zealand (Ogden, 1997, 2000; Kattel et al., 2010; Kattel et al., 2017). Cladocerans will reveal aquatic ecosystem response to environmental change and address the research questions in this project, as well as, advance the use of cladocerans as palaeoecological proxies in Australia.

3.12 CHARCOAL

Charcoal is a useful proxy in palaeoecological research for reconstructing past fire regimes and climate (Whitlock et al., 2001). Fire is limited by fuel, ignition, and climate (Parisien et al., 2009; Bowman et al., 2011; Murphy et al., 2013). In western Tasmania fire is likely limited by climate due to abundant fuel and ignition by Aboriginal burning practices for >40,000 years (Bowman et al., 1986a; Bowman et al., 2011). This is confirmed by antecedent evidence that rainfall is a key determinant of fire in Tasmanian rainforest (Styger et al., 2015).

Charcoal is produced by the incomplete combustion of organic matter at temperatures between 280-500°C. Hotter temperatures turn organic matter into ash, while lower temperatures scorch the plant material but do not produce charcoal (Figure 3.25) (Whitlock et al., 2001). Sediments with abundant charcoal fragments can provide a measure of past fire events in a given region (charcoal source area), the size of which can be inferred from the charcoal particle size being analysed (Whitlock et al., 1996; Whitlock et al., 2001; Mustaphi et al., 2014).

Charcoal is deposited into archive records by air or water with two key sources: (1) primary - deposits from current fire event; and (2) secondary - charcoal that has been introduced during non-fire events (Whitlock et al., 2001). Particle size can indicate local or regional fire activity where particles >1000 µm travel very short distances, and particles <100 µm can travel at least 100 m (Whitlock et al., 2001).

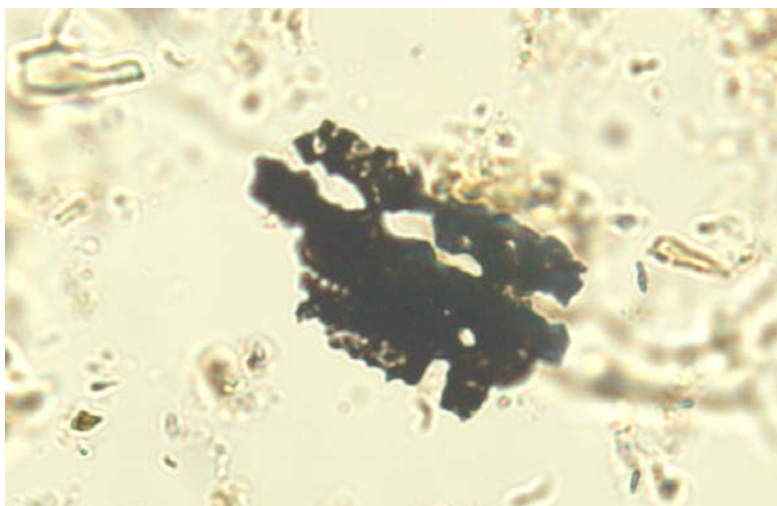


Figure 3.25: Photography of microscopic charcoal fragment under a light microscope at 20x magnification (TAS1508 N1C) (by: Kristen Beck, 2016).

3.12.1 STANDARD METHOD

Charcoal is processed using similar methods as described by Whitlock and Larsen (2001). Charcoal fragments are found on pollen slides, termed microscopic charcoal, are $<100\ \mu\text{m}$ in size and indicators of regional fire trends. These charcoal fragments are enumerated and accumulation rates are determined by methods similar to pollen (See Section 3.9.1). Macroscopic charcoal (particles $>100\ \mu\text{m}$) are enumerated separately and generally indicative of local fires. To process macroscopic charcoal, 1.25 mL of sediment is soaked in household bleach for one week to remove neighbouring organic material, then sieved through a $250\ \mu\text{m}$ and $125\ \mu\text{m}$ mesh and enumerated above $>250\ \mu\text{m}$ and between $250\text{-}125\ \mu\text{m}$ using a dissecting light microscope at 20x. Accumulation rates and charcoal peaks are determined in CharAnalysis (Higuera, 2009).

CharAnalysis is an analytical program designed to determine local fire history from sediment charcoal records. CharAnalysis provides several outputs of useful charcoal proxy data such as charcoal concentration, accumulation, peaks, magnitude, background charcoal, and fire return interval (Table 3.2). The outputs provide interpretation of locality and frequency thresholds of fire from sediment records (Higuera, 2009). More detailed methods on charcoal analysis can be found in discussion chapters 4, 5, 6 & 7.

Table 3.2: CharAnalysis outputs and definitions (Whitlock et al., 2001; Higuera, 2009).

CharAnalysis Outputs	Definition
Charcoal concentration	Interpolated charcoal concentration.
Charcoal accumulation rates	Interpolated charcoal accumulation rate.
Background charcoal	Lower-frequency charcoal accumulation often indicating changes in fuel availability.
Charcoal peak	Detrended charcoal, high frequency charcoal or a significant fire event.
Threshold value	Value to determine significant peaks in charcoal determined by modern calibration.
SNI index	Signal to noise index.
Peaks of significance	Determined by events above a threshold.
Peak magnitude	Size of charcoal peak exceeding the threshold value.
Mean fire return interval	Average time between fires.

3.12.2 ADVANTAGES TO CHARCOAL ANALYSIS

Charcoal analysis is a useful proxy in palaeoecology because:

1. It provides fire histories for longer time frames than dendrochronology (Whitlock et al., 2001);
2. It links fire history and climate change (Fletcher et al., 2015; Rees et al., 2015);
3. It can indicate the size, distribution, and location of past fire events (Whitlock et al., 1996; Whitlock et al., 2001).

3.12.3 LIMITATIONS OF CHARCOAL ANALYSIS

Limitations to charcoal analysis include:

1. Secondary charcoal can contaminate samples from non-fire periods (Whitlock et al., 2001);
2. Debated as to whether fire intensity or magnitude can be determined. Charcoal is most useful as an indicator of the presence or absence of fire events (Higuera, 2009);
3. Lack of consensus on a standardised method (Whitlock et al., 2001);

4. CharAnalysis does not differentiate the charcoal sizes to provide differences in regional or local charcoal (Higuera, 2009).

Even though there are limitations to charcoal analysis, the trends can be used to determine hydroclimate signals in Tasmania (Fletcher et al., 2015; Rees et al., 2015). In this thesis, fire history will be a useful metric for hydroclimate and understanding the aquatic ecosystem response to changing climate over the Holocene.

3.13 STATISTICAL METHODS AND DATA ANALYSIS

Statistical analyses appropriate to this project include: (1) Cluster analysis (CONISS); (3) Ordinations; (4) Lead and lag analysis; (5) Regime shift analysis; (6) Rate-of-change analysis; and (7) Generalised additive models.

Many statistical methods for time series data require even time steps. This is problematic for palaeoecological data because the results are rarely spaced evenly in time. Thus, many statistical methods require manipulation before analysis (such as interpolation or binning). Interpolating to even time steps uses functions (i.e. linear or smoothing) to determine a value between two time intervals (Birks, 2012c). However, interpolating time series data can unintentionally cause false correlations and remove important trends (Schulz et al., 1997; Dakos et al., 2012; Carstensen et al., 2013). Binning is typically a better method for creating even time steps as it takes averages of the data in selected time periods; however, it produces the coarsest resolution within the time series. Either method always results in a loss of data (Birks et al., 2006) and therefore, manipulating time series data can be problematic and should be avoided when possible.

3.13.1 CLUSTER ANALYSIS (CONISS)

Cluster analysis is commonly used in palaeoecology to determine stratigraphically constrained ecological groupings. It uses a dissimilarity coefficient to group data based on how much samples differ (Juggins et al., 2012; Legendre et al., 2012a). The most used metrics of dissimilarity employed in palaeoecology are Euclidean, Chord, Bray-Curtis, Hellinger distance, or Ward's method (Juggins et al., 2012). The constrained incremental sum of squares (CONISS) method is commonly used to identify shifts between ecological groups through time while maintaining the stratigraphy (Grimm, 1987; Legendre et al., 2012a). CONISS will be the method used in this research to determine ecological groupings.

3.13.1.1 Advantages to Cluster Analysis (CONISS)

CONISS cluster analysis is a useful palaeoecology analytical tool for several reasons.

1. It summarises stratigraphic patterns (Birks, 2012a).
2. CONISS stratigraphically constrains data (Grimm, 1987; Juggins et al., 2012).
3. CONISS maximises the similarity and dissimilarity between groups (Grimm, 1987; Juggins et al., 2012).

3.13.1.2 Limitations to Cluster Analysis (CONISS)

Some limitations of using CONISS cluster analyses are:

1. Visually heterogeneous data do not cluster well (Juggins et al., 2012);
2. CONISS can create groups that are not particularly viable, i.e. groups of one sample depth (Birks, 2012a);
3. CONISS does not necessarily cluster with the minimum variance possible and cannot change original clusters formed (Grimm, 1987; Juggins et al., 2012);
4. Ward's method can superimpose group structures that may not exist (Grimm, 1987; Juggins et al., 2012).

The results from CONISS can be further strengthened by performing a broken stick model to determine the number of significant groups. A broken stick model is a piece-wise regression model where the total variance of a dataset is represented by one length. The test operates by creating random break points along the length and if the variance of the groups represented by the random break points exceeds the variance of the dataset the group is considered significant (Birks, 2012d; Birks, 2012a). This test is recommended to determine significant number of ordination axes as well (Oksanen et al., 2016). The cluster analysis and broken stick model statistical tests will be employed to determine important ecological groupings through time (zones) of the various palaeoecological records of this project.

3.13.2 ORDINATION ANALYSIS

Ordination analyses are statistical methods used to reveal patterns in multivariate data and summarise complex relationships in two-dimensional space (Juggins et al., 2012; Legendre et al., 2012b). This statistical technique will be important to reveal relationships among and between proxy data. There are several ordination techniques commonly used in palaeoecology, with the most common being principal component analysis (PCA) (Rull, 1991; Korhola et al., 1996; Finkelstein et al., 2006; Juggins et al., 2012; Legendre et al., 2012b).

3.13.2.1 Principal Component Analysis

Principal component analysis (PCA) is an ordination that uses linear regression models or vectors to interpret directional variability in the multidimensional space of a dataset. PCA axis scores are determined by directional distance between data points using Euclidean distances and statistical strength of ordination axes use eigenvalues to measure explained variance (Hotelling, 1933; Juggins et al., 2012; Legendre et al., 2012b). PCA do not always capture the most important trends in compositional data due to long or dominant gradients (Simpson et al., 2012;

Bennion et al., 2015). Thus, when multivariate data demonstrates long gradients (three or more standard deviation units) Correspondence analysis (CA) or principal curves (PrCs) are more appropriate (Legendre et al., 2012a).

3.13.2.2 Detrended Correspondence Analysis

Detrended correspondence analysis (DCA) are typically more appropriate for ecological data because CA assumes a unimodal distribution, unlike PCA, which uses linear relationships to describe species' responses (Juggins et al., 2012; Legendre et al., 2012b). DCA estimates compositional change using chi-square distances to interpret differences between data to remove arch effects and edge effects (Juggins et al., 2012). Arch effects create highly skewed data by forcing data into a normal distribution. This typically indicates the gradient length is too long and other ordination methods are more appropriate (Legendre et al., 2012b). Proportional species data is distributed by non-linear rescaling using a unimodal weighted average approach (Legendre et al., 2012b).

Detrending by segment and non-linear rescaling estimates the DCA gradient length, expressed by standard deviation units. If the standard deviation is <2.5 the assemblage has a narrow variance and PCA is more appropriate (Legendre et al., 2012b). Detrending by segments, however, is an arbitrary method with no theoretical justification and the assumptions behind the nonlinear rescaling method have not been fully substantiated (Birks, 2012b; Legendre et al., 2012a). When working with species data, it is important to down weight the importance of rare taxa in the DCA (Hill et al., 1980; Juggins et al., 2012).

3.13.2.3 Principal Curves

Alternatively, principal curves (PrC) are another type of ordination analysis used to identify the most important trends in the multivariate time series data, particularly when gradient lengths are long causing arch effects (Simpson et al., 2012). PrC use linear relationships, the same metrics as a PCA, but data is fit with curves in multiple dimensions, thus, representing the optimal trend and most explained variance in the data (De' ath, 1999; Legendre et al., 2012b; Simpson et al., 2012). Species response is explained by smooth functions along the PrC

gradient, then fit similarly to PCA (De' ath, 1999). PrC penalise models that are too complex or overfit the data creating a trade-off between goodness-of-fit and the number of parameters within the model (Birks, 2012d). A penalty setting of 1.4 is recommended, ideal for fitting of the PrC to ecological data (pers. comm. Gavin Simpson). PrC typically outperform PCA and DCA >70% of the time (De' ath, 1999).

3.13.2.4 Advantages to Ordination Analyses

Ordinations are useful tools in palaeoecological research because:

1. They summarise trends in datasets with multiple variables in a few axes (Legendre et al., 2012b);
2. They constrain the sample (age-depth) to detect major patterns and variation (Birks, 2012a);
3. They are useful for comparing sites with differing stratigraphic sequences (e.g. diatoms vs. cladocerans) (Birks, 2012a);
4. They determine signal of the dataset (significant axes) from the noise (non-significant axes) (Birks, 2012a).

3.13.2.5 Limitations to Ordination Analyses

Ordinations analyses do have some limitations.

1. PCA can be subject to arch effects (Legendre et al., 2012b).
2. DCA does not perform particularly well for complex gradients or data that has a lot of outliers (Legendre et al., 2012b).
3. CA and DCA assume a unimodal distribution of species to an environmental driver, an unrealistic assumption of ecological data (Ejrnæs, 2000; Legendre et al., 2012b).
4. DCA can correct for the “arch effect”; however, the results are more random than methodological yet more consistent with species data (Hill et al., 1980; Ejrnæs, 2000; Juggins et al., 2012).

5. PrC do not perform well when a species response is small, constant, or multimodal (De' ath, 1999).
6. CA and PrC perform poorly when beta diversity is high. PCA perform better in this circumstance (Faith et al., 1987; De' ath, 1999).
7. PrC typically perform better than other ordination analyses but are not widely used in palaeoecological research (Legendre et al., 2012b).

Some of these limitations can be resolved by pre-treating data prior to ordination analysis. Appropriate methods include: (1) removing rare taxa, with low numbers of occurrence and low maximum abundance; (2) transformation - normalisation techniques using numerical standardisation of data; or (3) revitalisation - a normalisation technique scaling data around the mean by the use of standard deviation (z-scores). These techniques will also allow for more comparable data with unequal variance. These three ordination techniques will be used for different multivariate datasets in this research. Ordination selection will be dependent on individual datasets to avoid caveats of particular ordinations. Details of ordination methods and selection criteria for the individual datasets can be found in discussion chapters 4, 5, 6, and 7.

3.13.3 LEAD AND LAG ANALYSES

Statistical tests can be performed to understand leading and lagging relationships between time series datasets (e.g. between vegetation and aquatic ecosystem changes). To test for lead and lag relationships superposed epoch analysis (SEA) and cross-correlation analysis (CC) will be employed to explicitly test the hypotheses of this research.

3.13.3.1 Superposed Epoch Analysis

Superposed epoch analysis (SEA) is a response index developed for time series data to determine significant trends before and after response events (Haurwitz et al., 1981; Samson et al., 1986; Dunnette et al., 2014). These “response events” are known as the explanatory variable of the analysis (Prager et al., 1992). SEA determines significant changes between variables (leads and lags) in time (Hegerl et al., 2003; Fule et al., 2009; Dunnette et al., 2014). Older methods used a student’s t-test to determine the significance in time series surrounding the response events, but due to many limitations to this method (assumed normal distribution and autocorrelation) a Monte Carlo randomisation technique is now standard practice (Haurwitz et al., 1981; Prager et al., 1992). The Monte Carlo uses numerous iterations (i.e. 1,000) of the chosen response events from the dataset, to produce a probability distribution of the average departures and determine significant trends in the dataset before and after the response events (Haurwitz et al., 1981; Lough et al., 1987; Adams et al., 2003). The analysis can be run on multiple response events and the time window can be altered for different time series (in leading and lagging direction).

3.13.3.1.1 Advantages to SEA

SEA analysis has several advantages to palaeoecological research:

1. SEA reveals significant trends in the time series data in relation to response events (Dunnette et al., 2014);
2. Multiple response events can be chosen by the operator (Haurwitz et al., 1981; Prager et al., 1992);
3. The randomisation method (Monte Carlo) allows the elimination of normality, and equal variance requirements and serial correlations in the response index (Haurwitz et al., 1981).

3.13.3.1.2 Limitations to SEA

Drawbacks to SEA include:

1. Datasets must have the same time intervals, i.e. uneven time steps (Haurwitz et al., 1981);
2. It is difficult to determine the appropriate number of iterations needed in a SEA (Prager et al., 1992);
3. Response events close together in temporal space may cause problematic results (Prager et al., 1992).

The SEA assessment will allow the ability to test if time series data from multiple proxies are related temporally and measure the timing of trends in proxy data. Details of SEA methods and results can be found in discussion Chapter 8.

3.13.3.2 Cross-correlation Analysis

CC is a statistical method performed on two time series to determine if one time series is dependent on the other in leading and lagging time steps (Box et al., 1976; Green, 1981). CC uses probability statistics to determine correlation within a time window by differencing the variance and mean of a time series (Box et al., 2016). CC can only be performed on stationary or linear data with even time steps. Thus, non-stationary data must be detrended before cross-correlation is performed to avoid false correlations (Horvatic et al., 2011). Stationarity can be tested using a Ljung-Box test, an Augmented Dickey-Fuller test, or a Kwiatkowski-Phillips-Schmidt-Shin test. If the time series data are non-stationary they need to be detrended before cross correlation analysis is performed. Most commonly, and what is used in this study, is differential detrending:

$$x'_t = x_t - x_{t-1}$$

Where x_t is the value at time step of interest and x_{t-1} is the value of the previous time step. Once the data are stationary or detrended, CC can be performed with the chosen number of lead and lags.

3.13.3.2.1 Advantages to Cross-correlation Analysis

CC is advantageous to palaeoecological research because:

1. CC demonstrate correlative relationships between two time series datasets (SPSS Statistics, 2012);
2. The relationships are shown in lead and lag intervals and do not have to be instantaneous (Green, 1981; SPSS Statistics, 2012).

3.13.3.2.2 Limitations to Cross-correlation Analysis

CC have some limitations.

1. Data must be in even time steps (SPSS Statistics, 2012).
2. Data must be detrended if non-stationary and thus can also remove important trends in the time series data (Green, 1981; Horvatic et al., 2011).

CC will be a vital metric for testing the relationships between terrestrial and aquatic proxy datasets to answer the research questions regarding coupling of terrestrial-aquatic ecosystems. Details of CC methods and results can be found in discussion Chapter 5.

3.13.4 SEQUENTIAL T-TEST ANALYSIS OF REGIME SHIFTS

Regime shift tests define periods of reorganisation in an ecosystem by significant shifts in a time series.

Sequential t-test analysis of regime shifts (STARS) is the statistical method that will be employed to determine the occurrence, magnitude and length of a regime shift (Rodionov et al., 2005). Before STARS, the original application for determining regime shifts used student's or Mann-Kendall significance tests (Rodionov, 2004); however, this method had difficulty determining more than one shift in a time series. Another statistical method

for determining regimes shifts, known as the L method, used multivariate statistical functions, i.e. confirmatory statistics, to detect discontinuities in the data (Rodionov, 2004). However, there are problems with poor accuracy and statistical power near the end of the time series. Statistical power suggests the likelihood of a significant result being detected. Therefore, in the L method poor statistical power at the end of time series data meant significant shifts at the end of the time series would likely not be detected. These issue have since been resolved with the STARS method (Rodionov, 2004).

STARS uses sequential statistics. A t-test is used on a selected variable length, known as a window (number of data points in a test), to determine if the data significantly differs from the mean. If they do, a shift is detected (Rodionov, 2004). In time series data, this test is used as a running window to detect significant shifts which can be adjusted depending on the characteristics of the data. These calculations loop through the data using the mean window length to calculate regime shifts through the entire data set. The strength of the shift is represented by a regime shift index (RSI) value where negative values indicate the test has failed and positive values mean the regime shift is significant above a p-value of choosing (Rodionov, 2004).

3.13.4.1 Advantages to STARS

STARS will be used in this research because it has a number of advantages including:

1. Detection of multiple shifts in a dataset (Rodionov, 2004);
2. Analysis of uneven time steps (Rodionov, 2004);
3. The strength of shift detection stays constant (Rodionov, 2004);
4. Data can be used as anomalies or absolute values (Rodionov, 2004).

3.13.4.2 Limitations to STARS

STARS does have some limitations.

1. STARS only performs in two-dimensional space. Therefore, only one variable can be analysed at a time (Rodionov, 2004).
2. Smaller window lengths need stronger statistics (two standard deviations) to detect a significant shift. Larger windows only need one standard deviation (Rodionov, 2004).
3. STARS does not account for age uncertainty.
4. Gradual shifts may not be detected, STARS is designed for abrupt changes (Rodionov, 2004).

Some of these limitations do not apply to this research. For example, palaeoecological data exists in multivariate space, but STARS will be appropriate on two-dimensional curves (i.e. PCA axis 1). Gradual shifts in this research can be detected using other methods than STARS (See GAMs Section 3.13.6). STARS will be a useful statistical method in this research because it can test data with uneven time steps, as well as, find multiple shifts in a time series.

3.13.5 RATE-OF-CHANGE

Rate-of-change (ROC) is a simple metric to determine the rate of compositional change over time using dissimilarity measurements and can be used as an indicator of resilience (Lim et al., 2011; Birks, 2012a, c). Increased ROC reveals a system moving further away from equilibrium with longer recovery time (Scheffer et al., 2009; Lim et al., 2011; Scheffer et al., 2012; Siteur et al., 2016). Popular techniques for ROC typically run on data with even sampling intervals; however, interpolating data is problematic (Birks et al., 2006; Birks, 2012c; Carstensen et al., 2013). The ROC method used here will not require even time steps. It is performed on proportional multivariate data using a chosen method for dissimilarity (See Section 3.13.1) divided by the age intervals between samples to produce the ROC (Simpson, 2007).

3.13.5.1 Advantages of ROC

ROC is advantageous to this research because:

1. ROC is a simple and powerful statistic (Birks, 2012a);
2. It determines periods of increased ecological change (Birks, 2012a);
3. ROC can measure resilience. High ROC can reflect a system that is close to a bifurcation point between two alternative states (Lim et al., 2011; Dakos et al., 2012; Scheffer et al., 2012).

3.13.5.2 Limitations of ROC

ROC does have some limitations.

1. Sample interval (changes in resolution) may affect ROC results (Birks, 2012c). Interpolation can help remove the bias from uneven time interval; however, interpolation has its own problems of data manipulation (Schulz et al., 1997; Birks, 2012a).
2. Chronology can affect the ROC results (Birks, 2012c).

Even with the caveats of ROCs, a good chronology and sampling interval can reduce these problematic effects. Additionally, a method without interpolation will be more robust than issues of changes in resolution. Accounting for age variability in these analyses will help reduce these effects. Therefore, ROC will be important to assess the terrestrial and aquatic ecosystems change, variability, and non-linear shifts (critical transitions). Details of ROC methods and results can be found in discussion Chapter 7.

3.13.6 GENERALISED ADDITIVE MODELLING (GAMs)

Generalised additive models (GAMs) have enormous potential in palaeoecology, for instance modelling species responses to environmental variables (Birks, 2012d). GAMs are predicted models fitted with a response variable using complex mathematical functions such as smooth splines (Birks, 2012d). Their goal is to demonstrate true trends within a data series. Unlike linear models they assume that covariates and response variables are not necessarily linearly related. GAMs use a sum of smoothing functions to model the time series trends (Birks, 2012d). Three important components for fitting GAMs are: (1) the measure of the smooth in the data; (2) the fit to the data; and (3) penalty for overfitting the data.

Other valuable information from the fitted GAMs can be extracted and used for data analysis such as assessing change in variability of a time series (Bunting et al., 2016), or using the function derivatives to determine significant shifts in the data trends (Bennion et al., 2015). Variance becomes important for predicting non-linear shifts such as critical transitions and tipping points (Bunting et al., 2016).

3.13.6.1 Advantages of GAMs

The benefits to fitting GAMs in palaeoecological data are:

1. The mathematical modelling is automatic, no model selection is required to fit a GAM (Birks, 2012b; Simpson, 2017);
2. Model predictors and smooth selection can be controlled by the operator (Simpson, 2017);
3. They are more data driven than model driven (Birks, 2012d).

3.13.6.2 Limitations of GAMs

GAMs are powerful statistical tools but do have some limitations.

1. GAMs are more of a graphical and visual statistical technique than a numerical one (Birks, 2012d).
2. Sharp transitions are difficult to model using GAMs (Simpson, 2017).
3. The major assumption is that the functions are additive and smooth (Birks, 2012d).

GAMs will be imperative in the research to demonstrating gradual and true trends in the time series data, irrespective of the noise. Also, other important metrics from GAMs such as change in variance, will be used to understand non-linear shifts such as critical transitions (Chapter 7).

3.14 CHAPTER CLOSING

This chapter overviewed the methods used in this research; their justification, applications and limitations. Further details on exact methods performed (i.e. number of samples, proxies used on cores, and statistical methods) will be included in each discussion chapter relevant to the particular study site.

PART ONE: PADDY'S LAKE

CHAPTER 4: DISCUSSION

4.1 CHAPTER AIM

The aim of this chapter is to understand the terrestrial environmental response to climate change at Paddy's Lake. This chapter is comprised of the modified published article Beck, K.K., Fletcher, M.S., Gadd, P.S., Heijnis, H. & Jacobsen, G. (2017) An early onset of ENSO influence in the extra-tropics of the southwest Pacific inferred from a 14,600 year high resolution multi-proxy record from Paddy's Lake, northwest Tasmania. *Quaternary Science Reviews*, 157, 164-175 DOI:10.1016/j.quascirev.2016.12.001. Beck, K.K. and Fletcher, M.-S. conceived the ideas for this research. Beck, K.K. performed the pollen and statistical analyses, interpretation, and writing of this publication. Gadd, P.S., and Heijnis, H. performed the μ XRF geochemical analysis and Jacobsen, G. performed the radiocarbon analysis. All authors assisted in editing and interpretation of results for this publication.

4.2 ABSTRACT

Tropical El Niño Southern Oscillation (ENSO) is an important influence on natural systems and cultural change across the Pacific Ocean basin. El Niño events result in negative moisture anomalies in the southwest Pacific and are implicated in droughts and catastrophic wildfires across eastern Australia. An amplification of tropical El Niño activity is reported in the east Pacific after ca. 6.7 ka; however, proxy data for ENSO-driven environmental change in Australia suggest an initial influence only after ca. 5 ka. Here, we reconstruct changes in vegetation, fire activity and catchment dynamics (e.g. erosion) over the last 14.6 ka from part of the southwest Pacific in which ENSO is the main control of interannual hydroclimatic variability: Paddy's Lake, in northwest Tasmania (1,065 masl), Australia. Our multi-proxy approach includes analyses of charcoal, pollen, geochemistry, and radioactive isotopes. Our results reveal a high sensitivity of the local and regional vegetation to climatic change, with an increase of non-arboreal pollen between ca. 14.6 to 13.3 ka

synchronous with the Antarctic Cold Reversal, and a sensitivity of the local vegetation and fire activity to ENSO variability recorded in the tropical east Pacific through the Holocene. We detect local-scale shifts in vegetation, fire and sediment geochemistry at ca. 6.3, 4.8 and 3.4 ka, simultaneous with increases in El Niño activity in the tropical Pacific. Finally, we observe a fire-driven shift in vegetation from a pyrophobic association dominated by rainforest elements to a pyrogenic association dominated by sclerophyllous taxa following a prolonged (>1 ka) phase of tropical ENSO-amplification and a major local fire event at ca. 3.4 ka. Our results reveal the following key insights: (1) that ENSO has been a persistent modulator of southwest Pacific climate and fire activity through the Holocene; (2) that the climate of northwest Tasmania is sensitive to long-term shifts in tropical ENSO variability; and (3) that there has been possible stationarity in the spatial influence of ENSO over this region through the Holocene.

4.3 INTRODUCTION

The tropical Pacific El Niño-Southern Oscillation (ENSO) is an important component of the global climate system, influencing climatic, physical and ecosystem processes both within and beyond the Pacific Ocean basin. Over the historical period, changes in the intensity and frequency of ENSO events are correlated with a range of important processes; such as trends in rainfall (Ropelewski et al., 1987; Moy et al., 2002; Hoerling et al., 2003), biomass burning (Kitzberger et al., 2003; Fletcher et al., 2015), mammal population dynamics (Lima et al., 2002; Ogutu et al., 2003), and plant phenology (Asner et al., 2000; Dech et al., 2004; Fletcher et al., 2015). While longer-term changes in ENSO are implicated in major ecosystem transformations (Fletcher et al., 2014a), cultural shifts (Sandweiss et al., 1999; Sandweiss et al., 2001; Turney et al., 2006; Williams et al., 2008), and both terrestrial (Cao et al., 2004) and marine biogeochemical cycling (Karl et al., 1997). Indeed, the “switching on” of ENSO - the shift from a muted to ‘modern’ ENSO system that occurred in the mid-Holocene is implicated in changes in climate-driven processes across the entire Pacific Ocean basin (Sandweiss et al., 1996; Turney et al., 2004; Fletcher et al., 2012; Fletcher et al., 2015). Despite the

widespread recognition of the impact of the mid-Holocene amplification of ENSO, uncertainty exists over both where and when the effects were felt in natural systems (Conroy et al., 2008; Moreno et al., 2010). Here we use a high-resolution pollen, charcoal and geochemical analysis of lake sediment from northwest Tasmania, Australia, to assess the influence of millennial-scale ENSO variability over local climate variability and consequent landscape dynamics at a site located in the mid-latitudes (extra-tropics) of the southwest Pacific.

The dominant role of hydroclimatic variability over long-term Holocene terrestrial ecosystem dynamics in the mid- to high latitudes of the South Pacific Ocean basin is well described (e.g. Moreno, 2004; Lamy et al., 2010; Fletcher et al., 2012; Kilian et al., 2012; Fletcher et al., 2014a; Pesce et al., 2014; Fletcher, 2015; Fletcher et al., 2015; Rees et al., 2015; Mariani et al., 2016a; Stahle et al., 2016); and is understood as a dynamic interaction between zonally symmetric shifts in the extra-tropical southern westerly winds (SWW) and the meridionally asymmetric hydroclimatic signature of the ENSO system (Fletcher et al., 2012; Stahle et al., 2016). In other words, millennial-scale shifts in the SWW during the early to mid-Holocene (ca. 12,000 to 6,000 years ago – 12 to 6 ka) drove synchronous in-phase vegetation and fire regime changes across the South Pacific, while the mid- to late-Holocene (ca. 6 to 0 ka) was characterised by sub-millennial scale hydroclimatic oscillations across the region that reflect the influence of long-term phasing of tropical ENSO variability (Fletcher et al., 2012). Critically, while it is clear that ENSO variability approaching ‘modern’ appeared first at ca. 6.7 ka (Moy et al., 2002), the timing of the onset of ENSO inferred from proxy records within the Pacific Ocean basin varies widely (usually between ca. 6-3 ka). In east and southeast Australia, a region in which ENSO variability, in particular the warm (El Niño) phase, is a key determinant of rainfall variability and fire activity (Mariani et al., 2016a), a consensus of ca. 5 ka appears to have been reached from a range of proxy types (Turney et al., 2006; Donders et al., 2007; Fletcher, 2015; Rees et al., 2015). An initial onset of the effects of ENSO at ca. 5 ka is consistent with a substantial increase in the frequency of El Niño events recorded in the tropical east Pacific (Moy et al., 2002), but it post-dates the initial amplification of

ENSO by ca. 1.7 kyrs, suggesting a spatiotemporal complexity in how ENSO influences the climate of the Pacific Ocean basin.

Tasmania is a cool temperate continental island located in the extra-tropics of the Southern Hemisphere (41-44°S), at the extremity of the ENSO zone of influence in the southwest Pacific and positioned at the climatic interface between the tropical ENSO system and the extra-tropical SWW (Mariani et al., 2016a). Tasmania is, thus, critically located to assess how these two important systems interact in space and time (Figure 4.1).

Evidence for the influence of ENSO over the climate of Tasmania reveals substantial heterogeneity in where and when the impacts of ENSO were first felt in this complex landscape. Recent studies of lake sediment macroscopic charcoal sequences from southwest Tasmania, a region in which ENSO has little explanatory power over modern rainfall variability (Mariani et al., 2016a), reveal that the prominent spike in El Niño frequency at ca. 5 ka (Moy et al., 2002) was sufficient to teleconnect hydroclimatic anomalies to sites located in western Tasmania that are outside the modern ENSO area of influence (Fletcher et al., 2015; Rees et al., 2015). Initial burning of rainforest vegetation at ca. 6 ka in southern Tasmania, where both ENSO and the SWW are important in governing rainfall anomalies (Hill et al., 2009; Mariani et al., 2016a), is synchronous with a peak in tropical El Niño frequency and reveals an influence of ENSO almost 1 kyrs before the initial ENSO impacts reported in southeast Australia and western Tasmania (Fletcher et al., 2014a). Finally, a recent long-term vegetation and fire record from northwest Tasmania on the cusp of the SWW-ENSO zone, reports the first influence of ENSO at ca. 3.5 ka (Stahle et al., 2016), synchronous with a prolonged phase of amplified El Niño activity that is implicated in substantial changes in both natural and cultural systems across the entire Pacific Ocean basin (Sandweiss et al., 1999; Sandweiss et al., 2001; Williams et al., 2008), revealing a substantial lag at that site compared to elsewhere in the region.

Here, we aim to assess the role of tropical ENSO variability in governing fire, vegetation and sediment dynamics over the last 14.6 kyrs in part of western Tasmania where ENSO is currently the dominant driver of

interannual hydroclimatic variability. Our study site is Paddy's Lake in northwest Tasmania, a high altitude lake (1065 masl), located immediately above the modern treeline. We use a multi-proxy approach that employs analyses of charcoal, pollen, geochemistry, and radioactive isotopes to reconstruct fire, vegetation, and sediment dynamics at this site over the past 14.6 kyrs. We then compare our results to regional climate proxy data in an attempt to: (1) assess the long-term climatic framework proposed for this region; (2) determine the timing of the initial impacts of ENSO variability on the local ecosystem; and (3) ascertain the impact of changing tropical ENSO variability on the local ecosystem around Paddy's Lake.

4.4 WESTERN TASMANIA

4.4.1 REGIONAL GEOGRAPHY

Tasmania has a complex topography and a cool temperate maritime climate (Gentili, 1971). The roughly north-south trending mountain range that bisects Tasmania intercepts the dominant SWW flow and orographic rainfall results in up to 3,500 mm of precipitation annually on the west coast, while rainfall drops to as little as 400 mm p/a on the east side of the ranges (Macphail, 1979; Kitchener et al., 2013). Interannual rainfall variability in Tasmania is determined by both ENSO and the Southern Annular Mode (SAM - an index that describes interannual variability of the SWW). During the positive (negative) phase of SAM there is a decrease (increase) in precipitation in Tasmania due to a southward (northward) shift of the SWW resulting from a positive (negative) atmospheric pressure anomaly in the mid-latitudes and negative (positive) pressures in the high latitudes (Gillett et al., 2006; Stammerjohn et al., 2008). ENSO involves the Walker Circulation over the tropical Pacific Ocean: a weak (strong) SST gradient across the Pacific Ocean, the El Niño (La Niña) phase results in negative precipitation anomalies in the western (eastern) Pacific (Hill et al., 2009). Figure 4.1a shows the strong negative correlation between SAM and rainfall anomalies in the southwest of Tasmania over

the historical period, while Figure 4.1b demonstrates strong positive correlation between Southern Oscillation Index (an ENSO index) and rainfall anomalies in north Tasmania through the same period.

4.4.1.1 Paddy's Lake

Paddy's Lake (41°27' 04S, 145°57' 41E, 1065 masl) is a cirque lake located on the Black Bluff massif in northwest Tasmania. The lake is dystrophic, has a maximum depth of 21.5 m, a surface area of 26 km², and local catchment area of ca. 174.258 km². There is one outflow from Paddy's Lake draining to the north. The local geology is nutrient poor and consists of Quaternary deposits of quartzite, conglomerate and moraine deposits with traces of Cambrian volcanic conglomerate, sandstone and siltstone (Seymour et al., 1995; Pemberton et al., 2004). Average annual rainfall at the closest weather stations [Loongana 4.4 km (468masl) and Waratah 36 km (609 masl)] is 1,740 mm, with the wettest months in the Austral winter (JJA). The monthly maximum temperatures range from 7.2°C in July to 18.0°C in February, with an annual average of 12.3°C (Bureau of Meteorology, 2016c, b). Applying an adiabatic lapse rate of elevation on minimum (0.5°C per/100 m) and maximum (0.75°C per/100 m) temperature (Nunez et al., 1986) suggests that the approximate minimum and maximum monthly temperatures at Paddy's Lake are ~4.6°C and ~14°C.

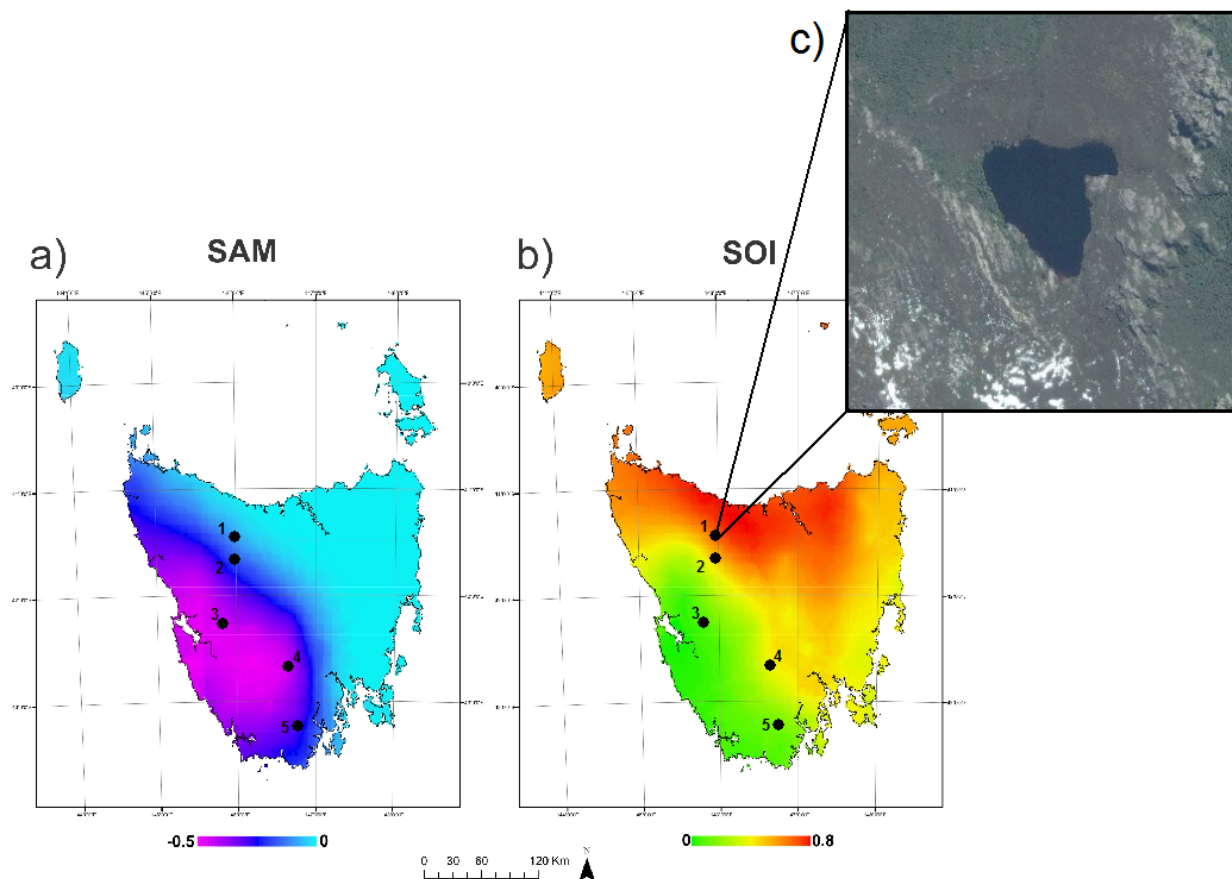


Figure 4.1: Maps of Tasmanian precipitation correlated to a) Southern Annular Mode and b) Southern Oscillation Index (modified from Mariani and Fletcher, 2016). Black dots indicate site locations: 1) Paddy's Lake, Black Bluff; 2) Wombat Pool, Cradle Mountain; 3) Lake Gwendolyn and Lake Nancy, Frenchman's Cap; 4) Lake Dobson, Mount Field National Park; and 5) Lake Osborne, Hartz Ranges. c) A satellite image of Paddy's Lake.

The vegetation in the local catchment is heathland comprised of *Nothofagus cunninghamii*, *Bauera rubioides*, *Beyeria* spp., *Eucalyptus coccifera*, *Athrotaxis selaginoides*, *Diselma archeri*, *Leptospermum* spp., *Orites revolutus*, *Oxylobium ellipticum*, *Baeckea gunniana*, epacrids, *Tasmannia lanceolata* and *Richea* spp. and is classed as eastern alpine heathland (Harris et al., 2005). The surrounding landscape is dominated by a fine-scale landscape mosaic of fire promoted plant communities and fire sensitive communities that have resulted from millennia of landscape management by people (Fletcher et al., 2010a). Slopes immediately to the north are blanketed in Eucalypt-dominant wet sclerophyll forest, a community in which Eucalypts overtop a rainforest understorey reflects the burning and recovery of rainforest vegetation (Jackson, 1968). The low

nutrient status of the local (and regional) geology and the cool wet climate conspire to promote the formation of organosols under most vegetation types, while the pervasive influence of fire in this landscape acts to control vegetation dynamics via a well-described fire-vegetation-organosol nutrient feedback mechanism. Frequent fires inhibit the establishment of trees and reduce the (primarily vegetation-derived) nutrient load of organosols, while the absence of fire allows the establishment of trees, the accumulation of nutrients, and the eventual establishment of pyrophobic rainforest. A series of vegetation states punctuates the extremes of this dynamic (moorland and rainforest) and are characterised by differing levels of shrub taxa that promote discrete and meta-stable vegetation states, such as shrubland/heath and Eucalypt (wet sclerophyll) forest (Jackson, 1968; Bowman et al., 2009b; Wood et al., 2012).

4.5 METHODS

4.5.1 SEDIMENT RECOVERY

Sediment cores were collected from a floating platform from the deepest point (20.78 m) of Paddy's Lake on 12 November 2014. A sediment-water interface core (TAS1401 SC1) was collected using a Bolivia coring system, a modified Livingstone system (Wright, 1967), while a long core (TAS1401 N1) was retrieved using a Nesje coring system (Nesje, 1992). All cores were packaged in the field and transported whole to allow for core scanning.

4.5.2 CHRONOLOGY

Nineteen samples were analysed for radiocarbon dating (two plant macrofossils and 17 bulk sediment samples) at Australian Nuclear Science and Technology Organisation (ANSTO) (5 samples) and DirectAMS

Radiocarbon Dating Service laboratory (14 samples) (Table 4.1). Lake sediments in Tasmania are susceptible to the lake reservoir effect whereby the lake and atmospheric ^{14}C are not in equilibrium causing bulk sediments to contain “old carbon” (MacDonald et al., 1991; Björck et al., 2001). Thus, paired macrofossil-bulk sediment samples were analysed where possible (n 2, Table 4.1) to estimate any age-offset present in the lake. An age-depth model was developed in *R v.3.1.1* (R Development Core Team, 2014) using the *clam v.2.2* package (Blaauw, 2010). Radiocarbon dates were calibrated with the Southern Hemisphere calibration curve - SHCal13 (Hogg et al., 2013) and a smooth spline model (smoothing factor set to 0.5) was applied to best fit the two sigma calibrated ages with a point estimates method of 1,000 iterations (Figure 4.2).

4.5.3 CHARCOAL ANALYSIS

Macroscopic charcoal was processed at 0.5 cm intervals for the entire length of the sedimentary sequence according to standard protocols: 1.25 mL of sediment was placed in store-bought bleach for at least seven days then sieved through 250 μm and 125 μm mesh and enumerated under a dissecting microscope at 10 to 20x magnification. Microscopic charcoal was also counted alongside pollen identification; charcoal was enumerated on prepared pollen slides until a total of 300 terrestrial pollen grains were identified.

Accumulation rates for microscopic charcoal were determined using concentration of an exotic pollen spike (*Lycopodium* spp.) by depositional time (yr cm^{-1}). Statistical analysis of macroscopic charcoal data was performed in CharAnalysis (Higuera, 2009). Charcoal data was interpolated to 30-year even time steps (the median age interval of the record) to calculate charcoal concentration and accumulation rates (CHAR).

Background charcoal ($\text{CHAR}_{\text{back}}$) was determined to represent the low-frequency trend of the interpolated charcoal data that is related to, among other factors, background biomass burning ($\text{particles cm}^{-2} \text{yr}^{-1}$).

$\text{CHAR}_{\text{back}}$ was estimated using a LOWESS smooth robust to outliers and was smoothed over a 500 year-window. The CharAnalysis output `peaksFinal` was determined to identify significant charcoal peaks and peak magnitude ($\text{particles cm}^{-2} \text{yr}^{-1}$) was used to identify the sum of all charcoal that exists above the charcoal peak

threshold. Signal-to-noise (SNI) index determined important peaks in charcoal above a noise threshold of 3 (Kelly et al., 2011). The fire return interval (FRI) identify interpolated fire return years smoothed over a 1,000 year-window. For further details on CharAnalysis see Higuera et al. (2009).

4.5.4 PALYNOLOGY

Pollen analysis was completed at 2 cm intervals, with the exception of 1 cm intervals from 50 to 87 cm in TAS1401 SC1. Pollen processing methods were conducted using the standard protocols by Faegri et al. (1989). At least 300 terrestrial pollen grains were identified in each sample. Percentage calculations of aquatic and spore pollen were based on a supersum inclusive of all pollen and spores, while a terrestrial pollen sum was used to calculate percentage values of plants identified as terrestrial in origin. Zonation of the pollen diagram was based on a constrained incremental sum of squares (CONISS) cluster analysis (Grimm, 1987) with a square root transformation of the data in *Tilia v. 2.0.37* (Grimm, 2013). A broken stick model was used to determine zones of significance using the rioja package (Juggins, 2016) in *R*. Detrended correspondence analysis (DCA) was performed using the terrestrial pollen percentage data using the rioja package in *R* where a square root transformation was applied (with rare taxa down weighted) to determine the main trends in the pollen dataset.

4.5.5 GEOCHEMISTRY

Non-destructive geochemical data was obtained using an Itrax X-ray fluorescence (ITRAX) core scanner at ANSTO at a resolution of 0.5 mm using a molybdenum (Mo) tube set at 30 kV and 55 mA with a dwell time of 10s. The geochemical dataset was normalised by kcps (Croudace et al., 2015). A subset of the main geochemical elements (Al, Si, P, S, Cl, K, Ca, Sc, Ti, Mn, Fe, Ni, Cu, Zn, Br, Rb, Sr, Zr, and Pb) and the Compton scattering incoherence/coherence ratio were converted to z-scores to meet the criteria for principal

component analysis (PCA) with variance/covariance analysis so the main trends in the geochemical dataset could be identified. The PCA was conducted in *PC-Ord v.4.27* (McCune et al., 2011).

4.6 RESULTS

4.6.1 SEDIMENT RECOVERY

Two cores, TAS1401 SC1 (93 cm) and TAS1401 N1 (227 cm), were collected from Paddy's Lake. Radiocarbon dating, charcoal and geochemistry were used to tie the cores into a master sequence. The composite core was 291 cm in length.

4.6.2 CHRONOLOGY

The results of radiocarbon analysis are presented in Table 4.1. A maximum radiocarbon age of $12,514 \pm 50$ ^{14}C yrs was obtained at 255 cm. Paired macrofossil-sediment dates reveal an average offset of 223.5 yrs (between 207 to 240 ^{14}C yrs). This mean offset was applied to the entire sequence to correct for the variable reservoir effect. The age-depth model (Figure 4.2) was fit with a smooth spline and demonstrates a high sedimentation rate (average 14.2 yrs/cm) until ~13 ka where sedimentation decreases dramatically (81.3 yrs/cm) with an almost linear sedimentation rate until present. This change in sedimentation rate is consistent with a marked change in sediment type from Gytia to pinkish-grey gravely clay at 177 cm (Appendix I Figure I.1). The selected age-depth model has two dates out of stratigraphic order that were considered as outliers in the selected age-depth model (Table 4.1 and Figure 4.2). The basis for selecting outlier dates is based on the following criteria: (1) the clear sedimentary change that indicates a change in depositional environment consistent with the selected age-depth model (fast accumulation of minerogenic sediment immediately after glacier retreat from the cirque); and (2) the higher likelihood of erroneously old dates resulting from old

carbon contamination of sediments by the in wash or glacial reworking of soil stored carbon into the lake (MacDonald et al., 1991). Further, interrogation of alternate age models that are free of outlier selection, while producing a basal age closer to cosmogenic ages of terminal Last Glacial Maximum moraines in Tasmania (Barrows et al., 2002), produces a substantial departure of key regionally-dispersed pollen types from the ‘regional’ signal (Macphail, 1979; Colhoun et al., 1991a; Colhoun, 1996).

Table 4.1: Radiocarbon laboratory results for Paddy's Lake. Dates are organised in chronological sequence and the core code is identified at the top of the depths. Samples measured at AMSDirect are labelled with lab code D-AMS and samples analysed at ANSTO are labelled with the lab code OZS. The two ***bold italicised*** dates were removed as outliers from the age model and * indicate the paired macrofossil-bulk sediment samples. Square brackets designate depths within the continuous sedimentary sequence.

Lab ID	Sample depths (cm) [in sediment sequence]	Material dated	$\delta^{13}\text{C}$ (per mil)	pMC (1σ)	Radiocarbon age (BP) (1σ)	Median calibrated age (cal yr BP)
<i>TAS1401 SC1</i>						
D-AMS 010530	14-14.5	bulk sediment	-15.7	86.65 ± 0.25	1,151 ± 23	937
D-AMS 009184	24-24.5	bulk sediment	-22.4	80.27 ± 0.30	1,765 ± 30	306
D-AMS 010531	47-47.5	bulk sediment	-26.3	68.42 ± 0.20	3,049 ± 23	1,245
D-AMS 009183	*65-65.5	plant macrofossil	-17.3	64.74 ± 0.23	3,493 ± 29	1,765
D-AMS 009185	*65-65.5	bulk sediment	-28.6	63.09 ± 0.20	3,700 ± 25	2,031
D-AMS 009186	79-79.5	bulk sediment	-21.0	55.22 ± 0.19	4,770 ± 28	3,524
D-AMS 010532	92-92.5	bulk sediment	-20.2	48.92 ± 0.20	5,743 ± 33	4,535
<i>TAS1401 N1</i>						
OZS591	*33.5-34 [97-97.5]	plant macrofossil	-25.6	46.51 ± 0.23	6,150 ± 40	5,037
OZS592	*33.5-34 [97-97.5]	bulk sediment	-24.9	45.14 ± 0.23	6,390 ± 45	5,334
OZS593	46-46.5 [109.5-110]	bulk sediment	-25.1	39.91 ± 0.19	7,380 ± 40	6,184
OZS594	64-64.5 [127.5-128]	bulk sediment	-25.7	33.04 ± 0.20	8,895 ± 50	8,011
D-AMS 010533	71.5-72 [135-135.5]	bulk sediment	-19.7	29.61 ± 0.14	9,777 ± 38	9,232
D-AMS 010534	87.5-88 [151-151.5]	bulk sediment	-22.7	26.38 ± 0.12	10,704 ± 37	10,700

	102.5-103	bulk				11,434
OZS595	[166-166.5]	sediment	-24.7	23.63 ± 0.14	$11,590 \pm 50$	
D-AMS	110.5-111	bulk				
010535	[174-174.5]	sediment	-25.3	23.98 ± 0.12	$11,471 \pm 40$	11,318
D-AMS	136.5-137	bulk				
013525	[200-200.5]	sediment	-27.2	18.27 ± 0.12	$13,655 \pm 53$	14,454
D-AMS	161.5-162	bulk				
012511	[225-225.5]	sediment	-21.3	18.43 ± 0.11	$13,585 \pm 48$	14,360
D-AMS	183.5-184	bulk				
012512	[247-247.5]	sediment	-17.4	20.23 ± 0.14	$12,837 \pm 56$	13,296
D-AMS	191.5-192	bulk				
013526	[255-255.5]	sediment	-25.8	21.06 ± 0.13	$12,514 \pm 50$	12,694

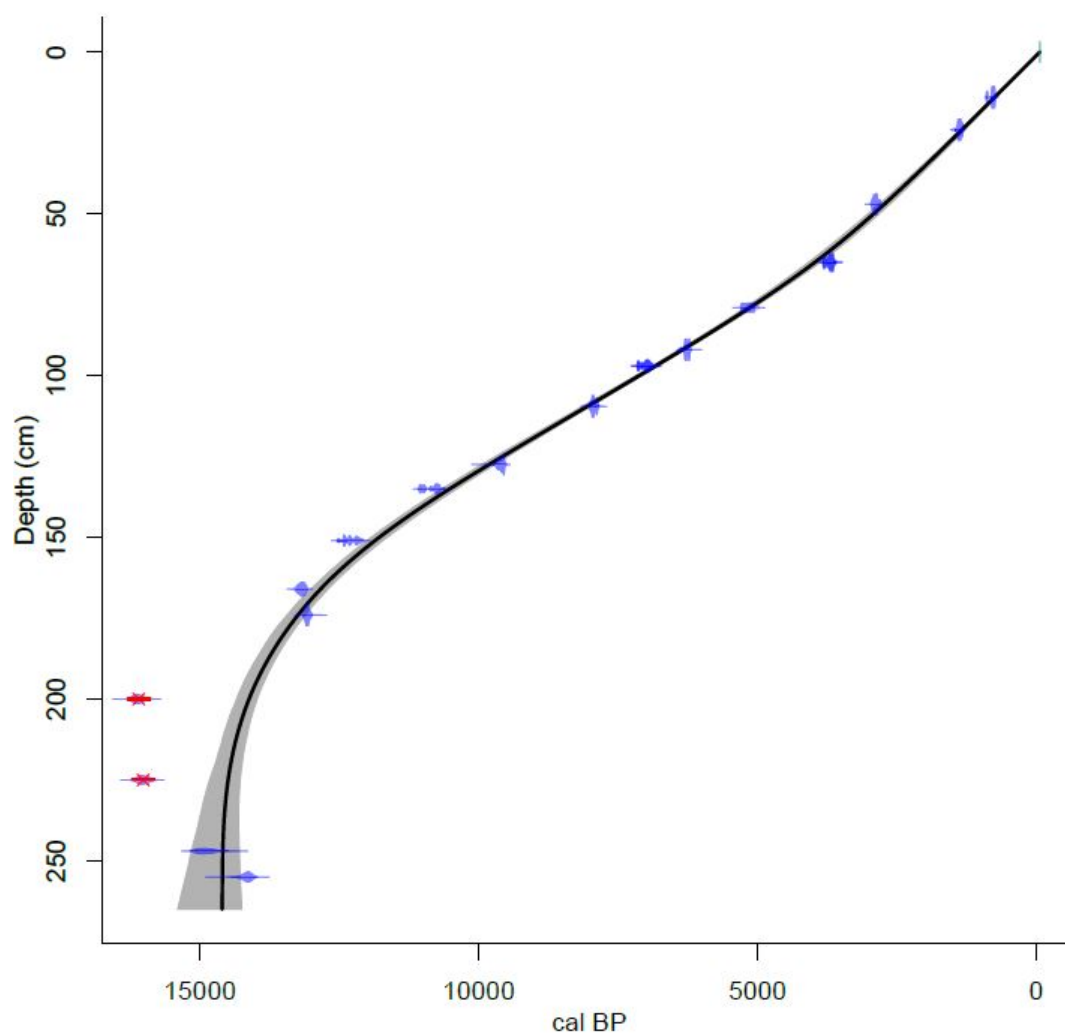


Figure 4.2: Age-depth model developed in clam v2.2 (Blaauw, 2010) using SHCal13 (Hogg et al., 2013) and employing a smooth spline (factor=0.50; goodness-of-fit of 83.38). Outliers are marked in red.

4.6.3 CHARCOAL

The macroscopic CHAR record reveals substantial changes in fire activity throughout the record.

CharAnalysis identified 35 significant charcoal peaks and their magnitudes, with the largest peaks occurring at 3.4 and 7.7 ka (Figure 4.3). Small $\text{CHAR}_{\text{back}}$ increases occur at 13.3 ka and 9.6 ka, at 6.3 ka the largest increase in $\text{CHAR}_{\text{back}}$ occurs until 4.3 ka where it declines and increases in a cyclical pattern to present. Fire return interval (FRI) identified peaks at 13.4, 12.3, 10.6, 9.1-6.4, 4.8 and 2.2 ka with the highest FRI identified from 3.6 to 2 ka. The SNI is above or close to 3 throughout the entire sequence, implying statistical robustness of the peak detection.

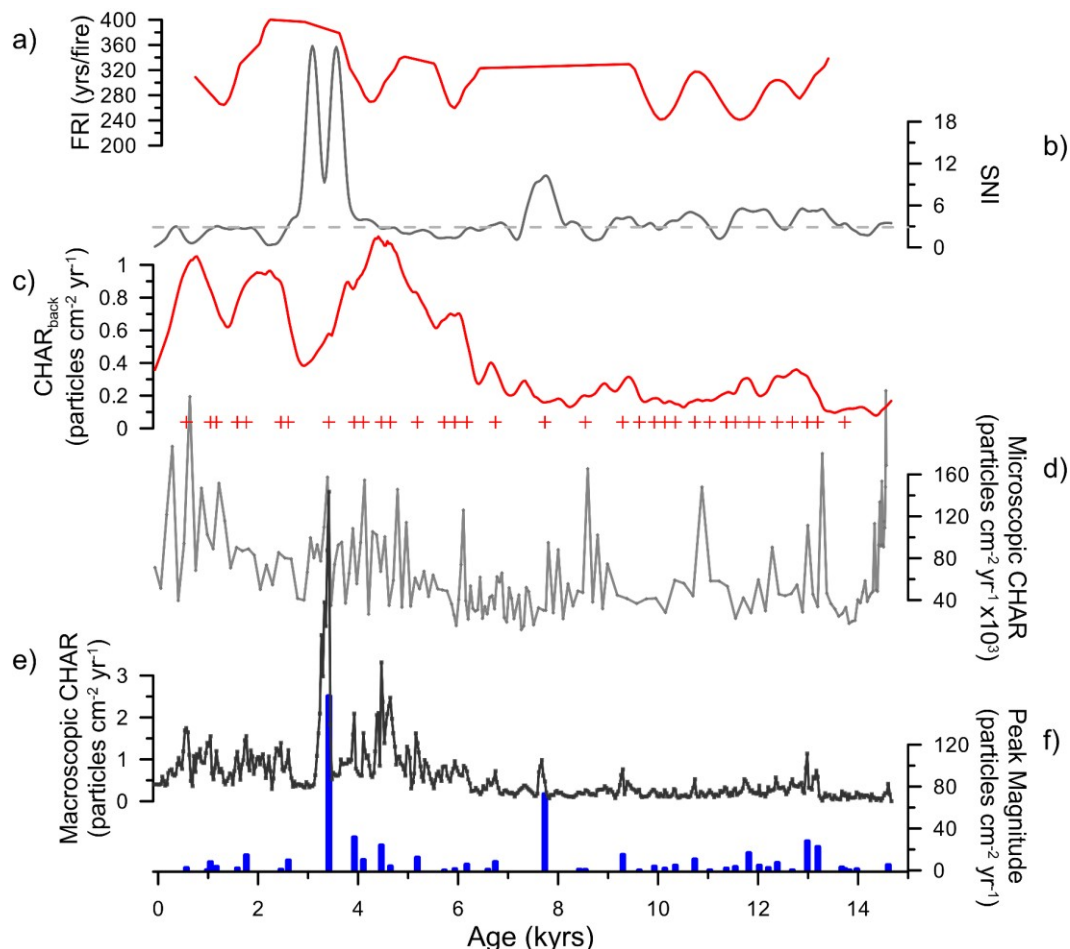


Figure 4.3: Paddy's Lake charcoal data: a) Fire return interval (FRI) (years per/fire); b) Signal-to-noise (SNI) index. SNI above the grey dashed line indicates fire events above the noise threshold (>3); c) background charcoal (particles/cm²yr⁻¹); d) Microscopic charcoal (particles/cm² yr⁻¹ x 10³); e) Macroscopic charcoal (particles/cm² yr⁻¹); and f) Peak Magnitude (particles/cm² yr⁻¹). Red plus symbols indicate significant charcoal peaks (peaksFinal).

4.6.4 PALYNOLOGY

A total of 185 samples were analysed for pollen, spore and microscopic charcoal with a total of 93 terrestrial pollen taxa identified throughout the sequence (Figure 4.4). Three significant CONISS zones were identified in the terrestrial pollen taxa: Zone 1-14,600 to 13,400 cal yr BP (265-177 cm), Zone 2-13,300 to 11,000 cal yr BP (175-141 cm), and Zone 3-11,000 to 65 cal yr BP (139-0 cm). Four subzones were identified in Zone 3. Following is a brief summary of the major trends in the pollen data [values in parentheses indicate averages and maximum percentages (<n)] and DCA axis 1 scores (explained variance = 52.0%):

4.6.4.1 Zone 1 - ca. 14.6-13.4 ka (265-177 cm)

Zone 1 is dominated by Poaceae (45%) and other non-arboreal pollen taxa: Asteraceae (15%), Chenopodiaceae (<10%), *Plantago* sp. (6%), and *Triglochin* sp. (<3%). Cupressaceae attains peak values for the record (3%) in this zone. The pollen DCA axis 1 has high stable values throughout Zone 1.

4.6.4.2 Zone 2- ca. 13.3-11.0 ka (175-141 cm)

Zone 2 is marked by a dramatic decline in Poaceae by 30% and a concomitant increase in *Pomaderris* sp., which dominates this zone (20%). *P. aspleniifolius* increases markedly through this zone (15-20%), while *N. cunninghamii* gradually increases. DCA axis 1 shows a sharp decline at the transition from Zone 1 and 2 with a slow decline for the remainder of the zone.

4.6.4.3 Zone 3 - ca. 11.0 ka -present (139-0 cm)

Zone 3 is dominated by tree and shrub taxa. *N. cunninghamii* dominates throughout (<50%) and other important taxa include: *P. aspleniifolius* (<15%), *Eucalyptus* spp. (15-20%), and *Bauera rubioides* (20%).

Zone 3 is divided into four subzones: Zone 3a [11,000 to 8,750 cal yr BP (139-117 cm)], Zone 3b [8,750 to

6,060 cal yr BP (116-89 cm)], Zone 3c [6,060 to 3,450 cal yr BP (88.5-58 cm)], and Zone 3d [3,450 to -65 cal yr BP (57-0 cm)]. The pollen DCA axis 1 remains fairly stable through the entirety of this zone.

Zone 3a - ca. 11.0-8.7 ka (139-117 cm). Subzone 3a is marked by a decline in *P. aspleniifolius*, an increase in *N. cunninghamii* (25%), and *B. rubioides* (10%). The aquatic fern *Isoetes* sp. increases sharply to ~20%.

Zone 3b - ca. 8.7-6.0 ka (116-89 cm). *N. cunninghamii* peaks toward the end of this subzone at 45%. *P. aspleniifolius* also increases in this zone (<10%) and *B. rubioides* slightly declines (5-10%).

Zone 3c - ca. 6.0-3.5 ka (88.5-58 cm). The beginning of subzone 3c is marked by a decline in *N. cunninghamii* (20%) and an increase in *B. rubioides* (15%) and *Melaleuca* sp. (3-4%), followed by an increase in *N. cunninghamii* toward a peak at ca. 4.8 ka (40%). *P. aspleniifolius* slowly declines through this zone.

Zone 3d - ca. 3.5 ka -present (57-0 cm). The final subzone is marked by a decline in *N. cunninghamii* (to 10%) with a slight incline in *Orites* sp. (3%). *N. cunninghamii* increases again (20%) toward the end of the subzone and *P. aspleniifolius* continues declining to the end of this zone.

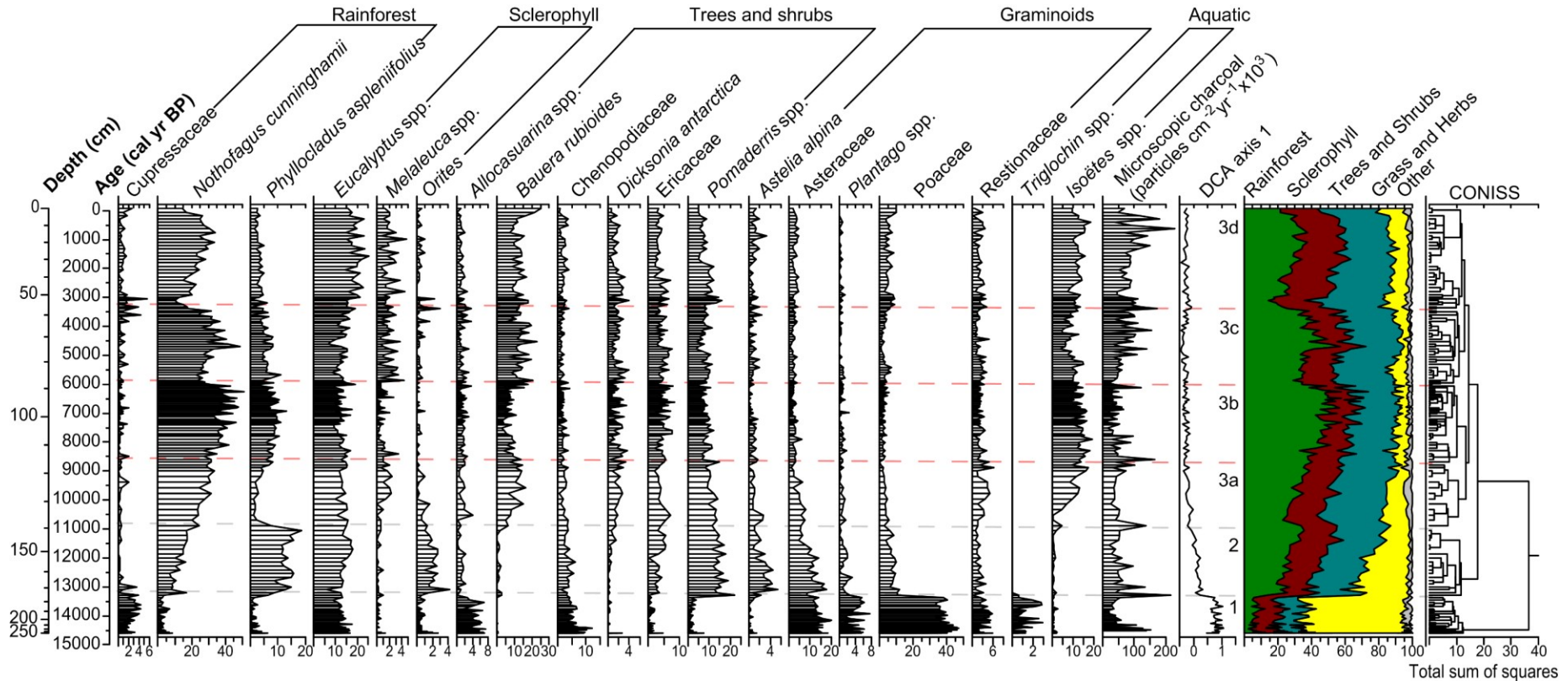


Figure 4.4: Pollen stratigraphy of Paddy's Lake important pollen types. Pollen data is presented as percentages and grouped by rainforest taxa (green), sclerophyll taxa (maroon), trees and shrubs (teal), graminoids (yellow) and aquatic taxa (grey). Group percentage totals are stacked by their associated colour. Microscopic charcoal is presented as particles $\text{cm}^{-2} \text{yr}^{-1} \times 10^3$. The DCA axis 1 scores estimate trends in the terrestrial pollen percentage data (variance=52.0%). CONISS cluster analysis represents the significant cluster groups and subzones of the terrestrial pollen types. The grey dashed line represents the break in Zones 1, 2, and 3 while the red dashed lines separate the subzones of Zone 3.

4.6.5 GEOCHEMISTRY

Elements associated with the PCA axis 1 scores (explained variance =42.39%) are Ti, K, Fe, Zr, Si, Rb, Zn, Br and the non-element incoherence/coherence ratio (Figure 4.5). Elements with a strong positive association with PCA axis 1 include Br and incoherence/coherence ratio while strong negative associations include elements Ti, K, Fe, Zr, Si, Rb and Zn. PCA axis 1 follows an opposing trends to the pollen DCA with low values in Zone 1 and a sharp increase at the zone transition while increasing slightly throughout the remainder of Zones 2 and 3. During Zone 3 there are two declines in the geochemical PCA axis 1 scores (Figures 4.5 & 4.6c). The first decline is at ca. 6.0 ka and the second at ca. 3.4 ka. Bromine is virtually absent between ca. 14.5 and 13.3 ka, increasing markedly to 9 ka, before declining after ca. 6.0 ka and remaining stable to present (Figure 4.7b).

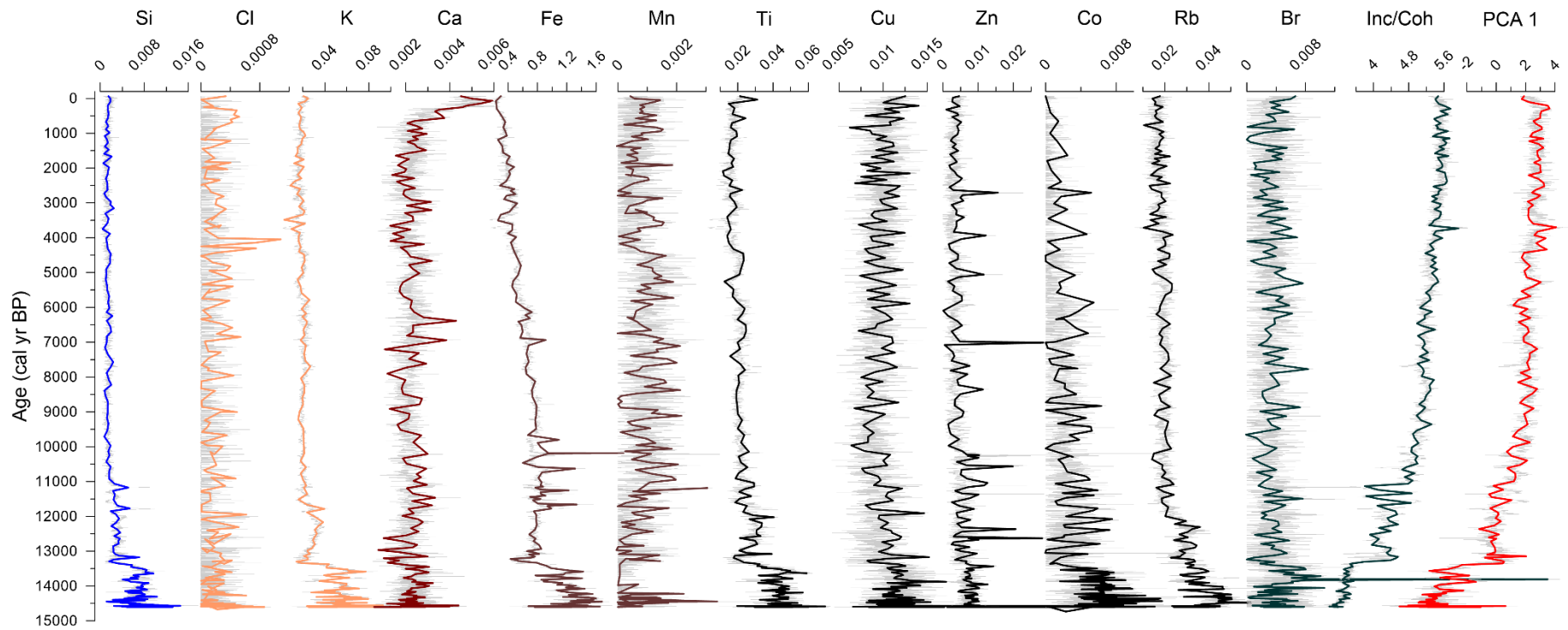


Figure 4.5: ITRAX stratigraphy for Paddy's Lake composite core of important μ XRF geochemicals, normalised by $k_{cps,n}$, with a 1.5 smooth spline.

4.7 DISCUSSION

4.7.1 PALAEOENVIRONMENTAL HISTORY

4.7.1.1 Late Pleistocene [ca. 14.6- 11.5 ka]

Our results demonstrate that Paddy's Lake was ice-free by ca. 14.6 ka (14,255-15,363 cal yr BP), ca. 2.4 kyrs after cosmogenic evidence of ice retreat following the Last Glacial Maximum (LGM) on the Central Plateau and West Coast Ranges of Tasmania (ca. 17-20 ka) (Barrows et al., 2002). The delayed onset of organic accumulation at Paddy's Lake, which lies at 1,065 masl, is consistent with other higher elevation lakes in Tasmania (e.g. Tarn Shelf, Upper Lake Wurawina, Tyndall Range (Macphail, 1979; Macphail et al., 1985; Colhoun, 1996)), at which postglacial organic accumulation occurs after ca. 13 ka. Interestingly, our selected age model indicates that the commencement of pelagic sedimentation at Paddy's Lake was coeval with the Antarctic Cold Reversal (ACR), a phase of depressed temperatures over Tasmania (Pedro et al., 2016). It is possible that a temperature threshold was crossed during the rapid temperature rise that occurred immediately prior to the ACR, initiating lacustrine development, and that any ACR temperature depression was insufficient to reinitiate ice formation within the cirque. This interpretation is consistent with the initial reduction in arboreal pollen at Paddy's Lake and the increase in Poaceae throughout the ACR chronozone (Figure 4.4), suggesting the establishment and persistence of alpine grassland vegetation through the ACR at the site (Figure 4.6b). This 'reversal' in vegetation development is consistent with the geochemical data, which shows a shift toward increased detrital input (Ti, Fe, K, and Si) (Figure 4.5) that reflects a reduction of arboreal vegetation and associated organosols and the establishment of a sparsely vegetated alpine landscape around Paddy's Lake through the ACR. Our inference of an ACR signal is supported regionally by evidence for the impact of the ACR on cool temperate terrestrial ecosystems across the southern extra-tropics, such as, a

decline in tall trees at Okarito Bog, New Zealand (Newnham et al., 2007) and an increase in cold resistant *Podocarpus* at Lago, Lepu  Patagonia from 14.6 to 12.7 ka (Pesce et al., 2014).

The return to rapid post-glacial warming recorded in Antarctica following the ACR is broadly synchronous with a sharp increase in arboreal pollen at Paddy's Lake, reflecting the influence of rising temperatures and the establishment of rainforest species within the local catchment and the broader region. Increasing biomass in the catchment is implied by the sharp increase in bromine (sediment organic matter, Figure 4.6g) at this time and supports the notion of a temperature and/or moisture-driven increase in productivity at the site. The notable increase in *P. aspleniifolius* between ca. 13.4 to 12.6 ka, while likely not reflecting establishment in the local catchment (Fletcher et al., 2007b), is a regional signal (Macphail, 1979; Markgraf et al., 1986; Colhoun et al., 1991a; Colhoun, 1996; Fletcher et al., 2007a; Stahle et al., 2016) that likely reflects the expansion of this rainforest pioneer into new habitats in response to climatic change (Macphail, 1979; Colhoun, 1996). *P. aspleniifolius* is a hygrophilous species and this phase likely reflects a cool and moist period. Fletcher and Moreno (2012) argue for a hemisphere-wide humid period between ca. 14 to 12 ka resulting from enhanced SWW flow across the mid-latitudes of the Southern Hemisphere and it is possible the *P. aspleniifolius* 'bulge' (Colhoun, 1996) reflects an increase in moisture resulting from this change in hemispheric circulation. Alternatively, McGlone et al. (2004) argue for an insolation-driven change in seasonality at this time resulting in increased winter and spring temperatures and wetter summers resulting in a phase of cool and cloudy conditions conducive to the development of hygrophilous forest in the extra-tropics and subantarctic islands of New Zealand (McGlone et al., 2010a; McGlone et al., 2010b). Supporting the seasonality hypothesis of McGlone et al. (2004, 2010ab) is evidence for a poleward displacement of the SWW at this time (Anderson et al., 2009), arguing against a more northerly position/enhancement of the SWW over the extra-tropics (sensu Fletcher et al., 2012). Our data only suggests a wetter period from ca. 13.4 to 12.6 ka and cannot discern between seasonality supporting either hypothesis.

4.7.1.2 Early to mid-Holocene [ca. 11-7 ka]

The onset of the Holocene is marked by a sharp decline in *P. aspleniifolius* and the establishment of both alpine 'rainforest' heath (*Bauera rubioides*) and littoral macrophyte communities dominated by *Isoetes* sp. (likely *I. gunnii*), implying that either changing lake levels inundated favourable *P. aspleniifolius* habitat or that lower water temperatures had inhibited the establishment of this alpine macrophyte prior to this time. The virtual absence of this pollen type during peak glacial conditions elsewhere in western Tasmania (Colhoun et al., 1999) supports the latter inference. The high values of *Pomaderris* sp. (cf. *P. apetala*) during this phase likely reflects transport into the lake from the wet sclerophyll forests on the lower slopes immediately north of the site. At Paddy's Lake, low CHAR (Figures 4.3e & 4.7g), CHAR_{back} (Figure 4.3c), the steady increase in organic matter content (Br) (Figure 4.7b), and both *N. cunninghamii* and *B. rubioides* (Figure 4.4) reflects the capture of the site by *N. cunninghamii*-dominant alpine heathland in the absence of significant disturbance by local fire. While low *P. aspleniifolius* values between ca. 11 to 9 ka (Figure 4.7c) is synchronous with regional drying and increased regional fire activity (Figure 4.7a) (Fletcher et al., 2015; Stahle et al., 2016), and likely reflects the impact of low moisture and fire on the regional dynamics of this hygrophilous rainforest species. This phase is synchronous with a hemisphere-wide low moisture phase likely resulting from combination of weak SWW flow (Fletcher et al., 2012) and increasing seasonality (McGlone et al., 2004). The steady increase in *P. aspleniifolius* after 9.4 ka (9,288 to 9,498 cal yr BP), then, likely reflects increasing regional moisture under an enhanced SWW regime and/or the influence of decreased regional fire activity, consistent with trends inferred from across Tasmania's southwest (Fletcher et al., 2011; Fletcher et al., 2015; Rees et al., 2015; Stahle et al., 2016) and with inferences of enhanced SWW dynamics over the South Island and Subantarctic Islands of New Zealand (McGlone et al., 2004; McGlone et al., 2010a; McGlone et al., 2010b) and southern South America (Moreno, 2004; Moreno et al., 2010).

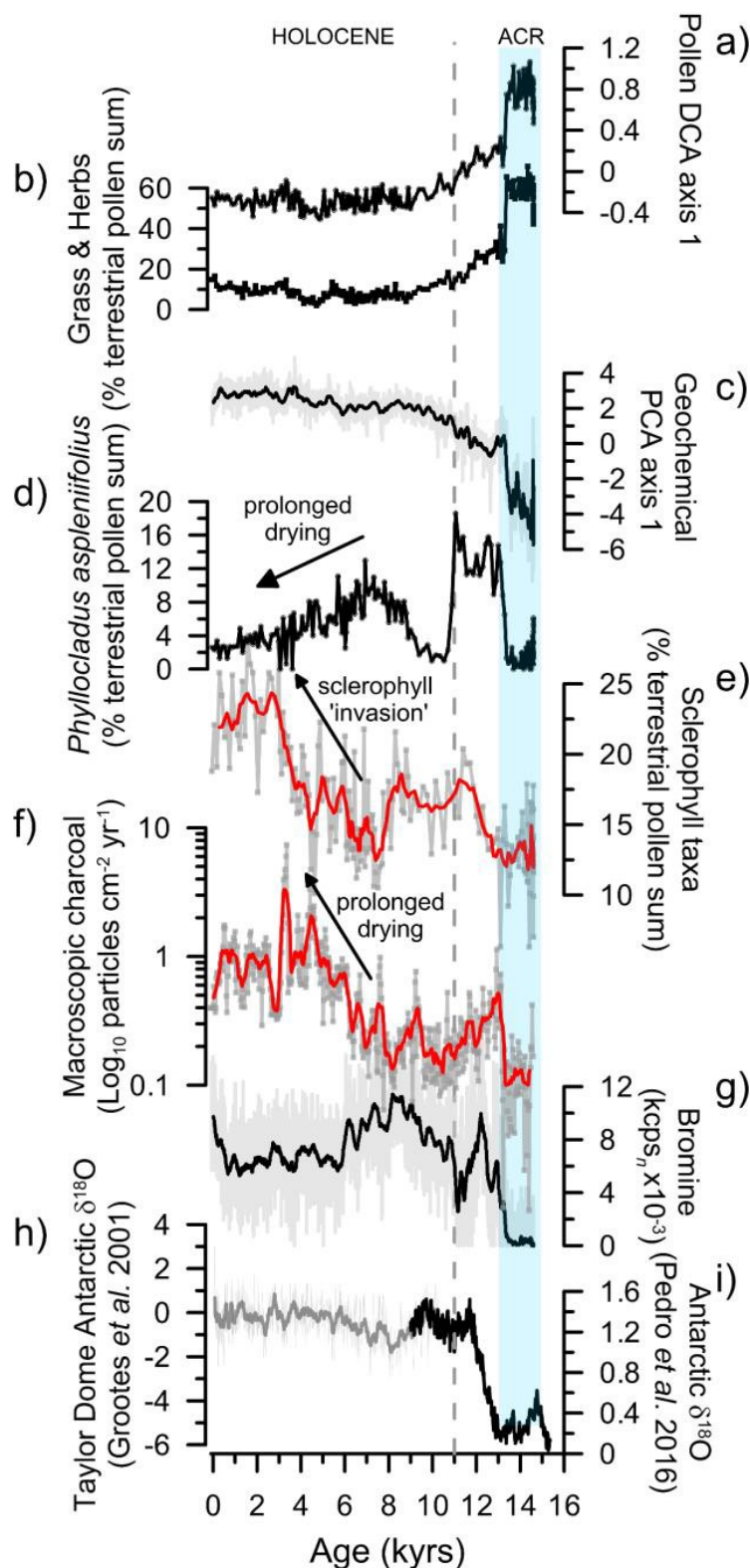


Figure 4.6: Summary plot of Paddy's Lake data including: a) terrestrial pollen DCA axis score 1; b) grass and herbs pollen percentages; c) geochemical PCA axis 1 scores with weighted average (window width=51); d) *Phyllocladus aspleniifolius* pollen percentages; e) sclerophyll taxa pollen percentages with weighted average in red (window width=7); f) macroscopic charcoal (particles/cm² yr⁻¹) on log scale with weighted average in red (window width=11); and g) bromine (kpcps₇ × 10⁻³) in grey with weighted average (black, window width=51). With Antarctic climate data from: h) δ¹⁸O record from Taylor Dome Antarctic (Grootes et al., 2001) raw data in grey with weighted average in dark grey (window width=11); and i) Antarctic ice core δ¹⁸O composite curve (Pedro et al., 2016). Blue box indicates the ACR and Zone 1 while the grey dashed line separates Zones 2 and 3.

4.7.1.3 Mid to late Holocene [ca. 7-0 ka]

The dominance of rainforest pollen types (>50% of the pollen sum) between ca. 7.5 to 6.5 ka indicates peak Holocene positive moisture balance at Paddy's Lake. The timing of this peak is synchronous with a minimum in fire activity in south western Tasmania (Figure 4.7a) (Fletcher et al., 2015); and with peak moisture across the mid-latitudes of the Southern Hemisphere during the extra-tropical mid Holocene SWW maximum (Fletcher et al., 2012). Despite peak regional rainforest development, the importance of non-arboreal pollen at Paddy's Lake suggests the persistence of an alpine shrubland community containing lowland rainforest elements with broad ecological tolerances (e.g. *N. cunninghamii*). A decline in *P. aspleniifolius* at ca. 6.7 ka (Figures 4.6d & 4.7c) signals a prolonged drying within the region and the end of the mid-Holocene humid phase prior to the first of a series of three high impact local fire events at ca. 6.3 ka (Figures 4.6f & 4.7g). We infer high impact fire events as macroscopic charcoal peaks associated with changes in either pollen composition and/or geochemistry (sensu Fletcher et al., 2014a). This local fire event drove a substantial decrease in *N. cunninghamii* and a major reduction in the amount of organic matter being delivered to the lake from the catchment organosols, revealing a local catchment response to this fire event (Figure 4.7b & d).

Two subsequent fire episodes occur at ca. 4.8 ka (4,690 to 4,850 cal yr BP) and 3.4 ka (3,385 to 3,565 cal yr BP) (Figure 4.3), with the former likely impacting extra-local vegetation (as indicated by the mild response in the pollen stratigraphy) and the latter driving substantial reduction in *N. cunninghamii* and concomitant increase in sclerophyllous species (Figure 4.7d & e). Sclerophyllous species in Tasmania are principally pyrogenic and the sharp increase in these taxa at Paddy's Lake reveals a marked shift in the vegetation-fire dynamic within the local catchment. The positive feedback between pyrogenic vegetation and fire is well described in Tasmania (e.g. Jackson, 1968; Wood et al., 2012), and the replacement of pyrophobic vegetation by pyrogenic vegetation is known to alter local fire regimes and subsequent charcoal stratigraphy (Fletcher et al., 2014a). We interpret the drop in macroscopic charcoal content of Paddy's Lake in concert with peak sclerophyll taxa as the sclerophyll 'invasion' (Figure 4.7e & g), a shift to more frequent and lower intensity burning at the site in response to the alteration of the local fuel type and structure in the catchment (sensu Fletcher et al., 2014a).

4.7.2 LONG-TERM CLIMATE CHANGE [SWW TO ENSO]

Our study represents the only well-dated continuous long-term proxy record of environmental change from outside of the modern SWW/SAM-dominant climate zone of Tasmania. Thus, our data is critical for assessing the prevailing model of long-term climatic change in the South Pacific, which depicts a shift from millennial scale SWW dominance between ca. 12-5 ka to ENSO dominant climate after ca. 5 ka (Fletcher et al., 2015; Rees et al., 2015). We identify a clear regional hydroclimatic signal based on the hygrophilous rainforest taxon, *P. aspleniifolius* (Figures 4.6d & 4.7c). Comparison of our data with a charcoal composite derived from two lakes located in the modern SWW/SAM-dominant climate zone of southwest Tasmania (Figure 4.7a) (Fletcher et al., 2015) highlights a clear divergence between local fire activity at Paddy's Lake and regional climate-driven fire activity in southwest Tasmania. Our evidence for low fire activity and lack of vegetation response to regional (south western Tasmanian) drying between ca. 11-9 ka demonstrates either a local vegetation resistance to the drying effects caused by attenuated SWW flow over Tasmania at this time or that the hydroclimatic impacts of this phase of attenuated SWW flow were less important outside of the modern western SWW/SAM-climate zone. The peak in rainforest pollen at Paddy's Lake between ca. 7.5-6.5 ka is synchronous with inferences of a hemisphere-wide mid-latitude enhancement of SWW flow that drove (1) low fire activity across western Tasmania, (2) hygrophilous rainforest expansion, and (3) high lake levels in SWW dominant landmasses across the hemisphere (Fletcher et al., 2012). Together, our data suggests that, while likely muted relative to sites further southwest in Tasmania, long-term climatic evolution change at Paddy's Lake closely follows the well-described SWW-dominant hemispheric signal between ca. 12-7 ka.

Critically, we identify an initial drying trend (reduction in *P. aspleniifolius*) at ca. 6.7 ka (6,676 to 6,794 cal yr BP) that is synchronous with the onset of the first phase of 'modern' ENSO variability in the Holocene based on the Moy et al. (2002) record (Figure 4.7c). Which predates any evidence we are aware of for ENSO-like climatic variability in the southwest Pacific (Gomez et al., 2004; Turney et al., 2006; Black et al., 2008; Donders et al., 2008; Fletcher et al., 2015; Rees et al., 2015; Stahle et al., 2016). Though the Moy et al. (2002) record is recording the eastern Pacific effects of El Niño, it has been successfully used to understand environmental response to ENSO in the Australasian region (Fletcher et al., 2014a; Fletcher et al., 2015;

Mariani et al., 2017b; Mariani et al., 2017c; Fletcher et al., 2018b). The subsequent local-scale fire events at ca. 6.3 ka and 3.4 ka also occur in concert with increased ENSO variability recorded in the tropical Pacific (Figure 4.7h) (Moy et al., 2002). We also observe a mild reduction in *N. cunninghamii* in concert with increasing charcoal at ca. 4.8 ka, synchronous with a major spike in ENSO activity that has been implicated in widespread changes in natural and human systems across the Pacific Ocean (Sandweiss et al., 1996; Sandweiss et al., 2001; Turney et al., 2004; Fletcher et al., 2012; Fletcher et al., 2015; Rees et al., 2015). The lack of catchment response (geochemical signal) and the mild response in the vegetation to this fire activity suggest that it was either extra-local or of low impact within the local catchment. We also observe a decrease in *P. aspleniifolius* at ca. 5.7 ka (5,624-5,757 cal yr BP), synchronous with a peak in tropical El Niño activity. Indeed, the hydrophile *P. aspleniifolius* decreases each time there is a peak in El Niño activity between ca. 6.7-3 ka, reflecting the high climatic sensitivity of the study region to ENSO variability through this period (Figure 4.7c & h).

Importantly, it is not possible to resolve whether our high impact fires are the result of single events or whether they are repeated fire episodes occurring within the sampling interval of our lake sediment. The Moy et al. (2002) El Niño reconstruction we have employed reports the number of El Niño events per century and it is possible that the ENSO-driven fires we hypothesise are the result of a cumulative drying of the landscape that coincides with fuel availability and ignition source, rather than single El Niño events. While biomass is, over the long term, not assumed to be a limitation for fires in temperate forested regions like Tasmania (Pausas et al., 2007; McWethy et al., 2013; Pausas et al., 2013), the charcoal minima that occurs during a phase of amplified El Niño activity following the high impact fire at ca. 3.4 ka likely reflects fuel limitation after severe burning of local vegetation around our site. Further, it is not possible to resolve whether the burning recorded at our study lake is either the result of an increased efficacy of Aboriginal burning during a more variable, and overall, drier climate or whether it is the result of an increase in the incidence of dry lightning strike following a protracted phase of below average rainfall. Analyses of historical ignitions in Tasmania reveal humans as the overwhelming cause of fires (Bowman et al., 1986a) and the long occupation (>35,000 years) of this landscape and clear evidence for landscape manipulation using fire argues strongly for

a human ignition source. However, recent (2016) landscape-scale fires in western Tasmania occurred following a combination of decades of protracted drying (Abram et al., 2014; Mariani et al., 2016a), a strong El Niño, and a series of intense dry lightning strikes (Sharp, 2016).

The synchrony we observe between tropical ENSO activity and environmental change at Paddy's Lake reveals a number of key insights about the spatiotemporal impact of the ENSO system: (1) it underscores the importance of ENSO over Australian climate and fire activity (Mariani et al., 2016a); (2) highlights the sensitivity of this part of Tasmania to long-term shifts in tropical ENSO variability; and (3) reveals possible stationarity in the spatial influence of ENSO over this region that likely results from the influence of the sharp relief in this alpine landscape over local climate expression. An apparent breakdown of the relationship between vegetation change and ENSO variability at Paddy's Lake occurs after ca. 3 ka, following a shift to local sclerophyll dominance of the vegetation (Figure 4.7e). This breakdown either reflects a greater resilience of this sclerophyll dominant vegetation to ENSO-driven hydroclimatic variability or an alteration to the fire-vegetation-charcoal signal dynamic through this period (Fletcher et al., 2014a).

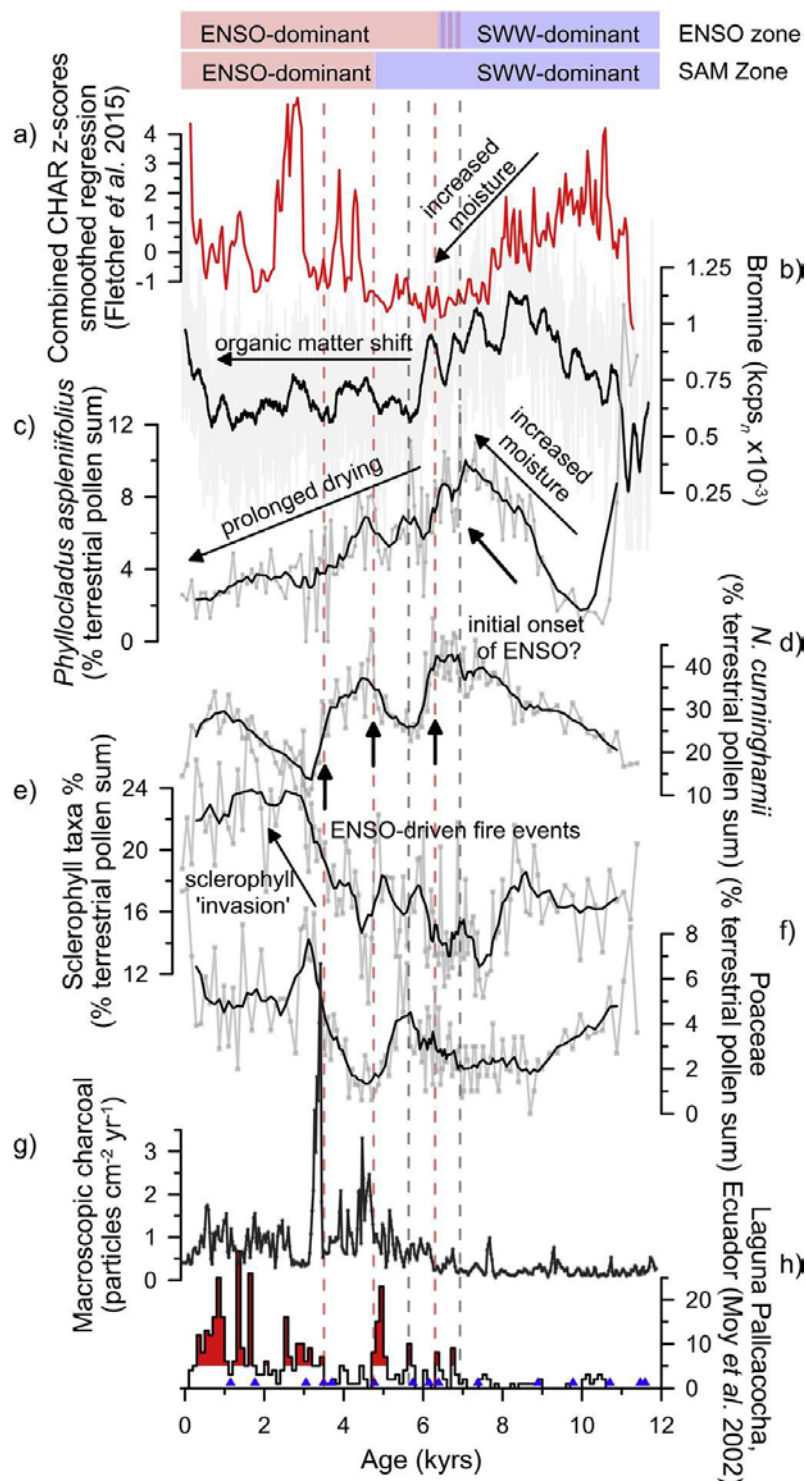


Figure 4.7: Summary plot of Holocene palaeoecological data: a) Lake Nancy and Lake Gwendolyn combined charcoal z-score regression (red) interpolated to 80-year time-steps and z-scores calculated from an average of pre-European (12-0.2 ka) charcoal values and smoothed weighted averaging regression (window width = 9) (Fletcher et al., 2015); b) Paddy's Lake bromine data ($\text{kpcps}_n \times 10^{-3}$) in grey with weighted grey dashed lines show shifts average (black, window width=51); Paddy's Lake pollen percent data (grey line - scatter) with a weighted average (black line, window width=7) for: c) *Phyllocladus aspleniifolius*; d) *Nothofagus cunninghamii*; e) sclerophyll taxa; f) Poaceae; g) Paddy's Lake macroscopic charcoal ($\text{particles}/\text{cm}^2 \text{yr}^{-1}$); and h) the number of El Niño events in 100-year overlapping windows from inorganic sediment deposits in Laguna Pallcacocha, Ecuador (Moy et al., 2002) with red shading indicates significant El Niño events. Red dashed lines indicate significant fire events and vegetation response and blue triangles indicate locations of ^{14}C dates. Grey dashed lines show shifts in *P. aspleniifolius* (signalling regional hydroclimate) that occur during periods of increased El Niño frequency.

4.7.3 SCLEROPHYLL INVASION

The onset of modern ENSO variability through the Holocene had dramatic consequences for natural and cultural systems across the Pacific Ocean basin (Sandweiss et al., 1996; Karl et al., 1997; Sandweiss et al., 1999; Asner et al., 2000; Sandweiss et al., 2001; Lima et al., 2002; Kitzberger et al., 2003; Ogutu et al., 2003). In the western Pacific, drought stress resulting from El Niño events contributed to demographic and technological change in Australian Aboriginal societies (Turney et al., 2006), while fires (human-lit and ‘natural’) drove ecosystem change, particularly in areas dominated by fire-sensitive plant communities (Fletcher et al., 2014a). The marked increase in charcoal delivery into Paddy's Lake after ca. 6.7 ka (6,587-6,711 cal yr BP) (Figures 4.3 and 4.7g) occurs in concert with an increase in pollen from sclerophyllous taxa (*Eucalyptus*, *Leptospermum*, *Melaleuca*, etc. Figure 4.7e). Elsewhere in Tasmania, the localised extinction of rainforest was facilitated by repeated burning over successive millennia that (1) irrevocably damaged the vegetation-organosol system, (2) resulted in nutrient loss from soils, and (3) facilitated the invasion of fire-promoting sclerophyllous species (Wood et al., 2012; Fletcher et al., 2014a). This suite of changes altered the vegetation-fire-soil dynamic and precipitated a vegetation state change from pyrophobic rainforest to pyrogenic Eucalypt-shrubland (Fletcher et al., 2014a). While likely never vegetated by rainforest (*sensu stricto*), the trends at Paddy's Lake reveal a clear fire-driven change in catchment sediment dynamics (Figure 4.7b), followed by an invasion of the local catchment by fire-promoting sclerophyll species resulting from ENSO-driven fire events (Figure 4.7e). The drop in macroscopic charcoal delivery into Paddy's Lake is consistent with a change in fire regime from less frequent-higher intensity fires (controlled largely by fuel moisture) that produce more charcoal to a more frequent-lower intensity fire regime (controlled principally by fuel type/flammability) (*sensu Fletcher et al., 2014a*) - i.e. a switch from pyrophobic to pyrogenic vegetation.

4.8 CONCLUSIONS

Climate variability is the key driver of change in fire regimes, geochemistry, and vegetation change at Paddy's Lake, Tasmania. The high percentage of non-arboreal pollen and dominance of Poaceae from ca. 14.5 to 13.3

ka indicate cold conditions during the ACR. Following the ACR, a significant shift in vegetation and geochemistry are confirmed by warming conditions toward the Holocene and an increase in fire activity. During the earliest Holocene, rainforest appears to have increased at Paddy's Lake in response to increased moisture. Following this, ENSO drove an increase in fire activity at ca. 6.3 ka and 3.4 ka; as well as, vegetation response with a decline in *N. cunninghamii* and increase in sclerophyll taxa. Indeed, it appears that the climate at Paddy's Lake is highly sensitive to ENSO, with an early spike in fire activity at ca. 6.3 ka coincident with an increase in tropical ENSO activity (Moy et al., 2002). Repeated local fire disturbance from ca. 6.3 to 3 ka culminated in a vegetation state shift, characterised by increased sclerophyll taxa, reduced organic sediment production and a defined change in the charcoal signature.

4.9 ACKNOWLEDGEMENTS

We acknowledge that our work was conducted on Tasmanian Aboriginal lands and thank the Tasmanian Aboriginal community for their ongoing support of our research. We would like to thank Alexa Benson, Agathe Lisé-Pronovost, Angelica Ramirez, William Rapuc, Scott Nichols, and Anthony Romano for their assistance in the field. The financial support of this project comes from the Australian Research Council (award: DI110100019 and IN140100050) and Australian Institute of Nuclear Science and Engineering (award: ALNGRA15003). We thank an anonymous reviewer for their constructive comments on an earlier draft that resulted in a substantial improvement of the manuscript.

Supplementary data in Appendix I

CHAPTER 5: DISCUSSION

5.1 CHAPTER AIM

The aim of this chapter is to understand the aquatic ecosystem response to climate at Paddy's Lake. This chapter is comprised of the modified published article Beck, K.K., Fletcher, M-S., Kattel, G., Barry, L., Gadd, P.S., Heijnis, H., Jacobsen, G., & Saunders, K.M. (2018) The indirect response of an aquatic ecosystem to long term climate-driven terrestrial vegetation in a subalpine temperate lake. *Journal of Biogeography*, 45, 713-725 DOI:10.1111/jbi.13144. Beck, K.K. and Fletcher, M.-S. conceived the ideas for this research. Beck, K.K. performed the cladoceran and statistical analyses, interpretation, and writing of this publication. Gadd, P.S., and Heijnis, H. performed the μ XRF geochemical analysis. Barry, L.A. performed the CN elemental and isotope analysis and Jacobsen, G. the radiocarbon analysis. All authors assisted in editing and interpretation of result for this publication.

5.2 ABSTRACT

Aim - To assess whether climate directly influences aquatic ecosystem dynamics in the temperate landscape of Tasmania or whether the effects of long-term climatic change are mediated through the terrestrial environment (indirect climate influence).

Location - Paddy's Lake is located at 1,065 masl in temperate north-west Tasmania, a continental island south-east of mainland Australia (41°15'-43°25'S; 145°00'-148°15'E).

Methods - We developed a new 13,400 year (13.4 kyr) palaeoecological dataset of lake sediment subfossil cladocerans (aquatic grazers), bulk organic sediment carbon (C%) and nitrogen (N%) and $\delta^{13}\text{C}$ and $\delta^{15}\text{N}$ stable isotopes. Comparison of this new data was made with a recently published pollen, geochemistry and charcoal record from Paddy's Lake.

Results - Low cladoceran diversity at Paddy's Lake is consistent with other temperate Southern Hemisphere lakes. The bulk sediment $\delta^{15}\text{N}$ values demonstrate a significant lagged negative response to pollen accumulation rate (pollen AR). Compositional shifts of dominant cladoceran taxa (*Bosmina meridionalis* and *Alona guttata*) occur following changes in both pollen AR and pollen (vegetation) composition throughout the 13.4 kyr record at Paddy's Lake. The $\delta^{15}\text{N}$ values demonstrate a significant positive lagged relationship to the oligotrophic:eutrophic cladoceran ratio.

Main conclusions - Long-term changes in cladoceran composition lag changes in both pollen AR and terrestrial vegetation composition. We interpret pollen AR as reflecting climate-driven changes in terrestrial vegetation productivity and conclude that climate-driven shifts in vegetation are the principal driver of the cladoceran community during the last ca. 13.4 kyrs. The significant negative lagged relationship between pollen AR and $\delta^{15}\text{N}$ reflects the primary control of vegetation productivity over within-lake nutrient status. Thus, we conclude that the effects of long-term climate change on aquatic ecosystem dynamics at our site are indirect and mediated by the terrestrial environment. Vegetation productivity controls organic soil development and has a direct influence over lake trophic status via changes in the delivery of terrestrial organic matter into the lake.

5.3 INTRODUCTION

Aquatic ecosystems are known to respond both 'directly' and 'indirectly' to climatic change (Battarbee, 2000; Ball et al., 2010). 'Direct' aquatic ecosystem responses to climate change are principally influenced by changes in temperature and lake level (Schindler, 1997; Smol et al., 2000; Gell et al., 2005), while 'indirect' responses include those that are mediated through the surrounding terrestrial environment via, for example, vegetation change that alters nutrient inputs and pH of watersheds (Huvane et al., 1996; Korsman et al., 1998; Lancashire et al., 2002; Augustinus et al., 2008; Wang et al., 2016). Despite the importance of climate in driving terrestrial ecosystem dynamics, and the clear relationship between terrestrial and aquatic ecosystems (Huvane et al., 1996; Korsman et al., 1998; Engstrom et al., 2000; Augustinus et al., 2008), a large portion of research into long-term aquatic ecosystem change focusses on the 'direct' role of climate in driving aquatic

ecosystem dynamics. Understanding how and when climate affects aquatic systems through both direct and indirect pathways is important if we are to understand how these systems will respond to the rapid climatic changes the earth is currently experiencing. Here we use multi-proxy palaeoecological data to assess the relationship between climatic change and long-term terrestrial and aquatic ecosystem dynamics in a temperate subalpine lake in Tasmania, Australia.

Direct aquatic ecosystem responses to climate change include changes to water temperature (Schindler, 1997, 2001), salinity/lake depth (De Deckker, 1982; Gasse et al., 1997; Smol et al., 2000; Saunders et al., 2007; Gell et al., 2012), and water chemistry (Schindler, 2001). Direct responses result in aquatic ecosystem changes that are either synchronous with (Prebble et al., 2005), or independent of (Tibby et al., 2012), changes in the terrestrial environment. In contrast, indirect aquatic ecosystem responses to climate that are mediated through the terrestrial environment are characterised by a lagged response of the aquatic environment to terrestrial change (Fritz et al., 2004; Heggen et al., 2010). Indirect effects of climate change include changes in the type and amount of terrestrial material entering an aquatic system (via erosion and/or vegetation productivity changes), which can alter critical factors such as pH (Whitehead et al., 1989; Pienitz et al., 1999), mixing/turbidity (Lotter, 2001; Augustinus et al., 2012), and the trophic status of water bodies (Engstrom et al., 2000; Heggen et al., 2010; Fritz et al., 2013; Perren et al., 2017).

In the cool high rainfall environment of western Tasmania, a combination of low temperatures, high humidity and extreme bedrock oligotrophy have resulted in a landscape blanketed in acid peats (Brown et al., 1982a; Jarman et al., 1982; Bowman et al., 1986b). As a result, waterbodies in this landscape are uniformly dystrophic, with nutrient inputs largely derived from the acid peat soils (Tyler, 1974, 1992; Vanhoutte et al., 2004). Indeed, the bedrock is so unyielding that the ionic composition of many lakes is near identical to sea water (i.e. low bedrock sources) (Buckney et al., 1973) and soil development is almost entirely dependent on the extant vegetation (Jackson, 1968; Wood et al., 2012). Despite the tight coupling between vegetation, peat development and water chemistry, there is a dearth of information about how terrestrial ecosystem change influences aquatic ecosystem dynamics in this landscape (Bradbury, 1986). This knowledge gap is critical, as

terrestrial systems in western Tasmania are currently experiencing unprecedented changes in response to anthropogenic climate change that are principally manifest as a reduction in rainfall and a concomitant increase in fire activity (McWethy et al., 2013; Fox-Hughes et al., 2014; Mariani et al., 2016a).

Here, we assess the relationship between long-term climatic change and changes in both aquatic and terrestrial ecosystems in a subalpine temperate environment in Tasmania, Australia. Given the tight coupling between vegetation, peat and water chemistry evident today, we hypothesise that the response of aquatic ecosystems to long-term climatic change in this landscape will be mediated by the terrestrial environment: i.e. ‘indirect’ response pathways. Further, we hypothesise that the principal pathway for mediation of climate signals through the terrestrial environment will be via vegetation-driven changes of nutrient inputs into the lake. To assess these hypotheses, we developed a new long-term (13,400 year; 13.4 kyr) multi-proxy lake sediment dataset of subfossil cladocerans (as a proxy for aquatic ecosystem dynamics), and organic carbon (elemental and $\delta^{13}\text{C}$) and nitrogen (elemental and $\delta^{15}\text{N}$) content. We compare our record to an existing record of pollen, charcoal and geochemistry from the same sediment sequence that shows clear climate-driven vegetation dynamics over the last ca. 14.6 kyrs (Chapter 4). To assess our hypotheses, we propose that ‘indirect’ climate-driven changes in aquatic ecosystem dynamics and nutrient cycling will be mediated by the terrestrial environment and, thus, will lag changes in the terrestrial system; while ‘direct’ climate-driven aquatic ecosystem dynamics and nutrient cycling will either precede, occur synchronously with, or be independent of changes in the terrestrial system.

5.4 GEOGRAPHICAL SETTING OF TASMANIA

Tasmania is a continental island with a cool temperate maritime climate (Gentilli, 1971) bisected by north-west—south-east mountain ranges that result in a steep gradient of westerly derived precipitation from 3,500 mm p/a west of the ranges to 400 mm p/a in the east (<http://www.bom.gov.au/>). These ranges create a clear division in the geography of Tasmania manifest as a stark east-west contrast in geology, climate, and ecology. Acidic organosols (peat), rainforests and fresh oligotrophic to dystrophic lakes prevail over much of the west,

lakes in the east are less acidic, (ultra) oligotrophic, turbid and more saline (Tyler, 1974, 1992; Vanhoutte et al., 2004). The zone of transition between the eastern and western provinces is often referred to as Tyler's Line (Figure 5.1). The rainforests of the Tasmania's west share remarkable taxonomic and physiologic similarities with the temperate rainforests in New Zealand and Chile, the so-called Gondwanan forests that are now restricted to tiny fire refugia in Tasmania (Wood et al., 2011b). Fires have decimated rainforest across all these southern regions (Veblen et al., 1982; McGlone, 1989), with more than 30% of Tasmanian subalpine rainforest lost to fire over the last two centuries (Holz et al., 2015).

5.4.1 CLADOCERANS OF SUBALPINE TEMPERATE AUSTRALASIA

Cladocerans are aquatic zooplankton that are an excellent proxy for changes in water temperature, lake level, water quality, trophic status of lakes, and food web dynamics (Lotter et al., 1997; Hofmann, 1998; Kamenik et al., 2007; Kattel et al., 2010; Kattel et al., 2015). In south-east Australia and New Zealand, important taxa include: *Alona guttata* (Sars, 1862), *Alonella excisa* (Fischer, 1854), *Bosmina meridionalis* (Sars, 1904) and *Chydorus sphaericus* (O.F. Müller, 1785) (Green, 1976; Geddes, 1988; Kattel et al., 2010; Augustinus et al., 2012; Kattel et al., 2015). *Alona guttata* is a cosmopolitan littoral taxon that is reported to be an indicator of wetland hydrology changes and nutrient status (Kattel et al., 2010; Kattel et al., 2015), as well as, warm climatic conditions (Frey, 1991b; Lotter et al., 2000; Kattel et al., 2010). *Bosmina meridionalis*, a pelagic cladoceran, is endemic to Australia and New Zealand and is an indicator of relatively clear water and oligotrophic conditions (Green, 1976; Geddes, 1988). *Chydorus sphaericus* is a eurytopic taxa, found in both littoral and pelagic habitats, showing responses to nutrient-enriched environments (Frey, 1980; Lotter et al., 1997; Kattel et al., 2010).

5.4.2 SITE DESCRIPTION

Paddy's Lake (41°27'04" S, 145°57'41" E) is a cirque lake situated at ca. 1,065 masl on the Black Bluff massif in north-west Tasmania, Australia (Figure 5.1). The lake is acidic and dystrophic; with one small,

outflow to the north and a maximum depth of ~21.5 m. The local geology is nutrient poor – consisting of quartz-dominated Quaternary glacial deposits and conglomerate, with minor surface expressions of slightly more fertile Cambrian volcanics (Seymour et al., 1995; Pemberton et al., 2004). Average monthly temperature ranges from ~4.6-14°C, with an annual average of ~12.3°C (Chapter 4; Bureau of Meteorology, 2016a, c). The local vegetation is classified as subalpine heathland (Harris et al., 2005), with the broader region composed of a complex mosaic of rainforest, *Eucalyptus*-dominant forest, scrub and open communities that reflects a long history of burning (Jackson, 1968; Fletcher et al., 2010a).

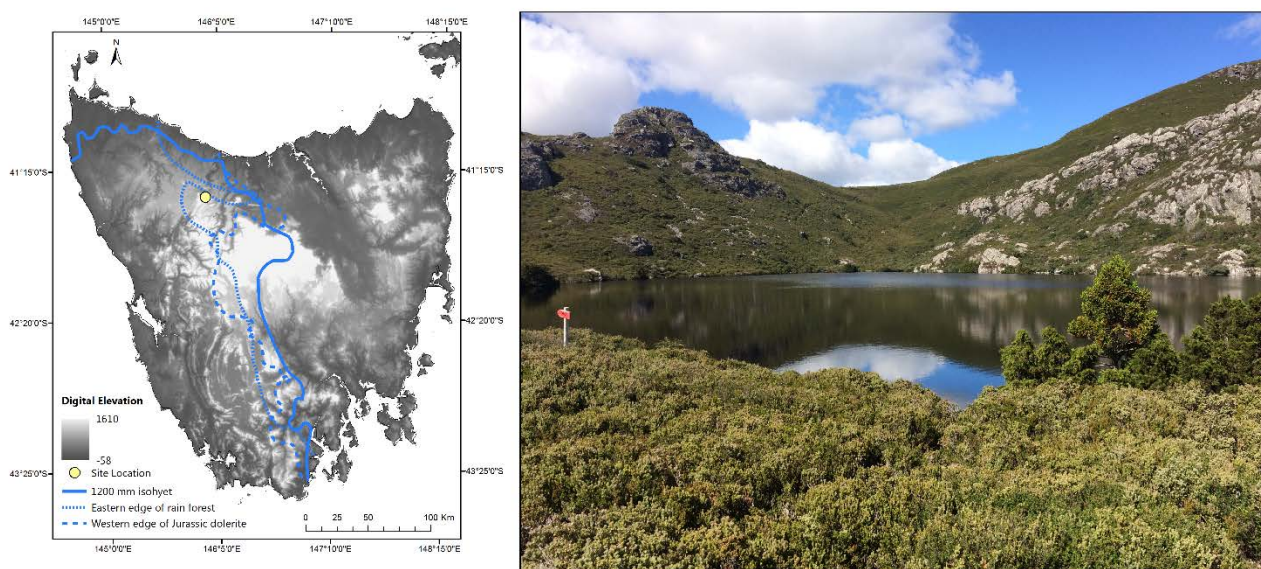


Figure 5.1: Digital elevation map of Tasmania and location of Paddy's Lake (yellow dot), on the left, featuring Tyler's Line (Tyler, 1992) determined by precipitation (solid blue line), rainforest boundary (dotted blue line) and the dolerite edge (blue dashed line). On the right, a photograph of Paddy's Lake (by: Kristen Beck, 2016).

5.5 MATERIALS AND METHODS

5.5.1 CORE COLLECTION AND CHRONOLOGY

An entire sediment sequence of 291 cm was developed using radiocarbon dating, charcoal and geochemistry from two cores (TAS1401 SC1 and TAS1401 N1) (Chapter 4) retrieved with a Bolivia coring system (a modified Livingstone system; Wright, 1967), and a Nesje coring system (Nesje, 1992). The core chronology was developed using 19 radiocarbon dates calibrated with the Southern Hemisphere calibration curve -

SHCal13 (Hogg et al., 2013) (Table II.1 in Appendix II). The age-depth model was produced in *R* v.3.1.1 (R Development Core Team, 2014) using a smooth spline regression with a smoothing factor of 0.5 in the *clam* v.2.2 package (Blaauw, 2010). Full details are in Chapter 4.

5.5.2 CLADOCERAN ANALYSIS

Processing for cladocerans followed standard methods (Korhola et al., 2001) at a resolution of 1 to 4 cm (ca. 60-350 yrs). Concentration values were determined using an exotic pollen spike (*Lycopodium* spp.) (sensu Faegri et al., 1989). A total of 100 cladoceran individuals were identified at 100-400x magnification (Kattel and Augustinus 2010). Identification was based on the following resources: Alonso, 1996; Brehm, 1953; Frey, 1991ab; Shiel and Dickson, 1995; Shiel, 1995; Smirnov and Timms 1983; and Szeroczyńska and Sarmaja-Korjonen, 2007. The oligotrophic:eutrophic ratio was calculated between *Bosmina meridionalis* (oligotrophic) and the sum of *Alona guttata* and *Chydorus sphaericus* (eutrophic).

5.5.3 GEOCHEMISTRY

Organic carbon (C%), nitrogen (N%), $\delta^{13}\text{C}$ and $\delta^{15}\text{N}$ were analysed at Australian Nuclear Science and Technology Organisation (ANSTO) at a resolution of 2 to 4 cm (ca. 50-530 yrs) using an Elementar VarioMICRO Elemental Analyser (C% and N%) and an Isotope Ratio Mass Spectrometer ($\delta^{13}\text{C}$ and $\delta^{15}\text{N}$) with a CO_2 trap (NaOH). An absence of carbonates was determined throughout the sequence by testing with HCl. The $\delta^{13}\text{C}$ results were normalised to an IAEA C8 reference (Le Clercq et al., 1998) and $\delta^{15}\text{N}$ to IAEA N-2 (Böhlke et al., 1995) and USGS-25 (Böhlke et al., 1995) normalisation references. Values for C% and N% were normalised to 'High Organic Sediment Standard OAS'. Normalised μXRF bromine (Br) data from Paddy's Lake is presented here to demonstrate trends in organic matter (Chapter 4).

5.5.4 POLLEN AND CHARCOAL ANALYSIS

Pollen and *Botryococcus* spp. accumulation rates (AR) were calculated from the existing Paddy's Lake pollen data (Chapter 4). Here, we use the pollen AR to track changes in vegetation biomass, consistent with data linking pollen influx and plant biomass (Sugita et al., 2010; Matthias et al., 2014). Background charcoal (particles cm⁻² yr⁻¹) was calculated with CharAnalysis (Higuera, 2009) from Chapter 4 and used as an indicator for local and regional drying. For further pollen and charcoal analysis methods see Chapter 4.

5.5.5 NUMERICAL ANALYSES

5.5.5.1 Detrended Correspondence Analysis (DCA) and Cluster Analysis

DCA was performed using the *vegan v.2.4-4* package (Oksanen et al., 2016) in *R* on square root transformed cladoceran percentage data with down-weighted rare taxa. Zonation was determined using CONISS cluster analysis (Grimm, 1987) in *TILIA v.2.0.37* (Grimm, 2013). Zone significance was determined using a broken stick model in *R* using *rioja v.0.9-15* (Juggins, 2016). Pollen ordination results (pollen DCA axis 2) from Chapter 4 were used to demonstrate the secondary vegetation composition changes on the landscape; primary shifts in the vegetation are dictated by the glacial-interglacial transition period (Chapter 4).

5.5.5.2 Cross-correlation

Cross-correlation analysis was performed on 400 year bins of the following data: cladoceran DCA axis 1, cladoceran oligotrophic:eutrophic ratio, bulk sediment $\delta^{15}\text{N}$, pollen DCA axis 2 and pollen AR to assess the significance of temporal relationships in the time series data (Green, 1981). Binning is an alternative to interpolation, where data are averaged within a selected age interval to create even time steps without creating non-existent trends (Carstensen et al., 2013; Seddon et al., 2014). Data was first binned using *R* script written by Seddon *et al.* 2014 then transformed by standardization in *R* using *analogue v.0.17-0* (Simpson et al., 2016)

to remove any non-stationarity, a violation of cross-correlation requirements (Horvatic et al., 2011). Cross-correlation analysis was run with four lags of 400 years in *R*.

5.6 RESULTS

5.6.1 CHRONOLOGY

Radiocarbon results are accessible in Appendix II Table II.1, with full details in Chapter 4. An age-offset estimate of 223.5 yrs was applied to all samples in the age-depth model and two dates (200 cm and 225 cm) were out of stratigraphic sequence and identified as outliers (Figure 5.2) (see Chapter 4).

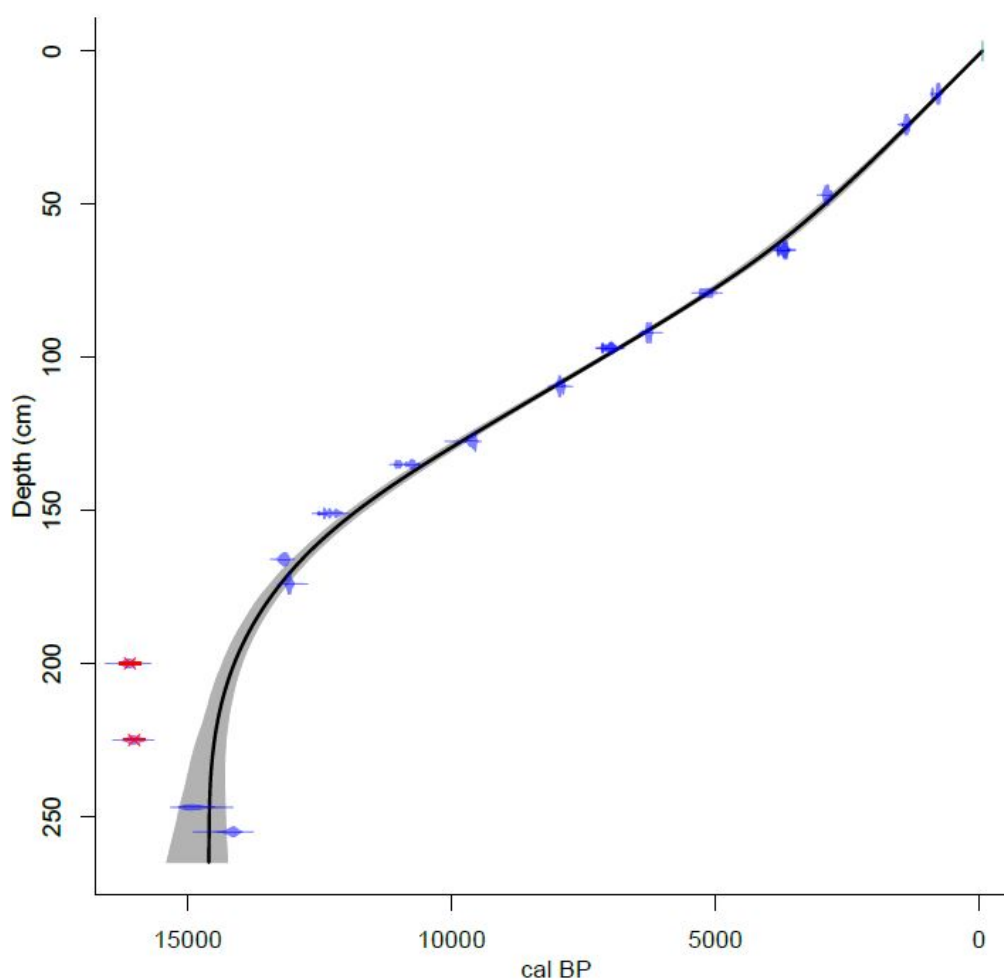


Figure 5.2: Age-depth model of Paddy's Lake, Tasmania with a smooth spline model (factor=0.50; goodness-of-fit of 83.38) calibrated using SHCal13 (Hogg et al., 2013). Outlier dates are marked in red (Chapter 4).

5.6.2 CLADOCERAN ANALYSIS

A total of 13 cladoceran taxa were identified throughout the Paddy's Lake record (Figure 5.3). Cladoceran diversity was very low; however, not abnormal for a Tasmanian alpine lake (pers. comm. A. Kotov and R. Shiel). Seven significant CONISS zones were produced and Table 5.1 lists the assemblage characteristics of each zone.

Table 5.1: Summary of significant CONISS cladoceran zones (N=7) from Paddy's Lake, displayed by age (ca. ka) and sample depths (cm). Key taxa are reported with their approximate mean, maximum and minimum percent abundance.

Zone	Age (ca. ka)	Sample Depths (cm)	Key Taxa	Mean % Abundance	Maximum % Abundance	Minimum % Abundance
1	> 13.4	177.5	<i>Alona guttata</i>	89.3	-	-
			<i>Bosmina meridionalis</i>	9.7	-	-
			<i>Chydorus sphaericus</i>	1.0	-	-
2	13.3-12.8	174.5-165.5	<i>Alona guttata</i>	8.2	10.7	6.7
			<i>Bosmina meridionalis</i>	88.8	92.4	82.5
			<i>Chydorus sphaericus</i>	1.9	3.9	0.0
			<i>Simocephalus spp.</i>	1.0	2.9	0.0
3	12.7-11.6	163.5-147.5	<i>Alona guttata</i>	57.6	81.4	39.8
			<i>Bosmina meridionalis</i>	9.9	16.5	4.3
			<i>Chydorus sphaericus</i>	30.6	46.6	10.8
			<i>Simocephalus spp.</i>	1.9	4.8	0.0
4	11.3-8.9	114.5-118.5	<i>Alona guttata</i>	10.6	17.0	5.6
			<i>Alona quadrangularis</i>	0.1	1.0	0.0
			<i>Bosmina meridionalis</i>	83.0	90.4	72.0
			<i>Chydorus sphaericus</i>	3.1	7.7	0.0
			<i>Diaphanosoma cf. unguiculatum</i>	0.2	1.0	0.0
			<i>Simocephalus spp.</i>	2.2	10.0	0.0
			Unknown	0.8	2.6	0.0
5	8.7-6.4	116.5-92.5	<i>Alona guttata</i>	49.4	80.0	15.3
			<i>Alona quadrangularis</i>	0.1	1.0	0.0
			<i>small Alona sp.</i>	0.2	2.4	0.0
			<i>Alonella excisa</i>	0.2	2.0	0.0
			<i>Alonella sp.</i>	0.2	2.4	0.0
			<i>Biapertura intermedia</i>	0.1	1.0	0.0
			<i>Bosmina meridionalis</i>	38.9	76.9	13.6
			<i>Chydorus sphaericus</i>	3.0	7.9	0.0
			<i>Daphnia spp.</i>	0.2	1.9	0.0

			<i>Diaphanosoma cf. unguiculatum</i>	0.4	3.0	0.0
			<i>Simocephalus spp.</i>	7.3	17.3	1.0
			Unknown	<0.1	1.2	0.0
6	6.2-0.3	90-6.5	<i>Alona guttata</i>	17.7	51.0	4.4
			<i>small Alona sp.</i>	0.1	1.0	0.0
			<i>Bosmina meridionalis</i>	80.3	94.7	45.9
			<i>Chydorus sphaericus</i>	0.8	3.5	0.0
			<i>Daphnia spp.</i>	<0.1	1.0	0.0
			<i>Pleuroxus spp.</i>	0.1	2.0	0.0
			<i>Simocephalus spp.</i>	0.9	3.7	0.0
			Unknown	0.4	1.7	0.0
7	< 0.1	2.5	<i>Alona guttata</i>	92.6	-	-
			<i>Bosmina meridionalis</i>	1.9	-	-
			<i>Chydorus sphaericus</i>	1.9	-	-
			<i>Simocephalus spp.</i>	3.7	-	-

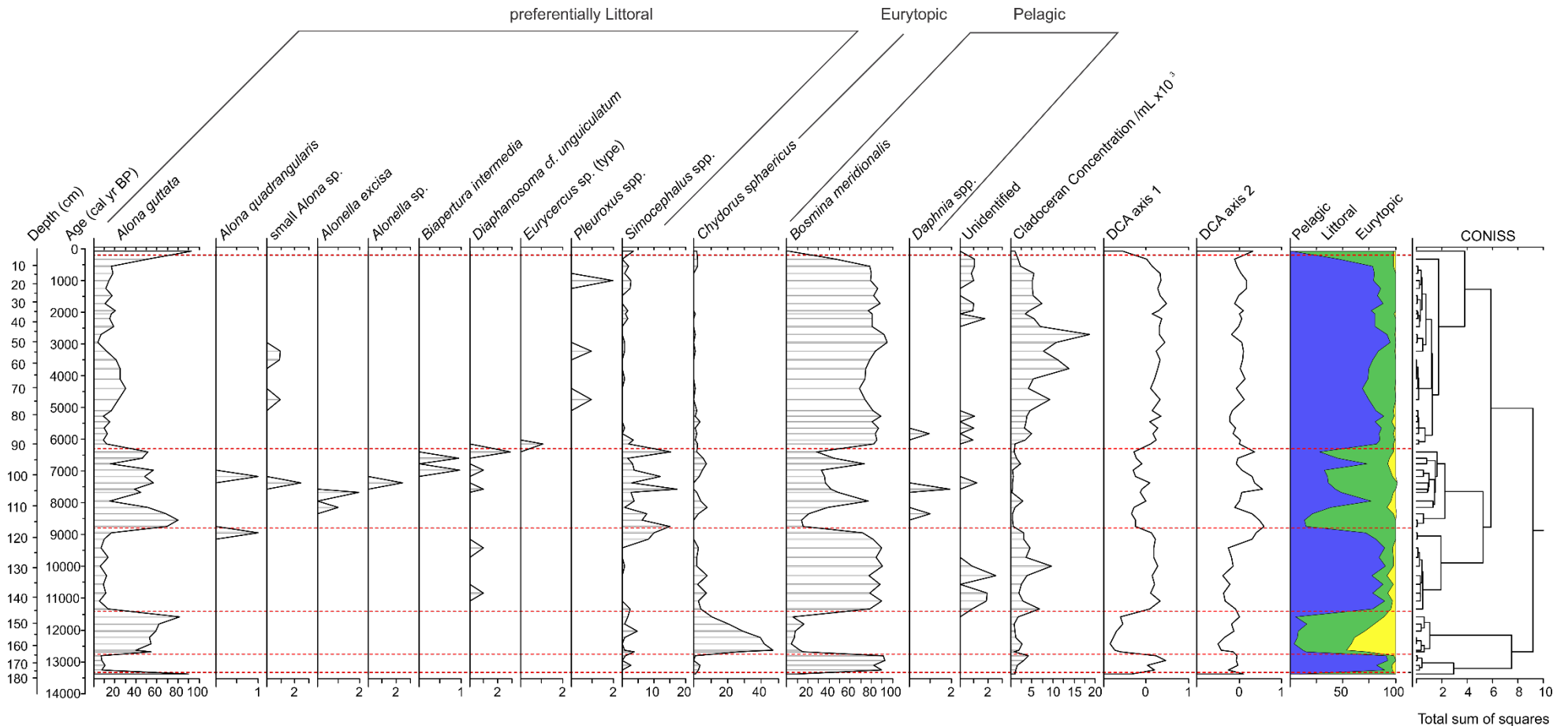


Figure 5.3: Stratigraphy of Paddy's Lake cladoceran taxa. Cladoceran species are presented as percentage composition and grouped by Pelagic (blue), Littoral (green) and Eurytopic (yellow) taxa. The DCA axis 1 (variance= 25.1%) and 2 (variance= 14.3%) scores estimate trends in the cladoceran percentage data. Red dashed lines indicate breaks in the seven significant CONISS zones.

5.6.3 GEOCHEMISTRY

All C%, N%, $\delta^{13}\text{C}$, and $\delta^{15}\text{N}$ results are the mean of replicate analyses, the standard deviation of the replicates are $\leq \pm 0.3$ for all $\delta^{13}\text{C}$ and $\leq \pm 0.4$ for all $\delta^{15}\text{N}$ results. These organic geochemical indicators show a distinct shift at ca. 13.4 ka (Figure 5.4). Distinct groupings are found before and after ca. 13.4 ka. C/N and $\delta^{13}\text{C}$ values before ca. 13.4 ka cluster with C/N below 16 and $\delta^{13}\text{C}$ above -25 ‰. After ca. 13.3 ka, C/N and $\delta^{13}\text{C}$ cluster above a C/N value of 16 and below a $\delta^{13}\text{C}$ value of -26 ‰ (Appendix Figure II.1). C%, N% and C/N are extremely low prior to ca. 13.4 ka followed by an increasing trend to maximum values by ca. 8 ka with relatively stable trends to present. High values of $\delta^{13}\text{C}$ occur prior to ca. 13.4 ka (maximum=-23.5 ‰) then decline to persistently low values. High $\delta^{15}\text{N}$ values (~2 ‰) occur prior to ca. 13.4 ka, then decline at ca. 13 ka and ca. 12 ka. $\delta^{15}\text{N}$ values peak at ca. 8.5 ka (~2.2 ‰) and ca. 6 ka (~2.3 ‰), a rise at ca. 2.5 ka is followed by stable values until present (Figures 5.4a & 5.5f). Trends in μXRF Br demonstrate very low values before ca. 13.4 ka, followed by a sharp increase to ca. 12 ka then decline to ca. 11 ka. From ca. 11 to 8 ka, Br increases with a declining trend from ca. 8.5 to 6 ka. At ca. 6 ka values drop with a stable trend until 0.1 ka after which it increases (Figures 5.4h & 5.5a).

5.6.4 POLLEN AND CHARCOAL ANALYSIS

Grass and herb pollen and woody plant percent pollen show opposite trends of high (low) values before ca. 13.3 ka, then a shift to decreasing (increasing) abundance for the remainder of the record (Figure 5.4f & g). The pollen AR increases from ca. 13.3 to 12.3 ka, ca. 6 to 4.5 ka, and ca. 3 ka to present. From ca. 9 to 6 ka high variability in pollen AR occurs (Figure 5.5h). Background charcoal remains relatively low from ca. 13.4 to 6 ka, followed by an increase to a maximum at ca. 4.3 ka. Values decline at ca. 4.3 ka with two more increasing trends at ca. 3 ka and 2 ka.

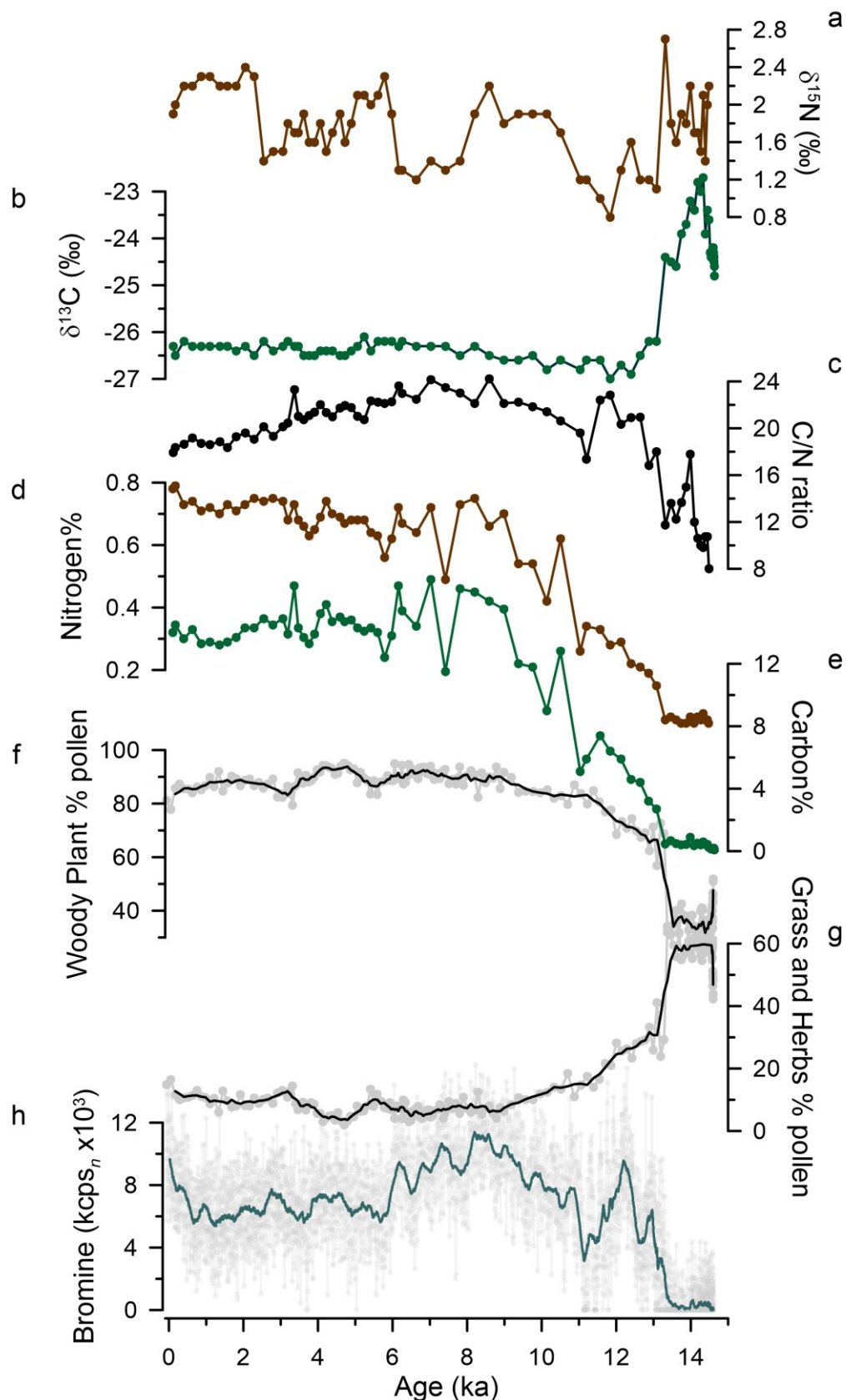


Figure 5.4: Summary figure of Paddy's Lake vegetation types and nutrient indicators. a) $\delta^{15}\text{N}$ (‰); b) $\delta^{13}\text{C}$ (‰); c) C/N ratio; d) sediment Nitrogen percentage; e) sediment Carbon percentage; f) percent woody plant pollen (grey) with a weighted average (black, window width=5); g) percent grass and herb pollen (grey) with a weighted average (black, window width=5); and h) bromine ($\text{kcp}_n \times 10^3$) (grey) and weighted average (dark green, window width=61) (Chapter 4).

5.6.5 NUMERICAL ANALYSES

5.6.5.1 Detrended Correspondence Analysis

Trends in the cladoceran DCA axis 1 scores (explained variance=25.1%) follow changes in the pelagic taxa *Bosmina meridionalis* (Figure 5.3 & 5.5e). DCA axis 2 (explained variance=14.3%) shows high stability throughout the entire record with high values from ca. 9.1 to 6.4 ka (Figure 5.3). The DCA biplot can be found in Figure II.2 in Appendix II. The terrestrial pollen DCA axis 2 scores follow opposing trends to the pollen AR from ca. 13.4 to 6 ka with an increasing trend from ca. 6 ka to present (Figure 5.5d). The pollen DCA axis 2 has a positive association with pollen types: Cupressaceae, *Oxylobium* spp., *Melaleuca* spp., *Eucryphia lucida*, *Lagarostrobos franklinii*, and *Banksia* spp. and negative association with *Phyllocladus aspleniifolius*, *Dodonaea* spp., *Acacia* spp., *Nothofagus cunninghamii*, Ericaceae, and *Pomaderris cf. apetala*.

5.6.5.2 Cross-Correlation

Cross-correlation analysis results are summarized in Table 5.2. Pollen AR has a positive correlation with $\delta^{15}\text{N}$ (-1,600 to 400 yr lag). A negative response in $\delta^{15}\text{N}$ occurs following an increase in pollen accumulation (1200 to 1600 yr lag). Cladoceran DCA axis 1 shows a positive response with pollen composition (Pollen DCA axis 2) prior to increase in cladoceran DCA 1 (-400 to 1,600 yr lag). The oligotrophic:eutrophic cladoceran ratio show a positive correlation with $\delta^{15}\text{N}$ (400 to 1,200 yr lag) (Figure 5.6).

Table 5.2: Cross Correlation analysis results including standard deviation, standard error, upper and lower confidence intervals (CI).

Lag yrs	Pollen DCA axis 2 vs. Cladoceran DCA 1	Pollen AR vs. $\delta^{15}\text{N}$	$\delta^{15}\text{N}$ vs. oligotrophic:eutrophic
-1600	0.057241282	0.435887572	-0.338392647
-1200	0.104607794	0.607734199	-0.32921518
-800	0.252291439	0.596098629	-0.198031424
-400	0.363491606	0.486169481	0.124005959
0	0.444837565	0.387560879	0.045055489
400	0.582469507	0.320976123	0.211265465
800	0.52400621	0.116601337	0.520772752
1200	0.417524413	-0.044240662	0.313163959
1600	0.402740946	-0.016726407	0.193827392
standard deviation	0.178993529	0.248003219	0.29544444
standard error	0.117419755	0.162690112	0.193811553
mean	0.349912307	0.321117906	0.060272418
Upper CI	0.467332062	0.483808018	0.254083971
Lower CI	0.232492552	0.158427794	-0.133539134

5.7 DISCUSSION

5.7.1 VEGETATION CHANGE AND LAKE NUTRIENT DYNAMICS

We observe a significant negative lagged relationship between pollen AR and the $\delta^{15}\text{N}$ content of organic matter within Paddy's Lake throughout the last ca. 13.4 kyrs (Figure 5.6a). Linear relationships between pollen ARs and plant biomass has been shown in temperate systems in the Northern Hemisphere (Sugita et al., 2010; Matthias et al., 2014), and anecdotal evidence suggests that this relationship occurs in subalpine Tasmanian ecosystems (Fletcher et al., 2014a). We interpret the negative lagged relationship between pollen AR and $\delta^{15}\text{N}$ as reflecting increased input of terrestrially derived ^{14}N into the lake as terrestrial vegetation productivity increases. The geochemical signature of Paddy's Lake suggests the organic elements preserved in the lake sediment are derived from terrestrial organic matter (Figure 5.4 & Appendix Figure II.1) (Lamb et al., 2004; Lamb et al., 2006). With high terrestrial biomass, more litter and microbial decomposition increase the available nitrate in surface waters (Morris et al., 2015). Thus, when available ^{14}N stocks are high, aquatic organisms discriminate against ^{15}N , resulting in organic matter low in $\delta^{15}\text{N}$. Once vegetation productivity

decreases (reduced pollen AR), available ^{14}N decreases and aquatic organisms are forced to use ^{15}N – classic Rayleigh Distillation (Talbot et al., 1992; Talbot, 2001) – resulting in an increase in organic matter $\delta^{15}\text{N}$ values. Low $\delta^{15}\text{N}$ values have also been shown to track precipitation (Hobbie et al., 2012), while this could be a contributing factor, there is not sufficient evidence to suggest the $\delta^{15}\text{N}$ is tracking precipitation at Paddy's Lake.

While the negative lagged relationship between pollen AR and $\delta^{15}\text{N}$ is significant over the entire ca. 13.4 kyr sequence, we observe an apparent decoupling of these variables after ca 3.4 ka. This decoupling is manifest as persistently high $\delta^{15}\text{N}$ values (Figure 5.5f) despite an increase in pollen AR (Figure 5.5h). We note that this decoupling is coeval with the establishment of both sclerophyll-dominant vegetation around the lake (Figure 5.5b) and a marked increase in the colonial algae *Botryococcus* spp. (Figure 5.5c). *Botryococcus* spp., likely *Botryococcus braunii* (Kützing), [$\delta^{15}\text{N}$ signature of 4-7 ‰ (Heyng et al., 2012)] is an algae common in oligotrophic waters that prefers shallow littoral environments (Aaronson et al., 1983; Clausing, 1999). We interpret this shift as reflecting increased nutrient consumption by *Botryococcus* spp. that depleted ^{14}N stocks within the lake. The shift toward sclerophyll-dominant vegetation was driven by successive fires beginning at ca. 6.3 ka (Chapter 4). Elsewhere, similar fire-driven vegetation shifts from pyrophobic rainforest communities to pyrophytic sclerophyll associations are marked by changes in both carbon and nitrogen content of lake sediment organic matter (Fletcher et al., 2014a). Sclerophylly is an adaptation to nutrient deficiency (Beadle, 1966; Beadle, 1968) and the nutrient content of soils under sclerophyllous vegetation in Tasmania is lower than under rainforest vegetation (Jackson, 1968; Bowman et al., 1986b; Orians et al., 2007; Wood et al., 2011a). It is possible, then, that the invasion of the catchment by sclerophyllous plant taxa lowered the nutrient status of the catchment organosols (C/N and Br; Figure 5.4c & h), lowering the available nutrient pool within the lake and favouring the increase in *Botryococcus* spp. The combination of reduced terrestrial nutrient input and increased aquatic nutrient demand would, thus, result in a rapid consumption of ^{14}N stocks, forcing aquatic organisms to use ^{15}N and, thus, increasing the $\delta^{15}\text{N}$ value of deposited organic matter.

The final decline in *B. meridionalis* and increase abundance of *A. guttata* at 0.1 ka may be attributed to anthropogenic climate change. Increased *A. guttata* favours warmer temperate conditions (Frey, 1991b; Lotter et al., 2000; Kattel et al., 2010); however, this final zone only contains one data point and more data is needed to determine if this final shift is a true result of warming climate.

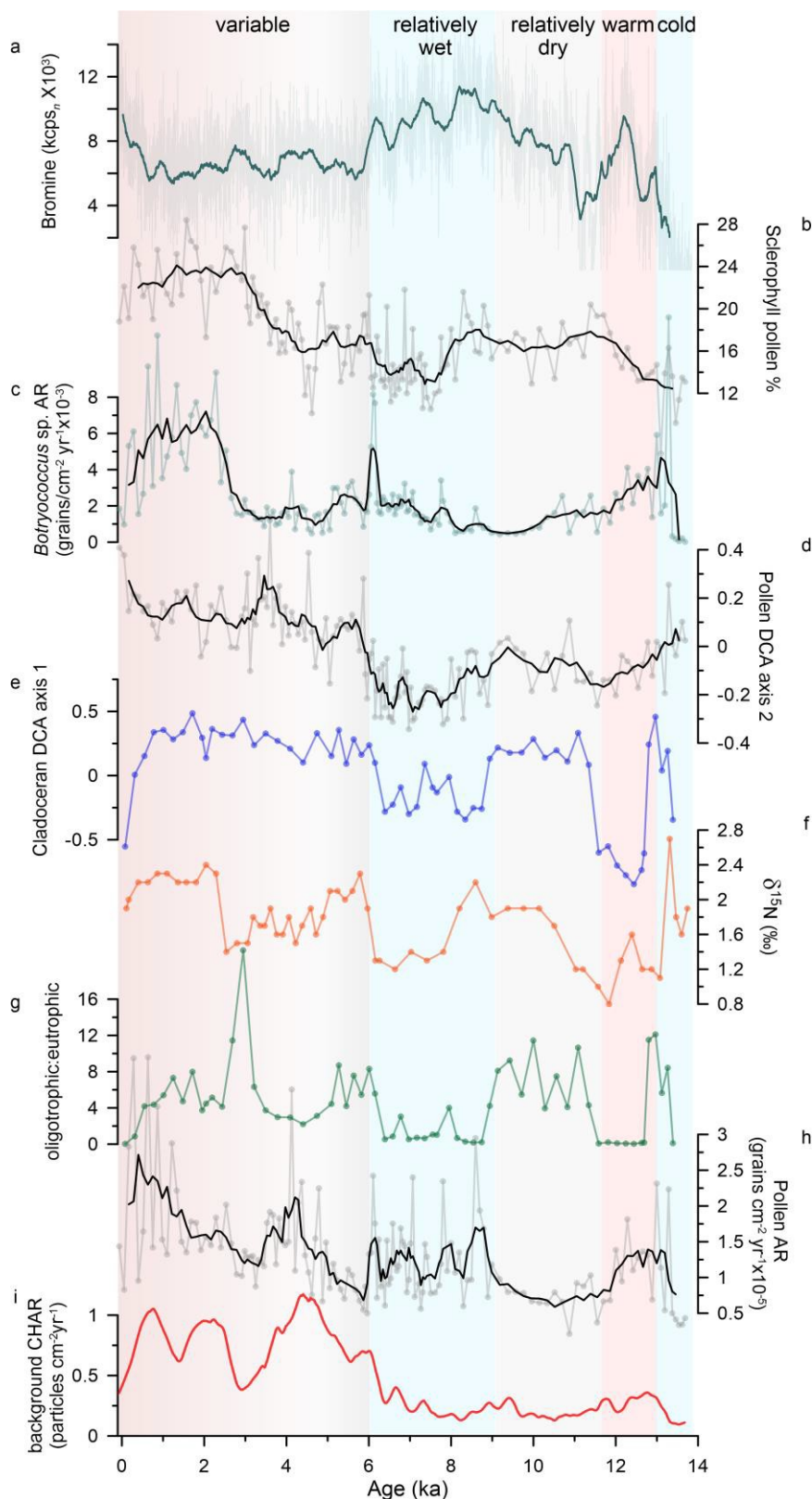


Figure 5.5: Summary figure of aquatic and terrestrial ecosystem changes at Paddy's Lake. a) bromine ($\text{kcpns}_n \times 10^3$) (grey) with a weighted average (dark green, window width=61) (Chapter 4); b) percent sclerophyll pollen (grey) with a weighted average (black, window width=3) (Chapter 4); c) *Botryococcus* spp. AR ($\text{grains/cm}^2 \text{ yr}^{-1} \times 10^{-3}$) (light green) with a weighted average (black, window width=3); d) Pollen DCA axis 2 (grey) with a weighted average (black, window width=5); e) Cladoceran DCA axis 1 (blue); f) $\delta^{15}\text{N}$ (‰) (orange); g) oligotrophic:eutrophic cladoceran taxa ratio (green); h) pollen AR ($\text{grains/cm}^2 \text{ yr}^{-1} \times 10^{-5}$) (grey) with a weighted average (black, window width=5); and i) background charcoal particles/ $\text{cm}^2 \text{ yr}^{-1}$ (red) (Chapter 4). Shaded background colours indicate generic climate transitions.

5.7.2 VEGETATION CHANGE AND AQUATIC ECOSYSTEM DYNAMICS

Our results reveal a significant relationship between terrestrial vegetation and aquatic ecosystem (cladoceran) change throughout the last ca. 13.4 kyrs at Paddy's Lake (Figure 5.6b). Importantly, shifts in terrestrial vegetation precede changes in cladoceran community composition, reflecting a clear link between terrestrial and aquatic ecosystem change through time. Long-term vegetation change at Paddy's Lake inferred from pollen data closely tracks long-term shifts in regional hydroclimate identified from a raft of local and regional palaeoecological and palaeoclimate data (Chapter 4; Macphail, 1979; Markgraf et al., 1986; Fletcher et al., 2012; Fletcher et al., 2014a; Stahle et al., 2016). Our results confirm that the influence of climate-driven changes in vegetation (composition and productivity) over nutrient delivery into the lake supersedes any direct influence of climatic change over aquatic ecosystem dynamics in this lake system. We, thus, accept our hypothesis that long-term aquatic ecosystem dynamics respond indirectly to climatic change in this landscape via changes in the terrestrial environment.

Whilst changes in hydroclimate could be expected to drive changes in lake level and a concomitant change in pelagic taxa (e.g. *B. meridionalis*) (Korhola et al., 2000; Kattal et al., 2010), we find no consistency between regional hydroclimatic trends and changes in pelagic cladoceran taxa at Paddy's Lake (Figure 5.3). Critically, we do observe a significant lagged relationship between $\delta^{15}\text{N}$ and the oligotrophic:eutrophic cladoceran ratio through the last ca. 13.4 kyrs (Figure 5.6c), indicating that changes in cladoceran composition at Paddy's Lake clearly tracks lake trophic status (oligotrophic:eutrophic ratio). Increases in the abundance of littoral cladocerans (*A. guttata* and *C. sphaericus*: low DCA axis 1 values) reflect characteristic of cosmopolitan communities that prefer higher lake nutrient levels (mesotrophic to eutrophic) (Kattal et al., 2010) (Figure 5.5e & g). Increases in pollen AR and pollen compositional change (pollen DCA axis 2) at Paddy's Lake occur during phases of elevated relative moisture, low regional fire activity and an increase in regional forest cover (Chapter 4; Fletcher et al., 2012; Stahle et al., 2016; Mariani et al., 2017a). These shifts in pollen AR and pollen DCA axis 2 are simultaneous with decreasing organic $\delta^{15}\text{N}$ values and an increase in the important occurrence of littoral cladocerans within the lake (Figure 5.3).

In contrast, 'pelagic' cladocerans (e.g. *B. meridionalis*) at Paddy's Lake favour oligotrophic lake conditions (Green, 1976; Geddes, 1988) and increases in these taxa occur during phases of low relative moisture, reduced regional forest cover, and increased regional fire activity (Chapter 4; Fletcher et al., 2012; Stahle et al., 2016; Mariani et al., 2017a), consistent with reduced terrestrial organic matter inputs (Br: Figure 5.5a) and $\delta^{15}\text{N}$ enrichment of organic matter within the lake (Figure 5.5f). Our results, then, reveal a shift toward more oligotrophic tolerant cladoceran community (dominated by *B. meridionalis*) that precedes $\delta^{15}\text{N}$ enrichment of organic matter within the lake (post ca. 3.4 ka), reflecting (1) a shift toward oligotrophic tolerant taxa due to reduced terrestrial nutrient input influencing the diet of these aquatic grazers, (2) a depletion of available ^{14}N stocks, and (3) a subsequent $\delta^{15}\text{N}$ enrichment of within-lake organic matter.

Given our established lagged relationship between terrestrial vegetation productivity and lake nutrient stocks, we interpret our results as indicating an aquatic ecosystem response to climate-driven changes in terrestrial nutrient inputs. Vegetation productivity decreases (increases) during relatively dry (wet) climate phases (Figure 5.5), resulting in a decrease (increase) in terrestrial nutrient inputs. Depletion (replenishment) of available nutrients for aquatic grazers leads to the development of a more (less) oligotrophic lake environment that favours an increase (decrease) in the abundance of cladoceran species, such as *B. meridionalis*, that have a competitive advantage in lower nutrient environments. During phases of low terrestrial nutrient delivery, the eventual depletion of ^{14}N stocks forces aquatic organisms to use ^{15}N – Rayleigh Distillation (Talbot et al., 1992; Talbot, 2001) – enriching organic matter in this isotope. P is also an important nutrient often limiting aquatic systems. While $\delta^{15}\text{N}$ is an indicator of available organic N, it may also relate to organic deposition which may include other important organic nutrients. Our results imply that cladoceran community dynamics respond indirectly to climatic change via the influence of temperature and precipitation over changes in terrestrial vegetation composition dynamics, as well as, their influence over lake nutrient status with no evidence of a direct climate response.

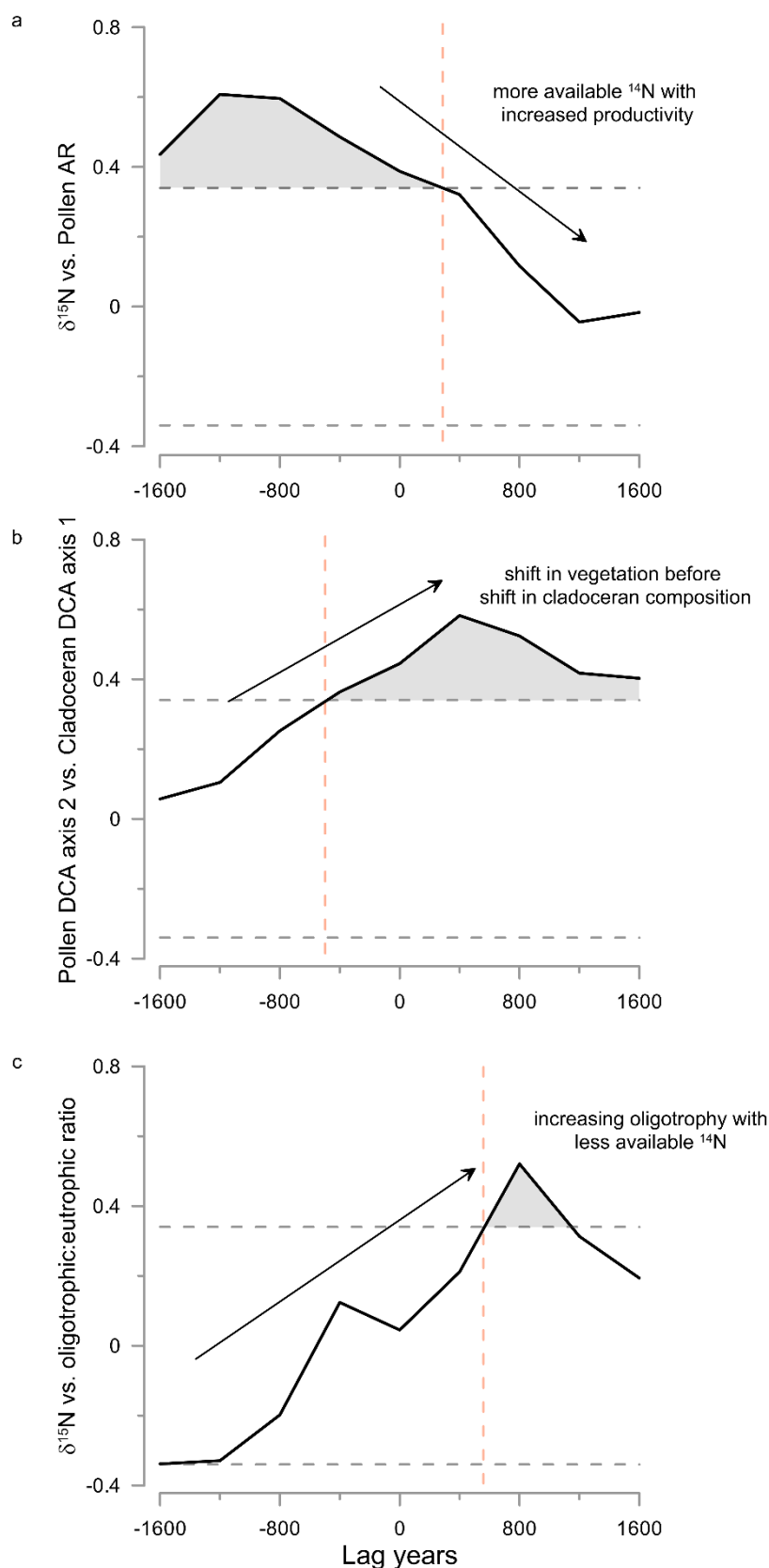


Figure 5.6: Cross-correlation analysis of Paddy's Lake data with four lags of 400 year bins for: a) $\delta^{15}\text{N}$ vs. pollen AR; b) pollen DCA axis 2 vs. cladoceran DCA axis 1; and c) $\delta^{15}\text{N}$ vs. oligotrophic:eutrophic cladoceran ratio. The grey dashed lines indicate the upper and lower confidence intervals of the Cross-correlation analysis. The grey shaded areas are the significant relationships between the two time series. The red dashed line indicates the start lag time which the two time series have a significant relationship.

5.8 CONCLUSION

In our study system, time series analysis of multi-proxy lake sediment data identified an indirect relationship between climatic change and aquatic ecosystem dynamics manifest as a lagged response of aquatic ecosystem change to terrestrial vegetation dynamics. Climate-driven terrestrial vegetation change exerts control over both within-lake nutrient cycling and cladoceran community composition, due principally to the low bedrock nutrient content promoting landscape-wide dominance of peat and associated dystrophy in fresh water systems. A fire-driven shift from rainforest to sclerophyll-dominant vegetation at ca. 3.4 ka is associated with a decoupling of vegetation productivity and lake nutrient cycling. Sclerophyll plants in this landscape produce peat with low nutrient content relative to rainforest, thus, lowering the within-lake nutrient status and favouring an increase in *Botryococcus* spp. The increase in *Botryococcus* spp. and reduction in terrestrial nutrient input, then, depleted nutrient stocks irrespective of changes in vegetation productivity. The increase in fire activity in western Tasmania over the last century is unprecedented throughout the last 12 kyrs and many Tasmanian rainforest systems are under threat of extinction in response to fire and invasion by fire-promoting plant species (Fletcher et al., 2014a; Holz et al., 2015). Paddy's Lake could also be experiencing the effects of anthropogenic climate change; however, our data was not sufficient to determine this and further investigation is needed. Our results indicate that aquatic ecosystem dynamics in subalpine western Tasmania are closely linked to climate-driven rainforest dynamics, and that fire-driven vegetation change has the potential to radically alter within-lake nutrient dynamics and aquatic ecosystem composition. All southern temperate rainforest systems are under threat of climatic and fire regime change and the lack of emphasis on how terrestrial and aquatic ecosystems are linked across these systems exposes a critical knowledge gap that must be addressed if we are to successfully manage aquatic ecosystems of the region into the future.

5.9 ACKNOWLEDGEMENTS

We acknowledge that our work was conducted on Tasmanian Aboriginal lands and thank the Tasmanian Aboriginal community for their support. The financial support of this project comes from the Australian Research Council (award: #DI110100019 and IN140100050) and Australian Institute of Nuclear Science and Engineering (award: ALNGRA15003 and ALNGRA16023). Giri Kattel would like to acknowledge CAS-PIFI Professorial Fellowship Program at the Chinese Academy of Sciences (NIGLAS) and the National Natural Science Foundation China (NSFC) Grants (#41530753 and #412723379). We would like to thank Alexa Benson, Agathe Lisé-Pronovost, Scott Nichols, Angelica Ramierez, William Rapuc, and Anthony Romano for their assistance in the field and Michela Mariani for her GIS support. Data will be accessible in the Neotoma database (<https://www.neotomadb.org/>). We would also like to acknowledge the reviewers for their excellent comments and suggestions.

Supporting information in Appendix II.

PART TWO: LAKE VERA

CHAPTER 6: DISCUSSION

6.1 CHAPTER AIM

This chapter uses a Holocene multiproxy record from Lake Vera to address the direct and indirect climate influences on aquatic ecosystems presented as an in-preparation manuscript written entirely by me. In this chapter Beck, K.K. and Fletcher, M.-S. conceived the ideas for this research. Beck, K.K. performed the diatom and statistical analyses, interpretation and writing of this manuscript. Gadd, P.S., and Heijnis, H. performed the μ XRF geochemical analysis and Zawadzki, A. performed the lead-210 analysis.

Potential author list:

Beck, K.K., Fletcher, Michael-Shawn, Gadd, P. S., Heijnis, H., Saunders, K. M. & Zawadzki, A. (*in prep*)

Direct and indirect aquatic ecosystem response to changes in climate variability: A Holocene diatom record from Tasmania, Australia

6.2 ABSTRACT

A multiproxy Holocene record of radiometric dating (^{14}C and ^{210}Pb), geochemistry (μ XRF scanning and CN isotopes), charcoal, pollen, and diatoms from Lake Vera, Tasmania was used to explore the direct and indirect influences of climate on aquatic ecosystem response. Lake Vera, shows hydroclimate driven vegetation changes that track both millennial-scale shifts in the southern westerly winds (SWW) (ca. 12 to 5 ka) and higher frequency climate variability with the onset of the El Niño-Southern Oscillation (5 ka to present). The aquatic ecosystem (diatoms) at Lake Vera is acidic and oligotrophic with increased acidity, an indirect climate response to wet periods (ca. 7 to 4 ka) via humic acids and tannins from rainforest and peat development. The onset of a more variable ENSO climate caused a direct response in the diatom community from ca. 4 ka via the influence of climate on lake level fluctuations and the emergence and disappearance of an expended

littoral zone in the lake. A period of increased fire (ca. 2.3 to 0.9 ka) caused a diatom community shift towards more alkaline and disturbance-tolerant taxa as a result of increased inorganic soil inputs and ash deposition from fire. The cumulative effects of the fire disturbance eventually caused a non-linear shift in the diatoms, from alkaline disturbance taxa to oligotrophic acidic taxa.

6.3 INTRODUCTION

Climate can directly influence aquatic ecosystem structure and function (Ball et al., 2010; Fritz et al., 2013; Mills et al., 2017) via changes in the precipitation/evaporation balance or temperature affecting lake level, ice coverage, salinity and/or the position of the lake thermocline (De Deckker, 1982; Schindler et al., 1996; Schindler, 1997; Smol et al., 2000; Gell et al., 2005; Prebble et al., 2005; Saunders, 2011; Gell et al., 2012; Saunders et al., 2012). Climate can also indirectly impact aquatic ecosystem response through changes in the catchment, such as shifts in vegetation composition altering nutrient input, organic matter, and hydrology into aquatic systems (Huvane et al., 1996; Korsman et al., 1998; Lancashire et al., 2002; Huxman et al., 2005; Tibby et al., 2007b; Augustinus et al., 2008; Moos et al., 2009; Ball et al., 2010; Fritz et al., 2013; Timbal et al., 2013; Law et al., 2015). However, there is a disproportionate amount of research on the direct impacts of climate compared to indirect impacts, and typically, these pathways are not explored in conjunction. Here we address this gap using a lake sediment record to determine direct and indirect climate impacts on aquatic ecosystem dynamics in southwest Tasmania, Australia. .

In the southwest Pacific, the temporal scale of climate variability over the mid-latitudes of the Southern Hemisphere shifted from low-frequency hydroclimatic variability (multi-millennial scale) between ca. 12 to 5 ka, driven by shifts in the strength and position of the SWW to higher frequency hydroclimatic variability (sub-millennial scale) after ca. 5 ka driven by changes in ENSO (Stanley et al., 2002; Moros et al., 2009; Fletcher et al., 2015; Rees et al., 2015). The SWW-dominant phase is marked by a mid-latitude hemisphere-wide multi-millennial phase of low relative moisture and high fire activity between ca. 12 to 8 ka and a phase of high relative moisture and low fire activity between ca. 8 to 5 ka (Moreno et al., 2003; Moreno, 2004;

Fletcher et al., 2012; Fletcher et al., 2015; Rees et al., 2015; Mariani et al., 2017b). The ENSO-dominant phase is characterised by anti-phased hydroclimatic variability across the mid-latitudes of the hemisphere, with a marked negative moisture anomaly and high fire activity over Tasmania after ca. 5 ka during a phase of increased frequency of El Niño events (Moy et al., 2002; Mariani et al., 2017b). This ENSO-driven increase in regional fire activity drove a region-wide shift in vegetation, with fire promoting sclerophyll taxa replacing fire-sensitive rainforest at many locations between ca. 6 to 2.5 ka (Macphail, 1979; Harle et al., 1999; Hopf et al., 2000; Fletcher et al., 2014a; Stahle et al., 2016; Beck et al., 2017; Mariani et al., 2017a; Stahle et al., 2017; Fletcher et al., 2018b). Though shifts in these climate systems are becoming well understood their relative impact on aquatic ecosystems is still uncertain.

Here we use a multi-proxy palaeoecological dataset to determine the effects of climate on the terrestrial and aquatic environment and determine which mechanisms of climate (direct or indirect) are driving aquatic ecosystem change. We employ diatoms to monitor aquatic ecosystem changes; charcoal as a proxy for fire and climate; Carbon and Nitrogen isotopes and elemental content as indicators of organic matter, nutrient cycling and sources; and μ XRF geochemistry as indicators of catchment processes. We compare these results to previous work on climate-driven vegetation changes. This approach aims to address the following questions: (1) how does the aquatic ecosystem respond to climate? (2) What are the relative impacts of direct vs. indirect changes? and (3) do these change through time?

6.4 REGIONAL GEOGRAPHY AND SITE DESCRIPTION

Tasmania has a cool temperate maritime climate (Gentilli, 1971). Northwest to southeast mountain ranges divide the island into two distinct climate and vegetation regions; a dry (400 mm rainfall p/a) sclerophyll savannah in the east and a wet (up to 3500 mm rainfall p/a) mixed rainforest and wet sclerophyll with acidic organosols in the west (Tyler, 1992; Jackson, 1999b; Kitchener et al., 2013). This geographical divide influences lake water characteristics with oligotrophic dystrophic waters in the west, and turbid, oligotrophic saline waters in the east (Tyler, 1974, 1992). The dystrophic western waters are characteristic of the terrestrial

organic matter and nutrients inputs (Tyler, 1974; Brown et al., 1982a; Steane et al., 1982). Peat soils high in humic acids and iron surround the western lakes and create the stained acidic dystrophic waters (Buckney et al., 1973; Tyler, 1974; Steane et al., 1982).

Lake Vera (42°16' 29" S, 145°52'44" E) is a small moraine-bound lake formed in a glacial valley located on Frenchman's Cap, western Tasmania at 550 masl (Figure 6.1) (Bradbury, 1986). The lake is dystrophic, oligotrophic and acidic with a maximum depth of ~50 m. The mean annual precipitation is ~2,800 mm and mean annual temperature of 8.7°C (Macphail, 1979; Bradbury, 1986; Markgraf et al., 1986; Fletcher et al., in review). Vegetation surrounding Lake Vera contains subalpine closed forest with underlying sclerophyll shrubs and open forest on the westward-facing slopes and a till plain of *Gymnoschoenus sphaerocephalus* sedgeland 30 m above the lake (Macphail, 1979). Dominant taxa consist of *Anodopetalum biglandulosum*, *Atherosperma moschatum*, *Athrotaxis selaginoides*, *Eucryphia lucida*, *Eucalyptus delegatensis*, *Lagarostrobos franklinii*, *Leptospermum nitidum*, *Nothofagus cunninghamii* and *Phyllocladus aspleniifolius* (Harris et al., 2005; Kitchener et al., 2013; Department of Primary Industries, 2017). Geology is described as mainly siliceous glacial deposits (Macphail, 1979; Bradbury, 1986). Lake Vera is located in the zone of strongest correlation between SAM and rainfall in Tasmania (Hill et al., 2009). The most recent increase in fire activity is the result of elevated SAM and ENSO activity causing regional drying (Mariani et al., 2016b; Mariani et al., 2017b; Fletcher et al., 2018a).

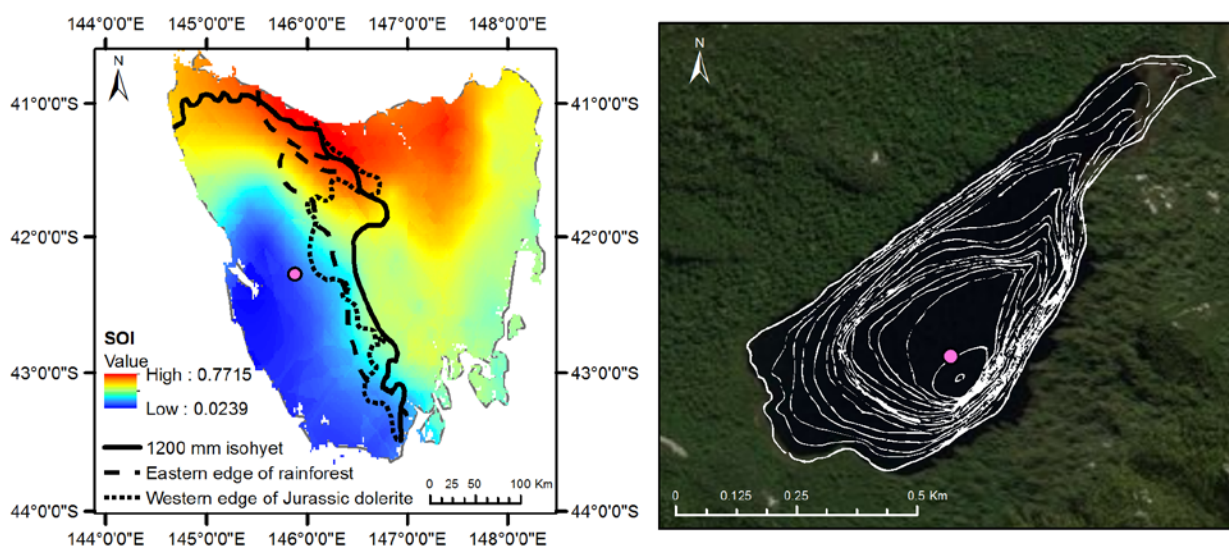


Figure 6.1: A map of Tasmania's Tyler's Line (Tyler, 1992) is on the left determined by precipitation (black solid line), rainforest boundary (black dashed line) and the dolerite edge (black dotted line) with a precipitation correlation heat map of the Southern Oscillation Index and location of Lake Vera (pink dot). On the right a satellite image of Lake Vera with the coring location (pink dot) overlaid with bathymetry determined by Peterson (1966), isobath intervals equal 10 feet (3.05 m).

6.5 METHODS

6.5.1 CORING AND CHRONOLOGY

Two cores were collected from Lake Vera to create a composite record. In 2011 a surface core of 105 cm in length (TAS1108 SC1) was collected from the deepest point in Lake Vera using the Universal coring system (Aquatic Research Instruments, 2016) and in 2015 a long continuous core (TAS1508 N1) was collected from the same deep basin using a Nesje system (Nesje, 1992).

Radiometric analysis was performed at Australian Nuclear Science and Technology Organisation (ANSTO) (five ^{210}Pb samples), the National Ocean Sciences Accelerator Mass Spectrometry (NOSAMS) (four radiocarbon bulk sediment samples) and DirectAMS (16 radiocarbon macrofossil samples) (Table 6.1).

Radiocarbon dates were calibrated with the Southern Hemisphere calibration curve - SHCal13 (Hogg et al., 2013) and ^{210}Pb ages were determined using a constant initial concentration (CIC) model (Appleby, 2001). A

Bayesian age-depth model was developed in *R* v. 3.4.1 (R Development Core Team, 2014) using the Bacon v. 2.2 package (Blaauw et al., 2013) for the composite core (TAS1108 SC1 & TAS1508 N1) (Figure 6.2). An age offset of 333 yrs (between 115 to 683 ¹⁴C yrs) was applied to the bulk sediment dates in the Bacon model determined by the average offset of paired macrofossil and bulk sediment radiocarbon dates (See Appendix III Table III.1).

6.5.2 μ XRF GEOCHEMISTRY

Non-destructive core scanning was used to acquire geochemical data. An Itrax micro-X-ray fluorescence (μ XRF) core scanner was used at ANSTO at a resolution of 0.2 mm for TAS1108 SC1 and 1.0 mm for TAS1508 N1 using a molybdenum (Mo) tube set to 30kV and 55mA with a dwell time of 10s. The geochemical dataset (Si, P, S, Cl, K, Ca, Ti, Mn, Fe, Co, Ni, Cu, Zn, Br, Rb, Pb, and Mo Inc/Coh) was normalised by Mo Incoherence/Coherence ratio (Croudace et al., 2015). Fe was used as an indicator of iron richness (Croudace et al., 2015). Fe/Mn ratio was calculated as an indicator of redox conditions (Koinig et al., 2003; Kylander et al., 2011). Bromine was used as an indicator of organic matter deposition (Chapters 4 & 5; Fletcher et al., 2015) and Ti as an indicator of erosion of mineral material (Koinig et al., 2003; Augustinus et al., 2011; Leys et al., 2016).

6.5.3 CARBON NITROGEN

Analyses of organic Carbon (%C) and Nitrogen (%N), and $\delta^{15}\text{N}$ were performed at on a Carlo Erba Elemental Analyser (CHNS-O EA1108 - Italy) coupled to a Delta^{plus} Continuous Flow Stable Isotope Ratio Mass Spectrometer for TAS1108 SC1 at the Elemental Isotope Laboratories, Wilfrid Laurier University and a EuroVector EuroEA Elemental Analyser in line with a Nu Instruments Nu Horizon IRMS for TAS1508 N1 at the University of Adelaide. Samples were analysed every 0.5 cm for TAS1108 SC1 and 5 cm intervals for TAS1508 N1 and calibrated to international standards (IAEA N1, N2, NO3, C6, and C7; USGS 24, 25, 32, 40, and 41; and NBS 22) (Fry et al., 1992).

6.5.4 CHARCOAL

Macroscopic charcoal was processed at 0.5 cm intervals for TAS1108 SC1 and 2.0 cm intervals for TAS1508 N1 according to standard protocols (Whitlock et al., 2001). Volume of 1.5 mL (TAS1108SC1) to 1.25 mL (TAS1508N1) of sediment was placed in household bleach for at least seven days then sieved through 250 μm and 125 μm mesh and enumerated under a dissecting microscope at 10-20x magnification. Composite charcoal accumulation rate (CHAR_{acc}) was calculated from TAS1108 SC1 and TAS1508 N1 macroscopic charcoal counts.

6.5.5 DIATOMS

Diatom analysis was performed on 137 sample depths of 0.5 mL by standard methods (Battarbee, 1986; Bradbury, 1986). Sample intervals varied depending on depositional rates of the cores. Known concentrations of residues were mounted using Naphrax® and a minimum of 300 diatom valves were identified per slide using an oil immersion DIC objective at 1000x magnification. Literature used for diatom identification included: Foged (1978); Krammer et al. (1986, 1988, 1991a, 1991b); Vyverman et al. (1995); Gell (1999); Sabbe et al. (2001); Kilroy et al. (2003); Vanhoutte et al. (2004); Spaulding et al. (2010). Diatom taxonomic nomenclature followed Algaebase (<http://www.algaebase.org/>), see Appendix III Table III.2 for authority names. Diatom concentration was calculated using known sediment concentrations and dilutions on slides.

Constrained incremental sum of squares (CONISS) cluster analysis (Grimm, 1987) and the principal component analysis (PCA) were performed on diatom percent data using the rioja package *v. 0.9-6* (Juggins, 2016) in *R*. Broken stick models were then used to determine the number of significant zones and ordination axes. The PCA was performed on diatom species that occurred more than three times with greater than 2% relative abundance and Hellinger transformed.

6.5.6 CANONICAL CORRESPONDENCE ANALYSIS

Canonical Correspondence Analysis (CCA) is a hybrid ordination and regression analysis used to plot relationships between data sets (Legendre et al., 2012b). CCA was performed on the Lake Vera diatom versus pollen data, and diatom versus geochemical data. Due to long gradient lengths, a CCA was chosen over a Canonical Redundancy Analysis. CCA can only be performed on datasets with corresponding sample depths, therefore the Lake Vera multi-proxy dataset was interpolated to 50-year intervals using *R*. After interpolation, pollen and diatom data were trimmed to include species above 2% maximum abundance and that occurred at least three times. The CCA was run in *R* using *vegan v. 2.4-4* (Oksanen et al., 2016) on the Hellinger-transformed diatom dataset with rare taxa down weighted. A forward selection approach was used to determine which variables (geochemical and pollen taxa) to include with an ANOVA test ($p < 0.05$) to determine variables with significant relationships to the diatom compositional data.

6.6 RESULTS

6.6.1 CORING AND CHRONOLOGY

The TAS1508 N1 sediment core did not reach the lake basement, the oldest radiocarbon date of $8,074 \pm 44$ ^{14}C years was at 526 cm. Table 6.1 summarises the radiocarbon dating results for TAS1108 SC1 and TAS1508 N1. Unsupported ^{210}Pb reached background at 5 cm. For more details on ^{210}Pb results see Appendix IV Table IV.1. The age model shows reasonably linear accumulation for the composite core (TAS1108 SC1 & TAS1508 N1) with a mean accumulation rate of 20 yr/cm (Figure 6.2) and a slight change in sedimentation rate between the two cores. An age offset of 333 yrs was applied to the bulk sediment radiocarbon dates (Table 6.1). See Appendix III Table III.1 for age offset calculations.

Table 6.1: Radiocarbon results table for Lake Vera (TAS1108 SC1 & TAS1508 N1), including the laboratory identification number, sample depth (cm), sample type, the F modern (pMC) and error (1σ), the radiocarbon age (BP) and error, and $\delta^{13}\text{C}$ (per mil).

Lab code	Depth	Type	pMC	Error (1σ)	Age	Age Error	$\delta^{13}\text{C}$
OS-92421	23-23.5	bulk organic sediment	0.9222	0.0028	650	25	-27.72
OS-92422	50-50.5	bulk organic sediment	0.8543	0.0034	1260	30	-27.6
OS-92423	81-81.5	bulk organic sediment	0.7758	0.0029	2040	30	-27.55
OS-89128	103.5-104	bulk organic sediment	0.7423	0.0025	2390	25	-27.15
D-AMS 015676	114-114.5	plant macrofossil	77.38	0.33	2060	34	-32.9
D-AMS 015678	131-131.5	plant macrofossil	76.32	0.34	2171	36	-27.7
D-AMS 015682	185-185.5	plant macrofossil	59.65	0.67	4150	90	-29.2
D-AMS 017892	195-195.5	plant macrofossil	68.32	0.24	3060	28	NA
D-AMS 015680	238.5-239	plant macrofossil	61.73	0.3	3875	39	-21
D-AMS 016846	298-298.5	plant macrofossil	57.1	0.17	4501	24	-30.5
D-AMS 015683	309.5-310	plant macrofossil	50.66	0.25	5463	40	-32.5
D-AMS 017893	358.5-359	plant macrofossil	43.41	0.2	6703	37	NA
D-AMS 016847	359-360	plant macrofossil	42.28	0.16	6915	30	-30.8
D-AMS 017894	383.5-384	plant macrofossil	46.26	0.31	6193	54	NA
D-AMS 016852	399-399.5	plant macrofossil	48.07	0.15	5884	25	-24.4
D-AMS 016848	419.5-420	plant macrofossil	46.92	0.23	6079	39	-19.4
D-AMS 016849	448-448.5	plant macrofossil	43.79	0.15	6633	28	-29.5
D-AMS 016850	462-462.5	plant macrofossil	42.07	0.14	6955	27	-27.6
D-AMS 016851	476-476.5	plant macrofossil	41.15	0.14	7133	27	-30
D-AMS 017895	525.5-526	plant macrofossil	36.6	0.2	8074	44	NA

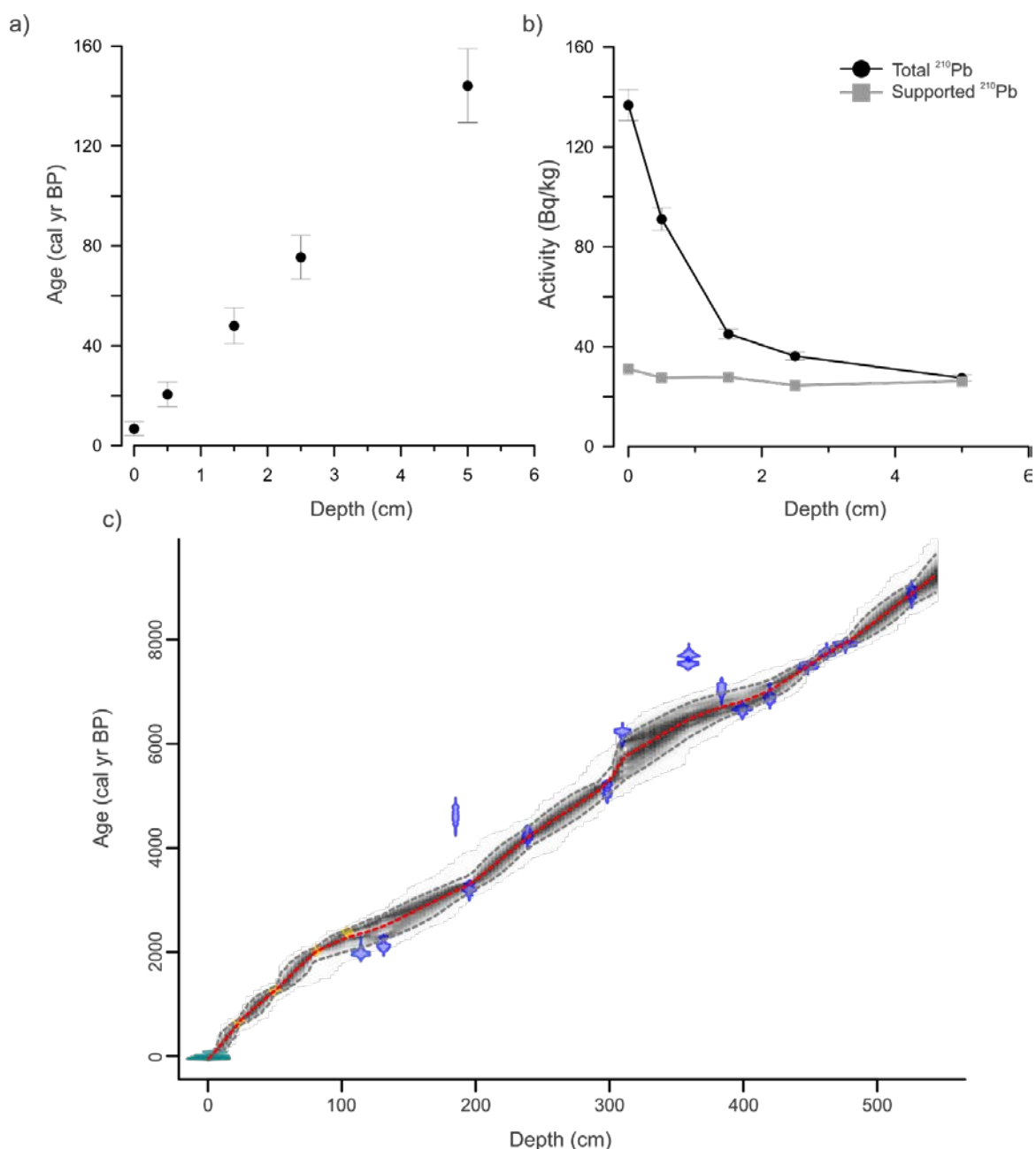


Figure 6.2: Age model for Lake Vera, Tasmania. a) ^{210}Pb CIC age-depth model with error bars. b) Activity of total and supported ^{210}Pb with errors by depth (cm). c) Bacon age-depth (red dotted line) model with probability distribution of the radiocarbon ages (blue) and age probability of ^{210}Pb dates (green). Yellow symbols represent the radiocarbon dates with an applied age offset. The 1000 iterations of potential depth ages (Bayesian statistic, black dotted lines) are shown with the 95% confidence interval (grey dotted lines).

6.6.2 μXRF GEOCHEMISTRY

Geochemical analysis had an average resolution of ca. 1 year from the composite core. Ti (kcps_n) shows high variability throughout the record. Peaks occur in the dataset at ca. 9.0, 8.0, 6.4, 5.8, 4.5, 2.5 to 2.2, 1.7, 0.9, and 0.5 ka (Figure 6.3f). Ca has an increasing trend from ca. 9.5 to 8.2 ka followed by a decrease to ca. 7.8 ka.

There is a stable, yet gradual increasing trend from 7.8 to 3.4 ka, followed by a decrease to 2.5 ka and increase to present. Peaks in the Ca data occur at ca. 7.0, 4.7, 3.5, 1.9, 1.2 and 0.6 ka (Figure 6.3e). Bromine shows overall stability from 9.2 ka to ca. 4 ka followed by an increasing trend to present. Decreases in Br occur at ca. 9.2, 8.1, 6.8, 6.2, 5.6 to 4.2, 2.9, 2.0, and 1.0 ka (Figure 6.3i). Fe has a general declining trend from ca. 9.2 to 8.0 ka followed by an increase to peak at ca. 6.8 ka. Fe has a general decline again until ca. 2.8 ka followed by a general increasing trend to present with peaks at ca. 2.3, 1.6, 0.9, and 0.5 ka (Figure 6.3h). Fe/Mn declines from ca. 9.4 to 7.8 ka followed by an increase to ca. 7.8 ka with an increase to present with peaks in the ratio occurring at ca. 9.0, 8.5, 8.0, 7.3, 6.8, 6.4, 5.7, .4, 2.3, 2.1, 1.6, and 0.9 ka. All geochemical proxies shift around ca. 2.2 ka (Figures 6.3 & III.7) represented by a break in the dendrogram of the μ XRF dataset (Figure III.8).

6.6.3 CARBON AND NITROGEN

Lake Vera Carbon Nitrogen analysis has an average resolution of ca. 31 years with high organic Carbon and low Nitrogen (%C median of ~15% and %N median of ~0.75%). $\delta^{13}\text{C}$ and C/N values cluster between -28.5 to -26 ‰ ($\delta^{13}\text{C}$) and 20 to 45 (C/N) (Appendix III Figure III.1). %C and %N have similar trends with gradual declines in both long-term records until ca. 2.5 ka. From ca. 2.5 ka to present %C and %N are variable with peaks at ca. 1.8, 1.4, and 0.6 ka and minimum values at ca. 2.1, 1.5, 0.9, and 0.5 ka (Figure 6.3c & d). C/N has a median of ~27 throughout the record with a gradual increase from ca. 9.2 to 6.7 ka followed by a decline then increase again from ca. 6.5 to 3.8 ka. Values decline to ca. 2.6 ka then become variable with peaks at ca. 2.5, 2.1, 1.6, 0.9, and 0.4 ka (Figure 6.3b). $\delta^{15}\text{N}$ is slightly variable at the start of the record with a decreasing trend (median of ~1.2 ‰) from 7.1 to 6.4 ka, low values at ca. 6.6 ka of 0.4 ‰. Stable values occur from ca. 6.4 to 2.6 ka (~1.5 ‰) then decline with high variability from ca. 2.6 ka to present (median of ~0.9‰). Low values at ca. 2.1, 1.6, 1.0 ka and peaks at ca. 2.0 and 1.2 ka. There is an increasing trend in $\delta^{15}\text{N}$ from ca. 0.6 ka to present.

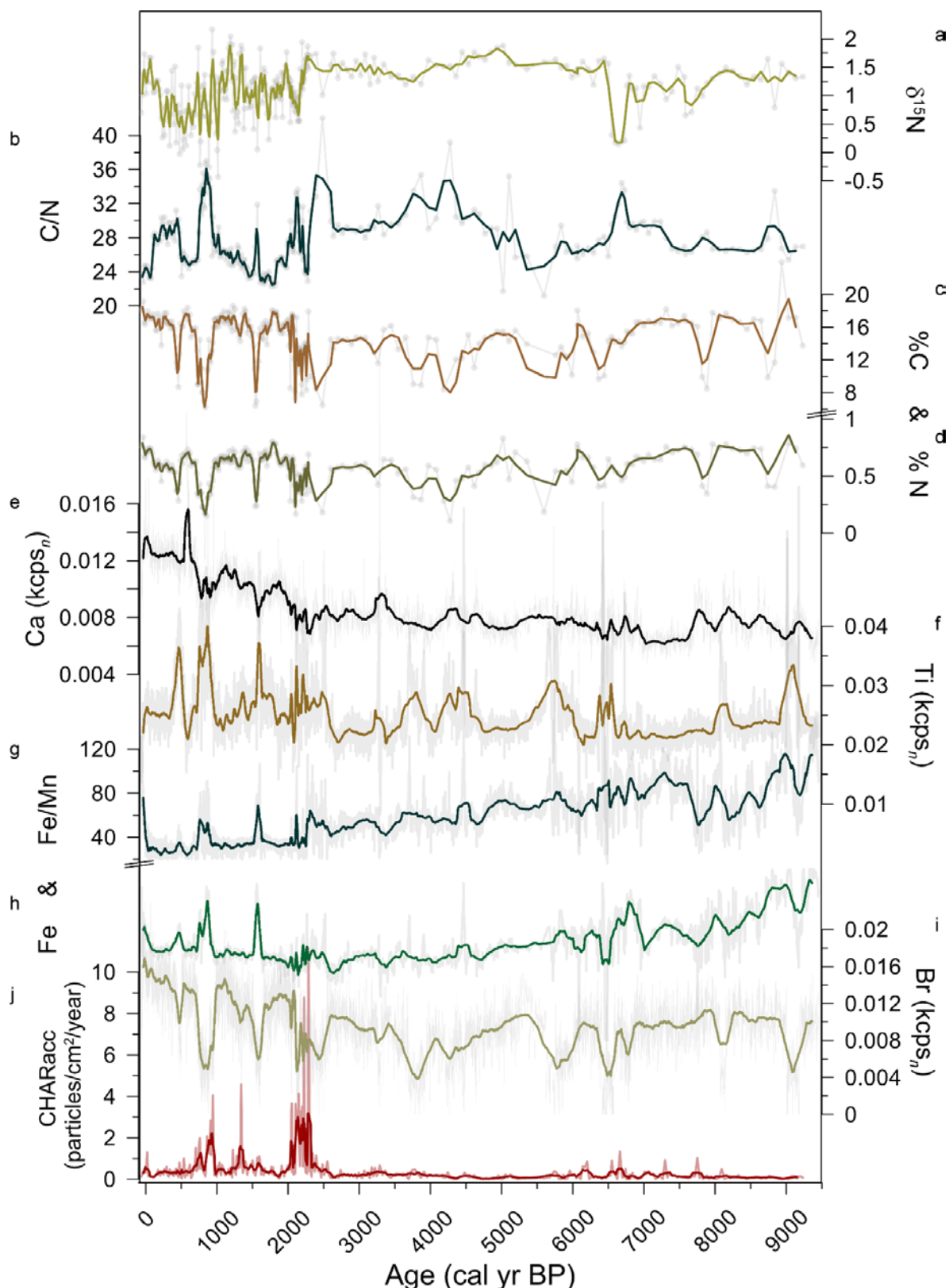


Figure 6.3: A summary of Paddy's Lake geochemistry results. a) $\delta^{15}\text{N}$ (‰) (grey) and weighted average (lime green, window width=3); b) Carbon/Nitrogen ratio (grey) and weighted average (dark green, window width=3); c) percent carbon (grey) and weighted average (light brown, window width=3) and d) percent nitrogen (grey) and weighted average (olive, window width=3); e) Ca (grey) and weighted average (black, window width=101); f) Ti (grey) and weighted average (brown, window width=101); g) Fe/Mn (grey) and weighted average (dark green, window width=101); h) Fe (grey) and weighted average (green, window width=101); i) Br (grey) and weighted average (light green, window width=101); and j) charcoal accumulation rate (light red) and weight average (dark red, window width=5).

6.6.4 CHARCOAL

Charcoal accumulation (CHAR_{acc}) has an average resolution of ca. 22 years and was calculated on the combined macroscopic charcoal records from TAS1108 SC1 and TAS1508 N1. The CHAR_{acc} shows very low values from ca. 9 to 2.6 ka. At ca. 2.6 ka values increase, then more rapidly at ca. 2.3 ka. Peaks in the remainder of the record occur at ca. 1.3, 0.9 and 0.8 ka (Figure 6.3j).

6.6.5 DIATOMS

Diatoms show good preservation throughout the composite record with ~325 species identified from 137 samples at an average resolution of ca. 68 years. Three significant zones were determined by the CONISS cluster analysis and three significant axes were identified in the PCA (PCA 1= 29.6 % variance, PCA 2= 13.7 % variance, and PCA 3 = 4.6% variance). PCA 1 has a strong negative association with *D. stelligera*, *Achnantheidium minutissimum*, and *Fragilaria capucina* and a strong positive relationship with *Eunotia diodon*, *S. exiguiformis*, *Gomphonema* spp. and *Eunotia implicata*. The PCA axis 1 increased from ca. 9.2 to 6.2 ka followed by a decline to ca. 3.6 ka, increased again to 2.8 ka then declined to its minimum at ca. 2.2 ka. The PCA axis 1 then slowly increased to present (Figure 6.5e).

6.6.5.1 Zone 1: 9,200 to 6,850 cal yr BP (TAS1508 N1)

This zone has a fairly stable species assemblage. From ca. 9.2 ka to 6.8 ka, *S. exiguiformis* increases from ~5 to 15%, *D. stelligera* has ~10% relative abundance. *Achnanthes subexigua*, *A. minutissimum*, *Brachysira styriaca*, *E. diodon*, *Eunotia incisa* and *Frustulia elongatissima* have ~5% relative abundance. There is a slight incline in *Aulacoseira distans* through this zone and a decline in *Tabellaria flocculosa*. The planktonic:benthic have low values during this zone. Total valve are relatively low peaking at ca. 8.0 ka in this zone (Figures 6.4 & III.4).

6.6.5.2 Zone 2: 6,050-3,850 cal yr BP (TAS1508 N1)

During this zone *S. exiguiformis* has a high relative abundance with a decreasing trend from ~15 to 7%. *D. stelligera* drops in relative abundance to ~5%. *Eunotia* spp. increases throughout this zone with a maximum relative abundance of *E. diodon* at ~20%, and *E. incisa* at 15%. *F. elongatissima* is more abundant (~7%), with increases in *Cocconeis placentula* (~3%) from ca. 6.9 to 5.5 ka and *Encyonema silesiacum* (~3%) from ca. 5.5 ka to the end of the zone. Achnanthaceae's and *Brachysira* spp. decline in abundance and the total valves and planktonic:benthic are lowest in this zone.

6.6.5.3 Zone 3: 3,800 cal yr BP to present (TAS1508 N1 & TAS1108 SC1)

From ca. 3.8 ka to present *D. stelligera* increases in relative abundance varying from ~20 to 45%. *E. diodon* and *F. elongatissima* decline from ca. 3.8 to 0.9 ka then increase again to present. *E. incisa* increases (~15%) then decreases (~5%) in relative abundance. *A. subexigua* (~5-10%), *A. minutissimum* (~10%), *B. styriaca* (~7%) and *Fragilaria capucina* (~5%) increase in abundance from ca. 2.3 to 0.9 ka and drop to lower abundances for the remainder of the zone. *Eunotia* spp. and *F. elongatissima* increase from ca. 0.9 ka to present. Planktonic:benthic increase at ca. 3.8 ka and remain high and variable throughout the remainder of the zone. Total valves are highest in this zone from ca. 2.3 to 1.0 ka with maximum values at ca. 1.6 ka, then decline to the lowest values from ca. 0.9 ka to present.

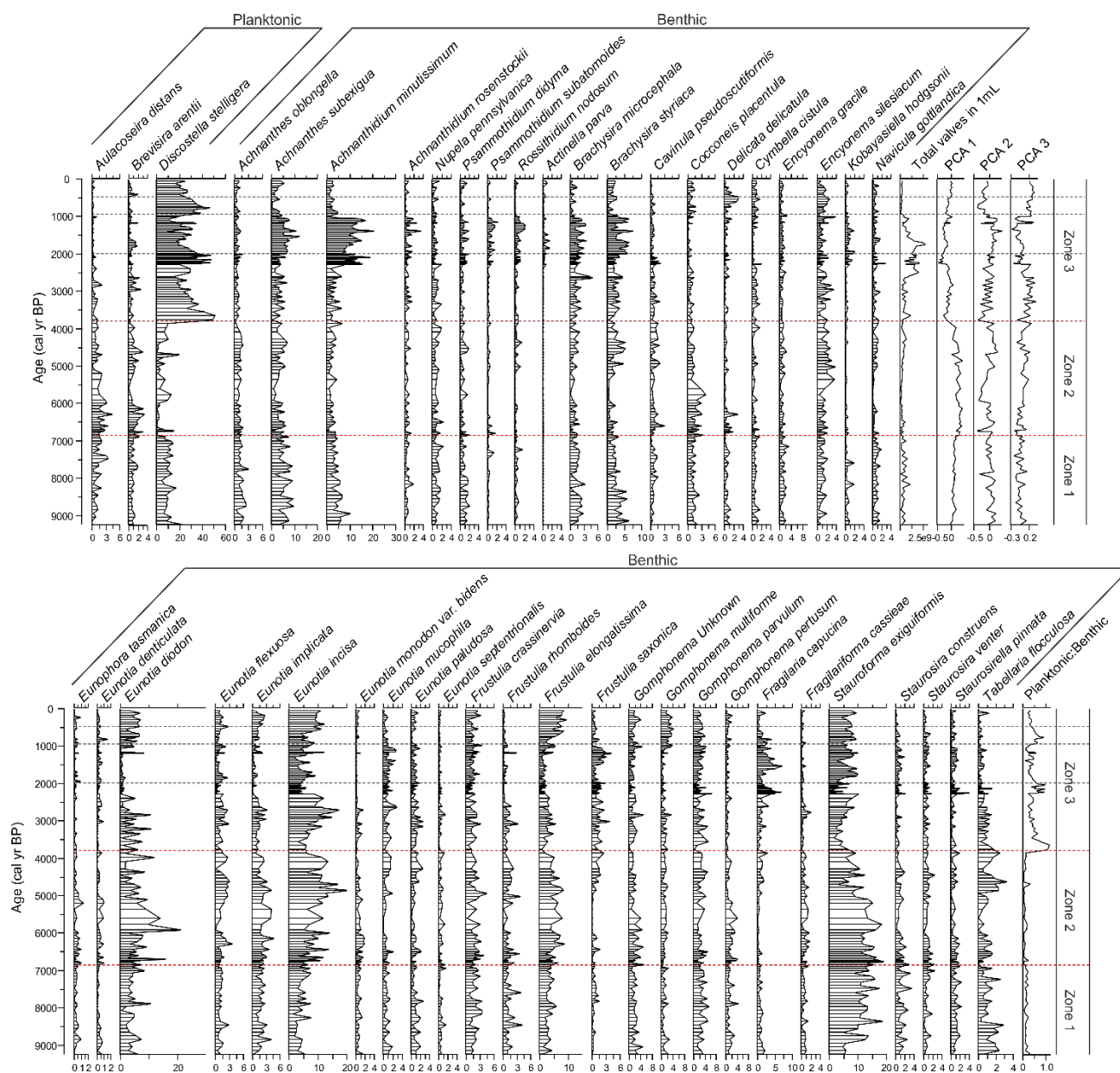


Figure 6.4: Stratigraphy of Lake Vera diatoms. Most abundant diatom species presented as relative abundance. The PCA axis 1, 2, and 3 estimate trends in the diatom percentage data (explained variance of PCA 1 =29.6 %, PCA 2=13.7 % and PCA 3= 4.6 %). Significant zones are separated by red dashed lines, significant zones from Chapter 7 are separated by grey dashed lines. Planktonic:benthic ratio estimate trends in the sum of planktonic taxa to benthic taxa.

6.6.6 CANONICAL CORRESPONDENCE ANALYSIS

The CCA analysis determines significant relationships between the diatom community and terrestrial environment (vegetation and geochemistry) independent of time. Eight geochemical indicators (Fe, Ni, N, C/N, Ca, Si, $\delta^{15}\text{N}$, and Rb) and 19 vegetation types (*Nothofagus gunnii*, *Lagarostrobos franklinii*,

Leptospermum/Baeckea, *Eucalyptus* spp., Cyperaceae, Cupressaceae, *Microsorium* spp., trilete spores, *Astelia*, *Dicksonia*, Restionaceae, Rhamnaceae, Proteaceae, *Pediastrum* influx, *Phyllocladus aspleniifolius*, *Isoetes*, Ericaceae, *Allocasuarina* spp., and *Eucryphia lucida*) were selected as significant variables (tested with an ANOVA $p < 0.05$). The overall significance of both CCA models as < 0.001 . Only select important geochemical and pollen types were displayed in Figure 6.7.

6.7 DISCUSSION

6.7.1 ECOLOGICAL INTERPRETATION OF DIATOMS

The Lake Vera diatom record reveals an oligotrophic acidic dystrophic lake, with periods of increasing dystrophic conditions (ca. 7 to 4 ka) and lower lake levels (4 ka to present) (Figure 6.4). From ca. 9.2 to 7 ka oligotrophic low light conditions are shown by the presence of pioneer tychoplanktonic taxa, tolerant of rapid changing environments (*S. exiguiformis*, *Staurosira construens*, *S. venter*, *S. pinnata* and *T. flocculosa*) (Augustinus et al., 2008; Saunders et al., 2013b; Gell et al., 2014; Law et al., 2015). Other taxa found in relatively high abundance during this period have wide ecological ranges from oligotrophic to mesotrophic and can also tolerate turbulence and acidic to alkaline conditions (*D. stelligera*, *A. subexigua*, *A. minutissimum* and *B. styriaca*) (Augustinus et al., 2008; Law et al., 2015). The bathymetry of Lake Vera suggests that a less full lake would decrease the littoral habitat and planktonic taxa would be more abundant (Figure 6.6) (Peterson, 1966). This assemblage indicates a relatively full oligotrophic acidic pioneer environment.

At ca. 7 ka increased acidity and dystrophy are apparent with increases in taxa tolerant of humic and dystrophic environments particularly, *Brachysira microcephala*, *B. styriaca*, *E. diodon*, *Eunotia flexuosa*, *E. incisa*, *E. monodon* var. *bidens*, *Frustulia crassinervia* and *F. elongatissima* other *Eunotia*, *Frustulia* and *Gomphonema* spp. (van Dam et al., 1981; Charles, 1985; Bradbury, 1986; Hodgson et al., 2000; Steinberg, 2003a; Thomas, 2007; Kattel et al., 2015). This period is followed by dominant planktonic *D. stelligera* indicating a decline in lake level (from ca. 4 ka). While absolute abundances only marginally increase at this

time, at ca. 2.3 ka total diatom valves and the absolute abundance of *D. stelligera*, Achnantheaceae, and tychoplanktonic taxa increases substantially in comparison to the previous portion of the record (Appendix III Figure III.4). This period is associated with increased fire disturbance (between ca. 2.3 ka and 0.9 ka) and an increase in benthic and less acidic disturbance taxa, such as Achnantheaceae spp. (van Dam et al., 1981; Robinson et al., 1987; Peterson et al., 1992; Law et al., 2015)

6.7.2 INDIRECT CLIMATE IMPACTS ON AQUATIC ECOSYSTEMS

From ca. 9 to 7 ka western Tasmania experienced an increase in moisture availability with the northern movement of the SWW (Fletcher et al., 2011; Fletcher et al., 2012; Fletcher et al., 2015; Rees et al., 2015). These climate conditions likely provide enough moisture to fill Lake Vera i.e. high littoral to planktonic habitat. During this period (ca. 9 to 7 ka) tychoplanktonic and pioneer taxa (*S. exiguiformis*, *Staurosira construens*, *S. venter*, *S. pinnata* and *T. flocculosa*) are associated with aquatic and terrestrial vegetation Restionaceae, *Isoëtes*, Proteaceae, Cupressaceae and Ericaceae (Figure 6.7b), as well as, geochemical indicators Fe and %N (Figure 6.7a). The association of tychoplanktonic diatoms with aquatic plants (*Restionaceae* and *Isoëtes*) suggests Lake Vera was relatively full with an extensive littoral environment. Organic elements Fe, C, and N are common in peats that dominate western Tasmania (Buckney et al., 1973; Steane et al., 1982). With development of this catchment the pioneer and tychoplanktonic taxa are prolific at the beginning of the record during a time of wetter conditions and a rapid changing environment. The Lake Vera catchment has always been heavily rainforested and vegetation tracks hydroclimate (Fletcher et al., in review). During these wetter conditions, peat formation would track rainforest development and thus develop more terrestrial derived cations, organic matter, and humic acids into Lake Vera. (Figures 6.4 & 6.5).

From ca. 7 to 5 ka peak moisture is consistent with the northern locality of the SWW supporting the highest abundance of rainforest to the region (Figure 6.5b) (Stahle et al., 2016; Mariani et al., 2017a; Stahle et al., 2017). At, ca. 7 ka, a peak in *Phyllocladus aspleniifolius* (Figure 6.5b) with high Fe and C/N (Figure 6.3b & h) indicate high precipitation and delivery of terrestrial matter. More terrestrial input would result in the

development of a dystrophic lake environment. The wet climate and forested conditions are also shown at Lake Vera with high lake levels and more dystrophic conditions. Low planktonic:benthic diatoms (Figure 6.4) and an increase in *Isoëtes*, a littoral macrophyte (Figure 6.5c), indicate a more extensive littoral habitat. During wet conditions, rainforest development increases the organic peat soils on the landscape increasing availability of acidic organic matter and nutrient rich soils (Jarman et al., 1982; Bowman et al., 1986b). This shift in climate is coincident with increased acidic dystrophic tolerant taxa (*Eunotia* spp.) (van Dam et al., 1981; Steinberg, 2003a) corroborated by association with rainforest taxa indicative of wet conditions (*Phyllocladus aspleniifolius*, *Nothofagus gunnii* and Rhamnaceae) and $\delta^{15}\text{N}$ of the CCA (Figure 6.7). Therefore, full lake conditions and increases in the dystrophic nature of the lake from ca. 9 to 5 ka suggests the diatom community at Lake Vera responded indirectly to shifts in climate through vegetation change and peat development.

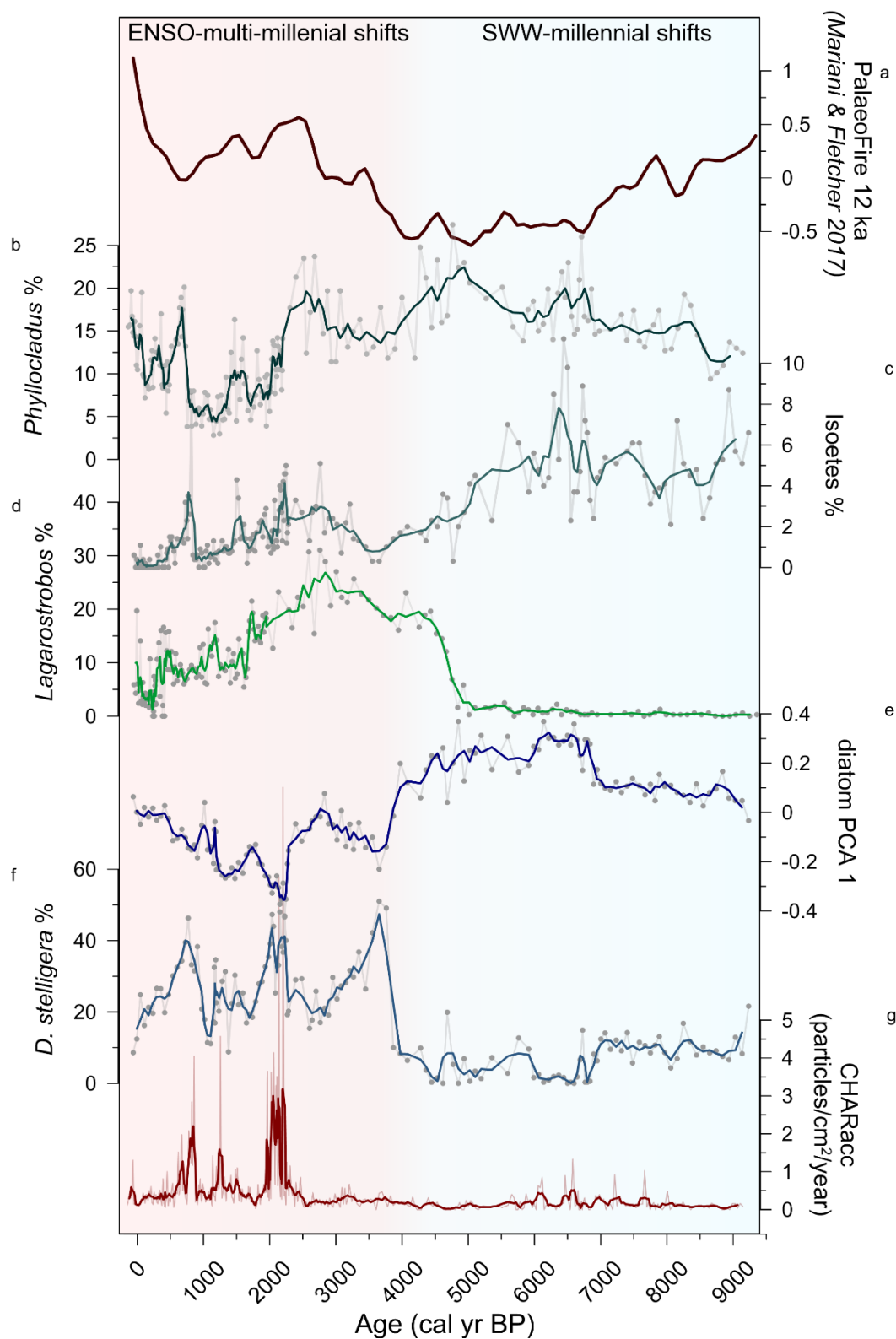


Figure 6.5: Summary plot of multi-proxy dataset from Lake Vera. a) western Tasmania palaeofire (Mariani et al., 2017b); b) *Phyllocladus aspleniifolius* pollen percent (grey) weighted average (dark green, window width=5); c) *Isoetes* pollen percent (grey) weighted average (teal, window width=5); d) *Lagarostrobos franklinii* pollen percent (grey) weighted average (light green, window width=5); e) diatom PCA axis 1 scores (grey) weighted average (dark blue, window width=3); f) *Discostella stelligera* percentage (grey) weighted average (light blue, window width=3); g) charcoal accumulation rate (light red) weighted average (dark red, window width=5).

6.7.3 DIRECT CLIMATE IMPACTS ON AQUATIC ECOSYSTEMS

A shift toward lower and more variable lake levels is the result of a drying regional trend from ca. 4 ka caused by increased magnitude and frequency of El Niño events as early as ca. 6.7 ka (Chapter 4; Stanley et al., 2002; Fletcher et al., 2015; Rees et al., 2015; Stahle et al., 2016; Stahle et al., 2017). Typically, planktonic taxa increase in abundance with lake level; however, the bathymetry at Lake Vera suggests that a fuller lake will have a larger littoral area, and thus, more benthic versus planktonic taxa (Figure 6.6). This relationship is substantiated by low *Isoëtes* (Figure 6.5c) and increases in planktonic:benthic diatom ratio, where benthic taxa occupy the littoral zone (Figures 6.4). Regional drying (Mariani et al., 2017b) causes declines in rainforest (*Phyllocladus aspleniifolius*; Figure 6.5b) and increases in vegetation that mast seeds during dry summers (*Lagarostrobos franklinii*; Figure 6.5d) indicating drought stressed environments (Chapter 4; Fletcher, 2015; Fletcher et al., in review). This drought stress is also shown by decreased lake levels, increases in planktonic *D. stelligera* (Figure 6.5f), and later fire (Figure 6.5g). Increasing Ca values from ca. 2.5 ka suggests high saturation of carbonates due to lower lake levels (Cohen, 2003; Kylander et al., 2011) (Figures 6.3d). Therefore, association between *D. stelligera*, Ca, and *Lagarostrobos franklinii* in the CCA indicates a drought stressed terrestrial environment with lower lake levels (Figure 6.7). This shift to a lake level response to climate suggests Lake Vera has transitioned from dominant indirect impacts of climate to direct impacts.

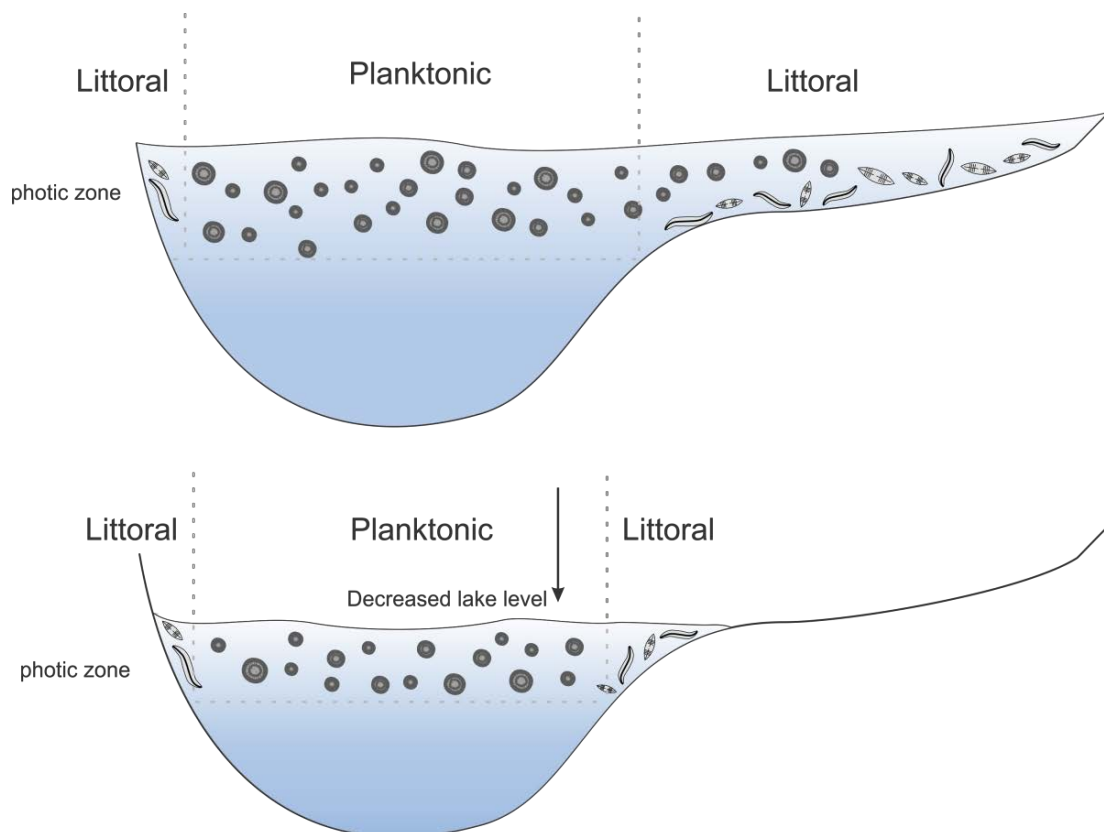


Figure 6.6: Schematic representative of Lake Vera bathymetry and planktonic versus littoral habitat extent at differing lake levels.

Burning of the local catchment from ca. 2.3 to 0.9 ka is the result of dry conditions caused by increased centennial scale trends in SWW variability of positive SAM phases (Mariani et al., 2016a; Fletcher et al., 2018a), in addition to continued increase in El Niño frequency (Mariani et al., 2016b; Mariani et al., 2017b). Increased local fires are coeval with increased abundance of *D. stelligera* and lower lake levels (Figure 6.5f & g). This burning has further impact on the aquatic ecosystem with more disturbance alkaline taxa (Figure 6.4 & Chapter 7). The CCA confirms a novel diatom assemblage of more alkaline disturbance taxa (Achnantheaceae) associated with *Leptospermum/Baেকেa*, sclerophyll species in the Myrtaceae family (Figure 6.7b). Sclerophyll vegetation are species adapt to frequently burned environments (Chapter 4; Jackson, 1968). With increased fire activity at Lake Vera (ca. 2.3 to 0.9 ka) alkaline and disturbance taxa increase (i.e. Achnantheaceae), as well as, planktonic *D. stelligera* coeval with decreases in organics (Br, %C and %N) and increases in erosion indicators (Ti) (Figure 6.3). In western Tasmania, fire activity is driven by changes in hydroclimate (Fletcher et al., 2015; Mariani et al., 2017b) and can cause increased erosion (Huvane et al., 1996; Korhola et al., 1996; Korsman et al., 1998; Klose et al., 2015) and lake alkalinity (Chapter 7; Renberg et

al., 1993; Korhola et al., 1996; Haberle et al., 2006). Fire also mobilises Fe and strips soil from the catchment increasing sediment deposition and water turbidity (Korhola et al., 1996; Ketterings et al., 2000) decreasing light penetration of the lake and increasing anoxic conditions of the lake bottom (Fe/Mn, Figure 6.3g) (Fee et al., 1996; Koinig et al., 2003). Repeated fire disturbance at Lake Vera from ca. 2.3 to 0.9 ka and extensive input of terrestrial material (Figure 6.3) caused a non-linear shift in the diatom community (Chapter 7).

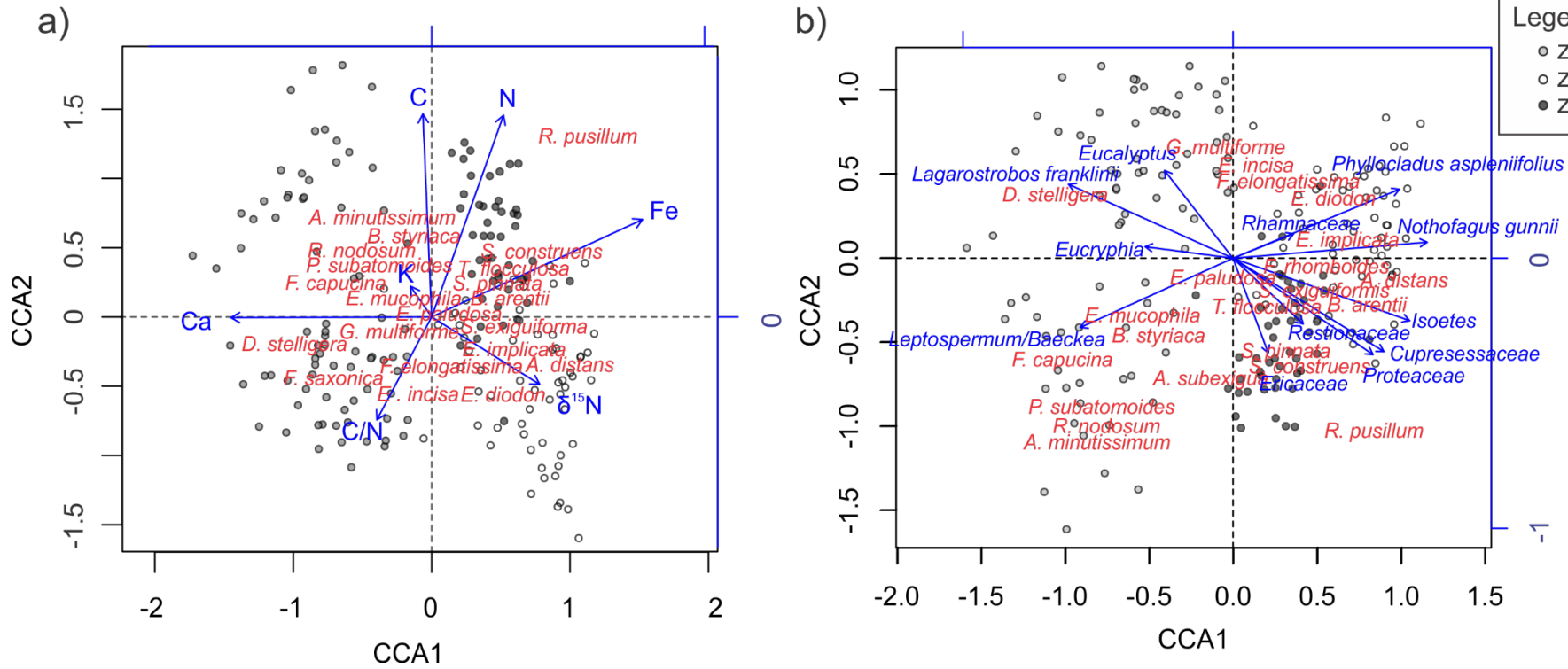


Figure 6.7: CCA biplot of important diatom taxa (red) and significant environmental geochemicals (a) and vegetation (b) (blue arrows) overlaying depth samples (grey circles). Zone 1 is indicated by black dots, Zone 2 is indicated by white dots and Zone 3 by grey dots.

6.7.4 MULTI-MILLENNIAL TO MILLENNIAL CLIMATE SHIFTS

A switch from multi-millennial (slow) climate variability (SWW) to sub-millennial (fast) climate variability (ENSO and SAM) during the Holocene (Stanley et al., 2002; Abram et al., 2014; Fletcher et al., 2015; Rees et al., 2015; Beck et al., 2017; Mariani et al., 2017b) results in a shift toward lower and more variable lake levels at Lake Vera. This shifts the pathway of climate influence over the lake (dominant indirect to dominant direct), principally due to the overriding effect that lake level fluctuations has on diatom composition. Understandably the unique bathymetry of Lake Vera allows this relationship to be possible, but the significant drop in lake level and the direct impact of climate on the diatom community is the result of the shift to high frequency climate variability (Moy et al., 2002; Mariani et al., 2017b). This shift in frequency of climatic change had a profound influence over the lake level and thus the diatom composition. In this system, it appears that changes in the frequency of climatic variability are also reflected in the variability and amplitude of the diatom compositional change (diatom PCA 1; Figure 6.5e). Given that we have entered a climate scenario characterised by unprecedented rates of change (IPCC, 2014), this finding is critical for understanding the potential effects of changing climate variability on aquatic systems in Tasmania and other similar systems.

6.8 CONCLUSION

This chapter has demonstrated that Lake Vera diatoms are responding to climate both directly and indirectly. During enhanced SWW dominant climate from the early to mid- Holocene (ca. 9 to 5 ka), Lake Vera remained relatively wet. The diatom community was more acidic and dystrophic, responding indirectly to climate with peat development under rainforest vegetation. With more variable climate after ca. 5 ka (ENSO), Lake Vera is responding more directly to climate via lake level changes. This is principally due to the lake bathymetry and the effects lake level declines have on the diatom composition. The shift in climate variability (SWW to ENSO) is also reflected in the diatom community with increased compositional variability. At ca. 2.3 ka, the onset of

burning results in increased input of terrestrial material and an alkaline disturbance aquatic environment. Continued disturbance causes a non-linear shift in the diatom community to a more acidic oligotrophic environment.

Supporting information in Appendix III.

CHAPTER 7: DISCUSSION

7.1 CHAPTER AIM

This chapter is comprised of the amended article Beck, K. K., Fletcher, M.-S., Gadd, P. S., Heijnis, H., Saunders, K. M., Simpson, G. L., & Zawadzki, A. (2018) Variance and rate-of-change as early warning signals for a critical transition in an aquatic ecosystem state: A test case from Tasmania, Australia. *Journal of Geophysical Research: Biogeosciences*, 123, 495–508 DOI:10.1002/2017JG004135. Beck, K.K. and Fletcher, M.-S. conceived the ideas for this Chapter. Beck, K.K. performed the diatom and statistical analyses, interpretation and writing of this publication. Gadd, P.S., and Heijnis, H. performed the μ XRF geochemical analysis and Zawadzki, A. performed the lead-210 analysis. Simpson, G.L. assisted with the statistically analysis and the writing of the R code. All authors assisted in editing and interpretation of this publication.

7.2 ABSTRACT

Critical transitions in ecosystem states are often sudden and unpredictable. Consequently, there is a concerted effort to identify measurable early warning signals (EWS) for these important events. Aquatic ecosystems provide an opportunity to observe critical transitions due to their high sensitivity and rapid response times. Using palaeoecological techniques, we can measure properties of time series data to determine if critical transitions are preceded by any measurable ecosystem metrics, i.e. identify EWS. Using a suite of palaeoenvironmental data spanning the last 2,400 years (diatoms, pollen, geochemistry, and charcoal influx) we assess whether a likely critical transition in diatom community structure was preceded by measurable EWS. Lake Vera in the temperate rainforest of western Tasmania, Australia, has a diatom community dominated by *Discostella stelligera* and undergoes an abrupt compositional shift at ca. 920 cal yr BP concomitant with increased fire disturbance of the local vegetation. This shift is manifest as a transition from less oligotrophic acidic diatom flora (*Achnantheidium minutissimum*, *Brachysira styriaca*, and *Fragilaria capucina*) to more oligotrophic acidic taxa (*Frustulia elongatissima*, *Eunotia diodon*, and *Gomphonema*

multiforme). We observe a marked increase in compositional variance and rate-of-change prior to this non-linear shift, revealing these metrics are useful EWS in this system. Interestingly, vegetation remains complacent to fire disturbance until after the shift in the diatom community. Disturbance taxa invade and the vegetation system experiences an increase in both compositional variance and rate-of-change. These trends in EWS imply an approaching critical transition in the vegetation and the probable collapse of the local rainforest system.

7.3 INTRODUCTION

Environmental pressures or perturbations can erode the resilience of an ecosystem such that, in cases where multiple stable states exist, a threshold is crossed and the system shifts into a new stable state (Carpenter et al., 2006; Wang et al., 2012; Bunting et al., 2016). These critical transitions are a non-linear ecosystem response to a change in conditions such as nutrient influx, climate, and/or land-use change (Scheffer et al., 2001; Scheffer et al., 2003; Scheffer et al., 2009; Lenton, 2011; Wang et al., 2012). Non-linear ecosystem dynamics and the existence of multiple stable states have profound implications, as state transitions can be sudden, unpredictable and difficult to reverse. Once a state shift has occurred in response to a perturbation, internal feedbacks can ‘fix’ the ecosystem in the new stable state irrespective of continued perturbation – i.e. hysteresis (Scheffer et al., 2003; Scheffer et al., 2009; Fletcher et al., 2014b). Consequently, an important endeavour is the attempt to detect early warning signals (EWS) that precede critical transitions in nature (Scheffer et al., 2009; Wang et al., 2012; Dakos et al., 2015). Whilst theory predicts that EWS should precede some types of critical transitions, detecting these signals empirically remains challenging; particularly for ecosystems with long generational timespans, such as temperate forests. Nevertheless, given the clear importance of critical transitions for ecosystem function and monitoring, considerable attention has been paid to theorising and attempting to measure EWS to improve predictive power (Carpenter et al., 2006; Scheffer et al., 2009; Scheffer et al., 2012; Wang et al., 2012; Dakos et al., 2015; Bunting et al., 2016; Seddon et al., 2016).

Modelling suggests critical transitions are often preceded by a reduction in resilience, the ability of a system to both resist and recover from perturbations (Scheffer et al., 2009; Hodgson et al., 2015). These factors of lost resilience are often associated with increased recovery time and variance, and a concerted effort has been made to measure these components in an attempt to understand how resilience changes through time (Carpenter et al., 2006; Scheffer et al., 2009; Dakos et al., 2015). A slowdown in recovery time as a system approaches a critical transition is termed “critical slowing down” (Scheffer et al., 2009), and it is this property that has received most attention when attempting to measure changes in resilience and detecting EWS (Scheffer et al., 2009; Wang et al., 2012). Some examples of EWS during a critical slowing down look at properties of time series data using statistical methods including: high autocorrelation at lag +1, increasing variance, and skewness from a fitted model to some ecosystem state measure (Scheffer et al., 2009; Scheffer et al., 2012; Wang et al., 2012; Dakos et al., 2015). Additionally, rate-of-change (ROC) can measure the change in state recovery for a critical transition, where increased ROC demonstrates an EWS of longer recovery and a loss in resilience (Lim et al., 2011). Despite a well-established theoretical underpinning, actual measurements of EWS in natural systems are few, particularly in ecology where species generational times often exceed observation windows, thus, precluding direct measurement. It is here that high resolution palaeoecological data are an important tool for testing the concepts underlying EWS.

Palaeoecological data can be used in the absence of monitoring data to comprehend long-term ecosystem dynamics, allowing an understanding of how ecosystems change through time, and an appreciation of the factors that can cause critical transitions and the formation of new stable states (Willis et al., 2010; Wang et al., 2012; Fletcher et al., 2014b). Importantly, palaeoecological data are rarely evenly spaced in time, thus, data are usually manipulated (often via interpolation) prior to application of many of the metrics of resilience, such as autocorrelation and skewness (e.g. Wang et al., 2012). Critically, the manipulation of time series data can unintentionally cause false correlations and remove important trends (Schulz et al., 1997; Dakos et al., 2012; Carstensen et al., 2013). In some cases, interpolation of data can artefactually cause an increase in standard deviation (i.e. variance), autocorrelation, and broadening of skew – all considered potential EWS that precede critical transitions (Carstensen et al., 2013). Thus, it is important to select appropriate metrics when using palaeoecological data to measure resilience and EWS. Variance, for example, has been a successfully

employed measure for palaeoecological data without interpolation, allowing an effective test for EWS of critical transitions (Dakos et al., 2012; Bunting et al., 2016). In addition, ROC (with no interpolation) can be used as a EWS to measure the erosion of resilience before a critical transition (Scheffer et al., 2012; Siteur et al., 2016).

Here we use a suite of palaeoecological data to understand the interconnection between changes in vegetation, nutrient cycling, sediment delivery, and diatom community structure through time. Our study site is Lake Vera in southwest Tasmania, Australia, a mountainous cool temperate landscape in which fire activity exerts a major influence over terrestrial ecosystem dynamics. Importantly, little is known about how fire-driven landscape change in this region influences aquatic ecosystem dynamics. We present data on temporal changes in diatom community composition, lake sediment geochemistry, pollen and charcoal spanning the last 2,400 years. Our objective is to test the response of the lentic ecosystem to changes in the local catchment. We specifically ask: (i) What is the response of the diatom community to fire-driven catchment change?; (ii) If changes in diatom community structure do occur, are they linear or non-linear?; and (iii) Can we detect EWS for any abrupt aquatic ecosystem change (i.e., critical transitions)?

7.3.1 BIOGEOGRAPHY OF TASMANIA

Tasmania (40-44°S) is a continental island that has a cool temperate maritime climate (Gentili, 1971). The island is bisected by northwest-southeast trending mountain ranges that intercept the prevailing mid-latitude westerly airflow, resulting in a steep west to east orographic precipitation gradient. The steep topography and rainfall gradient results in two distinct bioclimatic regions: a dry (ca. 400 mm p/a) open *Eucalyptus*-dominant savannah in the east of Tasmania and a wet (up to 3,500 mm p/a) west where moorland and rainforest dominate (Macphail, 1979; Fletcher et al., 2010b). The uniformly nutrient poor bedrock (Jurassic dolerite) and hyper-humid climate of western Tasmania results in the development of predominantly acidic organosols under all vegetation types (Pemberton, 1988, 1989; Isbell, 2002). Lake characteristics also follow this biogeographic divide, with acidic, oligotrophic and dystrophic waters in the west and turbid, less acidic,

(ultra)oligotrophic, saline lakes in the east (Tyler, 1974; Vanhoutte et al., 2004). Fire has shaped the regional vegetation of Tasmania. In the west, this has resulted in a failure of rainforest to occupy its climatic niche, and instead the landscape is dominated by fire-promoting plant communities. Fires are climate-limited in the west, where biomass is uniformly high, with interannual shifts in the strength and position of the westerly winds, the main control over fire activity (Mariani et al., 2016a).

7.3.2 STUDY SITE

Lake Vera (42°16' 29" S, 145°52'44" E) is a small moraine-bound lake formed in a glacial valley located near Frenchman's Cap in southwest Tasmania, Australia (Figure 7.1). The site lies within the region of strongest correlation between interannual shifts in the mid- latitude westerlies and rainfall anomalies on earth (Gillett et al., 2006; Hill et al., 2009). Lake Vera lies 550 masl, is dystrophic/oligotrophic and acidic with a maximum water depth of ~50 m. Annual mean precipitation is 2,800 mm and mean annual temperature is 8.7°C (Macphail, 1979; Bradbury, 1986; Markgraf et al., 1986). Surrounding vegetation includes: rainforest and related scrubland, heathland complexes, wet eucalypt forest and woodland, and non-eucalypt forest and woodland. Dominant taxa within the local catchment consist of *Atherosperma moschatum*, *Athrotaxis selaginoides*, *Eucryphia lucida*, *Eucalyptus delegatensis*, *Lagarostrobos franklinii*, *Leptospermum nitidum* and *Nothofagus cunninghamii* (Kitchener et al., 2013; Department of Primary Industries, 2017). Catchment geology contains mainly siliceous glacial deposits (Macphail, 1979; Bradbury, 1986).

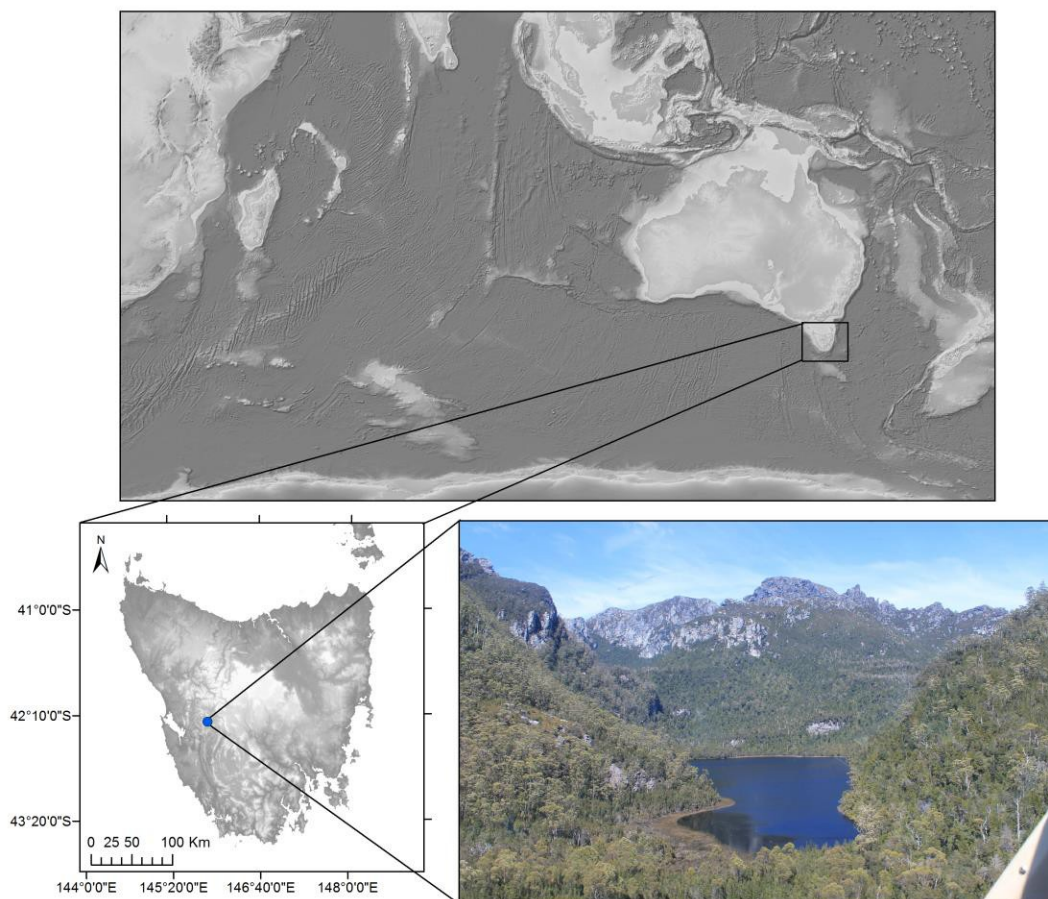


Figure 7.1: Map of Australia, inset map of Tasmania with site location (blue dot) and a photo of Lake Vera, Tasmania (by: Kristen Beck, 2015).

7.4 MATERIALS AND METHODS

7.4.1 CORING AND CHRONOLOGY

In 2011 a 105 cm core (TAS1108 SC1) was collected from 48 m depth in Lake Vera using the Universal coring system (Aquatic Research Instruments, 2016). Radiometric analysis was performed at the Australian Nuclear Science and Technology Organisation (ANSTO) (five ^{210}Pb samples) and The National Ocean Sciences Accelerator Mass Spectrometry (NOSAMS) (four radiocarbon samples) (Table 7.1). All radiocarbon samples were bulk sediment dried in a convention oven, rootlets removed and pre-treated in HCl to remove of any carbonates. Radiocarbon dates were calibrated to calendar years with Southern Hemisphere calibration curve to one standard deviation - SHCal13 (Hogg et al., 2013). ^{210}Pb ages were determined using a constant

initial concentration (CIC) model with an assumed constant sediment accumulation of 0.009 g/cm²/year. The constant rate of supply (CRS) and CIC model are in good agreement. However, due to the deep anoxic nature of this lake we would expect relative constant sedimentation throughout Lake Vera's history and, thus, CIC dates more appropriate for the age model (Appendix IV Table IV.1). A Bayesian age-depth model was developed in *R* v. 3.4.1 (R Development Core Team, 2014) using the Bacon v. 2.2 package (Blaauw et al., 2013) (Figure 7.2).

7.4.2 GEOCHEMICAL ANALYSIS

Geochemical data were obtained using a non-destructive Itrax X-ray fluorescence (μ XRF) core scanner at ANSTO at a resolution of 0.2 mm using a molybdenum (Mo) tube set at 30kV and 55mA with a dwell time of 10s. The geochemical data (Fe, Mn and Ti) were normalised by the Mo Incoherence/Coherence ratio (Croudace et al., 2015) and the Fe/Mn ratio was determined to demonstrate changes in redox conditions (Carignan et al., 1988; Koinig et al., 2003; Kylander et al., 2011) and alkalinity increases. Fe was used as an indicator of richness with fire (Korhola et al., 1996; Ketterings et al., 2000). Fe oxides are released from soils into waterbodies with fire (Korhola et al., 1996) and become soluble ferrous Fe that preserves in lake sediments when met with anoxic waters (Cohen, 2003).

Analysis for the percent Carbon (C%) and Nitrogen (N%) were performed at 0.5 cm intervals with an average sampling resolution of ca. 12 years. Samples were pre-treated with 10% HCl, freeze-dried and ground to create a homogeneous composition then analysed at the University of Waterloo on a Carlo Erba Elemental Analyser (CHNS-O EA1108 - Italy). Results were corrected to Carbon (IAEA-CH6, EIL-72 and USGS-40) and Nitrogen standards (IAEA-N1 and IAEA-N2) (Fry et al., 1992).

7.4.3 DIATOM ANALYSIS

Diatom analysis was performed at an average sampling resolution of ca. 45 years, at ~2.0 cm intervals, using 0.5 mL of sediment and standard methods (Battarbee, 1986; Bradbury, 1986). Known concentrations of residues were mounted using Naphrax® to determine diatom concentration. At least 300 diatom valves were identified per slide using an oil immersion DIC objective at 1000x magnification. Diatom concentration was calculated using known sediment concentrations. Constrained incremental sum of squares (CONISS) cluster analysis (Grimm, 1987) was performed using *Tilia v. 2.0.37* (Grimm, 2013). Taxa included in the cluster analysis occurred at least three times with an abundance of greater than 2%. To determine the significant number of zones (N =4) a broken stick model was used (Juggins, 2016).

7.4.4 PALYNOLOGY AND CHARCOAL ANALYSIS

Pollen analysis has an average sampling resolution of ca. 22 years, at 0.5-2.0 cm intervals. Pollen processing was performed on 0.5 mL of sediment using standard methods (Faegri et al., 1989). At least 300 terrestrial pollen grains were identified per slide using a bright field objective at 400x magnification. The terrestrial pollen sum was used to calculate percent of terrestrial pollen species and the supersum of all pollen grains was used to calculate pollen percent of non-terrestrial origin. Percent fern taxa (*Blechnum* spp., *Dicksonia* spp., *Histiopteris* spp., Hymenophyllaceae, *Microsorium* spp., Phymatodes, *Polystichum* spp.) were summed to represent lower canopy density. *Bauera rubioides* and Urticaceae pollen percentages were summed as an index for disturbance taxa. Cluster analysis (CONISS) was performed to identify pollen assemblage zones. Terrestrial taxa included in the cluster analysis occurred at least three times with an abundance greater than 2%. Significant zones (N =4) were identified using a broken stick model.

Macroscopic charcoal was processed at 0.5 cm intervals, an average sampling resolution of ca. 12 cal yr BP, for the entire core length according to standard protocols (Whitlock et al., 2001). A 1.5 mL sample was soaked in household bleach then sieved (250 µm and 125 µm) for identification at 10-20x magnification.

Microscopic charcoal was also enumerated during pollen identification. Charcoal particle size is a product of a range of factors including distance from fire, vegetation type, and fire intensity/severity (Whitlock et al., 2001; Mustaphi et al., 2014). To understand broad changes in fire activity irrespective of charcoal particle size, we created a composite charcoal record by averaging the sum of microscopic and macroscopic charcoal data after converting each charcoal series to z-scores using the entire sequence (i.e. 2,400 years).

7.4.5 NUMERICAL ANALYSES

7.4.5.1 Rate-of-change (ROC)

ROC analysis was run on proportional diatom and pollen data using the square chord distance measure standardised by the age intervals between samples to produce the ROC (Birks, 2012d) in *R*. This ROC method does not require interpolation of data to even time steps and we infer an increase in ROC as indicating a shift away from 'equilibrium', and a concomitant increase in recovery time that signals a loss in resilience (Scheffer et al., 2009; Lim et al., 2011; Scheffer et al., 2012; Siteur et al., 2016). ROC was performed on taxa that occurred more than three times with a maximum abundance great than 2% for both Lake Vera diatoms and terrestrial pollen.

7.4.5.2 Principal Curves (PrC) and Generalised Additive Models (GAMs)

A PrC was estimated on percentage diatom species and terrestrial pollen in analogue *v. 0.17-0* (Simpson et al., 2016) using *R*. PrCs are an alternative method to other ordination analyses for identifying the most important trend in the sediment sequence. A PrC is a non-linear curve fitted through data in multiple dimensions that, unlike the linear methods used by principal component analysis, can potentially represent greater explained variance if there is a single dominant gradient in the data (Hastie et al., 1989; De' ath, 1999; Simpson et al., 2012; Felde et al., 2014). The PrC was initialised using the first correspondence analysis axis and subsequently estimated by fitting smoothing splines to abundances of individual taxa. The generalised cross validation criterion was used to determine the wigglyness of each taxon's spline in the PrC. To avoid

overfitting, a penalty on the degrees of freedom of 1.4 was applied. The diatom and terrestrial pollen taxa included in the PrC occurred more than three times and above a 2% relative abundance.

GAMs were fitted to the diatom and pollen PrCs to identify the important trends in the community data using *mgcv v. 1.8-15* (Wood, 2016) in *R*. GAMs are semiparametric models that use a sum of smooth functions to model non-linear relationships between covariates and the response (Hastie et al., 1990; Yee et al., 1991; Simpson et al., 2009). Models were fitted using penalised residual maximum likelihood (REML), in which a penalty controls the degree of wigglyness of the estimated trends (smooth functions) (Wood, 2011). Here we use a location-scale Gaussian GAM, which enables simultaneous estimation of both the mean and variance of a time series. See Bunting et al., (2016) for further details on the GAM modelling approach. We account for the implicit non-constant variance which arises due to each sample representing a different amount of time by including this as a covariate in the linear predictor for the variance part of the model. This method is used to show the change in resilience of the lentic and terrestrial systems.

7.5 RESULTS

7.5.1 CORING AND CHRONOLOGY

A summary of the radiocarbon results is presented in Table 7.1. The age model shows somewhat linear sedimentation with some variability throughout sequence (Figure 7.2). Unsupported ^{210}Pb activity reached background at 5 cm. The Bayesian age-depth model determined a mean accumulation rate of 20 yr/cm (Figure 7.2). For more details on ^{210}Pb results see Appendix IV Table IV.1.

Table 7.1: Radiocarbon results for Lake Vera, including NOSAMS laboratory identification number, sample depth (cm), sample type, the F modern and error, the radiocarbon age (BP) and error (1σ), and $\delta^{13}\text{C}$ (per mil).

ID #	Depth (cm)	Sample Type	F Modern and error (1σ)	Radiocarbon	
				age and error	$\delta^{13}\text{C}$ (per mil)
OS-92421	23-23.5	Sediment Organic carbon	0.9222 ± 0.0028	650 ± 25	-27.72
OS-92422	50-50.5	Sediment Organic carbon	0.8543 ± 0.0034	1260 ± 30	-27.6
OS-92423	81-81.5	Sediment Organic carbon	0.7758 ± 0.0029	2040 ± 30	-27.55
OS-89128	103.5-104	Sediment Organic carbon	0.7423 ± 0.0025	2390 ± 25	-27.15

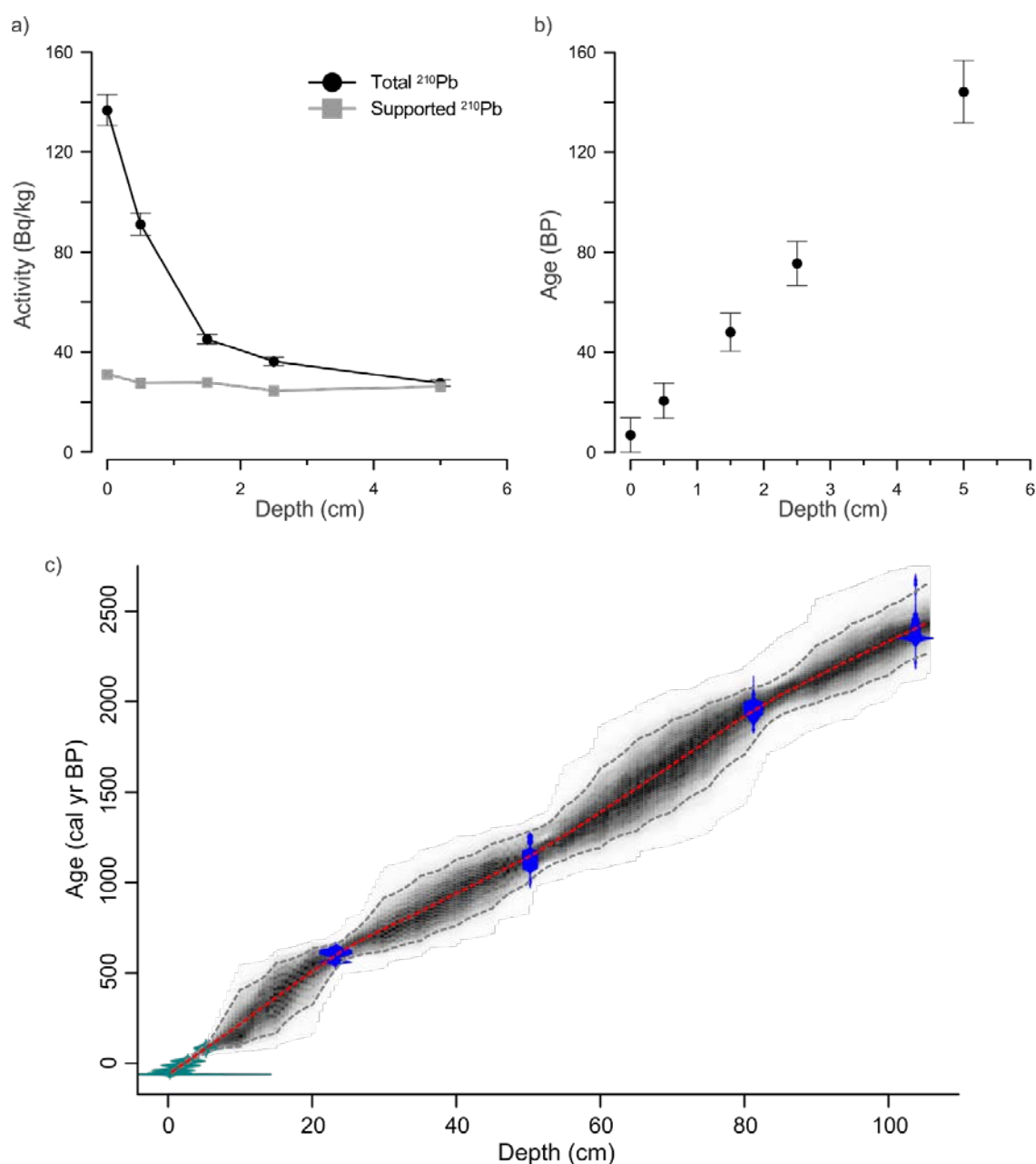


Figure 7.2: Age-depth model for Lake Vera, Tasmania. a) Total and supported ^{210}Pb activity concentrations with uncertainties, b) ^{210}Pb chronology based on the CIC model, c) Age-depth model developed in Bacon, the blue symbols indicate probability distribution of the ^{14}C ages and the green symbols age probability of ^{210}Pb dates. The black dotted lines demonstrate the 1,000 iterations of Bayesian statistic and potential depth ages in a 95% confidence interval. The red line demonstrates the weighted mean ages.

7.5.2 GEOCHEMICAL ANALYSIS

The Fe and Fe/Mn ratio demonstrates dynamic variability in this record. Fe has a general increasing trend (Figure 7.3e) and both datasets show peak values at ca. 2,200, from ca. 1,550 to 1,400 and ca. 800 to 600 cal yr BP. Rising values occur in Fe/Mn from ca. 0 cal yr BP to present and are likely the result of end effects from μ XRF scanning near the core end (Figure 7.3d). Ti shows similar trends as Fe and Fe/Mn with an opposing decreasing trend from 0 cal yr BP to present (Figure 7.3f). A further summary of the μ XRF geochemical results can be found in Appendix IV Figure IV.2.

Carbon and nitrogen percentages show similar trends, while C/N has opposing trends (Figure 7.3a, b & c). C/N (C% and N%) increases (decreases) from ca. 2,400 to 2,100 cal yr BP, followed by a decline (incline) to ca. 1,400 cal yr BP where a sharp peak (trough) occurs. Low (high) stable values occur until 880 cal yr BP where C/N (C% and N%) peaks (dips) rapidly from ca. 880 to 720 cal yr BP. Low (high) stable values resume when C/N (C% and N%) rapidly increases (decreases) at ca. 550 cal yr BP and slowly declines (inclines) until present (Figure 7.3a,b & c).

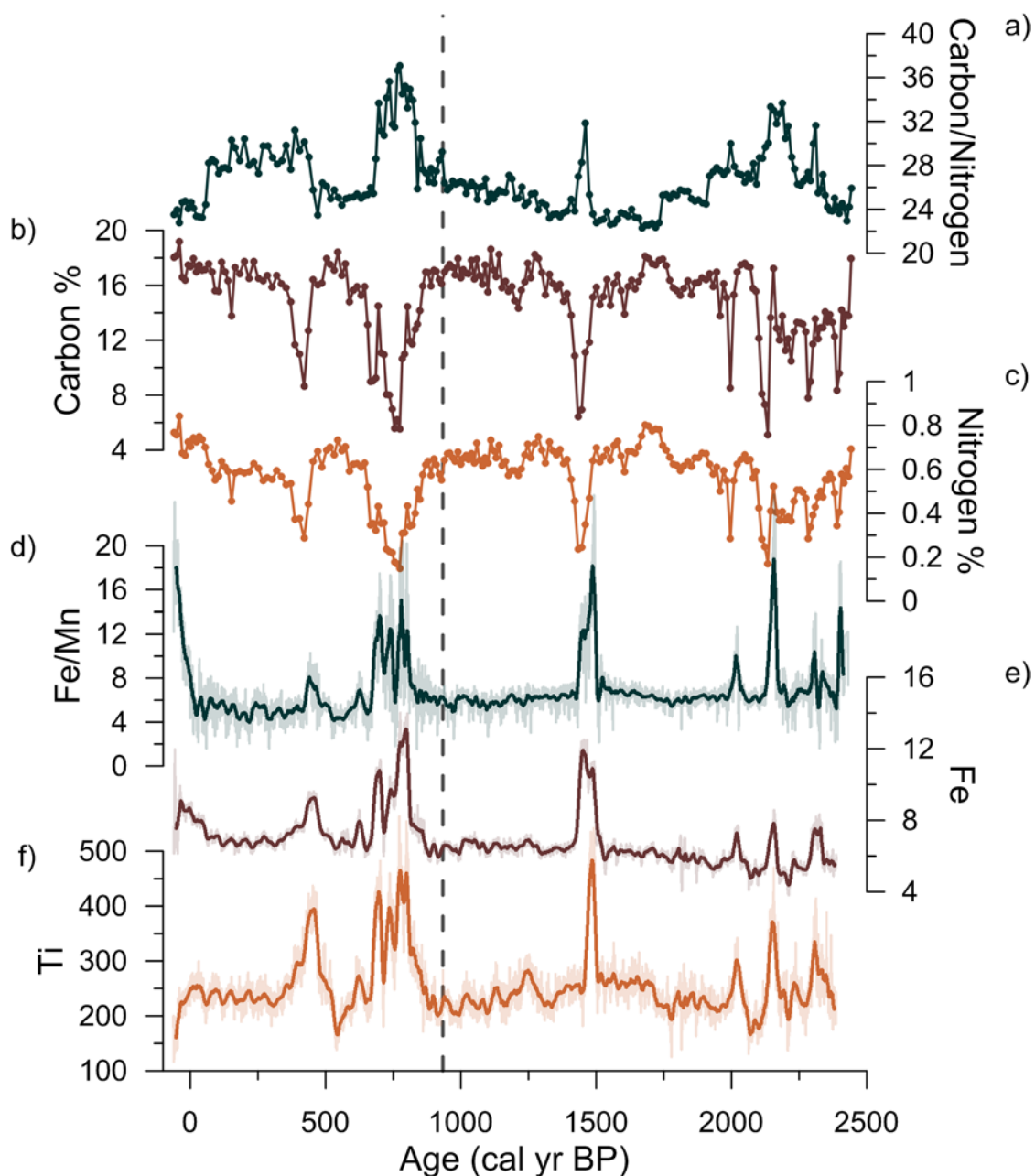


Figure 7.3: A summary of Lake Vera geochemical results of a) Carbon/Nitrogen ratio; b) Carbon percent; c) Nitrogen percent; d) Fe/Mn fit with a weighted average (window width= 51); e) Fe fit with a weighted average (window width= 51); and f) Ti ratios fit with a weighted average (window width= 51). Grey dashed line indicates the non-linear shift in the diatom community.

7.5.3 DIATOM ANALYSIS

Diatoms show good preservation throughout this record with 255 taxa identified from 57 depth samples. Four significant CONISS zones were identified in this record: Zone 1- 2,427 to 1,939 cal yr BP; Zone 2- 1,901 to 880 cal yr BP; Zone 3- 820 to 506 cal yr BP; and Zone 4- 448 cal yr BP to present (Figure 7.4).

Discostella stelligera dominates throughout the sediment record (>20%). In Zone 1 dominant taxa include: *Discostella stelligera* (30-40%), *Achnantheidium minutissimum* (~15%), *Stauroforma exiguiformis* (~5%), *Eunotia incisa* (~5%), *Achnanthes subexigua* (~4%), *Fragilaria capucina* (~4%) and *Gomphonema parvulum* (~3%) with high stability throughout this zone. Within this zone the total diatom valves are high, averaging around 1.6×10^8 valves/mL yr⁻¹. Zone 2 taxa are similar to Zone 1 with the exception of an increase in *Brachysira styriaca* (~4%) and *A. subexigua* (~5-10%), while *Discostella stelligera* (~20%) declines in abundance. In this zone, the total valves remain high, peaking at ca. 1,480 cal yr BP, before declining to the end of the zone. At ca. 920 cal yr BP *A. minutissimum* sharply declines to ~2% abundance.

Zone 3 begins at ca. 820 cal yr BP with low abundance of *A. subexigua* (~1-5%) and *B. styriaca* (~2%); and increased abundance of *D. stelligera* (~40-50%), *Eunotia diodon* (~5%), *Frustulia elongatissima* (~8-10%) and *Gomphonema multiforme* (~4%). Total valves are very low throughout this zone and the next. *D. stelligera* (~20%) begins to decline at ca. 700 cal yr BP through Zone 4 to present. In Zone 4 a slight increase in *A. subexigua* (~5%), *Brevisira arentii* (~1-2%), *B. styriaca* (~4%) and *E. incisa* (~10%) occurs.

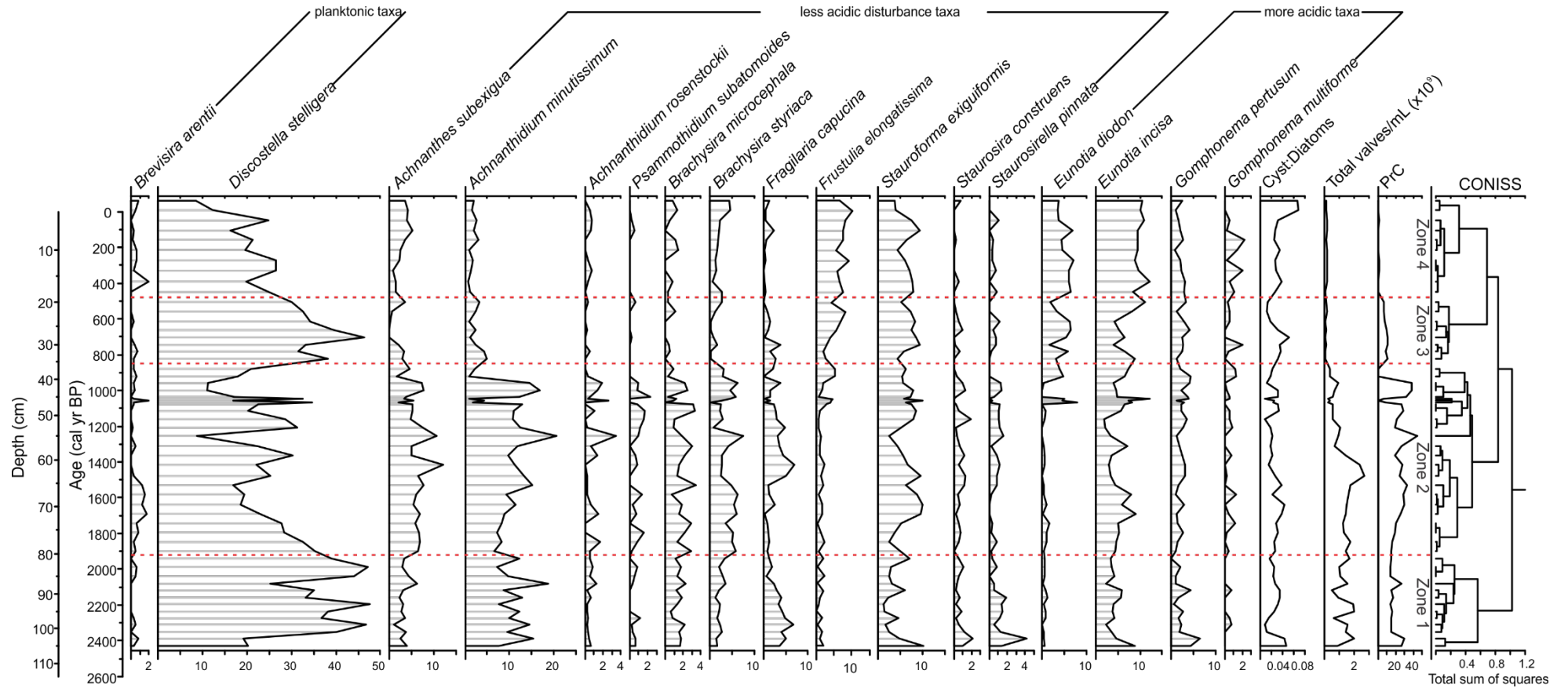


Figure 7.4: Stratigraphy of the important Lake Vera diatom species presented as percentage composition. The PrC estimate trends in the diatom percentage data (PrC explained variance=60.0%). Red dashed lines show breaks in CONISS cluster analysis for the diatoms (four significant zones). X-axis scale varies by taxa.

7.5.4 PALYNOLOGY AND CHARCOAL ANALYSIS

We observe four significant CONISS zones from the percent terrestrial pollen taxa: Zone 4- 2,429 to 2,098 cal yr BP; Zone 3- 2,078 to 802 cal yr BP; Zone 2- 783 cal yr BP to 562 cal yr BP; and Zone 1- 536 cal yr BP to present (Figure 6.5). *Pediastrum* spp. influx has low values from 2,440 to 1,250 cal yr BP followed by an increase to peak at 900 cal yr BP. *Pediastrum* spp. sharply declines with a slight increase and variable influx to present (Figure 7.6d). Total percent ferns remain low from ca. 2,430 cal yr BP until ca. 760 cal yr BP followed by a sharp increase with high variability. Ferns remain high for the remainder of the record with a decreasing trend (Figure 6.6b). Percent disturbance taxa (*Bauera rubioides* and Urticaceae) gradually increase from 2,430 to 880 cal yr BP followed by a decline to ca. 745 cal yr BP. Disturbance taxa then increase in abundance with high variability for the remainder of the record (Figure 6.6a). A pollen stratigraphy summarising the major taxa and compositional transitions are included in Figure 7.5. The charcoal sum z-scores show three time periods of increased charcoal from ca. 2,400 to 2,000 cal yr BP, at ca. 1,500 cal yr BP and from ca. 940 to 660 cal yr BP (Figure 7.6k).

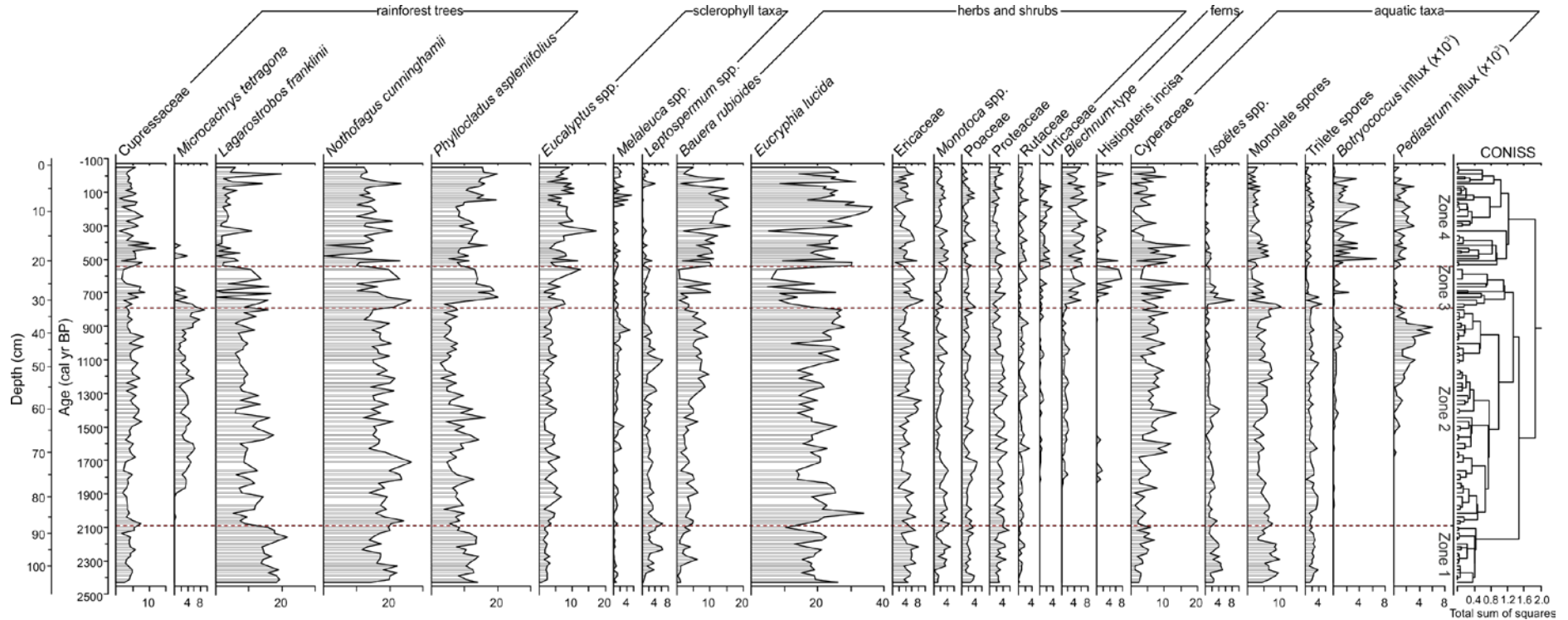


Figure 7.5: Summary stratigraphy of percent terrestrial pollen, ferns and aquatic taxa (x-axis varies) with four significant CONISS.

7.5.5 NUMERICAL ANALYSES

7.5.5.1 Rate-of-Change (ROC)

Diatom ROC is very low (below 0.5) until ca. 1,070 cal yr BP where peak values (3.5) occur until ca. 1,040 cal yr BP. Values decline again to below 0.5 for the remainder of the record (Figure 7.7a). The pollen ROC remains below 0.5 until ca. 780 cal yr BP then increases to 2.9 and becomes highly variable until present (Figure 7.7e).

7.5.5.2 Principal curves (PrC) and Generalised Additive Models (GAMs)

The PrC has an explained variance of 60.0% for diatoms and 60.7% for the terrestrial pollen. Low values of the diatom PrC are associated with more acidic taxa and high values with less acidic disturbance taxa. The diatom PrC is fairly stable with a slight declining trend from ca. 2,430 to 1,900 cal yr BP followed by a rapid increase with high variability until ca. 880 cal yr BP. From ca. 820 cal yr BP to present, the diatom PrC slowly declines with low stable values (Figure 7.7c). The pollen PrC, however, has a decreasing trend throughout the record, with abrupt increase and high variability from ca. 750 cal yr BP to present (Figure 7.7g). Low pollen PrC values are associated with disturbance taxa, middle values with wet rainforest taxa, and high values with low canopy cover taxa (*Ericaceae*, *Pomaderris* spp., *Proteaceae*, *Poaceae*). Species abundance gradients for both the diatoms and terrestrial pollen PrC are included in Appendix IV (See Figures IV.4 & IV.6).

The diatom fitted GAM declines from ca. 2,430 to 1,940 cal yr BP and increases to peak at ca. 1,450 cal yr BP then declines to low stable values from ca. 500 cal yr BP to present (Figure 7.7c). The variance of the diatom GAM residuals demonstrates a slight decline from ca. 2,430 to 1,780 cal yr BP followed by an increasing trend peaking at ca. 1,070 cal yr BP and declining to low values from ca. 500 cal yr BP to present (Figure 7.7b). The pollen GAM demonstrates a linear decreasing model through the PrC (Figure 7.7g). The variance of the pollen GAM increases and plateaus between ca. 1,850 and 1,450 cal yr BP, followed by a decline. The

pollen variance starts to rapidly increase at ca. 820 cal yr BP, peaking at ca. 490 cal yr BP followed by a gentle decline. The variance increases slightly from ca. 60 cal yr BP to present (Figure 7.7f).

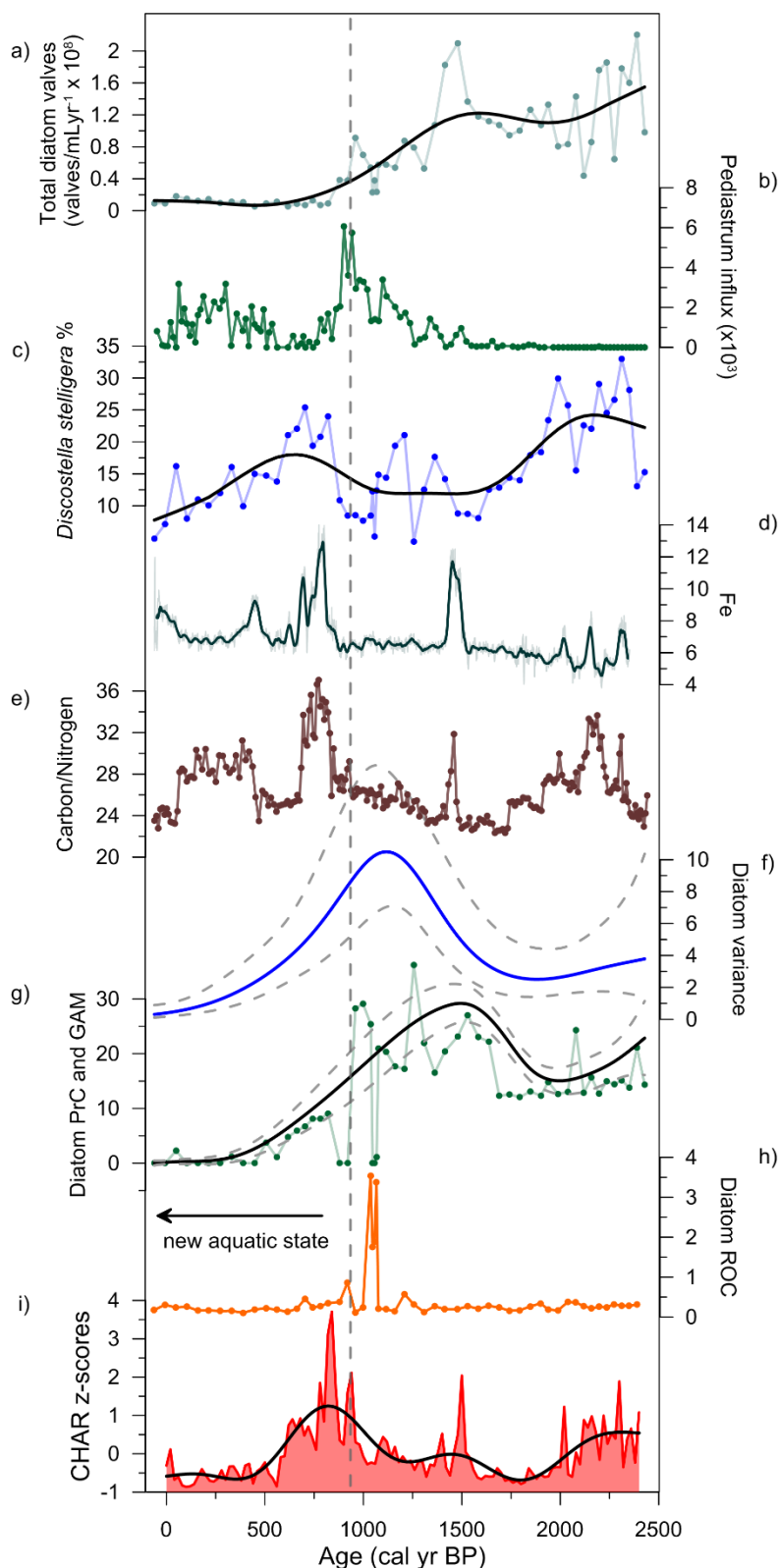


Figure 7.6: A summary plot of Lake Vera data. a) percent disturbance pollen taxa (*Urticaceae* and *Bauera rubioides*) (brown); b) total percent fern pollen taxa (orange); c) total diatom valves (valves/mL $\times 10^8$) (light green) fitted with a fitted GAM (black); d) *Pediastrum* spp. influx ($\times 10^3$) (green); e) *Discostella stelligera* percentages (blue) with a fitted GAM (black); f) Fe/Mn ratios (grey $\times 10^3$) fitted with a weighted average in black (window width= 33); g) Carbon/Nitrogen ratio (brown); h) diatom variance (blue) and confidence interval (grey dashed) of GAM residuals; i) diatom PrC (green) with fitted GAM (black) and confidence intervals (grey dashed); j) diatom ROC (orange); and k) charcoal sum z-scores (red) with a fitted GAM (black). Grey dotted line indicates the timing of the non-linear shift.

7.6 DISCUSSION

7.6.1 FIRE-DRIVEN CHANGES IN AQUATIC ECOSYSTEM DYNAMICS

The pivotal role of fire in the terrestrial ecology of western Tasmania is well understood (Jackson, 1968; Bowman et al., 2009a; Fletcher et al., 2014a), yet little is known about how fire-driven vegetation change influences aquatic ecosystems within this landscape. The deep organic soils that form under rainforest vegetation in this region are highly combustible when dry (Pemberton, 1988, 1989; di Folco et al., 2013). Indeed, fires within the rainforest only occur under anomalously dry conditions (Styger et al., 2015), and the substantial available biomass in these systems often results in high intensity forest fires that can completely incinerate the underlying organic soil profiles. Subsequent rainfall events can strip the soil profile from the landscape (Jackson, 1968; Bowman et al., 1981; Pemberton, 1988, 1989; di Folco et al., 2013), depositing large amounts of terrestrially-derived material into aquatic systems (Pemberton, 1988). Further, burning of the catchment organic soil profile causes a release of organically bound Fe into watersheds increasing preserved Fe in sediments (Korhola et al., 1996; Ketterings et al., 2000).

During this relatively stable diatom community from ca. 2,430 to 960 cal yr BP (Figure 7.6h & i), the relative importance of disturbance diatom taxa, i.e. *Achnantheidium minutissimum*, *Achnanthes subexigua*, *Achnantheidium rosenstockii*, *Psammothidium subatomoides*, *Brachysira styriaca*, *B. microcephala*, *Fragilaria capucina*, *Staurosira construens*, and *Staurosirella pinnata* (Figures 7.4 & 7.6i) are consistent with the effects of fire-related increases in terrestrial organic matter inputs into the lake (Hodgson et al., 1996; Saunders et al., 2013b). Damage to terrestrial vegetation by fire can destabilise soil profiles, resulting in erosion of terrestrial organic material (C/N; Figure 7.6g) and inorganic (Ti; Figure 7.3f) material into lakes that favours disturbance diatom. Additionally, increased ash deposition can increase the base cation content buffering lake pH, also favouring these less acidic diatom taxa (Korhola et al., 1996; Haberle et al., 2006).

While a series of fire events within the rainforest-dominant Lake Vera catchment (ca. 2,200, 1,500 and 800 cal yr BP) initially failed to provoke a shift in the pollen record (Figures 7.6a,b & 7.7g,h), these fire events are associated with an influx of terrestrially-derived carbon (Figure 7.6g), increases in the importance of the diatom *Discostella stelligera* (Figure 7.6e) and changes in other sediment geochemical properties (such as an increase in Ti and Fe/Mn; Figures 7.3f & d). Increased input of terrestrial material into lakes can result in less light penetration, less oxic conditions resulting from less stratification, and anoxic lake bottom waters (Carignan et al., 1988; Cohen, 2003; Koinig et al., 2003; Augustinus et al., 2012). *Discostella stelligera* (Figure 7.6e) is a planktonic diatom taxon with broad ecological tolerances that is favoured by relatively shallow mixing depths and increased nutrient availability (Korhola et al., 1996; Saros et al., 2012; Saros et al., 2015). At Lake Vera, lower lake levels would increase the relative abundance of planktonic diatoms. Additionally, increased input of terrestrial material, such as humics, can cause less light penetration into the upper water column, altering the thermocline and shallowing the lake mixing depth favouring *D. stelligera* (Figure 7.6e) (Steane et al., 1982; Carpenter et al., 1997; Bergström et al., 2000). We, thus, interpret our data as reflecting a lower lake levels and lower lake mixing depth resulting from a drier climate and less light availability following fire-driven influxes of organic matter into Lake Vera (Fee et al., 1996; Korhola et al., 1996).

A sudden diatom compositional shift occurs at ca. 880 cal yr BP (Figures 7.4 & IV.7): from the less acidophilus disturbance community to a more acidophilus oligotrophic community (i.e. *Brevisira arentii*, *Eunotia diodon*, *Eunotia incisa*, *Eunotia* spp., *Frustulia elongatissima*, *Gomphonema multiforme* and *Cocconeis placentula*) (Bradbury, 1986; Vyverman et al., 1995; Hodgson et al., 1996; Vyverman et al., 1996; Hodgson et al., 2000). This diatom shift is preceded by a decline in diatom productivity (Figure 7.6c), low charcoal deposition (low fire activity; Figure 7.6k), decreased terrestrial carbon input into the lake (Figure 7.6g) and an increase in *Pediastrum* influx (at ca. 1,420 cal yr BP; Figure 7.6d), a freshwater algae found in the littoral zones of clear oligotrophic acidic lakes (Weckström et al., 2010). These trends suggest a prolonged low fire period (between ca. 1,460 to 960 cal yr BP) and an associated reduction in terrestrial material inputs

(organic soil products and ash) into Lake Vera that led to clearer and more oligotrophic waters, lower diatom productivity and increased acidification of the lake (Figure 7.6i).

The remainder of the sequence is characterised by the decline in disturbance taxa (*A. minutissimum* and *F. capucina*) and a persistence of an oligotrophic/acidophilus diatom community (*E. diodon*, *E. incisa*, *F. elongatissima* and *G. multiforme*; Figure 7.4). While a fire event at ca. 960 cal yr BP drove an increase in terrestrially derived carbon, Fe/Mn and *D. stelligera*, the remaining diatom community appears complacent throughout the sequence to present (Figure 7.7c). The apparent permanence of this shift through the remaining ca. 920 years, despite fire activity until ca. 560 cal yr BP and indicators of input of terrestrially derived material into the lake, reveals a remarkably stable diatom community through this time (Figure 7.7b & c). The previous prolonged period of low fire likely drove the aquatic system to low productivity and oligotrophy where removed terrestrial soils by fire, declined inputs of important nutrients and organic matter into the lake. This shift would not easily be reversed with further fire disturbance, and thus, later disturbance does not return the system to its previous alkaline disturbed state.

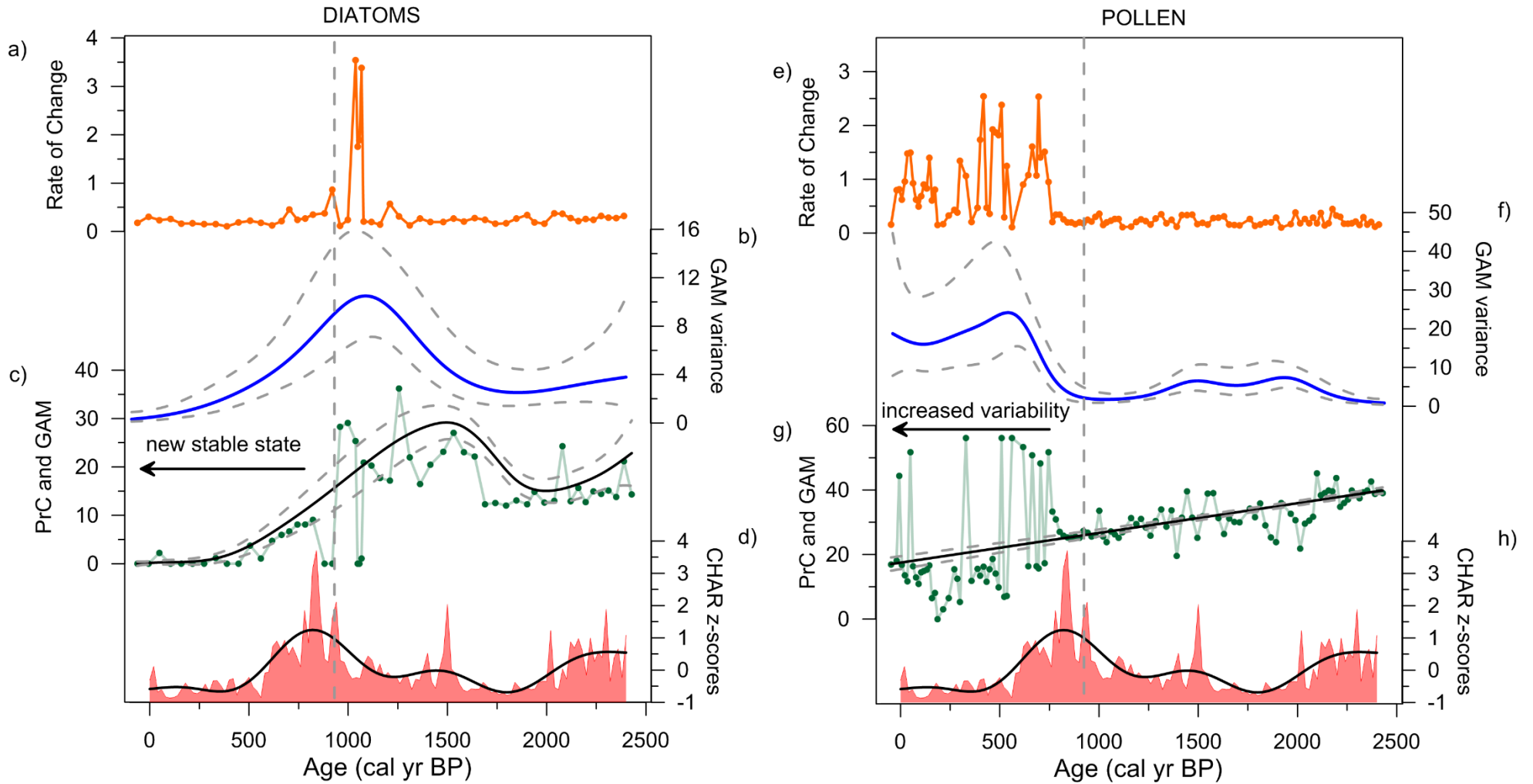


Figure 7.7: Early warning signals statistical summary of the Lake Vera diatoms (left) and pollen (right) including: a and e) ROC (orange); b and f) GAM fitted variance (blue) and confidence intervals (grey dashed line); c and g) PrC (green) fitted GAM (black) and confidence intervals (grey dashed); d and h) charcoal (CHAR in red) sum z-scores and fitted GAM (black). Vertical grey dashed lines indicate the timing of the diatom non-linear shift.

7.6.2 CRITICAL TRANSITIONS AND EARLY WARNING SIGNALS

7.6.2.1 The Aquatic System

We observe a non-linear diatom community shift at ca. 920 cal yr BP that we interpret as a response to the cumulative effect of fire-driven perturbations within the local catchment (Figures 7.6, 7.7 & IV.7). This shift affords us the opportunity to test for the presence of EWS of a potential critical transition in our data. Given the potential problems associated with data manipulation (i.e. interpolation), we focus on two measurements of ecosystem resilience considered robust for palaeoecological data: variance and ROC (Lim et al., 2011; Scheffer et al., 2012; Siteur et al., 2016). Ecological theory on critical transitions predicts that increased variance occurs as a system approaches a critical transition (Scheffer et al., 2009; Scheffer et al., 2012). While ROC is a measure of how rapidly a system state deviates from a stable steady state in response to a perturbation or a change in external conditions; with critical transitions, ROC increases when a system is unable to cope with the rapid changes (i.e. above some critical ROC threshold) and recovery slows (Scheffer et al., 2009; Lim et al., 2011; Dakos et al., 2012; Scheffer et al., 2012; Siteur et al., 2016).

At Lake Vera, fire-driven changes in the delivery of terrestrially derived organic and inorganic sediment into the lake had a profound influence on lake conditions and diatom community structure through the last ca. 2,400 years. These are manifest as shifts in lake water trophic status, pH, turbidity and mixing conditions that drove clear changes in diatom community dynamics. Importantly, we observe a clear increase in ecosystem variance between ca. 1,780 to 1,070 cal yr BP in response to this suite of changes and prior to the non-linear shift in the diatom community (Figure 7.6h & 7.7b). Further, we observe a marked decrease in variance of the new diatom community, suggesting a shift to a more resilient stable state, consistent with ecological theory, indicating that variance, as a measurable EWS in this system, is suggesting a critical transition (Carpenter et al., 2006; Scheffer et al., 2009; Dakos et al., 2012; Scheffer et al., 2012).

Further, we observe a marked increase in the ROC in the diatom community between ca. 1,070 to 1,040 cal yr BP (Figures 7.6j & 7.7a), reflecting rapid shifts in the system state away from equilibrium as it becomes unstable and potentially close to a bifurcation point. The shift to low ROC values following the non-linear shift suggests a potential critical transition to a new stable diatom community state, consistent with the reduction in variance. These results suggest that variance and ROC are potentially useful EWS metrics for detecting potential critical transitions in this aquatic system and that monitoring programs designed to detect potential critical transitions might benefit from measuring these variables. We conclude that the resilience of the diatom community was likely eroded by the cumulative influence of fire-driven catchment disturbance (principally via terrestrial organic matter inputs) on lake water trophic status, pH, turbidity and mixing conditions. While the diatom non-linear shift occurs in concert with a fire-driven influx of terrestrial organic matter, the fact that both variance and ROC increase through a phase of low catchment fire activity and low terrestrial matter influx (ca. 1,400 to 900 cal yr BP) implies that the loss of resilience of this system occurred in response to the cumulative effect of repeated fire events and changes within the catchment, rather than in response to a discrete event.

7.6.2.2 The Terrestrial System

Despite marked changes in the Lake Vera aquatic ecosystem driven by burning of the local catchment, the pollen from Lake Vera show a degree of complacency to fire (Figures 7.5 & 7.7 e-h). Indeed, the pollen PrC values remain remarkably stable between 2,430 to 800 cal yr BP, despite clear fire-driven disturbance of the local catchment (Figure 7.6a, b & k). This complacency to fire of the local rainforest stand contrasts the hyper-sensitivity displayed by rainforest to fire in this landscape (Chapter 4; Kirkpatrick et al., 1980; Bowman et al., 1981; Fletcher et al., 2014a). It is important to note that the source area airborne pollen into a lake is often considerably larger than the local lake catchment (Prentice, 1978; Sugita, 1993; Bunting et al., 2004). Consequently, the apparent complacency of the vegetation system to fire might reflect the discrepancy between

the size of burnt catchment area relative to the pollen source area (i.e. an insensitivity of pollen data to the scale of fire events and associated vegetation change, Figures 7.6a, b & 7.7g).

Importantly, we do observe a marked shift in variance and ROC of the pollen assemblage following the fire event that occurred at ca. 840 cal yr BP (Figure 7.7e-h), suggesting lost resilience within the local rainforest. The fire event at ca. 840 cal yr BP is associated with an increase in forest taxa found of disturbance (*Urticaceae* and *Bauera rubioides*; Figures 7.5 & 7.6a), ground ferns favoured by increased light penetration through a forest canopy (e.g. *Blechnum* spp.; Figures 7.5 & 7.6b) (Saldaña et al., 2010) and a sustained increase in *Eucalyptus* (Figure 7.5), a plant with highly flammable foliage that can alter local fire regimes and effectively out compete fire-sensitive rainforest vegetation (Bowman, 1998, 2000; Wood et al., 2012; Fletcher et al., 2014a; Fletcher et al., 2014b). We interpret this suite of changes in the terrestrial system as reflecting the cumulative effect of repeated fires on the resilience of this rainforest system via an opening of the canopy and an invasion by fire promoting species, thus, increasing the probability of future burning and the localised rainforest extinction (sensu Fletcher et al., 2014a; Fletcher et al., 2014b). If the non-linear shift in the diatoms is, in fact, a critical transition, the evidence for an increase in both variance and ROC of the vegetation, then, demonstrates the potential of these metrics as EWS for the rainforest system around Lake Vera. Importantly, this implies that these EWS metrics might be relevant and measurable indicators across a range of natural systems.

7.7 CONCLUSION

The diatom community demonstrates a non-linear shift from less acidic disturbance taxa to more oligotrophic acidic taxa at ca. 920 cal yr BP due to the cumulative effects of fire-driven changes in the amount and type of terrestrial material deposited into the lake system. This shift is preceded by measurable EWS: increased system state variability and ROC. The new diatom state displays less variability and a complacency to continued catchment disturbance by fire, suggesting a shift to a more resilient stable state. The terrestrial vegetation, on the other hand, appears complacent to repeated burning through the early part of the record, with a marked increase in

variability and ROC following the diatom state shift suggesting that this system may be approaching a critical transition. We conclude that (1) the diatom community is highly sensitive to fire-driven terrestrial ecosystem change; (2) that system state variance and ROC are useful EWS of aquatic and terrestrial ecosystem change; and (3) these metrics have the potential as EWS across a range of natural systems.

7.8 ACKNOWLEDGMENTS

The financial support of this project comes from the Australian Research Council (award: #DI110100019 and IN140100050) and Australian Institute of Nuclear Science and Engineering (award: ALNGRA12003P). Gavin L. Simpson was supported by the Natural Sciences and Engineering Research Council of Canada's Discovery Grant Program. We would like to thank Tasmania National Parks and Wildlife Service and the Tasmanian Aboriginal community for their support and allowing us to work on their lands. We would also like to thank Michela Mariani, Anthony Romano, Coralie Tate, and Valentina Vanghi for their assistance in the field. We would like to acknowledge Brent Wolfe and his laboratory from Wilfrid Laurier, Guelph, Canada for their isotopic analysis and interpretation assistance. The data presented is listed in the tables, references, and supplements, as well as, publicly available on Neotoma (<https://www.neotomadb.org/>) upon date of publication. We also thank two anonymous referees for their helpful comments on a previous draft.

Appendix IV contains supporting information.

CHAPTER 8: SYNTHESIS

8.1 CHAPTER AIMS

The aim of this chapter is to synthesise the findings presented in this thesis and address the research questions and broader significance of this work. A critique of this research will also be presented here, as well as, further gaps.

8.2 CHAPTER INTRODUCTION

The research questions of this thesis are:

1. *How does long-term climatic change influence aquatic ecosystems in Tasmania: directly, indirectly, or both?*
2. *If a direct pathway is evident, what is the principal mechanism influencing the aquatic ecosystem?*
3. *If an indirect pathway is evident, what is the principal mechanism through which terrestrial environmental change influences the aquatic environment?*
4. *How do aquatic ecosystems respond to fire disturbance in western Tasmania?*

Tasmania is an ideal region for understanding the influences of climate on aquatic ecosystems not only because the region is sensitive to climate and fire, but also, the aquatic ecosystems have unique characteristics, such as the oligotrophic/dystrophic nature of the lakes that require nutrients and organic input derived from terrestrial material (Buckney et al., 1973; Steane et al., 1982; Tyler, 1992). The findings from this thesis demonstrate a tightly linked aquatic and terrestrial environment (Chapters 5, 6, & 7), providing an opportunity to measure the mechanisms and processes in which climate indirectly impacts aquatic ecosystems. Though different aquatic proxies were used at each site (diatoms versus cladocerans), this chapter further investigates the generalities

across the differing biogeography (altitude, bathymetry, and vegetation cover) to reveal larger scale patterns in temperate regions.

8.3 AQUATIC ECOSYSTEM RESPONSE TO CLIMATE

HOW DOES LONG-TERM CLIMATIC CHANGE INFLUENCE AQUATIC ECOSYSTEMS IN TASMANIA: DIRECTLY, INDIRECTLY, OR BOTH?

Climate is the key driver of aquatic ecosystem change through complex direct (e.g. change in temperature and precipitation/evaporation balance) and indirect (terrestrial-mediated processes) pathways. Conclusions from discussion chapters reveal that aquatic ecosystems of Tasmania predominantly respond indirectly to climate via vegetation changes driven by hydroclimate (Chapters 5 & 6) and fire (Chapter 7). However, these relationships can be altered or transition from a dominant indirect climate response to a direct response. The findings of this thesis show that (1) the cladoceran community at Paddy's Lake respond indirectly to climate through nutrient cycling driven by vegetation production, where periods of increased productivity provide nutrients to the lake altering trophic status (Chapter 5). (2) Diatoms at Lake Vera respond indirectly to climate through increased peat formation during wet conditions resulting in increased humic acid delivery into the lake driving increased lake acidity. Followed by a shift to direct climate impacts through lake level fluctuations caused by increased climate variability (Chapter 6). To determine if these direct and indirect relationships are in fact occurring at these sites, further interrogation of the timing of these transitions are needed to determine which climate pathways are influencing the aquatic ecosystem. In this section I examine the timing of shifts in the time series data to test my primary hypotheses of direct and indirect climate impacts on aquatic ecosystems. They are as follows: if climate influences both aquatic and terrestrial environments directly, the aquatic ecosystem would respond before or synchronous with the terrestrial environment. In contrast, if the aquatic ecosystem is responding to climate mediated by the terrestrial environment, the terrestrial environment will respond first. Here I address question

No.1 of this thesis by testing the timing of the time series datasets (e.g. pollen, diatoms, C/N, etc.) using the same analyses for Paddy's Lake and Lake Vera of superposed epoch analysis (SEA).

SEA is used to determine significant changes between variables before and after response events (Hegerl et al., 2003; Fule et al., 2009; Dunnette et al., 2014). For this analysis, I used significant shifts in the aquatic ecosystems as response events to determine if trends in the terrestrial environment significantly shift before or after the aquatic ecosystem. The ordination axes from the original analyses, cladoceran DCA axis 1 from Paddy's Lake (Chapter 5) and the diatom PCA axis 1 from Lake Vera (Chapter 6), to summarize the aquatic trends. To identify response events in the aquatic ecosystems significant shifts in these ordinations axes were determined using a sequential t-test analysis of regime shifts (STARS). STARS is a statistical method, using moving t-tests, to define periods of reorganisation in an ecosystem by means of significant shifts in a time series (Rodionov et al., 2005). The regime shift index (RSI) retrieved from STARS provides the date of occurrence and strength of a regime shift for the response events. Before SEA can be performed, all time series data need corresponding sample depths. Pollen and diatom ordinations, μ XRF, CN geochemistry, and charcoal were interpolated in *R v.3.4.1* (R Development Core Team, 2014) using linear methods. Paddy's Lake was interpolated to 100-year intervals and Lake Vera to 50-year intervals using the *rioja v.0.9-15* package (Juggins, 2016) in *R*.

The Paddy's Lake cladoceran DCA axis 1 had five response events determined by significant RSI shifts (p value <0.05) using a window width of 6 (Figure 8.1a). The Lake Vera diatom PCA axis 1 had six events determined by significant RSI events (p value <0.05) using a window width of 20 (Figure 8.2a). The differences in window width between the two lake sites is due to difference in dataset resolution. The response events for Lake Vera were separated into two groups: Pre- 5 ka (6,900 and 9,150 cal yr BP) and Post- 5 ka (2,300, 3,850 and 4,400 cal yr BP) (Figure 8.2a & b) to test the hypothesised direct and indirect periods of the record from Chapter 6. The final response event (ca. 1 ka) was excluded from the analysis because it is a known non-linear shift driven by different mechanisms than the direct period i.e. fire disturbance (Chapter 7).

At Paddy's Lake vegetation productivity and composition significantly shift ($p < 0.05$) before the response events in the cladocerans (Figure 8.1). Pollen DCA axis 2 significantly shifts ($p < 0.01$) at -100 lag years and pollen AR significantly shifts at -500 and -200 lag years ($p < 0.05$) and 100 lag years ($p < 0.01$) (Figure 8.1b & c). At Lake Vera, the terrestrial indicators significantly shift ($p < 0.05$) before the diatom response events Pre- 5 ka (Figure 8.2 b-d). $\delta^{15}\text{N}$ significantly shifts from -350 to -250 lag years, Pollen PCA 1 shifts at -100 lag years, and Fe/Mn shifts from -400 to -300, -200, -100 to -50, 150, and 350 to 400 lag years. Post- 5 ka (with the exception of the most recent event), the diatom response events occur before significant changes in the terrestrial environment ($p < 0.05$) (Figure 8.2 e-g). The $\delta^{15}\text{N}$ significantly shifts at 50, 100 and 350 lag years, Fe/Mn shows a shift at 250 lag years, and Pollen PCA axis 1 shifts from 200 to 250 lag years but is not significant (Figure 8.2 g-j).

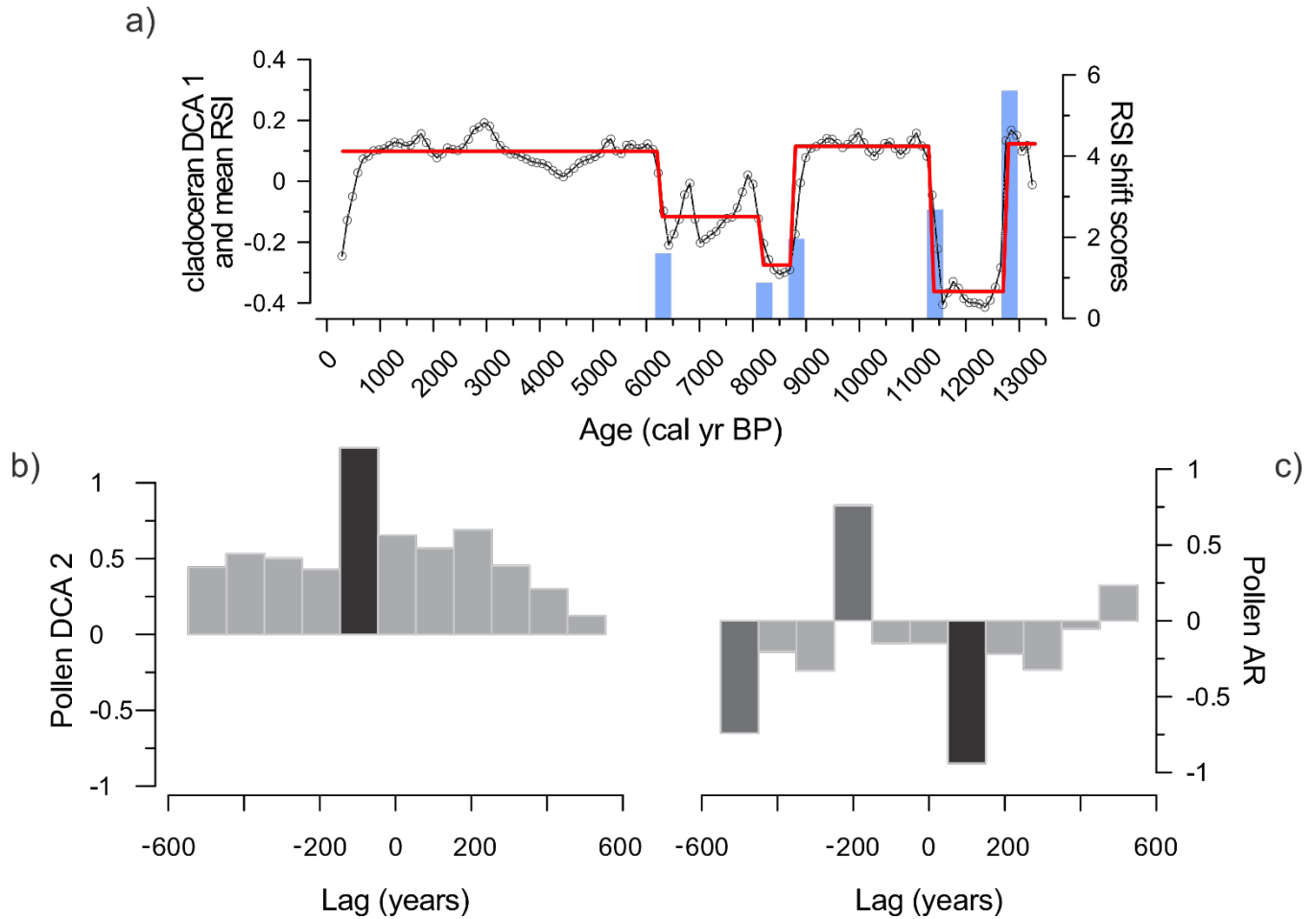


Figure 8.1: Paddy's Lake a) interpolated cladoceran DCA axis 1 scores (blue) with RSI curve (red, window width of 6); b) significant RSI shifts (p -value <0.05). SEA analysis on interpolated Paddy's Lake data for c) pollen DCA axis 2 scores and d) pollen accumulation rate (AR). Dark grey bars represent the significant SEA $p < 0.05$, black bars $p < 0.01$.

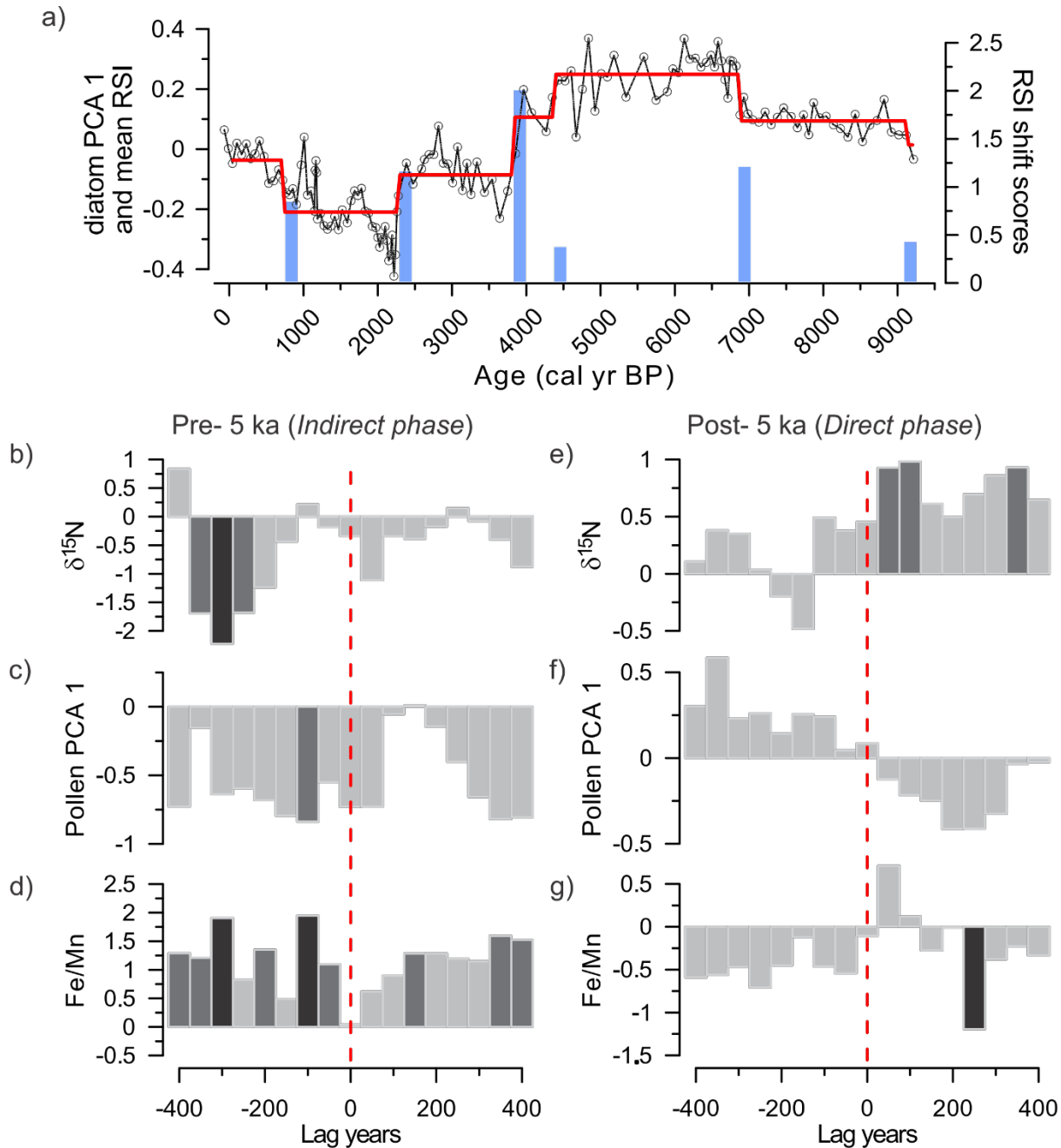


Figure 8.2: Lake Vera a) interpolated diatom PCA axis 1 scores (black) with RSI curve (red, window width of 20) and significant RSI shifts (blue, p -value < 0.05). Grey bar is the response event excluded from the analysis. b-g) SEA analysis on interpolated Lake Vera data split into response events pre 5 ka (right) and post 5 ka (left) for: b & e) $\delta^{15}\text{N}$; c & f) pollen PCA axis 1; and d & g) Fe/Mn. Dark grey bars represent the significant SEA $p < 0.05$, black bars $p < 0.01$.

The results for the SEA analysis confirm Paddy's Lake cladocerans are responding indirectly to climate (Figure 8.1). In this data, there is no evidence for direct influences of climate change on the aquatic ecosystem

(cladocerans) of Paddy's Lake (See extended SEA results Appendix V Figure V.1). The results from the Lake Vera SEA confirm the findings of Chapter 6; that diatoms are responding indirectly to climate Pre 5 ka and shift to a dominant direct influence of climate Post 5 ka (Figure 8.2). Lake Vera shows both the direct and indirect influences of climate during the Holocene (See extended SEA results Appendix V Figure V.2), but why does the pathway change?

IF A DIRECT PATHWAY IS EVIDENT, WHAT IS THE PRINCIPAL MECHANISM INFLUENCING THE AQUATIC ECOSYSTEM?

At ca. 4 ka at Lake Vera an increase in the planktonic diatom community emerges due to a drop in lake level from increased drying. This change in diatom assemblage is the result of bathymetry of Lake Vera where a drop in lake level results in a change in proportional aquatic habitat, i.e. less extensive littoral environment (Figure 6.6). The drop in lake level is a direct climate response caused by a shift in the dominant climatic system and variability.

The shift from low climate variability (i.e. SWW-driven) to high climate variability (i.e. ENSO-driven) caused a change in the climatic pathway influencing the aquatic ecosystem (Chapter 6). Climate variability prior to ENSO was not sufficient enough to alter diatom inferred lake level. The increased variability and frequency of drying events caused by ENSO forced the lake level to drop, possibly beyond a tipping point, resulting in less extensive littoral habitat (Figure 6.6). Though Paddy's Lake shows no evidence of direct influences of climate change, increased drying and fire (from ca. 6.3 to 3.4 ka), caused by the onset of ENSO, did alter the aquatic ecosystem relationship to the terrestrial environment. It appears the aquatic ecosystem remains oligotrophic and more complacent to changes in the terrestrial environment (i.e. terrestrial productivity and changes in ^{14}N), likely due to invasion of sclerophyll taxa resulting in a nutrient-depleted terrestrial and aquatic environment (Section 8.5). This is not an indicator of a direct response of the aquatic ecosystem to climate, rather that more variable climate and fire can alter the aquatic ecosystem response to the terrestrial environment. Therefore, the findings suggest

Tasmanian aquatic ecosystems are predominantly driven by climate indirectly. However, more variable climate and increased frequency of drying (i.e. ENSO) can alter the climate pathways of the aquatic ecosystem or their relationship to the terrestrial environment.

8.4 AQUATIC ECOSYSTEMS, CLIMATE AND CATCHMENT RELATIONSHIPS

IF AN INDIRECT PATHWAY IS EVIDENT, WHAT IS THE PRINCIPAL MECHANISM THROUGH WHICH TERRESTRIAL ENVIRONMENTAL CHANGE INFLUENCES THE AQUATIC ENVIRONMENT?

Aquatic ecosystems that respond indirectly to climate are driven by changes in the terrestrial environment (Battarbee, 2000; Ball et al., 2010; Fritz et al., 2013). For example, changing vegetation composition and productivity influence the surrounding catchment (via soil development, nutrient input, hydrology, and geochemistry) can alter aquatic ecosystem biota, chemistry, and thermal structure (Whitehead et al., 1989; Huvane et al., 1996; Korsman et al., 1998; Engstrom et al., 2000; Fritz et al., 2013). Although there is evidence of indirect climate influences on aquatic ecosystems, the mechanisms of these interactions are not well understood. Conclusions from this thesis and the above section (Section 8.3) reveal Tasmanian aquatic ecosystems are primarily indirectly driven by climate.

Western Tasmania is blanketed in acidic organic peats derived from terrestrial biomass (Tyler, 1974; Brown et al., 1982a; di Folco, 2007). In cool temperate regions peat accumulation is rapid due to slow decomposition rather than high primary productivity (Moore, 2002). In western Tasmania, these peaty organic soils of the terrestrial environment (Buckney et al., 1973; Steane et al., 1982) increase humic acid delivery (allochthonous carbon sources) into aquatic environments, important to nutrient delivery and local lake water chemistry (Gorham, 1961; Buckney et al., 1973; Tyler, 1974; Steane et al., 1982; Tyler, 1992). These features cause the dystrophic nature of these lakes (Hansen, 1962; Bergström et al., 2000). The climate and geology of Tasmania are the primary cause for the organic rich soils in an oligotrophic (dystrophic) environment (Tyler, 1974, 1992), similar biogeography is

found in temperate regions worldwide (Hansen, 1962; Steinberg, 2003b). Thus, climate driven vegetation-soil dynamics can alter lake physiology, such as: lake acidity, mixing regimes, and nutrient delivery (Chapters 5, 6, & 7).

Vegetation development in western Tasmania following deglaciation produced organic peats atop inert bedrock providing almost all the total dissolved solids and conductivity to water bodies (Buckney et al., 1973; Tyler, 1974; Macphail, 1979; di Folco, 2007). Following deglaciation, natural succession of rainforest vegetation (Macphail, 1979; Fletcher et al., in review), produces organic acidic peat soils high in humic acid (Round, 1957; Jackson, 1968; Tolonen, 1980; Jones et al., 1989; Tyler, 1992; Vanhoutte et al., 2004; di Folco, 2007; Kokfelt et al., 2010; Wood et al., 2012). Vegetation succession and catchment development slowly depleting soils of base cations resulting in lake acidification (Bradbury, 1986; Whitehead et al., 1989; Fritz et al., 2013). Previous work from Lake Vera suggests the aquatic transitions are the result of these successional processes known as lake ontogeny (Bradbury, 1986). Findings from this thesis also show aspects of lake ontogeny, where acidification is caused by the formation of thicker organic acidic peats with rainforest vegetation development (Chapter 6).

There is also evidence that terrestrial inputs from peat environments are important for lake stratification and mixing regimes. Thermocline and mixing depth of a lake can be altered by temperature and factors that alter light penetration (Fee et al., 1996; Schindler et al., 1996; Diehl et al., 2002; Winder et al., 2004; Saros et al., 2012). For example, increases in material that stains the lake cause less light penetration into the upper water column altering thermoclines and shallowing lake mixing depth (Steane et al., 1982; Carpenter et al., 1997; Bergström et al., 2000). Thus, the more dystrophic a lake the shallower the mixing depth. These processes result in increased benthic anoxia (Steane et al., 1982; Whitehead et al., 1989; Davison, 1993; Koinig et al., 2003), evident in Lake Vera (Chapter 6) and Lake Gordon (Steane et al., 1982), suggesting changes in dystrophic conditions could impact lake mixing and aquatic biota.

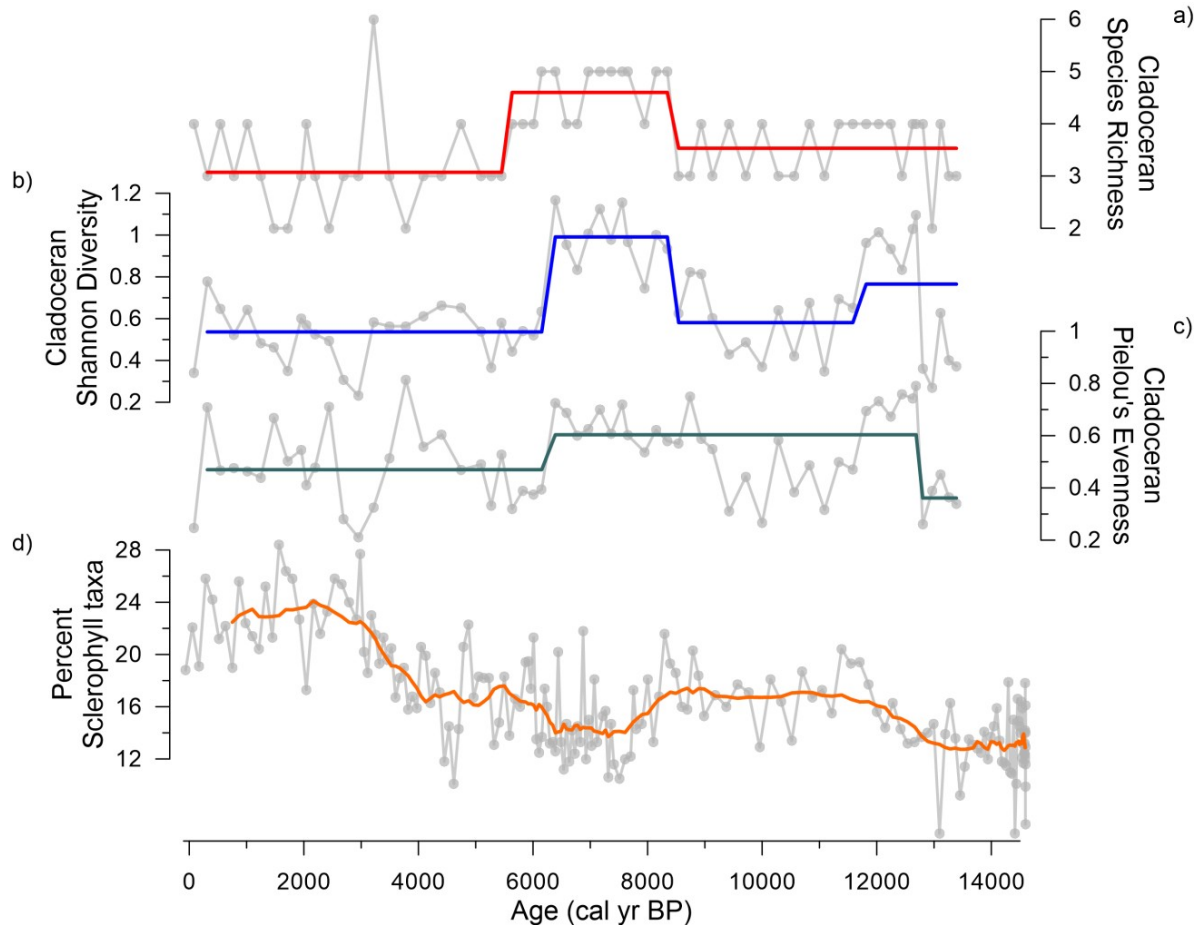


Figure 8.3: Summary figure of Paddy's Lake cladoceran diversity including a) cladoceran species richness with RSI index (red, window width=15); b) cladoceran Shannon diversity with RSI index (red, window width=15); c) cladoceran Pielou's evenness with RSI index (red, window width=15); and d) percent sclerophyll pollen with weighted average (orange, window width=15). Diversity indices were calculated using the package *vegan v.2.4-4* (Oksanen et al., 2016) in R.

Nutrient delivery from the terrestrial environment also impact aquatic ecosystems in Tasmania. Peat soils develop under rainforest vegetation and can increase lake dystrophy, lower light penetration, and lower mixing depth (Steane et al., 1982; Carpenter et al., 1997; Bergström et al., 2000). This will likely lead to increased anoxia and stratification (Steane et al., 1982; Whitehead et al., 1989; Davison, 1993; Koinig et al., 2003) and potential P release from lake sediments (Søndergaard et al., 2001), where iron bound phosphate is reduced and P is released into the water column in anoxic conditions (Nürnberg, 1984, 1988; Søndergaard et al., 2003). In contrast, sclerophyll vegetation are adapted to low nutrient environments and produce nutrient poor litter (Beadle, 1966; Beadle, 1968; Jackson, 1968; Orians et al., 2007; Wood et al., 2011a), and thus, soils with lower nutrient content (Bowman et al., 1986b). This thesis determines sclerophyll depletes the catchment, and thus, aquatic systems of

necessary nutrients (Chapter 5) essential to maximising diversity (Rosenzweig et al., 1993; Güsewell et al., 2005). For example, increased sclerophyll vegetation is associated with declines in the diversity of cladocerans at Paddy's Lake (Figure 8.3). These sclerophyllous taxa are widespread across the world including the North and South America, Europe, Africa, and mainland Australia (Axelrod, 1975; Prentice et al., 1992; Bowman, 2000; Crisp et al., 2009). Therefore, other aquatic ecosystems may be at risk of nutrient loss and decline in diversity with increasing distribution of sclerophyll vegetation caused by fire and climate change. These terrestrial-aquatic relationships are likely not restricted to western Tasmania, but widespread across other dystrophic environments in temperate regions that share similar terrestrial-aquatic ecosystem dynamics (Hansen, 1962; van Dam et al., 1981; Wetzel, 1992; Joniak et al., 1999; Bergström et al., 2000).

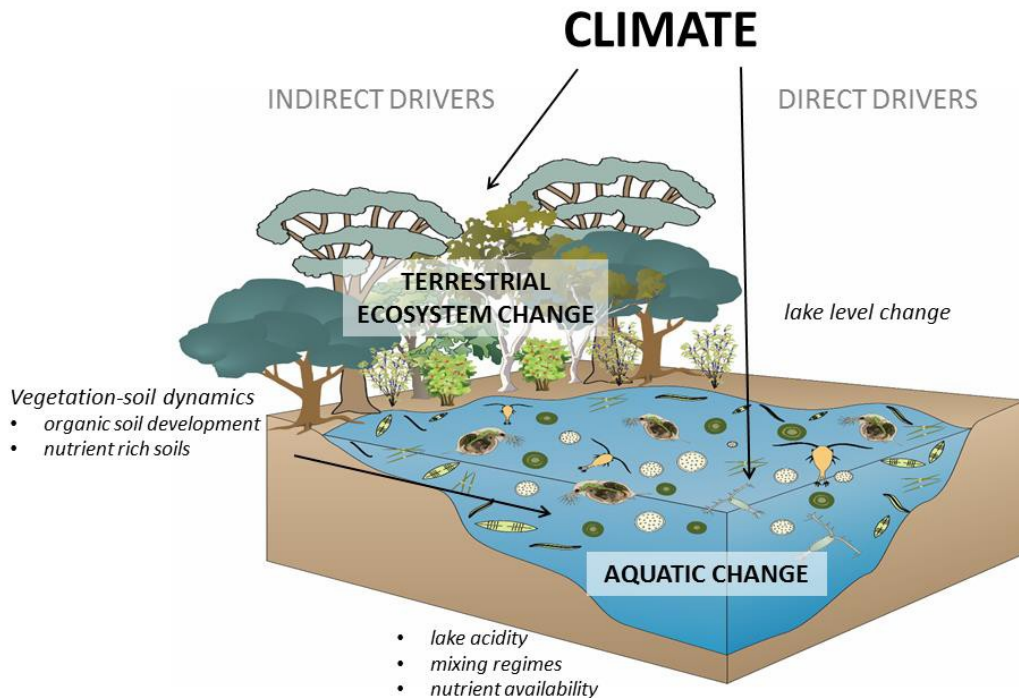


Figure 8.4: Revised Figure 1.1 schematic of the climate influences on aquatic ecosystem to highlight the important pathways determined by this thesis.

8.5 AQUATIC ECOSYSTEMS AND FIRE DISTURBANCE

HOW DO AQUATIC ECOSYSTEMS RESPOND TO FIRE DISTURBANCE IN WESTERN TASMANIA?

Tasmanian fire-vegetation-soil dynamics are well understood (Jackson, 1968; Macphail, 1979; Brown et al., 1982a; Kirkpatrick et al., 1984; Bowman et al., 1986b; Colhoun et al., 1999; Macphail et al., 1999; Wood et al., 2012; Fletcher et al., 2014a). However, impacts of fire on aquatic ecosystems are largely overlooked in fire-sensitive environments. More importantly, fire is predicted to increase in frequency in Tasmania and other arid regions of the world with anthropogenic climate change (Hennessy et al., 2005; Krawchuk et al., 2009; Bradstock, 2010; Fox-Hughes et al., 2014; Holz et al., 2015).

This thesis has revealed aquatic ecosystems are impacted by fire can alter available lake nutrients. While fire can initially mobilise nutrients (N and P) from soils (Kirkpatrick et al., 1984; Leys et al., 2016), the removal of organic soils and biomass caused by fire result in a loss of long-term available nutrients (Dunnette et al., 2014; Morris et al., 2015). There is also evidence that nutrient pulses caused by fire cannot be fully exploited by aquatic organisms due to corresponding inputs of inorganic material affecting light availability (Brown, 2016). In western Tasmania, the role of fire over vegetation structure alters available nutrients, where sclerophyll vegetation lower nutrient availability and organic soil thickness (Bowman et al., 1986b; Bradstock, 2010; Murphy et al., 2010) and thus aquatic ecosystem trophic status. Predictions of increased wildfire with climate change, will increase the extent sclerophyll vegetation and likely deplete lake systems of essential nutrients. In places like Tasmania where aquatic ecosystems are already highly oligotrophic it is uncertain what effect further nutrient depletion will have on these oligotrophic ecosystems.

Increased fire activity can also impact aquatic ecosystems through increased water pH and potentially lower mixing depth. Ash deposition increases the base cation lake content (Korhola et al., 1996; Korsman et al., 1998), buffering acidity and increasing the abundance of alkaline diatom taxa (Chapter 7). Further, fire releases

terrestrial and inorganic material from the catchment (Ti and C/N), as well as, Fe, common in burnt soils (Kutiel et al., 1993; Korhola et al., 1996; Ketterings et al., 2000; González-Pérez et al., 2004; di Folco et al., 2011). Deposition of terrestrial and inorganic material may result in lower light availability and favour taxa with lower mixing depth preferences, i.e. *Discostella stelligera* (Chapter 6) (Saros et al., 2012; Saros et al., 2015). As well, decreasing light penetration may prevent proliferation of aquatic taxa, and thus, the uptake of available nutrients (Brown, 2016). I hypothesise increases in organic and inorganic deposition from fire disturbance cause decreases in light penetration, shallowing of lake mixing depths, and favours *D. stelligera*. These effects of fire on mixing depth may be more widespread across fire impacted environments.

The cumulative effects of fire can stress an aquatic ecosystem and potentially result in a non-linear shift (Chapter 7). Though this is the first representation of fire causing a critical transition in aquatic ecosystems, terrestrial derived inputs of DOC have caused a critical transition in aquatic ecosystems (Carpenter et al., 1997). In extreme cases, sudden and abrupt ecosystem state shifts, that are largely unpredictable, can have major implications for ecosystem function (Scheffer et al., 2001; Scheffer et al., 2003; Scheffer et al., 2009; Scheffer et al., 2012; Wang et al., 2012).

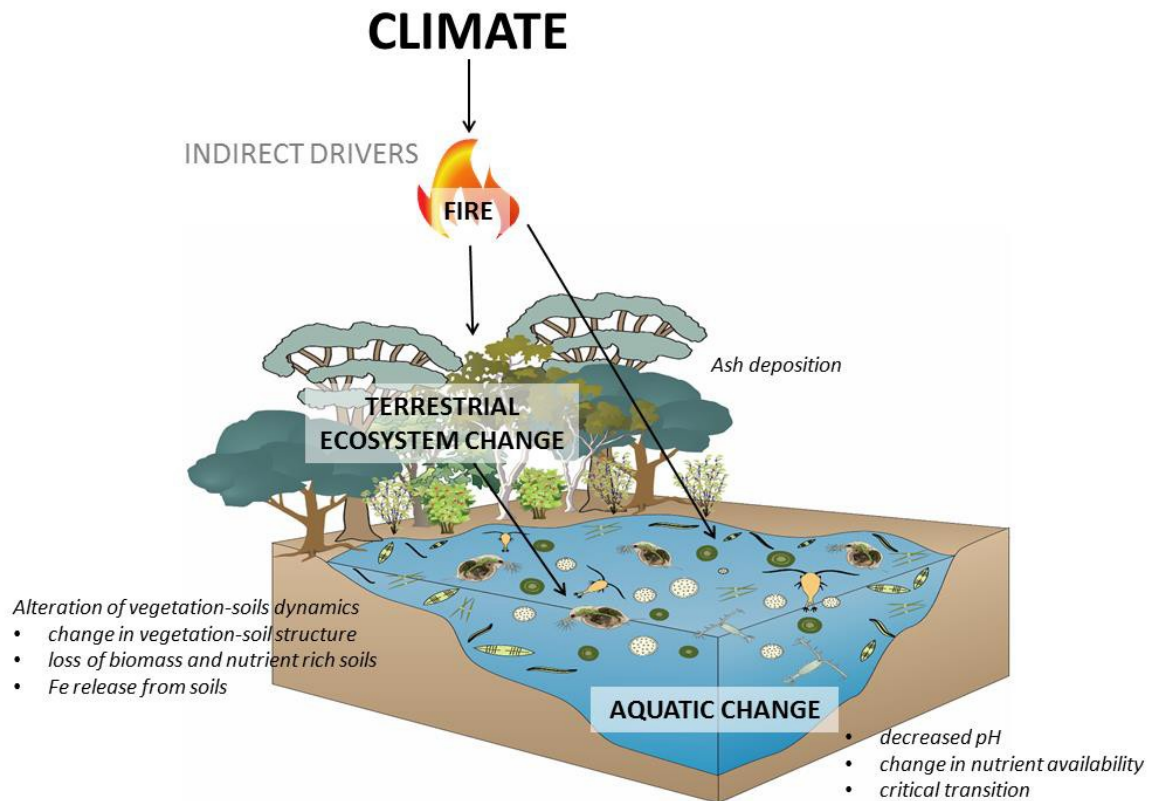


Figure 8.5: Revised Figure 1.1 schematic highlighting fire influences on an aquatic ecosystem.

8.6 CRITIQUE AND UNRESOLVED GAPS

The findings from this thesis were determined using different sites in different regions (Paddy's Lake, Black Bluff north west Tasmania and Lake Vera, Frenchman's Cap, western Tasmania) with two different aquatic indicators (cladocerans and diatoms). It is possible these differing climate impacts on aquatic ecosystem response are manifest from the different aquatic proxies used (diatoms versus cladocerans). As well, local site geography (altitude, bathymetry, vegetation cover) may determine, to some extent, the different terrestrial pathways influencing the aquatic ecosystems. Though, what is apparent, and the key aim of this thesis, is that both lakes are responding indirectly to climate through the tightly couple vegetation-soil dynamics regardless of aquatic indicator.

One major drawback to working with aquatic ecosystems in Tasmania is that aquatic taxonomy and ecology is limited. There is still a reliance on Northern Hemisphere taxonomy for interpreting palaeolimnological records even though there is likely more endemism in this region (Tyler, 1996; Vyverman et al., 2007; Vanormelingen et al., 2008). Tasmanian taxonomy and ecology of diatoms (Vyverman et al., 1995; Vyverman et al., 1996; Sabbe et al., 2001; Kilroy et al., 2003; Kociolek et al., 2004; Vanhoutte et al., 2004) and zooplankton (Shiel et al., 1995; Shiel, 1995; Walsh et al., 2001; Walsh et al., 2004) has had some attention. However, taxonomy is constantly being updated with new endemic taxa. Therefore, there is a need for updated ecological determinations for newly named species and determine ecological gradients of taxa.

One particular troubling diatom genus is *Discostella*. The taxonomy and ecology of this species is not well determined in Tasmania (Haworth et al., 1993; Vyverman et al., 1995; Vyverman et al., 1996) and is further problematic worldwide (Rühland et al., 2008; Saros et al., 2012; Fritz et al., 2013; Saros et al., 2014; Rühland et al., 2015; Saros et al., 2015; Perren et al., 2017). Abundant fossil evidence of this genus was found in Lake Vera with slight variations in the morphology (See Diatom Plate in Appendix VI). The limited resources made for unconvincing identification even following assistance from the expert community (pers. comm. W. Vyverman, J. Tibby, P. Gell, K. Saunders, and P. Tyler). Advice from these experts recommended lumping these species as *Discostella stelligera* because the ecology of *Cyclotella sensu lato* is fairly uniform, with broad ecological tolerances and some affinity for increased nutrients and lower mixing depth (Saros et al., 2012; Saros et al., 2014; Saros et al., 2015; Perren et al., 2017). While evidence from the CCA analysis in Chapter 6 (Figure 6.7) suggests *D. stelligera* is associated with Ca and *Lagarostrobos franklinii*, it is unclear if there is a more inherent relationship between these indicators or if climate is driving them. The modern ecological tolerances and classification of modern taxa need to be further explored in Tasmania.

Discostella stelligera may be a potential indicator of change in photic zone and dystrophy caused by increased terrestrial organic material inputs, and fire related to changes in mixing depth, stratification, and anoxic conditions of Tasmanian lakes. Again, this interpretation is made with very limited modern lake physiological data of

stratification or oxygen saturation conditions of these lakes (Steane et al., 1982). There are few modern measurements of Tasmanian lakes, but it is difficult to understand taxonomic ecology and change in lake physiology over time without a good benchmark of the current ecological conditions. There is a significant gap in Tasmanian limnology since the mid-1990s (Tyler, 1972; Tyler, 1974, 1992; Vyverman et al., 1995; Tyler, 1996), the region of highest concentration of freshwater in Australia (Tyler, 1974) and a climate sensitive landscape with a bleak future with projected climate change (Lenton, 2011; Power et al., 2013; Enright et al., 2015). To predict future conditions of these aquatic systems we need knowledge of their current state.

This research provides insight into the influences of fire on aquatic ecosystems in climate sensitive landscapes; however, the mechanisms related to fire and the impacts on aquatic ecosystems remain uncertain. The mechanisms behind the fire related stable state in the diatoms community is controversial (Chapter 7). While conclusions were based on the evidence and interpretations from the data collected, the data available could not determine with certainty if a critical transition had in fact occurred. The charcoal data is not conducive to model the hysteresis of this system, as well, the exact mechanisms related to cumulative fire disturbance and an acidic diatom state is complicated and speculative at times. Therefore, more research needs to be done to better understand these mechanisms and test the interpretations of this thesis. Fire impacts on aquatic ecosystems from this thesis have, thus, generated more questions: How does fire impact internal lake dynamics related to deposition of terrestrial material? Does increased terrestrial productivity and organic material decrease light penetration and create disturbed environments? Does increased terrestrial matter inputs influence mixing depth and anoxic lake conditions? Does fire produce enough ash to alter the base cation content of a lake? What are the internal mechanisms of fire that result in oligotrophic acidic aquatic ecosystem states?

This thesis demonstrates strong lines of evidence for the connection between the aquatic ecosystem and terrestrial environment driven by climate. However, more work needs to be done to understand the complex dynamics between terrestrial and aquatic ecosystems if we are to protect the future of these systems from the adverse effects of climate change.

8.7 CHAPTER CLOSING

This chapter has synthesised the findings from this thesis and draws from global biogeography to determine generalities of aquatic ecosystem response to climate change. I conclude aquatic ecosystems of Tasmania predominantly respond indirectly to the influences of climate via vegetation-soil dynamics with potentially altered relationships (direct) with increased climate variability. Further, fire impacts on aquatic ecosystem through vegetation-soil dynamics, ash, and sedimentary deposition and may result in critical transitions. The chapter closes with the caveats and knowledge gaps of this work.

Appendix V contains supporting information.

CHAPTER 9: CONCLUSION AND FUTURE WORK

9.1 THESIS CONCLUSION

This thesis has demonstrated the potential of palaeoecological records in assess the relationships between climate, the terrestrial environment, and aquatic ecosystem response.

Aquatic ecosystems of Tasmania display both direct and indirect relationships to climate during the Holocene. Direct responses to climate are manifest as changes in lake level while the indirect responses are mediated by climate-driven vegetation composition, productivity, and soil nutrient dynamics. Tasmanian vegetation produces thick organic soils imperative to these oligotrophic aquatic systems. Shifts in vegetation composition alter surrounding soils and catchment dynamics impacting aquatic ecosystems trophic status and pH.

Fire is also an important factor that impacts the aquatic environment. Sclerophyll and disturbance vegetation are favoured with increased fire frequency altering the nutrient profile of surrounding soils and loss of nutrient delivery to the aquatic environment. Fire also strips organic soils, increasing erosion and sediment delivery, mobilising Fe into nearby aquatic systems. Aquatic ecosystems respond to fire disturbance by increases in pH, oligotrophy, and lower mixing depth. Fire disturbance may also be the cause of critical transitions in aquatic ecosystems. The impact of fire on aquatic ecosystems is understudied and the findings of this thesis provide a platform to explore these relationships further.

These climate related terrestrial-aquatic ecosystem interactions have the potential to be more widespread across temperate peatlands and Southern Hemisphere biomes that share similar vegetation-soil dynamics.

9.2 FUTURE WORK

Future anthropogenic climate change will cause an increase in drying, temperature, and wildfire in Tasmania (Bradstock, 2010; Fox-Hughes et al., 2014) and worldwide (IPCC, 2013). Therefore, a better understanding of the impacts of climate on aquatic ecosystems is imperative if we are to manage the impacts of anthropogenic climate change. I am particularly interested in (1) global patterns of aquatic ecosystem response to climate change, (2) aquatic ecosystem responses to the terrestrial environment, (3) the ecologically complex genus *Discostella* as an indicator of fire stress in aquatic ecosystems, and (4) the effects of fire on aquatic ecosystems.

I also would like to create a baseline for the modern characteristics of Tasmanian lakes. It is very difficult to understand past aquatic ecological changes with poor determinations of taxa and ecological restraints. For example, attempting to understand changes in mixing regimes with lack of information on modern lake stratification. Additionally, Tasmanian lake physiology is unique compared to other temperate regions of the world. The majority of temperate lakes are located in the Northern Hemisphere and freeze annually resulting in dimictic lakes. However, Tasmanian lakes do not freeze and mixing regimes are mostly unknown. Understanding past aquatic ecosystem change and predicting future impact will continue to be a struggle without knowledge of the current state of Tasmanian lakes.

REFERENCES

- Aaronson, S., Berner, T., Gold, K., Kushner, L., Patni, N., Repak, A., Rubin, D., 1983. Some observations on the green planktonic alga, *Botryococcus braunii* and its bloom form. *Journal of Plankton Research* 5, 693-700.
- Abram, N.J., Mulvaney, R., Vimeux, F., Phipps, S.J., 2014. Evolution of the Southern Annular Mode during the past millennium. *Nature Climate Change* 4, 564-569.
- Adams, B.J., Mann, M.E., Ammann, C.M., 2003. Proxy evidence for an El Nino-like response to volcanic forcing. *Nature* 426, 274-278.
- Alhonen, P., 1970. On the significance of the planktonic-littoral ratio in the cladoceran stratigraphy of lake sediments. *Societas Scientiarum Fennica, Helsinki-Helsingfors*.
- Alonso, M., 1996. Crustacea, Branchiopoda. Editorial CSIC-CSIC Press, Madrid.
- Anderson, D., Goudie, A., Parker, A., 2007. *Global Environments Through the Quaternary: Exploring Environmental Change*. Oxford University Press Inc., New York, USA.
- Anderson, N.J., Bugmann, H., Dearing, J.A., 2006. Linking palaeoenvironmental data and models to understand the past and to predict the future. *TRENDS in Ecology and Evolution* 21, 696-704.
- Anderson, R.F., Ali, S., Bradtmiller, L.I., Nielsen, S.H.H., 2009. Wind-driven upwelling in the Southern Ocean and the deglacial rise in atmospheric CO₂. *Science* 323, 1443-1448.
- Appleby, P., 2001. Chronostratigraphic techniques in recent sediments, *Tracking environmental change using lake sediments*. Kluwer Academic Publishers, Dordrecht, The Netherlands, pp. 171-203.
- Aquatic Research Instruments, 2016. Universal Percussion Corer. Aquatic Research Instruments, Indiana, USA.

Asner, G.P., Townsend, A.R., Braswell, B.H., 2000. Satellite observation of El Nino effects on Amazon forest phenology and productivity. *Geophysical research letters* 27, 981-984.

Atlas of Living Australia, 2016. *Eucalyptus L'Hér.* National Research Infrastructure for Australia, Australia.

Augustinus, P., Bleakley, N., Deng, Y., Shane, P., Cochran, U., 2008. Rapid change in early Holocene environments inferred from Lake Pupuke, Auckland City, New Zealand. *Journal of Quaternary Science* 23, 435-447.

Augustinus, P., Cochran, U., Kattel, G., D'Costa, D., 2012. Late Quaternary paleolimnology of Onepoto maar, Auckland, New Zealand: implications for the drivers of regional paleoclimate. *Quaternary International* 253, 18-31.

Augustinus, P., D'Costa, D., Deng, Y., Hagg, J., Shane, P., 2011. A multi proxy record of changing environments from ca. 30 000 to 9000 cal. a BP: Onepoto maar palaeolake, Auckland, New Zealand. *Journal of Quaternary Science* 26, 389-401.

Axelrod, D.I., 1975. Evolution and biogeography of Madrean-Tethyan sclerophyll vegetation. *Annals of the Missouri Botanical Garden*, 280-334.

Ball, B.A., Kominoski, J.S., Adams, H.E., Jones, S.E., Kane, E.S., Loecke, T.D., Mahaney, W.M., Martina, J.P., Prather, C.M., Robinson, T.M.P., 2010. Direct and terrestrial vegetation-mediated effects of environmental change on aquatic ecosystem processes. *BioScience* 60, 590-601.

Balsam, W.L., McCoy, F.W., 1987. Atlantic sediments: glacial/interglacial comparisons. *Paleoceanography* 2, 531-542.

Barr, C., Tibby, J., Marshall, J.C., McGregor, G.B., Moss, P.T., Halverson, G.P., Fluin, J., 2013. Combining monitoring, models and palaeolimnology to assess ecosystem response to environmental change at monthly to millennial timescales: the stability of Blue Lake, North Stradbroke Island, Australia. *Freshwater Biology*, 1-17.

- Barrows, T.T., Stone, J.O., Fifield, L.K., 2002. The timing of the last glacial maximum in Australia. *Quaternary Science Reviews* 21, 159-173.
- Battarbee, R.W., 1986. Diatom analysis, in: Berglund, B.E. (Ed.), *Handbook Palaeoecology and Palaeohydrology*. John Wiley & Sons, Chichester, pp. 527-570.
- Battarbee, R.W., 2000. Palaeolimnological approaches to climate change, with special regard to the biological record. *Quaternary Science Reviews* 19.
- Battarbee, R.W., Jones, V.J., Cameron, N.G., Bennion, H., Carvalho, L., Juggins, S., 2001. Diatoms, in: Smol, J.P., Birks, H.J.B., Last, W.M. (Eds.), *Tracking Environmental Change Using Lake Sediments: Terrestrial, Algal and Siliceous Indicators*. Kluwer, Dordrecht, pp. 155-202.
- Beadle, N., 1968. Some aspects of the ecology and physiology of Australian xeromorphic plants. *Australian Journal of Science* 30, 348-355.
- Beadle, N.C.W., 1966. Soil Phosphate and Its Role in Molding Segments of the Australian Flora and Vegetation, with Special Reference to Xeromorphy and Sclerophylly. *Ecology* 47, 992-1007.
- Beck, K.K., Fletcher, M.-S., Gadd, P.S., Heijnis, H., Jacobsen, G.E., 2017. An early onset of ENSO influence in the extra-tropics of the southwest Pacific inferred from a 14, 600 year high resolution multi-proxy record from Paddy's Lake, northwest Tasmania. *Quaternary Science Reviews* 157, 164-175.
- Beck, K.K., Medeiros, A.S., Finkelstein, S.A., 2016. Drivers of Change in a 7300-Year Holocene Diatom Record from the Hemi-Boreal Region of Ontario, Canada. *PloS one* 11, e0159937.
- Benda, L.E., Miller, D.J., Dunne, T., Reeves, G.H., Agee, J.K., 1998. Dynamic Landscape Systems, in: Naiman, R.J., Bilby, R.E. (Eds.), *River Ecology and Management: Lessons from the Pacifica Coastal Ecoregion*. Springer-Verlag, New York, pp. 261-288.

Bengtsson, L., Enell, M., 1986. Chemical Analysis, in: Berglund, B.E. (Ed.), *Handbook Palaeoecology and Palaeohydrology*. John Wiley & Sons, Chichester, pp. 423-451.

Bennett, K.D., Willis, K.J., 2001. Pollen, in: Smol, J.P., Birks, H.J.B., Last, W.M. (Eds.), *Tracking Environmental Change Using Lake Sediments: Terrestrial, Algal, and Siliceous Indicators*. Kluwer Academic Publishers, Dordrecht, The Netherlands, pp. 5-32.

Bennion, H., Simpson, G.L., Goldsmith, B.J., 2015. Assessing degradation and recovery pathways in lakes impacted by eutrophication using the sediment record. *Frontiers in Ecology and Evolution* 3, 94.

Berglund, B.E., 1986a. Palaeoecological reference areas and reference sites, in: Berglund, B.E. (Ed.), *Handbook Palaeoecology and Palaeohydrology*. John Wiley & Sons, Chichester, pp. 111-126.

Berglund, B.E., 1986b. Pollen analysis and pollen diagrams, in: Berglund, B.E. (Ed.), *Handbook Palaeoecology and Palaeohydrology*. John Wiley & Sons, Chichester, pp. 455-484.

Bergström, A.-K., Jansson, M., Blomqvist, P., Drakare, S., 2000. The influence of water colour and effective light climate on mixotrophic phytoflagellates in three small Swedish dystrophic lakes. *Internationale Vereinigung für theoretische und angewandte Limnologie: Verhandlungen* 27, 1861-1865.

Bernhardt, E.S., Likens, G.E., Hall, R.O., Buso, D.C., Fisher, S.G., Burton, T.M., Meyer, J.L., McDowell, W.H., Mayer, M.S., Bowden, B.W., 2005. Can't see the forest for the stream? In-stream processing and terrestrial nitrogen exports. *Bioscience* 55, 219-230.

Birks, H., 1997. Reconstructing environmental impacts of fire from the Holocene sedimentary record, *Sediment Records of Biomass Burning and Global Change*. Springer, pp. 295-311.

Birks, H.H., Birks, J.H.B., 2006. Multi-proxy studies in palaeolimnology. *Vegetation history and Archaeobotany* 15, 235-251.

Birks, H.J.B., 2012a. Analysis of Stratigraphical Data, in: Birks, H.J.B., Lotter, A.F., Juggins, S., Smol, J.P. (Eds.), *Tracking Environmental Change Using Lake Sediments: Data Handling and Numerical Techniques*. Springer, Netherlands, pp. 355-378.

Birks, H.J.B., 2012b. Introduction and Overview of Part II: Numerical Methods for the Analysis of Stratigraphical Palaeolimnological Data, in: Birks, H.J.B., Lotter, A.F., Juggins, S., Smol, J.P. (Eds.), *Tracking Environmental Change Using Lake Sediments: Data Handling and Numerical Techniques*. Springer, Netherlands, pp. 101-121.

Birks, H.J.B., 2012c. Introduction and Overview of Part III: Numerical Methods for the Analysis of Stratigraphical Palaeolimnological Data, in: Birks, H.J.B., Lotter, A.F., Juggins, S., Smol, J.P. (Eds.), *Tracking Environmental Change Using Lake Sediments: Data Handling and Numerical Techniques*. Springer, Netherlands, pp. 331-353.

Birks, H.J.B., 2012d. Overview of Numerical Methods in Palaeolimnology, in: Birks, H.J.B., Lotter, A.F., Juggins, S., Smol, J.P. (Eds.), *Tracking Environmental Change Using Lake Sediments: Data Handling and Numerical Techniques*. Springer, Netherlands, pp. 19-92.

Birks, H.J.B., Birks, H.H., 1980. *Quaternary Palaeoecology*. Edward Arnold, London.

Birks, H.J.B., Gordon, A.D., 1985. *Numerical Methods in Quaternary Pollen Analysis*. Academic Press Inc., London.

Björck, S., Wohlfarth, B., 2001. ^{14}C Chronostratigraphic techniques in paleolimnology, in: Last, W.M., Smol, J.P. (Eds.), *Tracking Environmental Change Using Lake Sediments. Volume 1: Basin Analysis, Coring, Chronological Techniques*. Kluwer Academic Publishers, Dordrecht, The Netherlands, pp. 205-245.

Blaauw, M., 2010. Methods and code for 'classical' age-modelling of radiocarbon sequences. *Quaternary Geochronology* 5, 512-518.

Blaauw, M., Christen, J.A., 2011. Flexible Paleoclimate Age-Depth Models Using an Autoregressive Gamma Process. *Bayesian Analysis* 6, 457-474.

Blaauw, M., Christen, J.A., 2013. Bacon manual- v2.2, pp. 1-11.

Blaauw, M., Heegaard, E., 2012. Estimation of Age-Depth Relationships, in: Birks, H.J.B., Lotter, A.F., Juggins, S., Smol, J.P. (Eds.), *Tracking Environmental Change Using Lake Sediments. Volume 5: Data Handling and Numerical Techniques*. Kluwer Academic Publishers, Dordrecht, The Netherlands, pp. 379-413.

Black, M.P., Mooney, S.D., Attenbrow, V., 2008. Implications of a 14 200 year contiguous fire record for understanding human—climate relationships at Goochs Swamp, New South Wales, Australia. *The Holocene* 18, 437-447.

Böhlke, J., Coplen, T., 1995. Interlaboratory comparison of reference materials for nitrogen-isotope-ratio measurements, Consultants meeting on stable isotope standards and intercomparison materials, Vienna, Austria, pp. 51-66.

Bond, W.J., Woodward, F.I., Midgley, G.F., 2005. The global distribution of ecosystems in a world without fire. *New Phytologist* 165, 525-538.

Bowman, D., 1998. The impact of Aboriginal landscape burning on the Australian biota. *New Phytologist* 140, 385-410.

Bowman, D., 2000. *Australian rainforests: Islands of green in a land of fire*. Cambridge University Press, Cambridge UK.

Bowman, D., Balch, J.K., Artaxo, P., Bond, W.J., Carlson, J.M., Cochrane, M.A., D'Antonio, C.M., DeFries, R.S., Doyle, J.C., Harrison, S.P., 2009a. Fire in the Earth system. *science* 324, 481-484.

- Bowman, D., Brown, M.J., 1986a. Bushfires in Tasmania: a botanical approach to anthropological questions. *Archaeology in Oceania* 21, 166-171.
- Bowman, D., Jackson, W., 1981. Vegetation succession in southwest Tasmania. *Search* 12, 358-362.
- Bowman, D., Maclean, A.R., Crowden, R.K., 1986b. Vegetation-soil relations in the lowlands of south-west Tasmania. *Australian Journal of Ecology* 11, 141-153.
- Bowman, D., Wood, S.W., 2009b. Fire-driven land cover change in Australia and WD Jackson's theory of the fire ecology of southwest Tasmania, *Tropical Fire Ecology*. Springer, Berlin Heidelberg, pp. 87-111.
- Bowman, D.M.J.S., Balch, J., Artaxo, P., Bond, W.J., Cochrane, M.A., D'Antonio, C.M., DeFries, R., Johnston, F.H., Keeley, J.E., Krawchuk, M.A., Kull, C.A., Mack, M., Moritz, M.A., Pyne, S., Roos, C.I., Scott, A.C., Sodhi, N.S., Swetnam, T.W., 2011. The human dimension of fire regimes on Earth. *Journal of Biogeography* 38, 2223-2236.
- Box, G.E., Jenkins, G.M., 1976. *Time Series Analysis: Forecasting and Control*, 5 ed. Holden-Day, San Francisco, CA.
- Box, G.E., Jenkins, G.M., Reinsel, G.C., Ljung, G.M., 2016. *Time series analysis: forecasting and control*, 5 ed. John Wiley & Sons, Hoboken, New Jersey.
- Bradbury, P.J., 1986. Late Pleistocene and Holocene paleolimnology of two mountain lakes in western Tasmania. *PALAIOS* 1, 381-388.
- Bradstock, R.A., 2010. A biogeographic model of fire regimes in Australia: current and future implications. *Global Ecology and Biogeography* 19, 145-158.
- Brehm, V., 1953. Contributions to the freshwater microfauna of Tasmania-Part 1. *Papers and Proceedings of the Royal Society of Tasmania* 87, 33-62.

Bridle, K., Kirkpatrick, J., 1997. Local environmental correlates of variability in the organic soils of moorland and alpine vegetation, Mt Sprent, Tasmania. *Austral Ecology* 22, 196-205.

Bridle, K.L., Cullen, P.J., Russell, M., 2003. Peatland hydrology, fire management and Holocene fire regimes in southwest Tasmanian blanket bogs, Earth Science Section, Nature Conservation Report No. 03/07. Nature Conservation Branch of the Department of Primary Industries, Water and Environment, Hobart, Tasmania, Australia, p. 97.

Brooks, S.J., Birks, H.J.B., 2000. Chironomid-inferred late-glacial and early-Holocene mean July air temperatures for Kråkenes Lake, western Norway. *Journal of Paleolimnology* 23, 77-89.

Brown, M.J., Crowden, R.K., Jarman, S.J., 1982a. Vegetation of an alkaline pan — acidic peat mosaic in the Hardwood River Valley, Tasmania. *Australian Journal of Ecology* 7, 3-12.

Brown, M.J., Podger, F.D., 1982b. Floristics and fire regimes of a vegetation sequence from sedgeland-heath to rainforest at Bathurst Harbour, Tasmania. *Australian Journal of Botany* 30, 659-676.

Brown, S., 2016. Multi-proxy Holocene fire history reconstruction in Beartooth Mountains, Wyoming, Department of Earth and Environmental Systems. Indiana State University, Indiana, USA.

Bryant, R.H., 2013. *Physical Geography: Made Simple*. Elsevier Science, Burlington.

Buckney, R., Tyler, P., 1973. Chemistry of some sedgeland waters: Lake Pedder, south-west Tasmania. *Australian Journal of Marine and Freshwater Research* 24, 267-273.

Bunnell, F.L., Tait, D.E.N., Flanagan, P.W., 1977. Microbial respiration and substrate weight loss—I: A general model of the influences of abiotic variables. *Soil Biology and Biochemistry* 9, 33-40.

Bunting, L., Leavitt, P.R., Simpson, G.L., Wissel, B., Laird, K.R., Cumming, B.F., St. Amand, A., Engstrom, D.R., 2016. Increased variability and sudden ecosystem state change in Lake Winnipeg, Canada, caused by 20th century agriculture. *Limnology and Oceanography* 61, 2090-2107.

Bunting, M.J., Gaillard, M.J., Sugita, S., Middleton, R., Broström, A., 2004. Vegetation structure and pollen source area. *The Holocene* 14, 651-660.

Bureau of Meteorology, 2016a. Daily rainfall: Loongana (Serendipity). Commonwealth of Australia, Bureau of Meteorology, Australia.

Bureau of Meteorology, 2016b. Monthly mean maximum temperature: Loongana (Serendipity). Commonwealth of Australia, Bureau of Meteorology, Australia.

Bureau of Meteorology, 2016c. Monthly mean maximum temperature: Waratah (Mount Road). Commonwealth of Australia, Bureau of Meteorology, Australia.

Bureau of Meteorology, 2017. Climate Data Online, Monthly climate statistics. Australian Government, Bureau of Meteorology, Commonwealth of Australia.

Busby, J.R., 1986. A biogeoclimatic analysis of *Nothofagus cunninghamii* (Hook.) Oerst. in southeastern Australia. *Australian Journal of Ecology* 11, 1-7.

Cáceres, C., Soluk, D., 2002. Blowing in the wind: a field test of overland dispersal and colonization by aquatic invertebrates. *Oecologia* 131, 402-408.

Cai, W., Borlace, S., Lengaigne, M., van Rensch, P., Collins, M., Vecchi, G., Timmermann, A., Santoso, A., McPhaden, M.J., Wu, L., England, M.H., Wang, G., Guilyardi, E., Jin, F.-F., 2014. Increasing frequency of extreme El Niño events due to greenhouse warming. *Nature climate change* 4, 111-116.

- Cairns, M.A., Lajtha, K., 2005. Effects of succession on nitrogen export in the west-central Cascades, Oregon. *Ecosystems* 8, 583-601.
- Cameron, N.G., Tyler, P.A., Rose, N.L., Hutchinson, S., Appleby, P.G., 1993. The recent palaeolimnology of Lake Nicholls, Mount Field National Park, Tasmania. *Hydrobiologia* 269/270, 361-370.
- Cao, M., Prince, S.D., Small, J., Goetz, S.J., 2004. Remotely sensed interannual variations and trends in terrestrial net primary productivity 1981–2000. *Ecosystems* 7, 233-242.
- Capon, S.J., Lynch, J.A.J., Bond, N., Chessman, B.C., Davis, J., Davidson, N., Finlayson, M., Gell, P.A., Hohnberg, D., Humphrey, C., Kingsford, R.T., Nielsen, D., Thomson, J.R., Ward, K., Mac Nally, R., 2015. Regime shifts, thresholds and multiple stable states in freshwater ecosystems; a critical appraisal of the evidence. *Science of The Total Environment* 534, 122-130.
- Carignan, R., Tessier, A., 1988. The co-diagenesis of sulfur and iron in acid lake sediments of southwestern Quebec. *Geochimica et Cosmochimica Acta* 52, 1179-1188.
- Carpenter, S.R., Brock, W.A., 2006. Rising variance: a leading indicator of ecological transition. *Ecology Letters* 9, 311-318.
- Carpenter, S.R., Cole, J.J., Pace, M.L., Batt, R., Brock, W.A., Cline, T., Coloso, J., Hodgson, J.R., Kitchell, J.F., Seekell, D.A., Smith, L., Weidel, B., 2011. Early warnings of regime shifts: a whole-ecosystem experiment. *Science* 332, 1079-1082.
- Carpenter, S.R., Mooney, H.A., Agard, J., Capistrano, D., DeFries, R.S., Díaz, S., Dietz, T., Duraiappah, A.K., Oteng-Yeboah, A., Pereira, H.M., Perrings, C., Reid, W.V., Sarukhan, J., Scholes, R.J., Whyte, A., 2009. Science for managing ecosystem services: Beyond the Millennium Ecosystem Assessment. *Proceedings of the National Academy of Sciences* 106, 1305-1312.

- Carpenter, S.R., Pace, M.L., 1997. Dystrophy and eutrophy in lake ecosystems: implications of fluctuating inputs. *OIKOS* 78, 3-14.
- Carstensen, J., Telford, R.J., Birks, J.H.B., 2013. Diatom flickering prior to regime shift. *Nature* 498, E11-E13.
- Certini, G., 2005. Effects of fire on properties of forest soils: a review. *Oecologia* 143, 1-10.
- Chapman, A.D., 2009. Numbers of living species in Australia and the world, in: Department of the Environment, W., Heritage and the Arts (Ed.), 2nd ed. Australian Government, Canberra, Australia, p. 84.
- Chappell, J., 1978. Chronological Methods and the Ranges and Rates of Quaternary Physical Changes, in: Walker, D., Guppy, J.C. (Eds.), *Biology and Quaternary Environments*. Australian Academy of Science, Canberra, ACT, Australia.
- Chappellaz, J., Blunier, T., Raynaud, D., Barnola, J.M., 1993. Synchronous changes in atmospheric CH₄ and Greenland climate between 40 and 8 kyr BP. *Nature* 366, 443-445.
- Charles, D.F., 1985. Relationships between surface sediment diatom assemblages and lakewater characteristics in Adirondack lakes. *Ecology* 66, 994-1011.
- Chiew, F.H.S., Piechota, T.C., Dracup, J.A., McMahon, T.A., 1998. Seasonal streamflow forecasting in eastern Australia and the El Niño–Southern Oscillation. *Water Resources Research* 34, 3035-3044.
- Clausing, A., 1999. Palaeoenvironmental significance of the green alga *Botryococcus* in the lacustrine rotliedgen (upper carboniferous-lower permian). *Historical Biology* 13, 221-234.
- Cohen, A.S., 2003. *Paleolimnology: The History and Evolution of Lake Systems*. Oxford University Press, USA.
- Colhoun, E., 1996. Application of Iversen's glacial-interglacial cycle to interpretation of the late last glacial and holocene vegetation history of western Tasmania. *Quaternary Science Reviews* 15, 557-580.

- Colhoun, E., Pola, J.S., Barton, C.E., Heijnis, H., 1999. Late Pleistocene vegetation and climate history of Lake Selina, western Tasmania. *Quaternary International* 57-58, 5-23.
- Colhoun, E.A., Geer, G., 1991a. Late Glacial and Holocene Vegetation History at Dublin Bog North-Central Tasmania. *Australian Geographic Studies* 29, 337-354.
- Colhoun, E.A., van de Geer, G., Fitzsimons, S.J., 1991b. Late glacial and Holocene vegetation history at Governor Bog, King Valley, western Tasmania, Australia. *Journal of Quaternary Science* 6, 55-66.
- Conroy, J.L., Overpeck, J.T., Cole, J.E., Shanahan, T.M., Steinitz-Kannan, M., 2008. Holocene changes in eastern tropical Pacific climate inferred from a Galápagos lake sediment record. *Quaternary Science Reviews* 27, 1166-1180.
- Conroy, J.L., Restrepo, A., Overpeck, J.T., Steinitz-Kannan, M., Cole, J.E., Bush, M.B., Colinvaux, P.A., 2009. Unprecedented recent warming of surface temperatures in the eastern tropical Pacific Ocean. *Nature Geoscience* 2, 46-50.
- Cook, E., Bird, T., Peterson, M., Barbetti, M., Buckley, B., D'ARRIGO, R., Francey, R., Tans, P., 1991. Climatic change in Tasmania inferred from a 1089-year tree-ring chronology of Huon Pine. *Science* 253, 1266-1268.
- Costanza, R., d'Arge, R., de Groot, R., Farber, S., Grasso, M., Hannon, B., Limburg, K., Naeem, S., O'Neill, R.V., Paruelo, J., Raskin, R.G., Sutton, P., van den Belt, M., 1997. The value of the world's ecosystem services and natural capital. *nature* 387, 253-260.
- Cowling, S.A., 1999. Plants and Temperature-CO₂ Uncoupling. *Science* 285, 1500-1501.
- Cramer, W., Bondeau, A., Woodward, I.F., Prentice, C.I., Betts, R.A., Brovkin, V., Cox, P.M., Fisher, V., Foley, J.A., Friend, A.D., Kucharik, C., Lomas, M.R., Ramankutty, N., Sitch, S., Smith, B., White, A., Young-Molling, C., 2001. Global response of terrestrial ecosystem structure and function to CO₂ and climate change: results from six dynamic global vegetation models. *Global Change Biology* 7, 357-373.

- Crisp, M.D., Arroyo, M.T., Cook, L.G., Gandolfo, M.A., Jordan, G.J., McGlone, M.S., Weston, P.H., Westoby, M., Wilf, P., Linder, H.P., 2009. Phylogenetic biome conservatism on a global scale. *Nature* 458, 754-756.
- Crocker, R.L., Major, J., 1955. Soil Development in Relation to Vegetation and Surface Age at Glacier Bay, Alaska. *Journal of Ecology* 43, 427-448.
- Croome, R.L., 1986. Biological Studies of Meromictic Lakes, in: De Deckker, P., Williams, W.D. (Eds.), *Limnology in Australia*. Dr. W. Junk Publishers, Dordrecht/Boston/Lancaster, p. 113.
- Croome, R.L., Tyler, P.A., 1973. Plankton populations of Lake Leake and Tooms Lake—oligotrophic Tasmanian lakes. *British Phycological Journal* 8, 239-247.
- Croudace, I.W., Rindby, A., Rothwell, R.G., 2006. ITRAX: description and evaluation of a new multi-function X-ray core scanner, in: Rothwell, R.G. (Ed.), *New Techniques in Sediment Core Analysis*. Geological Society, London, Special Publications, London, pp. 51-63.
- Croudace, I.W., Rothwell, R.G., 2015. *Micro-XRF Studies of Sediment Cores: Applications of a non-destructive tool for the environmental sciences*. Springer Science + Business Media Dordrecht, Dordrecht Heidelberg New York London.
- CSIRO and Bureau of Meteorology, 2015. *Climate Change in Australia Information for Australia's Natural Resource Management Regions: Technical Report*, in: Meteorology, C.a.B.o. (Ed.). CSIRO and Bureau of Meteorology, Australia.
- Dakos, V., Carpenter, S.R., Brock, W.A., Ellison, A.M., Guttal, V., Ives, A.R., Kefi, S., Livina, V., Seekell, D.A., van Nes, E.H., Scheffer, M., 2012. Methods for detecting early warnings of critical transitions in time series illustrated using simulated ecological data. *PLoS one* 7, e41010.

- Dakos, V., Carpenter, S.R., van Nes, E.H., Scheffer, M., 2015. Resilience indicators: prospects and limitations for early warnings of regime shifts. *Philosophical Transactions of the Royal Society of London B: Biological Sciences* 370, 20130263.
- Dangles, O., Rabatel, A., Kraemer, M., Zeballos, G., Soruco, A., Jacobsen, D., Anthelme, F., 2017. Ecosystem sentinels for climate change? Evidence of wetland cover changes over the last 30 years in the tropical Andes. *PLoS one* 12, e0175814.
- Dansgaard, W., White, J.W.C., Johnsen, S.J., 1989. The abrupt termination of the Younger Dryas climate event. *Nature* 339, 532-533.
- Davidson, E.A., Janssens, I.A., 2006. Temperature sensitivity of soil carbon decomposition and feedbacks to climate change. *Nature* 440, 165-173.
- Davies, S.J., Lamb, H.F., Roberts, S.J., 2015. Micro-XRF Core Scanning in Palaeolimnology: Recent Developments, in: Croudace, I.W., Rothwell, R.G. (Eds.), *Micro-XRF Studies of Sediment Cores*. Springer Science + Business Media, Dordrecht, pp. 189-226.
- Davison, W., 1993. Iron and manganese in lakes. *Earth-Science Reviews* 34, 119-163.
- De' ath, G., 1999. Principal curves: a new technique for indirect and direct gradient analysis. *Ecology* 80, 2237-2253.
- De Deckker, P., 1982. Holocene ostracods, other invertebrates and fish remains from cores of four maar lakes in southeastern Australia. *Proceedings of the Royal Society of Victoria* 94, 183-220.
- Dech, J., Nosko, P., 2004. Rapid growth and early flowering in an invasive plant, purple loosestrife (*Lythrum salicaria* L.) during an El Niño spring. *International Journal of Biometeorology* 49, 26-31.

- Denham, T., Sniderman, K., Saunders, K.M., Winsborough, B., Pierret, A., 2009. Contiguous multi proxy analyses (X radiography, diatom, pollen, and microcharcoal) of Holocene archaeological features at Kuk Swamp, Upper Wahgi Valley, Papua New Guinea. *Geoarchaeology* 24, 715-742.
- Department of Primary Industries, P., Water and Environment (Tasmania), 2017. *TASVEG - The Digital Vegetation Map of Tasmania*, 3.0 ed. Tasmanian Government, Tasmania.
- di Folco, M.-B., 2007. *Tasmanian Organic Soils*. University of Tasmania, Tasmania, Australia, p. 421.
- di Folco, M.-B., Kirkpatrick, J.B., 2011. Topographic variation in burning-induced loss of carbon from organic soils in Tasmanian moorlands. *CATENA* 87, 216-225.
- di Folco, M.B., Kirkpatrick, J.B., 2013. Organic soils provide evidence of spatial variation in human-induced vegetation change following European occupation of Tasmania. *Journal of Biogeography* 40, 197-205.
- Diehl, S., Berger, S., Ptacnik, R., Wild, A., 2002. Phytoplankton, light, and nutrients in a gradient of mixing depths: field experiments. *Ecology* 83, 399-411.
- DirectAMS, 2017. *Sample Types: Sediment*, DirectAMS Radiocarbon dating service. DirectAMS, Washington, USA.
- Dixit, S.S., Smol, J.P., Kingston, J.C., Charles, D.F., 1992. Diatoms: powerful indicators of environmental change. *Environmental Science & Technology* 26, 22-33.
- Donders, T.H., Haberle, S.G., Hope, G., Wagner, F., Visscher, H., 2007. Pollen evidence for the transition of the Eastern Australian climate system from the post-glacial to the present-day ENSO mode. *Quaternary Science Reviews* 26, 1621-1637.
- Donders, T.H., Wagner-Cremer, F., Visscher, H., 2008. Integration of proxy data and model scenarios for the mid-Holocene onset of modern ENSO variability. *Quaternary Science Reviews* 27, 571-579.

- DPIPWE, 2016. Tasmanian Wilderness World Heritage Area Management Plan, in: Department of Primary Industries, P., Water and Environment (Ed.). Department of Primary Industries, Parks, Water and Environment, Hobart, Tasmania.
- Dunnette, P.V., Higuera, P.E., McLauchlan, K.K., Derr, K.M., Briles, C.E., Keefe, M.H., 2014. Biogeochemical impacts of wildfires over four millennia in a Rocky Mountain subalpine watershed. *New Phytologist* 203, 900-912.
- Durán, J., Rodríguez, A., Fernández-Palacios, J.M., Gallardo, A., 2008. Changes in soil N and P availability in a *Pinus canariensis* fire chronosequence. *Forest Ecology and Management* 256, 384-387.
- Ejrnæs, R., 2000. Can we trust gradients extracted by Detrended Correspondence Analysis? *Journal of Vegetation Science* 11, 565-572.
- Engstrom, D.R., Fritz, S.C., 2006. Coupling between primary terrestrial succession and the trophic development of lakes at Glacier Bay, Alaska. *Journal of Paleolimnology* 35, 873-880.
- Engstrom, D.R., Fritz, S.C., Almendinger, J.E., Juggins, S., 2000. Chemical and biological trends during lake evolution in recently deglaciated terrain. *Nature* 408, 161-166.
- Enright, N.J., Fontaine, J.B., Bowman, D.M.J.S., Bradstock, R.A., Williams, R.J., 2015. Interval squeeze: altered fire regimes and demographic responses interact to threaten woody species persistence as climate changes. *Frontiers in Ecology and Environment* 13, 265-272.
- Faegri, K., Iversen, J., 1989. Textbook of pollen analysis, 4 ed. John Wiley & Sons Ltd., London, Great Britain.
- Faith, D.P., Minchin, P.R., Belbin, L., 1987. Compositional dissimilarity as a robust measure of ecological distance. *Vegetatio* 69, 57-68.

- Fee, E.J., Hecky, R.E., Kasian, S.E.M., Cruikshank, D.R., 1996. Effects of lake size, water clarity, and climatic variability on mixing depths in Canadian Shield lakes. *Limnology and Oceanography* 41, 912-920.
- Felde, V.A., Bjune, A.E., Grytnes, J.A., of and, H.J.B., 2014. A comparison of novel and traditional numerical methods for the analysis of modern pollen assemblages from major vegetation–landform types. *Review of Palaeobotany and Palynology* 210, 22-36.
- Finkelstein, S.A., Gajewski, K., Viau, A.E., 2006. Improved resolution of pollen taxonomy allows better biogeographical interpretation of post-glacial forest development: analyses from the North American *Journal of Ecology* 94, 415-430.
- Flannigan, M.D., Krawchuk, M.A., de Groot, W.J., Wotton, M.B., Gowman, L.M., 2009. Implications of changing climate for global wildland fire. *International Journal of Wildland Fire* 18, 483-507.
- Fletcher, M.-S., 2015. Mast seeding and the El Niño-Southern Oscillation: a long-term relationship? *Plant Ecology* 216, 527-533.
- Fletcher, M.-S., Benson, A., Bowman, D.M.J.S., Gadd, P.S., Heijnis, H., Mariani, M., Saunders, K.M., Wolfe, B.B., Zawadzki, A., 2018a. Centennial-scale trends in the Southern Annular Mode revealed by hemisphere-wide fire and hydroclimatic trends over the last 2400 years. *Geology*.
- Fletcher, M.-S., Benson, A., Heijnis, H., Gadd, P.S., 2015. Changes in biomass burning mark the onset an ENSO-influenced climate regime at 42° S in southwest Tasmania, Australia. *Quaternary Science Reviews* 122, 222-232.
- Fletcher, M.-S., Bowman, D., Whitlock, C., Mariani, M., Stahle, L.N., 2018b. The changing role of fire in conifer-dominated temperate rainforest through the last 14,000 years. *Quaternary Science Reviews* 182, 37-47.
- Fletcher, M.-S., Wolfe, B.B., Whitlock, C., Pompeani, D.P., Heijnis, H., Haberle, S.G., Gadd, P.S., Bowman, D., 2014a. The legacy of mid-Holocene fire on a Tasmanian montane landscape. *Journal of Biogeography* 41, 476-488.

Fletcher, M.-S., Wood, S.W., Haberle, S.G., 2014b. A fire-driven shift from forest to non-forest: evidence for alternative stable states? *Ecology* 95, 2504-2513.

Fletcher, M.S., Bowman, D., Whitlock, C., Mariani, M., Stahle, L.N., Hopf, F., Benson, A., Heijnis, H., Zawadzki, A., in review. Long-term rain forest dynamics within a topographic fire refugia. *Journal of Biogeography*.

Fletcher, M.S., Moreno, P., 2012. Have the Southern Westerlies changed in a zonally symmetric manner over the last 14,000 years? A hemisphere-wide take on a controversial problem. *Quaternary International*.

Fletcher, M.S., Moreno, P.I., 2011. Zonally symmetric changes in the strength and position of the Southern Westerlies drove atmospheric CO₂ variations over the past 14 ky. *Geology* 39, 419-422.

Fletcher, M.S., Thomas, I., 2007a. Holocene vegetation and climate change from near Lake Pedder, south-west Tasmania, Australia. *Journal of Biogeography* 34, 665-677.

Fletcher, M.S., Thomas, I., 2007b. Modern pollen–vegetation relationships in western Tasmania, Australia. *Review of Palaeobotany and Palynology* 146, 146-168.

Fletcher, M.S., Thomas, I., 2010a. A Holocene record of sea level, vegetation, people and fire from western Tasmania, Australia. *The Holocene* 20, 351-361.

Fletcher, M.S., Thomas, I., 2010b. The origin and temporal development of an ancient cultural landscape. *Journal of Biogeography* 37, 2183-2196.

Fletcher, M.S., Thomas, I., 2010c. A quantitative Late Quaternary temperature reconstruction from western Tasmania, Australia. *Quaternary Science Reviews* 29, 2351-2361.

Foged, N., 1978. Diatoms in Eastern Australia. J. Cramer, Vaduz.

- Fox-Hughes, P., Harris, R., Lee, G., Grose, M., Bindoff, N., 2014. Future fire danger climatology for Tasmania, Australia, using a dynamically downscaled regional climate model. *International Journal of Wildland Fire* 23, 309-321.
- Frey, D., 1991a. The species of *Pleuroxus* and of three related genera (Anomopoda, Chydoridae) in Southern Australia and New Zealand. *Records of the Australian Museum* 43, 291-372.
- Frey, D.G., 1980. On the plurality of *Chydorus sphaericus* (OF Müller)(Cladocera, Chydoridae), and designation of a neotype from Sjaelsø, Denmark. *Hydrobiologia* 69, 83-123.
- Frey, D.G., 1986. Cladocera analysis, in: Berglund, B.E. (Ed.), *Handbook Palaeoecology and Palaeohydrology*. John Wiley & Sons, Chichester, pp. 667-692.
- Frey, D.G., 1991b. First subfossil records of *Daphnia* headshields and shells (Anomopoda, Daphniidae) about 10 000 years old from northernmost Greenland, plus *Alona guttata* (Chydoridae). *Journal of Paleolimnology* 6, 193-197.
- Fritz, S.C., Anderson, N.J., 2013. The relative influences of climate and catchment processes on Holocene lake development in glaciated regions. *Journal of Paleolimnology* 49, 349-362.
- Fritz, S.C., Cumming, B.F., Gasse, F., Laird, K.R., 1999. Diatoms as indicators of hydrologic and climatic change in saline lakes, in: Stoermer, E.F., Smol, J.P. (Eds.), *The diatoms: applications for the environmental and earth sciences*. Cambridge University Press, UK, pp. 41-72.
- Fritz, S.C., Engstrom, D.R., Juggins, S., 2004. Patterns of early lake evolution in boreal landscapes: a comparison of stratigraphic inferences with a modern chronosequence in Glacier Bay, Alaska. *The Holocene* 14, 828-840.
- Fritz, S.C., Juggins, S., Battarbee, R.W., 1993. Diatom Assemblages and Ionic Characterization of Lakes of the Northern Great Plains, North America: A Tool for Reconstructing Past Salinity and Climate Fluctuations. *Canadian Journal of Fisheries and Aquatic Sciences* 50, 1844-1856.

- Fry, B., Brand, W., Mersch, F.J., 1992. Automated analysis system for coupled $\delta^{13}\text{C}$ and $\delta^{15}\text{N}$ measurements. *Analytical Chemistry* 64, 288-291.
- Fule, P.Z., Korb, J.E., Wu, R., 2009. Changes in forest structure of a mixed conifer forest, southwestern Colorado, USA. *Forest Ecology and Management* 258, 1200-1210.
- Gasse, F., 2000. Hydrological changes in the African tropics since the Last Glacial Maximum. *Quaternary Science Reviews* 19, 189-211.
- Gasse, F., Barker, P., Gell, P., Fritz, S.C., Chalif, F., 1997. Diatom-inferred salinity in palaeolakes: An indirect tracer of climate change. *Quaternary Science Reviews* 16, 547-563.
- Geddes, M.C., 1988. The role of turbidity in the limnology of Lake Alexandrina, River Murray, South Australia; comparisons between clear and turbid phases. *Australian Journal of Marine and Freshwater Research* 39, 201-210.
- Gell, P., Mills, K., Grundell, R., 2012. A legacy of climate and catchment change: the real challenge for wetland management. *Hydrobiologia* 708, 133-144.
- Gell, P., Reid, M., 2014. Assessing change in floodplain wetland condition in the Murray Darling Basin, Australia. *Anthropocene* 8, 39-45.
- Gell, P., Tibby, J., Fluin, J., Leahy, P., Reid, M., 2005. Accessing limnological change and variability using fossil diatom assemblages, south-east Australia. *River Research and Applications* 21, 257-269.
- Gell, P.A., 1999. An illustrated key to common diatom genera from Southern Australia. Cooperative Research Centre for Freshwater Ecology, Thurgoona, NSW.
- Gentili, J., 1971. *Climates of Australia and New Zealand*. Elsevier Science Ltd, Amsterdam.

- Giles, M.P., Michelutti, N., Grooms, C., Smol, J.P., 2018. Long-term limnological changes in the Ecuadorian páramo: Comparing the ecological responses to climate warming of shallow waterbodies versus deep lakes. *Freshwater Biology* 00, 1-10.
- Gill, M.A., 1975. Fire and The Australian Flora: A Review. *Australian Forestry* 38, 4-25.
- Gillett, N.P., Kell, T.D., Jones, P.D., 2006. Regional climate impacts of the Southern Annular Mode. *Geophysical Research Letters* 33, 1-4.
- Glew, J.R., Smol, J.P., Last, W.M., 2001. Sediment Core Collection and Extrusion, in: Last, W.M., Smol, J.P. (Eds.), *Tracking environmental change using lake sediments 1: Basin Analysis, Coring and Chronological Techniques*. Kluwer Academic Publishers, Dordrecht, The Netherlands, pp. 73-105.
- Gomez, B., Carter, L., Trustrum, N.A., Palmer, A.S., 2004. El Niño–Southern Oscillation signal associated with middle Holocene climate change in intercorrelated terrestrial and marine sediment cores, North Island, New *Geological Society of America* 32, 653-656.
- Gonfiantini, R., Stichler, W., Rozanski, K., 1995. Standards and intercomparison materials distributed by the International Atomic Energy Agency for stable isotope measurements, pp. 13-29.
- González-Pérez, J.A., González-Vila, F.J., Almendros, G., Knicker, H., 2004. The effect of fire on soil organic matter—a review. *Environment International* 30, 855-870.
- Gorham, E., 1961. Factors influencing supply of major ions to inland waters, with special reference to the atmosphere. *Geological Society of America Bulletin* 72, 795-840.
- Green, D.G., 1981. Time series and postglacial forest ecology. *Quaternary Research* 15, 265-277.
- Green, J.D., 1976. Plankton of lake Ototoa, a sand dune lake in Northern New Zealand. *New Zealand Journal of Marine and Freshwater Research* 10, 43-59.

- Green, J.D., Shiel, R.J., 1992. Australia's neglected freshwater microfauna. *Australian Journal of Biological Sciences* 5, 118-123.
- Grimm, E.C., 1987. CONISS: a FORTRAN 77 program for stratigraphically constrained cluster analysis by the method of incremental sum of squares. *Computers & Geosciences* 13, 13-35.
- Grimm, E.C., 2013. Tilia, 2.0.37 ed. Illinois State Museum Research and Collection Centre, Illinois, USA.
- Grizzetti, B., Lanzanova, D., Liqueste, C., Reynaud, A., Cardoso, A.C., 2016. Assessing water ecosystem services for water resource management. *Environmental Science & Policy* 61, 194-203.
- Grootes, P.M., Steig, E.J., Stuiver, M., Waddington, E.D., Morse, D.L., Nadeau, M.-J., 2001. The Taylor Dome Antarctic 18 O record and globally synchronous changes in climate. *Quaternary Research* 56, 289-298.
- Güsewell, S., Bailey, K.M., Roem, W.J., Bedford, B.L., 2005. Nutrient limitation and botanical diversity in wetlands: can fertilisation raise species richness? *OIKOS* 109, 71-80.
- Haberle, S.G., 2005. A 23,000-yr pollen record from Lake Euramoo, Wet Tropics of NE Queensland, Australia. *Quaternary Research* 64, 343-356.
- Haberle, S.G., Tibby, J., Dimitriadis, S., Heijnis, H., 2006. The impact of European occupation on terrestrial and aquatic ecosystem dynamics in an Australian tropical rain forest. *Journal of Ecology* 94, 987-1002.
- Håkanson, L., Jansson, M., 1983. *Principles of Lake Sedimentology*. Springer-Verlag Berlin Heidelberg, Germany.
- Hall, R.I., Smol, J.P., 1992. A weighted-averaging regression and calibration model for inferring total phosphorus concentration from diatoms in British Columbia (Canada) lakes. *Freshwater Biology* 27, 417-434.
- Hansen, K., 1962. The dystrophic lake type. *Hydrobiologia* 19, 183-190.

- Harle, K.J., Hodgson, D.A., Tyler, P.A., 1999. Palynological evidence for Holocene palaeoenvironments from the lower Gordon River valley, in the World Heritage Area of southwest Tasmania. *The Holocene* 9, 149-162.
- Harris, S., Kitchener, A., 2005. From forest to fjældmark: descriptions of Tasmania's vegetation. Department of Primary Industries, Water and Environments, Hobart, Tasmania.
- Hastie, T., Stuetzle, W., 1989. Principal Curves. *Journal of the American Statistical Association* 84, 502-516.
- Hastie, T., Tibshirani, R., 1990. *Generalized Additive Models*. CRC Press.
- Haurwitz, M.W., Brier, G.W., 1981. A Critique of the Superposed Epoch Analysis Method: Its Application to Solar-Weather Relations. *American Meteorological Society* 109, 2074-2079.
- Haworth, E.Y., Tyler, P.A., 1993. Morphology and taxonomy of *Cyclotella tasmanica* spec. nov, a newly described diatom from Tasmanian lakes. *Hydrobiologia* 269-270, 49-56.
- Hedges, R.E.M., 1981. Radiocarbon dating with an accelerator: review and preview. *Archaeometry* 23, 3-18.
- Hegerl, G.C., Crowley, T.J., Baum, S.K., 2003. Detection of volcanic, solar and greenhouse gas signals in paleo-reconstructions of Northern Hemispheric temperature. *Geophysical Research Letters* 30.
- Heggen, M.P., Birks, H.H., Anderson, N.J., 2010. Long-term ecosystem dynamics of a small lake and its catchment in west Greenland. *The Holocene* 20, 1207-1222.
- Hennessy, K., Lucas, C., Nicholls, N., Bathols, J., Suppiah, R., Ricketts, J., 2005. Climate change impacts on fire-weather in south-east Australia, in: Group, C.I. (Ed.). *CSIRO Atmospheric Research and the Australian Government Bureau of Meteorology*, Aspendale, p. 91.
- Heyng, A.M., Mayr, C., Lücke, A., Striewski, B., Wastegård, S., Wissel, H., 2012. Environmental changes in northern New Zealand since the Middle Holocene inferred from stable isotope records (^{15}N , ^{13}C) of Lake Pupuke. *Journal of paleolimnology* 48, 351-366.

- Higuera, P., 2009. CharAnalysis 0.9: Diagnostic and analytical tools for sediment charcoal analysis. Montana State University, Bozeman, MT.
- Hill, K.J., Santoso, A., England, M.H., 2009. Interannual Tasmanian Rainfall Variability Associated with Large-Scale Climate Modes. *Journal of Climate* 22, 4383-4397.
- Hill, M.O., Gauch, H.G.J., 1980. Detrended correspondence analysis: an improved ordination technique. *Vegetation* 42, 47-58.
- Hill, R.S., Read, J., Busby, J.R., 1988. The temperature-dependence of photosynthesis of some Australian temperate rainforest trees and its biogeographical significance. *Journal of Biogeography* 15, 431-449.
- Hobbie, E.A., Hogberg, P., 2012. Tansley review: Nitrogen isotopes link mycorrhizal fungi and plants to nitrogen dynamics. *New Phytologist* 196, 367-382.
- Hodgson, D., McDonald, J.L., Hosken, D.J., 2015. What do you mean, 'resilient'? *Trends in ecology & evolution* 30, 503-506.
- Hodgson, D., Tyler, P., Vyverman, W., 1996. The palaeolimnology of Lake Fidler, a meromictic lake in south-west Tasmania and the significance of recent human impact. *Journal of Paleolimnology* 18, 313-333.
- Hodgson, D.A., Vyverman, W., Chepstow-Lusty, A., Tyler, P.A., 2000. From rainforest to wasteland in 100 years: The limnological legacy of the Queenstown mines, Western Tasmania. *Archiv fur Hydrobiologie* 146, 153-176.
- Hoerling, M., Kumar, A., 2003. The perfect ocean for drought. *Science* 299, 691-694.
- Hofmann, W., 1998. Cladocerans and chironomids as indicators of lake level changes in north temperate lakes. *Journal of Paleolimnology*.

- Hogg, A., Hua, Q., Blackwell, P., Niu, M., Buck, C., Guilderson, T., Zimmerman, S., 2013. SHCal13 Southern Hemisphere Calibration, 0-50,000 years cal BP. *Radiocarbon* 55, 1889-1903.
- Holden, J., 2011. *Physical Geography: The Basics*. Taylor and Francis, Hoboken.
- Holz, A., Wood, S.W., Veblen, T.T., Bowman, D., 2015. Effects of high severity fire drove the population collapse of the subalpine Tasmanian endemic conifer *Athrotaxis cupressoides*. *Global Change Biology* 21, 445-458.
- Hopf, F., Shimeld, P., Pearson, S., 2002. *The Newcastle Pollen Collection*, 3.01 ed. School of Environmental and Life Sciences at the University of Newcastle, Australia.
- Hopf, F.V.L., Colhoun, E.A., Barton, C.E., 2000. Late-glacial and Holocene record of vegetation and climate from Cynthia Bay, Lake St Clair, Tasmania. *Journal of Quaternary Science* 15, 725-732.
- Horvatic, D., Stanley, H.E., Podobnik, B., 2011. Detrended cross-correlation analysis for non-stationary time series with periodic trends. *EPL (Europhysics Letters)* 94, 18007.
- Hotelling, H., 1933. Analysis of a complex of statistical variables into principal components. *Journal of Educational Psychology* 24, 498-520.
- Howarth, R.W., Marino, R., Lane, J., Cole, J.J., 1988. Nitrogen fixation in freshwater, estuarine, and marine ecosystems. 1. Rates and importance. *Limnology and Oceanography* 33, 669-687.
- Hustedt, F., 1930-1966. *Die Kieselalgen. Deutschlands, Osterreichs und der Schweiz unter Berucksichtigung der Ubrigen Lander Europas Sowie der angrenzenden Meeresgebiete*. Koeltz, Koenigstein.
- Huvane, J.K., Whitehead, D.R., 1996. The paleolimnology of North Pond: watershed-lake interactions. *Journal of Paleolimnology* 16.

Huxman, T.E., Wilcox, B.P., Breshears, D.D., Scott, R.L., 2005. Ecohydrological implications of woody plant encroachment. *Ecology* 86, 308-319.

IPCC, 2013. *Climate Change 2013 The Physical Science Basis*, in: *Change*, W.G.I.C.t.t.F.A.R.o.t.I.P.o.C. (Ed.). Cambridge University Press, Cambridge.

IPCC, 2014. *Climate Change 2014: Synthesis Report.*, in: Core Writing Team, Pachauri, R.K., Meyer, L.A. (Eds.). Intergovernmental Panel on Climate Change, Geneva, Switzerland,, p. 151.

Isbell, R.F., 2002. *The Australian Soil Classification : Revised Edition*. CSIRO Publishing, Collingwood, VIC, Australia.

Iverson, J., 1964. Retrogressive vegetational succession in the post-glacial. *The Journal of Animal Ecology* 33, 59-70.

Jackson, W., 1968. Fire, air, water and earth—an elemental ecology of Tasmania, *Proceedings of the ecological society of Australia*, Canberra, Australia, pp. 9-16.

Jackson, W., 1999a. The Tasmanian Environment, in: Reid, J.B., Hill, R.S., Brown, M.J., Hovenden, M.J. (Eds.), *Vegetation of Tasmania*. Australian Biological Resources Study, Tasmania, Australia, pp. 11-38.

Jackson, W., 1999b. Vegetation Types, in: Reid, J.B., Hill, R.S., Brown, M.J., Hovenden, M.J. (Eds.), *Vegetation of Tasmania*. Australian Biological Resources Study, Tasmania, Australia, pp. 1-10.

Jacobson, G.L., Birks, H.J.B., 1980. Soil development on recent end moraines of the Klutlan Glacier, Yukon Territory, Canada. *Quaternary Research* 14, 87-100.

Jarman, S.J., Crowden, R.K., Brown, M.J., 1982. A descriptive ecology of the vegetation in the lower Gordon River basin, Tasmania. *Papers and Proceedings of Royal Society of Tasmania* 116, 165-177.

- Jeppesen, E., Leavitt, P., De Meester, L., Jensen, J.P., 2001. Functional ecology and palaeolimnology: using cladoceran remains to reconstruct anthropogenic impact. *Trends in Ecology & Evolution* 16, 191-198.
- John, J., 1983. The diatom flora of the Swan River estuary, Western Australia. *Bibliotheca Phycologia*.
- Johnson, C.R., Banks, S.C., Barrett, N.S., Cazassus, F., Dunstan, P.K., Edgar, G.J., Frusher, S.D., Gardner, C., Haddon, M., Helidoniotis, F., Hill, K.L., Holbrook, N.J., Hosie, Graham W., Last, Peter R. , Ling, Scott D., Melbourne-Thomas, J., Miller, K., Pecl, Gretta T. , Richardson, A.J., Ridgway, K.R., Rintoul, S.R., Ritz, D.A., Ross, J., Sanderson, J.C., Shepherd, S.A., Slotwinski , A., Swadling, K.M., Taw, N., 2011. Climate change cascades: Shifts in oceanography, species' ranges and subtidal marine community dynamics in eastern Tasmania. *Journal of Experimental Marine Biology and Ecology* 400, 17-32.
- Jones, R.N., Bowler, J.M., McMahon, T.A., 1998. A high resolution Holocene record of P/E ratio from closed lakes, western Victoria. *Palaeoclimates* 3, 51-82.
- Jones, V.J., Stevenson, A.C., Battarbee, R.W., 1989. Acidification of lakes in Galloway, south west Scotland: a diatom and pollen study of the post-glacial history of the Round Loch of Glenhead. *The Journal of Ecology* 77, 1-23.
- Joniak, T., Kraska, M., 1999. Contribution to the limnology of three dystrophic lakes of the Drawieński National Park, northern Poland. *Acta Hydrobiologica* 41, 191-196.
- Juggins, S., 2016. Package 'rioja', Analysis of Quaternary Science Data, 0.9-7 ed.
- Juggins, S., Simpson, G., 2012. Analysing Palaeolimnological Data with R, International Palaeolimnology Symposium 2012, University Marine Biological Station, Millport, Scotland.
- Kamenik, C., Szeroczyńska, K., Schmidt, R., 2007. Relationships among recent Alpine Cladocera remains and their environment: implications for climate-change studies. *Hydrobiologia* 594, 33-46.

- Kantvilas, G., Jarman, S.J., 1988. Lichens of buttongrass (*Gymnoschoenus*) moorland in Tasmania. *Papers and Proceedings of the Royal Society of Tasmania* 122, 1-17.
- Karl, D., Letelier, R., Tupas, L., Dore, J., Christian, J., Hebel, D., 1997. The role of nitrogen fixation in biogeochemical cycling in the subtropical North Pacific Ocean. *Nature* 388, 533-538.
- Kattel, G., Gell, P., Perga, M.E., Jeppesen, E., 2015. Tracking a century of change in trophic structure and dynamics in a floodplain wetland: integrating palaeoecological and palaeoisotopic evidence. *Freshwater Biology* 60, 711-723.
- Kattel, G., Gell, P., Zawadzki, A., Barry, L., 2017. Palaeoecological evidence for sustained change in a shallow Murray River (Australia) floodplain lake: regime shift or press response? *Hydrobiologia* 787, 269-290.
- Kattel, G.R., 2012. Can we improve management practice of floodplain lakes using cladoceran zooplankton? *River Research and Applications* 28, 1113-1120.
- Kattel, G.R., Augustinus, P.C., 2010. Cladoceran-inferred environmental change during the LGM to Holocene transition from Onepoto maar paleolake, Auckland, New Zealand. *New Zealand Journal of Geology and Geophysics* 53, 31-42.
- Kelly, R.F., Higuera, P.E., Barrett, C.M., Hu, F.S., 2011. A signal-to-noise index to quantify the potential for peak detection in sediment–charcoal records. *Quaternary Research* 75, 11-17.
- Kershaw, A.P., 1976. A Late Pleistocene and Holocene Pollen Diagram from Lynch's Crater, northeastern Queensland, Australia. *New Phytologist* 77, 469-498.
- Kershaw, A.P., 1986. Climatic change and Aboriginal burning in north-east Australia during the last two glacial/interglacial cycles. *Nature* 322, 47-49.
- Kershaw, A.P., 1995. Environmental change in Greater Australia. *Antiquity* 69, 656-675.

Ketterings, Q.M., Bigham, J.M., Laperche, V., 2000. Changes in soil mineralogy and texture caused by slash-and-burn fires in Sumatra, Indonesia. *Soil Science Society of America Journal* 64, 1108-1117.

Kilian, R., Lamy, F., 2012. A review of Glacial and Holocene paleoclimate records from southernmost Patagonia (49–55 S). *Quaternary Science Reviews* 53, 1-23.

Kilroy, C., Sabbe, K., Bergey, E.A., Vyverman, W., Lowe, R., 2003. New species of *Fragilariforma* (Bacillariophyceae) from New Zealand and Australia. *New Zealand Journal of Botany* 41, 535-554.

Kirkpatrick, J., 1983. Treeless plant communities of the Tasmanian high country, *Proceedings of the Ecological Society of Australia*, pp. 61-77.

Kirkpatrick, J., Bridle, K., 1998. Environmental relationships of floristic variation in the alpine vegetation of southeast Australia. *Journal of Vegetation Science* 9, 251-260.

Kirkpatrick, J., Hardwood, C.E., 1980. Vegetation of an infrequently burned Tasmanian mountain region. *Proceedings of the Royal Society of Victoria* 91, 79-102.

Kirkpatrick, J.B., Dickinson, K.J.M., 1984. The impact of fire on Tasmanian alpine vegetation and soils. *Australian Journal of Botany* 32, 613-629.

Kirschbaum, M.U.F., 1995. The temperature dependence of soil organic matter decomposition, and the effect of global warming on soil organic C storage. *Soil Biology and Biochemistry* 27, 753-760.

Kitchener, A., Harris, S., 2013. *From Forest to Fjaeldmark: Description of Tasmania's Vegetation*, 2 ed. Department of Primary Industries, Parks, Water and Environment, Tasmania.

Kitzberger, T., Veblen, T.T., 2003. Influences of climate on fire in northern Patagonia, Argentina, in: Montenegro, G., Swetnam, T.W. (Eds.), *Fire and Climatic Change in Temperate Ecosystems of the western Americas*. Springer, New York, pp. 296-321.

- Klose, K., Cooper, S.D., Bennett, D.M., 2015. Effects of wildfire on stream algal abundance, community structure, and nutrient limitation. *Freshwater Science* 34, 1494-1509.
- Kociolek, J.P.S., Sarah A., Sabbe, K., Vyverman, W., 2004. New *Gomphonema* (Bacillariophyta) species from Tasmania. *Phycologia* 43, 427-444.
- Köhler, S., Buffam, I., Seibert, J., Bishop, K., Laudon, H., 2009. Dynamics of stream water TOC concentrations in a boreal headwater catchment: Controlling factors and implications for climate scenarios. *Journal of Hydrology* 373, 44-56.
- Koinig, K.A., Shotyk, W., Lotter, A.F., Ohlendorf, C., Sturm, M., 2003. 9000 years of geochemical evolution of lithogenic major and trace elements in the sediment of an alpine lake—the role of climate, vegetation, and land-use history. *Journal of Paleolimnology* 30, 301-320.
- Kokfelt, U., Reuss, N., Struyf, E., Sonesson, M., Rundgren, M., Skog, G., Rosén, P., Hammarlund, D., 2010. Wetland development, permafrost history and nutrient cycling inferred from late Holocene peat and lake sediment records in subarctic Sweden. *Journal of Paleolimnology* 44, 327-342.
- Korhola, A., Olander, H., Blom, T., 2000. Cladoceran and chironomid assemblages as qualitative indicators of water depth in subarctic Fennoscandian lakes. *Journal of Paleolimnology* 24, 43-54.
- Korhola, A., Rautio, M., 2001. Cladocera and Other Branchiopod Crustaceans, in: Smol, J.P., Birks, H.J.B.L., W M. (Eds.), *Tracking Environmental Change Using Lake Sediments. Volume 4: Zoological Indicators*. Kluwer Academic Publishers, Dordrecht, The Netherlands, pp. 5-41.
- Korhola, A., Virkanen, J., Tikkanen, M., Blom, T., 1996. Fire-induced pH rise in a naturally acid hill-top lake, southern Finland: a palaeoecological survey. *Journal of Ecology* 84, 257-265.
- Korsman, T., Segerstrom, U., 1998. Forest fire and lake-water acidity in a northern Swedish boreal area: Holocene changes in lake-water quality at Makkassjon. *Journal of Ecology* 86, 113-124.

- Koste, W., Shiel, R., 1986. Rotifera from Australian inland waters. I. Bdelloidea (Rotifera: Digononta). *Marine and Freshwater Research* 37, 765-792.
- Koste, W., Shiel, R., 1987a. Rotifera from Australian inland waters. II. Epiphaniidae and Brachionidae (Rotifera: Monogononta). *Invertebrate Systematics* 1, 949-1021.
- Koste, W., Shiel, R., 1989a. Rotifera from Australian inland waters III. Euchlanidae, Mytilinidae and Trichotriidae (Rotifera: Monogononta). *Transactions of the Royal Society of South Australia* 113, 85-114.
- Koste, W., Shiel, R., 1989b. Rotifera from Australian inland waters. IV. Colurellidae (Rotifera: Monogononta). *Transactions of the Royal Society of South Australia* 113, 119-143.
- Koste, W., Shiel, R.J., 1987b. Tasmanian Rotifera: affinities with the Australian fauna. *Hydrobiologia* 147, 31-43.
- Krammer, K., Lange-Bertalot, H., 1986. *Susswasserflora von Mit- teleuropa. Bacillariophyceae. Vol. I.* Gustav Fischer Verlag Jena.
- Krammer, K., Lange-Bertalot, H., 1988. *Susswasserflora von Mit- teleuropa. Bacillariophyceae. Vol. II.* Gustav Fischer Verlag Jena.
- Krammer, K., Lange-Bertalot, H., 1991a. *Susswasserflora von Mit- teleuropa. Bacillariophyceae. Vol. III.* Gustav Fischer Verlag Jena.
- Krammer, K., Lange-Bertalot, H., 1991b. *Susswasserflora von Mit- teleuropa. Bacillariophyceae. Vol. IV.* Gustav Fischer Verlag Jena.
- Krawchuk, M.A., Moritz, M.A., Parisien, M.-A., Van Dorn, J., Hayhoe, K., 2009. Global pyrogeography: the current and future distribution of wildfire. *PloS one* 4, e5102.
- Kutiel, P., Inbar, M., 1993. Fire impacts on soil nutrients and soil erosion in a Mediterranean pine forest plantation. *Catena* 20, 129-139.

- Kylander, M.E., Ampel, L., Wohlfarth, B., Veres, D., 2011. High-resolution X-ray fluorescence core scanning analysis of Les Echets (France) sedimentary sequence: new insights from chemical proxies. *Journal of Quaternary Science* 26, 109-117.
- Laird, K.R., Fritz, S.C., Maasch, K.A., Cumming, B.F., 1996. Greater drought intensity and frequency before AD 1200 in the Northern Great Plains, USA. *Nature* 384, 552-554.
- Lal, R., 1993. Tillage effects on soil degradation, soil resilience, soil quality, and sustainability. *Soil and Tillage Research* 27, 1-8.
- Lamb, A.L., Leng, M.J., Mohammed, M.U., Lamb, H.F., 2004. Holocene climate and vegetation change in the Main Ethiopian Rift Valley, inferred from the composition (C/N and $\delta^{13}\text{C}$) of lacustrine organic matter. *Quaternary Science Reviews* 23, 881-891.
- Lamb, A.L., Wilson, G.P., Leng, M.J., 2006. A review of coastal palaeoclimate and relative sea-level reconstructions using $\delta^{13}\text{C}$ and C/N ratios in organic material. *Earth-Science Reviews* 75, 29-57.
- Lamy, F., Kilian, R., Arz, H.W., Francois, J.P., Kaiser, J., 2010. Holocene changes in the position and intensity of the southern westerly wind belt. *Nature Geoscience* 3, 695-699.
- Lancashire, A.K., Flenley, J.R., Harper, M., 2002. Late Glacial beech forest: an 18,000–5000-BP pollen record from Auckland, New Zealand. *Global and Planetary Change* 33, 315-327.
- Lane, P.N.J., Sheridan, G.J., Noske, P.J., Sherwin, C.B., 2008. Phosphorus and nitrogen exports from SE Australian forests following wildfire. *Journal of Hydrology* 361, 186-198.
- Last, W.M., Smol, J.P., 2001. *Tracking Environmental Change Using Lake Sediments: Volume 1: Basin Analysis, Coring, and Chronological Techniques*. Kluwer Academic Publishers, Dordrecht, The Netherlands.

- Law, A.C., Anderson, N.J., McGowan, S., 2015. Spatial and temporal variability of lake ontogeny in southwestern Greenland. *Quaternary Science Reviews* 126, 1-16.
- Le Clercq, M., Van Der Plicht, J., Gröning, M., 1998. New ^{14}C Reference Materials with Activities of 15 and 50 pMC. *Radiocarbon* 40, 295-297.
- Legendre, P., Birks, H.J.B., 2012a. Clustering and Partitioning, in: Birks, H.J.B., Lotter, A.F., Juggins, S., Smol, J.P. (Eds.), *Tracking Environmental Change using Lake Sediments: Data Handling and Numerical Techniques*. Springer Science, Dordrecht Heidelberg New York London.
- Legendre, P., Birks, H.J.B., 2012b. From Classical to Canonical Ordination, in: Birks, H.J.B., Lotter, A.F., Juggins, S., Smol, J.P. (Eds.), *Tracking Environmental Change using Lake Sediments: Data Handling and Numerical Techniques*. Springer Science, Dordrecht Heidelberg New York London.
- Lenton, T.M., 2011. Early warning of climate tipping points. *Nature Climate Change* 1, 201-209.
- Lenton, T.M., Held, H., Kriegler, E., Hall, J.W., Lucht, W., Rahmstorf, S., Schellnhuber, H., 2008. Tipping elements in the Earth's climate system. *Proceedings of the National Academy of Sciences* 105, 1786-1793.
- Leys, B., Higuera, P.E., McLauchlan, K.K., Dunnette, P.V., 2016. Wildfires and geochemical change in a subalpine forest over the past six millennia. *Environmental Research Letters* 11, 125003.
- Lian, O.B., Huntley, D.J., 2001. Luminescence Dating, in: Last, W.M., Smol, J.P. (Eds.), *Tracking Environmental Change Using Lake Sediments. Volume 1: Basin Analysis, Coring, Chronological Techniques*. Kluwer Academic Publishers, Dordrecht, The Netherlands, pp. 261-282.
- Lim, J., Epureanu, B.I., 2011. Forecasting a class of bifurcations: Theory and experiment. *Physical Review E* 83, 016203.

- Lima, M., Stenseth, N.C., Jaksic, F.M., 2002. Food web structure and climate effects on the dynamics of small mammals and owls in semi-arid Chile. *Ecology Letters* 5, 273-284.
- Liu, K.B., 1990. Holocene paleoecology of the boreal forest and Great Lakes-St. Lawrence forest in northern Ontario. *Ecological Monographs* 60, 179-212.
- Livingstone, D.A., 1955. A lightweight piston sampler for lake deposits. *Ecology* 36, 137-139.
- Lotter, A.F., 2001. The palaeolimnology of Soppensee (Central Switzerland), as evidenced by diatom, pollen, and fossil-pigment analyses. *Journal of Paleolimnology* 25, 65-79.
- Lotter, A.F., Birks, H.J.B., Eicher, U., Hofmann, W., 2000. Younger Dryas and Allerød summer temperatures at Gerzensee (Switzerland) inferred from fossil pollen and cladoceran assemblages. *Palaeogeography, Palaeoclimatology, Palaeoecology* 159, 349-361.
- Lotter, A.F., Birks, H.J.B., Hofmann, W., Marchetto, A., 1997. Modern diatom, cladocera, chironomid, and chrysophyte cyst assemblages as quantitative indicators for the reconstruction of past environmental conditions in the Alps. I. Climate. *Journal of Paleolimnology* 18, 395-420.
- Lough, J.M., Fritts, H.C., 1987. An assessment of the possible effects of volcanic eruptions on North American climate using tree-ring data, 1602 to 1900 AD. *Climatic Change* 10, 219-239.
- MacDonald, G.M., Beukens, R.P., Kieser, W., 1991. Radiocarbon dating of limnic sediments: a comparative analysis and discussion. *Ecology* 72, 1150-1155.
- MacDonald, G.M., Edwards, T.W.D., Moser, K.A., Pienitz, R., 1993. Rapid response of treeline vegetation and lakes to past climate warming. *Nature* 361, 243-246.
- Macphail, M., 1986. 'Over the top': pollen based reconstructions of past alpine floras and vegetation in Tasmania. *Flora and Fauna of Alpine Australia: Ages and Origins*. CSIRO, Melbourne, 173-204.

- Macphail, M., Colhoun, E., 1985. Late last glacial vegetation, climates and fire activity in southwest Tasmania. *Search* 16, 43-45.
- Macphail, M., Pemberton, M., Jacobson, G., 1999. Peat mounds of southwest Tasmania: possible origins. *Australian Journal of Earth Sciences* 46, 667-677.
- Macphail, M.K., 1979. Vegetation and climates in southern Tasmania since the last glaciation. *Quaternary Research* 11, 306-341.
- Mariani, M., Connor, S.E., Fletcher, M.S., Theuerkauf, M., Kuneš, P., Jacobsen, G., Saunders, K.M., Zawadzki, A., 2017a. How old is the Tasmanian cultural landscape? A test of landscape openness using quantitative land-cover reconstructions. *Journal of Biogeography* 44, 2410-2420.
- Mariani, M., Fletcher, M.S., 2016a. The Southern Annular Mode determines inter-annual and centennial-scale fire activity in temperate southwest Tasmania, Australia. *Geophysical Research Letters* 43, 1702-1709.
- Mariani, M., Fletcher, M.S., 2017b. Long-term climate dynamics in the southern extra-tropics revealed from sedimentary charcoal analysis. *Quaternary Science Reviews* 173, 187-192.
- Mariani, M., Fletcher, M.S., Drysdale, R.N., Saunders, K.M., Heijnis, H., Jacobsen, G., Zawadzki, A., 2017c. Coupling of the Intertropical Convergence Zone and Southern Hemisphere mid-latitude climate during the early to mid-Holocene. *Geology* 45, 1083-1086.
- Mariani, M., Fletcher, M.S., Holz, A., Nyman, P., 2016b. ENSO controls interannual fire activity in southeast Australia. *Geophysical Research Letters* 43, 10891-10900.
- Markgraf, V., Bradbury, P.J., Busby, J.R., 1986. Paleoclimates in Southwestern Tasmania during the Last 13,000 Years. *PALAIOS* 1, 368-380.

- Markgraf, V., Díaz, H.F., 2000. The past ENSO record: a synthesis, in: Diaz, H.F., Markgraf, V. (Eds.), *El Niño and the Southern Oscillation: Multiscale Variability and Global and Regional Impacts*. Cambridge University Press, Cambridge, UK, pp. 465-488.
- Matthias, I., Giesecke, T., 2014. Insights into pollen source area, transport and deposition from modern pollen accumulation rates in lake sediments. *Quaternary Science Reviews* 87, 12-23.
- McAndrews, J.H., Campbell, I.D., 1993. 6 ka Mean July Temperature in Eastern Canada from Bartlein and Webb's (1985) Pollen Transfer Functions: Comments and Illustrations, *Proxy Climate Data and Models of the Six Thousand Years before Present Time Interval: The Canadian Perspective*. Geological Survey of Canada, Canadian Global Change Program: Incidental Report Series, pp. 22-25.
- McBride, J.L., Nicholls, N., 1983. Seasonal relationships between Australian rainfall and the Southern Oscillation. *Monthly Weather Review* 111, 1998-2004.
- McCune, B., Mefford, M.J., 2011. *PC-ORD, Multivariate Analysis of Ecological Data*, 6.08 ed. MiM Software, Glendon Beach, Oregon, USA.
- McGlone, M.S., 1989. The Polynesian settlement of New Zealand in relation to environmental and biotic changes. *New Zealand Journal of Ecology* 12, 115-129.
- McGlone, M.S., Hall, G.M.J., Wilmshurst, J.M., 2010a. Seasonality in the early Holocene: Extending fossil-based estimates with a forest ecosystem process model. *The Holocene* 21, 517-526.
- McGlone, M.S., Turney, C., Wilmshurst, J.M., 2004. Late-glacial and Holocene vegetation and climatic history of the Cass Basin, central South Island, New Zealand. *Quaternary Research* 62, 267-279.
- McGlone, M.S., Turney, C., Wilmshurst, J.M., Renwick, J., Pahnke, K., 2010b. Divergent trends in land and ocean temperature in the Southern Ocean over the past 18,000 years. *Nature Geoscience* 3.

- McWethy, D.B., Higuera, P.E., Whitlock, C., Veblen, T.T., Bowman, D.M.J.S., Cary, G.J., Haberle, S.G., Keane, R.E., Maxwell, B.D., McGlone, M.S., Perry, G.L.W., Wilmshurst, J.M., Holz, A., Tepley, A.J., 2013. A conceptual framework for predicting temperate ecosystem sensitivity to human impacts on fire regimes. *Global Ecology and Biogeography*.
- Meyers, P.A., 1994. Preservation of elemental and isotopic source identification of sedimentary organic matter. *Chemical Geology* 114, 289-302.
- Meyers, P.A., Eadie, B.J., 1993. Sources, degradation and recycling of organic matter associated with sinking particles in Lake Michigan. *Organic Geochemistry* 20, 47-56.
- Meyers, P.A., Teranes, J.L., 2001. Sediment Organic Matter, in: Last, W.M., Smol, J.P. (Eds.), *Tracking environmental change using lake sediments*. Springer, Netherlands, pp. 239-269.
- Michelutti, N., Douglas, M.S., Smol, J.P., 2003. Diatom response to recent climatic change in a high arctic lake (Char Lake, Cornwallis Island, Nunavut). *Global and Planetary Change* 38, 257-271.
- Michelutti, N., Wolfe, A.P., Cooke, C.A., Hobbs, W.O., Vuille, M., Smol, J.P., 2015. Climate change forces new ecological states in tropical Andean lakes. *PloS one* 10, e0115338.
- Mills, K., Schillereff, D., Talbot, É., Gell, P., Anderson, J.N., Arnaud, F., Dong, X., Jones, M., McGowan, S., Massaferrò, J., Moorhouse, H., Perez, L., Ryves, D., B., 2017. Deciphering long term records of natural variability and human impact as recorded in lake sediments: a palaeolimnological puzzle. *Wiley Interdisciplinary Reviews: Water* 4, 1195.
- Mischke, S., Rajabov, I., Mustaeva, N., Zhang, C., Herzsuh, U., Boomer, I., Brown, E.T., Andersen, N., Myrbo, A., Ito, E., 2010. Modern hydrology and late Holocene history of Lake Karakul, eastern Pamirs (Tajikistan): a reconnaissance study. *Palaeogeography, Palaeoclimatology, Palaeoecology* 289, 10-24.

- Mook, W.G., 1986. Recommendations/resolutions adopted by the 12th International Radiocarbon Conference. *Radiocarbon*, 799.
- Mook, W.G., van de Plassche, O., 1986. Radiocarbon dating, in: van de Plassche, O. (Ed.), *Sea-level research: a manual for the collection and evaluation of data*. Free University, Amsterdam, pp. 525-560.
- Moore, P.D., 2002. The future of cool temperate bogs. *Environmental Conservation* 29, 3-20.
- Moos, M.T., Cumming, B.F., 2011. Changes in the parkland-boreal forest boundary in northwestern Ontario over the Holocene. *Quaternary Science Reviews* 30, 1232-1242.
- Moos, M.T., Laird, K.R., Cumming, B.F., 2009. Climate-related eutrophication of a small boreal lake in northwestern Ontario: a palaeolimnological perspective. *The Holocene* 19, 359-367.
- Moreno, P.I., 2004. Millennial-scale climate variability in northwest Patagonia over the last 15 000 yr. *Journal of Quaternary Science* 19, 35-47.
- Moreno, P.I., Francois, J.P., Moy, C.M., Villa-Martínez, R., 2010. Covariability of the Southern Westerlies and atmospheric CO₂ during the Holocene. *Geology* 38, 727-730.
- Moreno, P.I., León, A.L., 2003. Abrupt vegetation changes during the last glacial to Holocene transition in mid-latitude South America. *Journal of Quaternary Science* 18, 787-800.
- Moros, M., De Deckker, P., Jansen, E., Perner, K., Telford, R.J., 2009. Holocene climate variability in the Southern Ocean recorded in a deep-sea sediment core off South Australia. *Quaternary Science Reviews* 28, 1932-1940.
- Morris, J.L., McLauchlan, K.K., Higuera, P.E., 2015. Sensitivity and complacency of sedimentary biogeochemical records to climate-mediated forest disturbances. *Earth-Science Reviews* 148, 121-133.

- Moy, C.M., Moreno, P., Dunbar, R.B., Kaplan, M.R., Francois, J.-P., Villalba, R., Haberzettl, T., 2009. Climate Change in Southern South America During the Last Two Millennia, in: Vimeux, F. (Ed.), *Past climate variability in South America and surrounding regions*. Springer, Netherlands, pp. 353-393.
- Moy, C.M., Seltzer, G.O., Rodbell, D.T., Anderson, D.M., 2002. Variability of El Niño/Southern Oscillation activity at millennial timescales during the Holocene epoch. *Nature* 420, 162-165.
- Murphy, B.P., Bradstock, R.A., Boer, M.M., Carter, J., Cary, G.J., Cochrane, M.A., Fensham, R.J., Russell-Smith, J., Williamson, G.J., Bowman, D., 2013. Fire regimes of Australia: a pyrogeographic model system. *Journal of Biogeography* 40, 1048-1058.
- Murphy, B.P., Paron, P., Prior, L.D., Boggs, G.S., Franklin, D.C., Bowman, D., 2010. Using generalized autoregressive error models to understand fire–vegetation–soil feedbacks in a mulga–spinifex landscape mosaic. *Journal of Biogeography* 37, 2169-2182.
- Mustaphi, C.J.C., Pisaric, M.F.J., 2014. A classification for macroscopic charcoal morphologies found in Holocene lacustrine sediments. *Progress in Physical Geography* 38, 734-754.
- Nesje, A., 1992. A piston corer for lacustrine and marine sediments. *Arctic and Alpine Research*, 257-259.
- Newnham, R.M., Vandergoes, M.J., Hendy, C.H., 2007. A terrestrial palynological record for the last two glacial cycles from southwestern New Zealand. *Quaternary Science Reviews* 26, 517-535.
- Nicholls, N., Lucas, C., 2007. Interannual variations of area burnt in Tasmanian bushfires: relationships with climate and predictability. *International Journal of Wildland Fire* 16, 540-546.
- Niu, M., Heaton, T., Blackwell, P., Buck, C., 2013. The Bayesian approach to radiocarbon calibration curve estimation: the IntCal13, Marine13, and SHCal13 methodologies. *Radiocarbon* 55, 1905-1922.

- Nunez, M., Colhoun, E., 1986. A note on air temperature lapse rates on Mount Wellington, Tasmania, *Papers and Proceedings of the Royal Society of Tasmania*, pp. 11-15.
- Nürnberg, G.K., 1984. The prediction of internal phosphorus load in lakes with anoxic hypolimnia. *Limnology and Oceanography* 29, 111-124.
- Nürnberg, G.K., 1988. Prediction of Phosphorus Release Rates from Total and Reductant-Soluble Phosphorus in Anoxic Lake Sediments. *Canadian Journal of Fisheries and Aquatic Sciences* 45, 453-462.
- Ogden, R.W., 1997. The effects of European settlement on the biodiversity of chydorid Cladocera in billabongs of the south-east Murray Basin. *Memoirs of the Museum of Victoria* 56, 505-511.
- Ogden, R.W., 2000. Modern and historical variation in aquatic macrophyte cover of billabongs associated with catchment development. *Regulated Rivers: Research & Management* 16, 497-512.
- Ogutu, J.O., Owen-Smith, N., 2003. ENSO, rainfall and temperature influences on extreme population declines among African savanna ungulates. *Ecology Letters* 6, 412-419.
- Oksanen, J., Blanchet, F.G., Kindt, R., Legendre, P., Minchin, P.R., O'Hara, R.B., Simpson, G.L., Solymos, P., Stevens, M.H.H., Wagner, H., 2016. *vegan, Community Ecology Package*, 2.3-5 ed.
- Olsson, I.U., 1986. Radiometric dating, in: Berglund, B.E. (Ed.), *Handbook Palaeoecology and Palaeohydrology*. John Wiley & Sons, Chichester, pp. 273-312.
- Orians, G.H., Milewski, A.V., 2007. Ecology of Australia: the effects of nutrient-poor soils and intense fires. *Biological Reviews* 82, 393-423.
- Parisien, M.A., Moritz, M.A., 2009. Environmental controls on the distribution of wildfire at multiple spatial scales. *Ecological Monographs* 79, 127-154.

Parks & Wildlife Service, 2008. *Alpine and Subalpine Plants of Tasmania: Communities*. Department of Primary Industries, Parks, Water and Environment; Tasmanian Government, Tasmania.

Pastor, J., Post, W.M., 1986. Influence of climate, soil moisture, and succession on forest carbon and nitrogen cycles. *Biogeochemistry* 2, 3-27.

Pausas, J.G., Bradstock, R.A., 2007. Fire persistence traits of plants along a productivity and disturbance gradient in mediterranean shrublands of south-east Australia. *Global Ecology and Biogeography* 16, 330-340.

Pausas, J.G., Ribeiro, E., 2013. The global fire-productivity relationship. *Global Ecology and Biogeography* 22, 728-736.

Pearson, R.G., Dawson, T.P., 2003. Predicting the impacts of climate change on the distribution of species: are bioclimate envelope models useful? *Global Ecology and Biogeography* 12, 361-371.

Pedro, J.B., Bostock, H.C., Bitz, C.M., He, F., Vandergoes, M.J., Steig, E.J., Chase, B.M., Krause, C.E., Rasmussen, S.O., Markle, B.R., Cortese, G., 2016. The spatial extent and dynamics of the Antarctic Cold Reversal. *Nature Geoscience* 9, 51-55.

Pemberton, J., McKibben, J., 2004. Loongana, Digital Geological Atlas 1:25000 Scale Series. Mineral Resources Tasmania, Tasmania, p. Sheet 4041.

Pemberton, M., 1988. Soil erosion between Birchs Inlet and Elliott Bay, southwestern Tasmania. *Papers and proceedings of the Royal Society of Tasmania* 122, 109-114.

Pemberton, M., 1989. Land systems of Tasmania. Region 7, South west, in: Agriculture, D.o. (Ed.). Department of Agriculture, Tasmania, Australia.

Perren, B.B., Axford, Y., Kaufman, D.S., 2017. Alder, Nitrogen, and Lake Ecology: Terrestrial-Aquatic Linkages in the Postglacial History of Lone Spruce Pond, Southwestern Alaska. *PloS one* 12, e0169106.

- Pesce, O.H., Moreno, P.I., 2014. Vegetation, fire and climate change in central-east Isla Grande de Chiloé (43 S) since the Last Glacial Maximum, northwestern Patagonia. *Quaternary Science Reviews* 90, 143-157.
- Petchey, O.L., McPhearson, P.T., Casey, T.M., Morin, P.J., 1999. Environmental warming alters food-web structure and ecosystem function. *Nature* 402, 69-72.
- Peterson, B.J., Fry, B., 1987. Stable isotopes in ecosystem studies. *Annual Review of Ecology and Systematics* 18, 293-320.
- Peterson, C.G., Stevenson, R.J., 1992. Resistance and resilience of lotic algal communities: importance of disturbance timing and current. *Ecology* 73, 1445-1461.
- Peterson, J.A., 1966. Glaciation of Frenchmans Cap-National Park, *Papers and Proceedings of the Royal Society of Tasmania*, pp. 117-134.
- Philander, S.G.H., 1983. El Niño Southern Oscillation phenomena. *Nature* 302, 295-301.
- Pienitz, R., Smol, J.P., MacDonald, G.M., 1999. Paleolimnological Reconstruction of Holocene Climatic Trends from Two Boreal Treeline Lakes, Northwest Territories, Canada. *Arctic, Antarctic, and Alpine Research* 31, 82-93.
- Pitman, A.J., Narisma, G.T., McAneney, J., 2007. The impact of climate change on the risk of forest and grassland fires in Australia. *Climatic Change* 84, 383-401.
- Postel, S., Carpenter, S., 1997. Freshwater Ecosystem Services, in: Daily, G. (Ed.), *Nature's services: Societal dependence on natural ecosystems*. Island Press, USA, pp. 195-214.
- Power, S., Delage, F., Chung, C., Kociuba, G., Keay, K., 2013. Robust twenty-first-century projections of El Niño and related precipitation variability. *Nature* 502, 541-545.

- Prager, M.H., Hoenig, J.M., 1992. Can we determine the significance of key-event effects on a recruitment time series?—a power study of superposed epoch analysis. *Transactions of the American Fisheries Society* 121, 123-131.
- Prebble, M., Sim, R., Finn, J., Fink, D., 2005. A Holocene pollen and diatom record from Vanderlin Island, Gulf of Carpentaria, lowland tropical Australia. *Quaternary Research* 64, 357-371.
- Prentice, I.C., 1985. Pollen representation, source area, and basin size: toward a unified theory of pollen analysis. *Quaternary Research* 23, 76-86.
- Prentice, I.C., Cramer, W., Harrison, S.P., Leemans, R., Monserud, R.A., Solomon, A.M., 1992. A global biome model based on plant physiology and dominance, soil properties and climate. *Journal of Biogeography* 19, 117-134.
- Prentice, I.C., Harrison, S.P., 2009. Ecosystem effects of CO₂ concentration: evidence from past climates. *Climate of the Past* 5, 297-307.
- Prentice, L.C., 1978. Modern pollen spectra from lake sediments in Finland and Finnmark, north Norway. *Boreas* 7, 131-153.
- Punning, J.-M., Koff, T., 1997. The landscape factor in the formation of pollen records in lake sediments. *Journal of Paleolimnology* 18, 33-44.
- R Development Core Team, 2014. R: A language and environment for statistical computing., 3.1.1 ed. R Foundation for Statistical Computing, Vienna, Austria.
- Raison, R., 1979. Modification of the soil environment by vegetation fires, with particular reference to nitrogen transformations: a review. *Plant and soil* 51, 73-108.
- Ramsey, C., 2005. OxCal Program, 3.10 ed.

- Raper, D.J., Zander, H., 2009. Paleoeology: An Untapped Resource for Teaching Environmental Change. *International Journal of Environmental and Science Education* 4, 441-447.
- Read, J., Hill, R.S., 1985. Dynamics of *Nothofagus*-dominated rainforest on mainland Australia and lowland Tasmania. *Vegetatio* 63, 67-78.
- Reavie, E.D., Sgro, G.V., Estep, L.R., Bramburger, A.J., Chraïbi, V.L., Pillsbury, R.W., Cai, M., Stow, C.A., Dove, A., 2017. Climate warming and changes in *Cyclotella sensu lato* in the Laurentian Great Lakes. *Limnology and Oceanography* 62, 768-783.
- Rees, A.B.H., Cwynar, L.C., 2010a. Evidence for early postglacial warming in Mount field National Park, Tasmania. *Quaternary Science Reviews* 29, 443-454.
- Rees, A.B.H., Cwynar, L.C., 2010b. A test of Tyler's Line—response of chironomids to a pH gradient in Tasmania and their potential as a proxy to infer past changes in pH. *Freshwater Biology* 55, 2521-2540.
- Rees, A.B.H., Cwynar, L.C., Fletcher, M.S., 2015. Southern Westerly Winds submit to the ENSO regime: A multiproxy paleohydrology record from Lake Dobson, Tasmania. *Quaternary Science Reviews* 126, 254-263.
- Reeves, J.M., Barrows, T.T., Cohen, T.J., Kiem, A.S., 2013. Climate variability over the last 35,000 years recorded in marine and terrestrial archives in the Australian region: an OZ-INTIMATE compilation. *Quaternary Science Reviews* 74, 21-34.
- Reid, M.A., Tibby, J.C., Penny, D., 1995. The use of diatoms to assess past and present water quality. *Australian Journal of Ecology* 20, 57-64.
- Reimer, P.J., Bard, E., Bayliss, A., Beck, W.J., Blackwell, P.G., Ramsey, C., Buck, C.E., Cheng, H., Edwards, L.R., Friedrich, M., 2013. IntCal13 and Marine13 radiocarbon age calibration curves 0–50,000 years cal BP. *Radiocarbon* 55, 1869-1887.

- Renberg, I., Korsman, T., Birks, H.J.B., 1993. Prehistoric increases in the pH of acid-sensitive Swedish lakes caused by land-use changes. *Nature* 362, 824-827.
- Robinson, C.T., Rushforth, S.R., 1987. Effects of physical disturbance and canopy cover on attached diatom community structure in an Idaho stream. *Hydrobiologia* 154, 49-59.
- Rodionov, S., Overland, J., 2005. Application of a sequential regime shift detection method to the Bering Sea ecosystem. *ICES Journal of Marine Science* 62, 328-332.
- Rodionov, S.N., 2004. A sequential algorithm for testing climate regime shifts. *Geophysical Research Letters* 31, 1-4.
- Romanin, L.M., Hopf, F., Haberle, S.G., Bowman, D.M., 2016. Fire regime and vegetation change in the transition from Aboriginal to European land management in a Tasmanian eucalypt savanna. *Australian Journal of Botany* 64, 427-440.
- Ropelewski, C.F., Halpert, M.S., 1987. Global and regional scale precipitation patterns associated with the El Niño/Southern Oscillation. *Monthly weather review* 115, 1606-1626.
- Rosenzweig, M.L., Abramsky, Z., 1993. How are diversity and productivity related, in: Schluter, D., Ricklefs, R.E. (Eds.), *Species Diversity in Ecological Communities: Historical and Geographical Perspectives*. University of Chicago Press, USA, pp. 52-65.
- Rothwell, R.G., Rack, F.R., 2006. New techniques in sediment core analysis: an introduction. *Geological Society* 267, 1-29.
- Round, F.E., 1957. The Late-Glacial and Post-Glacial Diatom Succession in the Kentmere Valley Deposit. *New Phytologist* 56, 98-126.

- Round, F.E., 1993. A Review and Methods for the Use of Epilithic Diatoms for Detecting and Monitoring Changes in River Water. HMSO, London.
- Rühland, K., Paterson, A.M., Smol, J.P., 2008. Hemispheric-scale patterns of climate-related shifts in planktonic diatoms from North American and European lakes. *Global Change Biology* 14, 2740-2754.
- Rühland, K.M., Paterson, A.M., Smol, J.P., 2015. Lake diatom responses to warming: reviewing the evidence. *Journal of Paleolimnology* 54, 1-35.
- Rull, V., 1991. Palaeoecological significance of chrysophycean stomatocysts: a statistical approach. *Hydrobiologia* 220, 161-165.
- Running, S.W., Reid, C.P., 1980. Soil temperature influences on root resistance of *Pinus contorta* seedlings. *Plant Physiology* 65, 635-640.
- Ryves, D.B., Battarbee, R.W., Fritz, S.C., 2009. The dilemma of disappearing diatoms: Incorporating diatom dissolution data into palaeoenvironmental modelling and reconstruction. *Quaternary Science Reviews* 28, 120-136.
- Sabbe, K., Vanhoutte, K., Lowe, R.L., Bergey, E.A., Biggs, B., Francoeur, S., Hodgson, D., Vyverman, W., 2001. Six new *Actinella* (Bacillariophyta) species from Papua New Guinea, Australia and New Zealand: further evidence for widespread diatom endemism in the Australasian region. *European Journal of Phycology* 36, 321-340.
- Saldaña, A.O., Hernández, C., Coopman, R.E., Bravo, L.A., Corcuera, L.J., 2010. Differences in light usage among three fern species of genus *Blechnum* of contrasting ecological breadth in a forest light gradient. *Ecological Research* 25, 273-281.
- Samson, J., Yeung, K., 1986. Some generalizations on the method of superposed epoch analysis. *Planetary and space science* 34, 1133-1142.

- Sandweiss, D.H., Maasch, K.A., Anderson, D.G., 1999. Transitions in the mid-Holocene. *Science* 283, 499-500.
- Sandweiss, D.H., Maasch, K.A., Burger, R.L., Richardson, J.B., Rollins, H.B., Clement, A., 2001. Variation in Holocene El Niño frequencies: Climate records and cultural consequences in ancient Peru. *Geology* 29, 603-606.
- Sandweiss, D.H., Richardson III, J.B., Reitz, E.J., Rollins, H.B., Maasch, K.A., 1996. Geoarchaeological evidence from Peru for a 5000 years BP onset of El Niño. *Science* 273, 1531-1533.
- Saros, J.E., Anderson, N.J., 2015. The ecology of the planktonic diatom *Cyclotella* and its implications for global environmental change studies. *Biological Reviews* 90, 522-541.
- Saros, J.E., Stone, J.R., Pederson, G.T., Slemmons, K.E.H., Spanbauer, T., Schliep, A., Cahl, D., Williamson, C.E., Engstrom, D.R., 2012. Climate-induced changes in lake ecosystem structure inferred from coupled neo-and paleoecological approaches. *Ecology* 90, 2155-2164.
- Saros, J.E., Strock, K.E., McCue, J., Hogan, E., Anderson, J.N., 2014. Response of *Cyclotella* species to nutrients and incubation depth in Arctic lakes. *Journal of Plankton Research* 36, 450-460.
- Saunders, K.M., 2011. A diatom dataset and diatom-salinity inference model for southeast Australian estuaries and coastal lakes. *Journal of Paleolimnology* 46, 525-542.
- Saunders, K.M., Harrison, J.J., Butler, E.C.V., Hodgson, D.A., McMinn, A., 2013a. Recent environmental change and trace metal pollution in World Heritage Bathurst Harbour, southwest Tasmania, Australia. *Journal of Paleolimnology* 50, 471-485.
- Saunders, K.M., Harrison, J.J., Hodgson, D.A., Jong, d.R., Mauchle, F., McMinn, A., 2013b. Ecosystem impacts of feral rabbits on World Heritage sub-Antarctic Macquarie Island: A palaeoecological perspective. *Anthropocene* 3, 1-8.

Saunders, K.M., Kamenik, C., Hodgson, D.A., Hunziker, S., Siffert, L., Fischer, D., Fujak, M., Gibson, J.A.E., Grosjean, M., 2012. Late Holocene changes in precipitation in northwest Tasmania and their potential links to shifts in the Southern Hemisphere westerly winds. *Global and Planetary Change* 92, 82-91.

Saunders, K.M., McMinn, A., Roberts, D., Hodgson, D.A., Heijnis, H., 2007. Recent human-induced salinity changes in Ramsar-listed Orielton Lagoon, south-east Tasmania, Australia: a new approach for coastal lagoon conservation and management. *Aquatic Conservation: Marine and Freshwater Ecosystems* 17, 51-70.

Scheffer, M., Bascompte, J., Brock, W.A., Brovkin, V., Carpenter, S.R., Dakos, V., Held, H., van Nes, E.H., Rietkerk, M., Sugihara, G., 2009. Early-warning signals for critical transitions. *Nature* 461, 53-59.

Scheffer, M., Carpenter, S., Foley, J.A., Folke, C., Walker, B., 2001. Catastrophic shifts in ecosystems. *Nature* 413, 591-596.

Scheffer, M., Carpenter, S.R., 2003. Catastrophic regime shifts in ecosystems: linking theory to observation. *Trends in ecology & evolution* 18, 648-656.

Scheffer, M., Carpenter, S.R., Dakos, V., Van Nes, E.H., 2015. Generic indicators of ecological resilience: inferring the chance of a critical transition. *The Annual Review of Ecology, Evolution, and Systematics* 46, 145-167.

Scheffer, M., Carpenter, S.R., Lenton, T.M., Bascompte, J., Brock, W.A., Dakos, V., van de Koppel, J., van de Leemput, I.A., Levin, S.A., Van Nes, E.H., Pascual, M., Vandermeer, J., 2012. Anticipating critical transitions. *Science* 338, 344-348.

Schindler, D.W., 1997. Widespread effects of Climate Warming on Freshwater Ecosystems in North America. *Hydrological Processes* 11, 1043-1067.

Schindler, D.W., 2001. The cumulative effects of climate warming and other human stresses on Canadian freshwaters in the new millennium. *Canadian Journal of Fisheries and Aquatic Sciences* 58, 18-29.

- Schindler, D.W., Bayley, S.E., Parker, B.R., 1996. The effects of climate warming on the properties of boreal lakes and streams at the Experimental Lakes Area, northwestern Ontario. *Limnology and Oceanography* 41, 1004-1017.
- Schulz, M., Stattegger, K., 1997. SPECTRUM: Spectral analysis of unevenly spaced paleoclimatic time series. *Computers & Geosciences* 23, 929-945.
- Scott, A.C., Bowman, D.M.J.S., Bond, W.J., Pyne, S., Alexander, M.E., 2014. *Fire on Earth: An Introduction*. John Wiley & Sons, Ltd, UK.
- Seddon, A.W.R., Cole, L.E., Morris, J., Fletcher, M.S., Willis, K.J., 2016. EcoRe3- Resistance, Recovery and Resilience of Long-term Ecological Systems, *PAGES Magazine*, p. 75.
- Seddon, A.W.R., Froyd, C.A., Witkowski, A., Willis, K.J., 2014. A quantitative framework for analysis of regime shifts in a Galápagos coastal lagoon. *Ecology* 95, 3046-3055.
- Seymour, D.B., Calver, C.R., 1995. Stratotectonic Elements Map, in: Land Information Bureau, D.o.E.a.L.M. (Ed.), NGMA TASGO Project: Geological Synthesis. Mineral Resources Tasmania, Tasmania.
- Sharp, N., 2016. Lightning strikes and climate change. *Arena Magazine*, 13-14.
- Shiel, R., Dickson, J., 1995. Cladocera recorded from Australia. *Transactions of the Royal Society of South Australia* 119, 29-40.
- Shiel, R., Koste, W., 1986. Australian Rotifera: Ecology and Biogeography, in: De Deckker, P., Williams, W.D. (Eds.), *Limnology in Australia*. Dr. W. Junk Publishers, Dordrecht/Boston/Lancaster, pp. 141-150.
- Shiel, R., Koste, W., Tan, L., 1989. Tasmania revisited: rotifer communities and habitat heterogeneity. *Hydrobiologia* 186/187, 239-245.

Shiel, R.J., 1995. A guide to identification of rotifers, cladocerans and copepods from Australian inland waters. Co-operative Research Centre for Freshwater Ecology, Albury, NSW, Australia.

Shulmeister, J., 1999. Australasian evidence for mid-holocene climate change implies precessional control of Walker Circulation in the Pacific. *Quaternary International* 57-58, 81-91.

Shulmeister, J., Lees, B.G., 1995. Pollen evidence from tropical Australia for the onset of an ENSO-dominated climate at c. 4000 BP. *The Holocene* 5, 10-18.

Siegenthaler, U., Eicher, U., 1986. Stable oxygen and carbon isotope analyses, in: Berglund, B.E. (Ed.), *Handbook Palaeoecology and Palaeohydrology*. John Wiley & Sons, Chichester, pp. 407-422.

Simpson, G., 2017. Generalised Additive Models, in: Beck, K.K. (Ed.), *Numerical Analysis of Palaeoenvironmental Data*. 2010–2017 Gavin Simpson, Adelaide, Australia.

Simpson, G.L., 2007. Analogue methods in palaeoecology: using the analogue package. *Journal of Statistical Software* 22, 1-29.

Simpson, G.L., Anderson, N.J., 2009. Deciphering the effect of climate change and separating the influence of confounding factors in sediment core records using additive models. *Limnology and Oceanography* 54, 2529-2541.

Simpson, G.L., Birks, H.J.B., 2012. Statistical Learning in Palaeolimnology, in: Birks, H.J.B., Lotter, A.F., Juggins, S., Smol, J.P. (Eds.), *Tracking Environmental Change Using Lake Sediments: Data Handling and Numerical Techniques*. Springer, Netherlands, pp. 249-327.

Simpson, G.L., Oksanen, J., 2016. Package: analogue, Analogue and Weighted Averaging Methods for Palaeoecology, 0.17-0 ed.

- Siteur, K., Eppinga, M.B., Doelman, A., Siero, E., Rietkerk, M., 2016. Ecosystems off track: rate-induced critical transitions in ecological models. *Oikos* 125, 1689-1699.
- Smirnov, N.N., Timms, B., 1983. A revision of the Australian Cladocera (Crustacea). *Records of the Australian Museum*, 1-132.
- Smith, H.G., Sheridan, G.J., Lane, P.N.J., Nyman, P., 2011. Wildfire effects on water quality in forest catchments: a review with implications for water supply. *Journal of Hydrology* 396, 170-192.
- Smol, J.P., 1992. Paleolimnology: an important tool for effective ecosystem management. *Journal of Aquatic Ecosystem Health* 1, 49-58.
- Smol, J.P., 2010. The power of the past: using sediments to track the effects of multiple stressors on lake ecosystems. *Freshwater Biology* 55, 43-59.
- Smol, J.P., Cumming, B.F., 2000. Tracking long-term changes in climate using algal indicators in lake sediments. *Journal of Phycology* 36, 986-1011.
- Smol, J.P., Douglas, M.S.V., 2007. From controversy to consensus: making the case for recent climate change in the Arctic using lake sediments. *Frontiers in Ecology and the Environment* 5, 466-474.
- Sommaruga-Wögrath, S., Koinig, K.A., Schmidt, R., Sommaruga, R., Tessadri, R., Psenner, R., 1997. Temperature effects on the acidity of remote alpine lakes. *Nature* 387, 64-67.
- Søndergaard, M., Jensen, J.P., Jeppesen, E., 2003. Role of sediment and internal loading of phosphorus in shallow lakes. *Hydrobiologia* 506-509, 135-145.
- Søndergaard, M., Jensen, P.J., Jeppesen, E., 2001. Retention and internal loading of phosphorus in shallow, eutrophic lakes. *The Scientific World Journal* 1, 427-442.
- Spaulding, S.A., Lubinski, D.J., Potapova, M., 2010. *Diatoms of the United States*.

- SPSS Statistics, 2012. Cross-Correlations, in: Centre, I.K. (Ed.). IBM.
- Sreenivasa, M.R., Duthie, H.C., 1973. The postglacial diatom history of Sunfish Lake, southwestern Ontario. *Canadian Journal of Botany* 51, 1599-1609.
- St. Jacques, J.M., Douglas, M., McAndrews, J.H., 2000. Mid-Holocene hemlock decline and diatom communities in van Nostrand Lake, Ontario, Canada. *Journal of Paleolimnology* 23, 385-397.
- Stace, H.C.T., 1968. Handbook of Australian soils. Rellim Technical Publications, Glenside, South Australia.
- Stahle, L.N., Chin, H., Haberle, S., Whitlock, C., 2017. Late-glacial and Holocene records of fire and vegetation from Cradle Mountain National Park, Tasmania, Australia. *Quaternary Science Reviews* 177, 57-77.
- Stahle, L.N., Whitlock, C., Haberle, S.G., 2016. A 17,000-Year-Long Record of Vegetation and Fire from Cradle Mountain National Park, Tasmania. *Frontiers in Ecology and Evolution* 4, 1-17.
- Stammerjohn, S.E., Martinson, D.G., 2008. Trends in Antarctic annual sea ice retreat and advance and their relation to El Niño–Southern Oscillation and Southern Annular Mode variability. *Journal of Geophysical Research* 113, 1-20.
- Stanley, S., Patrick, D.D., 2002. A Holocene record of allochthonous, aeolian mineral grains in an Australian alpine lake; implications for the history of climate change in southeastern Australia. *Journal of Paleolimnology* 27, 207-219.
- Steane, M.S., Tyler, P.A., 1982. Anomalous Stratification Behaviour of Lake Gorden, Headwater Reservoir of the Lower Gorden River, Tasmania. *Marine and Freshwater Research* 33, 739-760.
- Steinberg, C.E.W., 2003a. Direct Effects on Organisms and Niche Differentiation, Ecology of Humic Substances in Freshwaters: Determinants from Geochemistry to Ecological Niches. Springer, Heidelberg, Germany.

Steinberg, C.E.W., 2003b. Ecology of Humic Substances in Freshwaters: Determinants from Geochemistry to Ecological Niches. Springer, Heidelberg, Germany.

Stoermer, E.F., Smol, J.P., 1999. Applications and uses of diatoms: prologue. The diatoms: Applications for the environmental and earth sciences, 3-8.

Styger, J., Kirkpatrick, J.B., 2015. Less than 50 millimetres of rainfall in the previous month predicts fire in Tasmanian rainforest, Papers and Proceedings of the Royal Society of Tasmania, pp. 1-5.

Sugita, S., 1993. A model of pollen source area for an entire lake surface. Quaternary Research 39, 239-244.

Sugita, S., Hicks, S., Sormunen, H., 2010. Absolute pollen productivity and pollen northern Finland. Journal of Quaternary Science 25, 724-736.

□vegetation rel

Szeroczyńska, K., Sarmaja-Korjonen, K., 2007. Atlas of Subfossil Cladocera from Central and Northern Europe. Friends of the Lower Vistula Society, Swiecie.

Taffs, K.H., Farago, L.J., Heijnis, H., Jacobsen, G., 2007. A diatom-based Holocene record of human impact from a coastal environment: Tuckean Swamp, eastern Australia. Journal of Paleolimnology 39, 71-82.

Talbot, M.R., 2001. Nitrogen Isotopes in Palaeolimnology, in: Last, W.M., Smol, J.P. (Eds.), Tracking Environmental Change Using Lake Sediments. Volume 2: Physical and Geochemical Methods. Kluwer Academic Publishers, Dordrecht, The Netherlands., pp. 401-439.

Talbot, M.R., Johannessen, T., 1992. A high resolution palaeoclimatic record for the last 27,500 years in tropical West Africa from the carbon and nitrogen isotopic composition of lacustrine organic matter. Earth and Planetary Science Letters 110, 23-37.

- Talbot, M.R., Lærdal, T., 2000. The Late Pleistocene-Holocene palaeolimnology of Lake Victoria, East Africa, based upon elemental and isotopic analyses of sedimentary organic matter. *Journal of Paleolimnology* 23, 141-164.
- Tamm, C.O., 1991. Nitrogen in terrestrial ecosystems: questions of productivity, vegetational changes, and ecosystem stability. Springer-Verlag, Berlin, Germany.
- Telford, R.J., Heegaard, E., Birks, H.J.B., 2004. All age–depth models are wrong: but how badly? *Quaternary Science Reviews* 23, 1-5.
- Thomas, E.J., 2007. Diatoms and Invertebrates as Indicators of pH in Wetlands of the South-west of Western Australia, *Environmental Biology*. Curtin University of Technology, Perth, Western Australia, p. 273.
- Tibby, J., Gell, P.A., Fluin, J., Sluiter, I.R.K., 2007a. Diatom–salinity relationships in wetlands: assessing the influence of salinity variability on the development of inference models. *Hydrobiologia* 591, 207-218.
- Tibby, J., Haberle, S.G., 2007b. A late glacial to present diatom record from Lake Euramoo, wet tropics of Queensland, Australia. *Palaeogeography, Palaeoclimatology, Palaeoecology* 251, 46-56.
- Tibby, J., Penny, D., Leahy, P., Kershaw, A.P., 2012. Vegetation and water quality responses to Holocene climate variability in Lake Purrumbete, western Victoria., in: Haberle, S., David, B. (Eds.), *Peopled landscapes: archaeological and biogeographic approaches to landscapes*, Terra Australis. ANU E Press, Canberra, pp. 359-374.
- Timbal, B., Fawcett, R., 2013. A Historical Perspective on Southeastern Australian Rainfall since 1865 Using the Instrumental Record. *Journal of Climate* 26, 1112-1129.
- Tolonen, K., 1980. Pollen, algal remains and macrosubfossils from Lake Gallträsk, S. Finland. *Annales Botanici Fennici* 17, 394-405.

- Tudhope, A.W., Chilcott, C.P., McCulloch, M.T., Cook, E.R., 2001. Variability in the El Niño-Southern Oscillation through a glacial-interglacial cycle. *Science* 291, 1511-1517.
- Turney, C.S., Hobbs, D., 2006. ENSO influence on Holocene Aboriginal populations in Queensland, Australia. *Journal of Archaeological Science* 33, 1744-1748.
- Turney, C.S.M., Kershaw, A.P., Clemens, S.C., Branch, N., 2004. Millennial and orbital variations of El Niño/Southern Oscillation and high-latitude climate in the last glacial period. *Nature* 428, 306-310.
- Tyler, P.A., 1972. Reconnaissance Limnology of Sub-Antarctic Islands I. Chemistry of Lake Waters from Macquarie Island and the Iles Kerguelen. *International Review of Hydrobiology* 57, 759-778.
- Tyler, P.A., 1974. Limnological Studies, in: Williams, W.D. (Ed.), *Biogeography and Ecology in Tasmania*. Dr. W. Junk b.v., Publishers, The Hague, Dordrecht, Netherlands, pp. 29-61.
- Tyler, P.A., 1992. A lakeland from the dreamtime the second founders' lecture. *British Phycological Journal* 27, 353-368.
- Tyler, P.A., 1996. 13. Endemism in freshwater algae: with special reference to the Australian region. *Hydrobiologia* 336, 127-135.
- van Dam, H., Suurmond, G., ter Braak, C.J., 1981. Impact of acidification on diatoms and chemistry of Dutch moorland pools. *Hydrobiologia* 83, 425-459.
- Van de Geer, G., Fitzsimons, S.J., Colhoun, E., 1991. Holocene vegetation history from King River railway bridge, western Tasmania, *Papers and Proceedings of the Royal Society of Tasmania*, pp. 73-77.
- van de Geer, G., Fitzsimons, S.J., Colhoun, E.A., 1989. Holocene to middle last glaciation vegetation history at Newall Creek, western Tasmania. *New Phytologist* 111, 549-558.

- van de Geer, V.G., Heusser, L.E., Lynch-Stieglitz, J., Charles, C.D., 1994. Paleoenvironments of Tasmania inferred from a 5–75 ka marine pollen record. *Palynology* 18, 33-40.
- Vander Zanden, M.J., Rasmussen, J.B., 2001. Variation in $\delta^{15}\text{N}$ and $\delta^{13}\text{C}$ trophic fractionation: implications for aquatic food web studies. *Limnology and Oceanography* 46, 2061-2066.
- Vandergoes, M.J., Newnham, R.M., Denton, G.H., Blaauw, M., 2013. The anatomy of Last Glacial Maximum climate variations in south Westland, New Zealand, derived from pollen records. *Quaternary Science Reviews* 74, 215-229.
- Vanhoutte, K., Verleyen, E., Vyverman, W., Chepurinov, V., A., Sabbe, K., 2004. The freshwater diatom genus *Kobayasiella* (Bacillariophyta) in Tasmania, Australia. *Australian Systematic Botany* 17, 483-496.
- Vanormelingen, P., Verleyen, E., Vyverman, W., 2008. The diversity and distribution of diatoms: from cosmopolitanism to narrow endemism. *Biodiversity and Conservation* 17, 393-405.
- Varma, V., Prange, M., Lamy, F., Merkel, U., Schulz, M., 2011. Solar-forced shifts of the Southern Hemisphere Westerlies during the Holocene. *Climate of the Past* 7, 339-347.
- Veblen, T.T., Ashton, D.H., 1982. The regeneration status of *Fitzroya Ccpressoides* in the Cordillera Pelada, Chile. *Biological Conservation* 23, 141-161.
- Verleyen, E., Vyverman, W., Sterken, M., Hodgson, D.A., De Wever, A., Juggins, S., Van der Vijver, B., Jones, V.J., Vanormelingen, P., Roberts, D., Flower, R., Kilroy, C., Souffreau, C., Sabbe, K., 2009. The importance of dispersal related and local factors in shaping the taxonomic structure of diatom metacommunities. *Oikos* 118, 1239-1249.
- Voigt, I., Chiessi, C.M., Prange, M., Mulitza, S., Groeneveld, J., Varma, V., Henrich, R., 2015. Holocene shifts of the Southern Westerlies across the South Atlantic. *Paleoceanography* 30, 39-51.

Vyverman, W., Verleyen, E., Sabbe, K., Vanhoutte, K., Sterken, M., Hodgson, D., A., Mann, D., G. , Juggins, S., de Vijver, B., Jones, V., Flower, R., Roberts, D., Chepurnov, V., A., Kilroy, C., Vanormelingen, P., Wever, A., 2007. Historical Processes Constrain Patterns in Global Diatom Diversity. *Ecology* 88, 1924-1931.

Vyverman, W., Vyverman, R., Hodgson, D., Tyler, P., 1995. Diatoms from Tasmanian mountain lakes: a reference data-set for environmental reconstruction. The TASDIAT diatom training set: a systematic and autoecological study. Cramer, Berlin.

Vyverman, W., Vyverman, R., Rajendran, V.S., Tyler, P., 1996. Distribution of benthic diatom assemblages in Tasmanian highland lakes and their possible use as indicators of environmental changes. *Canadian Journal of Fisheries and Aquatic Sciences* 53, 493-508.

Walsh, R., Shiel, R., Tyler, P., 2004. Reconnaissance limnology of Tasmania VIII. Tasmanian coastal lagoons-epicentres of endemism in the Australian aquatic microbiota, *Papers and proceedings of the Royal Society of Tasmania*, pp. 67-76.

Walsh, R.G.J., Shiel, R.J., Tyler, P.A., 2001. Reconnaissance limnology of Tasmania VII. Coastal lagoons of Bass Strait islands, with reference to endemic microflora and microfauna. *Archiv fur Hydrobiologie* 152, 489-510.

Wang, Q., Yang, X., Anderson, N.J., Dong, X., 2016. Direct versus indirect climate controls on Holocene diatom assemblages in a sub-tropical deep, alpine lake (Lugu Hu, Yunnan, SW China). *Quaternary Research* In Press, 1-12.

Wang, R., Dearing, J.A., Langdon, P.G., Zhang, E., Yang, X., Dakos, V., Scheffer, M., 2012. Flickering gives early warning signals of a critical transition to a eutrophic lake state. *Nature* 492, 419-422.

- Warfe, D.M., Pettit, N.E., Magierowski, R.H., Pusey, B.J., Davies, P.M., Douglas, M., Bunn, S.E., 2013. Hydrological connectivity structures concordant plant and animal assemblages according to niche rather than dispersal processes. *Freshwater Biology* 58, 292-305.
- Weckström, K., Weckström, J., Yliniemi, L.M., Korhola, A., 2010. The ecology of *Pediastrum* (Chlorophyceae) in subarctic lakes and their potential as paleobioindicators. *Journal of Paleolimnology* 43, 61-73.
- Wetzel, R.G., 1992. Gradient-dominated ecosystems: sources and regulatory functions of dissolved organic matter in freshwater ecosystems. *Hydrobiologia* 229, 181-198.
- Whitcraft, C.R., Levin, L.A., Talley, D., Crooks, J.A., 2008. Utilization of invasive tamarisk by salt marsh consumers. *Oecologia* 158, 259-272.
- White, I., Wade, A., Worthy, M., Mueller, N., Daniell, T., Wasson, R., 2006. The vulnerability of water supply catchments to bushfires: impacts of the January 2003 wildfire on the Australian Capital Territory. *Australian Journal of Water Resources* 10, 179-194.
- Whitehead, D.R., Charles, D.F., Jackson, S.T., Smol, J.P., Engstrom, D.R., 1989. The developmental history of Adirondack (N.Y.) lakes. *Journal of Paleolimnology* 2, 185-209.
- Whiteside, M.C., 1983. The mythical concept of eutrophication. *Hydrobiologia* 103, 107-111.
- Whiteside, M.C., Swindoll, M.R., 1988. Guidelines and limitations to cladoceran paleoecological interpretations. *Palaeogeography, Palaeoclimatology, Palaeoecology* 62, 405-412.
- Whitlock, C., Larsen, C., 2001. Charcoal as a fire proxy, in: Smol, J.P., Birks, H.J.B., Last, W.M. (Eds.), *Tracking Environmental Change Using Lake Sediments. Volume 3: Terrestrial, Algal, and Siliceous Indicators*. Kluwer Academic Publishers, Dordrecht, The Netherlands, pp. 75-97.

Whitlock, C., Millspaugh, S.H., 1996. Testing the assumptions of fire-history studies: an examination of modern charcoal accumulation in Yellowstone National Park, USA. *The Holocene* 6, 7-15.

Williams, A., Smith, M., Turney, C.S., Cupper, M., 2008. AustArch1: A Database of ¹⁴C and Luminescence Ages from Archaeological Sites in the Australian Arid Zone. *Australian Archaeology*, 99.

Williams, K.J., Potts, B.M., 1996. The natural distribution of Eucalyptus species in Tasmania. *Tasforests* 8, 39-149.

Williams, M., Cook, E., van der Kaars, S., Barrows, T., Shulmeister, J., Kershaw, A.P., 2009. Glacial and deglacial climatic patterns in Australia and surrounding regions from 35 000 to 10 000 years ago reconstructed from terrestrial and near-shore proxy data. *Quaternary Science Reviews* 28, 2398-2419.

Williams, W.D., 1974. Introduction, in: Williams, W.D. (Ed.), *Biogeography and Ecology in Tasmania*. Dr. W. Junk b.v., Publishers, The Hague, Dordrecht, Netherlands.

Willis, K.J., Bailey, R.M., Bhagwat, S.A., Birks, H.J.B., 2010. Biodiversity baselines, thresholds and resilience: testing predictions and assumptions using palaeoecological data. *Trends in Ecology & Evolution* 25, 583-591.

Winder, M., Schindler, D.E., 2004. Climatic effects on the phenology of lake processes. *Global Change Biology* 10, 1844-1856.

Wolfe, B.B., Edwards, T.W.D., Elgood, R.J., 2001. Carbon and Oxygen Isotope Analysis of Lake Sediment Cellulose: Methods and Applications, in: Last, W.M., Smol, J.P. (Eds.), *Tracking Environmental Change Using Lake Sediments. Volume 2: Physical and Geochemical Methods*. Kluwer Academic Publishers, Dordrecht, The Netherlands, pp. 373-400.

Wood, S., 2016. Package: mgcv, Mixed GAM Computation Vehicle with GCV/AIC/REML Smoothness Estimation, 1.8-15 ed.

- Wood, S.N., 2011. Fast stable restricted maximum likelihood and marginal likelihood estimation of semiparametric generalized linear models. *Journal of the Royal Statistical Society: Statistical Methodology Series B* 73, 3-36.
- Wood, S.W., Bowman, D.M.J.S., 2012. Alternative stable states and the role of fire–vegetation–soil feedbacks in the temperate wilderness of southwest Tasmania. *Landscape Ecology* 27, 13-28.
- Wood, S.W., Hua, Q., Bowman, D.M.J.S., 2011a. Fire-patterned vegetation and the development of organic soils in the lowland vegetation mosaics of south-west Tasmania. *Australian Journal of Botany* 59, 126-136.
- Wood, S.W., Murphy, B.P., 2011b. Firescape ecology: how topography determines the contrasting distribution of fire and rain forest in the south-west of the Tasmanian Wilderness World Heritage Area. *Journal of Biogeography* 38, 1807-1820.
- Woods, R., 2003. The relative roles of climate, soil, vegetation and topography in determining seasonal and long-term catchment dynamics. *Advances in Water Resources* 26, 295-309.
- Wright, H.E., Jr., 1967. A square-rod piston sampler for lake sediments. *Journal of Sedimentary Petrology* 37, 975-976.
- Xia, Q., Zhao, J.-x., Collerson, K., 2001. Early–Mid Holocene climatic variations in Tasmania, Australia: multi-proxy records in a stalagmite from Lynds Cave. *Earth and Planetary Science Letters* 194, 177-187.
- Yan, H., Sun, L., Wang, Y., Huang, W., Qiu, S., Yang, C., 2011. A record of the Southern Oscillation Index for the past 2,000 years from precipitation proxies. *Nature Geoscience* 4, 611-614.
- Yee, T.W., Mitchell, N.D., 1991. Generalized additive models in plant ecology. *Journal of Vegetation Science* 2, 587-602.

Zak, D.R., Holmes, W.E., MacDonald, N.W., 1999. Soil temperature, matric potential, and the kinetics of microbial respiration and nitrogen mineralization. *Soil Science Society of America Journal* 63.

Zuo, R., 2013. ITRAX: A potential tool to explore the physical and chemical properties of mineralized rocks in mineral resource exploration. *Journal of Geochemical Exploration* 132, 149-155.

APPENDIX I

This appendix contains the modified supplementary information for Chapter 4 from publication Beck, K.K., Fletcher, M.S., Gadd, P.S., Heijnis, H. & Jacobsen, G. (2017) An early onset of ENSO influence in the extra-tropics of the southwest Pacific inferred from a 14,600 year high resolution multi-proxy record from Paddy's Lake, northwest Tasmania. *Quaternary Science Reviews*, 157, 164-175.



Figure I.1: Optical image of Paddy's Lake recovered cores: TAS1401 SC1 (93 cm) and TAS1401 N1 (227 cm). TAS1401 N1 was cut in two [TAS1401 N1A (113 cm) and TAS1401 N1B (114 cm)] for analysis.

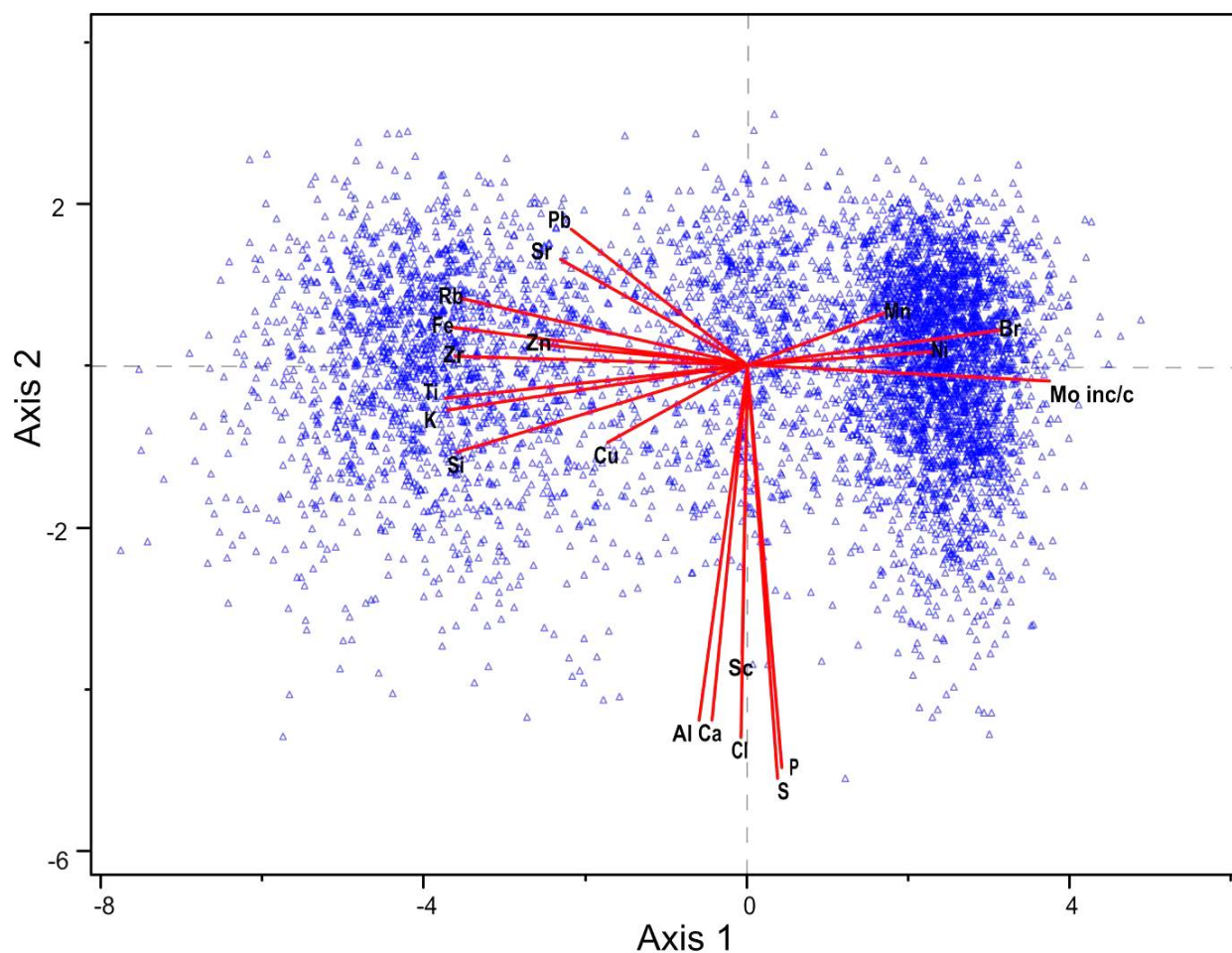


Figure I.2: PCA biplot for geochemical (ITRAX) of important geochemical elements (Al, Si, P, S, Cl, K, Ca, Sc, Ti, Mn, Fe, Ni, Cu, Zn, Br, Rb, Sr, Zr, and Pb) and Mo incoherence/coherence ratio axis 1 and 2. Data converted to z-scores and PCA analysis conducted in PC-Ord v4.27 (McCune et al., 2011), variance of axis 1= 42.391 and axis 2= 7.114.

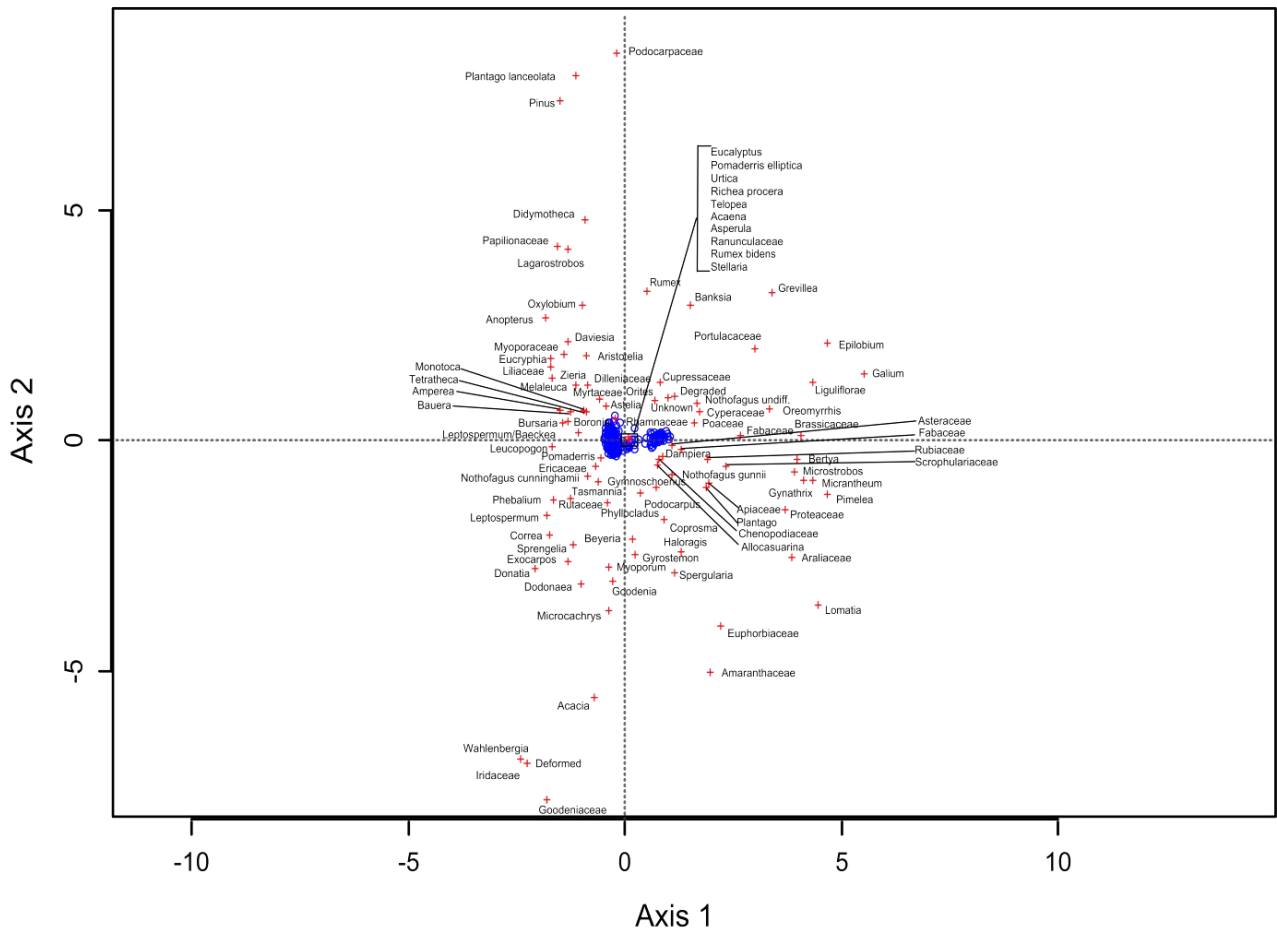


Figure I.3: DCA biplot for terrestrial pollen data axis 1 and 2. DCA was performed in *R* v3.1.1 (R Development Core Team, 2014) using the rioja package (Juggins, 2016) on square root transformed data with rare taxa down weighted. Percent variance described by axis 1 is 26.06% and 4.16% for axis 2.

APPENDIX II

This appendix contains the modified supporting information Beck, K.K., Fletcher, M-S., Kattel, G., Barry, L., Gadd, P.S., Heijnis, H., Jacobsen, G., & Saunders, K.M. (2018) The indirect response of an aquatic ecosystem to long term climate-driven terrestrial vegetation in a subalpine temperate lake. *Journal of Biogeography*, 45, 713-725 DOI:10.1111/jbi.13144 in Chapter 5.

Table II.1: Radiocarbon laboratory results for Paddy's Lake. Dates are organised in chronological sequence, core code identified at the top of depths. The two **bold italicised** dates were removed as outliers from the age model and * indicate the paired macrofossil-bulk sediment samples. Square brackets designate depths within the continuous sedimentary sequence (Chapter 4).

Lab ID	Analysis Location	Sample depths (cm) [in sediment sequence]	Material dated	Radiocarbon age (BP) + 1 σ error	$\delta(^{13}\text{C})$ per mil	pMC + 1 σ error
TAS1401 SC1						
D-AMS 010530	DirectAMS	14-14.5	bulk sediment	1151 \pm 23	-15.7	86.65 \pm 0.25
D-AMS 009184	DirectAMS	24-24.5	bulk sediment	1765 \pm 30	-22.4	80.27 \pm 0.30
D-AMS 010531	DirectAMS	47-47.5	bulk sediment	3049 \pm 23	-26.3	68.42 \pm 0.20
D-AMS 009183	DirectAMS	*65-65.5	plant macrofossil	3493 \pm 29	-17.3	64.74 \pm 0.23
D-AMS 009185	DirectAMS	*65-65.5	bulk sediment	3700 \pm 25	-28.6	63.09 \pm 0.20
D-AMS 009186	DirectAMS	79-79.5	bulk sediment	4770 \pm 28	-21.0	55.22 \pm 0.19
D-AMS 010532	DirectAMS	92-92.5	bulk sediment	5743 \pm 33	-20.2	48.92 \pm 0.20
TAS1401 N1						
OZS591	ANSTO	*33.5-34 [97-97.5]	plant macrofossil	6150 \pm 40	-25.6	46.51 \pm 0.23
OZS592	ANSTO	*33.5-34 [97-97.5]	bulk sediment	6390 \pm 45	-24.9	45.14 \pm 0.23
OZS593	ANSTO	46-46.5 [109.5-110]	bulk sediment	7380 \pm 40	-25.1	39.91 \pm 0.19
OZS594	ANSTO	64-64.5 [127.5-128]	bulk sediment	8895 \pm 50	-25.7	33.04 \pm 0.20
D-AMS 010533	DirectAMS	71.5-72 [135-135.5]	bulk sediment	9777 \pm 38	-19.7	29.61 \pm 0.14
D-AMS 010534	DirectAMS	87.5-88 [151-151.5]	bulk sediment	10704 \pm 37	-22.7	26.38 \pm 0.12

OZS595	ANSTO	102.5-103	bulk			
D-AMS		[166-166.5]	sediment	11590 ± 50	-24.7	23.63 ± 0.14
010535	DirectAMS	110.5-111	bulk			
D-AMS		[174-174.5]	sediment	11471 ± 40	-25.3	23.98 ± 0.12
013525	DirectAMS	136.5-137	bulk			
D-AMS		[200-200.5]	sediment	13655 ± 53	-27.2	18.27 ± 0.12
012511	DirectAMS	161.5-162	bulk			
D-AMS		[225-225.5]	sediment	13585 ± 48	-21.3	18.43 ± 0.11
012512	DirectAMS	183.5-184	bulk			
D-AMS		[247-247.5]	sediment	12837 ± 56	-17.4	20.23 ± 0.14
013526	DirectAMS	191.5-192	bulk			
D-AMS		[255-255.5]	sediment	12514 ± 50	-25.8	21.06 ± 0.13

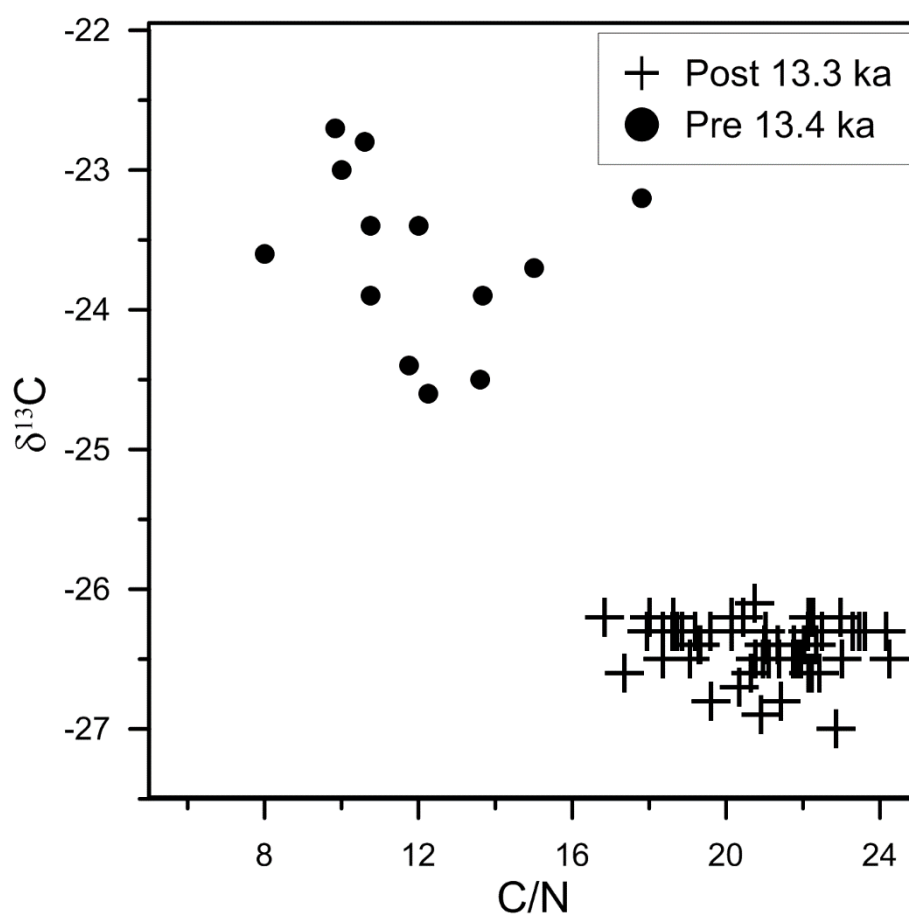


Figure II.1: Scatter plot of $\delta^{13}\text{C}$ and C/N results from Paddy's Lake. Pre 13.4 ka data is represented by black dots and post 13.3 ka is represented by plus signs.

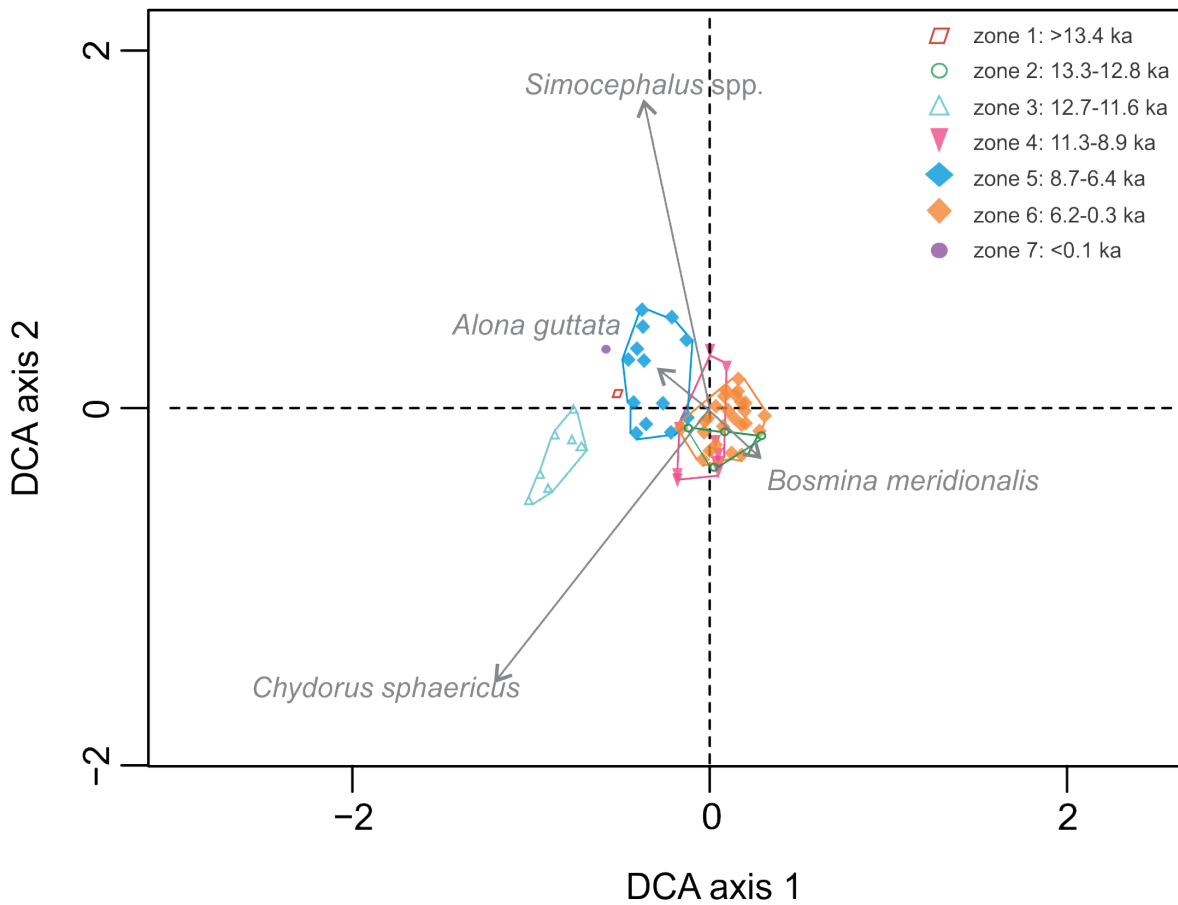


Figure II.2: Grey arrows demonstrate taxa with an axis correlation of $r^2 > 0.5$. DCA axis 1 explained variance is 25.1% and axis 2 explained variance is 14.3%. *Bosmina meridionalis* are positively associated with axis 1, and *Alona guttata* and *Chydorus sphaericus* are negatively associated. In axis 2 *spp.* shows strong positive affinity. Zones 2, 4, and 6 all cluster and overlap in the positive axis 1 direction, while Zones 1, 3, 5, and 7 do not overlap but cluster in the negative axis 1 direction. Zones 1 and 7 only include one data point.

APPENDIX III

This appendix contains the proposed supporting information for Chapter 6 planned manuscript: Beck, K.K., Fletcher, Michael-Shawn, Gadd, P. S., Heijnis, H., Saunders, K. M. & Zawadzki, A. (*in prep*) Direct and indirect aquatic ecosystem response to changes in climate variability: A Holocene diatom record from Tasmania, Australia

Table III.1: Age offset for bulk sediment dates. Calculated by differencing macrofossil and bulk sediment radiocarbon dates from the same depth sample.

¹⁴ C date	¹⁴ C error	Core ID	Depth (cm)	material	age difference (¹⁴ C)
2060	34	TAS1508 N1A	104	wood	683
2743	36	TAS1508 N1A	104	bulk sediment	
2171	36	TAS1508 N1A	131	wood	202
2373	38	TAS1508 N1A	131	bulk sediment	
3875	39	TAS1508 N1B	238.5	wood	115
3760	37	TAS1508 N1B	238.5	bulk sediment	
				age offset	333.3333

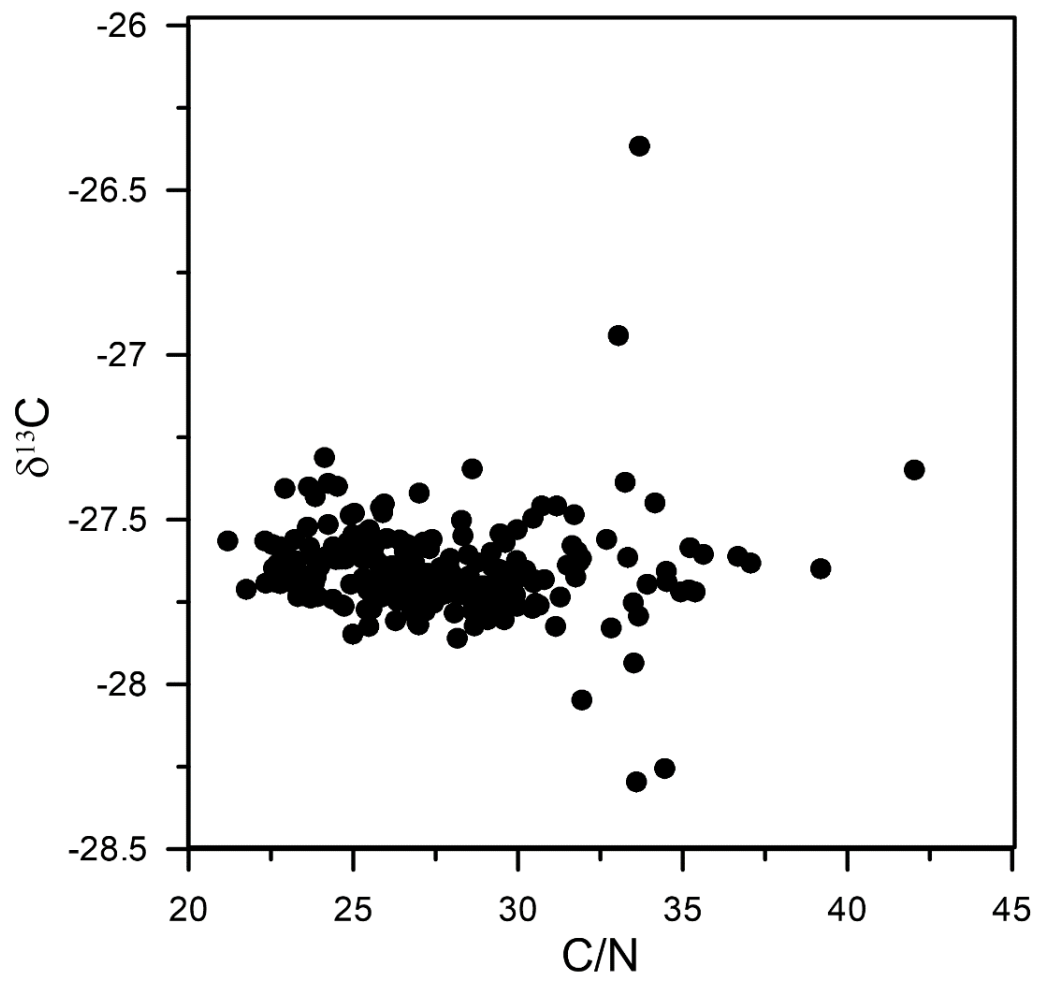


Figure III.1: Scatter plot of $\delta^{13}\text{C}$ and C/N results from Lake Vera.

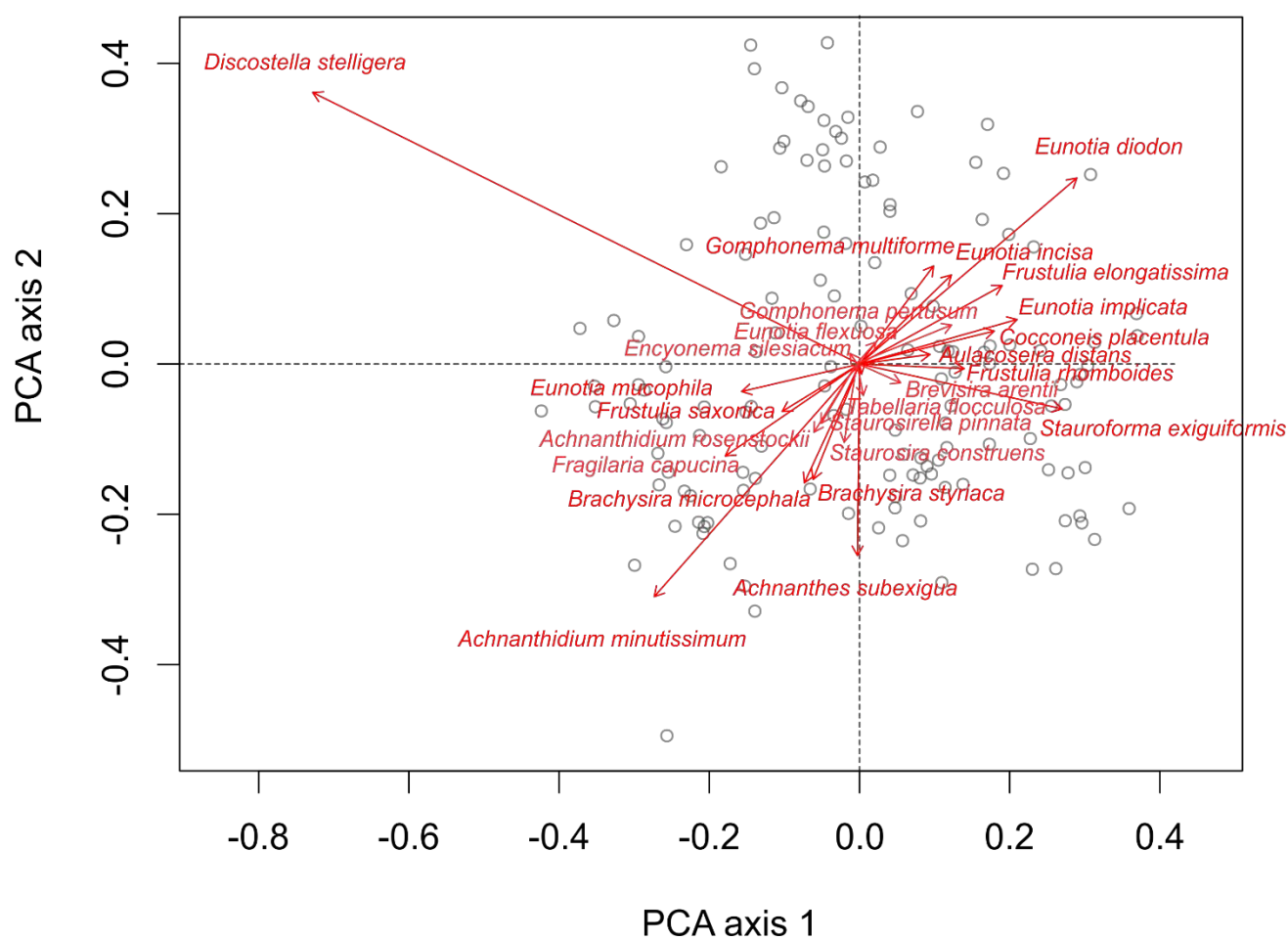


Figure III.2: PCA biplot of TAS1108SC1 +TAS1508 N1 Hellinger transformed fossil diatom data with important taxa presented here in red. Grey circles indicate sample depths. Explained variance of axis 1 is 29.6% and axis 2 is 13.7%.

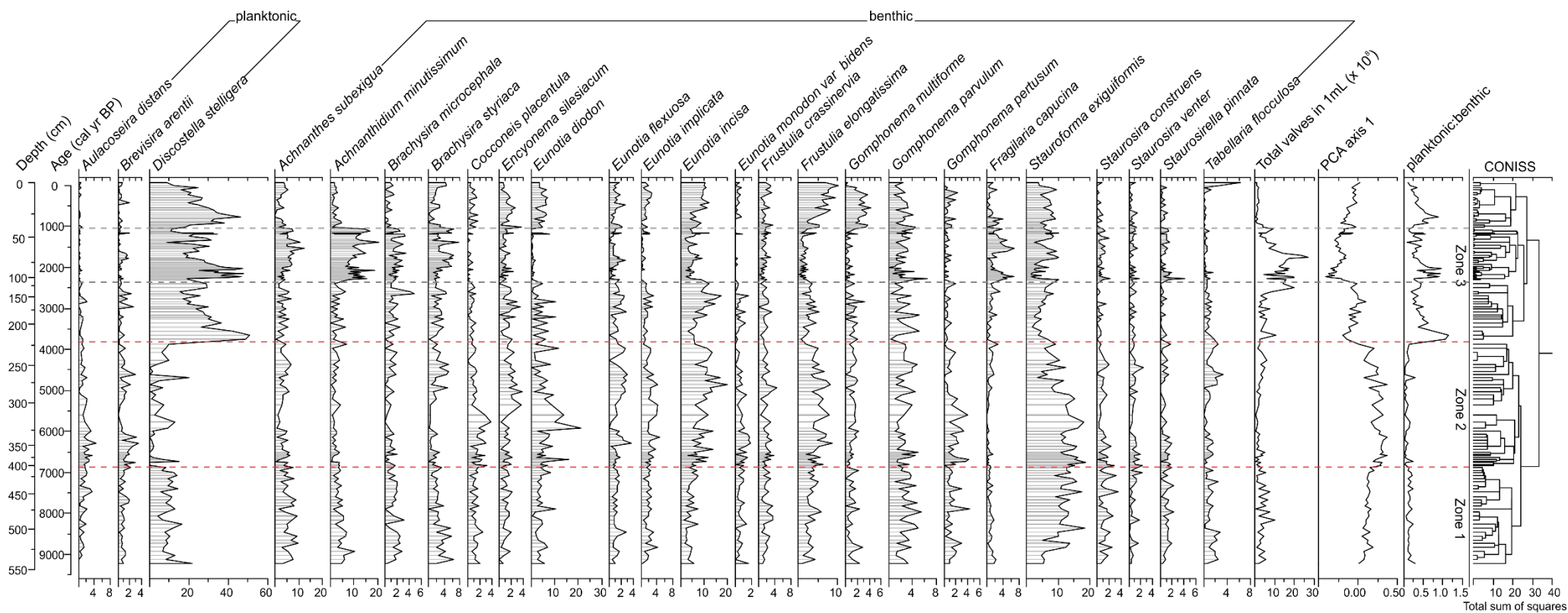


Figure III.3: Stratigraphy of Lake Vera diatoms. Most abundant diatom species presented as percentage composition. The PCA axis 1 estimate trends in the diatom percentage data (explained variance of PCA 1 29.6%). Significant zones determined by CONISS are separated by red dashed lines and significant zones from Chapter 7 are separated by grey dashed lines. Planktonic:benthic ratio estimate trends in the sum of planktonic taxa to benthic taxa.

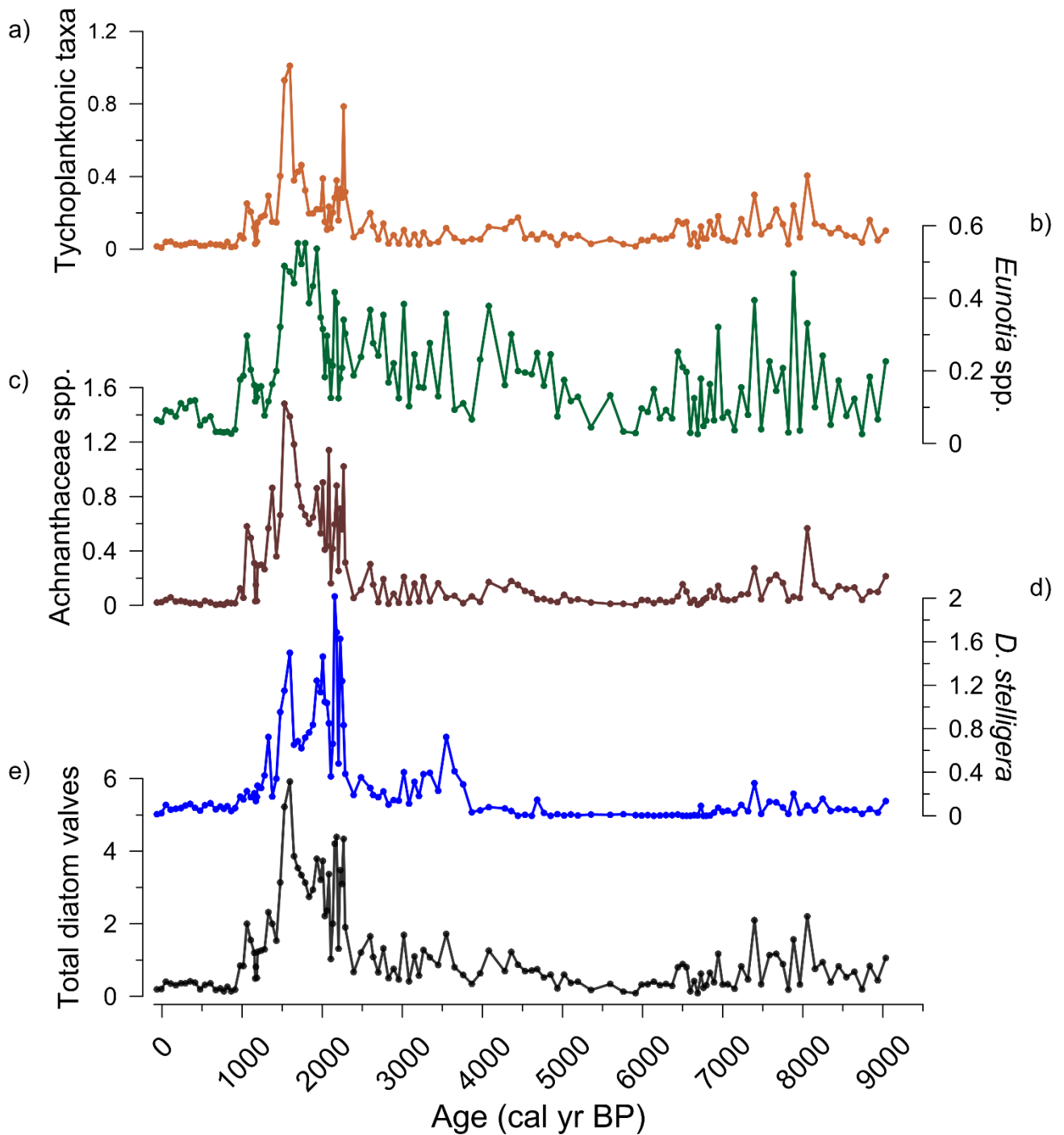


Figure III.4: Absolute abundance of a) tychoplanktonic taxa; b) *Eunotia* spp.; c) Achnantheaceae spp.; d) *Discostella stelligera*; and e) Total diatom valves for Lake Vera.

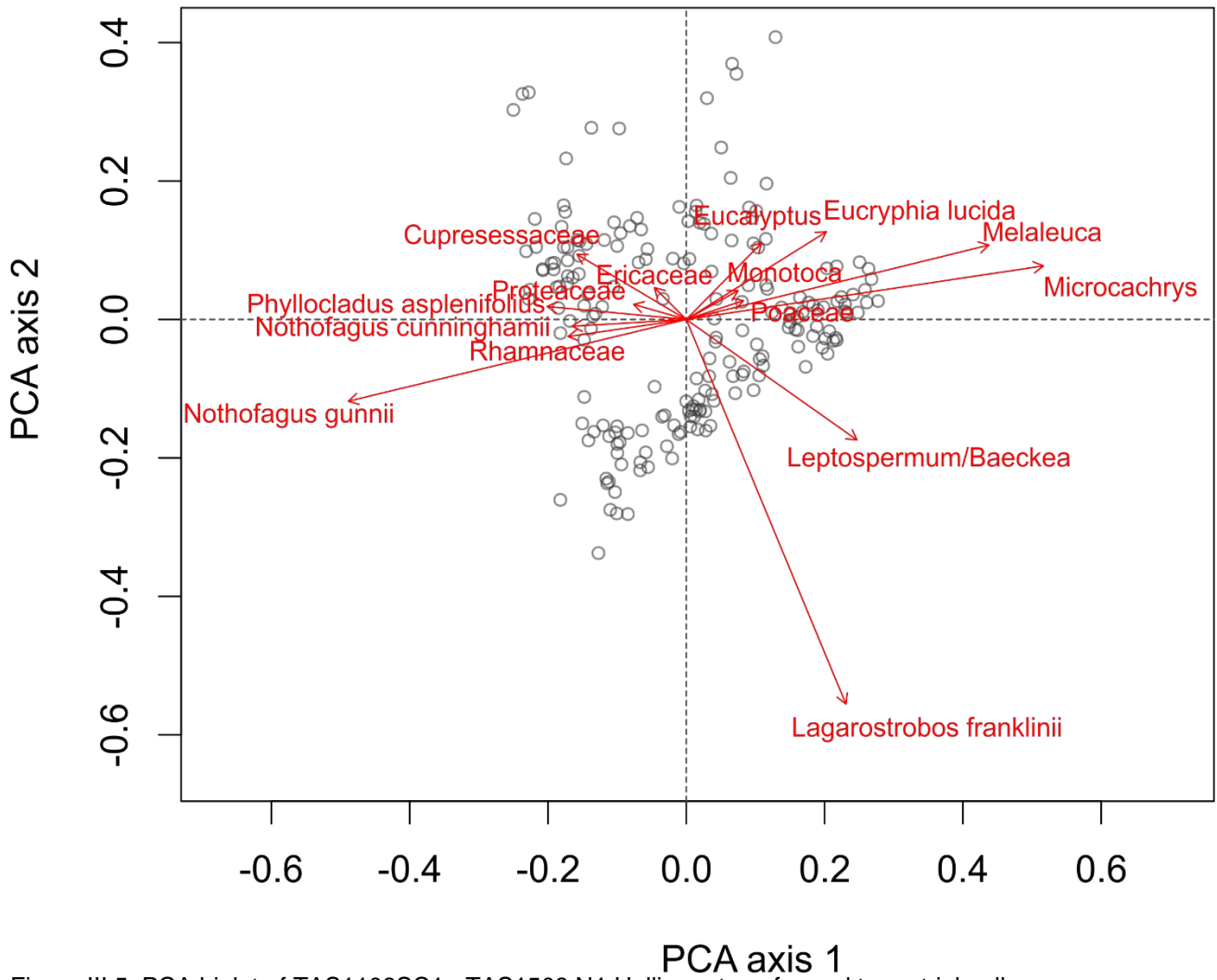


Figure III.5: PCA biplot of TAS1108SC1 +TAS1508 N1 Hellinger transformed terrestrial pollen percentages with important taxa presented here in red. Grey circles indicate sample depths. Explained variance of axis 1 is 37.2% and axis 2 is 15.3%.

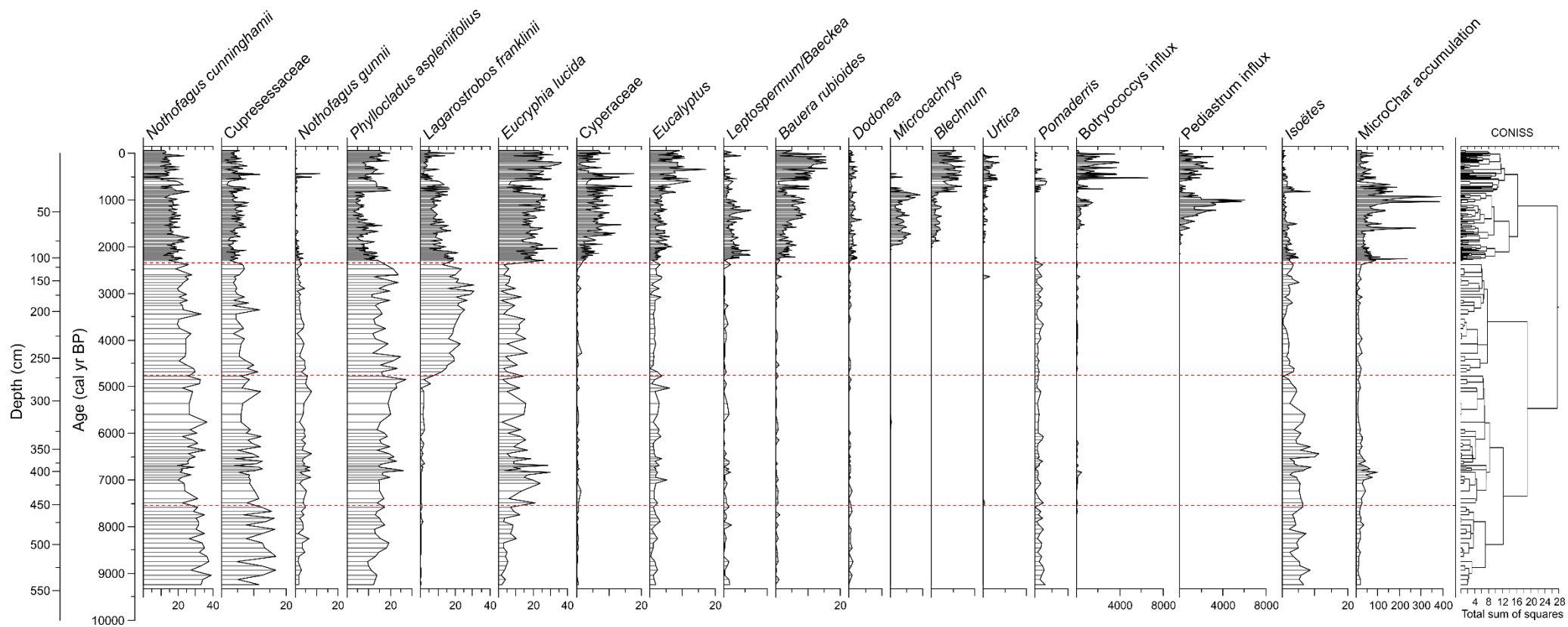


Figure III.6: Stratigraphy of Lake Vera pollen. Important pollen taxa are presented as percentage composition. *Botryococcus* and *Pediastrum* are presented as influx and microscopic charcoal as an accumulation rate. Zones determined by CONISS are separated by red dashed lines.

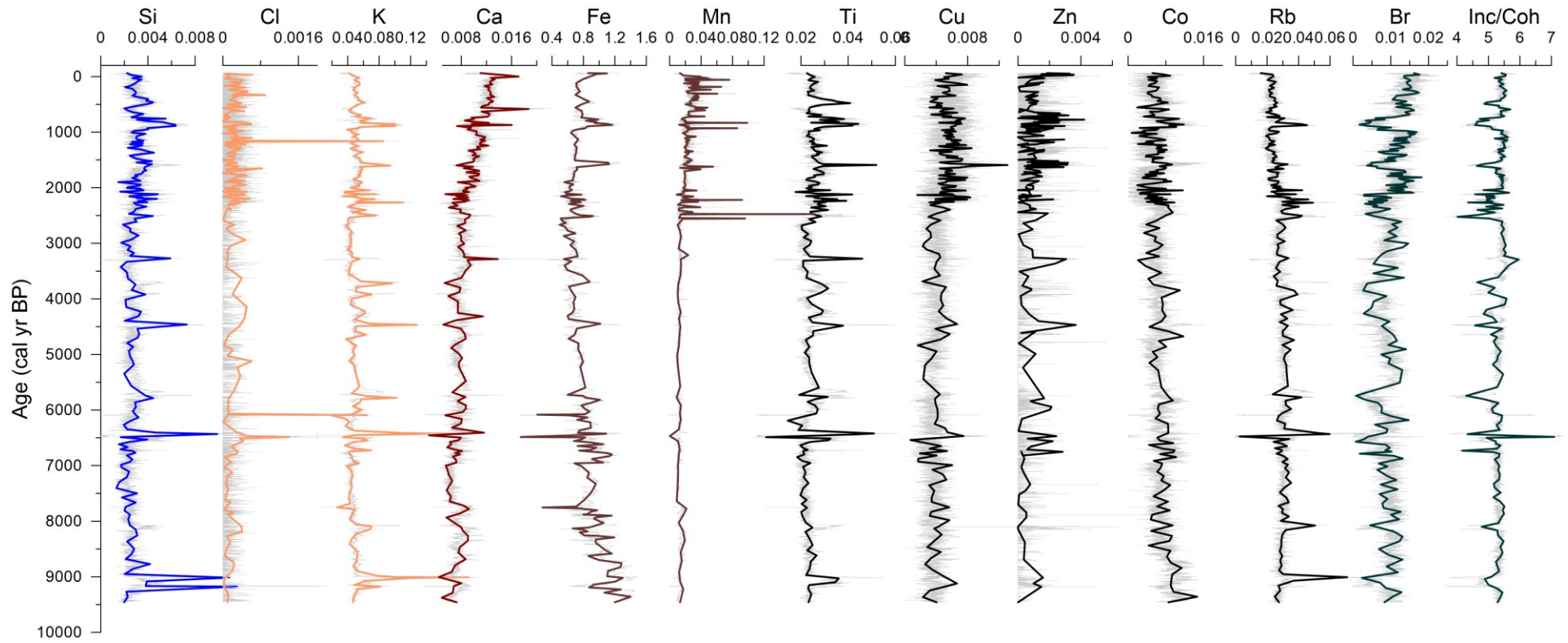


Figure III.7: μ XRF stratigraphy for Lake Vera composite core of important XRF geochemicals, normalised by Mo incoherence/coherence, with a smooth spline of 1.5.

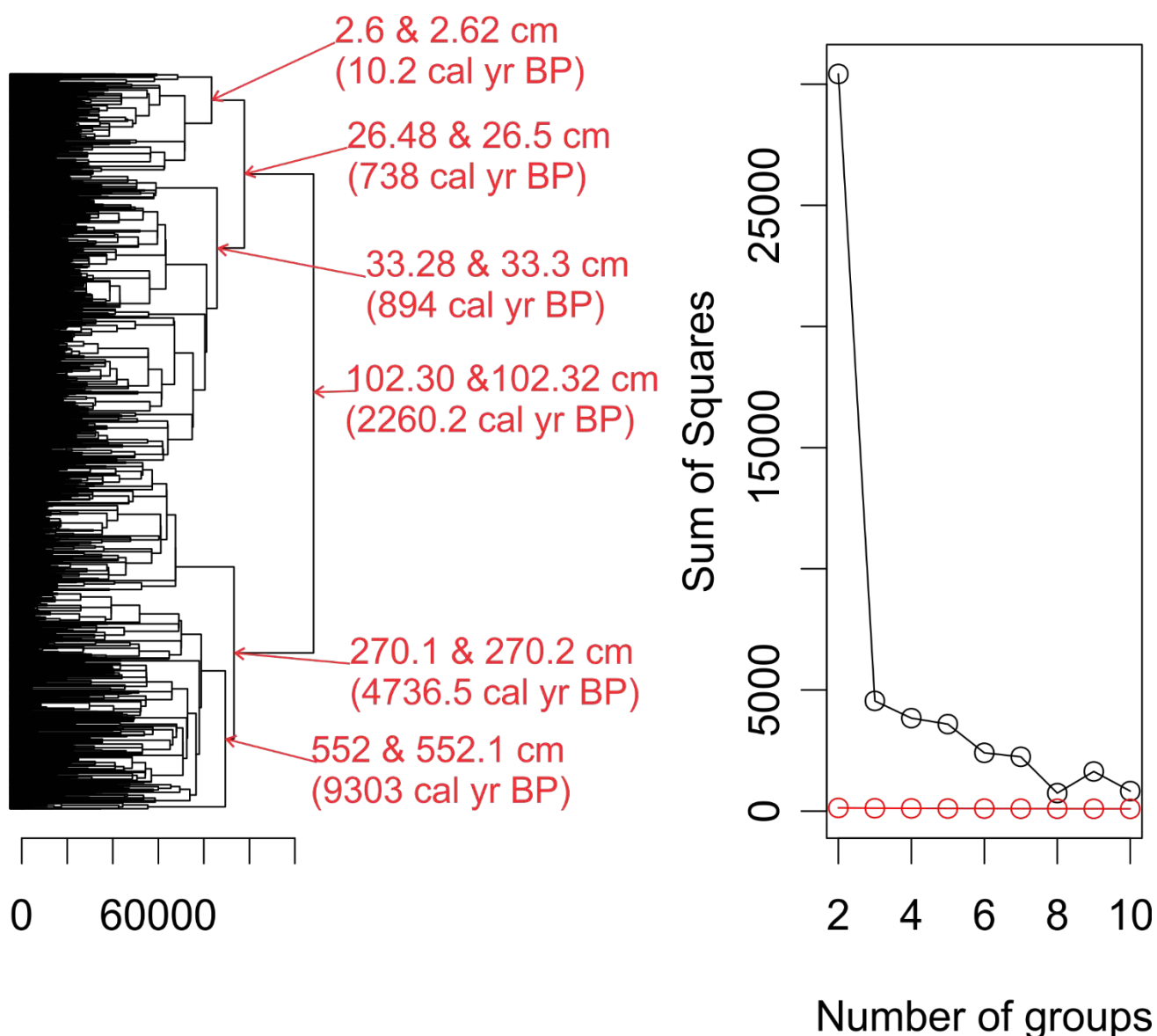


Figure III.8: Cluster analysis and broken stick model for Lake Vera μ XRF data. The broken stick shows up to 10 significant cluster. The age and depth of the first six significant breaks in the dendrogram are highlighted in red.

Table III.2: Diatom authorities Lake Vera TAS1108SC1+TAS1508 N1 composite core (Chapter 6). Diatom taxonomic nomenclature was verified using Algaebase (<http://www.algaebase.org/>).

Sample name	Authority
<i>Achnanthes bahusiensis</i>	(Grunow) Lange-Bertalot
<i>Achnanthes percava</i>	Carter
<i>Achnanthes pseudoswaki</i>	Carter
<i>Achnanthes sp. 1</i>	Vyverman et al. 1995
<i>Achnanthes coarctata</i>	(Brébisson ex W.Smith) Grunow
<i>Achnanthes delicatula subsp. hauckiana</i>	(Grunow) Lange-Bertalot & Ruppel
<i>Achnanthes delicatula subsp. septentrionalis</i>	(Østrup) Lange-Bertalot
<i>Achnanthes didyma</i>	Hustedt

<i>Achnanthes minutissima</i> var. <i>macrocephala</i>	Hustedt
<i>Achnanthes oblongella</i>	Østrup
<i>Achnanthes petersenii</i>	Hustedt
<i>Achnanthes stolidia</i>	(Krasske) Krasske
<i>Achnanthes subexigua</i>	Hustedt
<i>Achnanthes ventralis</i>	(Krasske) Lange-Bertalot
<i>Achnanthidium neomicrocephalum</i>	Lange-Bertalot & F.Staab, 2004
<i>Achnanthidium bioretii</i>	(H.Germain) Monnier, Lange-Bertalot & Ector
<i>Achnanthidium exiguum</i>	(Grunow) Czarnecki
<i>Achnanthidium kriegeri</i>	(Krasske) Hamilton, D.Antonini & Siver
<i>Achnanthidium minutissimum</i>	(Kützing) Czarnecki
<i>Achnanthidium pyrenaicum</i>	(Hustedt) H.Kobayasi
<i>Achnanthidium rosenstockii</i>	(Lange-Bertalot) Lange-Bertalot
<i>Achnanthidium subatomoides</i>	(Hustedt) O.Monnier, Lange-Bertalot & Ector
<i>Achnanthidium subatomus</i>	(Hustedt) Lange-Bertalot
<i>Actinella indistincta</i>	W.Vyverman & E.A.Bergey
<i>Actinella pulchella</i>	K.Sabbe & D.Hodgson
<i>Actinella parva</i>	K.Vanhoutte & K.Sabbe
<i>Actinella tasmaniensis</i>	Hustedt
<i>Amphora</i> sp. 1	Vyverman et al. 1995
<i>Amphora ovalis</i>	(Kützing) Kützing
<i>Aulacoseira valida</i>	(Grunow) Krammer
<i>Aulacoseira alpigena</i>	(Grunow) Krammer
<i>Aulacoseira crassipunctata</i>	Krammer
<i>Aulacoseira crenulata</i>	(Ehrenberg) Thwaites
<i>Aulacoseira distans</i>	(Ehrenberg) Simonsen
<i>Aulacoseira pfaffiana</i>	(Reinsch) Krammer
<i>Biremis tasmanica</i>	W.Vyverman, K.Sabbe & R.Vyverman
<i>Brachysira vitrea</i>	(Grunow) R.Ross
<i>Brachysira aponina</i>	Kützing
<i>Brachysira brebissonii</i>	R.Ross
<i>Brachysira microcephala</i>	(Grunow) Compère
<i>Brachysira styriaca</i>	(Grunow) R.Ross
<i>Brachysira zellensis</i>	(Grunow) Round & D.G.Mann
<i>Brevisira arentii</i>	(Kolbe) Krammer
<i>Caloneis bacillum</i>	(Grunow) Cleve 1894
<i>Caloneis molaris</i>	(Grunow) Krammer
<i>Caloneis silicula</i>	(Ehrenberg) Cleve 1894
<i>Caloneis sublinearis</i>	(Grunow) Krammer, nom. illeg. (Cleve) Lange-Bertalot in Werum and Lange-Bertalot 2004
<i>Cavinula pusio</i>	(Gregory ex Greville) Mann & Stickle in Round, Crawford & Mann 1990
<i>Cavinula cocconeiformis</i>	

<i>Cavinula pseudoscutiformis</i>	(Hustedt) D.G.Mann & A.J.Stickle
<i>Cavinula scutiformis</i>	(Grunow ex Schmidt) Mann and Stickle in Round et al. 1990
<i>Chamaepinnularia evanida</i>	(Hustedt) Lange-Bertalot
<i>Chamaepinnularia mediocris</i>	(Krasske) Lange-Bertalot & Krammer (Krasske) Lange-Bertalot & Krammer in Lange-Bertalot & Metzeltin 1996
<i>Chamaepinnularia soehrensii</i>	
<i>Cocconeis placentula</i>	Ehrenberg 1838
<i>Craticula halophila</i>	(Grunow) D.G.Mann
<i>Craticula subminuscula</i>	(Manguin) Wetzel and Ector 2015
<i>Cyclotella meneghiniana</i>	Kützing
<i>Cymbella affinis</i>	Kützing 1844
<i>Cymbella amphioxys</i>	(Kützing) Cleve
<i>Cymbella cistula</i>	(Ehrenberg) O.Kirchner
<i>Cymbella falaisensis</i>	(Grunow) Krammer & Lange-Bertalot
<i>Cymbopleura naviculiformis</i>	(Auerswald ex Heiberg) Krammer
<i>Cymbella reinhardtii</i>	Grunow
<i>Cymbopleura cuspidata</i>	(Kützing) Krammer
<i>Cymbopleura hauckii</i>	(Van Heurck) Krammer
<i>Cymbopleura inaequalis</i>	(Ehrenberg) Krammer
<i>Cymbopleura incerta</i>	(Grunow) Krammer
<i>Cymbopleura vasta</i>	(Hustedt) Krammer
<i>Delicata delicatula</i>	(Kützing) Krammer
<i>Diademsis gallica</i>	W.Smith
<i>Diploneis finnica</i>	(Ehrenberg) Cleve
<i>Diploneis interrupta</i>	(Kützing) Cleve
<i>Diploneis marginestriata</i>	Hustedt
<i>Diploneis oblongella</i>	(Nägeli ex Kützing) Cleve-Euler
<i>Diploneis ovalis</i>	(Hilse) Cleve
<i>Cyclotella pseudostelligera</i>	Hustedt
<i>Discostella stelligera</i>	(Cleve and Grunow) Houk and Klee 2004
<i>Encyonema alpinum</i>	(Grunow) D.G.Mann
<i>Encyonema caespitosum</i>	Kützing
<i>Encyonema gracile</i>	Rabenhorst
<i>Encyonema hebridicum</i>	Grunow ex Cleve
<i>Encyonema mesianum</i>	(Cholnoky) D.G.Mann
<i>Encyonema minutum</i>	(Hilse) D.G.Mann
<i>Encyonema muelleri</i>	(Hustedt) D.G.Mann
<i>Encyonema perpusillum</i>	(Cleve-Euler) D.G.Mann
<i>Encyonema rugosum</i>	(Hustedt) D.G.Mann
<i>Encyonema silesiacum</i>	(Bleisch) D.G.Mann
<i>Encyonopsis cesatii</i>	(Rabenhorst) Krammer
<i>Encyonopsis microcephala</i>	(Grunow) Krammer

<i>Eolimna minima</i>	(Grunow) Lange-Bertalot & W.Schiller, nom. illeg.
<i>Epithemia adnata</i>	(Kützing) Brébisson
<i>Epithemia soresx</i>	Kützing
<i>Eunophora indistincta</i>	R.Vyverman & D.G.Mann
<i>Eunophora sp. 2 (cf. oberonica)</i>	R.Vyverman & D.Hodgson
<i>Eunophora tasmanica</i>	R.Vyverman & K.Sabbe
<i>Eunotia denticula</i>	(L.A.Brébisson) G.Rabenhorst
<i>Eunotia sp. 1</i>	Vyverman et al. 1995
<i>Eunotia sp. 2</i>	Vyverman et al. 1995
<i>Eunotia sp. 3</i>	Vyverman et al. 1995
<i>Eunotia sp. 4</i>	Vyverman et al. 1995
<i>Eunotia sp. 5</i>	Vyverman et al. 1995
<i>Eunotia arculus</i>	Lange-Bertalot & Nörpel
<i>Eunotia bidentula</i>	W.Smith
<i>Eunotia bigibba</i>	Kützing
<i>Eunotia bilunaris</i>	(Ehrenberg) Schaarschmidt
<i>Eunotia crista-galli</i>	Cleve
<i>Eunotia diodon</i>	Ehrenberg
<i>Eunotia elegans</i>	Østrup
<i>Eunotia exigua</i>	(Brébisson ex Kützing) Rabenhorst
<i>Eunotia exigua var. bidens</i>	Hustedt
<i>Eunotia faba</i>	(Ehrenberg) Grunow, nom. illeg.
<i>Eunotia fallax</i>	A.Cleve
<i>Eunotia flexuosa</i>	(Brébisson ex Kützing) Kützing
<i>Eunotia implicata</i>	Nörpel, Lange-Bertalot & Alles
<i>Eunotia incisa</i>	W.Smith ex W.Gregory
<i>Eunotia intermedia</i>	(Krasske ex Hustedt) Nörpel & Lange-Bertalot
<i>Eunotia minor</i>	(Kützing) Grunow
<i>Eunotia monodon</i>	Ehrenberg
<i>Eunotia monodon var. bidens</i>	(Ehrenberg) Hustedt
<i>Eunotia mucophila</i>	(Lange-Bertalot, Nörpel-Schempp & Alles) Lange-Bertalot
<i>Eunotia muscicola</i>	Krasske
<i>Eunotia naegelii</i>	Migula
<i>Eunotia nymanniana</i>	Grunow
<i>Eunotia paludosa</i>	Grunow
<i>Eunotia pectinalis</i>	(Kützing) Rabenhorst
<i>Eunotia praerupta</i>	Ehrenberg
<i>Eunotia rhomboidea</i>	Hustedt
<i>Eunotia septentrionalis</i>	Østrup
<i>Eunotia soleirolii</i>	(Kützing) Rabenhorst
<i>Eunotia subarcuatoides</i>	Alles, Nörpel & Lange-Bertalot
<i>Fallacia pseudoforcipata</i>	(Hustedt) D.G.Mann
<i>Fallacia vitrea</i>	(Østrup) D.G.Mann

<i>Fragilaria acus</i>	Unchecked name-(Kützing) Lange-Bertalot
<i>Fragilaria brevistriata</i>	Grunow
<i>Fragilaria capensis</i>	Grunow
<i>Fragilaria capucina</i>	Desmazières
<i>Fragilaria construens</i>	(Ehrenberg) Grunow
<i>Fragilaria pseudoconstruens</i>	Marciniak
<i>Fragilariforma cassieae</i>	C.Kilroy & E.A.Bergey
<i>Fragilariforma exigua</i>	(Grunow) M.G.Kelly (Brébisson ex W.Smith) Lange-Bertalot & Krammer
<i>Frustulia crassinervia</i>	(Ehrenberg) De Toni
<i>Frustulia rhomboides</i>	Bourrelly & Manguin
<i>Frustulia rhomboides var. elongatissima</i>	Rabenhorst
<i>Frustulia saxonica</i>	Ehrenberg
<i>Gomphonema cf. turris</i>	Kociolek, Spaulding, Sabbe & Vyverman
<i>Gomphonema multiforme</i>	Vyverman et al. 1995
<i>Gomphonema sp. 2</i>	Ehrenberg
<i>Gomphonema acuminatum</i>	(Otto Müller) Cleve-Euler
<i>Gomphonema acutiusculum</i>	Kützing
<i>Gomphonema affine</i>	(Kützing) Rabenhorst
<i>Gomphonema angustatum</i>	Lange-Bertalot & E.Reichardt
<i>Gomphonema duplipunctatum</i>	Ehrenberg
<i>Gomphonema gracile</i>	W.Gregory
<i>Gomphonema hebridense</i>	(Hornemann) Brébisson
<i>Gomphonema olivaceum</i>	(Kützing) Kützing
<i>Gomphonema parvulum</i>	Kociolek, Spaulding, Sabbe & Vyverman
<i>Gomphonema pertusum</i>	Ehrenberg
<i>Gomphonema subtile</i>	(Ehrenberg) Grunow
<i>Hantzschia amphioxys</i>	(Grunow) Lowe, Kociolek, J.R.Johansen, Van de Vijver, Lange-Bertalot & Kopalová
<i>Humidophila contenta</i>	(Ehrenberg) Ruck & Nakov
<i>Iconella bifrons</i>	(Smith) Ruck & Nakov
<i>Iconella curvula</i>	(Hustedt) Bukhtiyarova
<i>Karayevia ploenensis</i>	(Grunow) Round & Bukhtiyarova
<i>Karayevia clevei</i>	(Hustedt) Bukhtiyarova
<i>Karayevia suchlandtii</i>	Vyverman
<i>Kobayasiella tasmanica</i>	Verleyen
<i>Kobayasiella hodgsonii</i>	(Kützing) D.G.Mann
<i>Luticola mutica</i>	(Ehrenberg) D.G.Mann
<i>Luticola nivalis</i>	(Kützing) Lange-Bertalot
<i>Mayamaea atomus</i>	(Krasske) Lange-Bertalot
<i>Mayamaea fossalis</i>	(Lange-Bertalot) Lange-Bertalot
<i>Microcostatus kuelbsii</i>	Vyverman et al. 1995
<i>Navicula sp. 11</i>	Vyverman et al. 1995
<i>Navicula sp. 3</i>	Vyverman et al. 1995
<i>Navicula sp. 4</i>	Vyverman et al. 1995
<i>Navicula sp. 6</i>	Vyverman et al. 1995

<i>Navicula cari</i>	Ehrenberg
<i>Navicula cincta</i>	(Ehrenberg) Ralfs
<i>Navicula cryptocephala</i>	Kützing
<i>Navicula cryptotenella</i>	Lange-Bertalot
<i>Navicula divaricata</i>	Hustedt
<i>Navicula gallica var. laevissima</i>	Unchecked name- (Cleve) Lange-Bertalot
<i>Navicula gerloffii</i>	Schimanski
<i>Navicula germainii</i>	J.H.Wallace
<i>Navicula gottlandica</i>	Grunow
<i>Navicula lundii</i>	E.Reichardt
<i>Navicula maceria</i>	Schimanski
<i>Navicula notha</i>	J.H.Wallace
<i>Navicula radiosa</i>	Kützing
<i>Navicula radiosafallax</i>	Lange-Bertalot
<i>Navigeia decussis</i>	(Østrup) Bukhtiyarova
<i>Neidium affine</i>	(Ehrenberg) Pfitzer
<i>Neidium ampliatum</i>	(Ehrenberg) Krammer
<i>Neidium iridis</i>	(Ehrenberg) Cleve
<i>Neidium productum</i>	(W.Smith) Cleve
<i>Nitzschia amphibia</i>	Grunow
<i>Nitzschia fonticola</i>	(Grunow) Grunow
<i>Nitzschia palea</i>	(Kützing) W.Smith
<i>Nitzschia perminuta</i>	(Grunow) M.Peragallo
<i>Nupela lapidosa</i>	(Krasske) Lange-Bertalot
<i>Nupela pennsylvanica</i>	(Patrick) Potapova, 2011
<i>Parlibellus protractus</i>	(Grunow) Witkowski, Lange-Bertalot & Metzeltin
<i>Pinnularia mesogongyla</i>	Ehrenberg
<i>Pinnularia acrosphaeria</i>	W.Smith
<i>Pinnularia aestuarii</i>	Cleve
<i>Pinnularia borealis</i>	Ehrenberg
<i>Pinnularia brebissonii</i>	(Kützing) Rabenhorst
<i>Pinnularia divergens</i>	W.Smith
<i>Pinnularia divergentissima</i>	(Grunow) Cleve
<i>Pinnularia gibbiformis</i>	Krammer
<i>Pinnularia lapponica</i>	Hustedt
<i>Pinnularia mesolepta</i>	(Ehrenberg) W.Smith
<i>Pinnularia microstauron</i>	(Ehrenberg) Cleve
<i>Pinnularia neomajor</i>	Krammer
<i>Pinnularia subcapitata</i>	W.Gregory
<i>Pinnularia subgibba</i>	Krammer
<i>Pinnularia viridis</i>	(Nitzsch) Ehrenberg
<i>Placoneis elginensis</i>	(W.Gregory) E.J.Cox
<i>Planothidium aueri</i>	(Krasske) Lange-Bertalot
<i>Planothidium distinctum</i>	(Messikommer) Lange-Bertalot
<i>Planothidium frequentissimum</i>	(Lange-Bertalot) Lange-Bertalot

<i>Planothidium lanceolatum</i>	(Brébisson ex Kützing) Lange-Bertalot
<i>Platessa conspicua</i>	(Ant.Mayer) Lange-Bertalot
<i>Psammothidium lacus-vulcani</i>	(Lange-Bertalot & Krammer) L.N.Bukhtiyarova
<i>Psammothidium levanderi</i>	(Hustedt) Bukhtiyarova & Round
<i>Psammothidium marginulatum</i>	(Grunow) Bukhtiyarova & Round
<i>Psammothidium montanum</i>	(Krasske) S.Mayama
<i>Psammothidium rossii</i>	(Hustedt) Bukhtiyarova & Round
<i>Pseudostaurosira elliptica</i>	(Schumann) Edlund, Morales & Spaulding
<i>Pseudostaurosira parasitica</i>	(W.Smith) Morales
<i>Pseudostaurosira subsalina</i>	(Hustedt) E.A.Morales
<i>Rhopalodia novae-zelandiae</i>	Hustedt
<i>Rossithidium nodosum</i>	(Cleve) Aboal
<i>Rossithidium pusillum</i>	(Grunow) Round & Bukhtiyarova
<i>Sellaphora americana</i>	(Ehrenberg) D.G.Mann
<i>Sellaphora bacillum</i>	(Ehrenberg) D.G.Mann
<i>Sellaphora difficillima</i>	(Hustedt) C.E.Wetzel, L.Ector & D.G.Mann
<i>Sellaphora laevisissima</i>	(Kützing) D.G.Mann
<i>Sellaphora medioconvexa</i>	(Hustedt) C.E.Wetzel
<i>Sellaphora mutata</i>	(Krasske) Lange-Bertalot
<i>Sellaphora pupula</i>	(Kützing) Mereschkovsky
<i>Sellaphora saugerresii</i>	(Desmazières) C.E.Wetzel & D.G.Mann
<i>Sellaphora seminulum</i>	(Grunow) D.G.Mann
<i>Sellaphora submuralis</i>	(Hustedt) C.E.Wetzel, L.Ector, B.Van de Vijver, Compère & D.G.Mann
<i>Sellaphora tridentula</i>	(Krasske) C.E.Wetzel
<i>Sellaphora utermoehlii</i>	(Hustedt) C.E.Wetzel & D.G.Mann
<i>Stauriforma exiguiformis</i>	(Lange-Bertalot) R.J.Flower, V.J.Jones & Round
<i>Stauroneis anceps</i>	Ehrenberg
<i>Stauroneis kriegeri</i>	R.M.Patrick
<i>Stauroneis obtusa</i>	Lagerstedt
<i>Stauroneis pachycephala</i>	P.T.Cleve
<i>Stauroneis phoenicenteron</i>	(Nitzsch) Ehrenberg
<i>Staurosira construens var. exigua</i>	(W.Smith) H.Kobayasi
<i>Staurosira venter</i>	(Ehrenberg) Cleve & J.D.Möller
<i>Staurosirella pinnata</i>	(Ehrenberg) D.M.Williams & Round
<i>Surirella sp. 2</i>	Vyverman et al. 1995
<i>Iconella linearis</i>	(W.Smith) Ruck & Nakov
<i>Tabellaria fenestrata</i>	(Lyngbye) Kützing
<i>Tabellaria flocculosa</i>	(Roth) Kützing
<i>Tryblionella scalaris</i>	(Ehrenberg) Siver & P.B.Hamilton

APPENDIX IV

This appendix contains the supporting information for Chapter 7 manuscript: Beck, K. K., Fletcher, M.-S., Gadd, P. S., Heijnis, H., Saunders, K. M., Simpson, G. L., & Zawadzki, A. (2018) Variance and rate-of-change as early warning signals for a critical transition in an aquatic ecosystem state: A test case from Tasmania, Australia. *Journal of Geophysical Research: Biogeosciences*, 123, 495–508

DOI:10.1002/2017JG004135

Table IV.1: Lead-210 extended results table, analysis conducted at Australian Nuclear Science and Technology Organisation.

ANSTO ID	Depth (cm)		Bulk Density (g/cm ³)	Cumulative Dry Mass (g/cm ²)		Total ²¹⁰ Pb (Bq/kg)		Supported ²¹⁰ Pb (Bq/kg)		Uncorrected Unsupported ²¹⁰ Pb (Bq/kg)		Unsupported ²¹⁰ Pb Decay corrected to 21/08/2012 (Bq/kg)		Calculated CIC Ages (years)		Calculated CRS Ages (years)		CRS model Mass Accumulation Rates (g/cm ² /year)	
	upper	lower																	
N950	0.0	0.5	0.27	0.07	± 0.07	136.8	± 6.22	31.1	± 2.47	105.7	± 6.69	105.7	± 6.70	6.9	± 6.88	7.8	± 2.78	0.030	± 0.0027
N951	0.5	1.0	0.24	0.20	± 0.07	91.1	± 4.45	27.6	± 2.09	63.5	± 4.92	63.5	± 4.92	20.6	± 7.02	24.2	± 4.92	0.030	± 0.0040
N952	1.5	2.0	0.25	0.44	± 0.06	45.1	± 1.88	27.8	± 2.16	17.3	± 2.86	17.3	± 2.86	48.0	± 7.69	51.5	± 7.18	0.048	± 0.0099
N953	2.5	3.0	0.25	0.69	± 0.06	36.2	± 1.61	24.5	± 1.95	11.7	± 2.53	11.7	± 2.53	75.5	± 8.76	76.6	± 8.75	0.032	± 0.0092
N954	5.0	5.5	0.22	1.29	± 0.06	27.5	± 1.25	26.2	± 2.03	1.3	± 2.38	1.3	± 2.39	144.1	± 12.46	218.0	± 14.77	0.003	± 0.0089

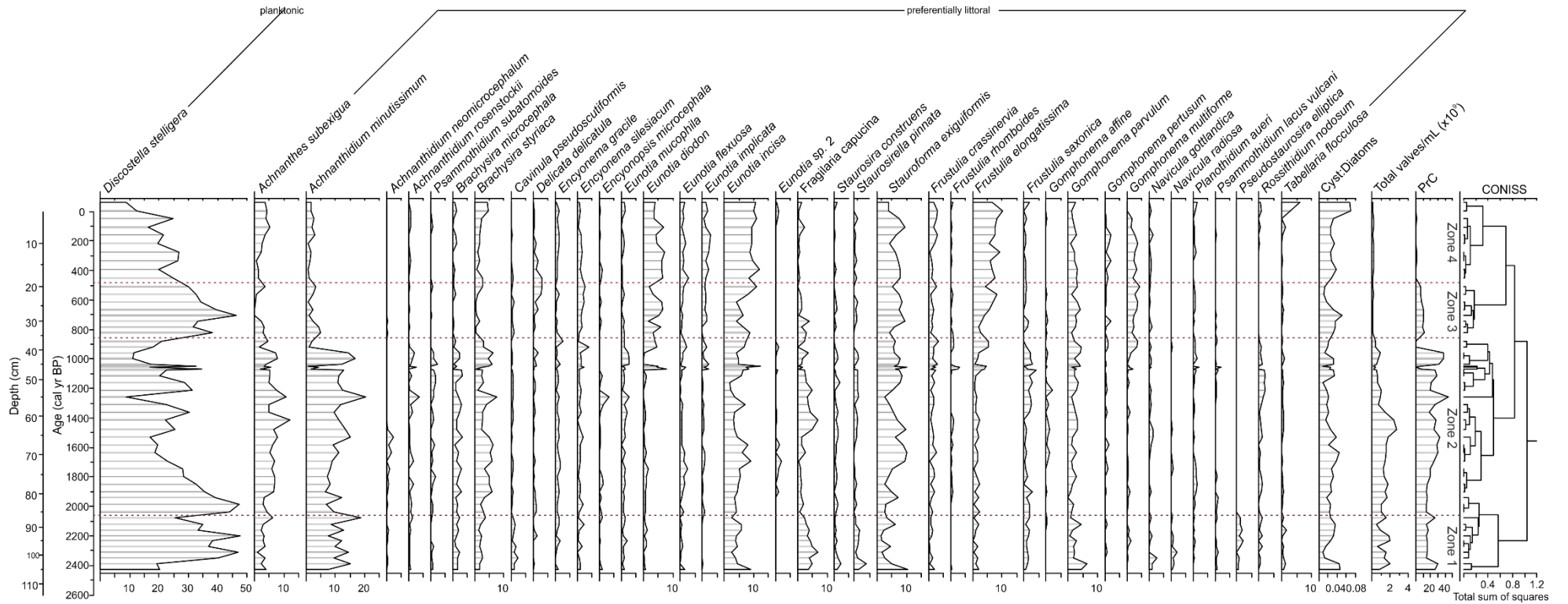


Figure IV.1: Extended diatom summary stratigraphy of percent diatoms (x-axis varies), cyst:diatoms, total valves (mLx10⁹) and PrC with four significant CONISS zones.

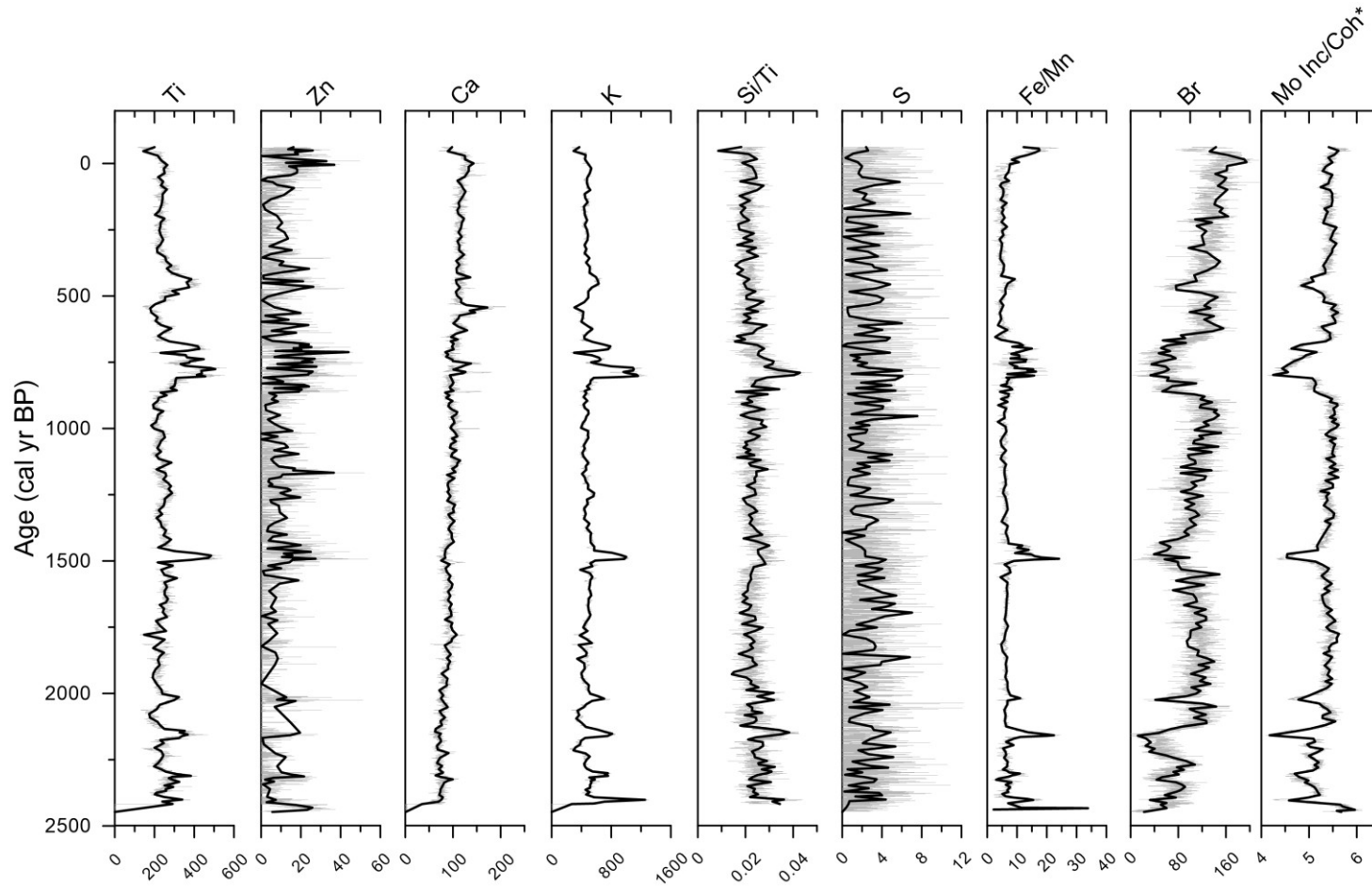


Figure IV.2: Geochemical μ XRF summary stratigraphy of important geochemical elements. Ti, Zn, Ca, K, include the detrital elements, Si/Ti is a bio indicator for diatom productivity, and S and Fe/Mn indicate terrestrial inputs and redox conditions, Br and Mo Inc/Coh are indicators of terrestrial organic matter inputs. All summarised elements are normalised values by Mo Inc/Coh with the exception of *.

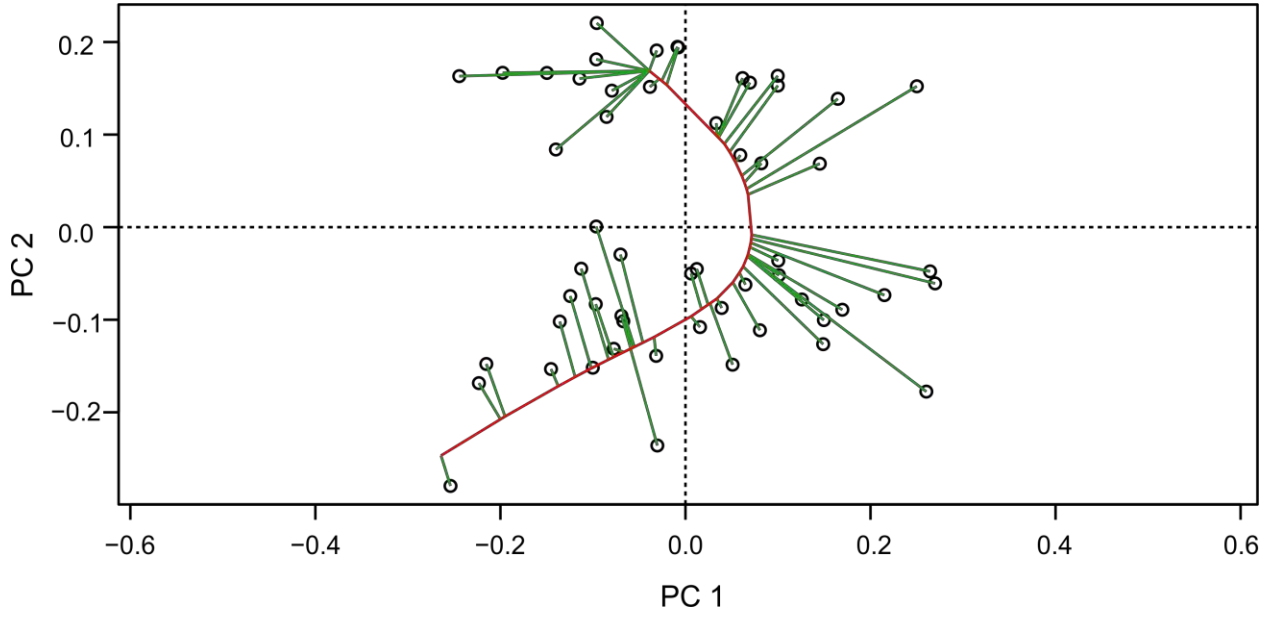
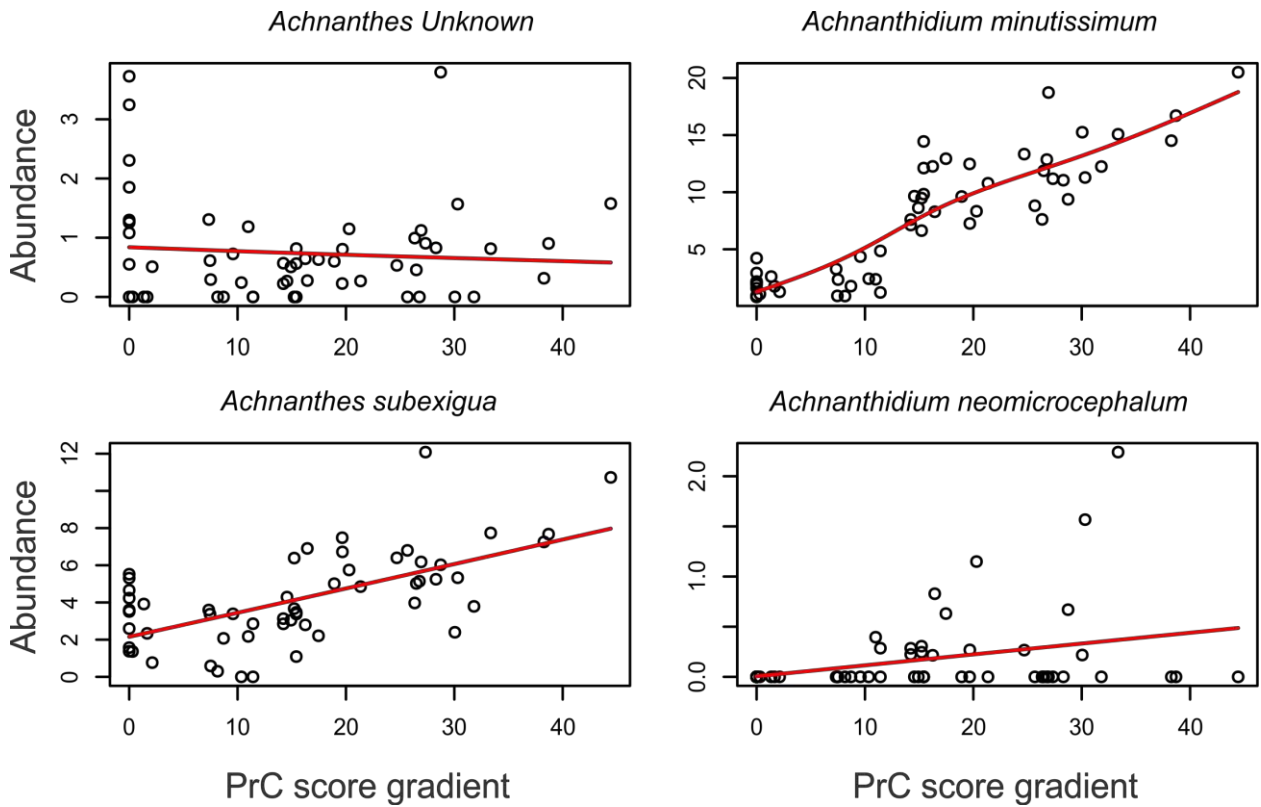
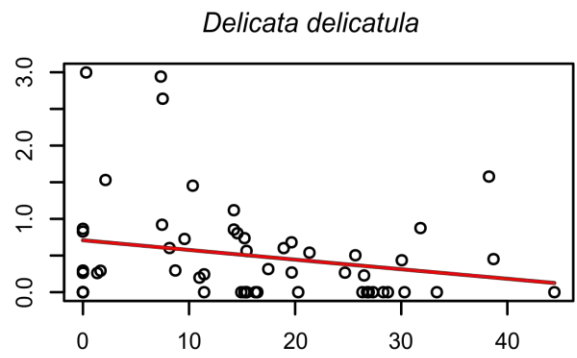
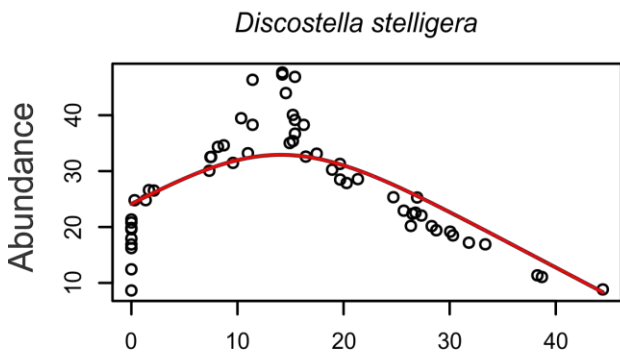
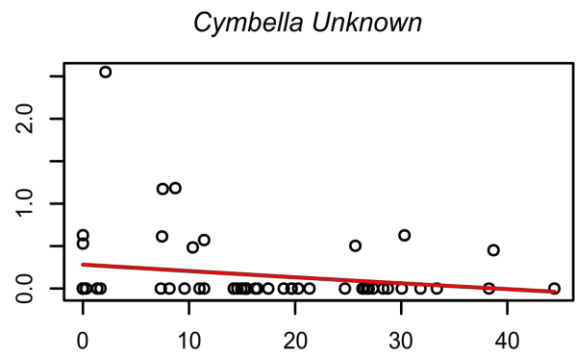
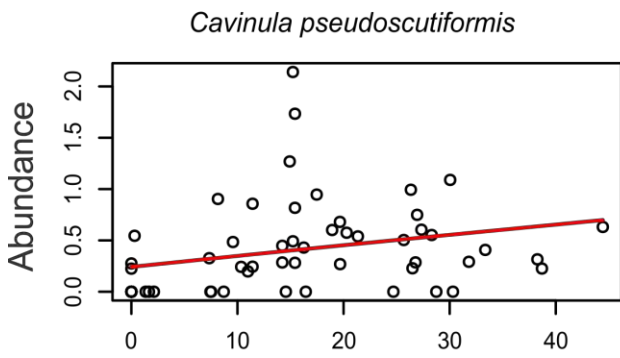
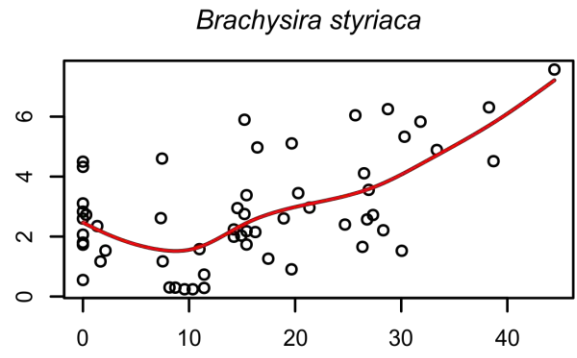
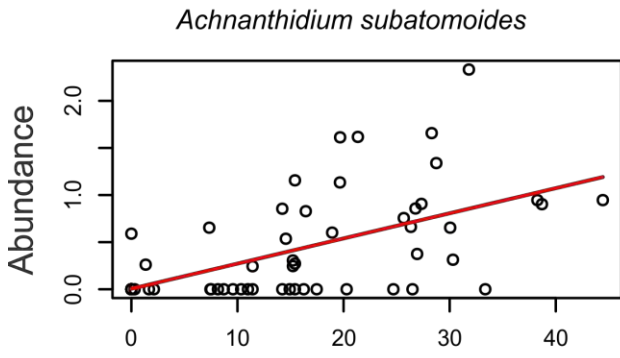
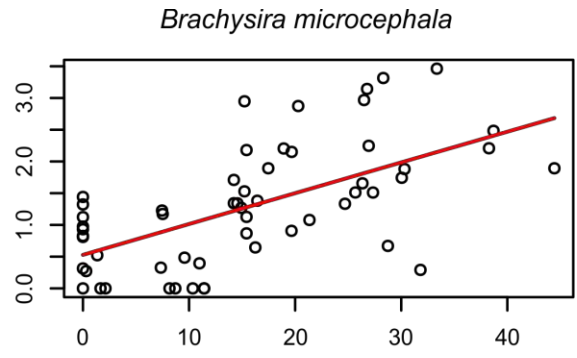
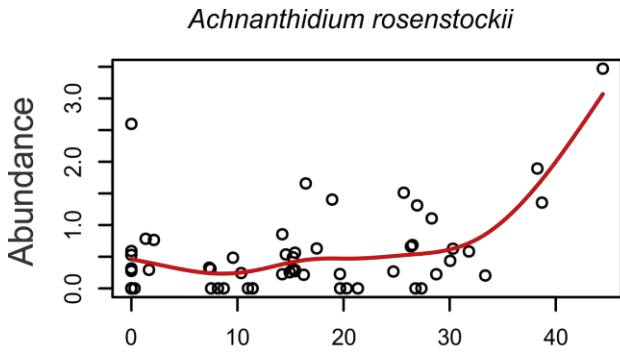


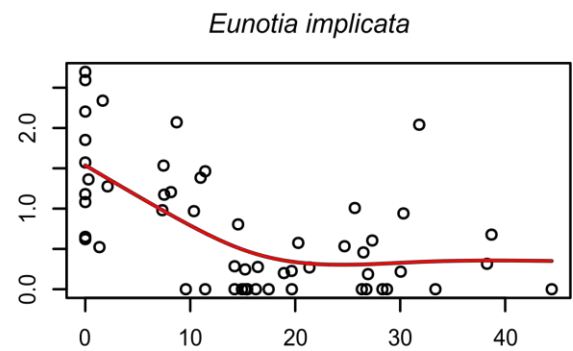
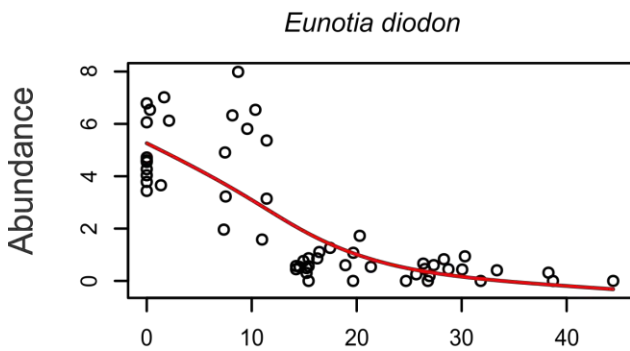
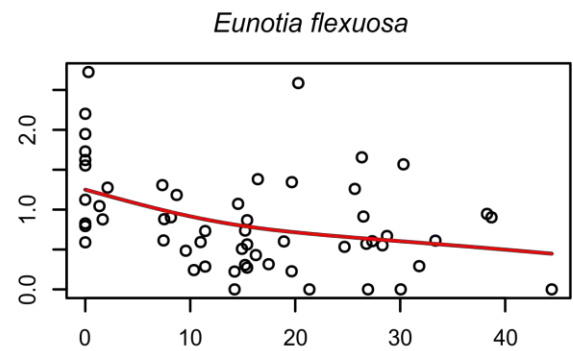
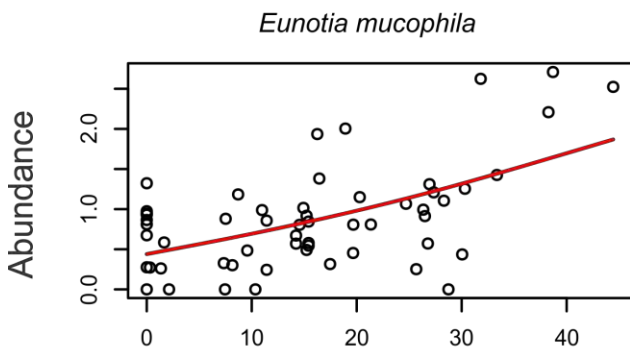
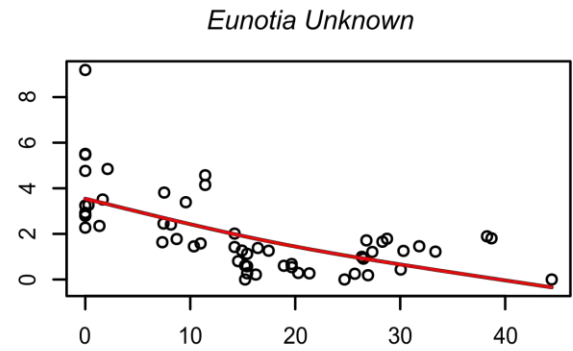
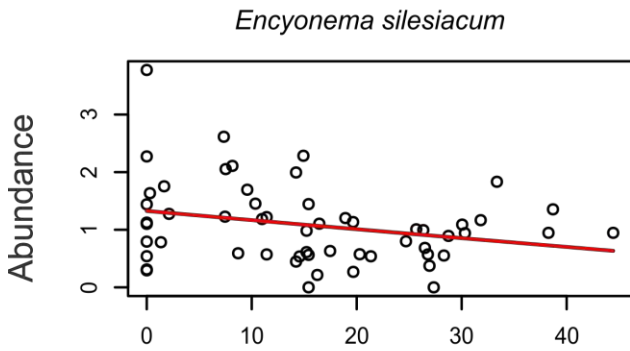
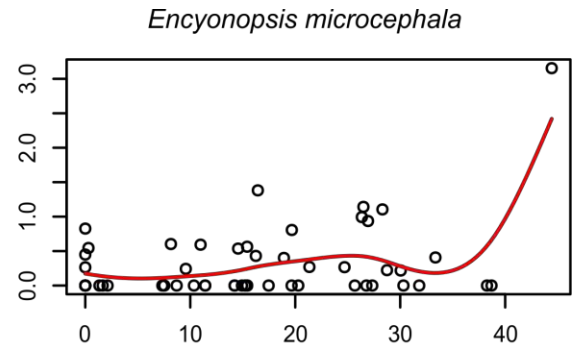
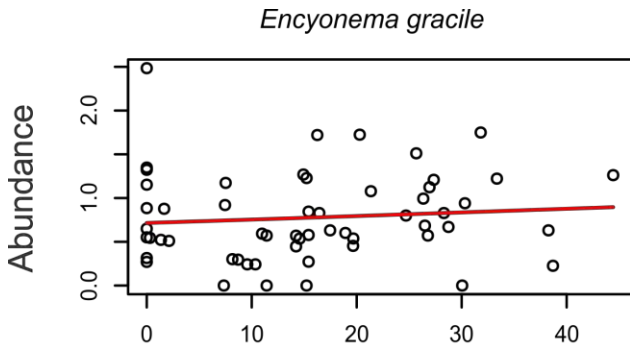
Figure IV.3: Diatom principal curve biplot with an explained variance of 60.0%. The fitted curve uses 133.978 degrees of freedom and correspondence analysis method with a penalty =1.4.





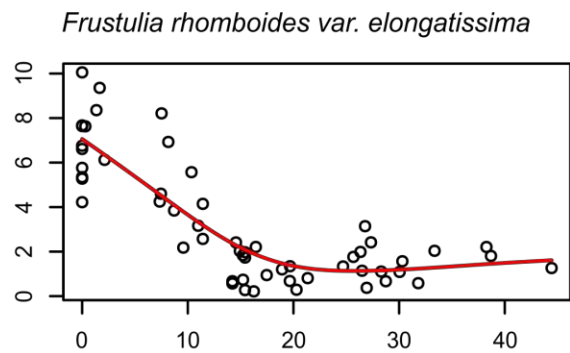
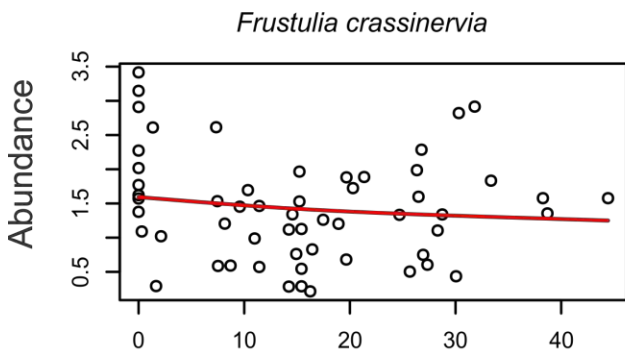
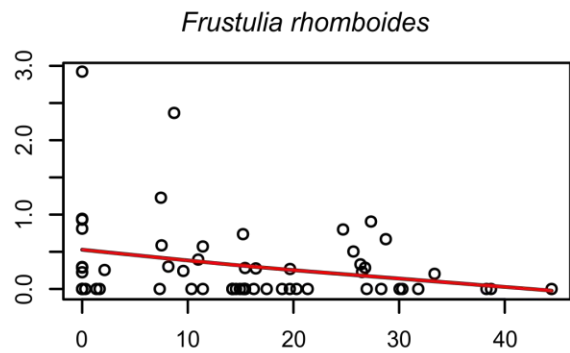
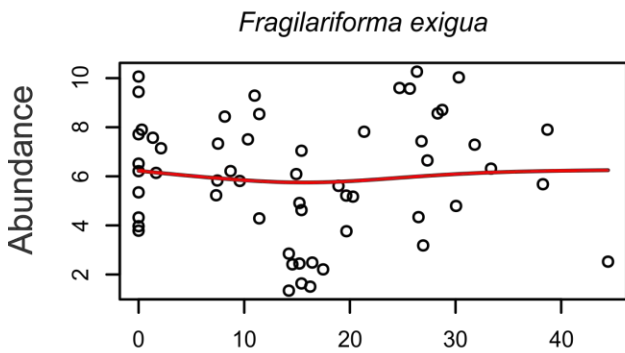
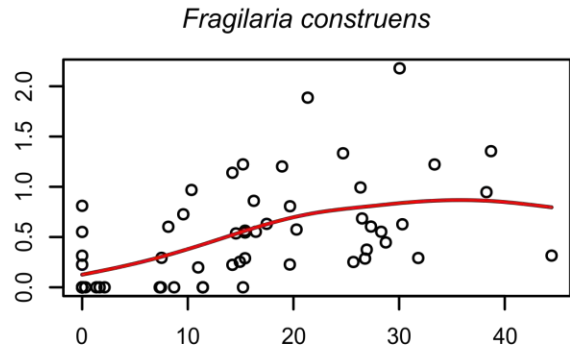
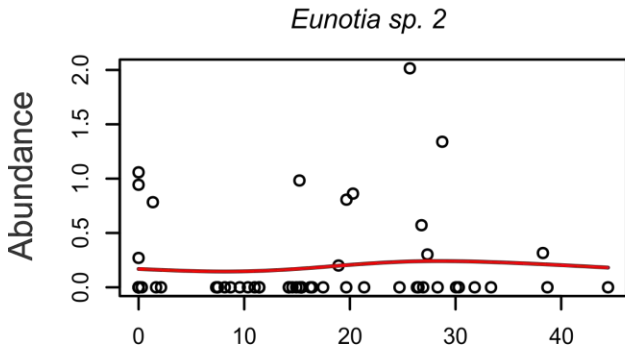
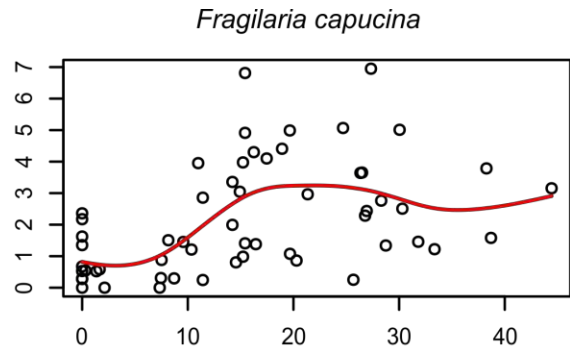
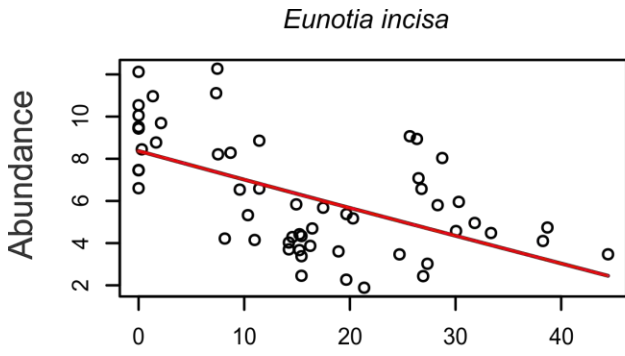
PrC score gradient

PrC score gradient



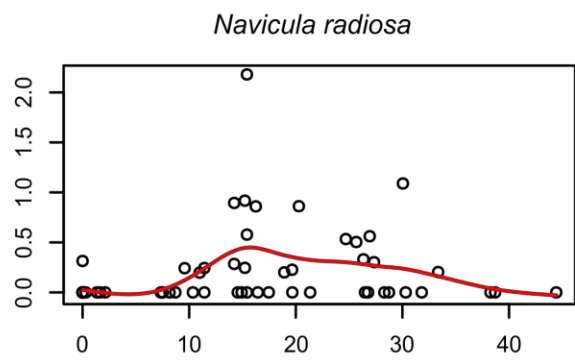
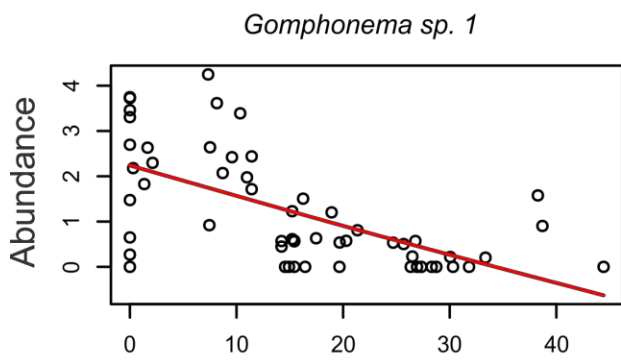
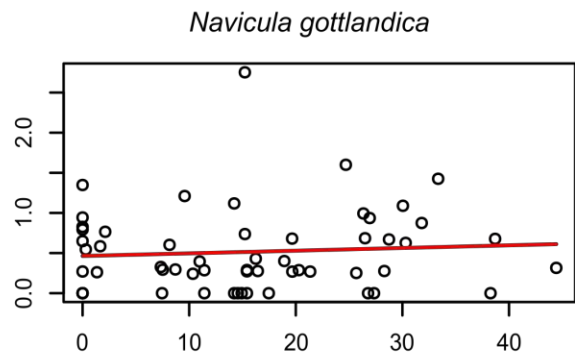
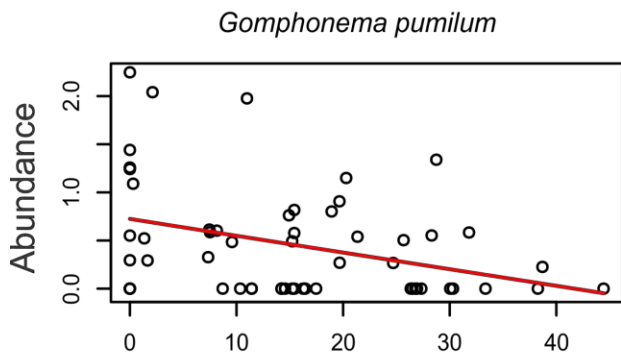
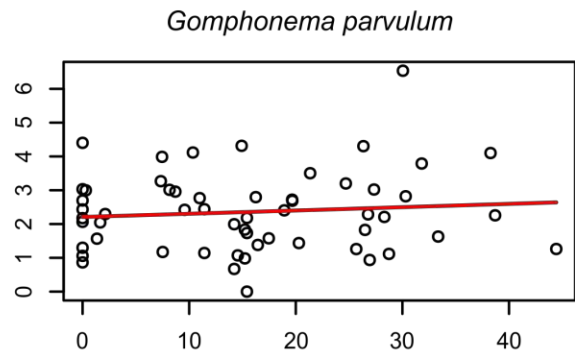
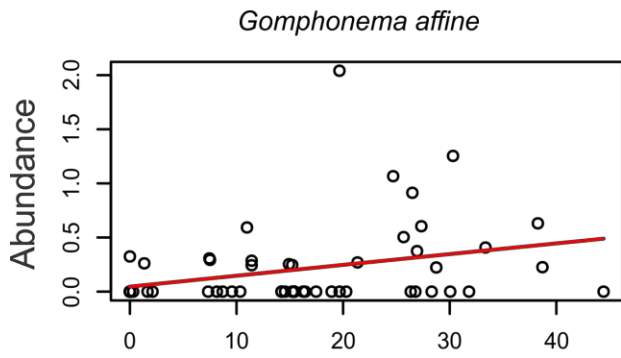
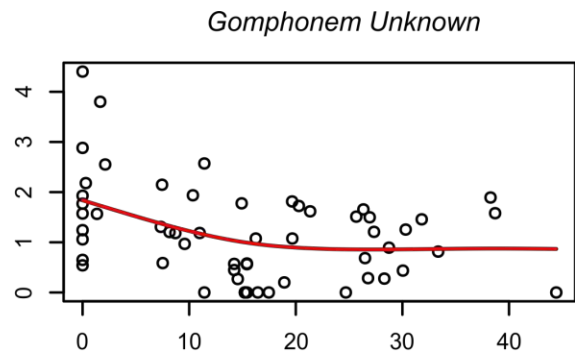
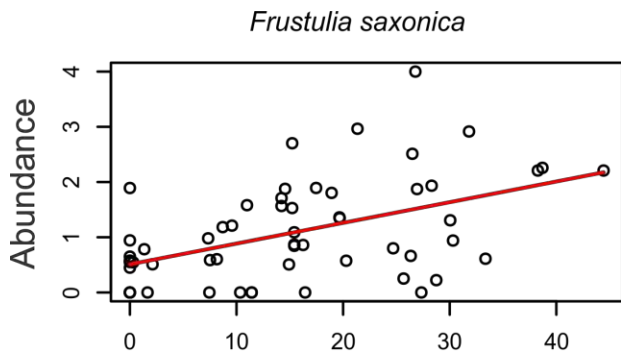
PrC score gradient

PrC score gradient



PrC score gradient

PrC score gradient



PrC score gradient

PrC score gradient

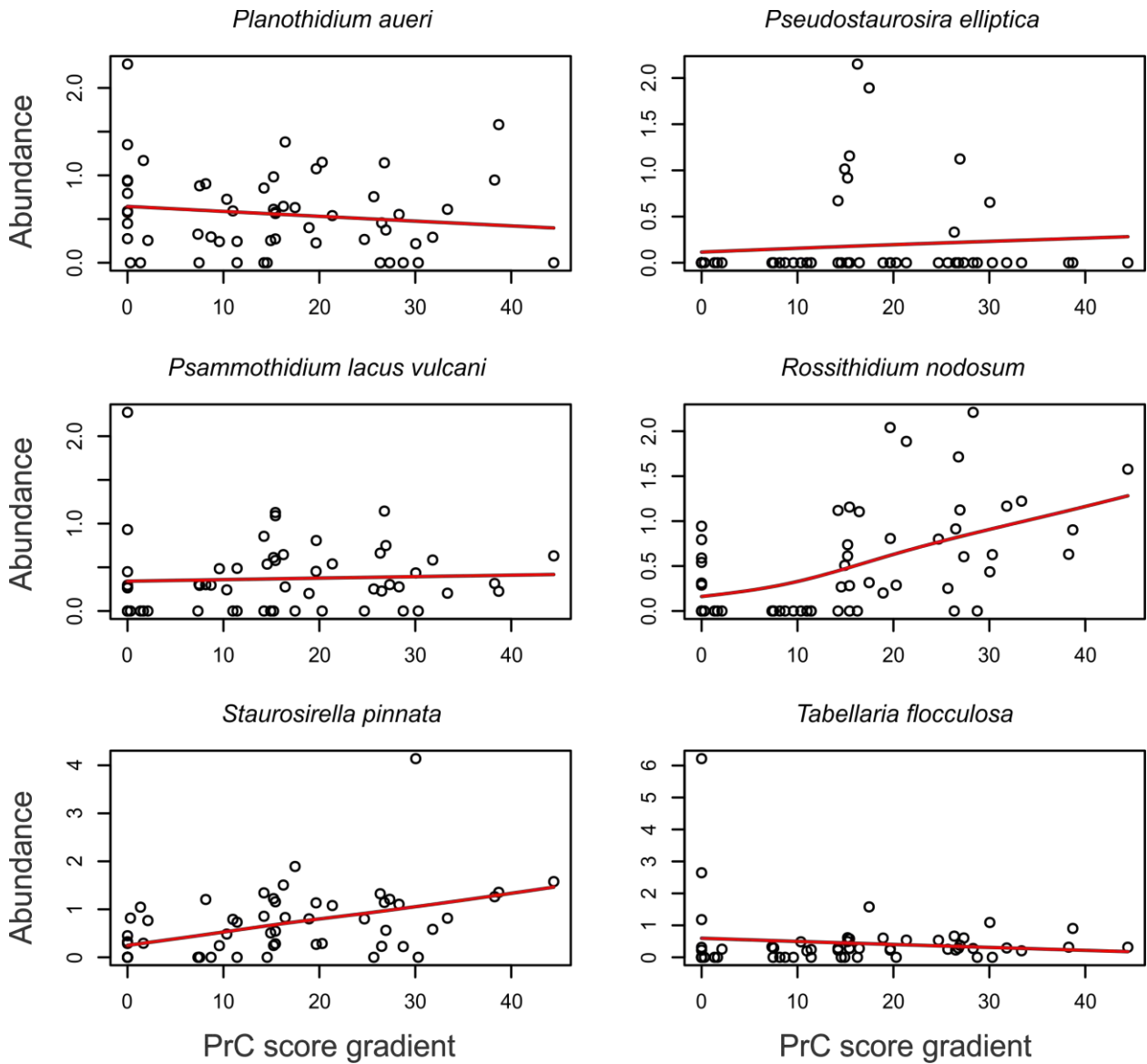


Figure IV.4: Species response plots of diatoms taxa included in the principal curve (PrC) performed using analogue (Simpson et al., 2016). Higher abundances indicate the PrC score the species is most associated with.

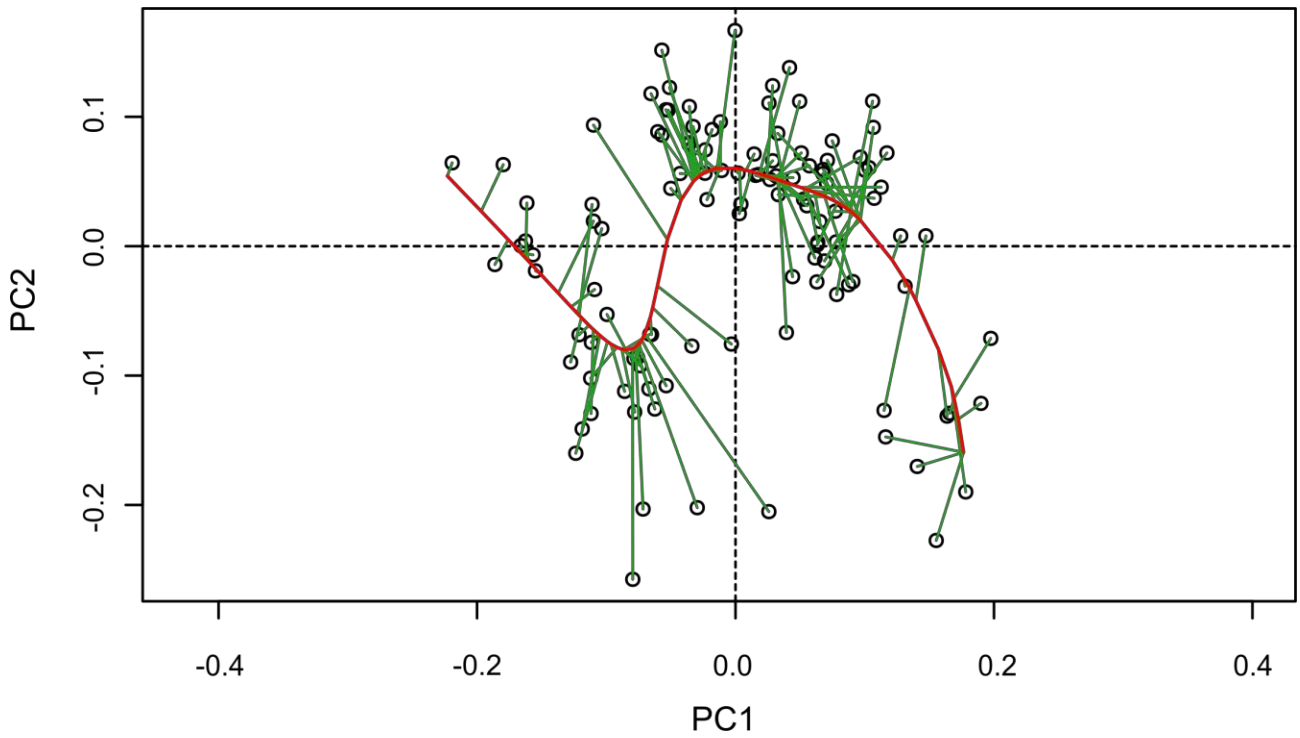
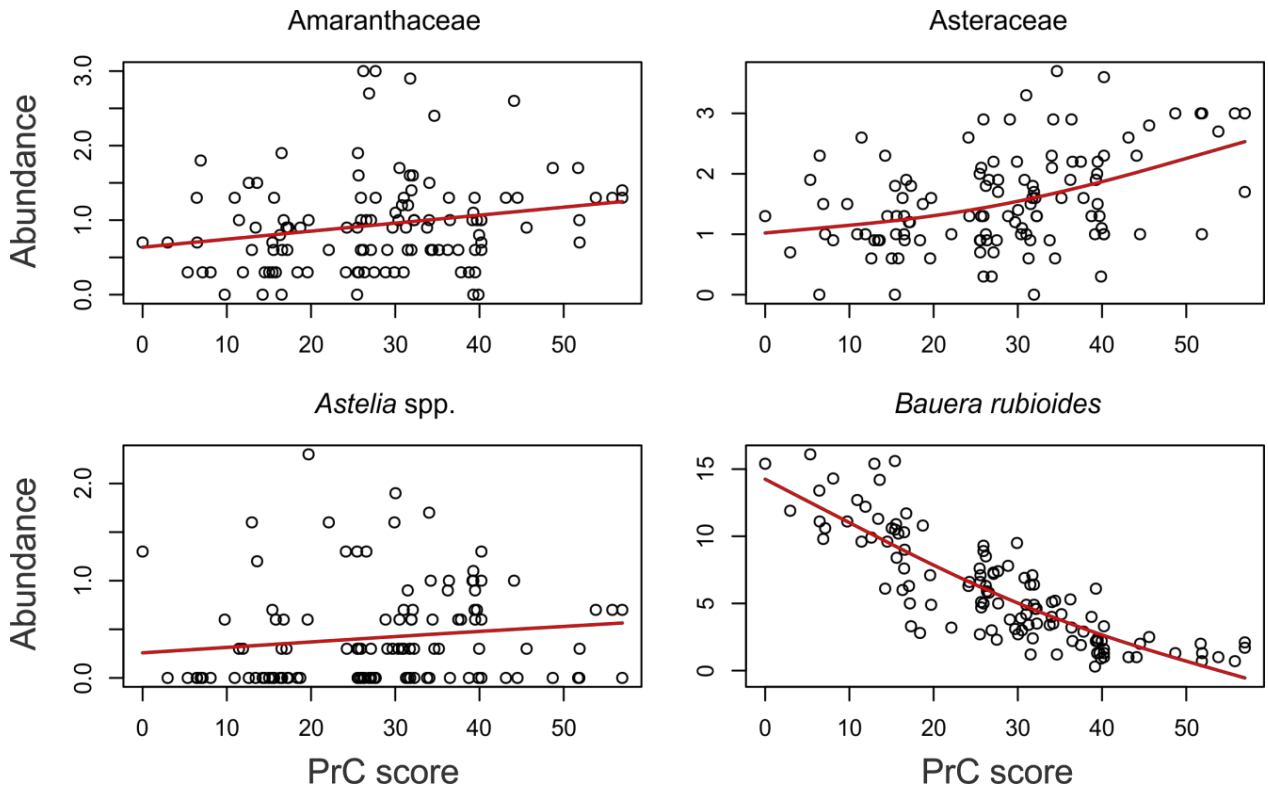
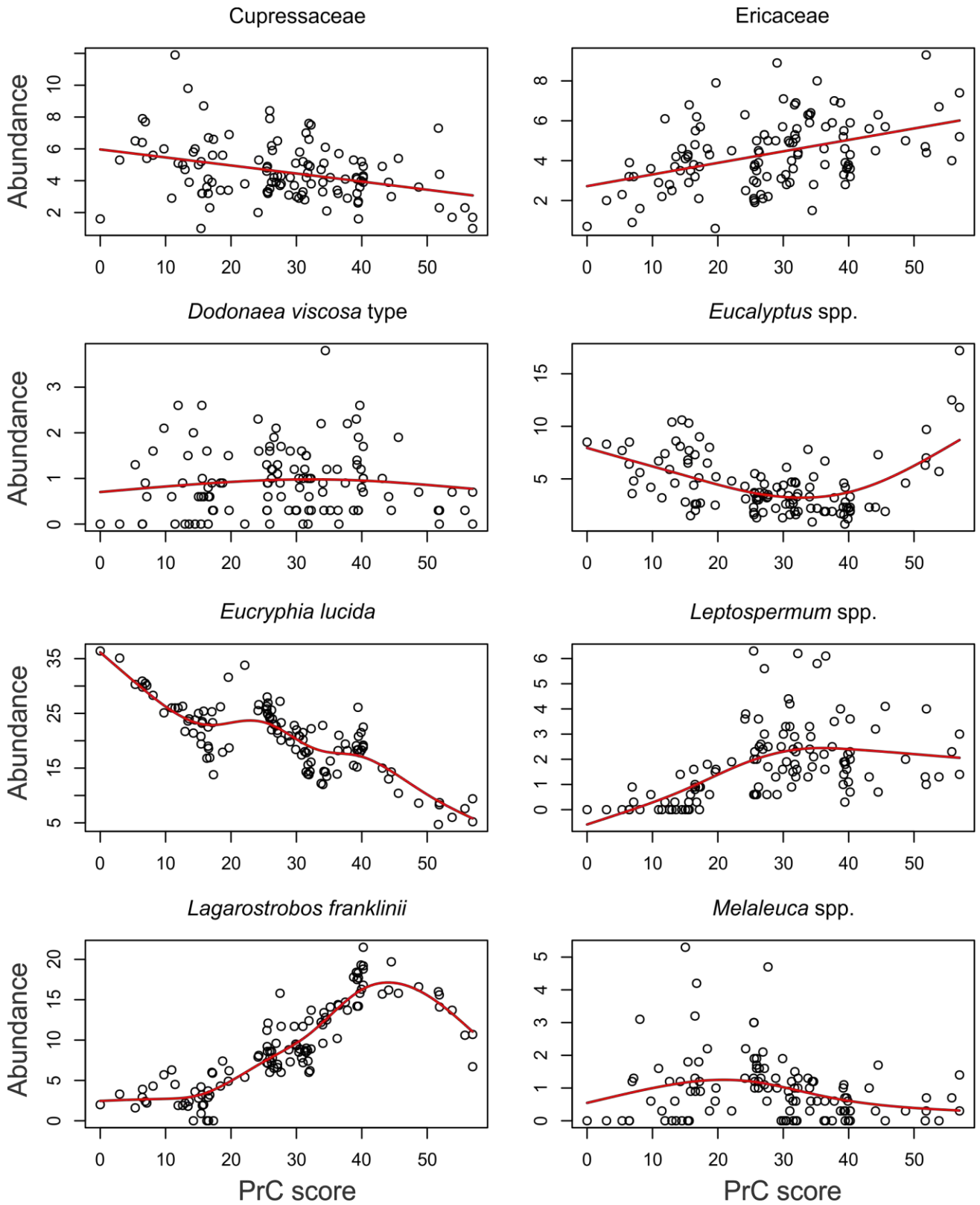
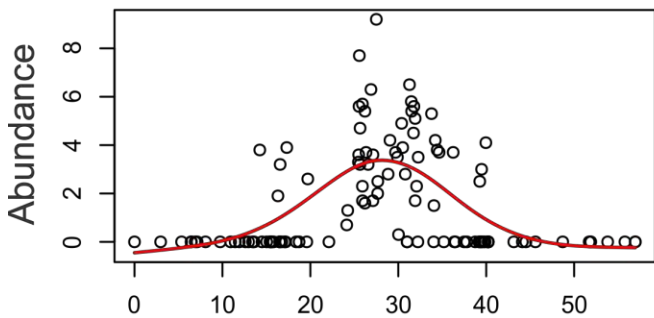


Figure IV.5: Pollen principal curve biplot with an explained variance 60.7 %. The fitted curve uses 75.2732 degrees of freedom and correspondence analysis method with penalty =1.4.

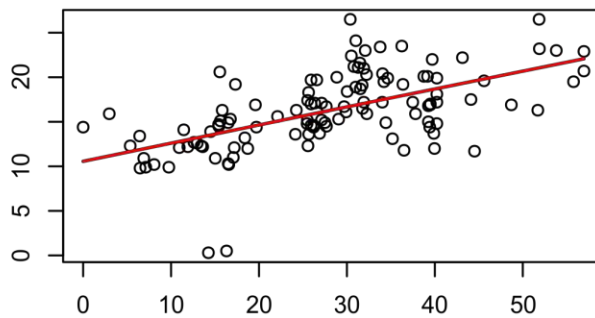




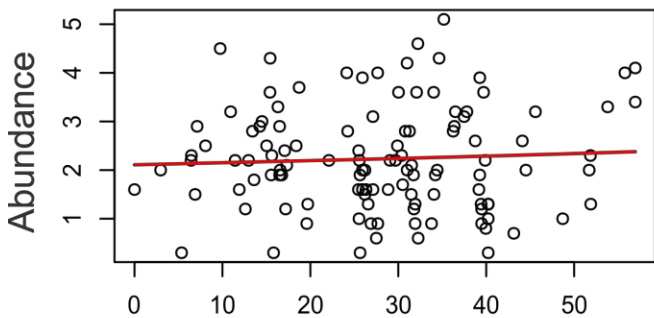
Microcachrys tetragona



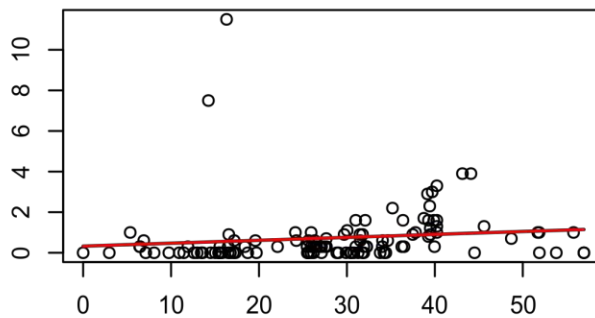
Nothofagus cunninghamii



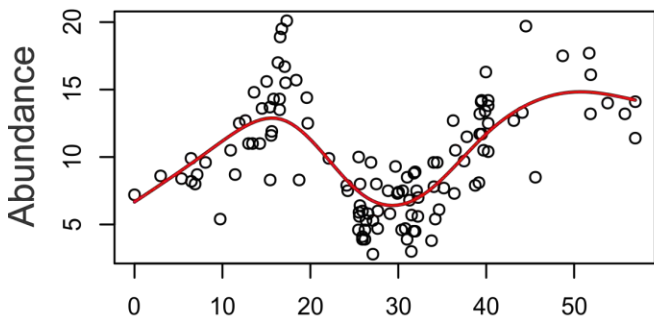
Monotoca spp.



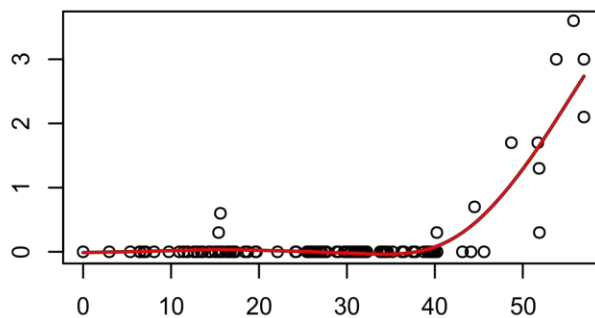
Nothofagus gunnii



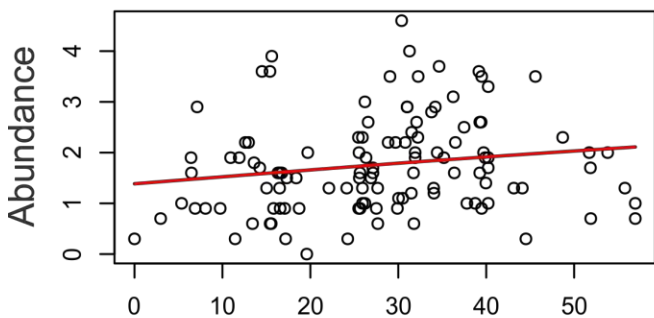
Phyllocladus aspleniifolius



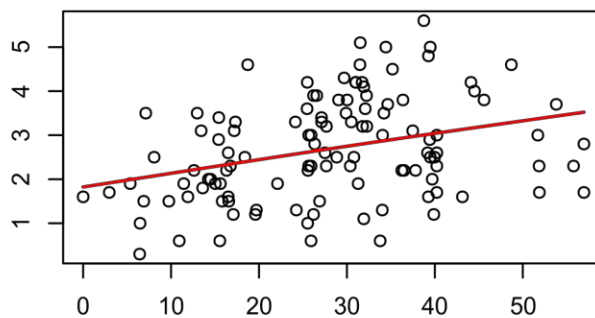
Pomaderris spp.



Poaceae



Proteaceae



PrC score

PrC score

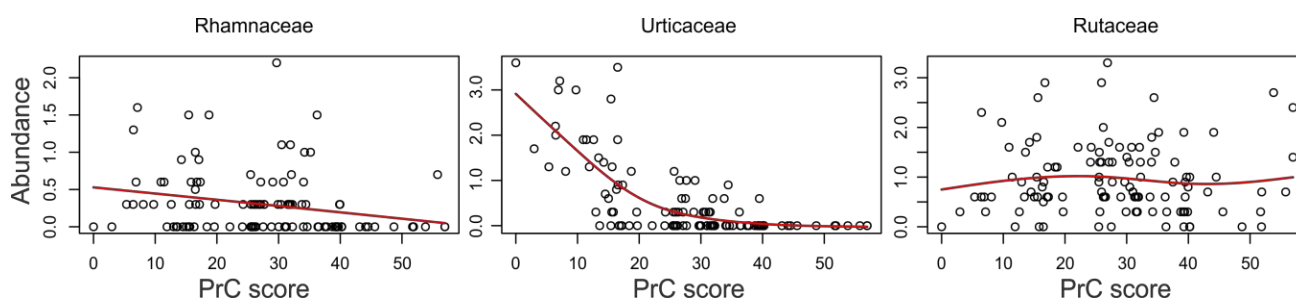


Figure IV.6: Species response plots of the terrestrial pollen for all taxa included in the PrC performed using analogue (Simpson et al., 2016). Higher abundances indicate the PrC score the species is most associated with.

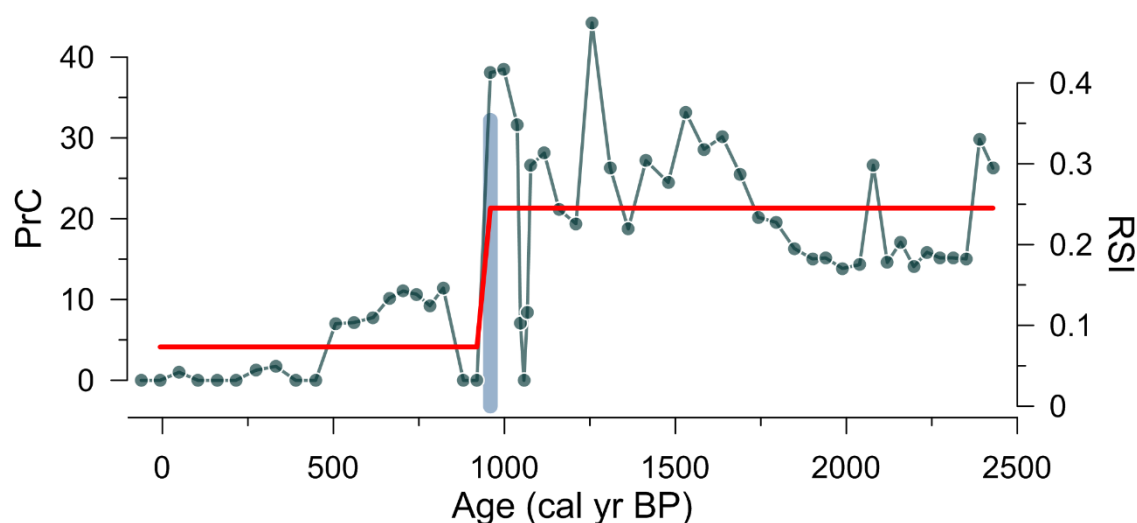


Figure IV.7: Lake Vera diatom PrC curve (green) fit with the mean RSI curve (red, window width of 5) and significant RSI shifts (blue bar, p-value <0.01). Outputs with larger window widths (i.e. 20 and 30) showed the same result.

Table IV.2: Diatom authorities for Lake Vera TAS1108SC1 (Chapter 7). Diatom taxonomic nomenclature was verified using Algaebase (<http://www.algaebase.org/>).

Species names	Authorities
<i>Achnanthes chlidanos</i>	M.H.Hohn & Hellerman
<i>Achnanthes didyma</i>	Hustedt
<i>Achnanthes minutissima</i> var. <i>macrocephala</i>	Hustedt
<i>Achnanthes oblongella</i>	Østrup
<i>Achnanthes percava</i>	Carter
<i>Achnanthes petersenii</i>	Hustedt
<i>Achnanthes pseudoswaki</i>	Carter
<i>Achnanthes rechtensis</i>	Leclercq
<i>Achnanthes</i> sp. 1	Vyverman et al. 1995
<i>Achnanthes</i> sp. 3	Vyverman et al. 1995
<i>Achnanthes</i> sp. 5	Vyverman et al. 1995
<i>Achnanthes stolida</i>	(Krasske) Krasske

<i>Achnanthes subexigua</i>	Hustedt
<i>Achnanthes thermalis</i>	(Rabenhorst) Schoenfeld
<i>Achnanthes ventralis</i>	(Krasske) Lange-Bertalot
<i>Achnantheidium exiguum</i>	(Grunow) Czarnecki
<i>Achnantheidium kranzii</i>	(Lange-Bertalot) Round & Bukhtiyarova
<i>Nupela lapidosa</i>	(Krasske) Lange-Bertalot
<i>Achnantheidium minutissimum</i>	(Kützing) Czarnecki
<i>Achnantheidium neomicrocephalum</i>	Lange-Bertalot & F.Staab, 2004
<i>Achnantheidium pyrenaicum</i>	(Hustedt) H.Kobayasi
<i>Achnantheidium rosenstockii</i>	(Lange-Bertalot) Lange-Bertalot
<i>Psammothidium subatomoides</i>	(Hustedt) Bukhtiyarova & Round
<i>Achnantheidium subatomus</i>	(Hustedt) Lange-Bertalot
<i>Achnantheidium subsalsum</i>	(J.B.Petersen) Aboal
<i>Achnantheidium bioretii</i>	(H.Germain) Monnier, Lange-Bertalot & Ector
<i>Actinella parva</i>	K.Vanhoutte & K.Sabbe
<i>Actinella indistincta</i>	W.Vyverman & E.A.Bergey
<i>Actinella tasmaniensis</i>	Hustedt
<i>Amphora sp. 1</i>	Vyverman et al. 1995
<i>Aulacoseira alpigena</i>	(Grunow) Krammer
<i>Aulacoseira crenulata</i>	(Ehrenberg) Thwaites
<i>Aulacoseira distans</i>	(Ehrenberg) Simonsen
<i>Aulacoseira valida</i>	(Grunow) Krammer
<i>Biremis leeawuliana</i>	W.Vyverman, K.Sabbe & R.Vyverman
<i>Biremis osbornii</i>	W.Vyverman, K.Sabbe & R.Vyverman
<i>Biremis tasmanica</i>	W.Vyverman, K.Sabbe & R.Vyverman
<i>Brachysira aponina</i>	Kützing
<i>Brachysira brebissonii</i>	R.Ross
<i>Brachysira microcephala</i>	(Grunow) Compère
<i>Brachysira styriaca</i>	(Grunow) R.Ross
<i>Brachysira zellensis</i>	(Grunow) Round & D.G.Mann
<i>Brevisira arentii</i>	(Kolbe) Krammer
<i>Caloneis bacillum</i>	(Grunow) Cleve 1894
<i>Caloneis dubia</i>	Krammer
<i>Caloneis silicula</i>	(Ehrenberg) Cleve 1894
<i>Caloneis undulata</i>	(W.Gregory) Krammer, nom. illeg. (Gregory ex Greville) Mann & Stickle in Round, Crawford & Mann 1990
<i>Cavinula cocconeiformis</i>	(Hustedt) D.G.Mann & A.J.Stickle
<i>Cavinula pseudoscutiformis</i>	(Cleve) Lange-Bertalot in Werum and Lange-Bertalot 2004
<i>Chamaepinnularia mediocris</i>	(Krasske) Lange-Bertalot & Krammer (Krasske) Lange-Bertalot & Krammer in Lange-Bertalot & Metzeltin 1996
<i>Chamaepinnularia soehrensii</i>	

<i>Cocconeis placentula</i>	Ehrenberg 1838
<i>Craticula subminuscula</i>	(Manguin) Wetzel and Ector 2015
<i>Cymbella affinis</i>	Kützing 1844
<i>Cymbella cistula</i>	(Ehrenberg) O.Kirchner
<i>Cymbella falaisensis</i>	(Grunow) Krammer & Lange-Bertalot
<i>Cymbella lanceolata</i>	(C.Agardh) C.Agardh
<i>Cymbella praerupta</i>	Hustedt
<i>Cymbopleura cuspidata</i>	(Kützing) Krammer
<i>Cymbopleura hauckii</i>	(Van Heurck) Krammer
<i>Cymbopleura incerta</i>	(Grunow) Krammer
<i>Cymbopleura naviculiformis</i>	(Auerswald ex Heiberg) Krammer
<i>Cymbopleura vasta</i>	(Hustedt) Krammer
<i>Delicata delicatula</i>	(Kützing) Krammer
<i>Diademsis gallica</i>	W.Smith
<i>Diploneis oblongella</i>	(Nägeli ex Kützing) Cleve-Euler
<i>Diploneis ovalis</i>	(Hilse) Cleve
<i>Discostella stelligera</i>	(Cleve and Grunow) Houk and Klee 2004
<i>Encyonema alpinum</i>	(Grunow) D.G.Mann
<i>Encyonema caespitosum</i>	Kützing
<i>Encyonema gracile</i>	Rabenhorst
<i>Encyonema mesianum</i>	(Cholnoky) D.G.Mann
<i>Encyonema minutum</i>	(Hilse) D.G.Mann
<i>Encyonema muelleri</i>	(Hustedt) D.G.Mann
<i>Encyonema perpusillum</i>	(Cleve-Euler) D.G.Mann
<i>Encyonema rugosum</i>	(Hustedt) D.G.Mann
<i>Encyonema silesiacum</i>	(Bleisch) D.G.Mann
<i>Encyonopsis cesatii</i>	(Rabenhorst) Krammer
<i>Encyonopsis descripta</i>	(Hustedt) Krammer
<i>Encyonopsis microcephala</i>	(Grunow) Krammer
<i>Encyonopsis angustissima</i>	(Hustedt) Krammer
<i>Epithemia sorex</i>	Kützing
<i>Eunophora indistincta</i>	R.Vyverman & D.G.Mann
<i>Eunophora tasmanica</i>	R.Vyverman & K.Sabbe
<i>Eunotia ambivalens</i>	Lange-Bertalot & Tagliaventi
<i>Eunotia arculus</i>	Lange-Bertalot & Nörpel
<i>Eunotia bidentula</i>	W.Smith
<i>Eunotia bigibba</i>	Kützing
<i>Eunotia bilunaris</i>	(Ehrenberg) Schaarschmidt
<i>Eunotia mucophila</i>	(Lange-Bertalot, Nörpel-Schempp & Alles) Lange-Bertalot
<i>Eunotia denticula</i>	(L.A.Brébisson) G.Rabenhorst- Unchecked
<i>Eunotia diodon</i>	Ehrenberg

<i>Eunotia faba</i>	(Ehrenberg) Grunow, nom. illeg.
<i>Eunotia fallax</i>	A.Cleve
<i>Eunotia flexuosa</i>	(Brébisson ex Kützing) Kützing
<i>Eunotia implicata</i>	Nörpel, Lange-Bertalot & Alles
<i>Eunotia incisa</i>	W.Smith ex W.Gregory
<i>Eunotia intermedia</i>	(Krasske ex Hustedt) Nörpel & Lange-Bertalot
<i>Eunotia minor</i>	(Kützing) Grunow
<i>Eunotia monodon</i>	Ehrenberg
<i>Eunotia monodon f. bidens</i>	(Ehrenberg) Hustedt
<i>Eunotia naegelii</i>	Migula
<i>Eunotia paludosa</i>	Grunow
<i>Eunotia pectinalis</i>	(Kützing) Rabenhorst
<i>Eunotia praerupta</i>	Ehrenberg
<i>Eunotia septentrionalis</i>	Østrup
<i>Eunotia sp. 2</i>	Vyverman et al. 1995
<i>Eunotia sp. 4</i>	Vyverman et al. 1995
<i>Eunotia sp. 5</i>	Vyverman et al. 1995
<i>Eunotia subarcuatoides</i>	Alles, Nörpel & Lange-Bertalot
<i>Eunotia exigua</i>	(Brébisson ex Kützing) Rabenhorst
<i>Fallacia pseudoforcipata</i>	(Hustedt) D.G.Mann
<i>Fallacia vitrea</i>	(Østrup) D.G.Mann
<i>Fragilaria brevistriata</i>	Grunow
<i>Fragilaria capucina</i>	Desmazières
<i>Fragilaria capucina var. gracilis</i>	(Oestrup) Hustedt
<i>Fragilaria pseudoconstruens</i>	Marciniak
<i>Fragilaria zeilleri</i>	Héribaud-Joseph
<i>Fragilariforma cassieae</i>	C.Kilroy & E.A.Bergey
<i>Stauroforma exiguiformis</i>	R.J.Flower, V.J.Jones & Round
<i>Frustulia crassinervia</i>	(Brébisson ex W.Smith) Lange-Bertalot & Krammer
<i>Frustulia rhomboides</i>	(Ehrenberg) De Toni
<i>Frustulia elongatissima</i>	(Manguin) Lange-Bertalot & Metzeltin - Unchecked
<i>Frustulia saxonica</i>	Rabenhorst
<i>Gomphonema affine</i>	Kützing
<i>Gomphonema angustum</i>	(Kützing) Rabenhorst
<i>Gomphonema exilissimum</i>	(Grunow) Lange-Bertalot & E.Reichardt
<i>Gomphonema gracile</i>	Ehrenberg
<i>Gomphonema grunowii</i>	R.M.Patrick & Reimer
<i>Gomphonema hebridense</i>	W.Gregory
<i>Gomphonema olivaceum</i>	(Hornemann) Brébisson
<i>Gomphonema parvulum</i>	(Kützing) Kützing
<i>Gomphonema pertusum</i>	Kociolek, Spaulding, Sabbe & Vyverman
<i>Gomphonema multiforme</i>	Kociolek, Spaulding, Sabbe & Vyverman
<i>Gomphonema trulliforme</i>	Kociolek, Spaulding, Sabbe & Vyverman
<i>Gomphonema subtile</i>	Ehrenberg
<i>Hantzschia amphioxys</i>	(Ehrenberg) Grunow

<i>Hantzschia virgata</i>	(Roper) Grunow
<i>Humidophila brekkaensis</i>	(Petersen) Lowe, Kociolek, Johansen, Van de Vijver, Lange-Bertalot & Kopalová
<i>Humidophila contenta</i>	(Grunow) Lowe, Kociolek, J.R.Johansen, Van de Vijver, Lange-Bertalot & Kopalová
<i>Humidophila perpusilla</i>	(Grunow) Lowe, Kociolek, Johansen, Van de Vijver, Lange-Bertalot & Kopalová
<i>Iconella curvula</i>	(Smith) Ruck & Nakov
<i>Iconella helvetica</i>	(Brun) Ruck & Nakov
<i>Iconella linearis</i>	(W.Smith) Ruck & Nakov
<i>Karayevia carissima</i>	(Lange-Bertalot) Bukhtiyarova
<i>Kobayasiella tasmanica</i>	Vyverman
<i>Kobayasiella hodgsonii</i>	Verleyen
<i>Luticola mutica</i>	(Kützing) D.G.Mann
<i>Mayamaea atomus</i>	(Kützing) Lange-Bertalot
<i>Mayamaea permitis</i>	(Hustedt) K.Bruder & Medlin
<i>Navicula angusta</i>	Grunow
<i>Navicula cari</i>	Ehrenberg
<i>Navicula cryptocephala</i>	Kützing
<i>Navicula digitulus</i>	Hustedt
<i>Navicula divaricata</i>	Hustedt
<i>Navicula gerloffii</i>	Schimanski
<i>Navicula gottlandica</i>	Grunow
<i>Navicula leptostriata</i>	Jørgensen
<i>Navicula lundii</i>	E.Reichardt
<i>Navicula minima</i>	Grunow- Unchecked
<i>Navicula notha</i>	J.H.Wallace
<i>Navicula pseudosilicula</i>	Hustedt
<i>Navicula radiosa</i>	Kützing
<i>Navicula recens</i>	(Lange-Bertalot) Lange-Bertalot
<i>Navicula sp. 1</i>	Vyverman et al. 1995
<i>Navicula sp. 2</i>	Vyverman et al. 1995
<i>Navicula sp. 3</i>	Vyverman et al. 1995
<i>Navicula sp. 4</i>	Vyverman et al. 1995
<i>Navicula sp. 6</i>	Vyverman et al. 1995
<i>Navicula sp. 7</i>	Vyverman et al. 1995
<i>Navicula sp. 8</i>	Vyverman et al. 1995
<i>Navicula stankovicii</i>	Hustedt
<i>Navicula tripunctata</i>	(O.F.Müller) Bory
<i>Neidium affine</i>	(Ehrenberg) Pfitzer
<i>Neidium ampliatum</i>	(Ehrenberg) Krammer
<i>Neidium perminutum</i>	Cleve-Euler
<i>Nitzschia bryophila</i>	(Hustedt) Hustedt

<i>Nitzschia fonticola</i>	(Grunow) Grunow
<i>Nitzschia intermedia</i>	Hantzsch
<i>Nitzschia palea</i>	(Kützing) W.Smith
<i>Nitzschia perminuta</i>	(Grunow) M.Peragallo
<i>Nupela pennsylvanica</i>	(Patrick) Potapova, 2011
<i>Nupela silvahercynia</i>	(Lange-Bertalot) Lange-Bertalot
<i>Pinnularia borealis</i>	Ehrenberg
<i>Pinnularia divergens</i>	W.Smith
<i>Pinnularia divergentissima</i>	(Grunow) Cleve
<i>Pinnularia gibbiformis</i>	Krammer
<i>Pinnularia hemiptera</i>	Brébisson ex Greville, nom. illeg.
<i>Pinnularia interrupta</i>	W.Smith
<i>Pinnularia microstauron</i>	(Ehrenberg) Cleve
<i>Pinnularia neomajor</i>	Krammer
<i>Pinnularia sp. 1</i>	Vyverman et al. 1995
<i>Pinnularia subcapitata</i>	W.Gregory
<i>Pinnularia viridis</i>	(Nitzsch) Ehrenberg
<i>Placoneis elginensis var. cuneata</i>	(M.Møller ex Foged) Lange-Bertalot
<i>Planothidium aueri</i>	(Krasske) Lange-Bertalot
<i>Planothidium frequentissimum</i>	(Lange-Bertalot) Lange-Bertalot
<i>Planothidium hauckianum</i>	(Grunow) Bukhtiyarova
<i>Planothidium lanceolatum</i>	(Brébisson ex Kützing) Lange-Bertalot
<i>Platessa conspicua</i>	(Ant.Mayer) Lange-Bertalot
<i>Psammothidium lacus-vulcani</i>	(Lange-Bertalot & Krammer) L.N.Bukhtiyarova
<i>Psammothidium levanderi</i>	(Hustedt) Bukhtiyarova & Round
<i>Psammothidium marginulatum</i>	(Grunow) Bukhtiyarova & Round
<i>Psammothidium rossii</i>	(Hustedt) Bukhtiyarova & Round
<i>Pseudostaurosira elliptica</i>	(Schumann) Edlund, Morales & Spaulding
<i>Pseudostaurosira subsalina</i>	(Hustedt) E.A.Morales
<i>Reimeria sinuata</i>	(W.Gregory) Kociolek & Stoermer
<i>Rossithidium nodosum</i>	(Cleve) Aboal
<i>Rossithidium pusillum</i>	(Grunow) Round & Bukhtiyarova
<i>Sellaphora americana</i>	(Ehrenberg) D.G.Mann
<i>Sellaphora arvensis</i>	(Hustedt) C.E.Wetzel & L.Ector
<i>Sellaphora difficillima</i>	(Hustedt) C.E.Wetzel, L.Ector & D.G.Mann
<i>Sellaphora laticeps</i>	(Hustedt) C.E.Wetzel, L.Ector, B.Van de Vijver, Compère & D.G.Mann
<i>Sellaphora pupula</i>	(Kützing) Mereschkovsky
<i>Sellaphora seminulum</i>	(Grunow) D.G.Mann
<i>Sellaphora tridentula</i>	(Krasske) C.E.Wetzel
<i>Sellaphora bacillum</i>	(Ehrenberg) D.G.Mann
<i>Sellaphora medioconvexa</i>	(Hustedt) C.E.Wetzel

<i>Stauroneis anceps</i>	Ehrenberg
<i>Stauroneis legumen</i>	Ehrenberg, nom. illeg.
<i>Stauroneis phoenicenteron</i>	(Nitzsch) Ehrenberg
<i>Stauroneis kriegeri</i>	R.M.Patrick
<i>Stauroforma exiguiformis</i>	(Lange-Bertalot) R.J.Flower, V.J.Jones & Round
<i>Staurosira construens</i>	(Ehrenberg) Grunow
<i>Staurosira construens var. exigua</i>	(W.Smith) H.Kobayasi
<i>Staurosira venter</i>	(Ehrenberg) Cleve & J.D.Möller
<i>Staurosirella pinnata</i>	(Ehrenberg) D.M.Williams & Round
<i>Stenopterobia densestriata</i>	(Hustedt) Krammer

APPENDIX V

This appendix contains extended results from SEA analysis in Chapter 8.

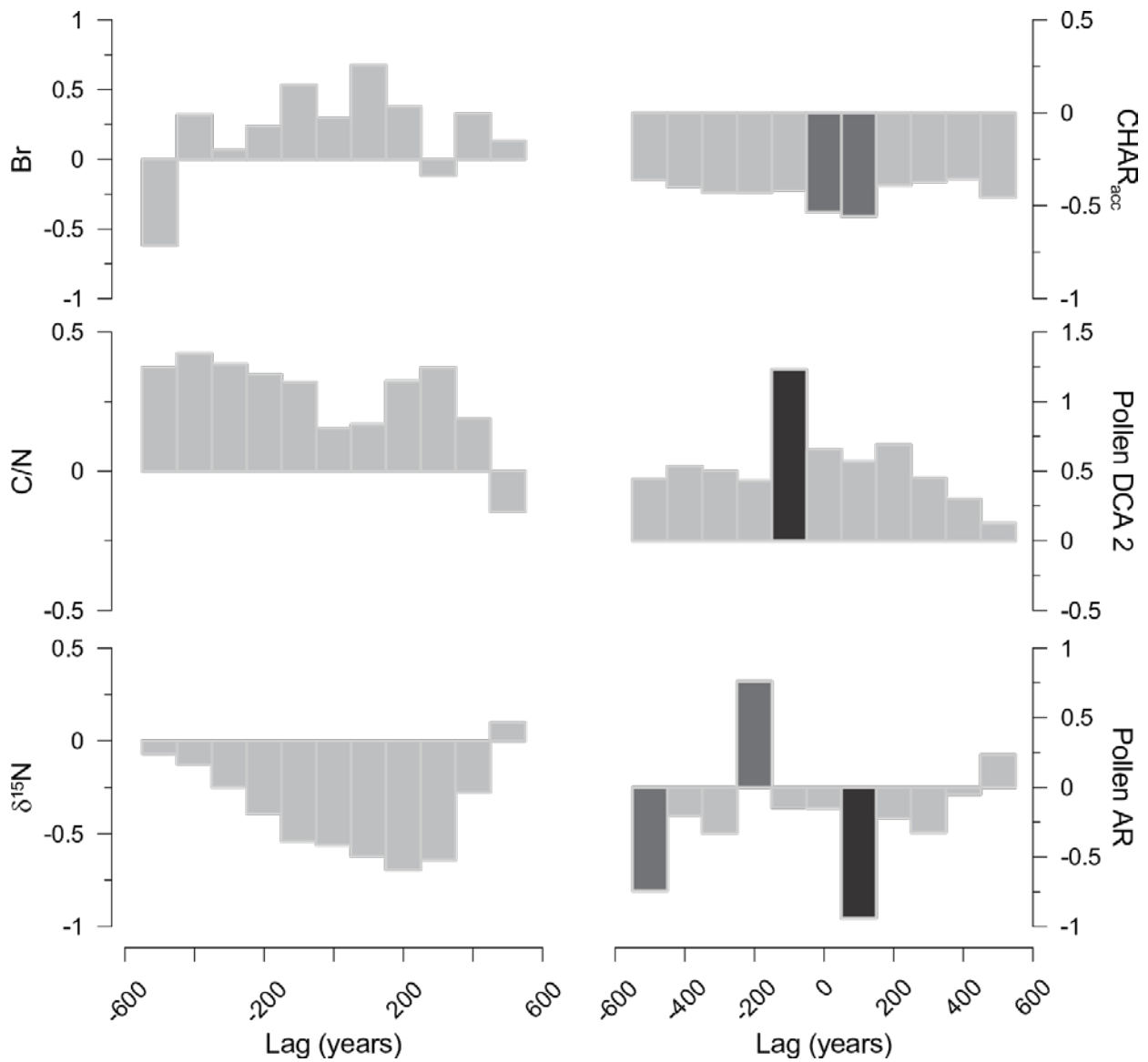


Figure V.1: Extended SEA analysis results for interpolated Paddy's Lake data (100 yrs) for Chapter 8. Dark grey bars represent the significant SEA $p < 0.05$, black bars $p < 0.01$.

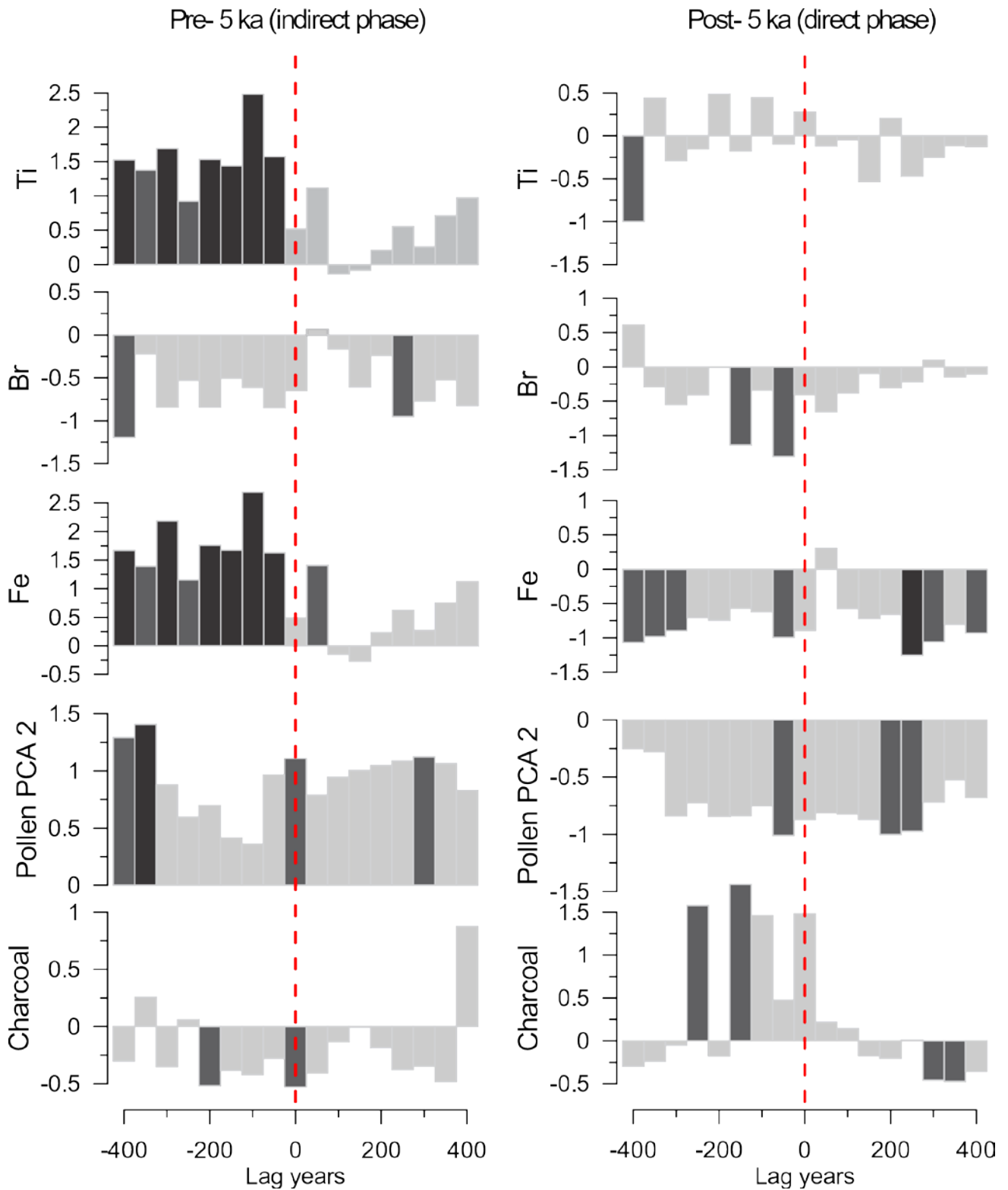
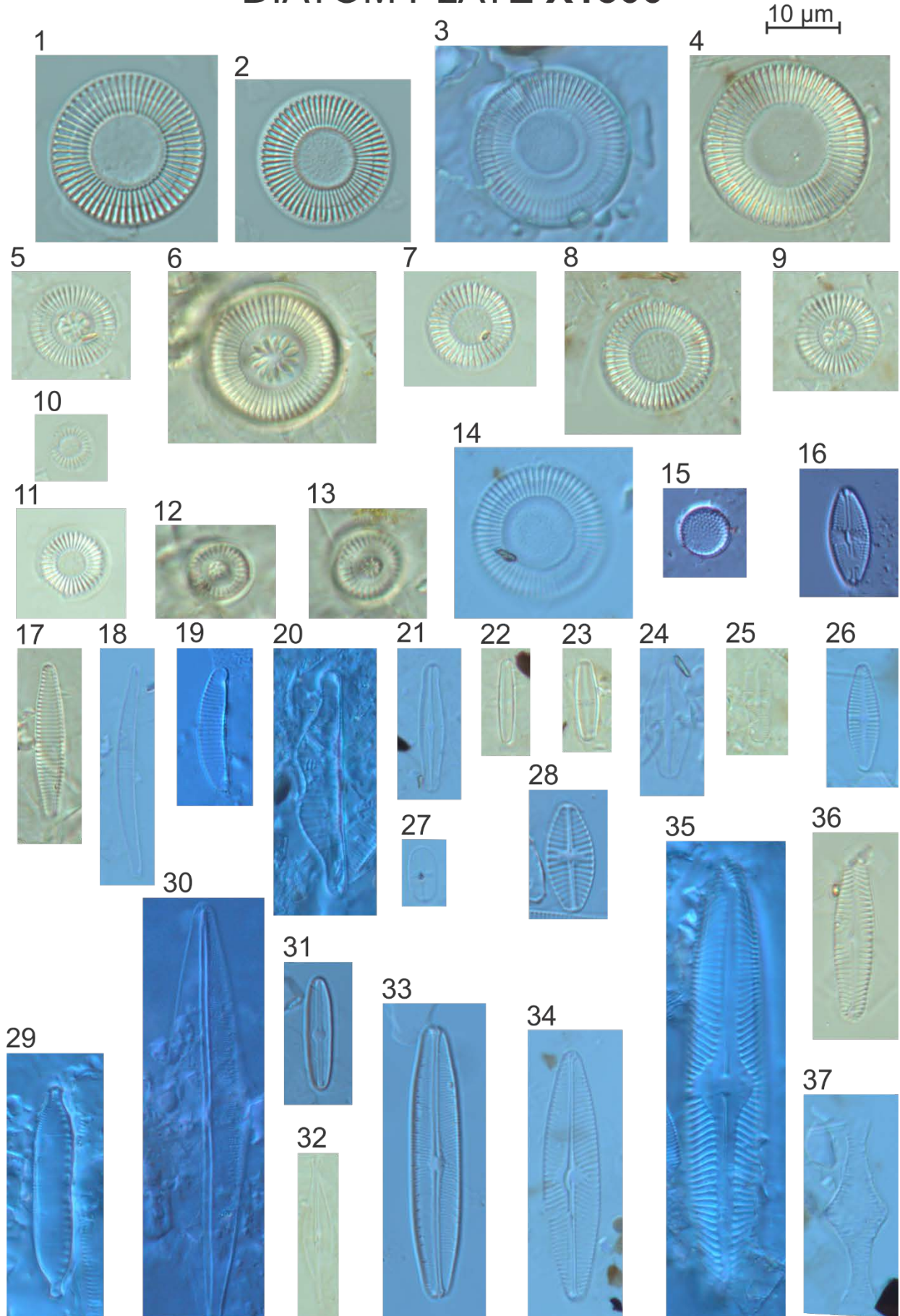


Figure V.2: Extended SEA analysis results for interpolated Lake Vera data (50 yrs) for Chapter 8. Dark grey bars represent the significant SEA $p < 0.05$, black bars $p < 0.01$.

APPENDIX VI

This appendix contains plates of some examples of microfossils identified in this thesis.

DIATOM PLATE X1500



Species Names Diatom Plate

- 1-14: *Discostella* cf. *stelligera* (Cleve & Grunow) Houk & Klee 2004
- 15: *Aulacoseira distans* (Ehrenberg) Simonsen
- 16: *Luticola mutica* (Kützing) D.G.Mann
- 17: *Stauroforma exiguiformis* (Lange-Bertalot) R.J.Flower, V.J.Jones & Round
- 18: *Eunotia bilunaris* (Ehrenberg) Schaarschmidt
- 19: *Eunotia incisa* W.Smith ex W.Gregory
- 20: *Eunotia bidentula* W.Smith
- 21-23: *Achnantheidium minutissimum* (Kützing) Czarnecki
- 24: *Psammothidium rossii* (Hustedt) Bukhtiyarova & Round - bottom valve
- 25: *Achnanthes pseudoswaki* Carter – bottom view
- 26: *Platessa conspicua* (Ant.Mayer) Lange-Bertalot
- 27: *Achnanthes didyma* Hustedt
- 28: *Achnanthes delicatula* subsp. *septentrionalis* (Østrup) Lange-Bertalot
- 29: *Hantzschia amphioxys* (Ehrenberg) Grunow
- 30: *Frustulia saxonica* Rabenhorst
- 31: *Brachysira zellensis* (Grunow) Round & D.G.Mann
- 32: *Brachysira microcephala* (Grunow) Compère
- 33: *Navicula* sp. 4 Vyverman *et al* (1995) - Plate 27
- 34: *Navicula lundii* E.Reichardt
- 35: *Pinnularia microstauron* (Ehrenberg) Cleve
- 36: *Pinnularia subcapitata* W.Gregory
- 37: *Tabellaria flocculosa* (Roth) Kützing

CLADOCERAN PLATE X1000

10 μm
└───┘

1



2



4



5



3



6

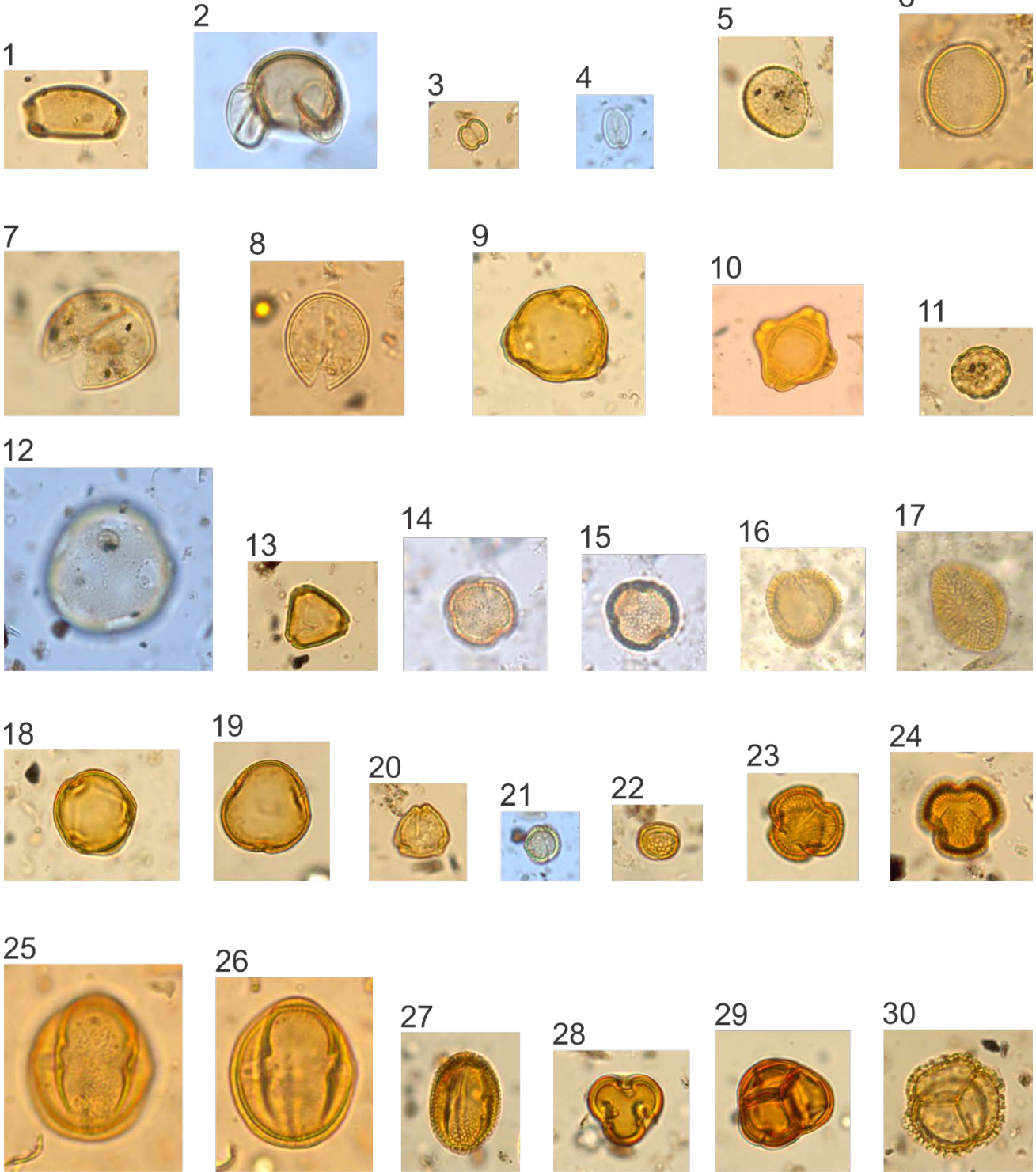


Species Names Cladoceran Plate

- 1: *Alona guttata* (Sars, 1862) - head shield
- 2: *Alona guttata* (Sars, 1862) - postabdomen
- 3: *Chydorus sphaericus* (O.F. Müller, 1785) - head shield
- 4: *Diaphanosoma cf. unguiculatum* (Gurney, 1927) - postabdomen
- 5: *Bosmina meridionalis* (Sars, 1904) - whole body
- 6: Ehippia

POLLEN PLATE X1000

10 μ m
└───┘



Species Names Pollen Plate

- 1: *Banksia* sp. (L.f.)
- 2: *Lagarostrobos franklinii* (Hook.f.) Quinn
- 3 and 4: *Bauera rubioides* (Andrews)
- 5: *Astelia alpine* (R.Br.)
- 6: *Atherosperma moschatum* (Labill.)
- 7 and 8: Cupressaceae (Bartlett)
- 9: *Allocasuarina* sp. (L.A.S. Johnson)
- 10: *Gonocarpus* sp. (Thunb.)
- 11: Chenopodiaceae (Vent.)
- 12: *Gymnoschoenus sphaerocephalus* [(R. Br.) Hook.f.]
- 13: *Eucalyptus* sp. (L'Hér. 1789)
- 14 and 15: Ranunculaceae (Juss.)
- 16 and 17: Brassicaceae (Burnett)
- 18: *Dodonaea* sp. (Mill.)
- 19: *Coprosma* sp. (J.R. Forst. & G.Forst.)
- 20: *Pomaderris cf. apetala* (Labill.)
- 21 and 22: *Bursaria spinose* (Cav.)
- 23 and 24: *Amperea xiphoclada* [(Sieber ex Spreng.) Druce]
- 25 and 26: Goodeniaceae (R.Br.)
- 27: *Zireria* sp. (Sm.)
- 28: *Gyrostemon thesioides* [(Hook.f.) A.S.George]
- 29: Ericaceae (Juss.)
- 30: *Tasmannia lanceolata* [(Poir.) A.C.Sm.]



Minerva Access is the Institutional Repository of The University of Melbourne

Author/s:

Beck, Kristen

Title:

Direct and indirect effects of long-term climatic change on terrestrial-aquatic ecosystem interaction in Tasmania

Date:

2018

Persistent Link:

<http://hdl.handle.net/11343/216441>

File Description:

Kristen Beck PhD Thesis: Direct and indirect effects of long-term climatic change on terrestrial-aquatic ecosystem interaction in Tasmania

Terms and Conditions:

Terms and Conditions: Copyright in works deposited in Minerva Access is retained by the copyright owner. The work may not be altered without permission from the copyright owner. Readers may only download, print and save electronic copies of whole works for their own personal non-commercial use. Any use that exceeds these limits requires permission from the copyright owner. Attribution is essential when quoting or paraphrasing from these works.